MAHMOUD NADIM NAHAS

FAILURE OF LAMINATED FIBRE-REINFORCED COMPOSITE STRUCTURES SUBJECTED TO COMBINED LOADINGS

COLLEGE OF AERONAUTICS
AIRCRAFT DESIGN

PH.D. THESIS.

CRANFIELD INSTITUTE OF TECHNOLOGY

COLLEGE OF AERONAUTICS

AIRCRAFT DESIGN DIVISION

Ph.D. THESIS

Academic Year 1979-1980

MAHMOUD NADIM NAHAS

"FAILURE OF LAMINATED FIBRE-REINFORCED COMPOSITE STRUCTURES SUBJECTED TO COMBINED LOADINGS"

Supervisors: R. TETLOW
C.K. TROTMAN
Prof. D. HOWE

SUMMARY

A new modified maximum strain failure criterion is proposed to predict the failure of the laminae of laminated fibre-reinforced composite structures when the laminate is subjected to combined loadings. The new criterion takes into account the layer non-linear behaviour which is an important factor in the failure prediction operation. The analysis of laminated structures containing laminae with non-linear stress-strain response is also studied and a new method is proposed for this analysis. The modified failure criterion introduces two levels of failure. The lower level is associated with the "yield" of the lamina, or the beginning of the lamina degradation, above which the lamina will exhibit irreversible damage. The higher failure level, however, is associated with the "ultimate" failure of the lamina, above which the lamina cannot sustain any load.

After the "ultimate" failure of a lamina in a certain direction, the post-failure model proposed in this study assumes the failed layer to unload in the failed direction only following a decreasing exponential function where the secant modulus decreases gradually to zero.

The theoretical results are compared with experimental results obtained from tests carried out on tubular composite specimens under combined loading conditions. Acoustic emission, C-scanning and photomicrographic tests were also conducted to examine the damage caused when the linear limit is exceeded.

The cylindrical specimens used in the experimental investigation introduced two additional problems which are also studied here. These are the design of the tubular test specimens, and the buckling of cylindrical shells under combined loading.

Comprehensive survey of the previous theories for all the problems studied in this thesis is presented, and where possible, the results obtained by previous investigators are compared with the present proposed solutions and commented on.

ACKNOWLEDGEMENT

I wish to express my gratitude to my supervisors: Mr. R. Tetlow*, Mr. C.K. Trotman** and Professor D. Howe for their help, encouragement and valuable comments.

I also wish to thank both Mr. R.A. Rawlinson (of Prodorite Limited) and Mr. J.F. Laurillard (of the M.O.D.P.E., Rocket Propulsion Establishment at Westcott) for providing the test specimens from Prodorite Limited and Bristol Aeroject Limited whose help is also acknowledged. Due thanks are made to the Reinforced Plastic Mouldings (Bedford) Limited for moulding the end reinforcements to the test specimens.

My thanks are due to Mr. R. Wilkins and his colleagues at the Rocket Propulsion Establishment for their help in the ultrasonic C-scanning and the acoustic emission tests.

I am much beholden to the staff of the laboratory and the workshop of the Aircraft Design Department, the Cranfield Computer Centre, the Library of the Institute and the Photographic Section for their help and cooperation.

I am also very grateful to my typist Mrs. S. Thompson for her dedication, skill and patience.

Last but not least, I am greatly indebted to my wife, Sahar, for the few years she has spent at Cranfield looking after a difficult husband and four active sons without too much complaint.

---

* now R. & D. Manager, Hepworth Industrial Plastics Limited.

** it is regretted that Mr. Trotman died before this thesis was submitted.

CONTENTS

TABLES

FIGURES

NOTATION

a	Factor defined in equation (2.4.17), parameter defined in equation (3.6.20).
[A]	In-plane stiffness matrix
b	Factor defined in equation (2.4.17), parameter defined in equation (3.6.21)
[B]	Stiffness coupling matrix
c	Parameter defined in equation (3.6.22)
C	Stiffness, constant
[C]	Stiffness matrix
d	Differentiation operator, factor defined in equation (2.4.17)
D	Diameter
[D]	Flexural stiffness matrix
e	Factor defined in equation (2.4.19)
E	Young modulus, stiffness
f	Function, factor defined in equation (2.4.19)
F	Constant defined in equation (3.3.5), strength tensor
g	Function, factor defined in equation (2.4.24)
G	Constant defined in equation (3.3.5)
h	Laminate thickness, factor defined in equation (2.4.24)
H	Constant defined in equation (3.3.5)
i	Imaginary factory.
k	= 1, 2, ..., n; proportional factor
K	Constant
[K]	Matrix of constants
ℓ	Length

L	Constant defined in equation (3.3.6)
m	= cos θ, root of the auxiliary polynomial, number of half-waves along the length of the cylinder.
M	Moment per unit length, constant defined in equation (3.3.6)
n	= sin θ, total number of layers in a laminate, square of the root of the auxiliary polynomial, number of waves in the circumferential direction.
N	Resultant force per unit length, constant defined in equation (3.3.6)
p	Internal pressure
P	Axial force, factor defined in equation (2.4.27)
[P]	Coefficient matrix
q	Factor defined in equation (2.4.24)
Q, Q'	Stiffness, shear force
[Q], [Q']	Stiffness matrix
r	Factor defined in equation (2.4.27)
R	Radius, shear strength in 1-3 plane
[R]	Matrix of the right hand side coefficients, strength matrix
s	Factor defined in equation (2.4.27)
S, S'	Strength, compliance, shear strength in 1-2 plane
[S], [S']	Compliance matrix
t	Thickness, constant defined in equation (2.4.55)
T	Torque, temperature, shear strength in 2-3 plane
[T]	Transformation matrix
u	Axial displacement
U	Strain energy, constant
v	Circumferential displacement

V	Volume, constant
w	Weight, radial displacement
W	Constant
x	Axial coordinate
X	Strength in 1-direction or x-direction
y	Circumferential coordinate
Y	Strength in 2-direction or y-direction
z	Radial coordinate
Z	Strength in 3-direction or z-direction
1	Longitudinal coordinate
2	Transverse coordinate
3	Through-the-thickness coordinate
α	Coefficient of thermal expansion, real part of the root of the auxiliary polynomial, interaction factor
β	Imaginary part of the root of the auxiliary polynomial, interaction factor
γ	Shear strain, real part of n, interaction factor
Δ	Difference
ϵ	Direct (normal) strain
θ	Angle of fibres from body axis
λ	Factor defined in equation (2.2.11), imaginary part of n, parameter defined in equation (3.6.8)
μ	Ratio characterizes shear strains induced by normal stresses (and vice versa)
ν	Poisson's ratio
π	= 3.1416
ρ	Density
σ	Direct (normal) stress

Σ	Summation
τ	Shear stress
ϕ	Stress ratio
χ	Change of curvature

Superscripts

i	Initial
k	kth layer in laminated composite
o	Middle surface properties
T	Transpose of a matrix
-T	Transpose and inverse of a matrix
-1	Inverse of a matrix
*	Normalized properties
Λ	Current value

Subscripts

a	Axial
c	Compression
e	End
f	Fraction, fibre
h	Homogeneous
i	Inside, interface
i, j	= 1, 2, ... 6 or x, y, z, zx, yz, xy
k	kth layer in laminated composite
L	Longitudinal
m	Matrix, mean
n	nth increment
o	Outside, nominal
p	Partial

s	Shear property
t	Tension, transverse
T	Transverse, laminate
u	Ultimate
x	Property in x-direction
y	Property in y-direction, yield properties
xy	Shear property in x-y plane
1	Property in the fibre direction
2	Transverse property
3	Through-the-thickness property
12	Shear property in 1-2 plane
13	Shear property in 1-3 plane
23	Shear property in 2-3 plane
45	Property in the 45° direction
θ	Property in θ-direction
,	Partial differentiation

Units

SI units and their symbols are used in this thesis unless otherwise stated. The computer programmes can be run with any consistent units.

ABBREVIATIONS USED IN THE LIST OF REFERENCES

AFFDL	Air Force Flight Dynamics Laboratory
AFML	Air Force Materials Laboratory
AGARD	Advisory Group for Aerospace Research and Development
AIAA	American Institute of Aeronautics and Astronautics
AMD	Applied Mechanics Division
ARPA	Advanced Research Project Agency
ASME	American Society of Mechanical Engineers
ASTM	American Society for Testing and Materials
CME	Chartered Mechanical Engineer
CR	Contract Report
ICCM	International Conference on Composite Materials
I.Mech.E.	Institute of Mechnical Engineers
Memo	Memorandum
NACA	National Advisory Committee of Aeronautics
NASA	National Aeronautics and Space Administration
NDT	Non-Destructive Testing
ONR	Office of Naval Research
RAPRA	Rubber and Plastics Research Association
SAE	Society of Automotive Engineers
SPI	Society of the Plastics Industry
TN	Technical Note
TR	Technical Report
TT	Technical Translation
UNIDO	United Nations Industrial Development Organization

Chapter 1

INTRODUCTION

1.1 WHY FIBRE-REINFORCED COMPOSITES?

If engineering materials are classified into the four main categories; metals, polymers, glasses and ceramics, then any combination of two (or more) of these materials on a macroscopic scale gives a composite material, Fig. (1.1.1).

The fibrous composites consist of fibres (which are much stiffer and stronger than the same material in bulk form) bonded together in a matrix. The laminated composites consist of layers of at least two different materials that are bonded together. Thus, the laminated fibrous composites are a bybrid class of composites involving both fibrous composites and lamination techniques. Only this type of composites is considered in this thesis.

The human body is one of the first high performance composite materials, for its bones and muscle tissue form a multi-directional fibrous laminate, (Ref. 1). Laminated structure

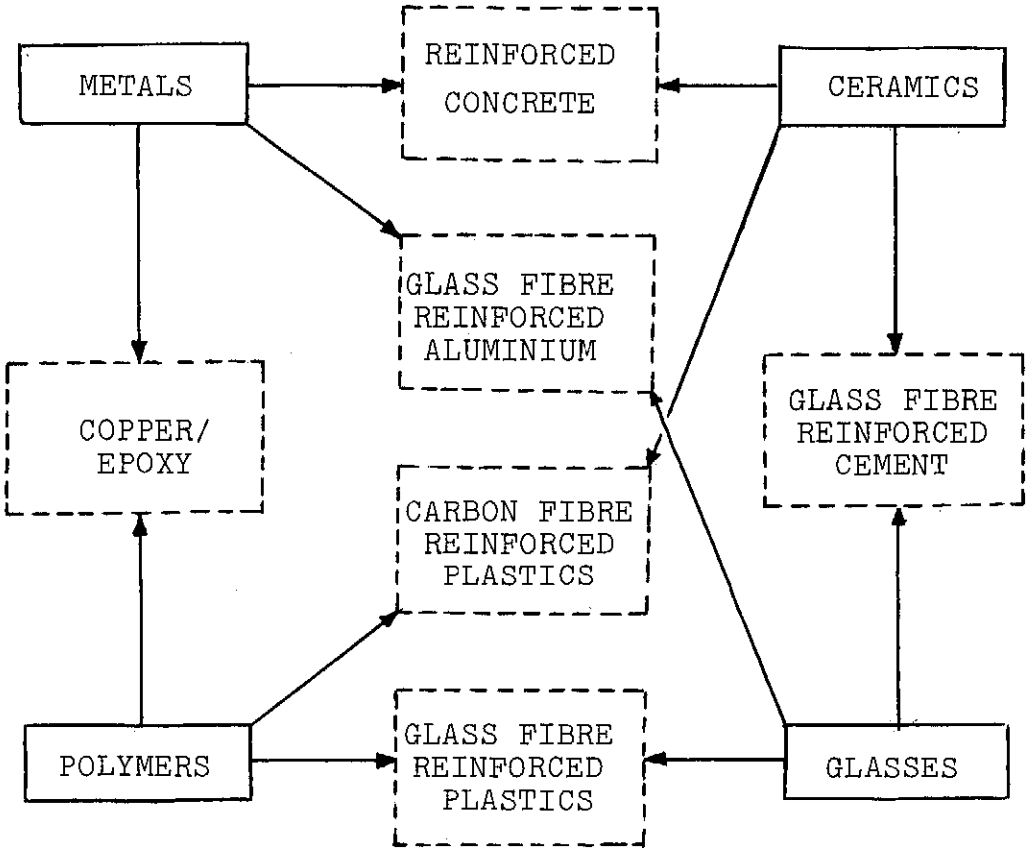

Fig. (1.1.1) Concept of composite materials

appeared in the plywood of the ancient Egyptians, (Ref. 2), the Mongol bow, the Damascus gun barrels and the Japanese ceremonial swords, (Ref. 1). Then in this century, advanced composite materials were introduced: the fabric-reinforced phenolic in the 1930's, the glass-fibre reinforced plastics in the 1940's, the boron and carbon fibres in the 1960's, the glass-fibre reinforced cement in the mid-1960's, the carbon-fibre and glass-fibre hybrid reinforced plastics in the late 1960's, Kevlar fibre in 1973, the jute-fibre reinforced plastics in 1973 (Ref. 3), and almost certainly the hybrid of Kevlar, carbon and glass fibres reinforced plastics in the 1980's.

What are the properties of fibre-reinforced composites which make them appealing as structural materials? The concept of composites is to obtain best qualities of their constituents, and often some qualities that neither constituent possesses. High specific stiffness, high specific strength, low thermal expansion, corrosion resistance, improved fatigue resistance, improved stress-rupture life time, formability, high damping, super finishing surface and economy of fabrication can all be exhibited in composites, though not necessarily at the same time.

The outcomes of these improved properties are: higher speed (e.g. aircraft and boats), higher load capacity or range (e.g. aircraft, missiles and general transportation), fuel economy (e.g. aircraft and general transportation), longer life time (e.g. aircraft, boats and chemical plants), improved manoeuverability (e.g. fighter planes, boats, tennis rackets, and skis), lower fabrication cost (e.g. boats).

To compare the stiffness and strength of composites with other materials, specific stiffness and specific strength are used for such comparison. These are the stiffness-to-density and strength-to-density ratios respectively. In this way the low weight of composites is accounted for. Many authors compare the unidirectional properties of composites with the properties of other materials. This is not a fair comparison, for composites have high properties in the fibre direction and low properties in the direction perpendicular to the fibres, and composites are usually used in the form of laminates which consist of several plies with different orientations. A fair comparison is to use the so-called quasi-isotropic laminate which has same properties in every direction and is a symmetric laminate of $0^{o}/90^{o}/\pm45^{o}$, table (1.1.1) and Fig. (1.1.2).

However, the fact that composite materials possess different properties in different directions is also an advantage, for the fibres can be aligned in the load directions, thus the designer can make op timum use of the material.

Cost of parts made of composites are in many cases higher than parts made of conventional materials. In order to justify the use of composites other savings must be possible,

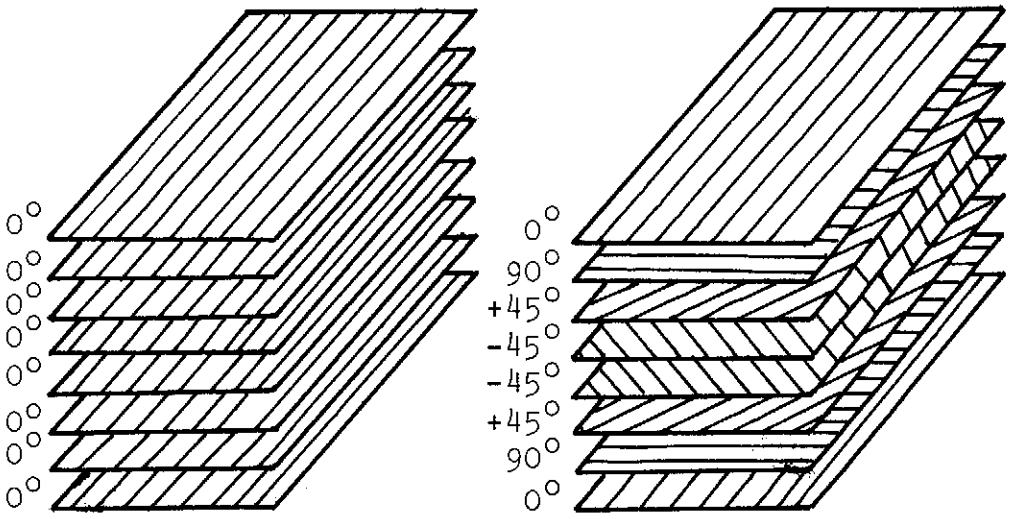

Unidirection Laminate Quasi-Isotropic Laminate

Fig. (1.1.2) Unbonded views of a Unidirectional and a Quasi-Isotropic Multidirectional Laminates

like savings in thickness, weight, trimming wastage and running cost. Many engineering applications of composites are listed in Refs.(4-15), essentially in road and rail transportation, aircraft, space vehicles, ocean engineering, building, chemical, electrical and nuclear industries, textile machines, measuring tools, mechanical engineering, bioengineering and sport equipment. Examples of very recent applications include the F-18 Advanced Fighter, (Ref. 11), which has composite laminated structures in the wing skins, vertical and horizontal tails, rudders, speed brakes, fuselage doors, covers and panels, flaps, and landing-gear doors. This reduces its weight by more than 500 lb. The Boeing 757 and 767 will employ composites in similar parts,(Ref. 12). All-composite helicopter rotor blades are in production status for UH60, CH47 and H46 helicopters, (Ref. 12). British Rail High Speed Train has a composite cab, (Ref. 14). The Royal Navy vessel, HMS Ledbury, is a complete GRP ship, (Ref. 16). And last, but not least, the revolutionary aircraft of Burt Rutan are constructed from a combination of plastic foam and G.R.P., (Ref. 17).

For the future of composites one can prophesy that these materials are the materials of the future. Mr. L.N. Phillips of the Royal Aircraft Establishment, (Ref. 13), concludes: "It is fairly certain that our children will fly in machines that are substantially of composite construction. They will do so, not to humour their dear old Dads, but because it will be a better way to fly."

Table (1.1.1)

Comparison of stiffness and strength for various structural materials

	Material	Density ρ (KN/m^3)	Tensile Stiffness E (GN/m^2)	Specific Stiffness E/ρ (Mm)	Tensile Strength S (MN/m^2)	Specific Strength S/ρ (Km)
Iso-tropic	Aluminium	27.1	69	2.5	414	15.3
	Titanium	46.1	100	2.2	1034	22.4
	Steel	76.5	200	2.6	1173	15.3
Unidirectional	E-Glass/Epoxy	18.5	34	1.9	1103	59.6
	S-Glass/Epoxy	17.8	50	2.8	1620	91.0
	Kevlar 49/Epoxy	13.0	66	5.0	1172	90.0
	Carbon-I/Epoxy	15.5	165	10.7	965	62.3
	Carbon-II/Epoxy	14.9	117	7.9	1241	83.3
	Carbon-III/Epoxy	14.9	100	6.7	1172	78.8
	Boron/Epoxy	18.6	210	11.3	1240	66.7
Quasi-Isotropic	E-Glass/Epoxy	18.5	15	0.8	328	17.7
	S-Glass/Epoxy	17.8	22	1.2	480	27.1
	Kevlar 49/Epoxy	13.0	22	1.7	414	31.8
	Carbon-I/Epoxy	15.5	52	3.3	324	20.9
	Carbon-II/Epoxy	14.9	38	2.5	414	27.8
	Carbon-III/Epoxy	14.9	33	2.2	414	27.8
	Boron/Epoxy	18.6	66	3.6	438	23.5

1.2 FAILURE OF FIBRE-REINFORCED COMPOSITES

Although composites have been in use in engineering applications for many years, the rigorous conditions under which materials have to operate led to the theory of composite materials, which is still in the development stage. On the other hand, the improvements in structural efficiency are the result of innovations in design criteria and better understanding of the behaviour of these new materials. With more reliable information about the behaviour of composite materials they will be used in primary structures and introduced in many other applications. Consequently, the production rates of composites will be higher which will result in lower material costs.

The strength of a structure is its ability to sustain a given load without failure. Failure is, therefore, the limit of load carrying capacity. Unlike homogeneous isotropic materials, laminated fibrous composite materials are non-homogeneous and anisotropic, which makes their strength difficult to determine.

The strength of homogeneous and isotropic materials is determined by first obtaining the material properties from simple test conditions (uniaxial tension, compression and shear), and then by generalising these data for more complex stress states to cover the entire spectrum of loading. For the generalisation process there exist various methods, e.g. Tresca, Von Mises ... etc.

The strength of a composite layer is also determined by first finding the layer properties from simple test conditions, though here there are more properties to obtain viz: longitudinal tension, longitudinal compression, transverse tension, transverse compression and in-plane shear. Then these data are generalised for complex states of stress. This procedure is not a unique one as there are many failure criteria with varying failure envelopes.

However, the strength of a liminated composite structure as a whole is a problem yet to be solved. This thesis is a contribution towards the strength of multilayered composites.

1.3 SCOPE OF PRESENT INVESTIGATION

The present theoretical and experimental research is meant to be a comprehensive study for the failure of laminated fibre-reinforced composite structures under complex stress states. It is appropriate to study the behaviour of these structures before any failure occurs in any of the plies of the multilayered laminate. The non-linear behaviour of fibrous composites is examined. This is very important in

understanding the failure process of composite materials.

The study is then directed towards the existing failure criteria which generalise the unidirectional data for the multidirectional loading state. These criteria produce dissimilar results. They are first verified against experimental results, and then, through different types of testing and examining composites, a new modified criteria is proposed for the failure of a layer in a laminated structure.

Once a particular lamina exceeds its strength, how and what proportion of its load can it carry, and what proportion of the load does it transfer to unfailed layers? What are the new laminate properties? And then what causes the total failure of the laminated structure as a whole? All these points are studied, and solutions for them are proposed.

An additional problem is imposed on the research programme and has to be studied. That is the analysis of the gripped specimen and the influence of the end-effect on the design of the test specimen in order to obtain uniform stress state in the characterisation section of the tubular specimen.

During the experimental investigation an instability failure may occur. This problem is studied to compare the critical load of instability with the limit load of strength in order to distinguish the type of failure.

1.4 REVIEW OF PREVIOUS STUDIES

As mentioned above this thesis is an all-embracing study of the problem of failure of composite structures starting from the pre-failure behaviour and ending with the post-failure behaviour of multilayer composites. Thus it is more appropriate to review previous work on different aspects of the problem where these matters arise as a comprehensive study of the subject is not known.

However, in the course of this research, two groups from two different academic institutions have separately published papers about their contribution to this important topic. These are from the University of Liverpool (Refs. 18-19) and the University of Manchester Institute of Science and Technology (Refs. 20-21). The methods of analysis, the theories derived and even objectives to some extent in both cases are different from those of this study. Non-linear response of composites is, for instance, ignored in Liverpool study, whereas the rule of mixtures is used in Manchester study to obtain the elastic properties of the composite lamina. Both of these studies are reviewed and compared with the present study in due course.

1.5 METHOD OF ANALYSIS

There are two methods of analysis of a composite lamina :

a) Micromechanical Behaviour

In the micromechanics approach a layer of a laminated fibre-reinforced composite structure is considered to be of two different materials: the fibre and the matrix. In this way it is heterogeneous.

b) Macromechanical Behaviour

In the macromechanics theory a ply of a laminate of composite structure is assumed homogeneous but anisotropic. The effects of the constituent materials, the fibre and the matrix, are allowed for only in a form of average apparent properties of the layer.

Thus, in the micromechanics the lamina properties are predicted, whereas they are measured by physical means in the macromechanics approach.

In general, due to the complexity of the microstructure of composite materials, many assumptions have to be made to simplify the solutions of various problems. These assumptions belong to filament shape, uniformity, array, homogeneity, alignment, continuity, properties of matrix and voids. Then, the analysis methods vary from strength-of-materials approach to rigorous three-dimensional theory of elasticity approach, (Refs. 22-32). In all cases, however, there is a difference between solutions and experimental data. Nevertheless, the micromechanics approach is useful in designing a new composite material to achieve certain properties.

In this present study the macromechanics approach is considered where the lamina properties are determined experimentally and then used to predict the laminate properties using the lamination theory which is itself a macromechanics analysis. In this way the properties of the lamina are more realistic and dependable for subsequent analysis in predicting the failure of the laminate. This failure of the laminated structure, according to the present theory, consists of a series of ply-failures. However, the macromechanics analysis is compared here with microscopic observations whenever possible.

It is worth mentioning that there exist another macromechanics method of analysis in which the laminate is characterised experimentally, as one unit, to determine its properties (e.g. Ref. 21). This theory does not involve a lamination

theory but necessitates mechanical testing for every laminate, a procedure to be compared with the lamina-laminate method in due course.

There is another micromechanics approach which is called "Netting Analysis". In this analysis, (Refs. 32, 33) the fibres carry the applied load, whereas the matrix is visualized as a medium necessary to keep the fibres bonded together and not as a load carrying agent. When compared with test data, netting analysis theory appears to be grossly conservative (Ref. 34). Such a theory is more appropriate for woven fabrics since they have no matrix to carry loads to begin with, (Ref. 2). Indeed, this theory becomes invalid for fibre-reinforced composites in special cases, e.g. when the fibre orientation is compatible with the applied loading.

1.6 EXPERIMENTAL TECHNIQUES

As mentioned above, the macromechanics approach of lamina-laminate theory is adopted in this present investigation. The first objective of the experimental programme is to obtain an individual layer properties. These properties are then used in the analysis of laminated structures, under combined loading states, where it is assumed that the behaviour of a single ply in a certain direction is the same as the behaviour of this ply in that direction when it constitutes part of a laminated structure.

The second objective for the experimental investigation is to establish biaxial data for known composite material in order to verify the theory developed here.

The experimental characterisation of composite materials is usually more difficult than homogeneous isotropic materials because, due to macroscopic anisotropic effects, there are more different kinds of independent data to obtain. On the other hand, the test specimen in case of composites is designed more carefully. It is not a surprise to see many conferences devoted completely to testing of composite materials, (e.g. Refs. 35-39).

Different types of composite specimens have been used by engineers and scientists to characterise composite materials. These are :

a) Off-Axis Coupon Specimen

The off-axis coupon, Fig. (1.6.1), has been of interest as an inexpensive means of obtaining data at a limited number of biaxial stress conditions. The coupon can be unidirectional or laminated composites. The problems of this type

of specimens are: the cut fibres at the edges which cause premature failure; obtaining homogeneous stress state; end constraints effects; the biaxial normal stresses are always of the same sign (first and third quadrants only); and the problem of limited biaxial loading ratios, (Refs. 40-45).

b) Plate-Type Specimens

Grimes et al, (Ref. 46), used a plate specimen for biaxial stress state testing, Fig. (1.6.2), but their specimens failed at the edges.

Cole et al, (Ref. 40), reported another plate-type biaxial test specimen which is called the Crossbeam, Fig. (1.6.3). The specimen consists of two sandwich beams intersecting at right angles. The composite to be tested is used as a skin facing on the beam. The beams are subjected to four point bending which places the test section in pure bending. A known state of biaxial stress is produced at the point of intersection of the centre-lines of the beams, point O.

The advantages of this type of specimens are: it can characterise the behaviour of composites in the four quadrants, in a wide range of stress ratios, and the theoretical analysis uses simple beam theory. The disadvantages are: the stress concentrations at the intersections of the edges of the beam skins, and possible effects of the core-to-facing bond on the strength of the facing.

Bert et al, (Ref. 47), developed a plate-type specimen to overcome the disadvantages of the Grimes et al specimen. Their specimen is of reduced-thickness test section and loaded by means of four bonded loading tabs. However, it is limited to two biaxial-stress ratios (1:1 and 1:2), both in tension only.

c) Shell-Type Specimens

Circular cylindrical specimens are the most important among the shell-type specimens because they possess many advantages over other shells. Among other types of specimens thin-walled cylindrical test specimens constitute the most unified procedure available for characterising the static mechanical properties of fibre-reinforced composite materials, (Ref. 48). This is because an approximate state of uniform stress can be induced in this type of specimen when subjected to combined loading. As in other types of specimens, there are some practical problems regarding the end effects which lead to complicated test rigs. There is no doubt that cylindrical specimens cost more than any other type of specimen. But this configuration allows for complete characterisation from unidirectional laminae to multidirectional laminates, thus it reduces the cost of test rigs and equipment, whereas in other types of biaxial test specimens mentioned above the undirectional properties have

to be determined by other techniques, as described in Refs. (49-53), which means more test costs and another error source.

Unlike other specimens, the cylindrical specimen represents end-product structures such as pressure vessels, pipe lines, rocket motor cases, launcher tubes, storage tanks and any similar structures. This, of course, does not limit the applications of tests carried out on tubular specimens only to these types of structures as the results obtained are usually general.

In the experimental investigation of the present work circular cylindrical shell specimens are used. A test rig was designed to fit the testing machines available in the Aircraft Design Laboratories. The rig is suitable for uniaxial loading as well as for combined loadings of axial, internal pressure and/or torsion. In this way the stated objectives of the experimental work are catered for in one test rig. The specimens used were unidirectional, angle-ply and multi-layered specimens.

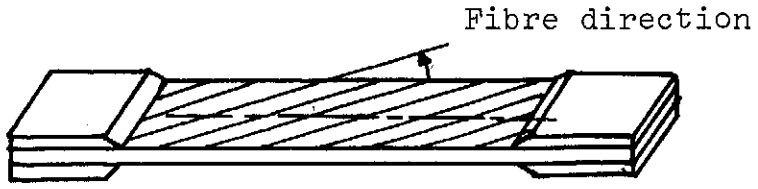

Fig. (1.6.1) Off-axis Coupon Specimen

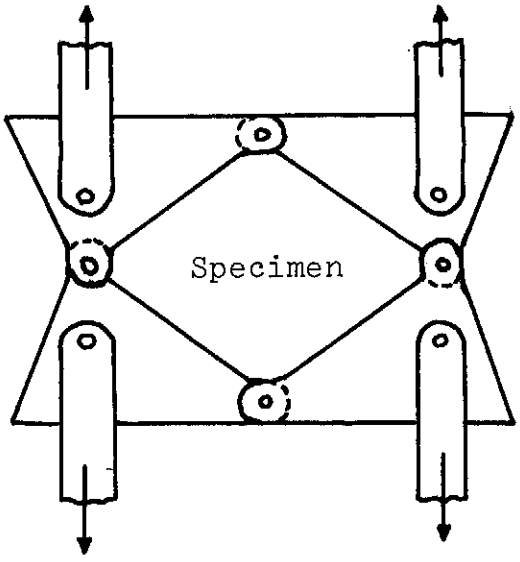

Fig. (1.6.2) Plate specimen of Grimes et al

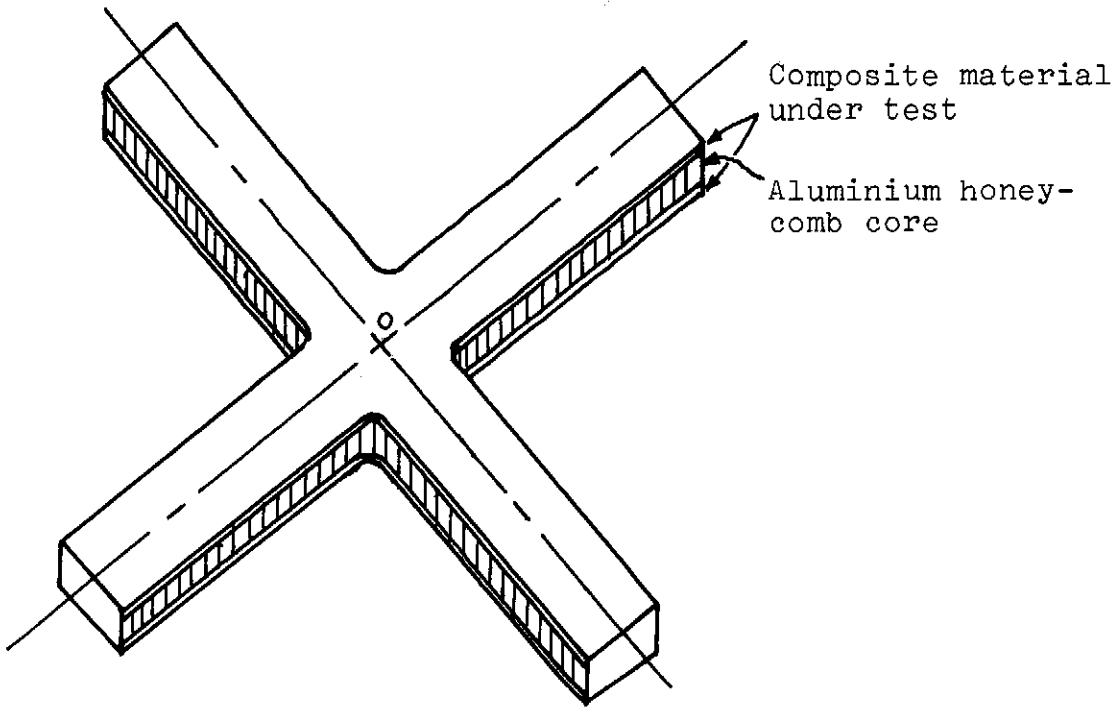

Fig. (1.6.3) Crossbeam specimen

CHAPTER 2

PRE-FAILURE BEHAVIOUR OF LAMINATED COMPOSITES

2.1 INTRODUCTION

Although the aim of this work is to investigate the progressive failure of fibre-reinforced composite materials, it is necessary to know the behaviour of these materials before any failure occurs. As discussed earlier, the currently popular idea of considering a composite material, consisting of oriented fibres in a supporting matrix, to behave macroscopically as a homogeneous, anisotropic material, is used here. It will be discussed later, in Chapter 3, why it is more appropriate to consider the lamina as the basic building block in a laminated fibre-reinforced composite rather than using the laminate as whole to be the basic block in a laminated structure.

Consequently, a knowledge of the mechanical behaviour of a lamina is essential to understand the mechanical behaviour of laminated fibre-reinforced composite structures. In this Chapter the behaviour of a lamina and then of a laminate is focused upon. The study will be oriented towards laminated tubes because tubular specimens are used in the experimental investigation of the present research.

A tubular specimen is shown schematically in Fig. (2.1.1), from which it can be seen that there exists discontinuity in the loading near the ends of the tube. The tube can thus be considered to have two different regions: the test section region, and the end region. The test section is located at sufficient distance from the ends of the tube so that it will be subjected to membrane loading only when the tube is

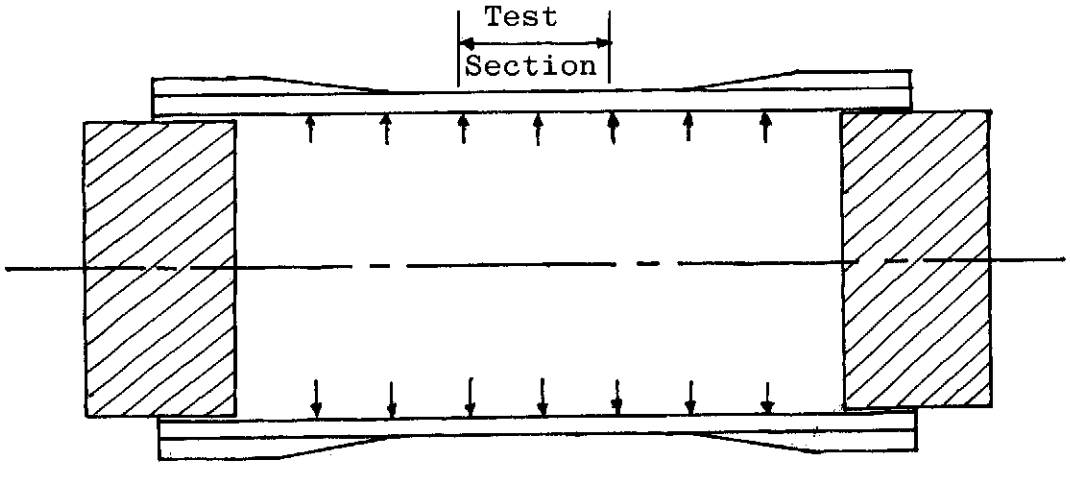

Fig. (2.1.1) Schematic drawing of the test specimen

subjected to combinations of axial load, internal pressure, and torsion.

In Sec. 2.2 the linear stress analysis in the test section will be focused upon, whereas the non-linear analysis will be discussed in Sec. 2.3; and the stress analysis of the tube near its ends will be studied in Sec. 2.4.

2.2 ELASTIC PROPERTIES OF INFINITELY LONG LAMINATED COMPOSITE CYLINDRICAL SHELLS

2.2.1 Review of Shell Theories

A laminated composite structure consists of layers of fibre-reinforced composites bonded together to form one material capable of bearing load in desired directions. The elastic properties of this laminated composite are calculated from the elastic properties of the individual plies whose fibres may be aligned in any arbitrary directions chosen by the designer to resist certain loads. The procedure which relates the laminate behaviour to the laminae behaviour is called "lamination theory".

Three-dimensional stress analysis of composites is possible, (Refs. 54-58), but the experimental determination of the "out-of-plane" characteristics is tedious and necessitates many assumptions, especially when the non-linear behaviour is to be considered. Therefore, in all characterization studies of composite materials "thin" structures are considered. In this way only the "in-plane" properties are included in the analysis. The lamination theory for thin infinite flat laminates subjected to in-plane loading is well established, (Refs. 1, 2, 59-63). For an infinitely long circular cylindrical shell the situation is different. In this type of structures the combination of internal pressure, axial (tension or compression) and torsional loads, results in an in-plane stress state in the wall of the cylinder. But for these stresses to be uniform across the wall thickness (or approximately so) this wall must be thin, or the radius-to-thickness ratio must be large. The different shell theories to determine stresses in laminated hollow cylinders are reviewed here briefly.

Sherrer, (Ref. 64), developed a theory which treats the problem using the micromechanics approach. A mathematical model for the composite element is necessary. Sherrer used two different models for the fibres and the way they are arranged in the resin matrix. The difficulty of determining the exact properties of the resin made it difficult to assess the validity of the theoretical model. The numerical calculations associated with this theory are extremely cumbersome and chances for error are numerous.

Franklin, (Ref. 65), determined a membrane solution of fibre-reinforced corrugated shells of revolution.

Dong et al, (Ref. 66), used the so called Donnell shallow curvature approximations of isotropic shells, (Ref. 124), to formulate a small deflection theory for thin laminated composite shells. Later, Dong R.G. and Dong, S.B. (Ref. 67), used a perturbation method to reduce the system of anisotropic shell equations to successive systems of orthotropic shell equations.

Donnell approximations were also used by Pagano et al, (Ref. 68), on unidirectional filament wound tubes, and later by Whitney et al, (Ref. 69), on multidirectional tubes.

Donnell type shell theory does not predict the minimum radius-to-thickness ratio which defines "thin-wall tube". Solutions of exact elasticity equations were, therefore, sought to overcome this difficulty. The study of Rizzo and Vicario, (Refs. 70, 71), is a finite element solution which can deal with the general three-dimensional anisotropic axisymmetric composite tubes.

Pagano et al, (Refs. 72, 73) developed a procedure to determine the proper geometry of laminated anisotropic tubes such that the elastic stress gradients across the wall thickness can be reduced to a predetermined limit. Their approach consists of combining a modified plane strain elasticity solution with shell theory based on Donnell approximations as discussed in Ref. (66).

Since elastic solutions are lengthy a simple solution would be desirable provided it gives acceptable results. Whitney et al, (Refs. 74, 75), applied Vlasov-Ambartsumyan shell theory, (Refs. 76, 77), to laminated anisotropic cylindrical shells and developed equations for calculating the stresses in a composite tube. Results compared well with results obtained from elasticity solutions.

Earlier, Cheng and Ho, (Ref. 78), extended Flügge's theory of isotropic shells, (Ref. 79), to develop a theory for laminated cylindrical shells. This study, however, was more general than Whitney et al study, but same equations are obtained when all unwanted terms are dropped. Chao et al, (Ref. 80), used Cheng and Ho equations to investigate the optimum fibre orientations in laminated cylindrical shells under combined loadings.

Widera and Chung, (Ref. 81), used the method of asymptotic integration of the elasticity equations to derive a first approximation theory governing the non-homogeneous anisotropic cylindrical shells. For homogeneous isotropic material the equations derived in this method reduce to the linearized Donnell equations.

Reuter, (Ref. 82), analysed, using Donnell eqautions, angle-ply cylindrical shells under internal pressure only. This study is limited to balanced-unsymmetric and unbalanced-symmetric constructions under unidirectional loading.

The problem of bending of laminated anisotropic composite cylinders was studied by Zien, (Ref. 83), whereas thin anisotropic shells with arbitrary geometry are analysed by Bert, (Ref. 84).

Whitney and Sun, (Ref. 85), developed a refined theory for anisotropic cylinders of moderate radius-to-thickness ratio. Another technique for thickness correction was also used by Widera and Logan, (Ref. 86). Bert and Guess, (Ref. 87), used another refinement technique to allow for materials whose stiffness matrix is not symmetric, i.e., the reciprocal relation among the Young's moduli and Poisson's ratios: $\nu_{21}/E_2 = \nu_{12}/E_1$ does not hold. An example of these materials is carbon-carbon composite. More about analysis of laminated composite shells can be found in (Refs. 62, 88).

In this present investigation, Vlasov-Ambartsumyan type shell theory is adopted for the analysis of laminated composite tubes. This is because it predicts the stress gradients across the wall thickness fairly accurately, and is simpler than the elasticity solutions.

2.2.2 A Single Orthotropic Layer

The properties of anisotropic materials depend on the directional orientation. The generalized Hooke's law is used to relate stresses to strains for such materials. It is of the form :

$$\left[\sigma_i\right] = \left[C_{ij}\right]\left[\varepsilon_j\right] \qquad (2.2.1)$$

where $i, j = 1, 2, \ldots 6$.

$\left[\sigma_i\right]$ is column vector representing the stress components

$\left[\varepsilon_j\right]$ is column vector representing the strain components

$\left[C_{ij}\right]$ is square matrix of stiffness coefficients.

For orthotropic layer, Fig. (2.2.1), the stiffness matrix is (Ref. 89) :

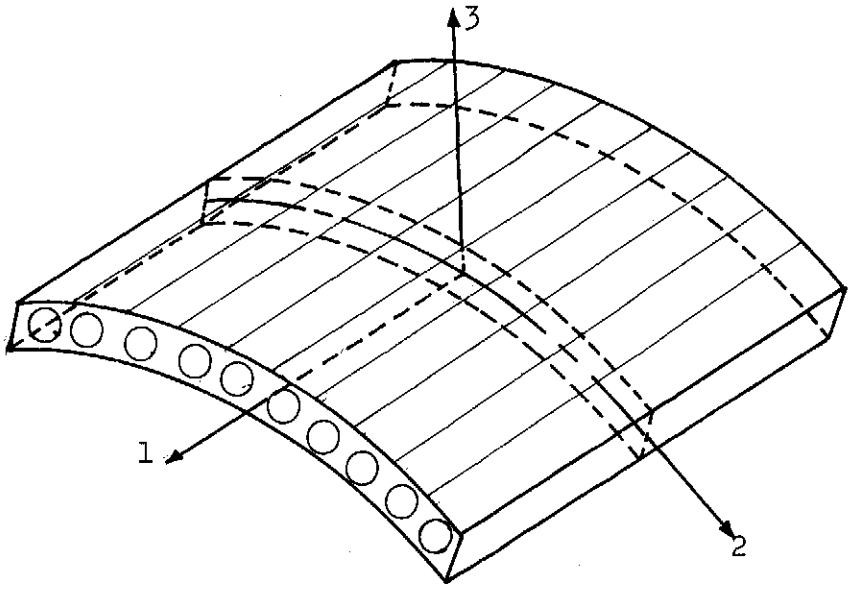

Fig. (2.2.1) Shell lamina with unidirectional fibres in the direction of the body axis

$$[C] = \begin{bmatrix} C_{11} & C_{12} & C_{13} & 0 & 0 & 0 \\ & C_{22} & C_{23} & 0 & 0 & 0 \\ & & C_{33} & 0 & 0 & 0 \\ & & & C_{44} & 0 & 0 \\ & & & & C_{55} & 0 \\ \text{(symmetric)} & & & & & C_{66} \end{bmatrix} \qquad (2.2.2)$$

The stiffness matrix (2.2.2) can be reduced to the state of generalized plane stress when the layer is sufficiently thin compared with the radius of the tube. In this case the three components of stress in the thickness direction are negligible, i.e.:

$$\sigma_3 = 0, \quad \tau_{23} = 0, \quad \tau_{31} = 0 \qquad (2.2.3)$$

From equations (2.2.3) :

$$C_{13}\,\varepsilon_1 + C_{23}\,\varepsilon_2 + C_{33}\,\varepsilon_3 = 0,$$

$$\gamma_{23} = 0, \quad \gamma_{31} = 0 \qquad (2.2.4)$$

where the shear stress σ_4, σ_5 and σ_6 are denoted by τ_{23}, τ_{31} and τ_{12}; and the shear strains ε_4, ε_5 and ε_6 by γ_{23}, γ_{31} and γ_{12}.

From above, it can be seen that the normal strain ε_3 is not zero in general, but it can be expressed in terms of ε_1 and ε_2 (the first of equations 2.2.4).

Thus, for a thin orthotropic layer, Fig. (2.2.1), the stress-strain relations reduce to :

$$\begin{bmatrix} \sigma_1 \\ \sigma_2 \\ \tau_{12} \end{bmatrix} = \begin{bmatrix} Q'_{11} & Q'_{12} & 0 \\ Q'_{12} & Q'_{22} & 0 \\ 0 & 0 & Q'_{66} \end{bmatrix} \begin{bmatrix} \varepsilon_1 \\ \varepsilon_2 \\ \gamma_{12} \end{bmatrix} \qquad (2.2.5)$$

where the reduced stiffness coefficients Q'_{ij} are related to the three-dimensional stiffness coefficients by :

$$Q'_{ij} = C_{ij} - (C_{i3}C_{j3}/C_{33}) \qquad (2.2.6)$$

The stiffness coefficients discussed above have no direct meaning for engineers, and the engineering constants are usually used instead. These are : Young's elastic moduli E_1 and E_2, Poisson's ratios ν_{12} and ν_{21}, and shear modulus G_{12}. These constants are measured in simple tests on unidirectional ply. They can be defined by writing the strains in terms of the stresses as follows :

$$\begin{bmatrix} \varepsilon_1 \\ \varepsilon_2 \\ \gamma_{12} \end{bmatrix} = \begin{bmatrix} 1/E_1 & -\nu_{21}/E_2 & 0 \\ -\nu_{12}/E_1 & 1/E_2 & 0 \\ 0 & 0 & 1/G_{12} \end{bmatrix} \begin{bmatrix} \sigma_1 \\ \sigma_2 \\ \tau_3 \end{bmatrix} \qquad (2.2.7)$$

From the symmetry condition :

$$\nu_{21}/E_2 = \nu_{12}/E_1 \qquad (2.2.8)$$

Then, for thin orthotropic layer the four independent engineering constants are : E_1, E_2, ν_{12} and G.

The matrix :

$$[S'] = \begin{bmatrix} 1/E_1 & -\nu_{21}/E_2 & 0 \\ -\nu_{12}/E_1 & 1/E_2 & 0 \\ 0 & 0 & 1/G_{12} \end{bmatrix} \qquad (2.2.9)$$

is called the compliance matrix, whose inverse is the stiffness matrix Q' :

$$[Q'] = \begin{bmatrix} E_1/\lambda & \nu_{21}E_1/\lambda & 0 \\ \nu_{12}E_2/\lambda & E_2/\lambda & 0 \\ 0 & 0 & G_{12} \end{bmatrix} \qquad (2.2.10)$$

where : $\lambda = 1 - \nu_{12}\nu_{21}$ (2.2.11)

2.2.3 Lamina of Arbitrary Orientation

It is not always possible to use coordinate directions which coincide with the principal directions of orthotropy. Rather it is more convenient to use coordinate directions appropriate to the particular problem under consideration, e.g. coordinate directions coinciding with the load directions, Fig. (2.2.2).

In this case the elastic onstants must be referred to the body axes. The x - y stresses transform to the orthogonal axes 1 - 2 by :

$$\begin{bmatrix} \sigma_1 \\ \sigma_2 \\ \tau_{12} \end{bmatrix} = [T] \begin{bmatrix} \sigma_x \\ \sigma_y \\ \tau_{xy} \end{bmatrix} \qquad (2.2.12)$$

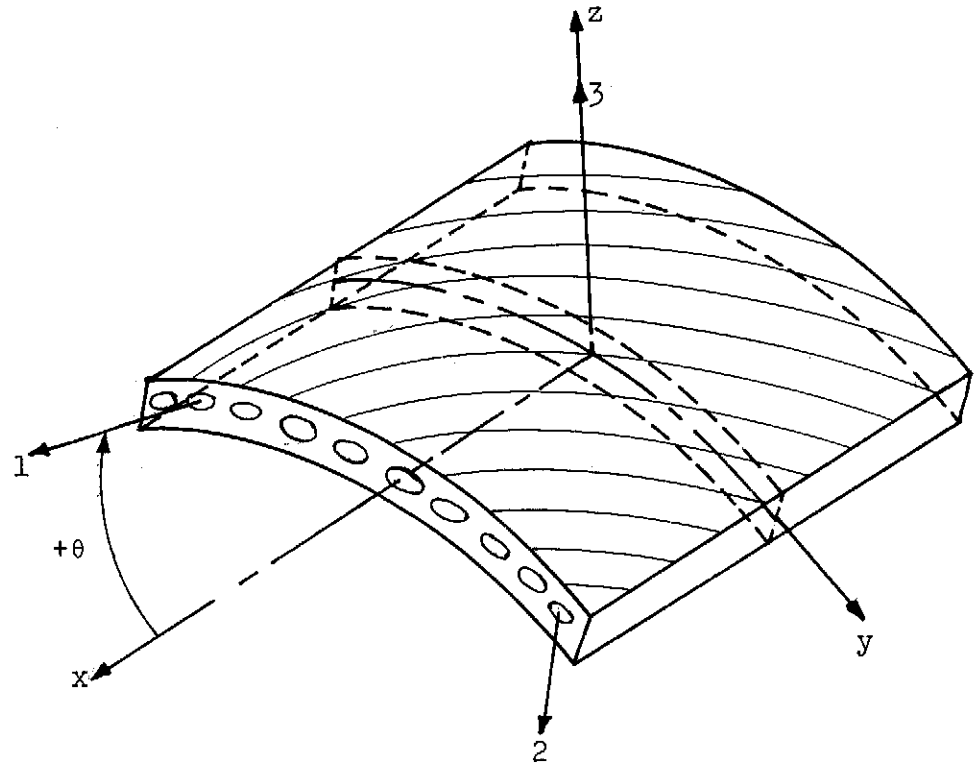

Fig. (2.2.2) Shell lamina with unidirectional fibres aligned at angle θ from the direction of the body axis.

Similarly, the strains transform by :

$$\begin{bmatrix} \varepsilon_1 \\ \varepsilon_2 \\ \frac{1}{2}\gamma_{12} \end{bmatrix} = [T] \begin{bmatrix} \varepsilon_x \\ \varepsilon_y \\ \frac{1}{2}\gamma_{xy} \end{bmatrix} \qquad (2.2.13)$$

where :

$$[T] = \begin{bmatrix} m^2 & n^2 & -2mn \\ n^2 & m^2 & 2mn \\ mn & -mn & m^2-n^2 \end{bmatrix} \qquad (2.2.14)$$

$$m = \cos\theta, \; n = \sin\theta \qquad (2.2.15)$$

θ is positive in the clockwise direction, Fig. (2.2.2)

Alternatively, the strain transformation equations can be written as follows :

$$\begin{bmatrix} \varepsilon_x \\ \varepsilon_y \\ \gamma_{xy} \end{bmatrix} = [T]^T \begin{bmatrix} \varepsilon_1 \\ \varepsilon_2 \\ \gamma_{12} \end{bmatrix} \qquad (2.2.16)$$

where the superscript T denotes the matrix transpose.

Thus, from eqautions (2.2.5), (2.2.12) and (2.2.16) the stress-strain relations in the x - y coordinate directions are :

$$\begin{bmatrix} \sigma_x \\ \sigma_y \\ \tau_{xy} \end{bmatrix} = [Q] \begin{bmatrix} \varepsilon_x \\ \varepsilon_y \\ \gamma_{xy} \end{bmatrix} \qquad (2.2.17)$$

where the transformed elastic coefficients Q_{ij} are related to the elastic coefficients Q'_{ij} of equation (2.2.10) by :

$$[Q] = [T]^{-1} [Q'] [T]^{-T} \qquad (2.2.18)$$

When the matrix multiplication of (2.2.18) is performed the following relations between Q_{ij} and Q'_{ij} are obtained :

$$\begin{bmatrix} Q_{11} \\ Q_{12} \\ Q_{16} \\ Q_{22} \\ Q_{26} \\ Q_{66} \end{bmatrix} = \begin{bmatrix} m^4 & 2m^2n^2 & n^4 & 4m^2n^2 \\ m^2n^2 & m^4+n^4 & m^2n^2 & -4m^2n^2 \\ -m^3n & mn(m^2-n^2) & mn^3 & 2mn(m^2-n^2) \\ n^4 & 2m^2n^2 & m^4 & 4m^2n^2 \\ -mn^3 & -mn(m^2-n^2) & m^3n & -2mn(m^2-n^2) \\ m^2n^2 & -2m^2n^2 & m^2n^2 & (m^2-n^2)^2 \end{bmatrix} \begin{bmatrix} Q'_{11} \\ Q'_{12} \\ Q'_{22} \\ Q'_{66} \end{bmatrix} \qquad (2.2.19)$$

The stress-strain relations, equation (2.2.17), can be written in inverted form as :

$$\begin{bmatrix} \varepsilon_x \\ \varepsilon_y \\ \gamma_{xy} \end{bmatrix} = [S] \begin{bmatrix} \sigma_x \\ \sigma_y \\ \tau_{xy} \end{bmatrix} \qquad (2.2.20)$$

where :

$$[S] = [Q]^{-1} \tag{2.2.21}$$

is the transformed compliance matrix, whose elements are related to the compliance coefficients S'_{ij} by :

$$\begin{bmatrix} S_{11} \\ S_{12} \\ S_{16} \\ S_{22} \\ S_{26} \\ S_{66} \end{bmatrix} = \begin{bmatrix} m^4 & 2m^2n^2 & n^4 & m^2n^2 \\ m^2n^2 & m^4+n^4 & m^2n^2 & -m^2n^2 \\ -2m^3n & 2mn(m^2-n^2) & 2mn^3 & mn(m^2-n^2) \\ n^4 & 2m^2n^2 & m^4 & m^2n^2 \\ -2mn^3 & -2mn(m^2-n^2) & 2m^3n & -mn(m^2-n^2) \\ 4m^2n^2 & -8m^2n^2 & 4m^2n^2 & (m^2-n^2)^2 \end{bmatrix} \begin{bmatrix} S'_{11} \\ S'_{12} \\ S'_{22} \\ S'_{66} \end{bmatrix} \tag{2.2.22}$$

The matrix $[S]$ gives the apparent engineering constants of the lamina as follows :

$$\begin{aligned} E_x &= 1/S_{11}, \quad E_y = 1/S_{22}, \quad G_{xy} = 1/S_{66} \\ \nu_{xy} &= -S_{12}/S_{11}, \quad \nu_{yx} = -S_{21}/S_{22} \\ \mu_{xs} &= S_{61}/S_{11}, \quad \mu_{ys} = S_{62}/S_{22} \\ \mu_{sx} &= S_{16}/S_{66} \quad \mu_{sy} = S_{26}/S_{66} \end{aligned} \tag{2.2.23}$$

where the new engineering constants μ are similar to Poisson's ratios ν but characterise the shear strains induced by normal stresses (μ_{xs} and μ_{ys}) or the normal strains induced by shear stress (μ_{sx} and μ_{sy}).

If the coefficients S_{ij} are substituted by the apparent engineering constants (equations 2.2.23), and the coefficients S'_{ij} are substituted by the real engineering constants (equations 2.2.9), then equation (2.2.22) gives the relations between the apparent and real engineering constants.

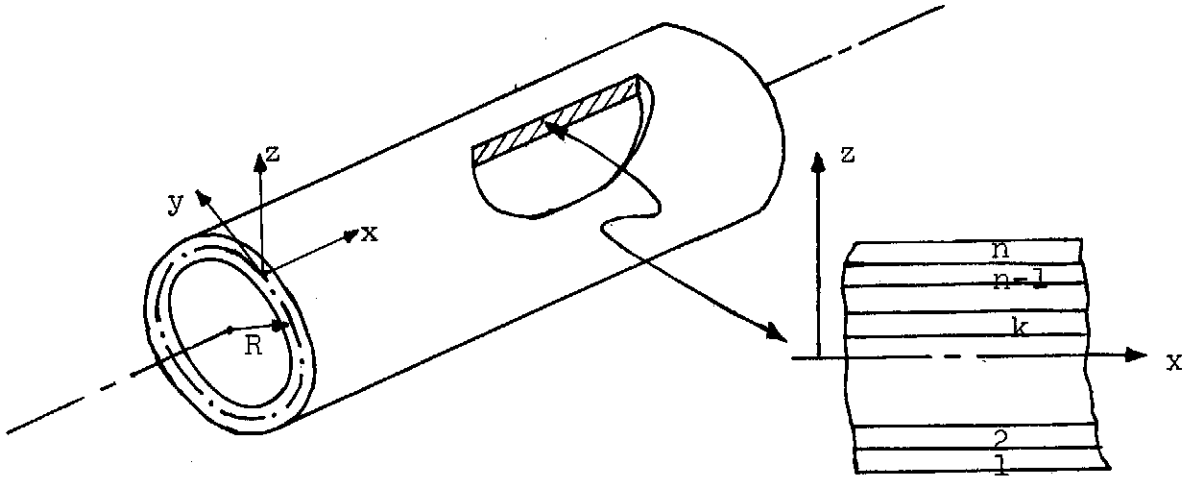

Fig. (2.2.3) Coordinate directions for laminated composite tube

2.2.4 Laminated Composite Tubes

The coordinate directions for laminated composite tube are selected as shwon in Fig. (2.2.3). The origin is taken to be in the middle surface of the tube with x, y and z measured along the longitudinal, circumferential, and radial directions respectively.

The usual method in analysing multi-layered flat composites in the plane stress case is to assume that the strains of the laminate are constant across the thickness of the composite structures, (Refs. 59, 60). However, the stresses in an anisotropic tube subjected to combinations of axial load (tension or compression), internal pressure, and torsion are uniform across the wall thickness if the tube is sufficiently thin.

The terminology "thin-walled tube" must be used with considerable care in the case of anisotropic materials, (Ref. 74). A large radius-to-thickness ratio will be necessary to obtain acceptable uniform stress across the wall thickness for highly anisotropic materials or within each layer for laminated tube.

However, as shown in (Ref. 75), the necessary radius-to-thickness ratio depends on the materials of the tube; the lamination sequence and orientation; and the type of loading, e.g. for radius-to-thickness ratio (R/h) of 10.5 and winding angle (θ) of 30° in axial loading case the ratio of

the axial stress in the inner surface $(\sigma_x)_i$ to that in the outer surface $(\sigma_x)_o$ for glass/epoxy tube (with $E_1:E_2:G_{12}$ = 6:2:08) was 1.016, whereas for graphite/epoxy tube (with $E_1:E_2:G_{12}$ = 20:1:0.6) it was 1.3. Thus, in the graphite/epoxy case larger R/h ratio is required to attain small gradient or variation in stress, especially in torsion, though, in this case the tube becomes highly susceptible to shear buckling.

The stress gradient across the wall thickness can be obtained from the solutions of the exact elasticity equations. But these solutions are rather difficult. As mentioned before, Vlasov-Ambartsumyan shell theory (Refs. 76, 77) can be used to obtain approximate solutions, which are in good agreement with the exact solutions. The Vlasov-Ambartsumyan shell theory for anisotropic laminates is based on Love's first approximations (Ref. 89) which are :

1. transverse shear and transverse normal strains are neglected, i.e. $\gamma_{xz} = \gamma_{yz} = \varepsilon_z = 0$;

2. the thickness of the shell h is small compared with other dimensions, i.e. terms of the order h/R are neglected; and

3. only small deflections are considered, i.e. second and higher order terms are neglected.

These assumptions lead to the following relations for the strains at any point :

$$\begin{bmatrix} \varepsilon_x \\ \varepsilon_y \\ \gamma_{xy} \end{bmatrix} = \begin{bmatrix} \varepsilon_x^o \\ \varepsilon_y^o \\ \gamma_{xy}^o \end{bmatrix} + z \begin{bmatrix} \chi_x \\ \chi_y \\ \chi_{xy} \end{bmatrix} \qquad (2.2.24)$$

where ε^{o}'s are the middle surface strains; χ's are the changes of curvature ; and z is the distance from the reference surface. These strains and changes of curavture are given in terms of displacements by, (Ref. 74) :

$$\begin{bmatrix} \varepsilon_x^o \\ \varepsilon_y^o \\ \gamma_{xy}^o \end{bmatrix} = \begin{bmatrix} u^o_{,x} \\ v^o_{,y} + w^o/R \\ u^o_{,y} + v^o_{,x} \end{bmatrix} \qquad (2.2.25)$$

$$\begin{bmatrix} \chi_x \\ \chi_y \\ \chi_{xy} \end{bmatrix} = \begin{bmatrix} w^o_{,xx} \\ -(w^o_{,yy} + w^o/R^2) \\ -(2w^o_{,xy} + u^o_{,y}/R - v^o_{,x}/R) \end{bmatrix} \qquad (2.2.26)$$

where :

u^o, v^o and w^o are the middle surface displacements in the x, y and z directions respectively; and (,) denotes partial differentiation, (e.g. $u^o_{,x} = \partial u^o/\partial x$).

In the case of cylindrical shell subjected to combinations of axial load, internal pressure and torsion the displacements are independent of y variable as the cylinder is axisymmetrically loaded. Thus, from equations (2.2.25) :

$$\begin{bmatrix} u^o \\ v^o \\ w^o \end{bmatrix} = \begin{bmatrix} \varepsilon^o_x \cdot x \\ \gamma^o_{xy} \cdot x \\ \varepsilon^o_y \cdot R \end{bmatrix} \qquad (2.2.27)$$

Where ε^o_x, ε^o_y and γ^o_{xy} are assumed to be constant along the test section of infinitely long cylinder. Then, from equations (2.2.26) :

$$\begin{bmatrix} \chi_x \\ \chi_y \\ \chi_{xy} \end{bmatrix} = \begin{bmatrix} 0 \\ -\varepsilon^o_y/R \\ \gamma^o_{xy}/R \end{bmatrix} \qquad (2.2.28)$$

Each layer of the laminated tube is assumed to be orthotropic with respect to a plane perpendicular to the z-axis and in an approximate state of plane stress. Thus equations (2.2.17) are applicable to each layer. Equations (2.2.17), when integrated across the thickness of the laminated tube, give the resultant forces acting per unit length of the reference surface arc :

$$\begin{bmatrix} N_x \\ N_y \\ N_{xy} \end{bmatrix} = \int_{-h/2}^{h/2} \begin{bmatrix} \sigma_x \\ \sigma_y \\ \tau_{xy} \end{bmatrix} dz$$

or

$$\begin{bmatrix} N_x \\ N_y \\ N_{xy} \end{bmatrix} = [A] \begin{bmatrix} \varepsilon_x^o \\ \varepsilon_y^o \\ \gamma_{xy}^o \end{bmatrix} + [B] \begin{bmatrix} \chi_x \\ \chi_y \\ \chi_{xy} \end{bmatrix} \qquad (2.2.29)$$

where

$$A_{ij} = \int_{-h/2}^{h/2} Q_{ij}\, dz = \sum_{k=1}^{n} Q_{ij}^{(k)} (z_{k+1} - z_k)$$

(2.2.30)

$$B_{ij} = \int_{-h/2}^{h/2} Q_{ij} \cdot z dz = \tfrac{1}{2} \sum_{k=1}^{n} Q_{ij}^{(k)} (z_{k+1}^2 - z_k^2)$$

$k = 1, 2, \ldots, n$, where n is the total number of layers in the laminated tube.

Equations (2.2.29), when considering equations (2.2.28), can be written as follows :

$$\begin{bmatrix} N_x \\ N_y \\ N_{xy} \end{bmatrix} = h \, [Q]_T \begin{bmatrix} \varepsilon_x^o \\ \varepsilon_y^o \\ \gamma_{xy}^o \end{bmatrix} \qquad (2.2.31)$$

where $[Q]_T$ is the effective stiffness matrix of the laminated tube and is given by :

$$[Q]_T = \frac{1}{h}\begin{bmatrix} A_{11} & (A_{12} - \frac{B_{12}}{R}) & (A_{61} + \frac{B_{16}}{R}) \\ A_{21} & (A_{22} - \frac{B_{22}}{R}) & (A_{62} + \frac{B_{26}}{R}) \\ A_{61} & (A_{62} - \frac{B_{62}}{R}) & (A_{66} + \frac{B_{66}}{R}) \end{bmatrix} \tag{2.2.32}$$

Equations (2.2.31) are written in the inverted form as follows:

$$\begin{bmatrix} \varepsilon_x^o \\ \varepsilon_y^o \\ \gamma_{xy}^o \end{bmatrix} = \frac{1}{h} [S]_T \begin{bmatrix} N_x \\ N_y \\ N_{xy} \end{bmatrix} \tag{2.2.33}$$

where $[S]_T$ is the compliance matrix of the laminated tube, i.e.

$$[S]_T = [Q]_T^{-1} \tag{2.2.34}$$

The strains in the k^{th} layer of the tube are given by equations (2.2.24) or, taking equations (2.2.28) into account, by :

$$\begin{bmatrix} \varepsilon_x \\ \varepsilon_y \\ \gamma_{xy} \end{bmatrix}_k = \begin{bmatrix} \varepsilon_x^o \\ \varepsilon_y^o \\ \gamma_{xy}^o \end{bmatrix} + z_k \begin{bmatrix} 0 \\ -\varepsilon_y^o/R \\ \gamma_{xy}^o/R \end{bmatrix} \tag{2.2.35}$$

Substituting equations (2.2.33) into equations (2.2.35) yields the following relations for the strains in the k^{th} layer of the tube :

$$\begin{bmatrix} \varepsilon_x \\ \varepsilon_y \\ \gamma_{xy} \end{bmatrix}_k = \left\{ [S]_T + \frac{z_k}{R} [S^o]_T \right\} \begin{bmatrix} \sigma_x^o \\ \sigma_y^o \\ \tau_{xy}^o \end{bmatrix} \qquad (2.2.36)$$

where :

$$[S^o]_T = \begin{bmatrix} 0 & 0 & 0 \\ -(S_{21})_T & -(S_{22})_T & -(S_{26})_T \\ (S_{61})_T & (S_{62})_T & (S_{66})_T \end{bmatrix} \qquad (2.2.37)$$

and

$$\begin{bmatrix} \sigma_x^o \\ \sigma_y^o \\ \sigma_{xy}^o \end{bmatrix} = \begin{bmatrix} \frac{N_x}{h} \\ \frac{N_y}{h} \\ \frac{N_{xy}}{h} \end{bmatrix} = \begin{bmatrix} \frac{P_x}{2\pi Rh} \\ \frac{R \cdot p}{h} \\ \frac{T}{2\pi R^2 h} \end{bmatrix} \qquad (2.2.38)$$

where P_x, p and T are the axial load, the internal pressure and the torque respectively.

The stresses in the k^{th} layer of the tube are given by equation (2.2.17) or :

$$\begin{bmatrix} \sigma_x \\ \sigma_y \\ \tau_{xy} \end{bmatrix}_k = [Q]_k \left\{ [S]_T + \frac{z_k}{R} [S^o]_T \right\} \begin{bmatrix} \sigma_x^o \\ \sigma_y^o \\ \tau_{xy}^o \end{bmatrix} \qquad (2.2.39)$$

The in-plane engineering constants of the laminated tube are calculated from the laminate compliance matrix $[S]_T$ using equations (2.2.23).

If the cylinder radius, R, is chosen to be big, then the above analysis will reduce to plate analysis of infinite length.

2.2.5 Thermal Stresses

Thermal stresses arise in composites when they operate at temperatures different from their curing temperatures. The thermal strains, ε^T, for single orthotropic layer are given by, (Refs. 90-92) :

$$\varepsilon_i^T = \alpha_i \Delta T \qquad (2.2.40)$$

where

$i = 1, 2, \ldots, 6$

ΔT is the temperature difference, and

α_i are the coefficients of thermal expansion

These thermal strains are measured from stress-free state, and they are added to the mechanical strains to give the total strains.

Equations (2.2.1) becomes :

$$[\sigma_i] = [C_{ij}] [\{\varepsilon_j - \alpha_i \Delta T\}] \qquad (2.2.41)$$

and for thin orthotropic layer, equations (2.2.5) become :

$$\begin{bmatrix} \sigma_1 \\ \sigma_2 \\ \sigma_3 \end{bmatrix} = \begin{bmatrix} Q'_{11} & Q'_{12} & 0 \\ Q'_{12} & Q'_{22} & 0 \\ 0 & 0 & Q_{66} \end{bmatrix} \begin{bmatrix} \varepsilon_1 - \alpha_1 \Delta T \\ \varepsilon_2 - \alpha_2 \Delta T \\ \gamma_{12} \end{bmatrix} \qquad (2.2.42)$$

i.e. the coefficients of thermal expansion do not affect the shear strain. These coefficients, α_1 and α_2, are determined experimentally, (Refs. 93, 94).

The above analysis of orthotropic layer can be extended to the laminate analysis by including the thermal stresses in the eqautions of Secs. 2.2.3 and 2.2.4. But is it necessary?

If the macromechanics approach is adopted, then the experimentally characterized lamina properties will include the thermal expansion effects as the measured strains represent the total of the mechanical and the thermal strains. These effects will be included automatically in any further characterization.

However, if the operating temperature of a composite material is different from that under which the composite was characterized, or if the micromechanics approach was used to calculate the lamina properties, then, the laminate analysis of Sec. 2.2.4 must be modified to include the thermal stresses.

In the present research, the experimental investigation was carried out under a relatively constant temperature, that is the laboratory temperature, hence, the analysis of thermal stresses is omitted.

2.2.6 Application of the Theory to the Test Specimens

In the experimental investigation in this work, Chapter 5, about fifty tubular specimens were tested under different combinations of axial load (tension/compression), internal pressure and torsion. These specimens were cut from seven long GRP tubes of different stacking and orientation whose data are given in Appendix A.

To ascertain that all specimens are "thin" under whatever external load they were subjected to, the preceding shell theory was applied. Numerical results for the stresses and the strains across the wall thickness were obtained and are shown in Figs. (2.2.4) - (2.2.10). These results are given in normalized coordinates defined by :

$$z^* = \frac{z}{h} \tag{2.2.43}$$

$$\begin{bmatrix} \sigma_x^* \\ \sigma_y^* \\ \tau_{xy}^* \end{bmatrix} = \begin{bmatrix} \frac{\sigma_x}{\sigma_x^o} \\ \frac{\sigma_y}{\sigma_y^o} \\ \frac{\tau_{xy}}{\tau_{xy}^o} \end{bmatrix} \tag{2.2.44}$$

$$\begin{bmatrix} \varepsilon_x^* \\ \varepsilon_y^* \\ \gamma_{xy}^* \end{bmatrix} = \begin{bmatrix} \frac{\varepsilon_x}{\varepsilon_x^o} \\ \frac{\varepsilon_y}{\varepsilon_y^o} \\ \frac{\gamma_{xy}}{\gamma_{xy}^o} \end{bmatrix} \tag{2.2.45}$$

The stress distributions across the thickness of a specimen give an idea about the validity of the "thin-walled shell theory" when applied to that particular specimen. The strain distributions, however, give the ratios between the specimen middle surface strains and the strains at the outer surface of the specimen. These are needed because in the experimental programme the strain gauges were bonded on the outer surface of the tubes, whereas in the analysis the middle surface strains were considered to represent the laminate strains. It is worth mentioning that internal strain measurements have been used by Daniel et al, (Ref. 123), by implementing an embedded strain gauge technique. The technique was tested successfully by them and was consequently used to determine surface and subsurface strains in coupon specimens. In case of filament-wound tubular specimens the technique would be much more difficult.

Figs. (2.2.4) - (2.2.10) show that all test specimens can be regarded as thin shells because the stress variations across the wall thickness (for angle-ply laminates) or across each layer (for multilayered laminates) are small.

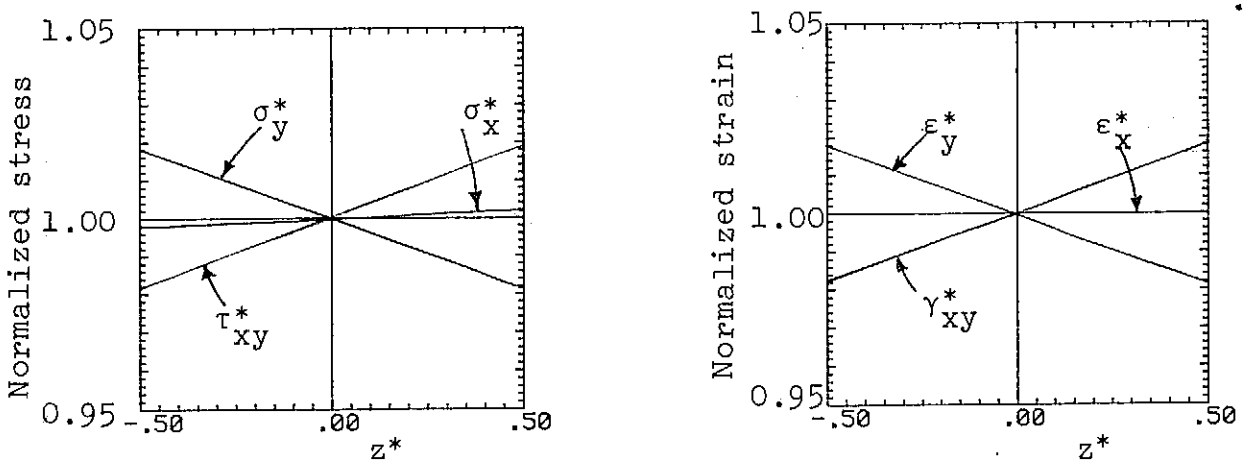

Fig. (2.2.4) Stress and strain distributions in specimens of tube B1

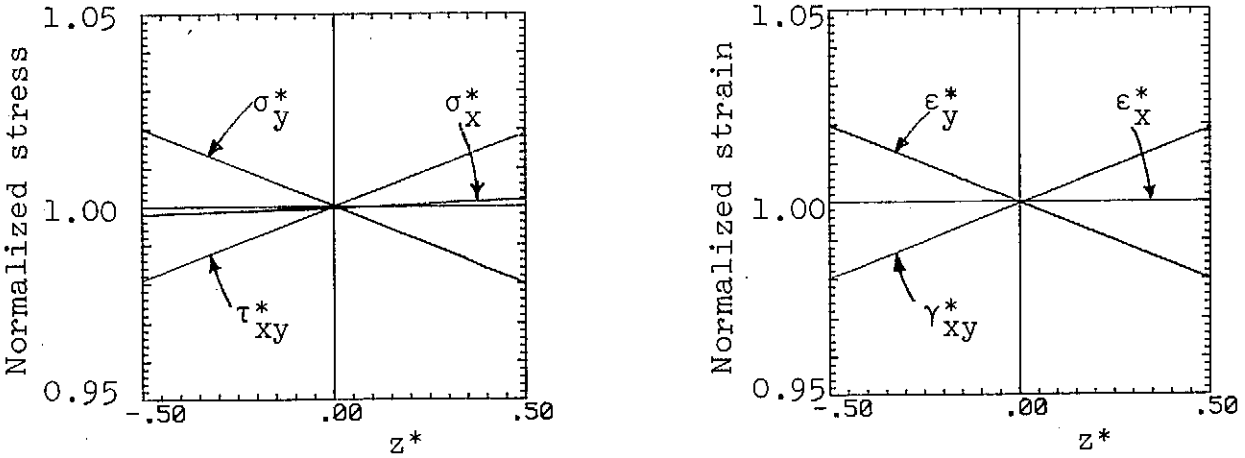

Fig. (2.2.5) Stress and strain distributions in specimens of tube B2

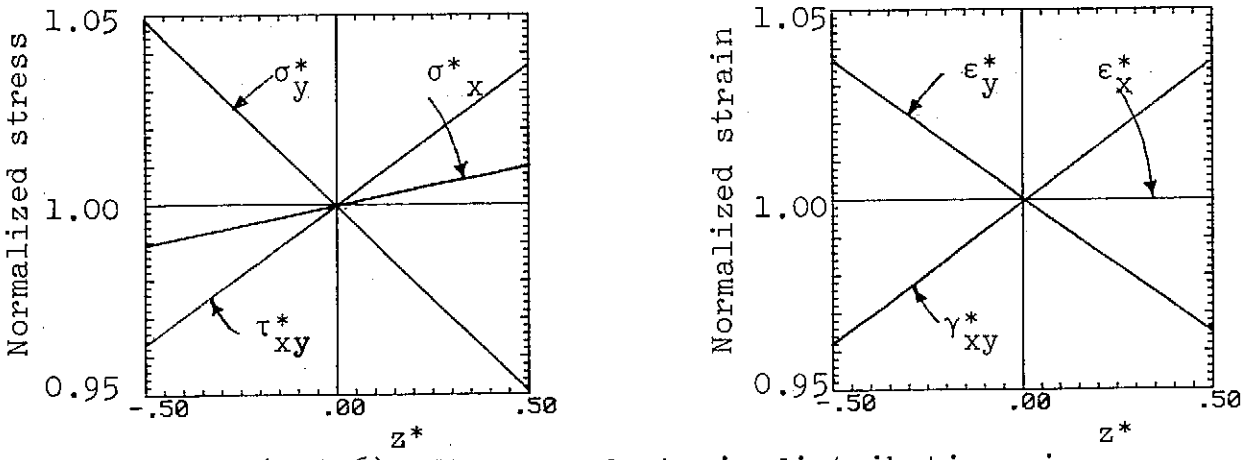

Fig. (2.2.6) Stress and strain distributions in specimens of tube B3

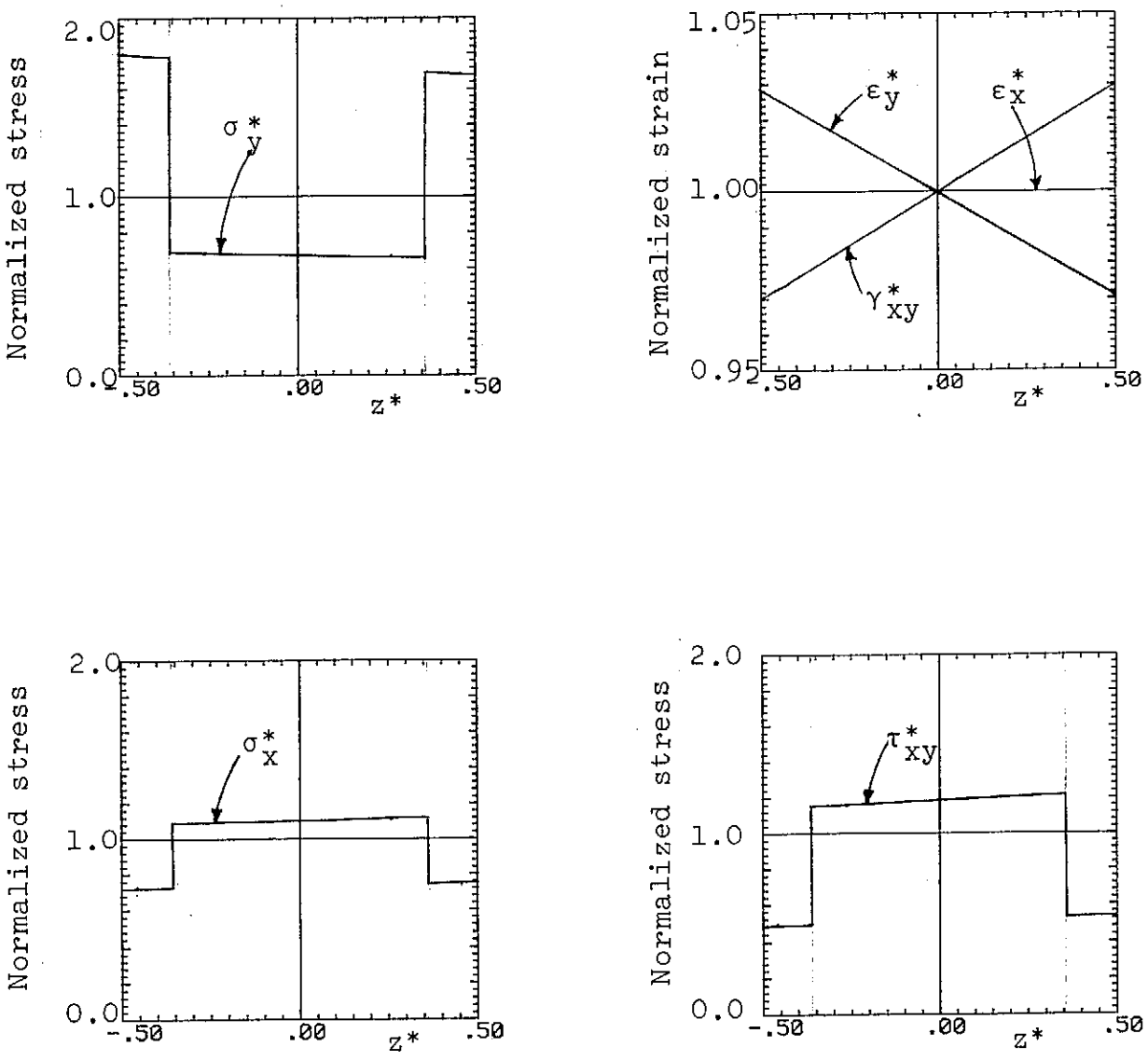

Fig. (2.2.7) Stress and strain distributions in specimens in tube B4

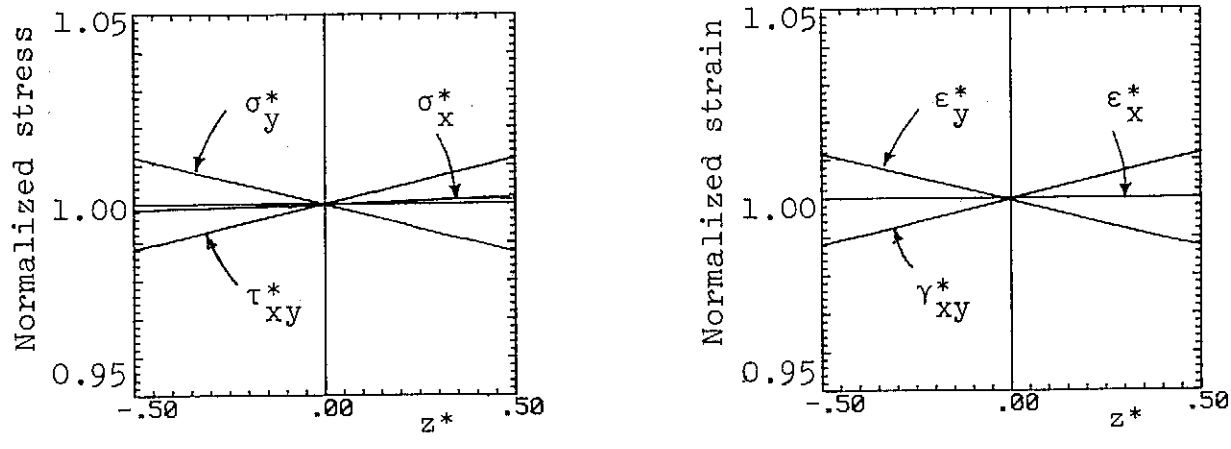

Fig. (2.2.8) Stress and strain distributions in specimens in tube B6

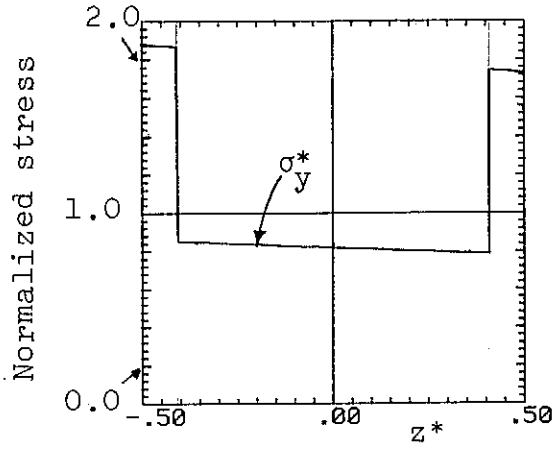

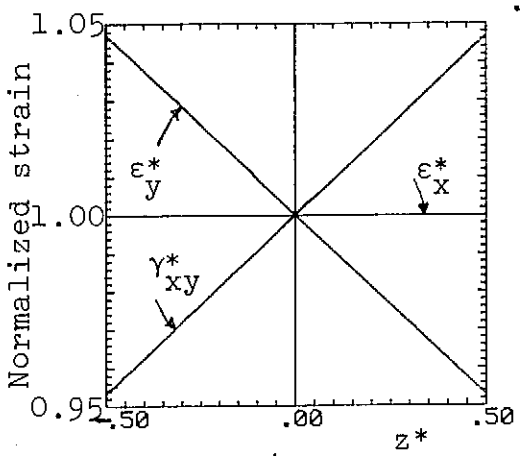

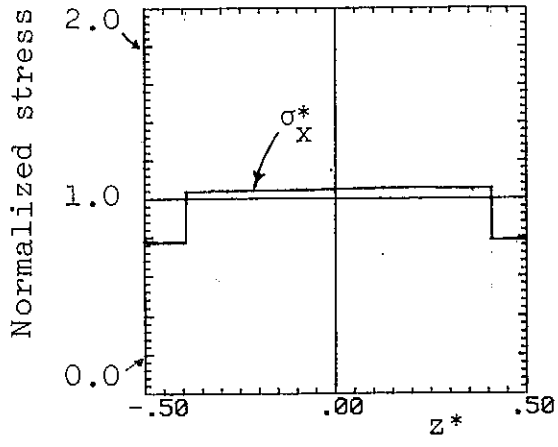

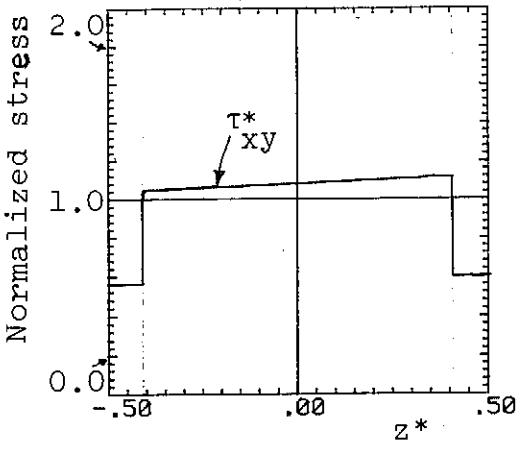

Fig. (2.2.9) Stress and strain distributionsin specimens in tube B5

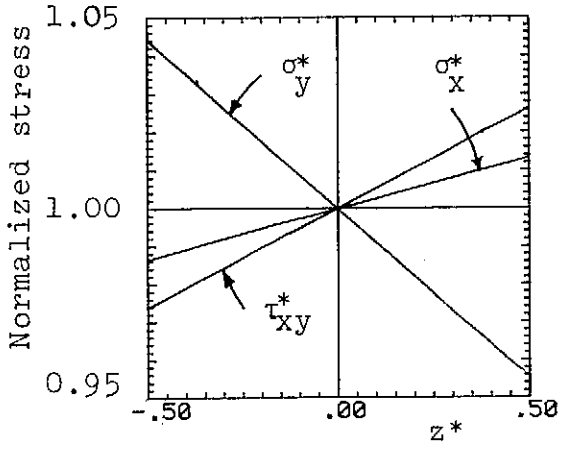

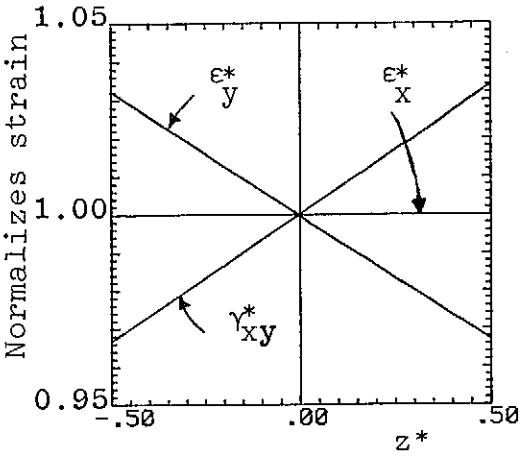

Fig. (2.2.10) Stress and strain distributionsin specimens in tube P1

2.3 ANALYSIS OF NON-LINEAR STRESS-STRAIN BEHAVIOUR

2.3.1 Introduction

Most fibre-reinforced composite materials exhibit non-linear stress-strain behaviour. Fig. (2.3.1) shows typical stress-strain behaviour of most fibre-reinforced composites, from which it can be seen that in the fibre direction the lamina behaves linearly even at high stress levels, though it might have different muduli in tension and compression. In the direction transverse to the fibres the lamina behaves linearly to some stress level but the response becomes non-linear after that level, whereas the shear response is not linear at all stress levels.

Non-linearity is also observed in Poisson's ratio curve as shown in Fig. (2.3.2).

The degree of non-linearity varies from composite to composite and is due mainly to the non-linear behaviour of the matrix materials, Fig. (2.3.3). From this figure it can be seen that the rule of mixtures will not give good results in predicting the lamina strength properties.

In Sec. 2.3.2 the existing methods for analysing non-linar behaviour of fibre-reinforced composites are outlined and commented upon. In Sec. 2.3.3 a new method is introduced, and then results of different methods are compared with test data in Sec. 2.3.4.

Fig. (2.3.1) Typical stress-strain behaviour of most fibre-reinforced composite materials

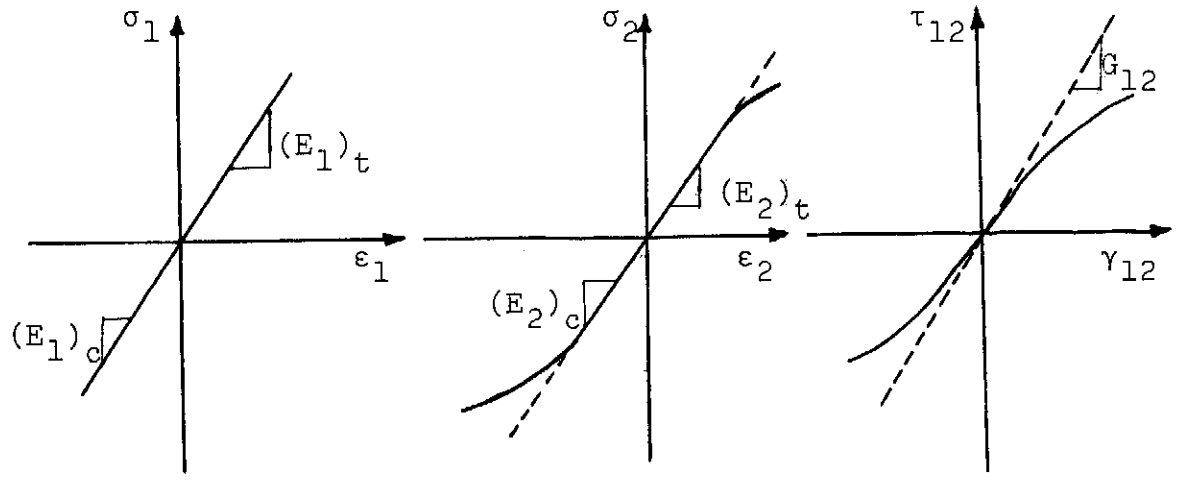

(a) in the fibre direction

(c) transverse to the fibres

(c) shear response

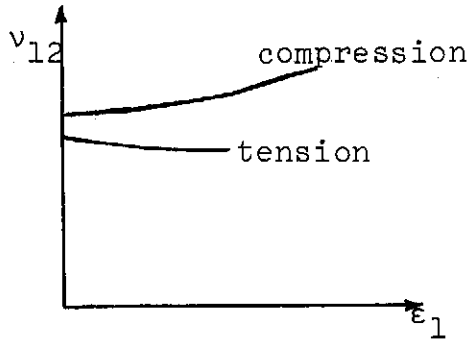

Fig. (2.3.2) Typical Poisson's ratio curves

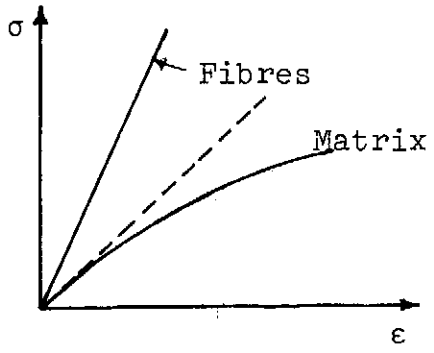

Fig. (2.3.3) Typical (σ - ε) curves for the fibres and the matrix materials

2.3.2 Previous Methods for Analysing Non-Linear Behaviour

a) Hahn-Tsai Method

Hahn and Tsai, (Ref. 98), used complementary elastic energy density to derive a stress-strain relation which is linear in uniaxial loadings in the longitudinal and transverse directions, but non-linear in shear. In case of a composite lamina under plane stress, they introduced one additional fourth-order constant to account for the non-linear shear behaviour.

For lamina with unidirectional fibres parallel to the body axis, Fig. (2.2.1), the stress-strain relations are given by :

$$\begin{bmatrix} \varepsilon_1 \\ \varepsilon_2 \\ \gamma_{12} \end{bmatrix} = \begin{bmatrix} S'_{11} & S'_{12} & 0 \\ S'_{12} & S'_{22} & 0 \\ 0 & 0 & S'_{66} \end{bmatrix} \begin{bmatrix} \sigma_1 \\ \sigma_2 \\ \tau_{12} \end{bmatrix} + S_{6666}\, \tau_{12}^2 \begin{bmatrix} 0 \\ 0 \\ \tau_{12} \end{bmatrix} \qquad (2.3.1)$$

i.e.

$$\gamma_{12} = S'_{66}\, \tau_{12} + S_{6666}\, \tau_{12}^3 \qquad (2.3.2)$$

where :

$$S_{6666} > 0 \tag{2.3.3}$$

The inverse of (2.3.1) can be written as :

$$\begin{bmatrix} \sigma_1 \\ \sigma_2 \\ \tau_{12} \end{bmatrix} = \begin{bmatrix} Q'_{11} & Q'_{12} & 0 \\ Q'_{12} & Q'_{22} & 0 \\ 0 & 0 & Q'_{66} \end{bmatrix} \begin{bmatrix} \varepsilon_1 \\ \varepsilon_2 \\ \gamma_{12} \end{bmatrix} + f(\gamma_{12}) \begin{bmatrix} 0 \\ 0 \\ \gamma_{12} \end{bmatrix} \tag{2.3.4}$$

where $f(\gamma_{12})$ is the real root of the equation

$$f^3 + \frac{3}{S'_{66}} f^2 + \left(\frac{3}{S'^2_{66}} + \frac{S'_{66}}{S_{6666}} \frac{1}{\gamma^2_{12}}\right) f + \frac{1}{S'^3_{66}} = 0 \tag{2.3.5}$$

Later, Hahn, (Ref. 99) extended the above method of unidirectional laminae to laminated composites.

First the lamina properties are transformed to coordinate system other than the material coordinates. In order to make use of the transformation properties of Sec. 2.2, equation (2.3.1) is written as :

$$\begin{bmatrix} \varepsilon_1 \\ \varepsilon_2 \\ \gamma_{12} \end{bmatrix} = \left[\bar{S} \right] \begin{bmatrix} \sigma_1 \\ \sigma_2 \\ \tau_{12} \end{bmatrix} \tag{2.3.6}$$

where :

$$\left[\bar{S}\right] = \begin{bmatrix} S'_{11} & S'_{12} & 0 \\ S'_{12} & S'_{22} & 0 \\ 0 & 0 & S'_{66} + S_{6666}\,\tau_{12}^2 \end{bmatrix} \qquad (2.3.7)$$

The stress-strain relation in the x-y coordinates, Fig. (2.2.2), becomes :

$$\begin{bmatrix} \varepsilon_x \\ \varepsilon_y \\ \gamma_{xy} \end{bmatrix} = [S]\begin{bmatrix} \sigma_x \\ \sigma_y \\ \tau_{xy} \end{bmatrix} + S_{6666}\,\tau_{12}^2 \begin{bmatrix} \frac{1-\cos 4\theta}{8} & -\frac{1-\cos 4\theta}{8} & -\frac{\sin 4\theta}{4} \\ & \frac{1-\cos 4\theta}{8} & \frac{\sin 4\theta}{4} \\ \text{(symmetric)} & & \frac{1+\cos 4\theta}{2} \end{bmatrix} \begin{bmatrix} \sigma_x \\ \sigma_y \\ \tau_{xy} \end{bmatrix} \qquad (2.3.8)$$

where :

$$\tau_{12}^2 = \frac{1-\cos 4\theta}{8}(\sigma_x-\sigma_y)^2 - \frac{\sin 4\theta}{2}\tau_{xy}(\sigma_x-\sigma_y) + \tfrac{1}{2}(1+\cos 4\theta)\,\tau_{xy}^2 \qquad (2.3.9)$$

or in the inverted form:

$$\begin{bmatrix} \sigma_x \\ \sigma_y \\ \tau_{xy} \end{bmatrix} = [Q]\begin{bmatrix} \varepsilon_x \\ \varepsilon_y \\ \gamma_{xy} \end{bmatrix} + g(\varepsilon_1,\varepsilon_2,\gamma_{12}) \begin{bmatrix} \frac{1-\cos 4\theta}{2} & -\frac{1-\cos 4\theta}{2} & -\frac{\sin 4\theta}{2} \\ & \frac{1-\cos 4\theta}{2} & \frac{\sin 4\theta}{2} \\ \text{(symmetric)} & & \frac{1+\cos 4\theta}{2} \end{bmatrix} \begin{bmatrix} \varepsilon_x \\ \varepsilon_y \\ \gamma_{xy} \end{bmatrix} \qquad (2.3.10)$$

where $g(\varepsilon_1,\varepsilon_2,\gamma_{12})$ is the root of equation (2.3.5) with ε_{12}^2 replaced by:

$$\varepsilon_{12}^2 = \frac{1-\cos 4\theta}{2}(\varepsilon_x-\varepsilon_y)^2 - \sin 4\theta\ \gamma_{xy}\ (\varepsilon_x-\varepsilon_y) + \frac{1+\cos 4\theta}{2}\tau_{xy}^2$$

(2.3.11)

Hahn restricted the analysis to laminates of the type $(0^o/\pm\alpha^o/90^o)$ for which he obtained the following stress-strain relations :

$$\begin{bmatrix} N_x \\ N_y \\ N_{xy} \end{bmatrix} = [A] \begin{bmatrix} \varepsilon_x^o \\ \varepsilon_y^o \\ \gamma_{xy}^o \end{bmatrix} + t_\alpha \begin{bmatrix} \frac{g_e(1-\cos 4\alpha)}{2} & \frac{g_e(1-\cos 4\alpha)}{2} & \frac{g_o(\sin 4\alpha)}{2} \\ & \frac{g_e(1-\cos 4\alpha)}{2} & \frac{g_o(\sin 4\alpha)}{2} \\ \text{(symmetric)} & & \frac{t_o+t_{90}}{t_\alpha} f(\tau_{xy}) + \frac{g_e(1+\cos 4\alpha)}{2} \end{bmatrix} \begin{bmatrix} \varepsilon_x^o \\ \varepsilon_y^o \\ \gamma_{xy}^o \end{bmatrix}$$

(2.3.12)

where:

t_o, t_α, t_{90} are the thicknesses of the different laminae

$$g_e = \tfrac{1}{2}\left[g(\varepsilon_x, \varepsilon_y, \gamma_{xy}, \alpha) + g(\varepsilon_x, \varepsilon_y, \gamma_{xy}, -\alpha)\right]$$
$$g_o = \tfrac{1}{2}\left[g(\varepsilon_x, \varepsilon_y, \gamma_{xy}, \alpha) - g(\varepsilon_x, \varepsilon_y, \gamma_{xy}, -\alpha)\right] \quad (2.3.13)$$

The above analysis has the following shortcomings :

1. It does not account for non-linear response in the longitudinal and transverse direction.

2. It introduces a new constant, S_{6666}, which must be determined by test. Hahn, (Ref. 99), showed that it could be determined from unidirectional tension test on $\pm 45^o$ laminate.

3. The analysis will be extremely difficult for a general laminate, especially for laminated tubes where, as shown in Sec. 2.2, the stress gradient is of some importance.

b) Petit-Waddoups Method

Petit and Waddoups, (Refs. 100, 101), used the lamina empirical stress-strain curves and the linear laminate constitutive relations of Sec. 2.2 to obtain the laminate stress-strain response. Thus, their method accounts for non-linear behaviour in the longitudinal and transverse directions as well as in-plane shear.

The use of the linear lamina and laminate constitutive relations in the non-linear analysis of the laminate was made possible by incrementally applying the average laminate stresses (σ_x^o, σ_y^o and τ_{xy}^o), and by using a piecewise linear representation of the stress-strain curves. That is, an increment of average laminate stresses ($\Delta\sigma_x^o$, $\Delta\sigma_y^o$ and $\Delta\tau_{xy}^o$) is placed on the laminate, and, by using the initial laminate compliance matrix, $[S]_T$, the first increment in the laminate strains is calculated with the assumption that the laminate behaves linearly over the applied stress increment, i.e.

$$\left[\Delta\varepsilon^o\right]_{n+1} = \left[S_T\right]_n \left[\Delta\bar{\sigma}^o\right]_{n+1} \qquad (2.3.14)$$

the increment in the laminate strains, $[\Delta\varepsilon^o]$, is added to any previous strains to determine the current total laminate strains :

$$\left[\varepsilon^o\right]_{n+1} = \left[\varepsilon^o\right]_n + \left[\Delta\varepsilon^o\right]_{n+1} \qquad (2.3.15)$$

These strains are used to determine the lamina strains through the usual procedure of the linear analysis. As the incremental loading proceeds, the individual lamina strains may be monitored, and, by referring to the empirical lamina stress-strain curves the corresponding lamina tangent moduli and stiffness for the strain levels present can be calculated from the following :

$$[Q']_n = \begin{bmatrix} \frac{E_{11}}{1 - \nu_{12}\,\nu_{21}} & \frac{\nu_{21}\,E_{11}}{1 - \nu_{12}\,\nu_{21}} & 0 \\ \frac{\nu_{21}\,E_{11}}{1 - \nu_{12}\,\nu_{21}} & \frac{E_{22}}{1 - \nu_{12}\,\nu_{21}} & 0 \\ 0 & 0 & G_{12} \end{bmatrix} \qquad (2.3.16)$$

where, E_{11}, E_{22} and G_{12} are the lamina tangent moduli which are determined from their respective stress-strain curves at the current or nth values of lamina strains. The above lamina stiffness matrix is used to compute the laminate compliance matrix for the (n + 1)th stress increment, equation (2.3.14).

The shortcomings of this method are :

1. It uses a piecewise linear representation which is not accurate enough to represent the real stress-strain curves.

2. It uses the n^{th} values of lamina strain to obtain the laminate compliance for the next $(n + 1)^{th}$ load increment. This is a predictor technique. A predictor-corrector technique would be better to give more accurate results.

3. Resulting from the previous point, the laminate stress-strain curves depend very much on the size of load increments giving rise to cumulative error.

c) Hashin-Bagchi-Rosen Method

Hasin et al., (Ref. 102), used Ramberg-Osgood representation of the lamina transverse and shear strain curves in conjunction with deformation theory to describe the resultant laminate non-linear behaviour.

In this analysis the lamina strains ε are split into elastic strains ε' and inelastic strains ε''. Thus :

$$\begin{bmatrix} \varepsilon_1 \\ \varepsilon_2 \\ \gamma_{12} \end{bmatrix} = \begin{bmatrix} \varepsilon_1' \\ \varepsilon_2' \\ \gamma_{12}' \end{bmatrix} + \begin{bmatrix} \varepsilon_1'' \\ \varepsilon_2'' \\ \gamma_{12}'' \end{bmatrix} \qquad (2.3.17)$$

The elastic strains are given by :

$$\begin{bmatrix} \varepsilon_1' \\ \varepsilon_2' \\ \gamma_{12}' \end{bmatrix} = [S'] \begin{bmatrix} \sigma_1 \\ \sigma_2 \\ \tau_{12} \end{bmatrix} \qquad (2.3.18)$$

where S' is the linear compliance matrix and given by equation (2.2.7).

The inelastic strains are given by Ramberg-Osgood form :

$$\begin{bmatrix} \varepsilon_1'' \\ \varepsilon_2'' \\ \varepsilon_{12}'' \end{bmatrix} = \begin{bmatrix} 0 \\ \frac{\sigma_2}{E_2} \left[\left(\frac{\sigma_2}{\sigma_y'}\right)^2 + \left(\frac{\tau_{12}}{\tau_y'}\right)^2 \right]^{\frac{M-1}{2}} \\ \frac{\tau_{12}}{2G_{12}} \left[\left(\frac{\sigma_2}{\sigma_y'}\right)^2 + \left(\frac{\tau_{12}}{\tau_y'}\right)^2 \right]^{\frac{N-1}{2}} \end{bmatrix} \qquad (2.3.19)$$

where :

the inelastic longitudinal strain is neglected,

σ_y', τ_y' are called the nominal yield stresses,

M, N are Ramberg-Osgood parameters for the composite.

σ'_y, τ'_y, M and N are obtained by curve fitting.

The laminate analysis is rather complicated. It is based on writing 3n equations for the 3n stresses in a laminate with n layers. First the layer strains are transformed to the laminate axes and written in terms of compliances and stresses. Then the 3n equations are written using the following conditions which must be satisfied :

1) Equilibrium of stresses :

$$\sum_{k=1}^{n} \sigma_x^{(k)} = \sigma_x^o$$

$$\sum_{k=1}^{n} \sigma_y^{(k)} = \sigma_y^o \qquad (2.3.20)$$

$$\sum_{k=1}^{n} \tau_{xy}^{(k)} = \tau_{xy}^o$$

2) Traction continuity at laminae interfaces :

$$\varepsilon_x^{(k)} = \varepsilon_x^{(k+1)}$$

$$\varepsilon_y^{(k)} = \varepsilon_y^{(k+1)} \qquad (2.3.21)$$

$$\tau_{xy}^{(k)} = \tau_{xy}^{(k+1)}$$

$$k = 1, 2, \ldots, n$$

The above 2 sets of equations form the required 3n equations which are solved numerically by an iteration method.

The above analysis has the following shortcomings :

1. It does not account for non-linear behaviour in the fibre direction. Some fibre-reinforced composites, e.g. carbon-carbon, have non-linearities in all principal material directions. Thus, it is important for any method to account for these non-linearities.

2. It is based on equal strain through the thickness. Thus, it is not suitable to calculate the stress gradient.

3. The convergence in the iteration is not guaranteed.

d) Sandhu Method

Sandhu, (Refs. 103, 104), introduced a new method which tries to overcome the shortcomings of Petit-Waddoups method. First, this method uses piecewise cubic spline functions to represent the basic stress-strain data. Second, it uses a predictor-corrector and iteration technique instead of the predictor technique used in Petit-Waddoups method. That is, this method proceeds in the same way described in Petit-Waddoups method till equation (2.3.14). In Petit-Waddoups method the elastic properties at the end of the nth load increment are used to compute the laminate strain increments $\Delta\varepsilon^{o}$ for the (n+1)th load increment. In this method, however, the lamina strains obtained are used to determine average laminate compliance for the same load increment, and a new set of laminate strains are obtained. This procedure is repeated until the difference between two consecutive sets of laminate strains is less than a prescribed value. Thus, in this method the dependence of laminate stress-strain curves on the size of load increments is reduced.

The only disadvantage of this method is that, as in Petit-Waddoups method, it uses tangent moduli which are not easy to obtain correctly from the test data, thus, giving possibility to errors to rise.

e) Jones-Nelson-Morgan Method

In this method, (Ref. 105-110), the non-linear mechanical properties are functions of the strain energy density :

$$(\text{Mechanical Property})_i = A_i \left[1 - B_i \left(U/U_{oi}\right)^{C_i}\right] \qquad (2.3.22)$$

where :

$$U = (\sigma_1\varepsilon_1 + \sigma_2\varepsilon_2 + \tau_{12}\gamma_{12})/2 \qquad (2.3.23)$$

for a lamina under plane stress, and A_i, B_i and C_i are the initial slope, initial curvature, and change of curvature of the ith stress-strain curve. The quantity U_o is used to nondimensionalize the strain energy portion of the mechanical property equation.

It is obvious from equation (2.3.23) that the strain energy is calculated at a particular point of the stress-strain curve using the secant modulus, Fig. (2.3.4).

The maximum strain energy, U_{max}, is the limit of the defined data, Fig. (2.3.5). However, Jones and Morgan states that the actual strain energy can exceed the defined range of the mecanical property versus strain energy curve because the non-linear analysis is applied in multiaxial stress states for which the strain energy is higher than in the uniaxial stress states in which the mechanical properties are measured. Thus, Jones and Morgan extrapolate the curves as shown in Fig. (2.3.6). This is done in a complicated procedure.

The next step in the analysis is to evaluate the non-linear behaviour. In (Refs. 105-110), however, the method is applied to single lamina structure under uniaxial loading. The constants A, B and C of equation (2.3.22) are determined from the best fit to the data from Fig. (2.3.6). Then an iteration technique is used to obtain the stress-strain behaviour. At each iteration of the non-linear procedure, a linear elastic system with properties determined from the strain energy of the preceding iteration is analysed. The elastic properties are used to start the procedure.

Later, Morgan and Jones, (Ref. 111), extended the above method to the laminate behaviour using iteration technique to satisfy the stress-strain relations, stress equilibrium and strain compatibility throughout the laminate.

This method seems to be comprehensive for the analysis of non-linear behaviour of fibrous laminated structures, but as mentioned by Morgan and Jones, (Ref. 111), is quite complicated. This complexity did not prove to produce better results when compared with the simple method of Hahn-Tsai, (Refs. 109, 110).

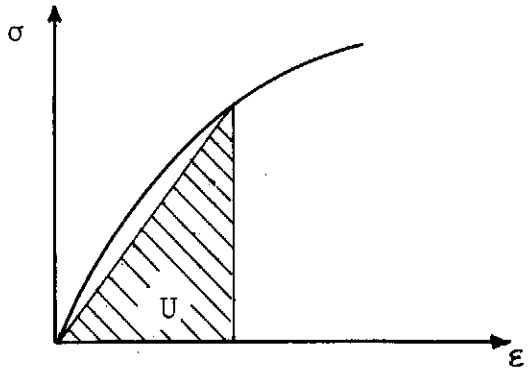

Fig. (2.3.4) Calculation of strain energy in Jones-Nelson-Morgan analysis

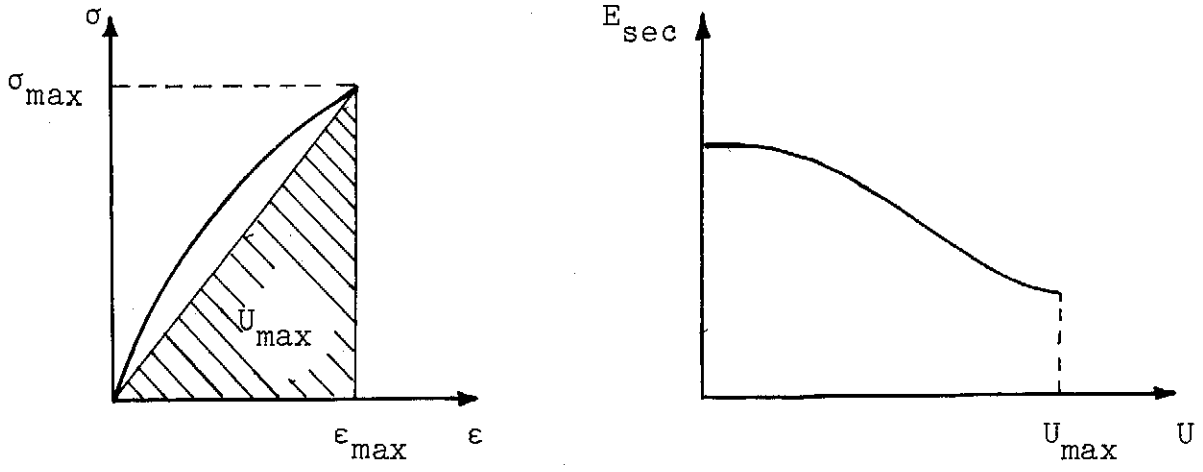

Fig. (2.3.5) Limit of measured data for mechanical property versus strain energy curve

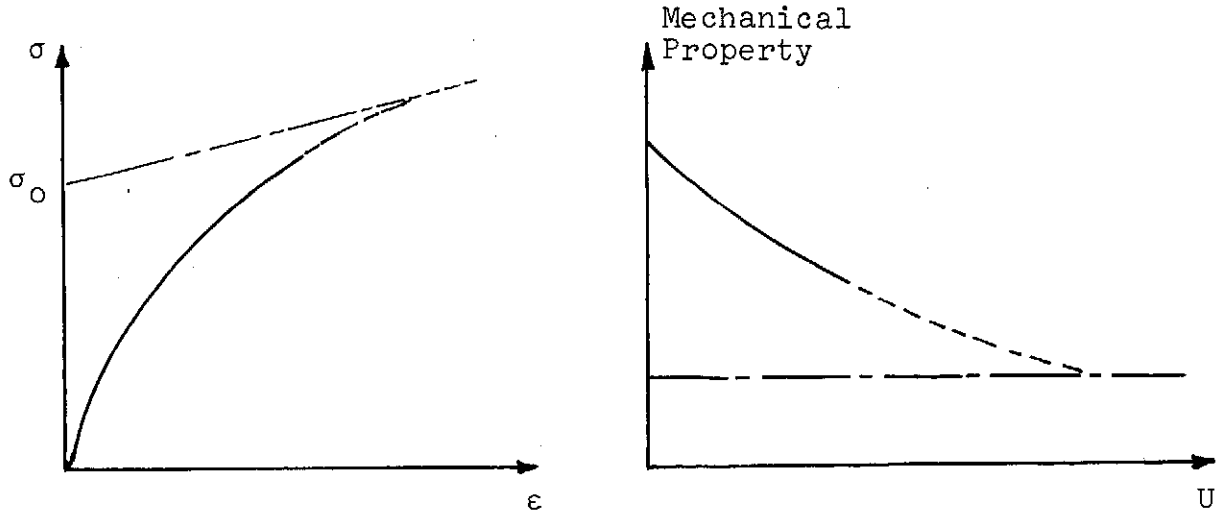

Fig. (2.3.6) Extended stress-strain curve approach

f) Amijima-Adachi Method

Although appeared recently, (Ref. 112), this method did not introduce a fundamentally new technique. It is restricted to shear non-linearity only and this non-linearity is represented by series of linear lines, i.e. the shear stress-strain curve is divided properly into n small sections where it is considered as a linear line within each increment as follows :

$$(G_{12})_n = \frac{(\Delta\tau_{12})_n}{(\Delta\gamma_{12})_n} = \text{variable} \qquad (2.3.24)$$

In (Ref. 112) only uniaxial loading case is considered, thus equations between the in-plane principal shear strain increment of the lamina, $\Delta\gamma_{12}$, and the stress resultant increment of the laminate in the loading direction, ΔN_x, are obtained easily for both unidirectional and angle-ply laminates. Then the laminate strain increments are obtained from equation similar to equation (2.2.31), and the non-linear stress-strain curve of the laminate is predicted from these calculated values.

Laminates of multidirectional configurations are analysed by superposing the stress-strain responses of the individual unidirectional or angle-ply laminae.

The limitations of this method are obvious from the foregoing description.

g) Other Methods

In addition to the preceding macromechanics methods of analysing the non-linear behaviour of composite structures there exist some micromechanics methods to predict the effect of matrix non-linearity on the behaviour of fibrous composite materials (Refs. 113-121). These methods are not discussed here as the macromechanics approach is adopted in this thesis.

2.3.3 A Proposed Method for Analysis of Non-Linear Behaviour

This method is based on the analysis of Sec. 2.2, and is meant to be simple and easy for computation even by a calculator.

The aim of the method is to obtain the non-linear behaviour of a laminate which results from the non-linear behaviour of its constituent laminae. The stress-strain response of a unidirectional layer must, therefore, be obtained first. These are obtained from experiments and presented as shown in Fig. (2.3.1). All the lamina stress-strain curves are allowed to be non-linear even with different behaviour in tension and compression, Fig. (2.3.1).

A curve fitting technique is then employed on the experimental data. Any reliable method can be used for this procedure. Cubic spline functions are used in the computer programme which has been developed for this analysis in this thesis, Appendix C.

Using the lamina "linear" properties the elastic properties of the laminate are obtained employing the relations of Sec. 2.2. The external loadings $[N]$ are then applied to the laminate and the linear laminate strains are obtained from equations (2.2.33). The stresses and strains in the individual layers are computed from equations (2.2.36) and (2.2.39) and then transformed to the layer axis system, equations (2.2.12) and (2.2.13).

The above calculations are the start of the iteration procedure which follows. This procedure is schematically shown in Fig. (2.3.7). For sake of explanation, Fig. (2.3.7) shows only the relationship of the laminate response under uniaxial loading to the shear response of one of its laminae, though, in the analysis the effects of longitudinal and transverse (whether in tension or compression) of all layers of the laminate are allowed for to obtain the behaviour of the laminate under multi-axial loading state.

The external load σ_x^o results in lamina stress τ_{12} and lamina strain γ_{12} when the lamina linear properties are used. The point (γ_{12}, τ_{12}) does not lie on the experimental non-linear lamina curve. Then the strain γ_{12} is used to find the corresponding lamina stress, τ'_{12}, from the lamina test data. The point $(\gamma_{12}, \tau'_{12})$ is then used to calculate a secant lamina modulus

$$(G'_{12})_{\text{secant}} = \frac{\tau'_{12}}{\gamma_{12}} \qquad (2.3.25)$$

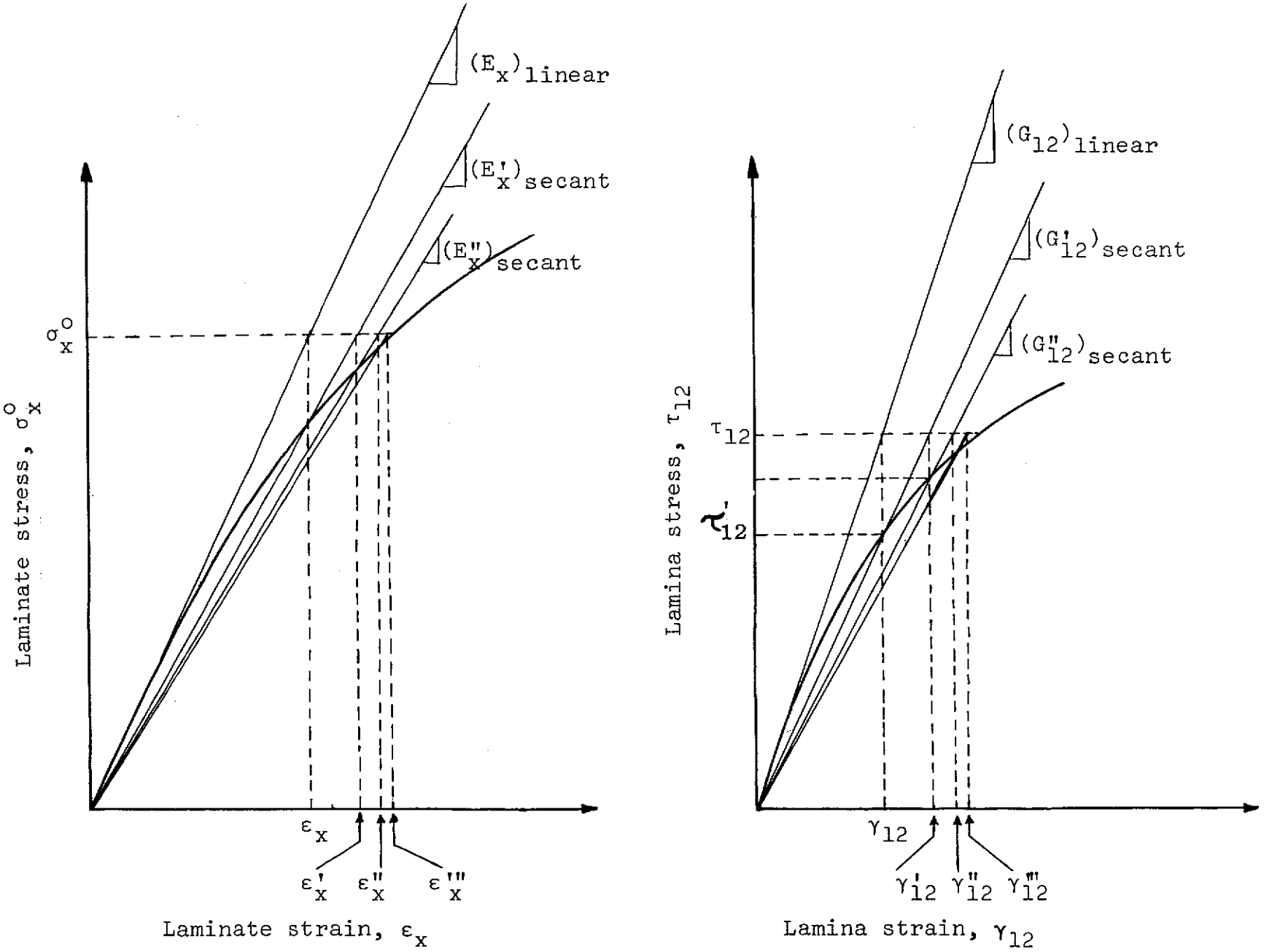

Fig. (2.3.7) Iteration technique for non-linear behaviour

The secant modulus is then used instead of the linear modulus in all equations of Sec. 2.2. This leads to a new laminate compliance and produces a new laminate strain ε'_x which, in turn, gives a new lamina strain γ'_{12} which is nearer to the test curve than γ_{12}. The procedure is repeated with the new laminate strain γ'_{12} and the modification continues until some convergence for the lamina strain is achieved. Practically, the convergence is considered to have taken place when the difference of two successive values of the laminate strains is too small (smaller than a desired value).

The whole stress-strain curve for the laminate is obtained by changing the applied load and employing the above procedure for each load. One advantage of this method of analysis is that the technique converges rapidly, but convergence depends on the value of the applied load, for it is obvious that higher load will require more iterations than small load. Another advantage of the method is that the response of the laminate under a single load ratio can be computed without any need to obtain the complete stress-strain curve as it is the case in other techniques.

Convergence for one layer laminate is defined to occur when all the lamina strains converge to their experimental values. In case of multi-layered laminate convergence is defined to be achieved when the convergence criterion is simultaneously satisfied for all layers.

2.3.4 Correlation of Predicted and Observed Results

The new method described above was included in the general computer programme which was developed to analyse the behaviour of laminated composite structures. To verify this new method it is compared here with experimental data and results obtained from other techniques. Since it is not convenient to develop a computer programme for all previous methods, the comparison is made with available data from another reference. This also helps to ensure that this part of the analysis of the failure is checked before any further development.

Results from Hahn-Tsai, Petit-Waddoups and Sandhu methods were found available in (Ref. 104) where they were compared with experimental data extracted from (Refs. 40, 122).

These data belong to boron-epoxy (type: NARMCO 5505) which possesses the following elastic properties :

$$E_1 = 207.5 \times 10^9 \text{ N/m}^2$$

$$E_2 = 19.8 \times 10^9 \text{ N/m}^2$$

$$G_{12} = 6.4 \times 10^9 \text{ N/m}^2$$

$$\nu_{12} = 0.225$$

and exhibits non-linear behaviour in transverse and shear properties as shown in Figs. (2.3.8) and (2.3.9).

Stress-strain curves under uniaxial tensile load for 15°, 30°, 45°, 60° and 75° unidirectional laminates obtained experimentally (Ref. 40) and analytically are compared in Figs. (2.3.10) - (2.3.14). It can be seen that a similar or better agreement exists between the experimental results and the analytical results of the present approach than those obtained by other analytical techniques. In particular, Hahn-Tsai method, which allows for shear non-linearity only, seems to be inadequate especially in the 75° laminate where the contribution of the transverse response to the response in the load direction is very high.

Experimental responses of $\pm 30^\circ$, $\pm 45^\circ$ and $\pm 60^\circ$ angle-ply laminates subjected to uniaxial loads are compared with the theoretical results of the present method and other techniques in Figs. (2.3.15) - (2.3.17). Here again good agreement exists between the experimental data and results of the present theory.

Regarding the Hashin-Bagchi-Rosen and the Jones-Nelson-Morgan methods there is no available data to be compared with the present analysis results. However, in (Ref. 102) comparison was made between the Hashin-Bagchi-Rosen method, Petit-Waddoups method and experimental data which showed moderately good agreement. In (Ref. 110) comparison was made between the Jones-Nelson-Morgan method, the Hahn-Tsai method and experimental data which showed that agreement was poor in some cases and good in some cases. The complexity of these two methods is another factor which should be taken into account.

Regarding the Amijima-Adachi method there is also no available data for comparison, but in (Ref. 112) it is stated that the analytical results of that technique will fairly fit to the experimental one. As mentioned earlier this method is limited.

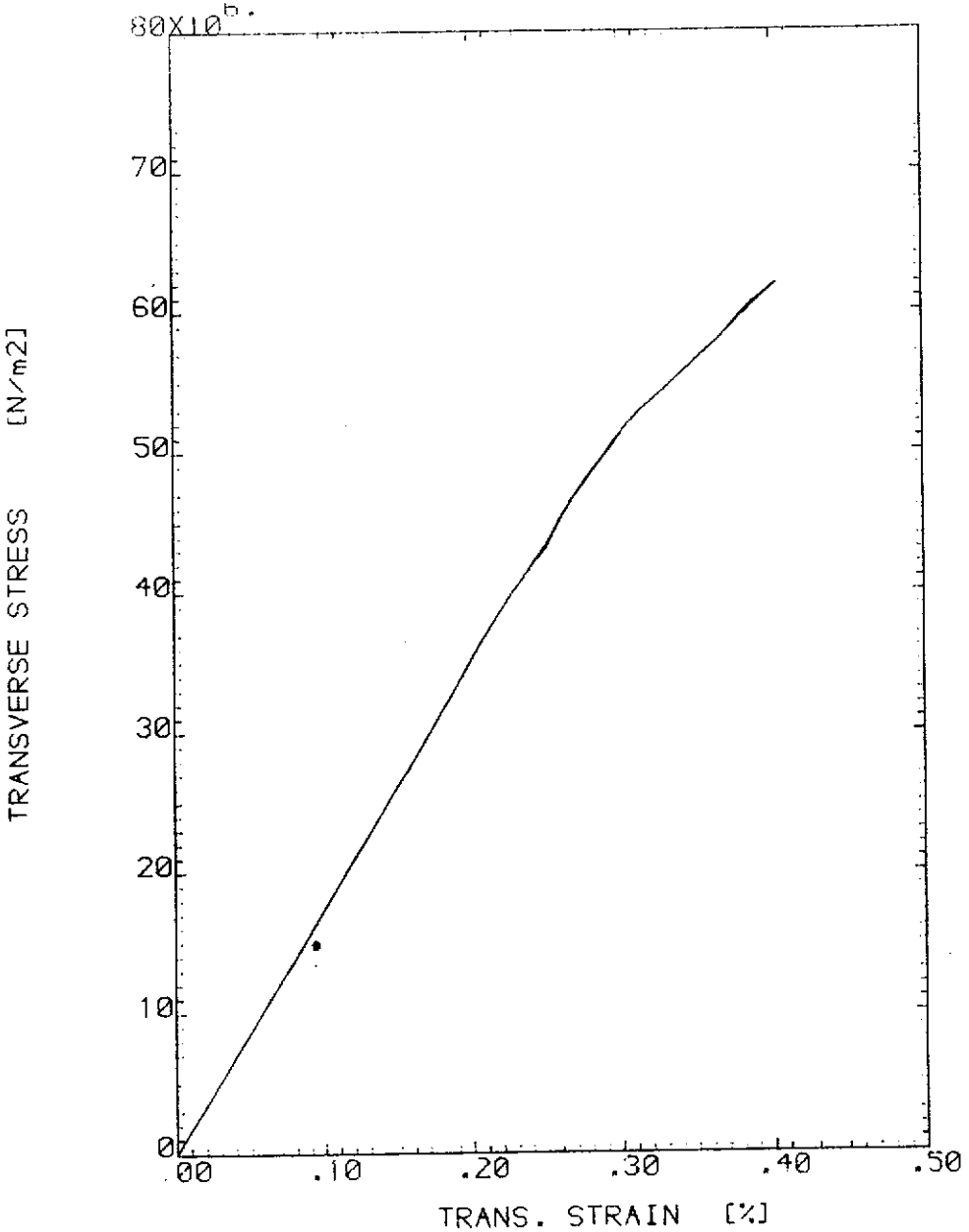

Fig.4

LAMINA TRANSVERSE CURVE

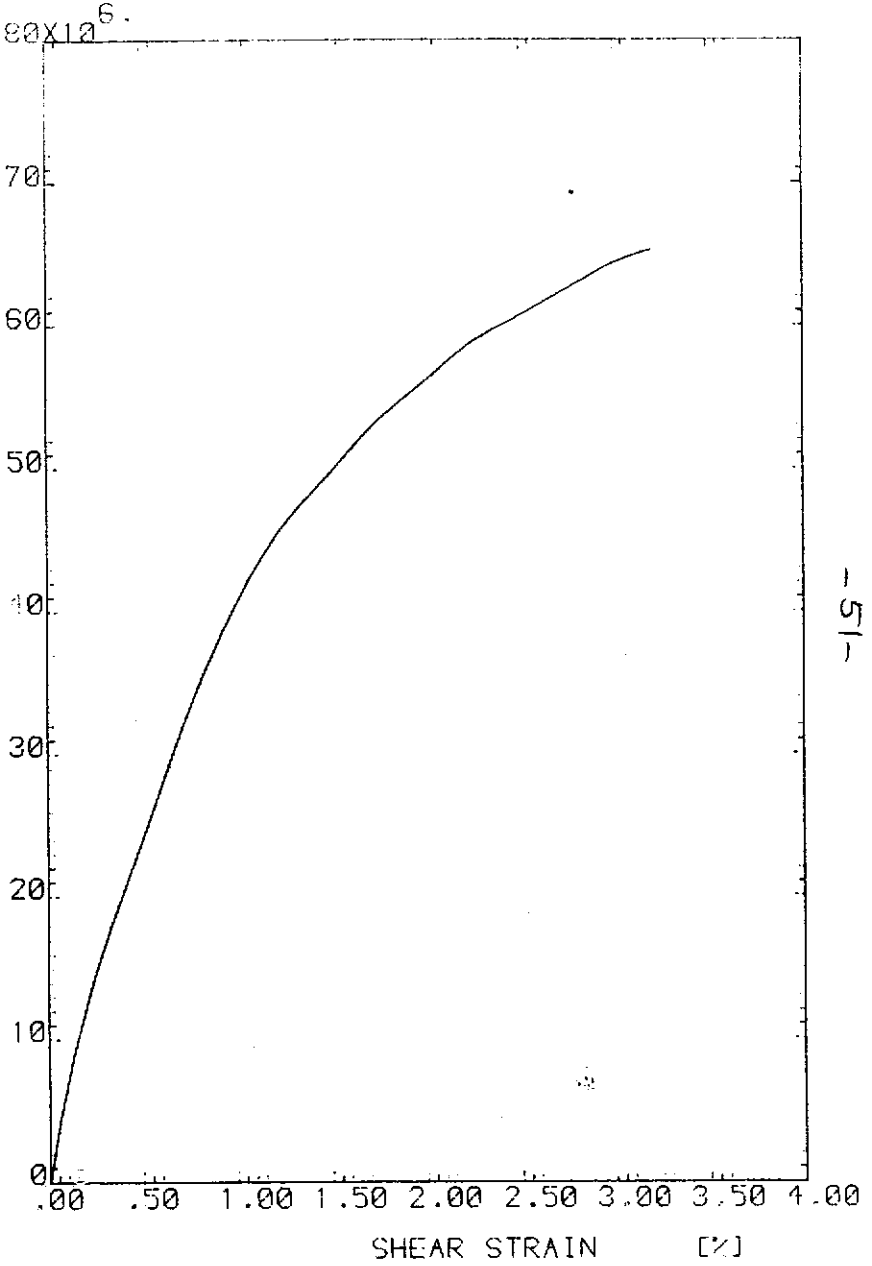

Fig.5

LAMINA SHEAR CURVE

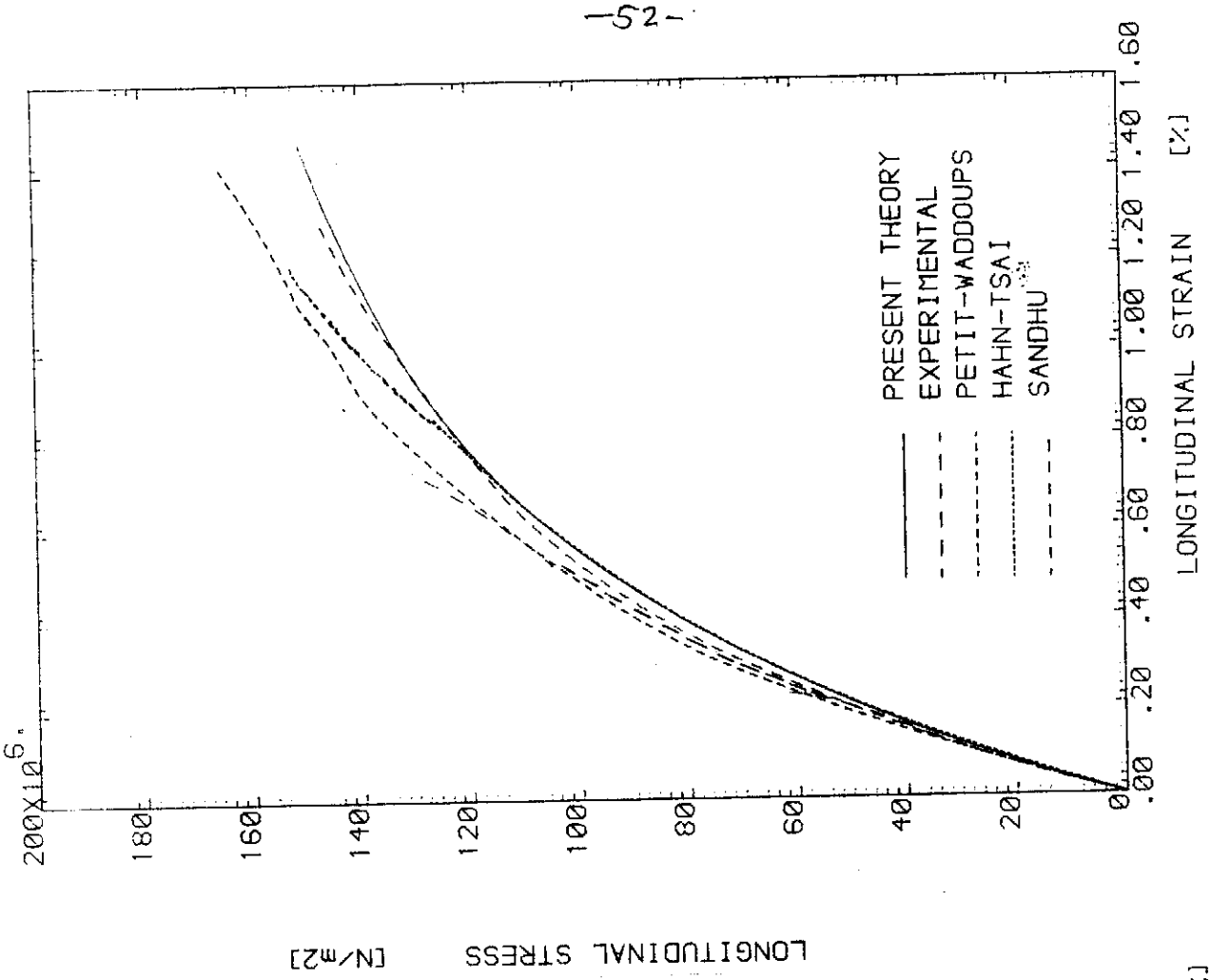

Fig. 7 RESPONSE OF 30° OFF AXIS PLY

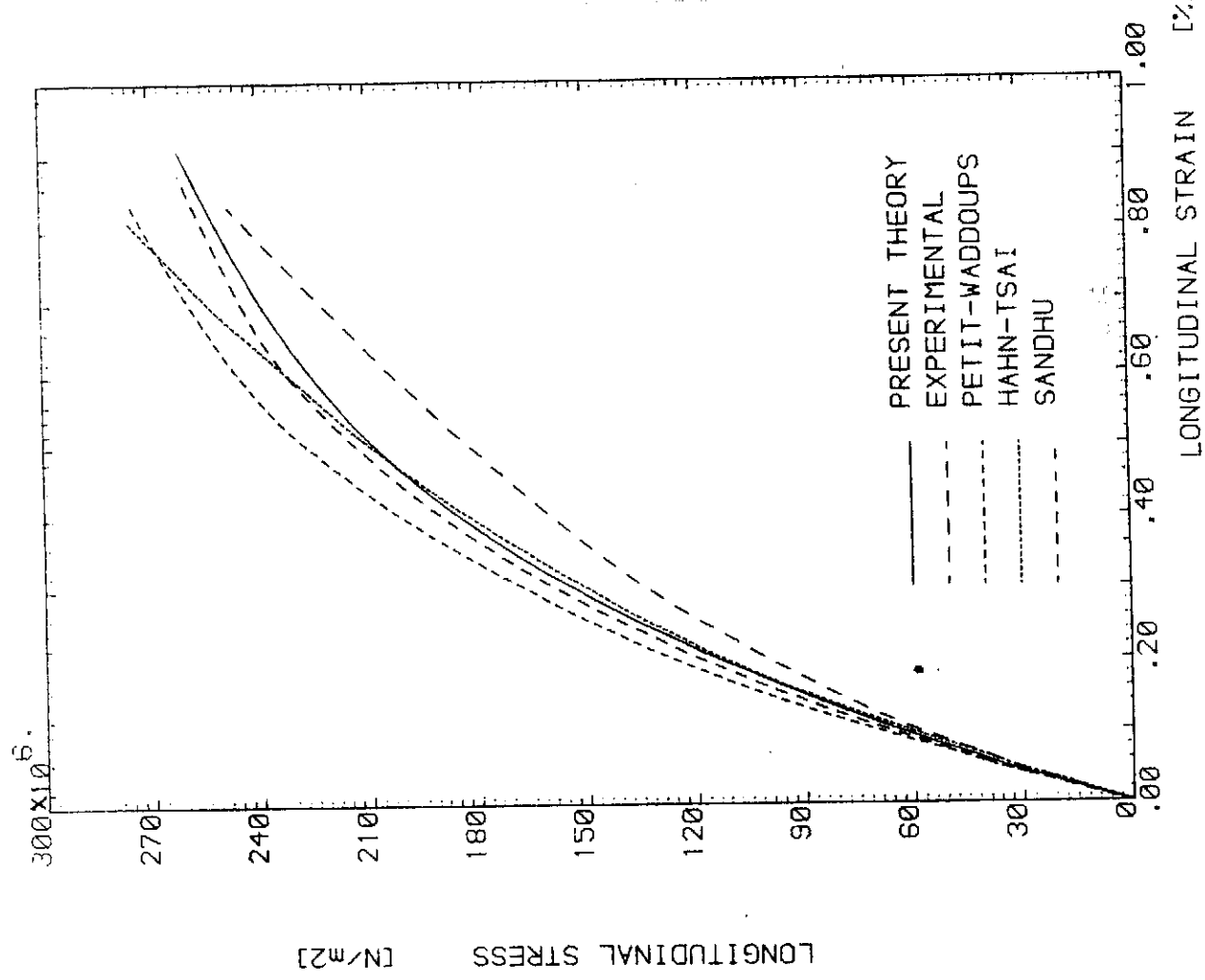

Fig. 6 RESPONSE OF 15° OFF AXIS PLY

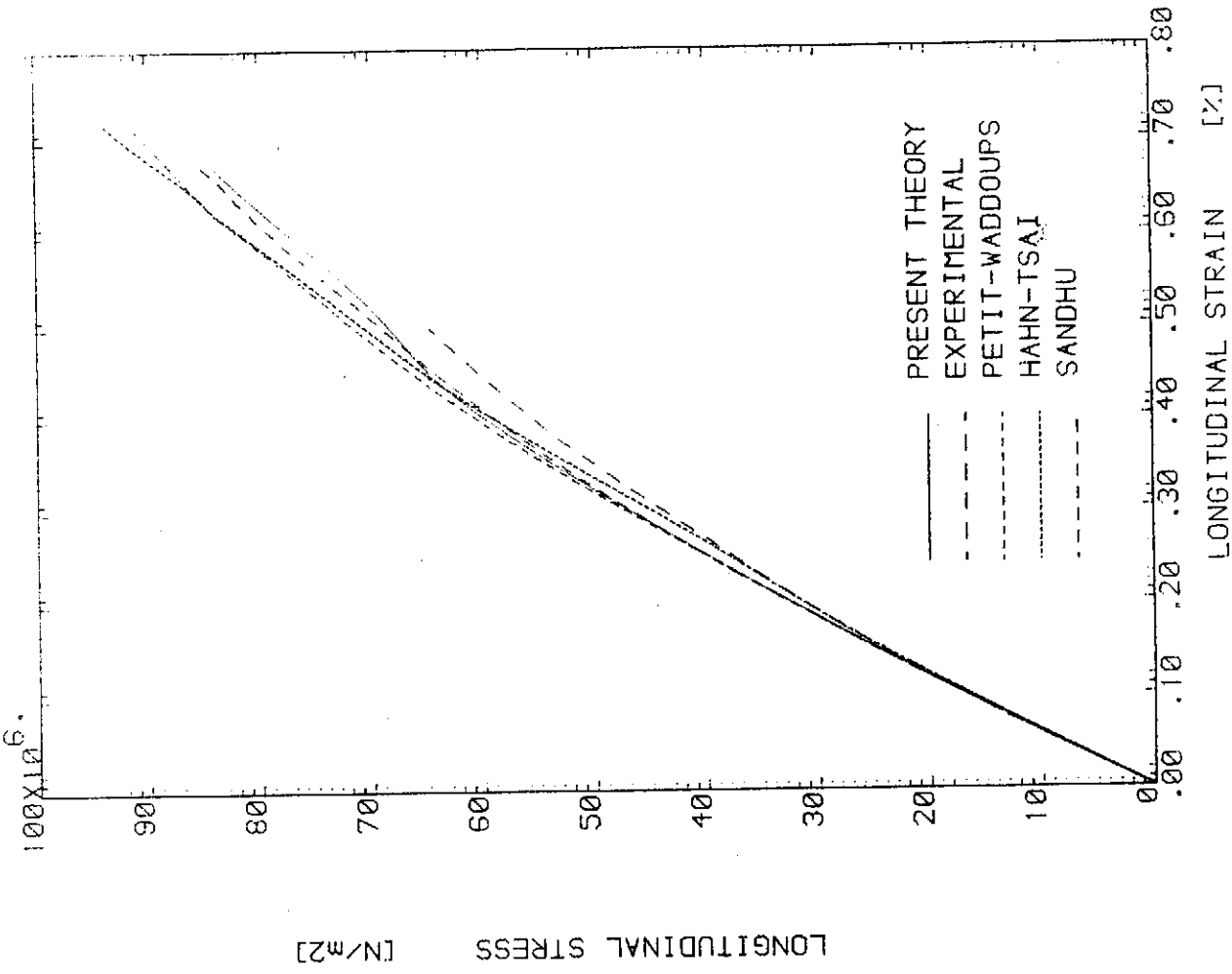

Fig. 9 RESPONSE OF 60° OFF AXIS PLY

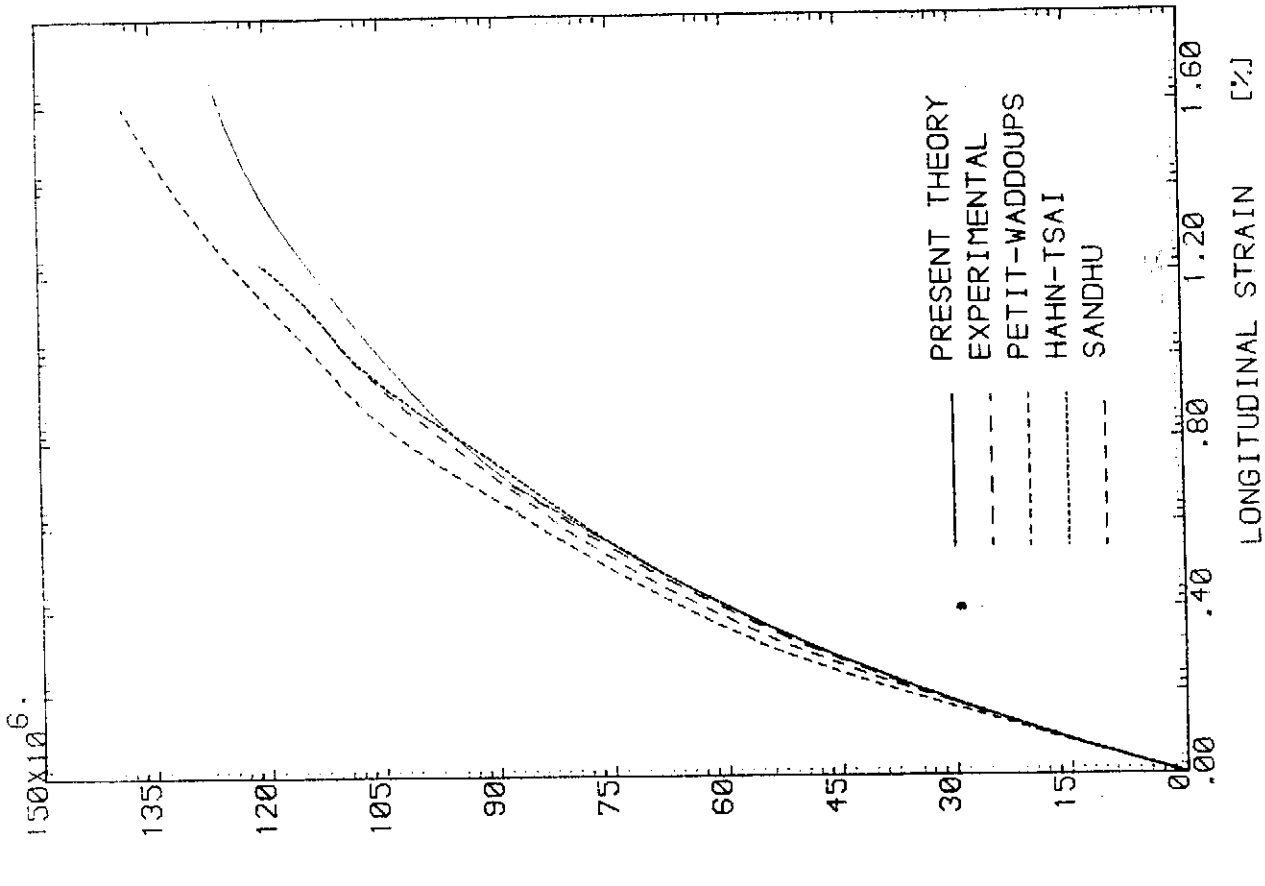

Fig. 8 RESPONSE OF 45° OFF AXIS PLY

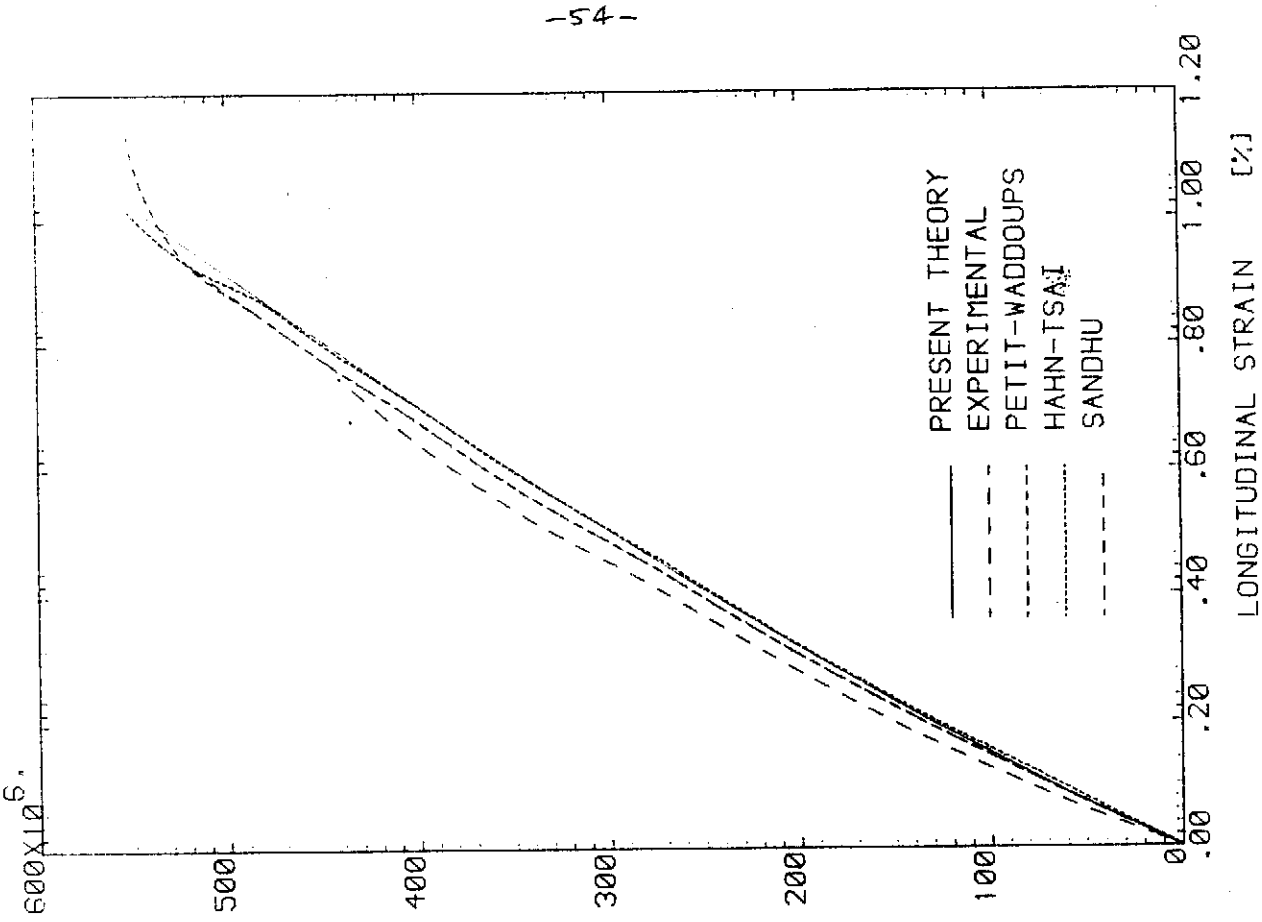

Fig.11 RESPONSE OF +/-30° LAMINATE, LOAD: SX

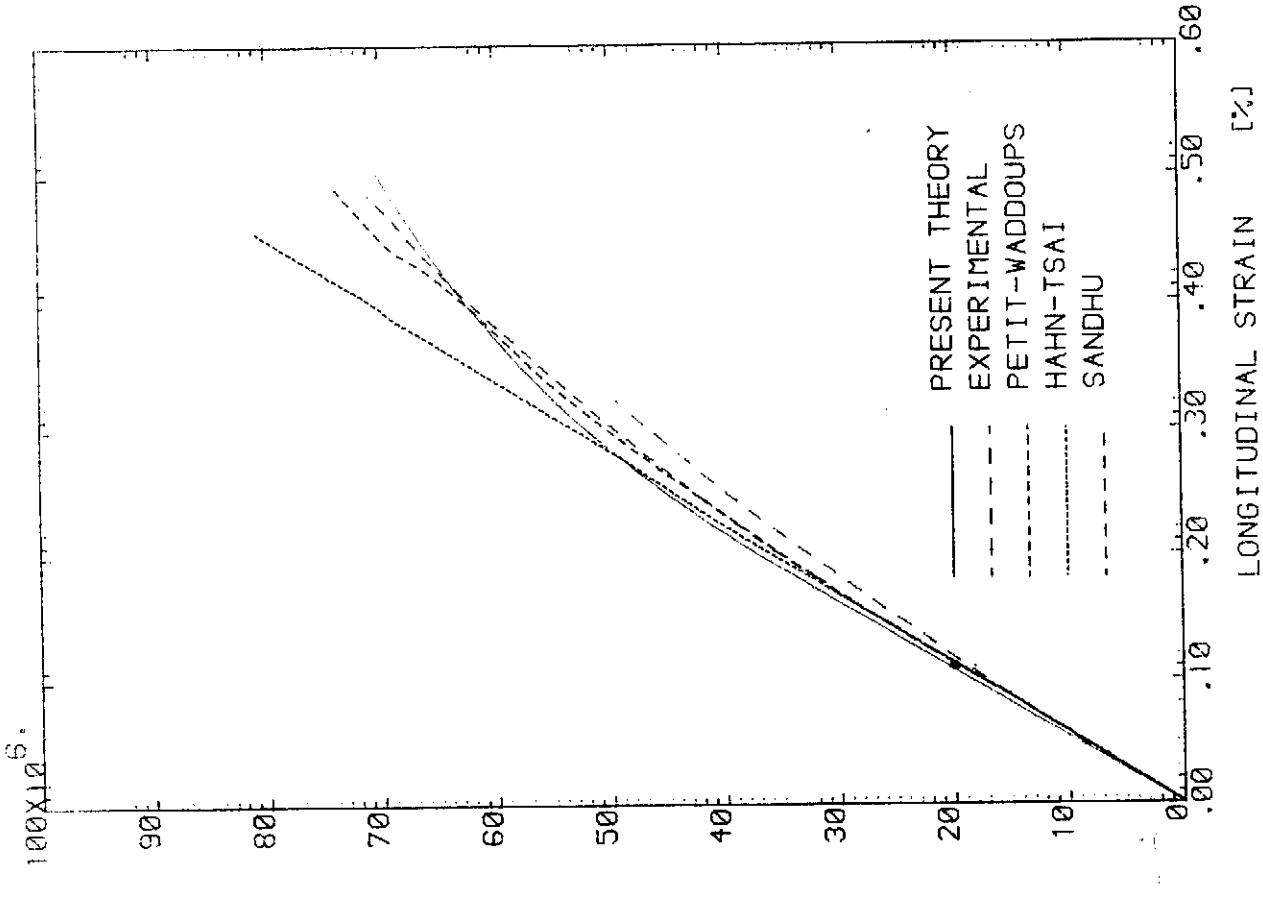

Fig. 10 RESPONSE OF 75° OFF AXIS PLY

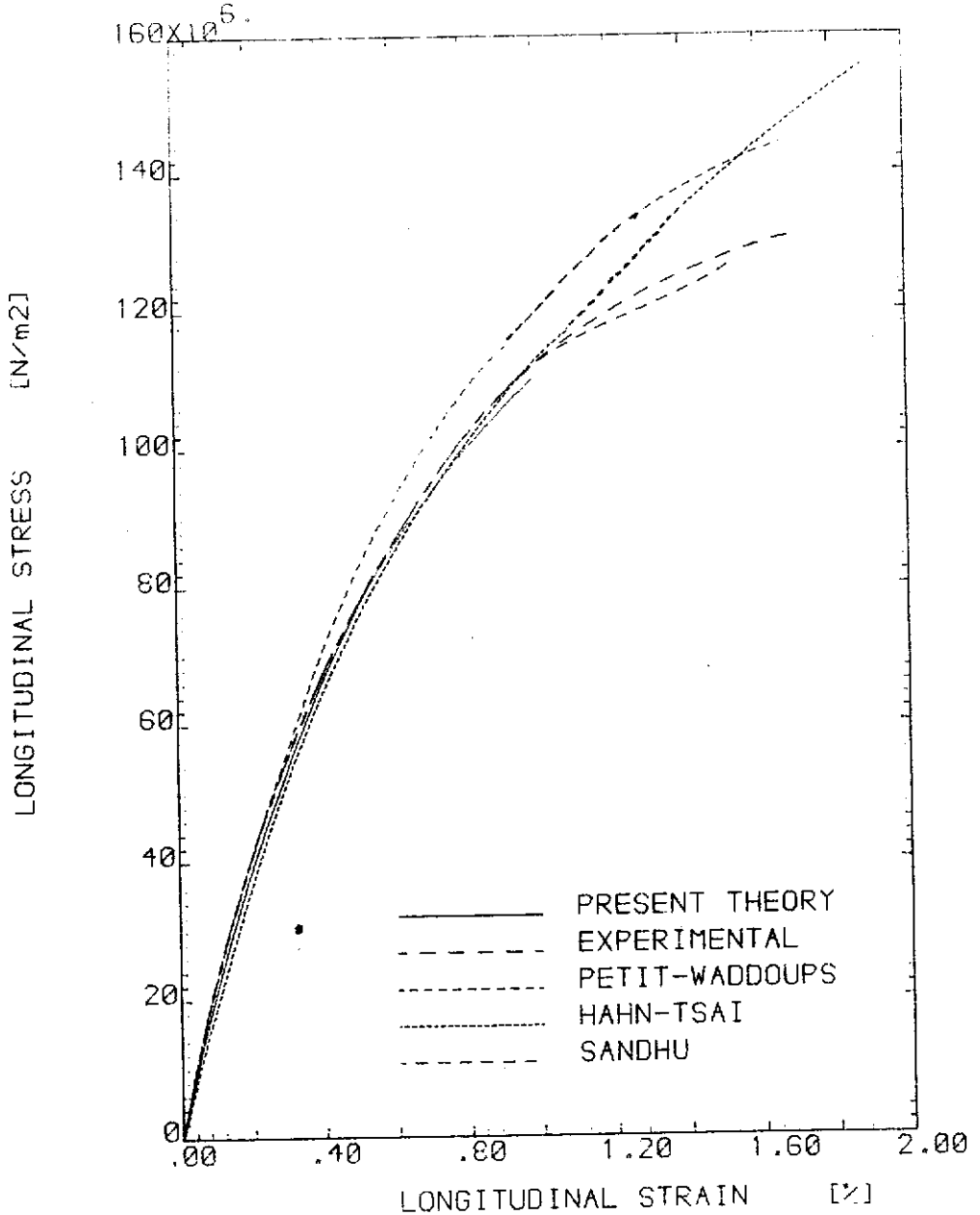

Fig. 12

RESPONSE OF +/-45° LAMINATE, LOAD: SX

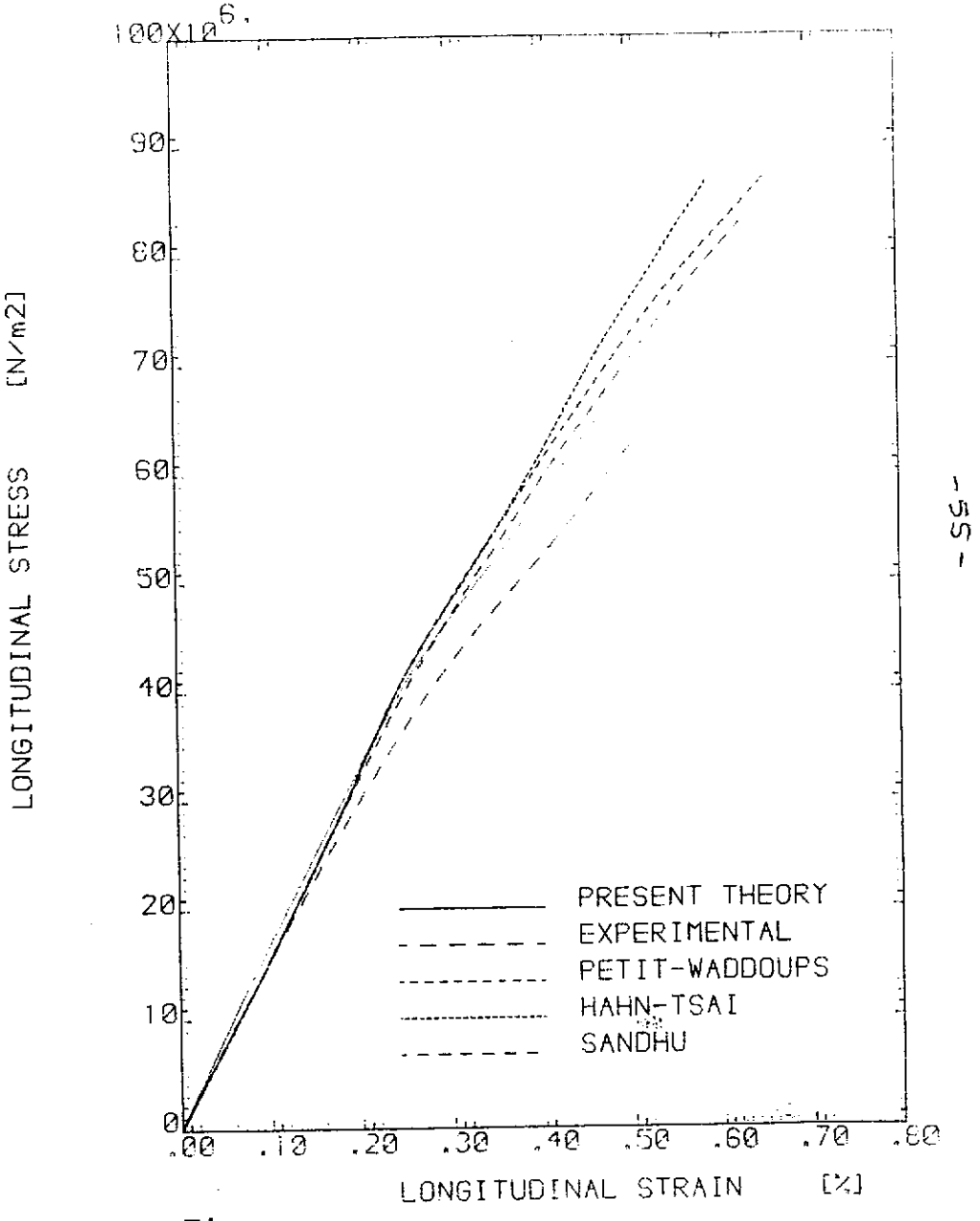

Fig. 13

RESPONSE OF +/-60° LAMINATE, LOAD: SX

2.4 ANALYSIS OF LAMINATED COMPOSITE CYLINDERS OF FINITE LENGTH

2.4.1 Introduction

In Sec. 2.2 the laminated composite shells of infinite length were analysed. The study of that section concentrated on the membrane stress state which exists in any section of infinitely long laminated tube subjected to combination of internal pressure, axial and torsional loadings. The tubular specimen for composite characterization, however, cannot be of infinite length. Discontinuities, therefore, exist at the ends of the tube (due to the unpressurised overhang) leading to presence of bending in these regions. Moreover, the specimen is gripped at its ends (for some test configurations) and the effects of end constraints must be studied.

It is the purpose of this section to determine the layered cylinder geometry, namely the length, l, such that there exists, in the middle of the cylinder, a region, called the test section, in which the stress state is membrane, Fig. (2.1.1). On the other hand, the presence of bending at the ends of the cylindrical specimen and the clamping constraints result in stresses and strains in the end regions higher than their values at the test section. This means that specimens will fail at sections other than their test sections preventing full characterization of the tubes. To overcome this, the ends of the tubular specimens are reinforced by tapered tabs of fibre-reinforced composites (or any other material). This necessitates full analysis to obtain the tabs geometry which ensures that failure will occur in the test section. The aim of this section, therefore, is to design the laminated cylindrical specimens to achieve complete characterization of composite structures.

2.4.2 Review of Previous Work

The different theories of laminated composite shells were reviewed in Sec. 2.2.1. Here, the works related to the problem of gripped laminated anisotropic tubes of finite length are reviewed.

Pagano et al, (Ref. 68), were the first to draw the attention to the influence of end constraints. They demonstrated that in case of a unidirectional cylinder subjected to uniaxial tension, the end clamps, owing to the presence of induced shear, introduced instability under a particular value of the applied tension. They called this phenomenon the "tension buckling" of anisotropic cylinders. However, in case of symmetric (about the middle surface) laminate this phenomenon does not exist. Later, Pagano and Whitney, (Ref. 72), used shell theory based on Donnell approximations to determine the cylindrical specimen length.

Herrmann and Chan, (Ref. 125), presented analyses in which they neglected the end effects due to the complexity of their three-dimensional analysis.

Vicario and Rizzo analysed the problem using shell theory at first, (Ref. 126), and then they used exact elasticity equations in developing finite element programme to gain insight into the effect of the geometry on the response of laminated tubes in material characterization tests, (Refs. 70, 71).

Flugge's shell theory, (Ref. 79), was used by Whitney et al, (Ref. 127), to study the effect of end fixity on the strength of composite cylindrical specimens. They suggested that more detailed analytical techniques would be helpful for predicting end-tab stresses and strains.

Reuter and Guess, (Ref. 128), used the analysis of (Ref. 82) which is based on Donnell shell theory to analyse filament wound composite tubular specimens under internal pressurization loading. Laplace transform technique was used in the solution of the differential equations, and the effect of the material overhang on the magnitude of the strength was studied.

The interlaminar stresses induced by the end effects were studied by Waltz and Vinson, (Ref. 129), where they presented solutions for both two laminae and three laminae shells subjected to internal pressure with clamped or simply supported boundary conditions.

Pipes and Whitney, (Ref. 130), analysed the anisotropic cylinder of finite length using elasticity equations and finite difference method. They compared their results with results obtained from Flugge's shell theory and found that the distributions of the in-plane stresses and strains were similar for both theories, but some differences in predictions of the through-the-thickness distributions were shown.

Guess and Haizlip, (Ref. 131), studied two different gripping configurations to determine their affect on stress distributions within the specimen test section. Finite element analyses were used in this study. The study illustrated the importance of the end effects on the stress distributions along the specimen.

Miller, (Ref. 135), presented a method to reduce moment and shear loads which occur at the end plugs of orthotropic cylinders subjected to external radial pressure.

Finally, Lemoine, (Ref. 132), used large displacements theory in the study of filament-wound motor chambers during internal pressurization. In the cylindrical part of the chamber the difference in the radial deflection predicted by small deflection theory and large deflection theory was negligible, whereas, this difference was significant in the domes of the

of the chamber. This means that small deflection shell theories are suitable for the analysis of the problem.

In this present work, Vlasov-Ambartsumyan type shell theory used in Sec. 2.2 is used here again for the analysis of laminated composite tubes of finite length. And because the wall thickness is varying near the ends of the tube, Fig. (2.1.1), finite element analysis is employed using "ring" or "short cylinder" elements to obtain the deflections, the stresses and the strains along the tube. Since lamination theory is used at the same time, the stresses and strains at any point in the wall can be found by making use of the analysis of Sec. 2.2. This method, in terms of computer time, is cheaper than the full finite element analysis of Vicario and Rizzo, (Refs. 70, 71).

2.4.3 Derivation of Governining Equations

Assuming a state of generalized plane stress in each of the orthotropic layers of the n-layer laminated composite cylinder the stress-strain relations of Sec. 2.2.2 and Sec. 2.2.3 are still applicable here.

Using the coordinate directions of Fig. (2.2.3) the strains at any point distant z from the middle surface of the tube are given by (see equation 2.2.24):

$$\begin{bmatrix} \varepsilon_x \\ \varepsilon_y \\ \gamma_{xy} \end{bmatrix} = \begin{bmatrix} \varepsilon_x^o \\ \varepsilon_y^o \\ \gamma_{xy}^o \end{bmatrix} + z \begin{bmatrix} \chi_x \\ \chi_y \\ \chi_{xy} \end{bmatrix} \qquad (2.4.1)$$

where ε^o's are the middle surface strains; χ's are the changes of curvature. These strains and changes of curvature, according to Vlasov-Ambartsumyan shell theory, are given in terms of the middle surface displacements by equations (2.2.25) and (2.2.26). For cylindrical shell subjected to axisymmetric loading the displacements are independent of y variable. All the derivatives with respect to y can therefore be dropped leading to the following equations for the middle surface strains and the changes of curvature :

$$\begin{bmatrix} \varepsilon_x^o \\ \varepsilon_y^o \\ \gamma_{xy}^o \end{bmatrix} = \begin{bmatrix} u^o{}_{,x} \\ w^o/R \\ v^o{}_{,x} \end{bmatrix} \qquad (2.4.2)$$

$$\begin{bmatrix} \chi_x \\ \chi_y \\ \chi_{xy} \end{bmatrix} = \begin{bmatrix} - w^o_{,\,xx} \\ - w^o/R^2 \\ + v^o_{,\,x}/R \end{bmatrix} \qquad (2.4.3)$$

where: u^o, v^o and w^o are the middle surface displacements in the x, y and z directions respectively; and (,) denotes partial differentiation.

The resultant forces and moments acting per unit length of the reference surface arc are obtained by integrating the stresses, equation (2.2.17), across the thickness of each layer and then summing over n plies :

$$\begin{bmatrix} N_x \\ N_y \\ N_{xy} \end{bmatrix} = \int_{-h/2}^{h/2} \begin{bmatrix} \sigma_x \\ \sigma_y \\ \tau_{xy} \end{bmatrix} dz \qquad (2.4.4)$$

$$\begin{bmatrix} M_x \\ M_y \\ M_{xy} \end{bmatrix} = \int_{-h/2}^{h/2} \begin{bmatrix} \sigma_x \\ \sigma_y \\ \tau_{xy} \end{bmatrix} z\, dz \qquad (2.4.5)$$

or

$$\begin{bmatrix} N_x \\ N_y \\ N_{xy} \end{bmatrix} = [A] \begin{bmatrix} \varepsilon^o_x \\ \varepsilon^o_y \\ \gamma^o_{xy} \end{bmatrix} + [B] \begin{bmatrix} \chi_x \\ \chi_y \\ \chi_{xy} \end{bmatrix} \qquad (2.4.6)$$

$$\begin{bmatrix} M_x \\ M_y \\ M_{xy} \end{bmatrix} = [B] \begin{bmatrix} \varepsilon_x^o \\ \varepsilon_y^o \\ \gamma_{xy}^o \end{bmatrix} + [D] \begin{bmatrix} \chi_x \\ \chi_y \\ \chi_{xy} \end{bmatrix} \qquad (2.4.7)$$

where :

$$A_{ij} = \int_{-h/2}^{h/2} Q_{ij}\, dz = \sum_{k=1}^{n} Q_{ij}^{(k)} (z_{k+1} - z_k) \qquad (2.4.8)$$

$$B_{ij} = \int_{-h/2}^{h/2} Q_{ij}\, z\, d_z = \frac{1}{2} \sum_{k=1}^{n} Q_{ij}^{(k)} (z_{k+1}^2 - z_k^2) \qquad (2.4.9)$$

$$D_{ij} = \int_{-h/2}^{h/2} Q_{ij}\, z^2\, dz = \frac{1}{3} \sum_{k=1}^{n} Q_{ij}^{(k)} (z_{k+1}^3 - z_k^3) \qquad (2.4.10)$$

To establish the differential equations for the displacements u^o, v^o and w^o which define the deformation of the cylinder one begins with the equations of equilibrium of a shell element cut from the cylinder by two adjacent axial sections and by two adjacent sections perpendicular to the axis of the cylinder, Fig. (2.4.1). The equations of equilibrium were derived by Timoshenko, (Ref. 133), and for thin shell they are :

$$\frac{\partial N_x}{\partial x} + \frac{\partial N_{yx}}{\partial y} = 0$$

$$R\frac{\partial N_y}{\partial y} + R\frac{\partial N_{xy}}{\partial x} + \frac{\partial M_{xy}}{\partial x} + \frac{\partial M_y}{\partial y} = 0 \qquad (2.4.11)$$

$$-N_y + R\frac{\partial^2 M_{yx}}{\partial x \partial y} + R\frac{\partial^2 M_x}{\partial x^2} + R\frac{\partial^2 M_{xy}}{\partial x \partial y} + R\frac{\partial^2 M_y}{\partial y^2} + p.R = 0$$

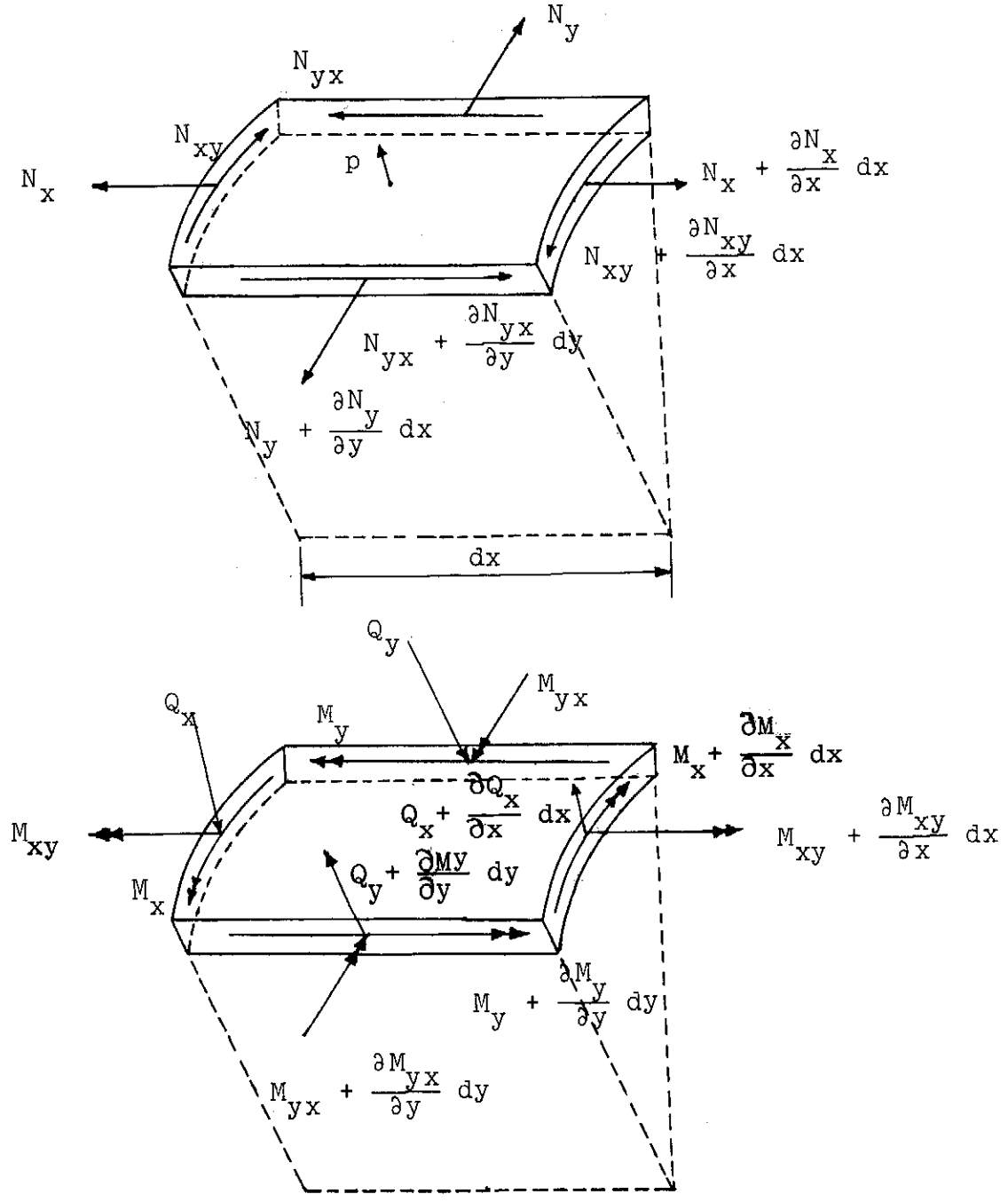

Fig. (2.4.1) Resultant forces and moments on a cylindrical shell element

Here also all the derivitives with respect to y are zero because of the axisymmetric loading condition. The equilibrium equation therefore becomes :

$$N_{x,x} = 0$$

$$(N_{xy} + \frac{1}{R} M_{xy})_{,x} = 0 \qquad (2.4.12)$$

$$M_{x,xx} - \frac{1}{R} N_y + p = 0$$

From equations (2.4.2), (2.4.3), (2.4.6), (2.4.7) and (2.4.12) the differential equations for the displacements u^o, v^o and w^o of laminated composite circular cylindrical shell can be derived. They are :

$$A_{11} u^o_{,xx} + (A_{13} + \frac{1}{R}B_{13}) v^o_{,xx} + (\frac{1}{R}A_{12} - \frac{1}{R^2}B_{12}) w^o_{,x} - B_{11} w^o_{,xxx} = 0 \qquad (2.4.13)$$

$$(A_{31} + \frac{1}{R}B_{31}) u^o_{,xx} + (A_{33} + \frac{2}{R}B_{33} + \frac{1}{R^2}D_{33}) v^o_{,xx} +$$

$$(\frac{1}{R}A_{32} - \frac{1}{R^3}D_{32}) w^o_{,x} - (B_{31} + \frac{1}{R}D_{31}) w^o_{,xxx} = 0 \qquad (2.4.14)$$

$$-B_{11} u^o_{,xxx} + \frac{1}{R}A_{21} u^o_{,x} - (B_{13} + \frac{1}{R}D_{13}) v^o_{,xxx} +$$

$$(\frac{1}{R}A_{23} + \frac{1}{R^2}B_{23}) v^o_{,x} + D_{11} w^o_{,xxxx}$$

$$- (\frac{1}{R}B_{12} + \frac{1}{R}B_{21} - \frac{1}{R^2}D_{12}) w^o_{,xx} + (\frac{1}{R^2}A_{22} - \frac{1}{R^3}B_{22}) w^o = p \qquad (2.4.15)$$

2.4.4 Solution of the Differential Equations

To solve the differential equations (2.4.13), (2.4.14) and (2.4.15) the variables are first uncoupled. From equation (2.4.13) :

$$u^{o}_{,xx} = a\, v^{o}_{,xx} + b\, w^{o}_{,x} + d\, w^{o}_{,xxx} \qquad (2.4.16)$$

where :

$$a = -\frac{1}{A_{11}}\left(A_{13} + \frac{1}{R} B_{13}\right)$$

$$b = -\frac{1}{A_{11}}\left(\frac{1}{R} A_{12} - \frac{1}{R^2} B_{12}\right) \qquad (2.4.17)$$

$$d = \frac{B_{11}}{A_{11}}$$

when the value of $u^{o}_{,xx}$ from equation (2.4.16) is substituted in equation (2.4.14) the value of $v^{o}_{,xx}$ is obtained :

$$v^{o}_{,xx} = e\, w^{o}_{,x} + f\, w^{o}_{,xxx} \qquad (2.4.18)$$

where :

$$e = -\frac{\frac{A_{32}}{R} - \frac{D_{32}}{R^3} - \frac{1}{A_{11}}\left(A_{31} + \frac{B_{31}}{R}\right)\left(\frac{A_{12}}{R} - \frac{B_{12}}{R^2}\right)}{A_{33} + \frac{2}{R} B_{33} + \frac{1}{R^2} D_{33} - \frac{1}{A_{11}}\left(A_{31} + \frac{B_{31}}{R}\right)\left(A_{13} + \frac{B_{13}}{R}\right)}$$

$$f = -\frac{B_{11}\left(A_{31} + \frac{B_{31}}{R}\right)/A_{11} - \left(B_{31} + \frac{D_{31}}{R}\right)}{A_{33} + \frac{2}{R} B_{33} + \frac{1}{R^2} D_{33} - \frac{1}{A_{11}}\left(A_{31} + \frac{B_{31}}{R}\right)\left(A_{13} + \frac{B_{13}}{R}\right)} \qquad (2.4.19)$$

then equation (2.4.16) becomes :

$$u^{o}_{,xx} = (ae + b)\, w^{o}_{,x} + (af + d)\, w^{o}_{,xxx} \qquad (2.4.20)$$

From equations (2.4.18) and (2.4.20) :

$$u^{o}_{,x} = (ae + b)\, w^{o} + (af + d)\, w^{o}_{,xx} + K_1$$

$$u^{o} = (ae + b) \int w^{o}\, dx + (af + d)\, w^{o}_{,x} + K_1 x + K_3$$

$$u^{o}_{,xxx} = (ae + b)\, w^{o}_{,xx} + (af + d)\, w^{o}_{,xxxx}$$

(2.4.21)

$$v^{o}_{,x} = e\, w^{o} + f\, w^{o}_{,xx} + K_2$$

$$v^{o} = e \int w^{o}\, dx + f\, w^{o}_{,x} + K_2\, x + K_4 \qquad (2.4.22)$$

$$v^{o}_{,xxx} = e\, w^{o}_{,xx} + f\, w^{o}_{,xxxx}$$

where:

K_1, K_2, K_3 and K_4 are integration constants.

Thus, equation (2.4.15) becomes :

$$g\, w^{o}_{,xxxx} + h\, w^{o}_{,xx} + q\, w^{o} = p - \frac{A_{21}}{R} K_1 - \left(\frac{A_{23}}{R} + \frac{B_{23}}{R^2}\right) K_2$$

(2.4.23)

where:

$$g = D_{11} - B_{11}(af + d) - f\left(B_{13} + \frac{D_{13}}{R}\right)$$

$$h = \frac{A_{21}}{R}(af + d) + f\left(\frac{A_{23}}{R} + \frac{B_{23}}{R^2}\right) - e\left(B_{13} + \frac{D_{13}}{R}\right) - B_{11}(ae + b) - \left(\frac{B_{12}}{R} + \frac{B_{21}}{R} - \frac{D_{12}}{R^2}\right)$$

$$q = \frac{A_{21}}{R}(ae + b) + e\left(\frac{A_{23}}{R} + \frac{B_{23}}{R^2}\right) + \left(\frac{A_{22}}{R^2} - \frac{B_{22}}{R^3}\right)$$

(2.4.24)

Equation (2.4.23) is a non-homogeneous fourth-order linear differential equation with constant coefficients. Its solution is, (Ref. 134) :

$$w^o = w_h^o + w_p^o \qquad (2.4.25)$$

where :

w_h^o is the solution of the corresponding homogeneous equation; and

w_p^o is any particular solution of the non-homogeneous equation.

The particular solution, using the undetermined coefficients method, is :

$$w_p^o = P + r K_1 + s K_2 \qquad (2.4.26)$$

where :

$$P = \frac{p}{q}$$

$$r = -\frac{A_{21}}{Rq} \qquad (2.4.27)$$

$$s = \frac{1}{q}\left(\frac{B_{23}}{R} + \frac{A_{23}}{R}\right)$$

The solution of the corresponding homogeneous equation is :

$$w_h^o = e^{mx} \tag{2.4.28}$$

where m is the root of the auxiliary polynomial :

$$g\, m^4 + h\, m^2 + q = 0 \tag{2.4.29}$$

To obtain the roots of this polynomial let $m^2 = n$, then :

$$g\, n^2 + h\, n + q = 0 \tag{2.4.30}$$

$$n = \frac{-h \pm \sqrt{h^2 - 4gq}}{2g} = \gamma \pm i\lambda \tag{2.4.31}$$

thus :

$$m = \pm \sqrt{\gamma \pm i\lambda} \tag{2.4.32}$$

or

$$m = \pm (\alpha \pm i\beta) \tag{2.4.33}$$

where :

$$(\alpha \pm i\beta) = \sqrt{\gamma \pm i\lambda} \tag{2.4.34}$$

The solution (2.4.28) becomes in its general form as follows:

$$w_h^o = e^{\alpha x} (C_1 \cos \beta x + C_2 \sin \beta x) + e^{-\alpha x}(C_3 \cos \beta x + C_4 \sin \beta x) \tag{2.4.35}$$

where : C_1, C_2, C_3 and C_4 are constants.

However, when a relatively long cylinder is considered the boundary conditions at one end do not affect the boundary conditions at the other end. In the middle of the long cylinder there exist a region of steady state where the deflection w^o equals the value w_p^o, i.e. w_h^o must vanish. This can be satisfied if the term $e^{\alpha x}$ disappears from the solution (2.4.35), i.e. for long cylinder the solution (2.4.35) becomes:

$$w_h^o = e^{-\alpha x} (C_3 \cos \beta x + C_4 \sin \beta x) \qquad (2.4.36)$$

2.4.5 Finite Element Technique for the Design of Test Specimens

The preceding theory is now to be used in designing the test specimens. The test specimen, Fig. (2.1.1). is divided into finite segments as shown in Fig. (2.4.2) where only half of the cylinder is considered due to the symmetry. Element (1) represents the parallel part of tube and is taken as long cylindrical element, whereas the rest of the elements are short cylindrical elements. For each short element there are 8 constants to be determined, namely, C_1, C_2, C_3, C_4, K_1, K_2, K_3 and K_4, as it is obvious from equations (2.4.21), (2.4.22) and (2.4.35). For the long element only 6 of these are there, i.e. without C_1 and C_2 as shown in equation (2.4.36). Thus, for the example shown in Fig. (2.4.2), there are 46 constants to be determined which require 46 boundary conditions. These conditions are :

1) at point 1, the middle of the tube, both u and v deflections are zero due to the symmetry, i.e.

$$u_1^o = 0$$
$$v_1^o = 0 \qquad (2.4.37)$$

2) at the joint 2-3 the following relationsexist :

$$u_2^o = u_3^o$$
$$v_2^o = v_3^o$$
$$w_2^o = w_3^o \qquad (2.4.38)$$
$$(w^o_{,x})_2 = (w^o_{,x})_3$$
$$(M_x)_2 = (M_x)_3$$

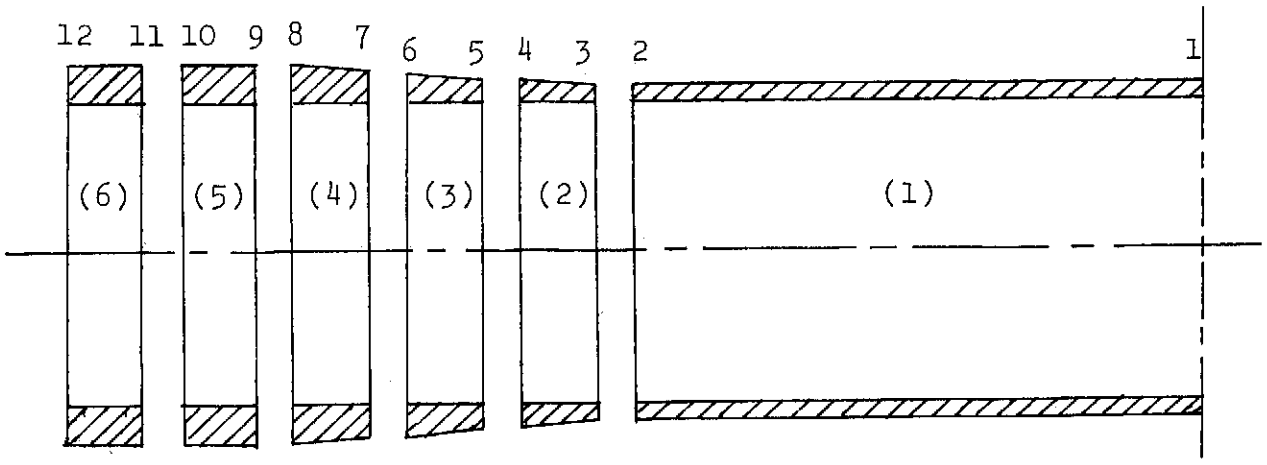

Fig. (2.4.2) The test specimen divided into finite elements.

$$(Q_x)_2 = (Q_x)_3$$

$$(N_x)_2 = (N_x)_3$$

$$(N_{xy} + \frac{1}{R} M_{xy})_2 = (N_{xy} + \frac{1}{R} M_{xy})_3 \qquad (2.4.38)$$

where $(N_{xy} + \frac{1}{R} M_{xy})$ represents the effective shear and Q_x represents the thickness-shearing force :

$$Q_x = M_{x,\,x} \qquad (2.4.39)$$

3) at the joints 4-5, 6-7, 8-9 and 10-11 there exist relations similar to those of equations (2.4.38).

4) at point 12 there are five different possibilities according to the clamping conditions :

   a) for completely free ends (case of internal pressure only) :

$$(M_x)_{12} = (Q_x)_{12} = (N_x)_{12} = (N_{xy} + \frac{1}{R} M_{xy})_{12} = 0 \qquad (2.4.40)$$

b) for completely clamped ends without axial or torsional loadings :

$$w^{o}_{12} = (w^{o}_{,x})_{12} = u^{o}_{12} = v^{o}_{12} = 0 \qquad (2.4.41)$$

c) for clamped ends with axial load only :

$$w^{o}_{12} = (w^{o}_{,x})_{12} = v_{12} = 0$$

$$(N_x)_{12} = \frac{P_x + \pi R^2 p}{2\pi R} \qquad (2.4.42)$$

d) for clamped ends with torsional load only :

$$w^{o}_{12} = (w^{o}_{,x})_{12} = u_{12} = 0$$

$$(N_{xy} + \frac{1}{R} M_{xy})_{12} = \frac{T}{2\pi R^2} \qquad (2.4.43)$$

e) for clamped ends with axial and torsional loads :

$$w^{o}_{12} = (w^{o}_{,x})_{12} = 0$$

$$(N_x)_{12} = \frac{P_x + 2\pi R^2 p}{2\pi R} \qquad (2.4.44)$$

$$(N_{xy} + \frac{1}{R} M_{xy})_{12} = \frac{T}{2\pi R^2}$$

where P_x, p and T are the axial load, the internal pressure and the torque respectively.

The above conditions give 46 equations to determine the 46 unknowns. In matrix form they can be written as :

$$[P]\,[K] = [R] \qquad (2.4.45)$$

where :

$[K]$ is a column matrix representing the constants;

$[P]$ is a square matrix representing the coefficients of the equations; and

$[R]$ is a column matrix representing the coefficients which are independents of the unknowns, (i.e. the right hand sides of the equations).

The unknowns are then given by :

$$[K] = [P]^{-1}\,[R] \qquad (2.4.46)$$

To establish the matrix $[P]$, the parameters u^o, v^o etc., must be written in terms of the constants C_1, C_2, etc.

For the general case of short cylinder the following equations can be obtained (see Appendix D) :

$$w^o = e^{\alpha x}\cos\beta x\, C_1 + e^{\alpha x}\sin\beta x\, C_2 + e^{-\alpha x}\cos\beta x\, C_3 + e^{-\alpha x}\sin\beta x\, C_4 + r\,K_1 + s\,K_2 + P \qquad (2.4.47)$$

$$w^o_{,x} = e^{\alpha x}(\alpha\cos\beta x - \beta\sin\beta x)\,C_1 + e^{\alpha x}(\beta\cos\beta x + \alpha\sin\beta x)\,C_2 - e^{-\alpha x}(\alpha\cos\beta x + \beta\sin\beta x)C_3 + e^{\alpha x}(\beta\cos\beta x - \alpha\sin\beta x)C_4 \qquad (2.4.48)$$

$$u^{o} = e^{\alpha x}\left[\frac{ae+b}{\alpha^2+\beta^2}(\alpha \cos \beta x+\beta \sin \beta x)+(af+d)(\alpha \cos \beta x-\beta \sin \beta x)\right] C_1$$

$$+e^{\alpha x}\left[\frac{ae+b}{\alpha^2+\beta^2}(-\beta \cos \beta x+\alpha \sin \beta x)+(af+d)(\beta \cos \beta x+\alpha \sin \beta x)\right] C_2$$

$$+e^{-\alpha x}\left[\frac{ae+b}{\alpha^2+\beta^2}(-\alpha \cos \beta x+\beta \sin \beta x)-(af+d)(\alpha \cos \beta x+\beta \sin \beta x)\right] C_3$$

$$+e^{-\alpha x}\left[-\frac{ae+b}{\alpha^2+\beta^2}(\beta \cos \beta x+\alpha \sin \beta x)+(af+d)(\beta \cos \beta x-\alpha \sin \beta x)\right] C_4$$

$$+\left[(ae+b)r + 1\right] \times K_1 + (ae+b)\ s \times K_2 + K_3 + (ae+b) \times P$$

(2.4.49)

$$v^{o} = e^{\alpha x}\left[\frac{e}{\alpha^2+\beta^2}(\alpha \cos \beta x+\beta \sin \beta x)+f(\alpha \cos \beta x-\beta \sin \beta x)\right] C_1$$

$$+e^{\alpha x}\left[\frac{e}{\alpha^2+\beta^2}(-\beta \cos \beta x+\alpha \sin \beta x)+f(\beta \cos \beta x+\alpha \sin \beta x)\right] C_2$$

$$+e^{-\alpha x}\left[\frac{e}{\alpha^2+\beta^2}(-\alpha \cos \beta x+\beta \sin \beta x)-f(\alpha \cos \beta x+\beta \sin \beta x)\right] C_3$$

$$+e^{-\alpha x}\left[-\frac{e}{\alpha^2+\beta^2}(\beta \cos \beta x+\alpha \sin \beta x)+f(\beta \cos \beta x-\alpha \sin \beta x)\right] C_4$$

$$+e\ r \times K_1 + (e\ s +1) \times K_2 + K_4 + e \times P \qquad (2.4.50)$$

$$M_x = e^{\alpha x}\left[t\cos\beta x + t'\{(\alpha^2-\beta^2)\cos\beta x - 2\alpha\beta\sin\beta x\}\right]C_1$$

$$+e^{\alpha x}\left[t\sin\beta x + t'\{2\alpha\beta\cos\beta x + (\alpha^2-\beta^2)\sin\beta x\}\right]C_2$$

$$+e^{-\alpha x}\left[t\cos\beta x + t'\{(\alpha^2-\beta^2)\cos\beta x + 2\alpha\beta\sin\beta x\}\right]C_3$$

$$+e^{-\alpha x}\left[t\sin\beta x + t'\{-2\alpha\beta\cos\beta x + (\alpha^2-\beta^2)\sin\beta x\}\right]C_4$$

$$+(t\,r + B_{11})K_1 + (t\,s + B_{13} + D_{13}/R)K_2 + t\,P \qquad (2.4.51)$$

$$Q_x = e^{\alpha x}\left[t(\alpha\cos\beta x - \beta\sin\beta x) + t'\{(\alpha^3 - 3\alpha\beta^2)\cos\beta x + (-3\alpha^2\beta+\beta^3)\sin\beta x\}\right]C_1$$

$$+e^{\alpha x}\left[t(\beta\cos\beta x + \alpha\sin\beta x) + t'\{(3\alpha^2\beta-\beta^3)\cos\beta x + (\alpha^3-3\alpha\beta^2)\sin\beta x\}\right]C_2$$

$$+e^{-\alpha x}\left[-t(\alpha\cos\beta x + \beta\sin\beta x) + t'\{-(\alpha^3-3\alpha\beta^2)\cos\beta x + (-3\alpha^2+\beta^3)\sin\beta x\}\right]C_3$$

$$+e^{-\alpha x}\left[t(\beta\cos\beta x - \alpha\sin\beta x) + t'\{(3\alpha^2\beta-\beta^3)\cos\beta x - (\alpha^3-3\alpha\beta^2)\sin\beta x\}\right]C_4$$

$$N_x = A_{11}K_1 + \left(A_{13} + \frac{B_{13}}{R}\right)K_2 \qquad (2.4.53)$$

$$N_{xy} + \frac{1}{R} M_{xy} = (A_{31} + \frac{B_{31}}{R}) K_1 + (A_{33} + \frac{2}{R} B_{33} + \frac{1}{R^2} D_{33}) K_2 \qquad (2.4.54)$$

where :

$$t = B_{11}(ae + b) + e (B_{13} + \frac{D_{13}}{R}) + (\frac{B_{12}}{R} - \frac{D_{12}}{R^2})$$

$$t' = B_{11}(af + d) + f (B_{13} + \frac{D_{13}}{R}) - D_{11} \qquad (2.4.55)$$

For the case of long cylinder $C_1 = C_2 = 0$ in all the above equations.

For every element, x is measured from the left, Fig. (2.4.3). Therefore, the values of u^o, v^o, etc., at the different points of Fig. (2.4.2) are obtained by substituting $x = 0$ or $x = \ell$, where ℓ represents the length of the element.

Then, upon substitution in the boundary conditions equations, the matrix [P] is obtained, hence the unknowns K can be calculated from equation (2.4.46).

When the constants of the solutions of the differential equations are obtained the deflections, the moments, the strains and the stresses along the tube can be calculated.

2.4.6 Application of the Theory to the Test Specimens

The preceding theory was used to design the test specimens and their end reinforcements. The results obtained from one of the specimens are shown in Figs. (2.4.4) to (2.4.8). These figures show the extraneous bending stresses which are induced at the unreinforced ends of the tubular specimens and cause premature end failures preventing full characterization of the specimens. The functions in Figs. (2.4.4) to (2.4.8) are given in normalized forms where the deflection, the strains and the stresses are divided by their own values at the test sections, while the bending moment and the shearing force are divided by $p.h^2$ and p.h. respectively. The results were obtained from a computer program developed

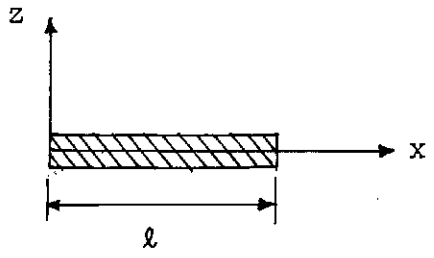

Fig. (2.4.3) Coordinate directions for an element

for this purpose, the details of which are given in Appendix D.

In the experimental investigation, when testing specimens of tube B1 (Appendix A), strain gauges were mounted in the centre of the tube as well as at 50mm from the cntre towards both ends. The strain measurments, Appendix B, showed the uniformity of the strains along the test section.

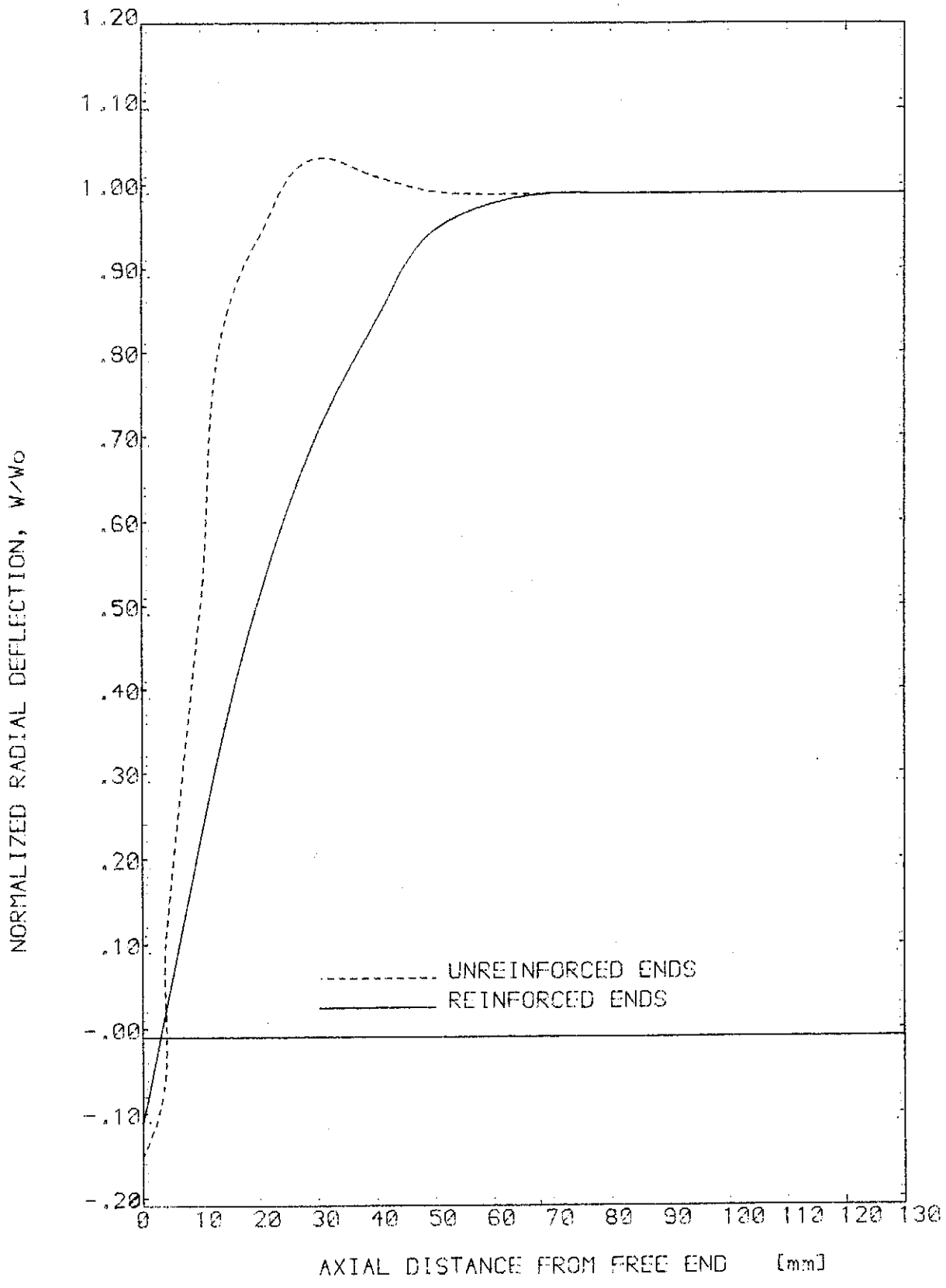

Fig.(2.4.4) RADIAL DEFLECTION DISTRIBUTION OF SPECIMEN 1B3

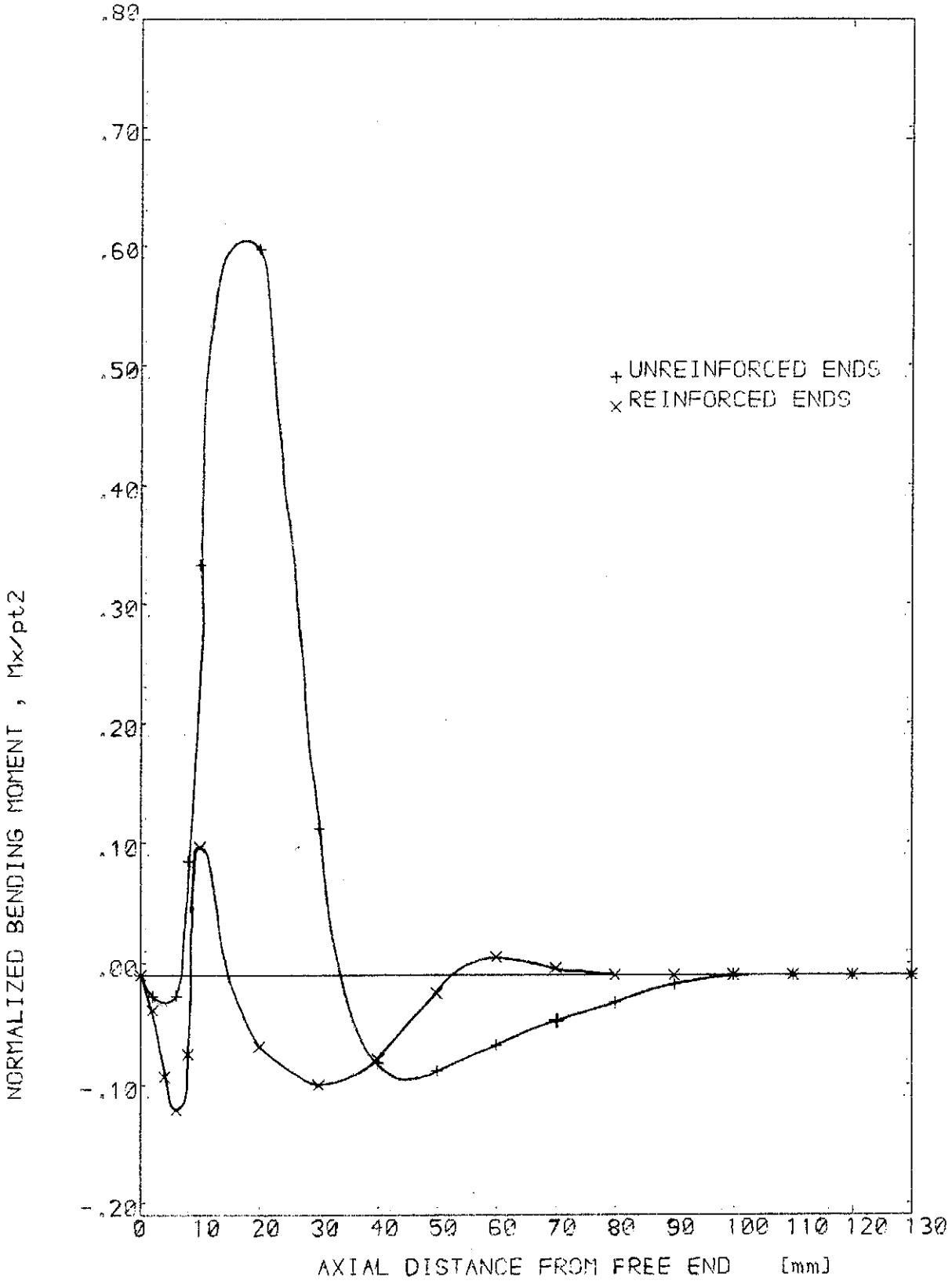

Fig.(2.4.5) BENDING MOMENT DISTRIBUTION OF SPECIMEN 1B3

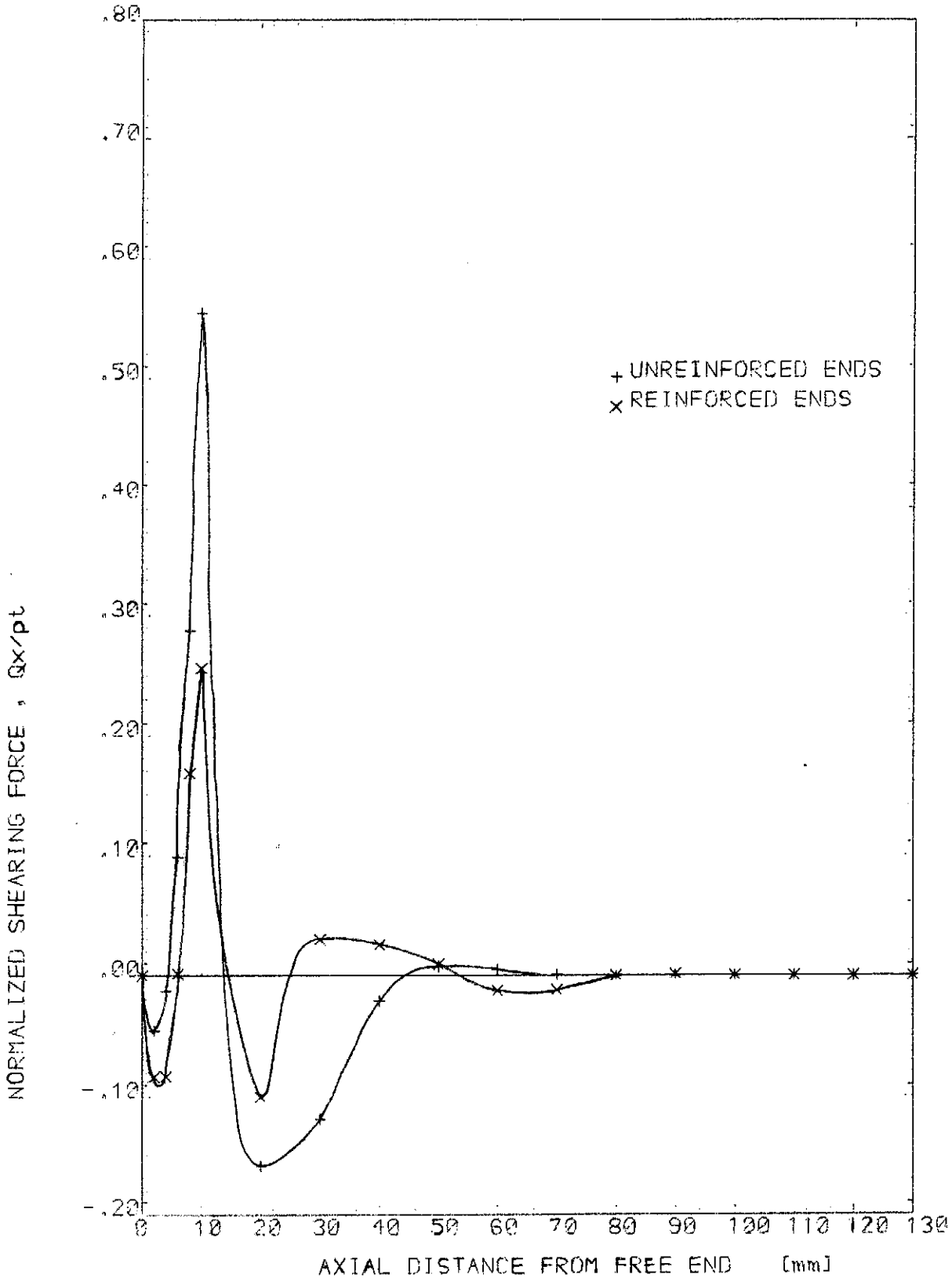

Fig.(2.4.6) SHEAR FORCE DISTRIBUTION OF SPECIMEN 1B3

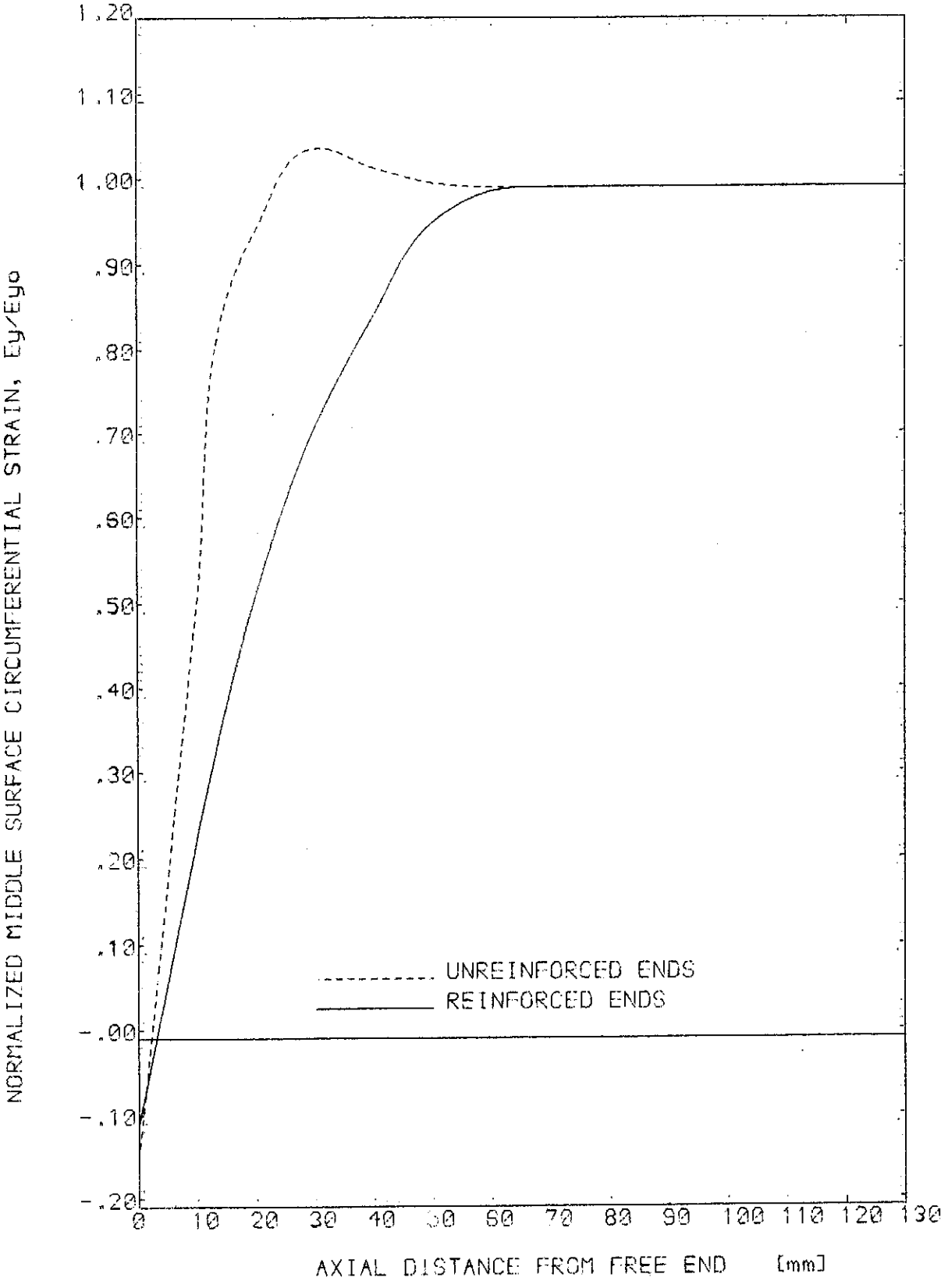

Fig.(2.4.7) CIRCUMFERENTIAL STRAIN DISTRIBUTION OF SPECIMEN 1S3

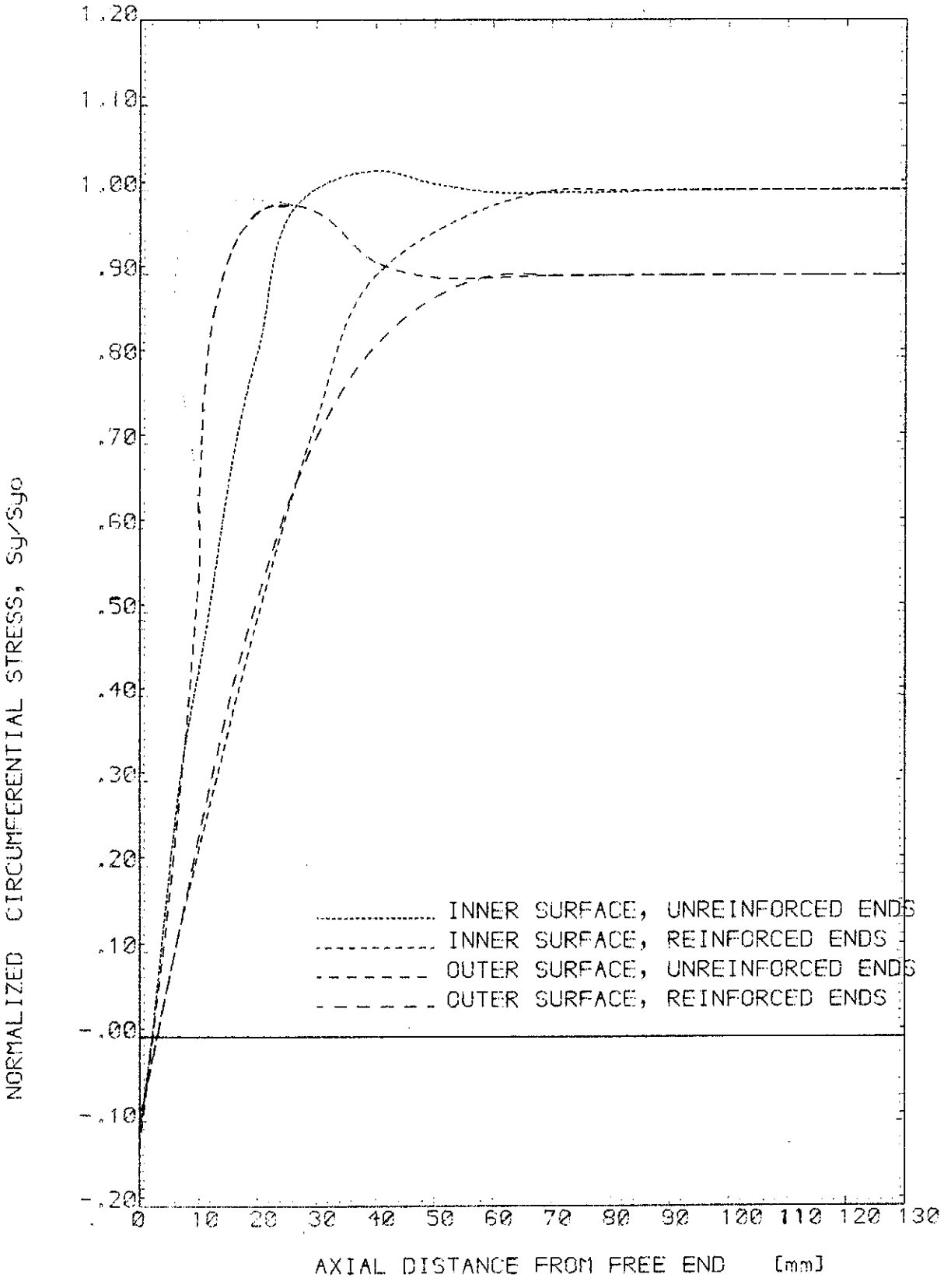

Fig.(2.4.8) CIRCUMFERENTIAL STRESS DISTRIBUTION OF SPECIMEN 1B3

CHAPTER 3

FAILURE ANALYSIS OF LAMINATED COMPOSITE MATERIALS

3.1 INTRODUCTION

Failure of a material is the limit of its load carrying capacity. The failure in this way determines the strength of this material. The strength of a material is an important property in the design of any structure which uses that material. Since it is an expensive task to establish strength characteristics of materials for every complex stress state, the idea of "failure criterion" has been introduced to predict the strength of materials under any loading using data obtained from simple tests. The "failure envelope", which is established from the failure criterion to cover the entire spectrum of loading, is a surface (or curve in the case of two dimensional stresssystem) in the stress space describes the stress states which the material can sustain without failure.

Several failure criteria for composite materials have been proposed. Many of these were developed from the failure theories of homogeneous isotropic materials. These theories for conventional materialswhich define yield or ultimate strengths will be described briefly before the existing failure criteria of composite materials are described.

The results obtained from ultrasonic C-scanning test, acoustic emission test, scanning electron microscope test, and the main experimental investigation, are then used to introduce a "modified failure criterion".

Since the main subject of this Chapter is failure, the instability failure of the tubular test specimens is also studied for completion.

3.2 FAILURE THEORIES OF ISOTROPIC MATERIALS

Before any failure criterion is applied, the applied stresses σ_x, σ_y, σ_z, τ_{xy}, τ_{yz} and τ_{xz} are transformed to the principal stresses σ_1, σ_2 and σ_3 via Mohr's circle.

3.2.1 Tresca Theory (Maximum Shear Stress Theory)

For ductile materials Tresca proposed the following yeild criterion :

$$\max \{\tfrac{1}{2}|\sigma_1 - \sigma_2|, \tfrac{1}{2}|\sigma_2 - \sigma_3|, \tfrac{1}{2}|\sigma_3 - \sigma_1|\} = \tau_y \quad (3.2.1)$$

where $\frac{1}{2}|\sigma_1 - \sigma_2|$ etc. represent the maximum values of the shear stresses, and τ_y is the yield limit in simple shear which is, for ductile material, set equal to the shearing stress at yield in simple tension or compression, i.e.,

$$\tau_y = \tfrac{1}{2}\sigma_y \quad (3.2.2)$$

Thus, equation (3.2.1) becomes :

$$\max \{|\sigma_1 - \sigma_2|, |\sigma_2 - \sigma_3|, |\sigma_3 - \sigma_1|\} = \sigma_y \quad (3.2.3)$$

For the special case of plane stress, this equation becomes :

$$\max \{|\sigma_1 - \sigma_2|, |\sigma_2|, |\sigma_1|\} = \sigma_y \quad (3.2.4)$$

Fig. (3.2.1) shows a graphical representation of equation (3.2.4) compared with other criteria. Any stress state outside the failure envelope represents non-elastic behaviour.

3.2.2. Von Mises-Hencky Theory (Maximum Distorted Energy Theory)

The distorsional energy is that part of the strain energy which remains when the energy due to change of volume is subtracted. In this theory, a ductile material under a general stress state yields when its shear distortional energy reaches the value of the shear distortional energy under simple tension. This gives the following mathematical expression :

$$(\sigma_1 - \sigma_2)^2 + (\sigma_2 - \sigma_3)^2 + (\sigma_3 - \sigma_1)^2 = 2\sigma_y \quad (3.2.5)$$

For plane stress case, equation (3.2.5) becomes :

$$\sigma_1^2 - \sigma_1\sigma_2 + \sigma_2^2 = \sigma_y \quad (3.2.6)$$

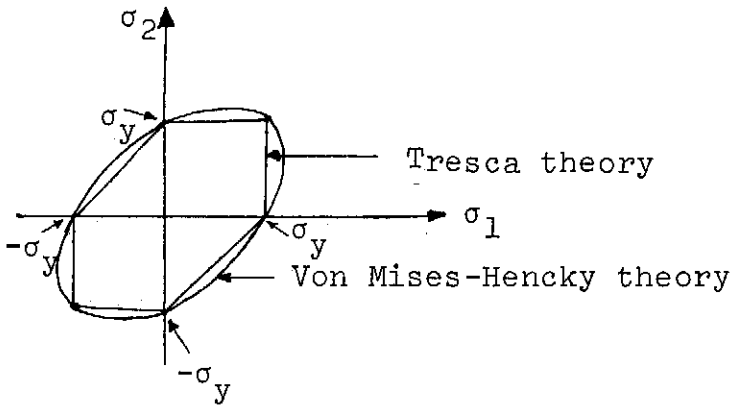

Fig. (3.2.1) Yield criteria for ductile materials

This equation represents an ellipse enclosing the Tresca hexagon, Fig. (3.2.1).

3.2.3 Maximum Normal Stress Theory

In this theory, a brittle material fails when any of the principal stresses reaches the ultimate value, i.e.,

$$\max \{|\sigma_1|, |\sigma_2|, |\sigma_3|\} = \sigma_u \qquad (3.2.7)$$

where σ_u is the ultimate stress in simple tension or compression depending on the sign of the maximum stress. For two-dimensional stress state equation (3.2.7) becomes :

$$\max \{|\sigma_1|, |\sigma_2|\} = \sigma_u \qquad (3.2.8)$$

This equation represents a square which its centre does not necessarily coincide with the origin of the coordinates as most brittle materials have different strengths in tension and compression, Fig. (3.2.2).

3.2.4 Mohr Theory

This theory is similar to that of Tresca but it is used for brittle materials with different strengths in tension and compression. For the plane stress case the equation which defines the failure is :

$$\max \{|\sigma_1|, |\sigma_2|, |\sigma_1 - \frac{(\sigma_u)_c}{(\sigma_u)_t} \sigma_2|\} = \sigma_u \qquad (3.2.9)$$

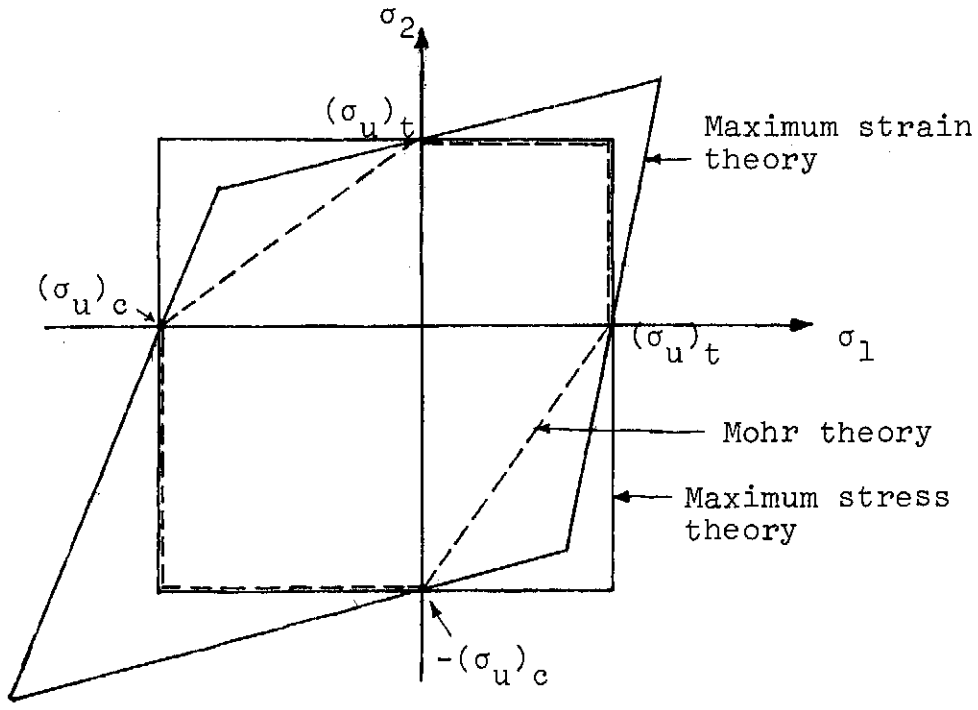

Fig. (3.2.2) Failure criteria for brittle materials

where t denotes tension, c denotes compression, and σ_u in the right hand side is either $(\sigma_u)_t$ or $(\sigma_u)_c$ depending on the sign of the maximum stress, Fig. (3.2.2). When $(\sigma_u)_t = (\sigma_u)_c$ Mohr's strength theory reduces to Tresca theory.

3.2.5 St. Venant Theory (Maximum Principal Strain Theory)

This theory is similar to that of maximum stress theory except that it places a restriction on the maximum normal strains rather than maximum normal stresses. In this theory, a brittle material fails under any stress state when any of the principal strains reaches an ultimate value obtained from simple tests, i.e.,

$$\max \{|\varepsilon_1|, |\varepsilon_2|, |\varepsilon_3|\} = \varepsilon_u \qquad (3.2.10)$$

where ε_u represents ultimate strain.

For plane stress state the following relations exist :

$$\varepsilon_1 = \frac{1}{E}(\sigma_1 - \nu\sigma_2)$$

$$\varepsilon_2 = \frac{1}{E}(\sigma_2 - \nu\sigma_1) \qquad (3.2.11)$$

where ν is Poisson's ratio and E is Young's modulus.

From simple tests :

$$\varepsilon_u = \frac{1}{E}\sigma_u \qquad (3.2.12)$$

Thus, equation (3.2.10) becomes :

$$\max\{|\sigma_1 - \nu\sigma_2|, |\sigma_2 - \nu\sigma_1|\} = \sigma_u \qquad (3.2.13)$$

This equation is shown graphically in Fig. (3.2.2).

3.3 EXISTING FAILURE CRITERIA FOR COMPOSITE MATERIALS

3.3.1 General Considerations

All the existing failure theories are phenomenological (macromechanical) design criteria. The mechanistic (micromechanics) analysis can be used to predict the unidirectional strength properties from the strength properties of the constituent materials. These unidirectional strength properties (i.e. the strength in the fibres direction, the strength in the direction perpendicular to the fibres direction, and the shear strength) can also be obtained experimentally from simple test conditions.

There are two different approaches to predict the laminate strength, namely: the ply-for-ply approach, and the whole laminate approach. In the first approach, the laminate is considered to be consisting of bonded layers. Each layer is considered to be homogeneous and orthotropic. The lamination theory of Sec. 2.2 is used to obtain the stresses and strains in each layer. These stresses and strains are transformed to the layer principal axes before the failure criterion is applied to each lamina. The failure envelope for the laminate is obtained by superimposing the failure envelopes of all the layers and determining the innermost envelope. In the second approach, however, the lamination theory is not needed as the failure criterion is applied directly to the entire laminate which is considered homogeneous but anisotropic. This approach requires the strength characterization of each laminate under consideration, whereas in the first approach the strength characterization is carried out on a layer and then the strength of any laminate under any stress state is predicted. It should be noted here that, due to the different assumptions used in these two different procedures, the criteria derived for one approach are not applicable for the other.

Any failure criterion is established either through empirical approach or mathematical modelling. In the former procedure extensive experimental measurements are made in all components of the stress space. This is, of course, a costly approach both in time and effort in addition to being cumbersome in application. In the second approach the mathematical model reduces the required number of experimental measurements. Some failure criteria, however, are semi-empirical theories.

The lamina failure criteria are either with independent failure modes (e.g. maximum stress criterion) where the onset as well as the mode of failure are predicted, or interaction failure criterion (e.g. Azzi-Tsai criterion) where only the onset of failure is predicted. The interaction failure criteria are basically empirical curve-fitting techniques, and lack sound theoretical basis but they are simple to use.

Most of the failure criteria for composite materials are extension or generalization of the yield or the failure criteria of the isotropic homogeneous materials discussed in Sec. 3.2. In what follows in this section a comprehensive survey of the failure theories of composite materials is given. It should be mentioned here that incomplete surveys for some of these criteria exist, (Refs. 136-145).

For isotropic materials, the failure envelope was presented in the principal stress space (σ_1, σ_2 and σ_3) or (σ_1 and σ_2) in the case of plane stress. In the case of composite materials, however, the situation is different as these principal stresses are of no use even for a unidirectional laminate. The failure envelopes for composite materials is then represented in the laminate six stress component space (σ_x, σ_y, σ_z, τ_{xy}, τ_{yz} and τ_{zx}), or, for a plane stress case, in the three stress component space (σ_x, σ_y and τ_{xy}). For convenience two dimensional failure envelopes will be presented here. These are generated for fixed values of the shearing stress and then projected on the (σ_x, σ_y) plane.

In the failure criteria presented below a unified notation system is used. This implies that the original notations used by the previous investigators may be different from those used here.

3.3.2 Maximum Stress Theory

In this theory, a composite layer fails when any of the stress components in the principal material directions reaches its corresponding strength value as determined from simple unidirectional stress experiments. There is no interaction between the stresses. Failure occurs when any of the following

conditions is not satisfied :

$$-X_c < \sigma_1 < X_t$$

$$-Y_c < \sigma_2 < Y_t \qquad (3.3.1)$$

$$|\tau_{12}| < S$$

where:

X_t is the axial tensile strength;
X_c is the axial compressive strength;
Y_t is the transverse tensile strength;
Y_c is the transverse compressive strength; and
S is the in-plane shear strength (which is independent of the sign of τ_{12}, i.e. it retains the same value for both positive and negative shear stress components).

The failure envelope for a lamina in the (σ_1, σ_2) stress space, as described in the first two of equations (3.3.1), is a rectangular and schematically shown in Fig. (3.3.1) for a particular value of τ_{12} ($|\tau_{12}| < S$). When the lamina loading axes do not coincide with the material axes the failure envelope in the $\sigma_x\sigma_y$ stress space (for a fixed value of τ_{xy}) is represented by six lines given by equations (3.3.1), and the non-failure region is the inmost envelope, Fig. (3.3.2).

3.3.3 Stowell-Liu Theory

This theory, (Ref. 146), is essentially a maximum stress theory but tries to take into account the strength of the constituent materials. In this theory, the failure stress of the fibres is taken as the limiting strength of the lamina in the fibre direction, while the limiting transverse and shear stresses are those of the matrix. Stowell and Liu applied their criterion to only the case of uniaxial lading at any arbitrary angle from the fibre axis.

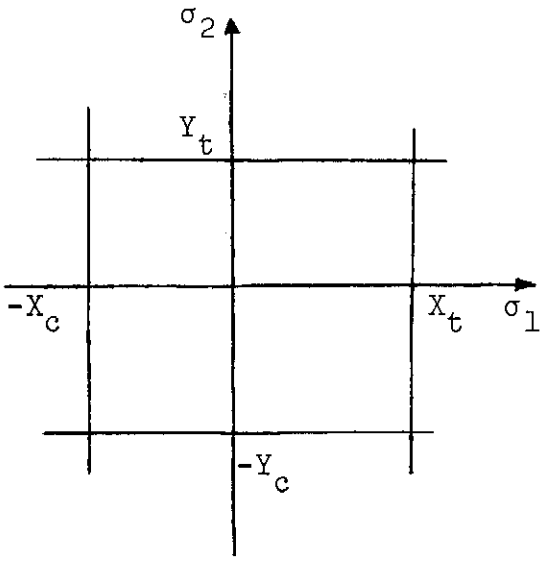

Fig. (3.3.1) Maximum stress criterion in $\sigma_1\sigma_2$ stress space ($\theta = 0^o$)

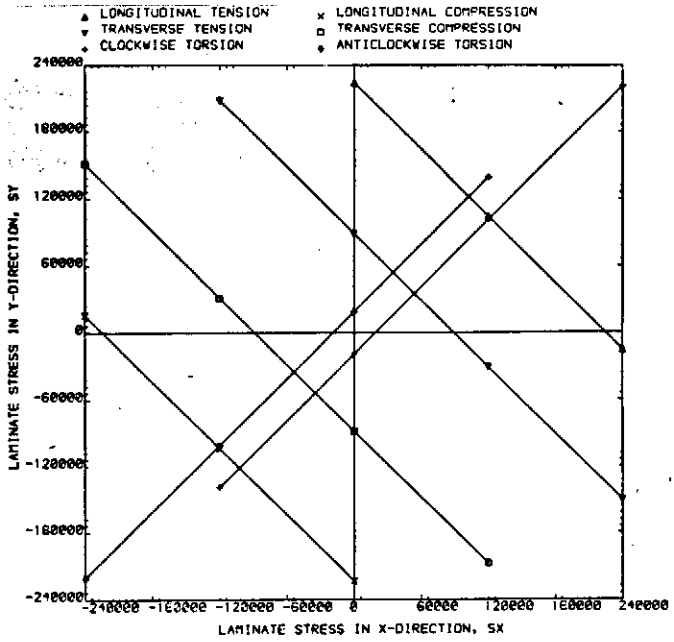

Fig. (3.3.2) Maximum stress criterion in $\sigma_x\sigma_y$ stress space ($\theta = 45^o$)

3.3.4 Kelly-Davies Theory

Kelly and Davies, (Refs. 147-149), have studied the effect of fibre orientation on a fibre reinforced metal with the metal matrix in the plastic form. Their strength theory is similar to that of Stowell-Liu theory except that they allowed for the fibre-matrix interaction, which is ignored by Stowell-Liu theory, by using matrix strengths greater than the ultimate strengths obtained from simple test conditions. The factors used for this purpose are: 1.15 for the matrix tensile strength, and 1.5 for the matrix shear strength.

3.3.5 Prager Theory

This theory, (Ref. 150), is a modification to that of Stowell-Liu theory. It states that the matrix failure in the transverse direction and in shear are not independent of each other but interact. Accordingly, Prager derives the failure loads of a unidirectional laminate under biaxial loading and of angle-ply laminate under uniaxial tension.

3.3.6 Maximum Strain Theory

Failure of a layer by this theory occurs when any one of the strains in the principal material axes reaches its corresponding ultimate strain values as determined from simple unidirectional loading conditions. There is no interaction between the strain components but interaction exists between the stress components due to the Poisson ratio. The following inequalities determine the unfailed regions :

$$-\varepsilon_{1c} < \varepsilon_1 < \varepsilon_{1t}$$

$$-\varepsilon_{2c} < \varepsilon_2 < \varepsilon_{2t} \qquad (3.3.2)$$

$$|\gamma_{12}| < \gamma_u$$

where :

ε_{1t} is the ultimate axial tensile strain;
ε_{1c} is the ultimate axial compressive strain;
ε_{2t} is the ultimate transverse tensile strain;
ε_{2c} is the ultimate transverse compressive strain; and
γ_u is the ultimate in-plane shear strain.

The lamina failure envelope in the space of its principal stresses is a parallelogram (for a fixed value of τ_{12} with $|\gamma_{12}| < \gamma_u$) determined by the first two of equations (3.3.2), Fig. (3.3.3). For a lamina with fibres aligned at an angle from the body axis, the failure envelope is drawn in the $\sigma_x \sigma_y$ stress space and it is determined by the innermost envelope of the six intersecting lines of equations (3.3.2), Fig. (3.3.4). A graphical method to determine the strength envelope in the strain space is described in (Ref.151).

Although this theory have an advantage over the maximum stress theory due to the interaction of the stress components, it exhibits one difficulty in the application that is the definition of the ultimate strains due to the non-linear behaviour.

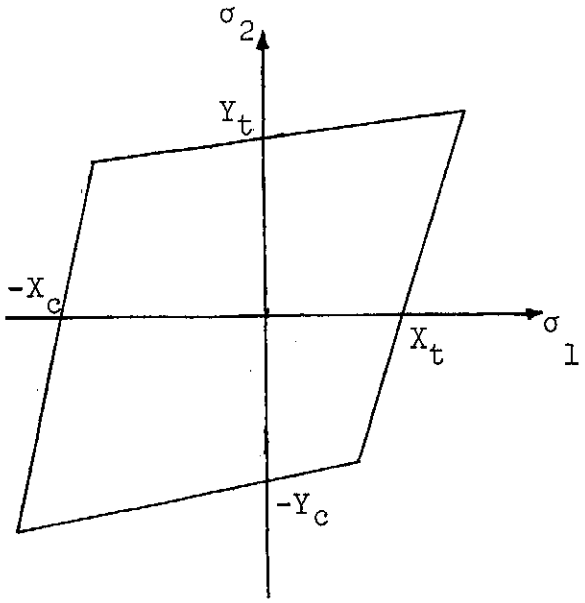

Fig. (3.3.3) Maximum strain criterion in $\sigma_1\sigma_2$ stress space ($\theta = 0^o$)

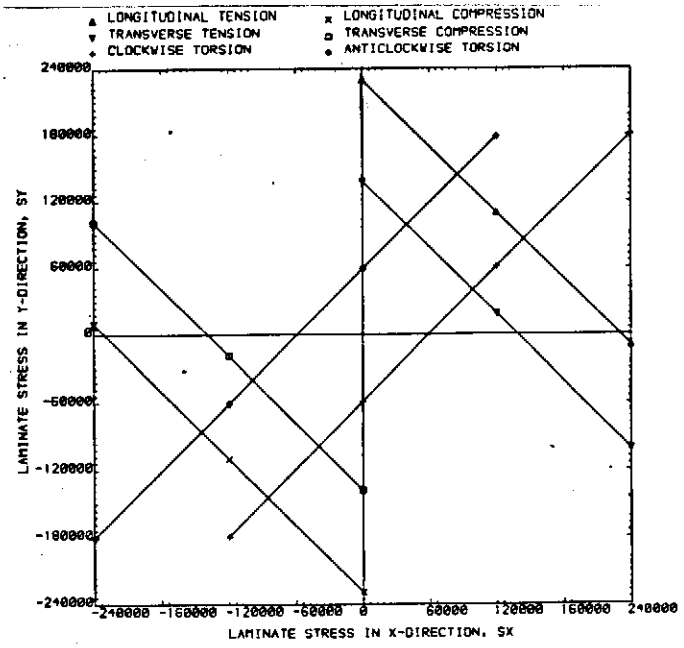

Fig. (3.3.4) Maximum strain criterion in $\sigma_x\sigma_y$ stress space ($\theta = 45^o$)

3.3.7 Maximum Shear Stress Theory

There have been many attempts to generalize Tresca maximum shear stress yield criterion to composite materials, (Refs. 152-155). The most general theory is that of Lance and Robinson, (Ref. 154), which states that a composite material will yield when: (1) the shearing stress on planes parallel to the fibres, and in a direction perpendicular to them; or (2) the shearing stress on the same planes, but in a direction parallel to the fibres; or (3) the maximum shear stress on planes oriented at 45° to the fibre direction; reaches a critical value of stress associated with the failure planes. No interaction between these stresses is considered in this theory. In the state of plane stress the above yielding conditions are given by :

$$\begin{aligned}
\tfrac{1}{2}|(\sigma_x - \sigma_y)\sin 2\theta| &= S_a \\
\tfrac{1}{2}|\sigma_x \cos^2\theta + \sigma_y \cos^2\theta| &= S_t \\
\tfrac{1}{2}|\sigma_x \cos^2\theta + \sigma_y \sin^2\theta| &= S_s \\
\tfrac{1}{2}|(\sigma_x - \sigma_y)\cos 2\theta| &= S_s
\end{aligned} \qquad (3.3.3)$$

where :

σ_x and σ_y are the stresses in x and y directions.

Θ is the fibre angle with x-axis.

S_a, S_t and S_s are the critical values of the shear stresses associated with the above mentioned planes.

3.3.8 Hill Theory

This theory is a generalization of Von Mises-Hencky maximum distortional energy theory to include anisotropic materials. It was proposed by Hill, (Ref. 156), and its critical equation is given by :

$$(G + H)\,\sigma_1^2 + (F + H)\,\sigma_2^2 + (F + G)\,\sigma_3^2 - 2H\,\sigma_1\sigma_2 - 2G\,\sigma_1\sigma_3 - 2F\,\sigma_2\sigma_3 + 2L\,\tau_{23}^2 + 2M\,\tau_{13}^2 + 2N\,\tau_{12}^2 = 1 \qquad (3.3.4)$$

where F, G, H, L, M and N are constants characteristic of the material and can be regarded as failure strengths as they, from the failure of simple loading conditions, can be written as :

$$2H = \frac{1}{X^2} + \frac{1}{Y^2} - \frac{1}{Z^2}$$

$$2G = \frac{1}{X^2} + \frac{1}{Z^2} - \frac{1}{Y^2} \qquad (3.3.5)$$

$$2F = \frac{1}{Y^2} + \frac{1}{Z^2} - \frac{1}{X^2}$$

$$2L = \frac{1}{R^2}$$

$$2M = \frac{1}{S^2} \qquad (3.3.6)$$

$$2N = \frac{1}{T^2}$$

Where X, Y and Z are the strengths in the directions 1, 2 and 3 respectively; and R, S and T are the shear strengths in the principal planes of orthotropy.

For the plane stress case, equation (3.3.4) becomes :

$$\frac{\sigma_1^2}{X^2} + \frac{\sigma_2^2}{Y^2} - \left(\frac{1}{X^2} + \frac{1}{Y^2} - \frac{1}{Z^2}\right)\sigma_1\sigma_2 + \frac{\tau_{12}^2}{S^2} = 1 \qquad (3.3.7)$$

Unlike all the previously discussed criteria, this theory considers "interaction" between the failure strengths, whereas in the preceding theories, failures in different modes are presumed to occur independently.

This results in a smooth failure envelope rather than the intersecting straight lines obtained before.

One disadvantage for this criterion is that it does not consider different strengths for the tensile and compressive modes, i.e. the material has to exhibit the same strength in tension and compression. Another disadvantage is that the mode of failure is not predicted, only the onset to failure is.

3.3.9 Azzi-Tsai Theory

This is a modified Hill criterion where Azzi and Tsai, (Refs. 157-159), assumed the lamina to be transversely isotropic (i.e. Y = Z) to obtain the following equation for the failure envelope :

$$\frac{\sigma_1^2}{X^2} - \frac{\sigma_1\sigma_2}{X^2} + \frac{\sigma_2^2}{Y^2} + \frac{\tau_{12}^2}{S^2} = 1 \qquad (3.3.8)$$

Furthermore, Tsai et al, (Ref. 25), state this criterion remains applicable for materials with properties different in tension and compression. It is only necessary to use the principal strengths compatible with the prevailing stress components, i.e. tensile strength for positive normal stress and compressive strength for negative normal stress. The failure envelope is, therefore, piecewise continuous in the stress space.

When a failure occurs in a lamina, i.e. the stress state reaches the failure surface, the mode of failure is then determined by simple comparison between the stress components and their corresponding strengths.

For the three dimensional stress state, Tsai, (Ref. 34), presents another two equations, similar to equation (3.3.8), for the other two planes using the appropriate strengths.

Because of its simplicity, this theory is recommended or used by many authors for quick design checks, (e.g. Refs. 160-164).

3.3.10 Marin Theory

This theory is also a generalization of the Von Mises-Hencky theory to account for the difference in tensile and compressive yield strengths and the variation of strength with direction. Marin, (Ref. 165), limited his theory to principal stresses. This is an advantage in the case of isotropic material as it eliminates the shear from the analysis. For anisotropic materials, however, the concept of principal stresses is of no use as the mechanical properties depend on the direction of the applied load, and axes of principal stress are not always coincident with axes of principal strain.

The mathematical form for Marin's strength criterion is :

$$(\sigma_1 - a)^2 + (\sigma_2 - b)^2 + (\sigma_3 - c)^2 +$$

$$q\,[(\sigma_1 - a)(\sigma_2 - b) + (\sigma_2 - b)(\sigma_3 - c) + (\sigma_3 - c)(\sigma_1 - a)]$$

$$= \sigma^2 \qquad (3.3.9)$$

Where a, b, c, q and σ can be found from various stress states, and σ_1, σ_2 and σ_3 are the principal stresses.

Topping, (Ref. 166), states that this criterion is not only questionable but untenable, whereas Coleman, (Ref. 167), states that Topping's comments have helped in determining the restrictions on the constant q, but did not make equation (3.3.9) untenable for some cases. He, therefore, suggests that the theory should be compared with test results before any final judgement can be made.

For the case of plane stress the failure envelope is given by :

$$\sigma_1^2 + K_1\,\sigma_1\sigma_2 + \sigma_2^2 + K_2\,\sigma_1 + K_3\,\sigma_2 = K_4 \qquad (3.3.10)$$

where the K's are experimentally determined constants, and, in terms of the strengths, they are given by :

$$K_1 = 2 - \frac{X_t X_c - S\left[X_c - X_t - X_c\,(X_t/Y_t) + Y_t\right]}{S^2}$$

$$K_2 = X_c - X_t$$

$$K_3 = X_c\,(X_t/Y_t) - Y_t \qquad (3.3.11)$$

$$K_4 = X_T X_c$$

Equation (3.3.10) represents a smooth curve in the principal stress state.

3.3.11 Franklin Theory

Franklin, (Ref. 137), has modified Marin's criterion to overcome its shortcoming of using principal stress concept. Moreover, Franklin includes a biaxial stress condition in each quadrant such that the failure surface must pass through three points in each quadrant instead of two at its endpoints. These modifications result in the following formula :

$$K_1\sigma_1^2 + K_2\,\sigma_1\sigma_2 + K_3\,\sigma_2^2 + K_4\,\sigma_1 + K_5\,\sigma_2 + K_6\,\tau_{12}^2 = 1 \qquad (3.3.12)$$

The constants K_1 and K_4 are evaluated from uniaxial loading to failure in 1-direction, (i.e. $\sigma_1 = X_t$ and $\sigma_1 = -X_c$), the constants K_3 and K_5 from $\sigma_2 = Y_t$ and $\sigma_2 = -Y_c$, and the constants K_6 from $\tau_{12} = S$. The constants K_2 is allowed to exist as a "floating constant" to be determined from a biaxial stress failure condition.

Although this criterion seems more accurate than other criteria due to the floating constant which allows the failure envelope to have different shapes in each quadrant, it has the disadvantage of requiring four biaxial test data to determine the four different values of this floating constant in the four quadrants.

3.3.12 Stassi-D'Alia Theory

Stassi-D'Alia, (Ref. 168), proposed the following relation for the case of biaxial principal stresses aligned with the material symmetry axes :

$$\sigma_1^2 + \sigma_2^2 - \sigma_1\sigma_2 + X_t\,(X_c/X_t - 1)(\sigma_1 + \sigma_2) = X_c \qquad (3.3.13)$$

It is assumed here that the shear strength is a function of X_t and $Y_c/Y_t = X_c/X_t$. Unfortunately, composite materials do not generally satisfy these two assumptions.

3.3.13 Norris Theory

Norris and McKinnon, (Ref. 169), proposed the following interaction empirical strength formula :

$$\frac{\sigma_1^2}{X^2} + \frac{\sigma_2^2}{Y^2} + \frac{\tau_{12}^2}{S^2} = 1 \qquad (3.3.14)$$

Later, Norris, (Ref. 170), presented a strength theory, which is a generalization of Von Mises-Hencky distortional energy theory, and given by the following set of equations, one for each plane :

$$\begin{aligned}
&\frac{\sigma_1^2}{X^2} - \frac{\sigma_1\sigma_2}{XY} + \frac{\sigma_2^2}{Y^2} + \frac{\tau_{12}^2}{S^2} = 1 \\
&\frac{\sigma_2^2}{Y^2} - \frac{\sigma_2\sigma_3}{YZ} + \frac{\sigma_3^2}{Z} + \frac{\tau_{23}^2}{T^2} = 1 \qquad (3.3.15) \\
&\frac{\sigma_3^2}{Z^2} - \frac{\sigma_3\sigma_1}{ZX} + \frac{\sigma_1^2}{X^2} + \frac{\tau_{31}^2}{R^2} = 1
\end{aligned}$$

where the strengths X, Y and Z are either tensile or compressive strengths according to the signs of the stresses σ_1, σ_2 and σ_3.

For the case of plane stress state, equations (3.3.15) become :

$$\frac{\sigma_1^2}{X^2} - \frac{\sigma_1\sigma_2}{XY} + \frac{\sigma_2^2}{Y^2} + \frac{\tau_{12}^2}{S^2} = 1$$

$$\frac{\sigma_2^2}{Y^2} = 1 \qquad (3.3.16)$$

$$\frac{\sigma_1^2}{X^2} = 1$$

3.3.14 Fischer Theory

The Fischer criterion, (Ref. 171), is a modification of Norris criterion. The idea is to include different elastic constants in the failure envelope formula which is :

$$\frac{\sigma_1^2}{X^2} + \frac{\sigma_2^2}{Y^2} + \frac{\tau_{12}^2}{S^2} - K\frac{\sigma_1\sigma_2}{XY} = 1 \qquad (3.3.17)$$

where :

$$K = \frac{E_1\,(1 + \nu_{21}) + E_2\,(1 + \nu_{12})}{2\sqrt{E_1E_2\,(1 + \nu_{12})(1 + \nu_{21})}} \qquad (3.3.18)$$

3.3.15 Yamada-Sun Theory

Yamada and Sun, (Ref. 172), proposed a failure criterion of the form :

$$\frac{\sigma_1^2}{X^2} + \frac{\tau_{12}^2}{S^2} = 1 \qquad (3.3.19)$$

They used this criterion in their statistical analysis to investigate the probabilistic nature of composite faiure. The criterion could be regarded as a degenerated form of many of the preceding criteria.

Yamada and Sun conclude that their proposed equation was proved simple and effective in predicting failure in both deterministic and probabilistic sense.

3.3.16 Griffith-Baldwin Theory

This theory, (Ref. 173), is an extension of the distortional energy theory. Griffith and Baldwin calculated the distortional energy, U_d, by subtracting the volumetric strain energy from the total strain energy. For the case of plane stress state, U_d is given by :

$$U_d = \frac{\sigma_1^2}{3}\left(S_{11} - \frac{S_{12} + S_{13}}{2}\right) + \frac{\sigma_2^2}{3}\left(S_{22} - \frac{S_{12} + S_{23}}{2}\right) + \frac{\sigma_1\sigma_2}{3}\left(2S_{12} - \frac{S_{11} + S_{22} + S_{13} + S_{23}}{2}\right) + S_{66}\tau_{12}^2 \qquad (3.3.20)$$

where: $[S]$ is the compliance matrix.

Failure (yield or fracture) occurs when U_d is equal to its critical value U_c which is obtained by a single uniaxial test.

3.3.17 Chamis Theory

Chamis theory, (Ref. 174, 175), is also an extension of the distortional energy theory but it accounts for fabrication variables such as filament and void content and distribution, fibre-matrix bonding, residual stresses, etc. The criterion is expressed as :

$$\frac{\sigma_1^2}{X^2} + \frac{\sigma_2^2}{Y^2} + \frac{\tau_{12}^2}{S^2} - KK' \frac{\sigma_1\sigma_2}{XY} = 1 \qquad (3.3.21)$$

This criterion is similar to that of Fischer, equation (3.3.17), except that the coefficient K there is replaced here by a product of two coefficients KK'. The coefficient K is derived here as :

$$K = \frac{(1 + 4\nu_{12} - \nu_{13})\, E_2 + (1 - \nu_{23})\, E_1}{[E_1 E_2 (2 + \nu_{12} + \nu_{13})(2 + \nu_{21} + \nu_{23})]^{1/2}} \qquad (3.3.22)$$

whereas the coefficient K' is a theory-experiment correlation coefficient and it accounts for different tensile and compressive strengths and for variable interaction between stresses. K' takes different value in each stress quadrant in order that calculated and experimental results are in good agreement. Thus, the failure envelope consists of four different curves, one curve for each quadrant in the $\sigma_1\sigma_2$ stress space.

The strength X and Y can take the values X_t or X_c and Y_t or Y_c to be consistent with the stresses σ_1 and σ_2.

3.3.18 Hoffman Theory

Hoffman, (Ref. 176), has generalized Hill theory to account for different strengths in tension and compression. The failure envelope is described by :

$$K_1 (\sigma_2 - \sigma_3)^2 + K_2 (\sigma_3 - \sigma_1)^2 + K_3 (\sigma_1 - \sigma_2)^2 + K_4 \sigma_1 +$$

$$K_5 \sigma_2 + K_6 \sigma_3 + K_7 \tau_{23}^2 + K_8 \tau_{31}^2 + K_9 \tau_{12}^2 = 1 \qquad (3.3.23)$$

where the nine coefficients $K_1, \ldots, K_9$ are uniquely determined by nine basic strength data, namely: the three uniaxial tensile strengths, the three uniaxial compressive strengths, and the three pure shear strengths. The following expressions are obtained :

$$K_1 = \frac{1}{2}\left(\frac{1}{Y_t Y_c} + \frac{1}{Z_t Z_c} - \frac{1}{X_T X_c}\right)$$

$$K_2 = \frac{1}{2}\left(\frac{1}{Z_t Z_c} + \frac{1}{X_t X_c} - \frac{1}{Y_t Y_c}\right)$$

$$K_3 = \frac{1}{2}\left(\frac{1}{X_t X_c} + \frac{1}{Y_t Y_c} - \frac{1}{Z_t Z_c}\right)$$

$$K_4 = \frac{1}{X_t} - \frac{1}{X_c}$$

$$K_5 = \frac{1}{Y_t} - \frac{1}{Y_c}$$

$$K_6 = \frac{1}{Z_t} - \frac{1}{Z_c}$$

$$K_7 = \frac{1}{T^2}, \quad K_8 = \frac{1}{R^2}, \quad K_9 = \frac{1}{S^2} \qquad (3.3.24)$$

For transversely isotropic lamina in the plane stress state, the criterion becomes :

$$\frac{\sigma_1^2 - \sigma_1 \sigma_2}{X_t X_c} + \frac{\sigma_2^2}{Y_t Y_c} + \frac{X_c - X_t}{X_t X_c} \sigma_1 + \frac{Y_c - Y_t}{Y_t Y_c} \sigma_2 + \frac{\tau_{12}^2}{S^2} = 1$$

(3.3.25)

This equation is, in fact, a special case of Franklin criterion as, if $K_2 = 1$ in equation (3.3.12), one obtains equation (3.3.25).

3.3.19 Puck-Schneider Theory

In the work of Puck and Schneider the strengths of the constituent materials are taken into account, though interaction formulae are used. Three types of failure are consisered, namely: the fracture of the fibre, the yield of the matrix, and the adhesive failure of the interface, (Refs. 177-180). The following set of equations represent these three failure :

$$\frac{\sigma_1}{X_f} = 1$$

$$\frac{\sigma_1^2}{X_m^2} + \frac{\sigma_2^2}{Y_m^2} - \frac{1}{3} \frac{\sigma_1 \sigma_2}{X_m Y_m} + \frac{\tau_{12}^2}{S_m} = 1 \qquad (3.3.26)$$

$$\frac{\sigma_2}{Y_i} + \frac{\tau_{12}^2}{S_i^2} = 1$$

where f denotes fibre, m denotes matrix, and i denotes interface.

Hütter et al, (Ref. 144), state that this theory did not give satisfactory results when was applied to multilayer laminates.

Later, Schneider and Bardenheier, (Ref. 203), used the following equation for the matrix failure (for $\sigma_2 > 0$) :

$$\left(\frac{\sigma_2}{Y}\right)^2 + \left(\frac{\tau_{12}}{S}\right)^2 = 1 \qquad (3.3.27)$$

With more data available about the compressive strength, the following equation gives better approximations.

$$\frac{\sigma_2^2}{Y_t Y_c} + \sigma_2 \frac{Y_c - Y_t}{Y_t Y_c} + \frac{\tau_{12}^2}{S^2} = 1 \qquad (3.3.28)$$

Equation (3.3.27) was also used by Liverpool University group, (Ref. 19).

3.3.20 Haga-Hayashi-Kasuya Theory

This theory, (Ref. 182), is restricted to glass fabric reinforced plastics under tension, compression and combined tension-compression loads, Fig. (3.3.5).

If the strengths in L - T coordinate system are: X (in L - direction, tensile or compressive, Y (in T-direction, tensile or compressive), and S (for shear stress τ_{LT}), then the strength (tensile or compressive) in x-direction under uni-axial loading (tensile or compressive) is given by :

$$F_\theta = \frac{XYS}{\sqrt{m^4X^2S^2 + n^4X^2S^2 + m^2n^2X^2Y^2}} \qquad (3.3.29)$$

where : $m = \cos\theta$ and $n = \sin\theta$

For $\theta = 45^\circ$, results obtained by equation (3.3.29) deviate from experimental values, therefore equation (3.3.29) is replaced by :

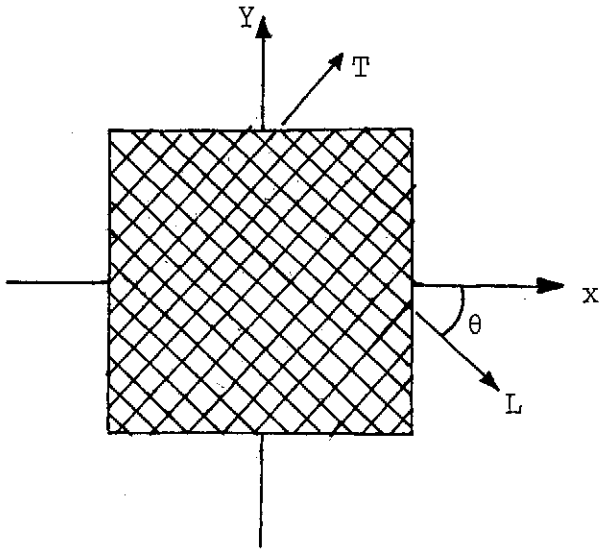

Fig. (3.3.5) Coordinate system for glass fabric reinforced plastic laminates.

$$F_\theta = \frac{1}{\sqrt{(m^2 - n^2)\left(\frac{m^2}{X^2} - \frac{n^2}{Y^2}\right) + \left(\frac{2mn}{F_{45}}\right)^2}} \qquad (3.3.30)$$

where F_{45} is the compressive strength for $\theta = 45^\circ$.

In the case of biaxial loading state for combined tension (in x-direction) and compression (in y-direction) of ratio $\sigma_x/\sigma_y = -\varphi$, failure may occur in any of the following modes :

1) When σ_x or σ_y reaches the appropriate F_θ of equation (3.3.30);

2) When the shear stress τ_{LT} reaches S, i.e. when

$$\sigma_x - \sigma_y = \frac{S}{mn} \qquad (3.3.31)$$

or

3) When any of the combined stresses :

$$\sigma_{eL} = \sqrt{\sigma_L^2 + \tau_{LT}^2} = \sigma_x \sqrt{m^2 + \frac{n^2}{\varphi^2}}$$

or

$$\sigma_{eT} = \sqrt{\sigma_T^2 + \tau_{LT}^2} = \sigma_x \sqrt{n^2 + \frac{m^2}{\varphi^2}} \qquad (3.3.32)$$

reaches the uniaxial strength of equation (3.3.30).

Failure, then, is predicted from the minimum of σ_x values which cause the above failures.

3.3.21 Sandhu Theory

Sandhu has proposed a failure theory based on total strain energies to be used in conjunction with his analysis of non-linear behaviour of composite materials which was discussed in Sec. 2.3.2(d),(Refs. 103, 104). Assuming strain energies as independent parameters, the failure criterion for orthotropic materials is expressed as :

$$\sum_{i=1}^{3} \sum_{j=1}^{3} \left[K_{ij} \int_{\hat{\varepsilon}_{ij}} \sigma_{ij} \, d\, \varepsilon_{ij} \right]^{m_{ij}} = 1 \qquad (3.3.33)$$

where :

$\hat{\varepsilon}_{ij}$ are the current strain components :

m_{ij} are parameters define the shape of the failure surface in the strain-energy space; and

K_{ij} are material characteristics

For the plane stress state and using the notation of this thesis, equation (3.3.33) becomes :

$$K_1 \left[\int_{\hat{\varepsilon}_1} \sigma_1 \, d\, \varepsilon_1 \right]^{m_1} + K_2 \left[\int_{\hat{\varepsilon}_2} \sigma_2 \, d\, \varepsilon_2 \right]^{m_2} +$$

$$+ K_{12} \left[\int_{\hat{\gamma}_{12}} \tau_{12} \, d\, \gamma_{12} \right]^{m_{12}} = 1 \qquad (3.3.34)$$

Using the resutls of tests under simple load conditions, the parameters K can be written as :

$$K_1 = \left[\int_{\varepsilon_{1u}} \sigma_1 \, d\,\varepsilon_1\right]^{-m_1}, \quad K_2 = \left[\int_{\varepsilon_{2u}} \sigma_2 \, d\,\varepsilon_2\right]^{-m_2},$$

$$K_{12} = \left[\int_{\gamma_{12u}} \tau_{12} \, d\,\gamma_{12}\right]^{-m_{12}} \qquad (3.3.35)$$

where u denotes ultimate (tensilre or compressive). Then the failure criterion becomes :

$$\left[\frac{\int_{\hat{\varepsilon}_1} \sigma_1 \, d\,\varepsilon_1}{\int_{\varepsilon_{1u}} \sigma_1 \, d\,\varepsilon_1}\right]^{m_1} + \left[\frac{\int_{\hat{\varepsilon}_2} \sigma_2 \, d\,\varepsilon_2}{\int_{\varepsilon_{2u}} \sigma_2 \, d\,\varepsilon_2}\right]^{m_2} + \left[\frac{\int_{\hat{\gamma}_{12}} \tau_{12} \, d\,\gamma_{12}}{\int_{\gamma_{12u}} \tau_{12} \, d\,\gamma_{12}}\right]^{m_{12}} = 1$$

(3.3.36)

The shape of the failure surface given by this equation depends strongly on m_1, m_2 and m_{12}, e.g. for $m_1 = m_2 = m_{12} = 2$, it is spherical, and for $m_1 = m_2 = m_{12} = 1$, it is a pyramidal surface. These shape factors cause inconvenience as they must be determined from biaxial experimental information.

3.3.22 Gol'denblat-Kopnov Theory

The work of Gol'denblat and Kopnov, (Ref. 183), is the first attempt towards a general theory of strength for anisotropic materials. They proposed a general theory of the form :

$$(F_{ij}\,\sigma_{ij})^{\alpha} + (F_{ijkl}\,\sigma_{ij}\,\sigma_{kl})^{\beta} + (F_{ijklmn}\,\sigma_{ij}\,\sigma_{kl}\,\sigma_{mn})^{\gamma}$$

$$+ \ \ldots\ = 1 \qquad (3.3.37)$$

where :

$i, j, k, l, m, n, \ldots = 1, 2, 3$

F_{ij}, F_{ijkl}, ... are strength tensors of different orders

$\alpha, \beta, \gamma, \ldots$ are constants

They also fixed the values of the exponents by requiring that the criterion be homogeneous in the Euler sense. This gives

$\alpha = 1$, $\beta = 1/2$, $\gamma = 1/3$, ... The simplest form of equation (3.3.37) is :

$$F_{ij}\,\sigma_{ij} + (F_{ijkl}\,\sigma_{ij}\,\sigma_{kl})^{1/2} = 1 \qquad (3.3.38)$$

3.3.23 Ashkenazi Theory

The early work of Ashkenazi suggested a failure criterion similar to that of Norris, i.e. equation (3.3.16), (Ref. 138). Later, he developed a fairly complicated strength criterion for the plane state of stress of highly anisotropic materials which is expressed in the form of a fourth-order polynomial as, (Ref. 184) :

$$\left[\frac{\sigma_1^2}{X} + \frac{\sigma_2^2}{Y} + \sigma_1\,\sigma_2\left(\frac{4}{X_{45}} - \frac{1}{X} - \frac{1}{Y} - \frac{1}{S}\right) + \frac{\tau_{12}^2}{S}\right]^2 +$$

$$2\,\frac{\sigma_1\,\sigma_2 - \tau_{12}^2}{S}\left[\sigma_1\,\sigma_2\left(\frac{1}{X} + \frac{1}{Y}\right) + \frac{\sigma_1^2}{X} + \frac{\sigma_2^2}{Y}\right]$$

$$-(\sigma_1\,\sigma_2 - \tau_{12}^2)\left[\sigma_1\,\sigma_2\,(\lambda + \mu) + \lambda\,\sigma_1^2 + \mu\,\sigma_2^2\right] +$$

$$\rho\,(\sigma_1\,\sigma_2 - \tau_{12}^2)(\sigma_1 + \sigma_2) - (\sigma_1^2 + \sigma_2^2 + \sigma_1\,\sigma_2 + \tau_{12}^2) = 1$$

(3.3.39)

where λ, μ and ρ are coefficients which must be determined from three biaxial stress states, and X_{45} is the strength for the direction 45° to the fibre direction. The strengths, X, Y and X_{45} can be replaced by the compressive strengths when $\sigma_1 + \sigma_2 < 0$, and the constants μ, λ and ρ will have different values in this case. The main drawback of this criterion is the need to determine these coefficients from experimental data for biaxial states of stress.

3.3.24 Malmeister Theory

Malmeister theory, (Ref. 185), is a generalization of Ashkenazi theory and is expressed by :

$$F_{ij}\,\sigma_{ij} + F_{ijkl}\,\sigma_{ij}\,\sigma_{kl} + F_{ijklmn}\,\sigma_{ij}\,\sigma_{kl}\,\sigma_{mn} + \ldots = 1 \qquad (3.3.40)$$

where :

$i, j, k, l, m, n, \ldots = 1, 2, 3$; and

F_{ij}, F_{ijkl}, ... are strength tensors of different order.

Equation (3.3.40) is a special case of equation (3.3.37) with $\alpha = \beta = \gamma = \ldots = 1$, (Ref. 186).

3.3.25 Tsai-Wu Theory

Tsai and Wu, (Ref. 187), have proposed a tensor polynomial failure criterion and considered it to be the general theory of strength for anisotropic materials. Wu, (Ref. 188), has shown that most of the previous criteria are degenerated cases of this theory. The theory says that a failure surface in the stress space exists in the form :

$$F_i\,\sigma_i + F_{ij}\,\sigma_i\,\sigma_j = 1 \qquad (3.3.41)$$

where :

$i, j = 1, 2, \ldots, 6$

F_i and F_{ij} are second and fourth order strength tensors.

The non-interaction F terms are related to the engineering strengths by :

$$F_1 = \frac{1}{X_t} - \frac{1}{X_c}$$

$$F_2 = \frac{1}{Y_t} - \frac{1}{Y_c}$$

$$F_3 = \frac{1}{Z_t} - \frac{1}{Z_c} \qquad (3.3.42)$$

$$F_4 = \frac{1}{T_+} - \frac{1}{T_-}$$

$$F_5 = \frac{1}{R_+} - \frac{1}{R_-}$$

$$F_6 = \frac{1}{S_+} - \frac{1}{S_-} \qquad (3.3.43)$$

$$F_{11} = \frac{1}{X_t X_c}, \quad F_{22} = \frac{1}{Y_t Y_c}, \quad F_{33} = \frac{1}{Z_t Z_c} \qquad (3.3.44)$$

$$F_{44} = \frac{1}{T_+ T_-}, \quad F_{55} = \frac{1}{R_+ R_-}, \quad F_{66} = \frac{1}{S_+ S_-} \qquad (3.3.45)$$

where (+) denotes positive shear strength and (-) denotes negative shear strength.

The interaction F terms are determined from biaxial test conditions. These biaxial tests must be selected with care to obtain accurate values for these strength tensors, (Refs. 189, 190). The magnitude of these interaction terms are constrained by the following inequality :

$$F_{ii} F_{jj} - F_{ij}^2 \geq 0 \qquad (3.3.46)$$

Under plane-stress conditions, the failure criterion becomes :

$$F_1 \sigma_1 + F_2 \sigma_2 + F_6 \tau_{12} + F_{11} \sigma_1^2 + F_{22} \sigma_2^2 + 2F_{12} \sigma_1 \sigma_2$$

$$+ F_{66} \tau_{12}^2 = 1 \qquad (3.3.47)$$

where F_{16} and F_{26} vanish due to the orthotropy.

This theory has not yet been applied to the extent of its potential due to the difficulty associated with the determination of the terms F_{ij}, though some applications have appeared, e.g. the study of the strength of molded discontinuous fibre composites, (Ref. 191), and the analysis of fracture modes of composites, (Ref. 181). On the other hand there have been some studies to evaluate the criterion, e.g. Collins and Crane, (Ref. 192), discussed the graphical representation of the failure surface of equation (3.3.47); Narayanaswami and Adelman, (Ref. 193), used the criterion with $F_{12} = 0$ and concluded that it had been sufficiently accurate for engineering applications;

Collins and Thomas, (Ref. 194, 195), state that F_{12} changes sign from stress quadrant to another stress quadrant; and finally, Tennyson et al, (Refs. 196, 197), conclude that the quadratic formulation of equation (3.3.41) is too conservative and a cubic representation of the form :

$$F_i \sigma_i + F_{ij} \sigma_i \sigma_j + F_{ijk} \sigma_i \sigma_j \sigma_k = 1 \qquad (3.3.48)$$

is required.

3.3.26 Huang-Kirmser Theory

This theory, (Ref. 198), is more general than that of Tsai-Wu and it is of the form :

$$(F_i \sigma_i)^{\alpha} + (F_{ij} \sigma_i \sigma_j)^{\beta} + (F_{ijk} \sigma_i \sigma_j \sigma_k)^{\gamma} = 1 \qquad (3.3.49)$$

Huang and Kirmser, however, did not use this criterion in its comprehensive form. They set $\alpha = \beta = \gamma = 1$ and then they dropped the cubic term which resulted in Tsai-Wu criterion.

3.3.27 Puppo-Evensen Theory

All the failure criteria which have been discussed in the preceding sections are applicable to unidirectional laminae of composite materials. This means that the laminated structures is first analysed to obtain the stresses acting on each layer whereupon the desired failure criterion is applied to check the failure in each ply. The theory of Puppo and Evensen, however, is fundamentally different as it can be applied to the laminate as a whole, (Ref. 199). The laminate is assumed homogeneous and anisotropic but not necessarily orthotropic. Interaction is accounted for through the interaction factors which are defined by :

$$\alpha = \frac{3T^2}{YZ}, \quad \beta = \frac{3R^2}{ZX}, \quad \gamma = \frac{3S^2}{XY} \qquad (3.3.50)$$

where the strengths, X, Y, Z, R, S and T are relative to a general coordinate system. The failure criterion is then stated in three quadratic expressions of the form :

$$[\sigma]^T [R]_i [\sigma] = 1 \qquad (3.3.51)$$

where :

$i = 1, 2, 3$

σ is the stress vector; and

$[R]_i$ are the strength matrices of the form :

$$[R]_i = \left[\begin{array}{c|c} A_i & 0 \\ \hline 0 & B \end{array}\right] \qquad (3.3.52)$$

The symmetric submatrices A_1, A_2, A_3 and B are defined by :

$$[A]_1 = \begin{bmatrix} \frac{1}{X^2} & -\frac{\gamma}{2Y^2} & -\frac{\beta}{2Z^2} \\ & \frac{\gamma}{Y^2} & -\frac{1}{2X^2} \\ \text{(symmetric)} & & \frac{\beta}{Z^2} \end{bmatrix} \qquad (3.3.53)$$

$$[A]_2 = \begin{bmatrix} \frac{\gamma}{X^2} & -\frac{\gamma}{2X^2} & -\frac{1}{2Y^2} \\ & \frac{1}{Y^2} & -\frac{\alpha}{2Z^2} \\ \text{(symmetric)} & & \frac{\alpha}{Z^2} \end{bmatrix} \qquad (3.3.54)$$

$$[A]_3 = \begin{bmatrix} \frac{\beta}{X^2} & -\frac{1}{2Z^2} & -\frac{\beta}{2X^2} \\ & \frac{\alpha}{Y^2} & -\frac{\alpha}{2Y^2} \\ \text{(symmetric)} & & \frac{1}{Z^2} \end{bmatrix} \qquad (3.3.55)$$

$$[B] = \begin{bmatrix} \frac{1}{T_2} & 0 & 0 \\ 0 & \frac{1}{R^2} & 0 \\ 0 & 0 & \frac{1}{S^2} \end{bmatrix} \qquad (3.3.56)$$

For a material in a state of plane stress the criterion can be written in explicit form as follows :

$$\left(\frac{\sigma_x}{X}\right)^2 - \gamma\left(\frac{X}{Y}\right)\left(\frac{\sigma_x}{X}\right)\left(\frac{\sigma_y}{Y}\right) + \gamma\left(\frac{\sigma_y}{Y}\right)^2 + \left(\frac{\tau_{xy}}{S}\right)^2 = 1$$

$$\gamma\left(\frac{\sigma_x}{X}\right)^2 - \gamma\left(\frac{Y}{X}\right)\left(\frac{\sigma_x}{X}\right)\left(\frac{\sigma_y}{Y}\right) + \left(\frac{\sigma_y}{Y}\right)^2 + \left(\frac{\tau_{xy}}{S}\right)^2 = 1 \qquad (3.3.57)$$

These two equations are valid for $\gamma \leq 1$. For $\gamma > 1$, the following set of equations is valid :

$$\left(\frac{\sigma_x}{X}\right)^2 + \left(\frac{\sigma_y}{Y}\right)^2 + \left(\frac{\tau_{xy}}{S}\right)^2 - 2h(\gamma)\left(\frac{\sigma_x}{X}\right)\left(\frac{\sigma_y}{Y}\right)$$

$$\pm 2g(\gamma)\left(\frac{\tau_{xy}}{S}\right)\left(\frac{\sigma_x}{X} + \frac{\sigma_y}{Y}\right) = 1 \qquad (3.3.58)$$

where the functions $h(\gamma)$ and $g(\gamma)$ are defined by :

$$h(\gamma) = 1 - \frac{1}{2} f(\gamma)$$

$$f(\gamma) = \frac{1}{10} \{ - (\frac{3}{\gamma} + 4) + \left[(\frac{3}{\gamma} + 4)^2 + \frac{240}{\gamma} \right]^{1/2} \}$$

$$g(\gamma) = (\frac{\gamma}{12})^{1/2} \left[3 f(\gamma)/(f(\gamma) - 4) + 1 \right] . f(\gamma)$$

(3.3.59)

Although direct laminate failure criteria do not require the lamination theory to analyse the stresses in the layers, they are more difficult than the lamina failure theories because they require the strengths X, Y, etc., for every designed laminate, whereas in the lamina criteria the strengths of a ply are determined once.

3.3.28 Wu-Scheublein Theory

This theory, (Refs. 200, 201), is also applied directly to the laminates. It is expressed in terms of a tensor polynomial in the form of Tsai-Wu lamina criterion. The principal directions of strength are not necessarily orthogonal, hence the failure surface may not be ellipsoidal, and higher-order terms need to be included in the tensor polynomial which takes the form :

$$F_i \sigma_i + F_{ij} \sigma_i \sigma_j + F_{ijk} \sigma_i \sigma_j \sigma_k = 1 \qquad (3.3.60)$$

For a two-directional planar laminated composites the number of F coefficients is 39, but considerations of symmetry and redundancy reduce this number. The non-interaction terms are determined from uniaxial tests, but the interaction terms are determined by biaxial tests under prescribed optimum stress ratios. But these ratios depend on the required terms which means that iteration must be employed. To reduce the number of iterations required, Wu and Scheublein suggest "hybrid" analysis which is a combination of lamina failure and laminate failure analyses. In this way better agreement between the experimental and the failure envelope is also obtained, but the analysis is prohibitively expensive.

3.3.29 Chou-McNamee Theory

This theory, (Ref. 202), can be regarded as a "hybrid" analysis. It employs Tsai-Wu criterion and takes the form :

$$\hat{F}_i^k \sigma_i + \hat{F}_{ij}^k \sigma_i \sigma_j = 1 \qquad (3.3.61)$$

where :

$$\hat{F}_i^k = F_j^k U_{ji}^k$$

$$\hat{F}_{ij}^k = F_{mn}^k U_{im}^k U_{jn}^k \qquad (3.3.62)$$

$$U_{ij}^k = Q_{im}^k S_{mj}$$

$i, j, m, n = 1, 2, 3, \ldots 6$

k denotes the k^{th} layer

Equation (3.3.61) is the failure condition for a laminate with anisotropic layers caused by failure in the k^{th} layer.

3.3.30 UMIST Theory

Soden et al at the University of Manchester Institute of Science and Technology (UMIST), (Refs. 20, 21), have proposed two failure theory. The first theory employs the maximum stress lamina failure criterion taking into account the non-linearity in shear. Hahn-Tsai method of non-linear analysis of Sec. 2.3.2(a) is employed for this purpose. The second failure theory is a modification of Puppo-Evensen theory, i.e. it is applied directly to the laminate. The criterion, for two-dimensional stress system with no shear load, is expressed by the following set of equations :

$$\left(\frac{\sigma_x}{X}\right)^2 - \gamma_1\left(\frac{\sigma_x\sigma_y}{Y^2}\right) + \gamma_1\left(\frac{\sigma_y}{Y}\right)^2 = 1$$

$$\gamma_2\left(\frac{\sigma_x}{X}\right)^2 - \gamma_2\left(\frac{\sigma_x\sigma_y}{Y^2}\right) + \left(\frac{\sigma_y}{Y}\right)^2 = 1 \qquad (3.3.63)$$

where X and Y are the strengths in the loading directions x and y and can either be tensile or compressive according to the signs of σ_x and σ_y. The constants γ_1 and γ_2, however, must be determined experimentally under biaxial test conditions. Their values differ from a stress quadrant to another.

3.3.31 Guess-Gerstle Theory

Guess and Gerstle, (Refs. 230-231), used two laminate failure criteria. The first is the maximum stress criterion applied directly a composite laminate. To include the interaction among the stress components, they used a second criterion again applied directly to the laminate and is similar to that of Norris lamina criterion. In the absence of shear loading, their strength equation is :

$$\left(\frac{\sigma_x}{X}\right)^2 - \frac{\sigma_x}{X}\frac{\sigma_y}{Y} + \left(\frac{\sigma_y}{Y}\right)^2 = 1 \qquad (3.3.64)$$

where X and Y are the laminate strengthsin x and y directions.

3.3.32 Summary

The thirty failure criteria described briefly above can be classified into the following four categories :

a) the limit criteria: failure occurs when a stress (or strain) parameter reaches its limit. No interaction between the stress components is accounted for (some interaction exists in the case of maximum strain theory). Unequal tensile and compressive strengths are usually allowed for. The onset to failure as well as the failure mode are predicted. These features introduce operational simplicity in the analysis.

b) the interaction criteria: these are basically curve-fitting techniques and lack sound theoretical basis. Failure occurs when a simple-to-use quadratic formula of stress is satisfied. Only the onset to failure is predicted and not the mode of failure. The use of different tension and compression strengths is allowed for in some criteria. Some criteria require biaxial tests to evaluate the interaction terms.

c) the tensor polynomial criteria: these are also curve-fitting techniques but more general and more difficult than the criteria of the previous category. The failure mode is not predicted, only its onset.. Different tension and compression strengths are accounted for. The evaluation of

the interaction terms requires biaxial tests which must be chosen carefully. To have better fitting a cubic formula has been suggested which means more interaction parameters to be determined by inconvenient biaxial tests.

d) the direct laminate criteria: these do not involve a lamination theory nor constitutive assumptions. The mode of failure is not predicted. Biaxial tests are required to evaluate the interaction terms. The most important shortcoming is that there is no generality in these criteria as the laminate strengths must be determined experimentally for every new design. The laminate criteria are best used to verify the failure envelope obtained by ply-to-ply analysis.

3.4 A PROPOSED FAILURE CRITERION

3.4.1 Introduction

With so many failure criteria in existence, the choice of a reliable and easy-to-use criterion has become a difficult task. One typical assumption in most of the failure criteria is that the mechanical behaviour of the lamina is linear-elastic. As shown in Sec. 2.3 this assumption is far from reality. Sandhu criterion, however, considers non-linearity in the stress-strain response, but it is inconvenient as its shape factors must be determined from biaxial experimental information.

It is also generally assumed in the described criteria that "yield" and "Ultimate" strengths are the same. Although the stress-strain behaviour of a composite material and an isotropic material may look alike, what happens beyond the linear limits in both cases is absolutely different. The yeild in metals is associated with dislocations, whereas the onset to non-linearity in composites is an indication to the beginning of degradation as cracks, though at micro-level, commence to initiate. To elaborate this point a series of ultrasonic C-scanning, acoustic emission, and photomicrographic techniques were conducted. These are basically non-destructive testing methods and are usually used to detect damage in structures during the regular inspection routines, (Refs. 204-213). These tests and the results obtained from them are given in Appendices E, F and G respectively. The conclusion obtained from these tests is that the non-linear characteristic of a composite material is associated with crack propagation. This can explain the non-reversible behaviour of the composites when the stress level exceeds the elastic limit. These observations have led to propose the following failure criterion for composite materials.

3.4.2 Modified Maximum Strain Criterion

The present criterion is to be used to predict the failure of a lamina in a composite structure as well as the failure of the laminate as a whole, i.e., the criterion will be used to predict the behaviour of a laminated structure after one of its layers has failed.

The latter part of the criterion, which is referred to as the post-failure behaviour, is to be discussed in Chapter 4. It is enough to mention here that the "mode" of failure of the lamina is needed to predict the post-failure behaviour of the laminate. The only two failure criterion which predict the mode of failure as well as the onset to failure are the maximum stress criterion and the maximum strain criterion.

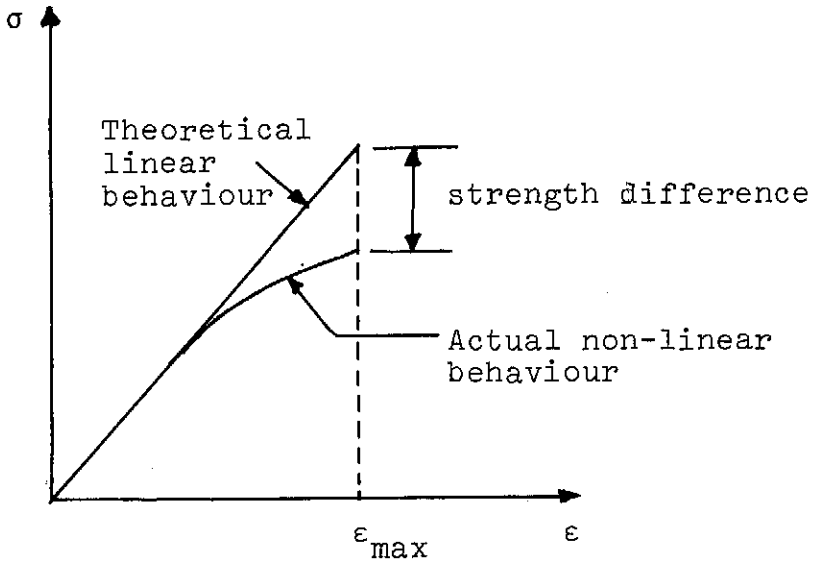

Fig. (3.4.1) The importance of considering non-linear behaviour in strength prediction.

The maximum strain criterion has an advantage over the maximum stress criterion because some interaction exists between the stress components due to Poisson's ratio. Another advantage of using "strain" rather than "stress" as a limit criterion is that the "strain" is a measured quantity, whereas the "stress" is a calculated quantity.

The maximum strain criterion, as it stands now, always predict higher failure loads than the experimental loads, (Ref. 159). This can easily be explained when one refers to Fig. (3.4.1). It is obvious that the theoretical linear stress-strain curve will predict higher strength than the actual non-linear response.

The preceding points were taken into account in forming the present modified maximum strain criterion. Two modifications are introduced. First, the non-linear stress-strain curves of the lamina, as analysed in Sec. 2.3.3, are considered allowing different response for tension and compression. Second, two levels of failure are proposed: the lower failure level represents the beginning of the degradation, i.e., the onset to non-linearity, while the higher failure level represents the total failure of the lamina in a particular mode. In this way, both the "yield" as well as the "ultimate" strengths are predicted. In general, these are not the same, but can be the same in some cases, e.g., if the longitudinal stress-strain curve is linear and its contribution to degradation is high, then the two levels of failure coincide.

The designer must judge which level of failure is more appropriate for the case under consideration bearing in mind that above the low failure level the lamina will exhibit irreversible damage as shown in Appendix E, F and G, i.e., the cracks which initiate at the beginning of the degradation will not close tight during unloading.

3.5 CORRELATION OF THEORETICAL AND EXPERIMENTAL RESULTS

The new modified maximum strain criterion was included in a general computer program which calculates the stress and strength of laminated composites, (Appendix C). Six of the already existing failure criteria were also included in the program for comparison purpose. These are the maximum stress, the maximum strain, Hill-Azzi-Tsai, Hoffman, Tsai-Wu, and Puppo-Evensen failure criteria. These were chosen from the available failure criteria because they are widely used by different designers. The criteria were then applied to the specimens of tubes B2 ($\pm 70^{\circ}$) and B3 ($\pm 45^{\circ}$), the experimental data of which are given in Appendix B.

Figs. (3.5.1) to (3.5.6) show the six failure criteria applied to the specimens of tube B2, and every criterion is compared with the present modified criterion. The inner envelope of the modified criterion belongs to the beginning of degradation, while the outer envelope belongs to the ultimate failure. The maximum strain criterion predicts high failure load, while the predictions of the other lamina criteria are very conservative as they compare fairly well with the inner envelope of the present criterion. The laminate failure criterion of Puppo-Evensen agrees as well as the present modified theory with the experimental results, but this theory is applied directly to the laminate and does not give any information about the failure of the layers nor the mode of failure.

When the new failure criterion is compared with the maximum strain criterion for $\pm 45^{\circ}$ tubes, Fig. (3.5.7), the invalidity of the maximum strain criterion becomes very obvious as the failure in these laminates is dominated by shear, and non-linearity here is very important. The other criteria, Figs. (3.5.8) to (3.5.12), compare well with the inner envelope, but their predictions are still conservative when they are compared with the outer envelope.

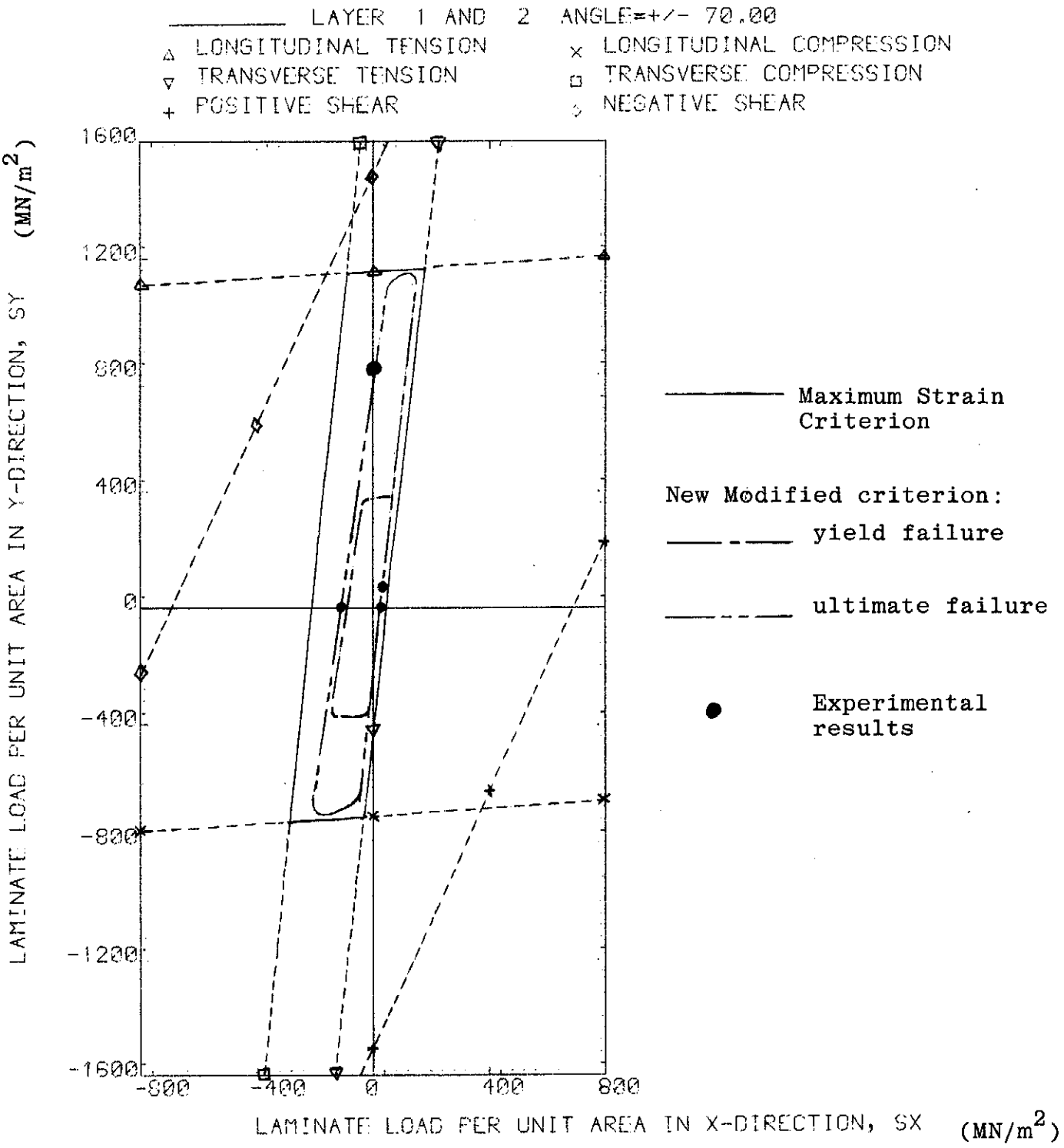

Fig.(3.5.1) MAXIMUM STRAIN FAILURE ENVELOPE FOR $\pm$ 70^{o} tube compared with the present modified criterion

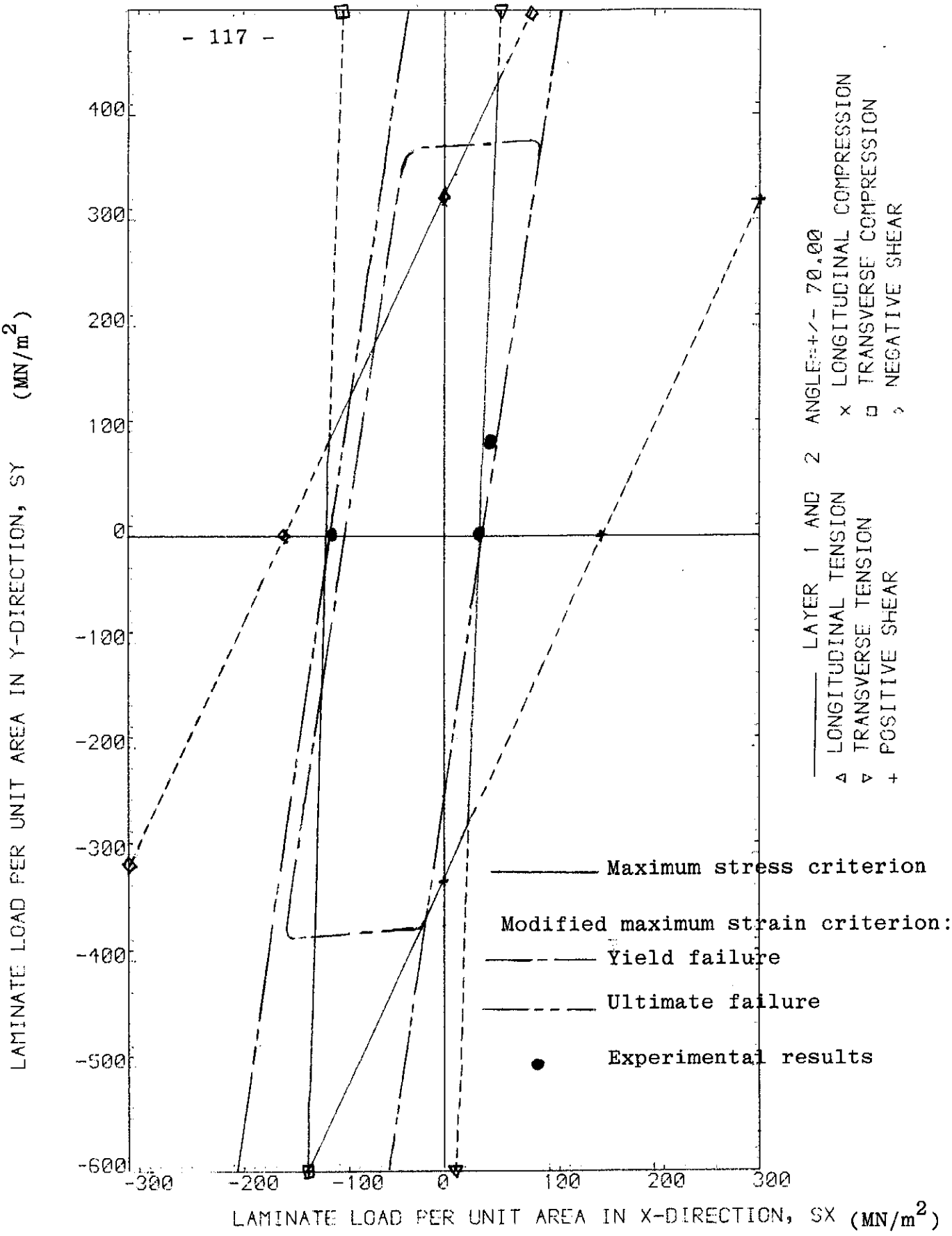

Fig.(3.5.2) MAXIMUM STRESS FAILURE ENVELOPE FOR $\pm 70^{o}$ tube compared with the present modified criterion

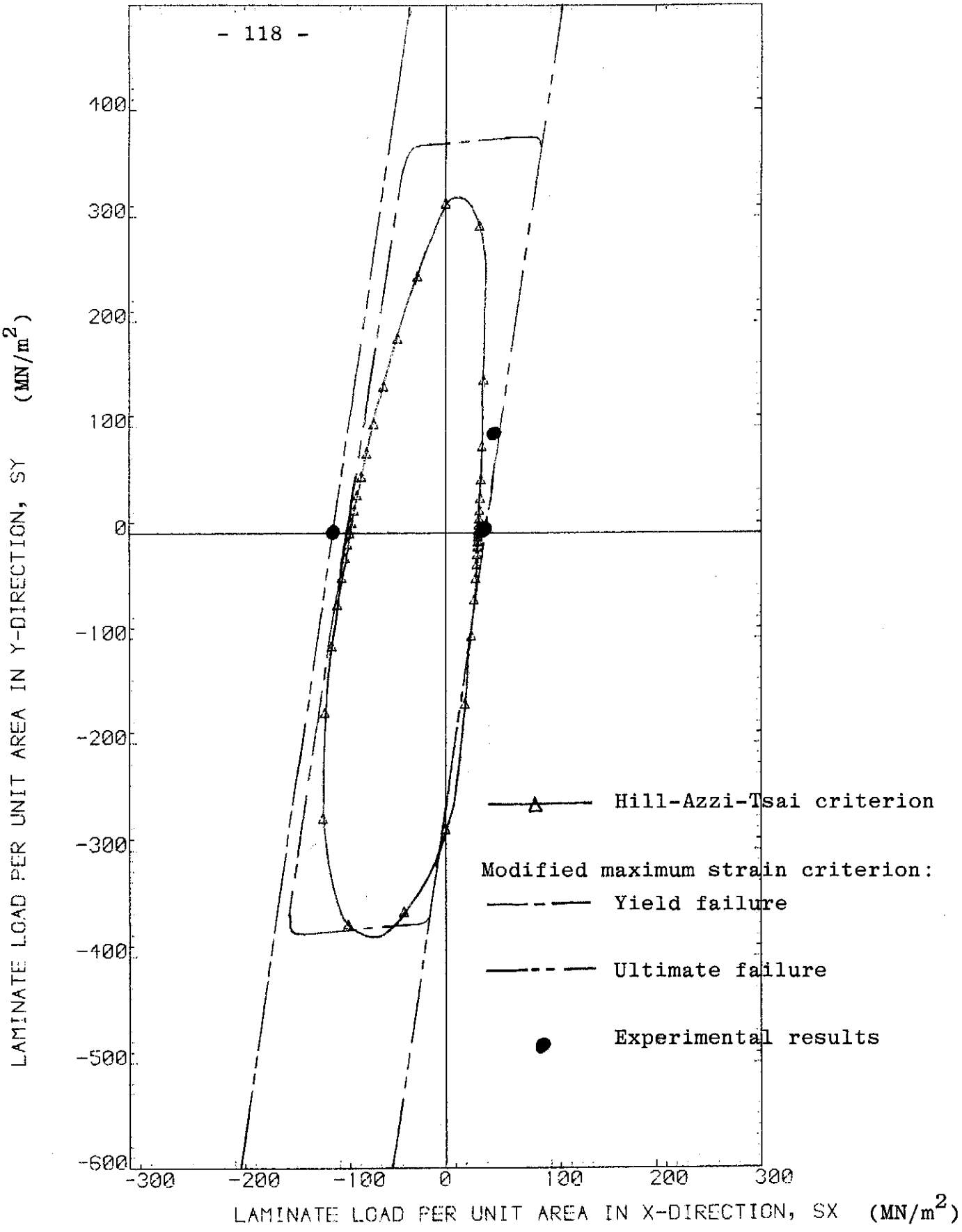

Fig.(3.5.3) HILL-TSAI FAILURE ENVELOPE FOR $\pm 70^{o}$ tube
compared with the present modified criterion

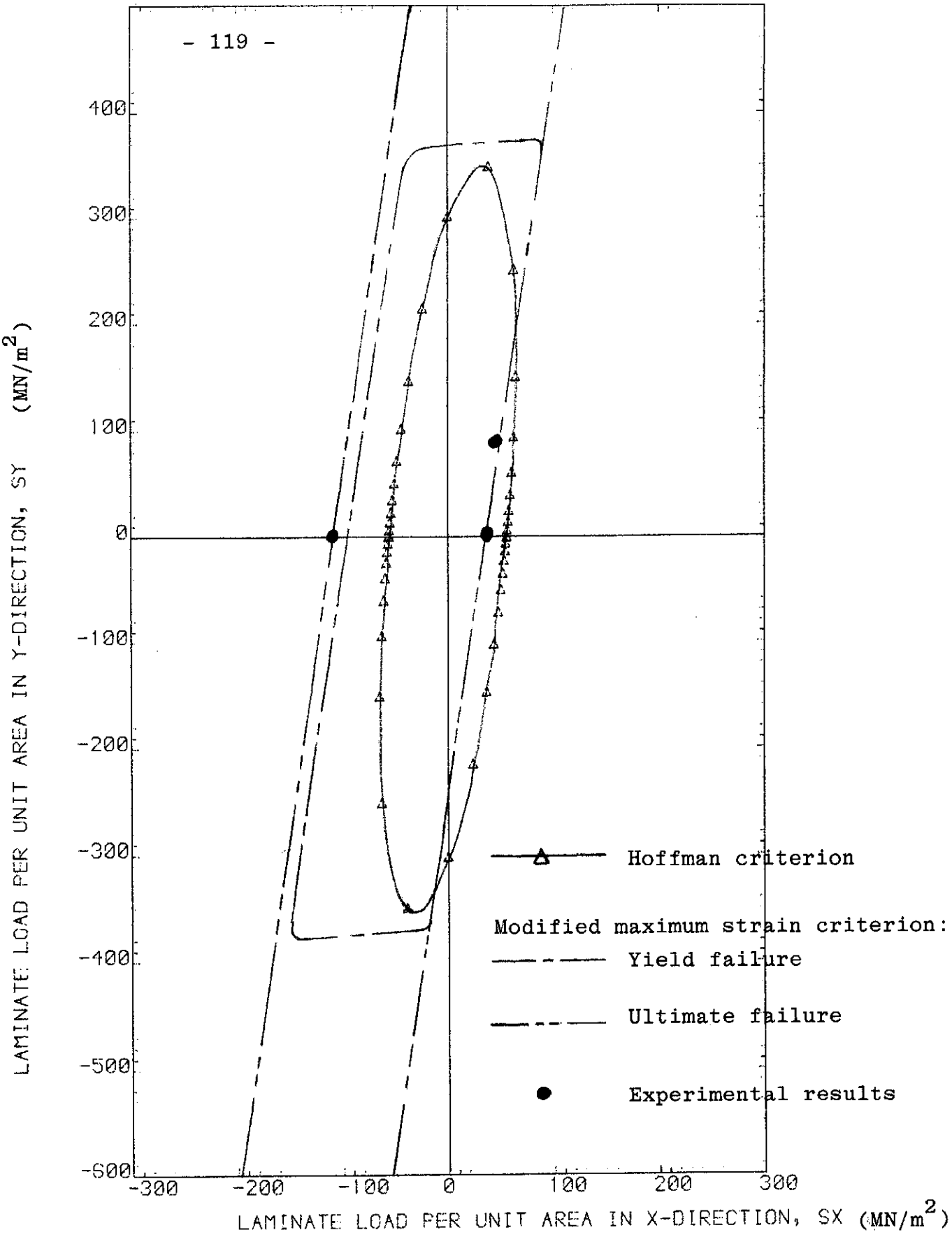

Fig.(3.5.4) HOFFMAN FAILURE ENVELOPE FOR $\pm 70^{o}$ tube compared with the present modified criterion

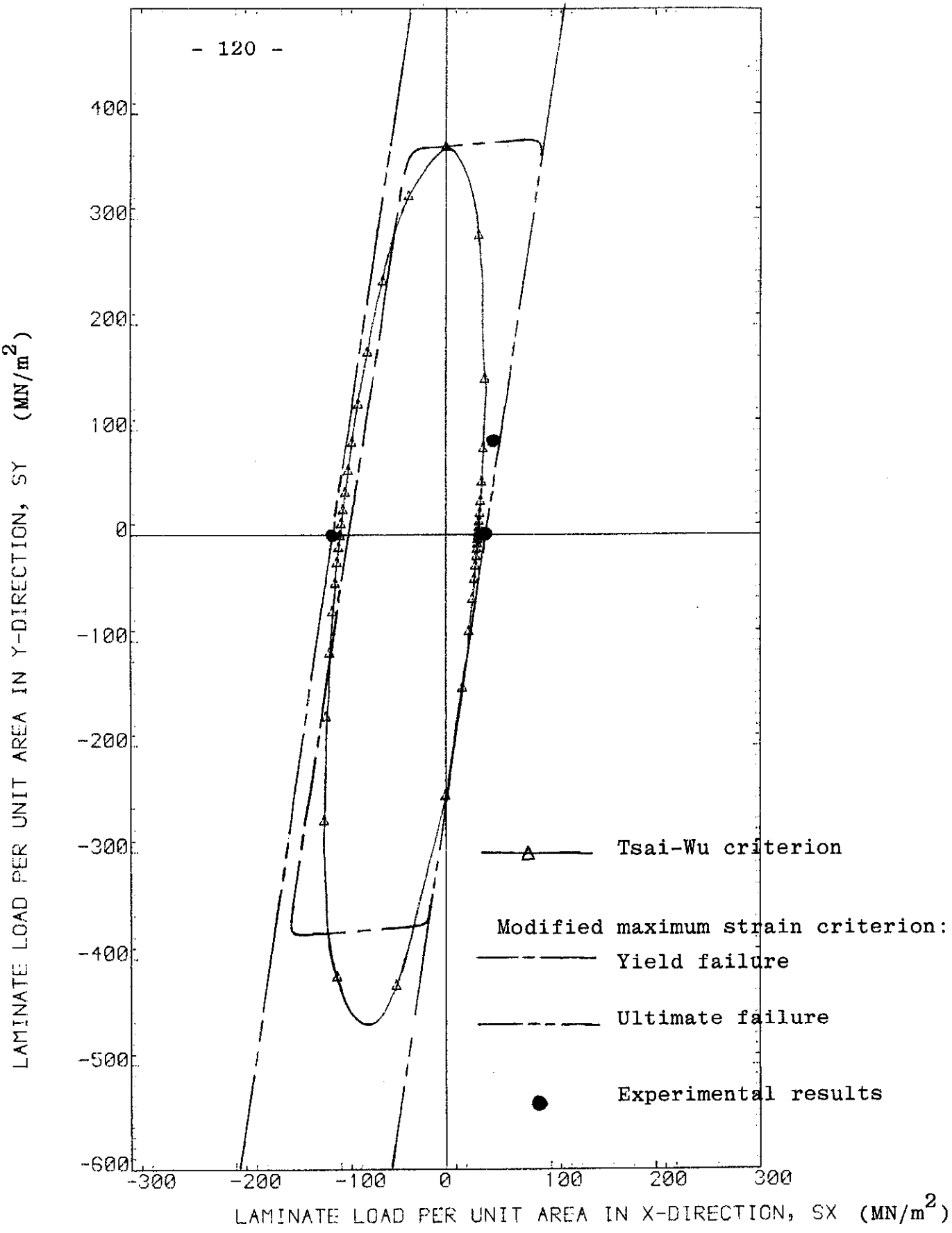

Fig.(3.5.5) TSAI-WU FAILURE ENVELOPE FOR $\pm 70^{\circ}$ tube compared with the present modified criterion

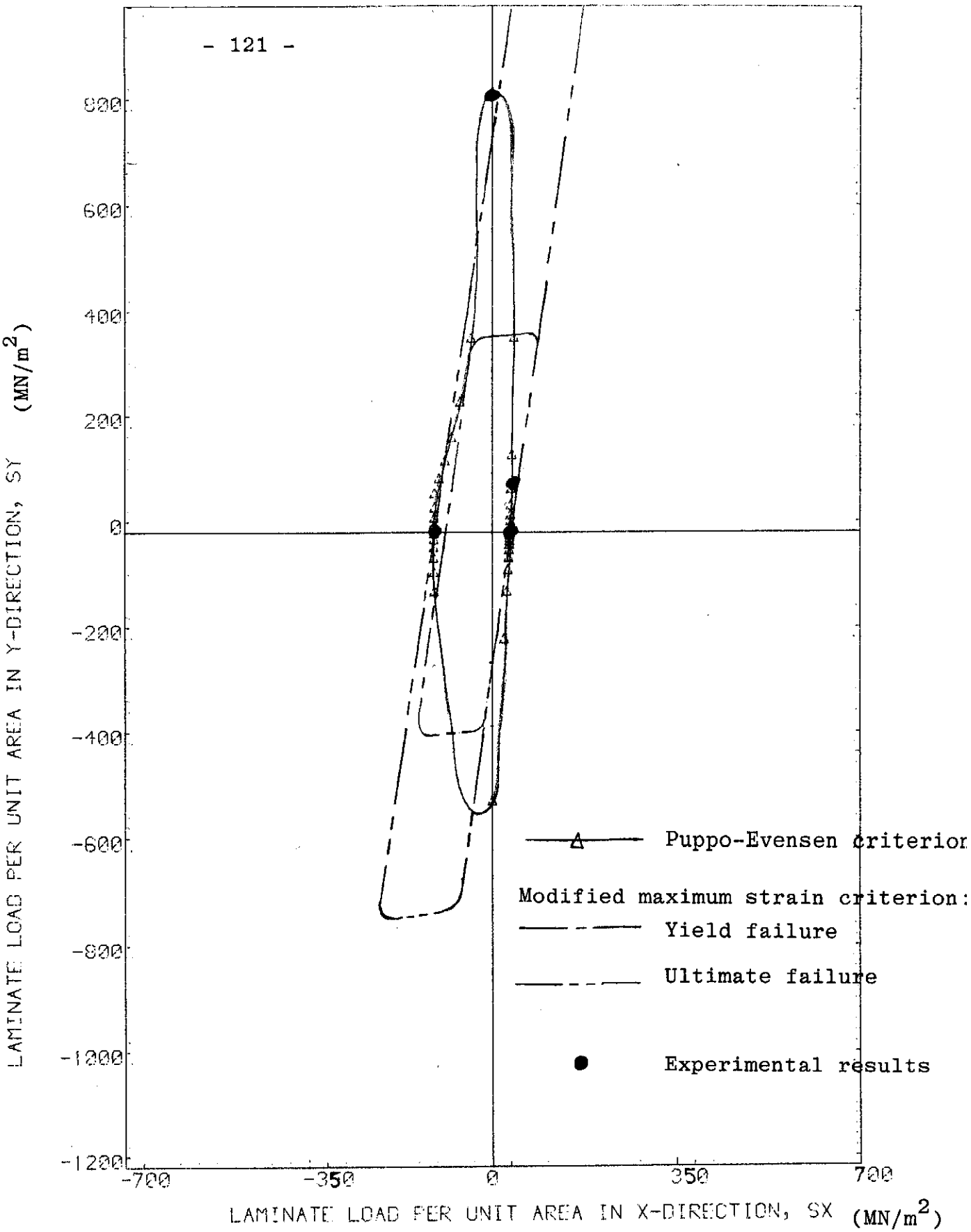

Fig.(3.5.6) PUPPO-EVENSEN FAILURE ENVELOPE FOR $\pm 70^{\circ}$ tube compared with the present modified criterion

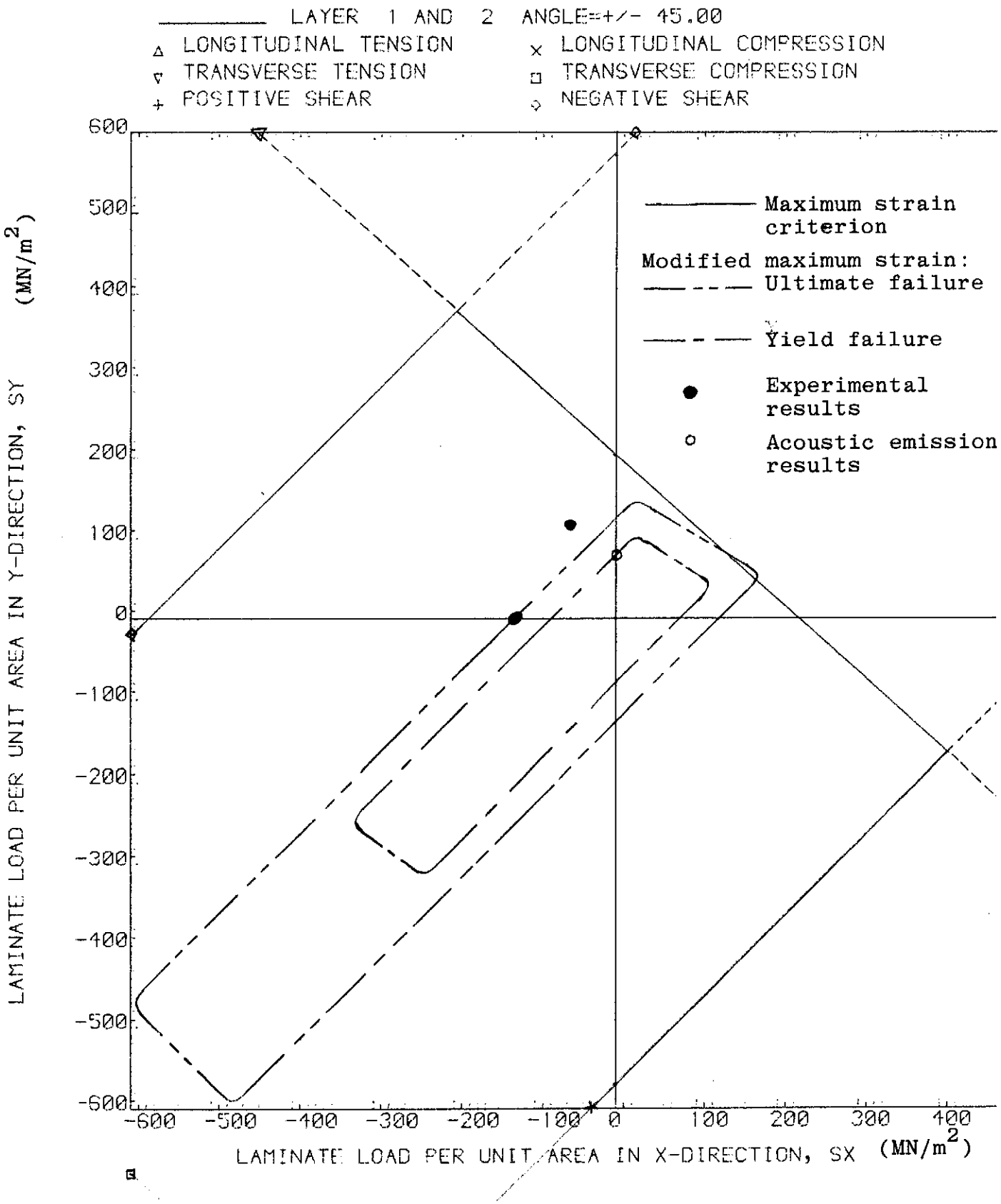

Fig.(3.5.7) MAXIMUM STRAIN FAILURE ENVELOPE FOR $\pm 45^{o}$ tube compared with the present modified criterion

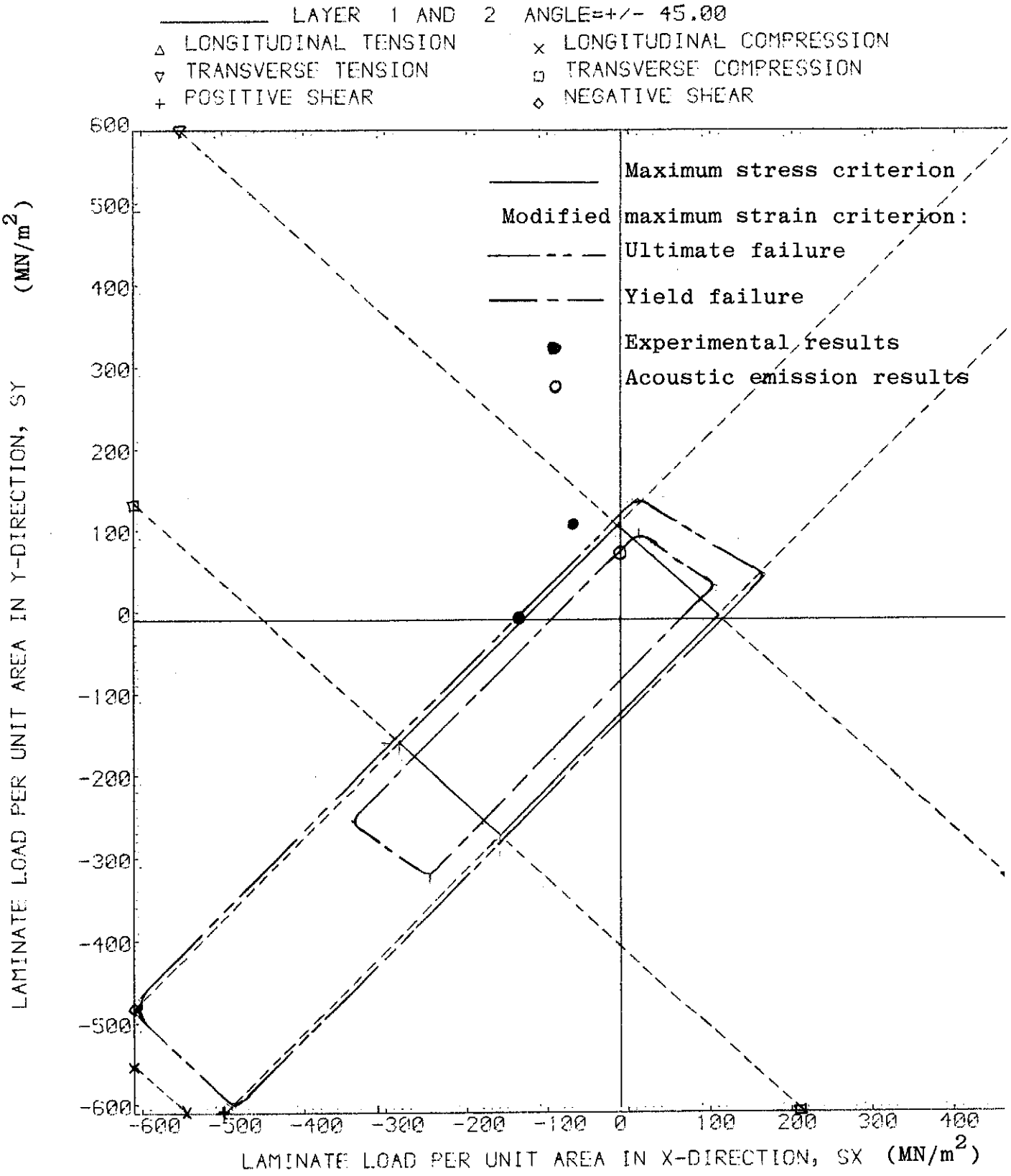

Fig.(3.5.8) MAXIMUM STRESS FAILURE ENVELOPE FOR $\pm 45^{o}$ tube compared with the present modified criterion

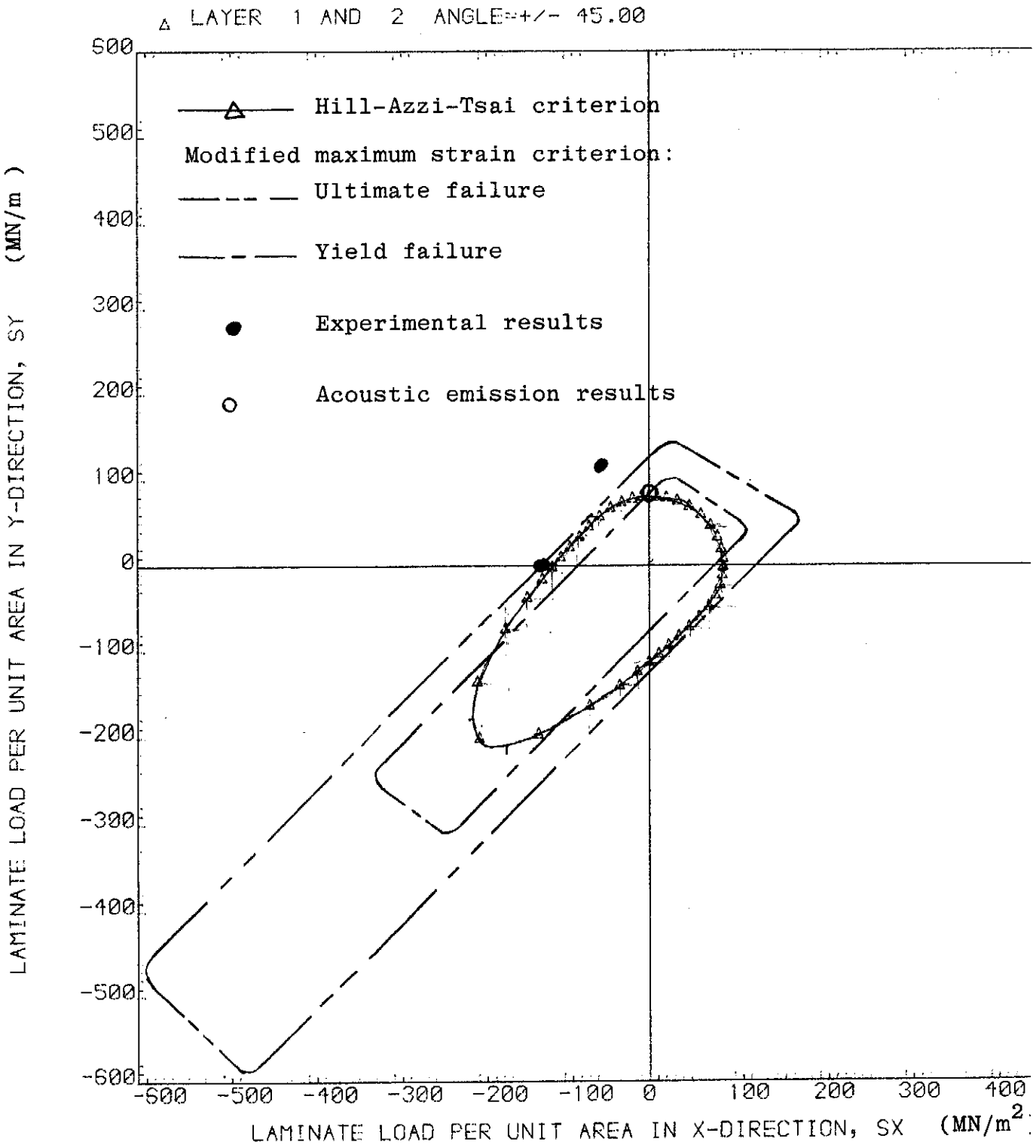

Fig.(3.5.9) HILL-TSAI FAILURE ENVELOPE FOR $\pm 45^{o}$ tube compared with the present modified criterion

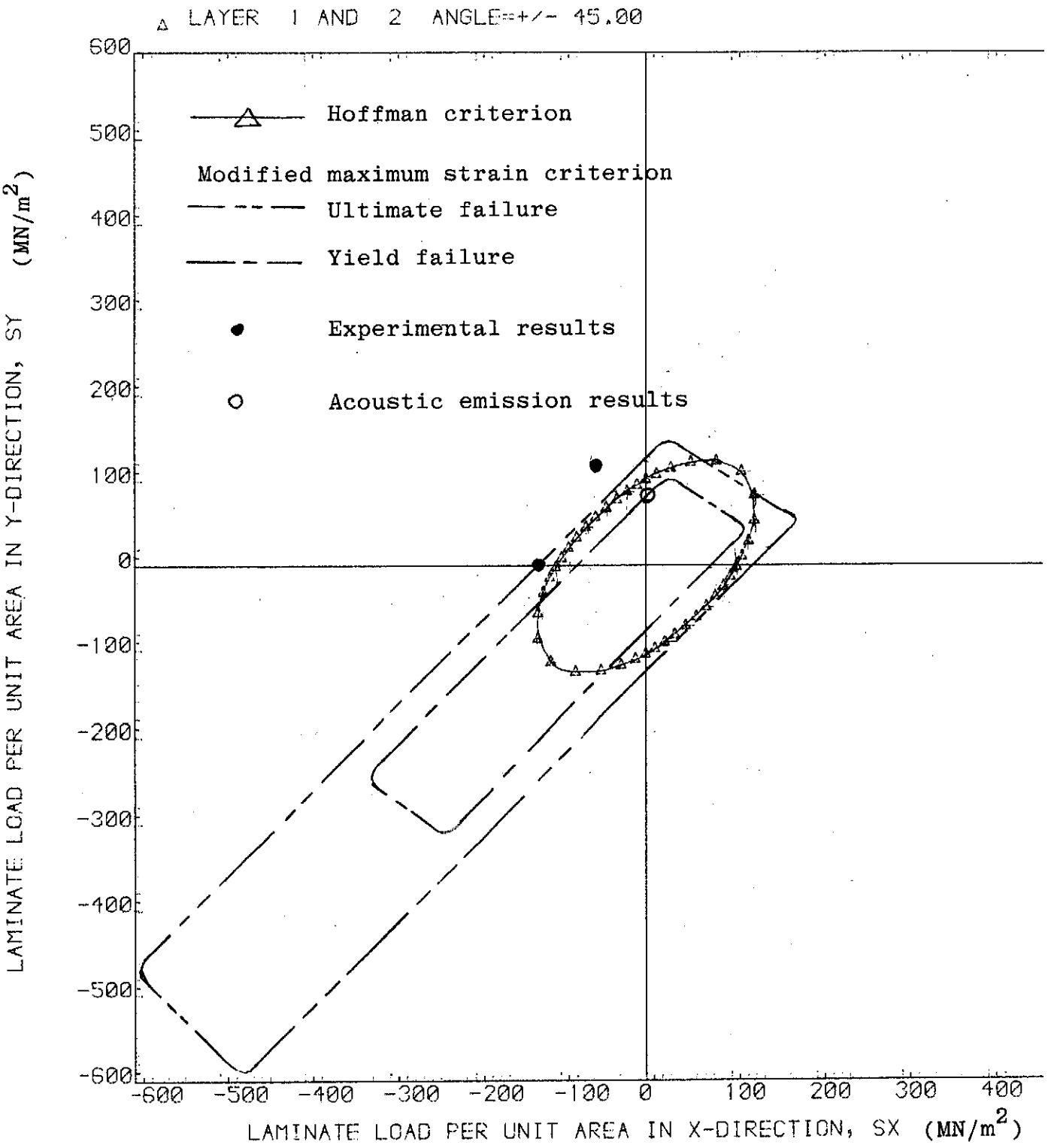

Fig.(3.5.10) HOFFMAN FAILURE ENVELOPE FOR $\pm 45^{o}$ tube compared with the present modified criterion

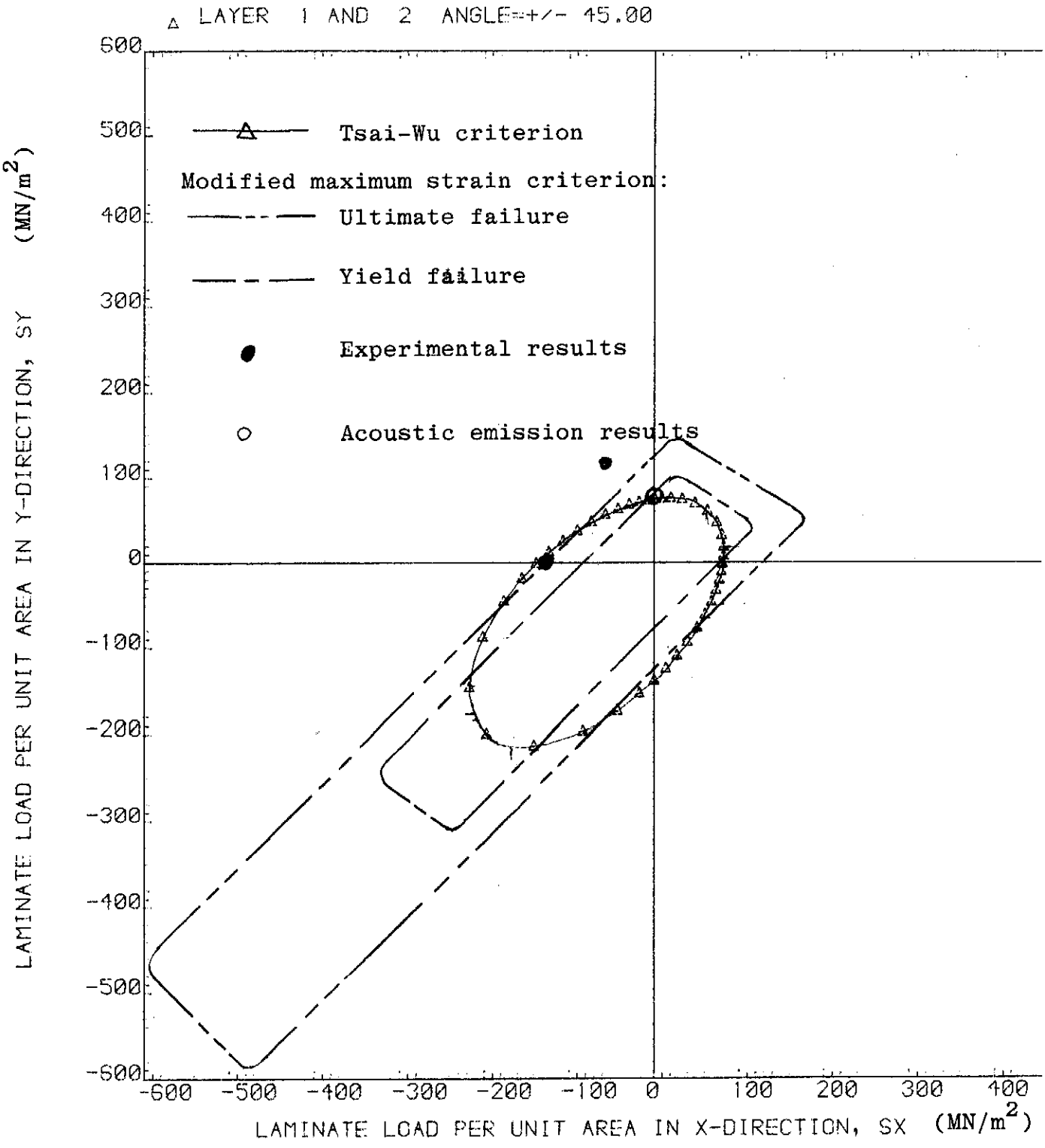

Fig.(3.6.11) TSAI-WU FAILURE ENVELOPE FOR $\pm 45^{o}$ tube compared with the present modified criterion

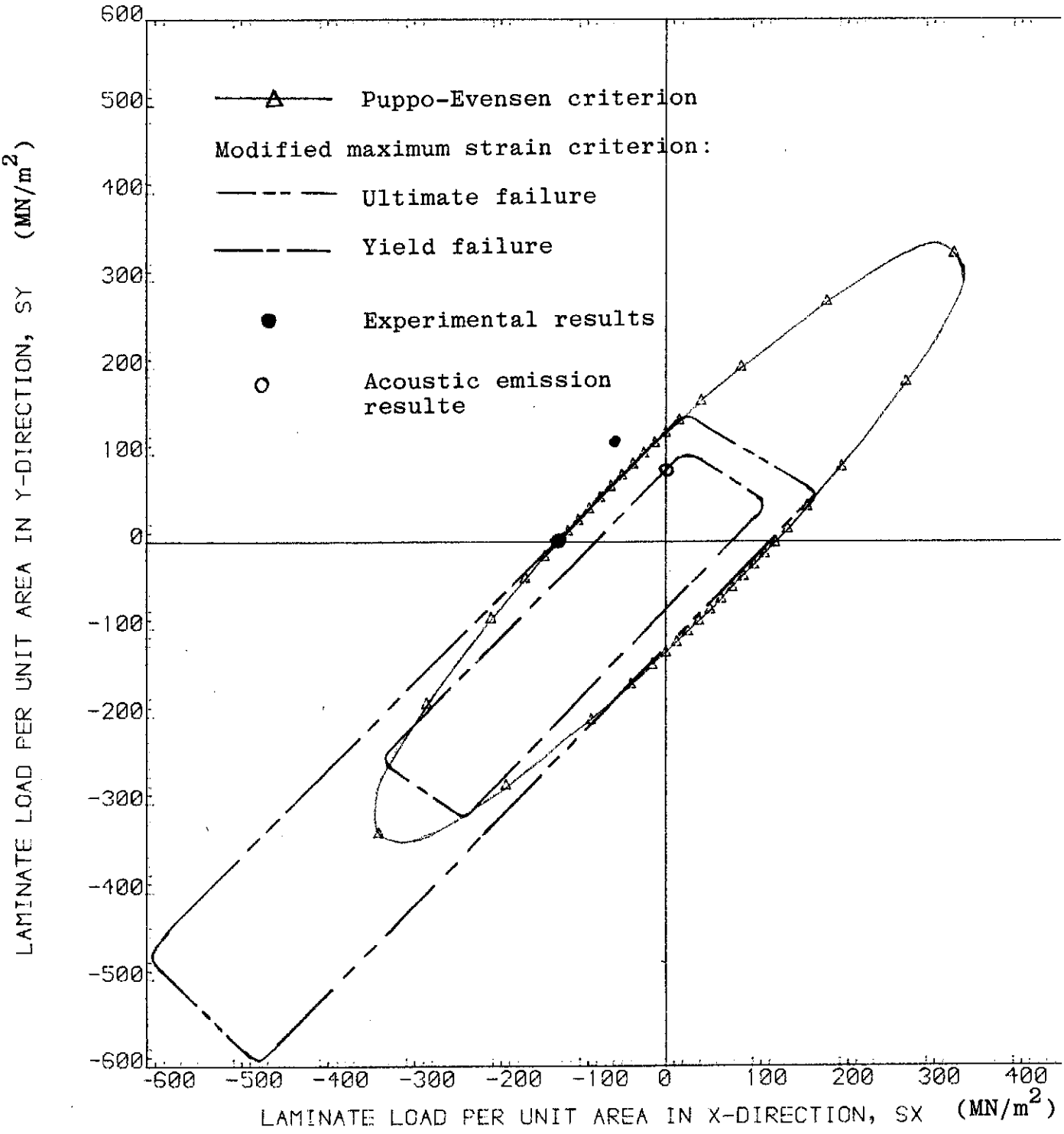

Fig.(3.5.12) PUPPO-EVENSEN FAILURE ENVELOPE FOR $\pm 45^{o}$ tube compared with the present modified criterion

3.6 INSTABILITY FAILURE OF COMPOSITE CYLINDRICAL SPECIMENS

3.6.1 Introduction

It was not intended to study the problem of buckling of cylindrical shells in this thesis, because this problem is quite different from the main theme of the present research, but because "thin" tubular specimens were used in the experimental investigation under combined loadings, the instability problem of these specimens has imposed itself. This section describes the method used to estimate the buckling loads of the test specimens under the appropriate test conditions.

3.6.2 Review of the Theory of Buckling of Composite Shells

Tennyson, (Ref. 232), and Bert, (Ref. 88), have reviewed the work done on buckling of composite cylindrical shells. In general, shell theories used for buckling studies are either Flügge's shell theory, (Ref. 79), Donnell-type stability theory (Ref. 124), or large deflection shell theory, (Ref. 233). Cheng and Ho, (Refs. 78, 234), and Whitney and Sun, (Ref. 236), for instance used Flügge's shell theory, Tsai, (Ref. 235), and Hirano, (Ref. 237), used Donnell's shell theory, whereas Chao, (Ref. 238), employed Timoshenko's buckling equilibrium equations.

Later, Booton and Tennyson, (Ref. 239), studied the buckling of imperfect anisotropic cylinders under combined loading, while Jones et al, (Refs. 240-241), studied the effect of prebuckling deformations and the difference of behaviour in tension and compression on the buckling of laminated composite tubes.

There have also been some experimental work in this field. Most experimental results on composite cylinders under axial compression seem to be in good agreement with theoretical predictions. Under torsion, however, there is some discrepancy (Ref. 242).

In this thesis, Flügge's shell theory is used as it is consistent with the shell theory used in Sec. 2.2 and 2.4. Only the equilibrium equations for buckling differ from the equilibrium equations which are given in Sec. 2.4. All other equations (strains, curvatures, resultant forces and moments) are still the same.

3.6.3 Governing Differential Equations

The governing buckling differential equations of a circular cylindrical shell of mean radius R and subjected simultaneously to combination of axial compression internal pressure, and torsional loads are given by (Ref. 79) :

$$N_{x,x} + N_{xy,y} + N_x^i u^o_{,xx} + N_y^i(u^o_{,yy} - \frac{1}{R} w^o_{,x}) + 2N_{xy}^i u^o_{,xy} = 0 \qquad (3.6.1)$$

$$(N_y + \frac{1}{R}M_y)_{,y} + (N_{xy} + \frac{1}{R}M_{xy})_{,x} + N_x^i v^o_{,xx} + N_y^i(v^o_{,yy} + \frac{1}{R}w^o_{,y}) + 2N_{xy}^i(v^o_{,xy} + \frac{1}{R}w^o_{,x}) = 0 \qquad (3.6.2)$$

$$M_{x,xx} + 2M_{xy,xy} + M_{y,yy} - \frac{1}{R}N_y + N_x^i w_{,xx} + N_y^i(\frac{1}{R}u_{,x} - \frac{1}{R}v_{,y} + w_{,yy}) - 2N_{xy}^i(\frac{1}{R}v_{,x} - w_{,xy}) = 0 \qquad (3.6.3)$$

where N_x^i, N_y^i and N_{xy}^i represent the initial or pre-buckling loads. The superscript (i) is used here to distinguish these loads from the additional loads which appear when the cylinder buckles.

Using equations (2.2.24), (2.2.25), (2.2.26), (2.4.6) and (2.4.7) the differential equations of buckling can be written in terms of the mid-surface displacements (u^o, v^o and w^o) and their derivatives as follows :

$$u^o_{,xx}(A_{11} + N_x^i) + u^o_{,xy}(A_{13} + A_{31} - \frac{1}{R}B_{13} + 2N_{xy}^i) + u^o_{,yy}(A_{33} - \frac{1}{R}B_{33} + N_y^i) + v^o_{,xx}(A_{13} + \frac{1}{R}B_{13}) + v^o_{,xy}(A_{12} + A_{33} + \frac{1}{R}B_{33}) + v^o_{,yy} A_{32} - w^o_{,xxx} B_{11}$$

$$- w^{o}_{,xxy}(2B_{13} + B_{31}) - w^{o}_{,xyy}(B_{12} + 2B_{33}) - w^{o}_{,yyy}\, B_{32}$$

$$+ w^{o}_{,x}\,\frac{1}{R}(A_{12} - \frac{1}{R}B_{12} - N^{i}_{y}) + w^{o}_{,y}\,\frac{1}{R}(A_{32} - \frac{1}{R}B_{32})$$

(3.6.4)

$$u^{o}_{,xx}(A_{31} + \frac{1}{R}B_{31}) + u^{o}_{,xy}(A_{21} + A_{33} + \frac{1}{R}B_{21} - \frac{1}{R^2}D_{33})$$

$$+ u^{o}_{,yy}(A_{23} - \frac{1}{R^2}B_{23}) + v^{o}_{,xx}(A_{33} + \frac{2}{R}B_{33} + \frac{1}{R^2}D_{33} + N^{i}_{x})$$

$$+ v^{o}_{,xy}(A_{23} + A_{32} + \frac{2}{R}B_{23} + \frac{1}{R}B_{32} + \frac{1}{R^2}D_{23} + 2N^{i}_{xy})$$

$$+ v^{o}_{,yy}(A_{22} + \frac{1}{R}B_{22} + N^{i}_{y}) - w^{o}_{,xxx}(B_{31} + \frac{1}{R}D_{31})$$

$$- w^{o}_{,xxy}(B_{21} + 2B_{33} + \frac{1}{R}D_{21} + \frac{2}{R}D_{33})$$

$$- w^{o}_{,xyy}(2B_{23} + B_{32} + \frac{2}{R}D_{23} + \frac{1}{R}D_{32}) - w^{o}_{,yyy}(B_{22} + \frac{1}{R}D_{22})$$

$$+ w^{o}_{,x}\,\frac{1}{R}(A_{32} - \frac{1}{R^2}D_{32} + 2N^{i}_{xy}) + w^{o}_{,y}\,\frac{1}{R}(A_{22} - \frac{1}{R^2}D_{22} + N^{i}_{y}) = 0$$

(3.6.5)

$$u_{,xxx}\, B_{11} + u_{,xxy}(B_{13} + 2B_{31} - \frac{1}{R}D_{13}) + u_{,xyy}(2B_{33} + B_{21} - \frac{2}{R}D_{33})$$

$$+u_{,yyy}(B_{23} - \frac{1}{R}D_{23}) + u_{,x}\,\frac{1}{R}(-A_{21} + N^{i}_{y}) + u_{,y}\,\frac{1}{R}(-A_{23} + \frac{1}{R}B_{23})$$

$$+v_{,xxx}(B_{13} + \frac{1}{R}D_{13}) + v_{,xxy}(B_{12} + 2B_{33} + \frac{2}{R}D_{33})$$

$$+ v_{,xyy}(2B_{32} + B_{23} + \frac{1}{R}D_{23}) + v_{,yyy}\, B_{22}$$

$$- v_{,x}\,\frac{1}{R}(A_{23} + \frac{1}{R}B_{23} + 2N^{i}_{xy}) - v_{,y}\,\frac{1}{R}(A_{22} + N^{i}_{y})$$

$$- w_{,xxxx}\, D_{11} - w_{,xxxy}\,(2D_{13} + 2D_{31}) - w_{,xxyy}(D_{12} + D_{21} + 4D_{33})$$

$$- w_{,xyyy}(2D_{32} + 2D_{23}) - w_{,yyyy}\, D_{22}$$

$$+ w_{,xx}(\frac{1}{R}B_{12} + \frac{1}{R}B_{21} - \frac{1}{R^2}D_{12} + N^{i}_{x})$$

$$+ w_{,xy}\, 2(\frac{1}{R}B_{32} + \frac{1}{R}B_{23} - \frac{1}{R^2}D_{32} + N^{i}_{xy})$$

$$+ w_{,yy}(\frac{2}{R}B_{22} - \frac{1}{R^2}D_{22} + N^{i}_{y}) + w\,\frac{1}{R^2}(-A_{22} + \frac{1}{R}B_{22})$$

(3.6.6)

3.6.4 Solution of the Differential Equations

The equations above are coupled partial differential equations and not easy to solve directly. Fourier series solution is suggested by Flügge, (Ref. 69), and Whitney and Sun, (Ref. 236). Whitney and Sun state that this solution is very cumbersome and advise that for quick estimate of the buckling load the following solution be used :

$$\left.\begin{aligned} u^{o} &= U \sin \frac{1}{R}(\lambda x + ny) \\ v^{o} &= V \sin \frac{1}{R}(\lambda x + ny) \\ w^{o} &= W \cos \frac{1}{R}(\lambda x + ny) \end{aligned}\right\} \qquad (3.6.7)$$

where : U, V and W are constants

$$\lambda = \frac{m \pi R}{\ell} \qquad (3.6.8)$$

m is the number of half-waves along the length of the cylinder

n is the number of waves in the circumferential direction

ℓ is the length of the cylinder

R is the mean radius of the cylinder

The solution (3.6.7) is an exact solution for the partial differential equations (3.6.4), (3.6.5.) and (3.6.6), but it does not satisfy all boundary conditions. In particular, it does not satisfy the fixed ends conditions. This is not a problem if the length of the cylinder is long enough to the extent that the constraints at the ends do not affect much the critical loads, (Ref. 78). On the other hand, the solution (3.6.7) yields a more conservative estimate of the buckling loads than the solution which satisfies the boundary conditions (Refs. 234, 236).

If the solution (3.6.7) is substituted in the differential equations the following equation is obtained :

$$\begin{bmatrix} F_{11} - a N_o & F_{12} & F_{13} + c N_o \\ F_{21} & F_{22} - a N_o & F_{23} - b N_o \\ F_{31} + c N_o & F_{32} - b N_o & F_{33} - a N_o \end{bmatrix} \begin{bmatrix} U \\ V \\ W \end{bmatrix} = 0 \qquad (3.6.9)$$

where

$$F_{11} = - \lambda^2 A_{11} - \lambda n (A_{13} + A_{31} - \frac{1}{R} B_{13}) - n^2 (A_{33} - \frac{1}{R} B_{33}) \qquad (3.6.10)$$

$$F_{12} = - \lambda^2 (A_{13} + \frac{1}{R} B_{13}) - \lambda n (A_{12} + A_{33} + \frac{1}{R} B_{33}) - n^2 A_{32} \qquad (3.6.11)$$

$$F_{13} = -\frac{1}{R}\lambda^3 B_{11} - \frac{1}{R}\lambda^2 n(2B_{13} + B_{31}) - \frac{1}{R}\lambda n^2(B_{12} + 2B_{33})$$

$$- \frac{1}{R} n^3 B_{32} - \lambda(A_{12} - \frac{1}{R}B_{12}) - n(A_{32} - \frac{1}{R}B_{32}) \qquad (3.6.12)$$

$$F_{21} = -\lambda^2(A_{31} + \frac{1}{R}B_{31} - \lambda n(A_{21} + A_{33} + \frac{1}{R}B_{21} - \frac{1}{R^2}D_{33})$$

$$- n^2(A_{23} - \frac{1}{R^2}D_{23}) \qquad (3.6.13)$$

$$F_{22} = -\lambda^2(A_{33} + \frac{2}{R}B_{33} + \frac{1}{R^2}D_{33})$$

$$- \lambda n(A_{23} + A_{32} + \frac{2}{R}B_{23} + \frac{1}{R}B_{32} + \frac{1}{R^2}D_{23})$$

$$- n^2(A_{22} + \frac{1}{R}B_{22}) \qquad (3.6.14)$$

$$F_{23} = -\frac{1}{R}\lambda^3(B_{31} + \frac{1}{R}D_{31}) - \frac{1}{R}\lambda^2 n(B_{21} + 2B_{33} + \frac{1}{R}D_{21} + \frac{2}{R}D_{33})$$

$$- \frac{1}{R}\lambda n^2(2B_{23} + B_{32} + \frac{2}{R}D_{23} + \frac{1}{R}D_{32})$$

$$- \frac{1}{R}n^3(B_{22} + \frac{1}{R}D_{22}) - \lambda(A_{32} - \frac{1}{R^2}D_{32}) - n(A_{22} - \frac{1}{R^2}D_{22}) \qquad (3.6.15)$$

$$F_{31} = -\frac{1}{R}\lambda^3 B_{11} - \frac{1}{R}\lambda^2 n(B_{13} + 2B_{31} - \frac{1}{R}D_{13})$$

$$- \frac{1}{R}\lambda n^2(2B_{33} + B_{21} - \frac{2}{R}D_{33}) - \frac{1}{R}n^3(B_{23} - \frac{1}{R}D_{33})$$

$$- \lambda A_{21} - n A_{23} \qquad (3.6.16)$$

$$F_{32} = -\frac{1}{R}\lambda^3(B_{13} + \frac{1}{R}D_{13}) - \frac{1}{R}\lambda^2 n(B_{12} + 2B_{33} + \frac{2}{R}D_{33})$$

$$- \frac{1}{R}\lambda n^2(2B_{32} + B_{23} + \frac{1}{R}D_{23}) - \frac{1}{R}n^3 B_{22}$$

$$- \lambda(A_{23} + \frac{1}{R}B_{23}) - n A_{22} \qquad (3.6.17)$$

$$F_{33} = \frac{1}{R^2}\lambda^4 D_{11} - \frac{2}{R^2}\lambda^3 n(D_{13} + D_{31}) - \frac{1}{R^2}\lambda^2 n^2(D_{12} + D_{21} + 4D_{33})$$

$$- \frac{2}{R^2}\lambda n^3(D_{32} + D_{23}) - \frac{1}{R^2}n^4 D_{22}$$

$$- \frac{1}{R}\lambda^2(B_{12} + B_{21} - \frac{1}{R}D_{12}) - \frac{2}{R}\lambda n(B_{32} + B_{23} - \frac{1}{R}D_{32})$$

$$- \frac{1}{R}n^2(2B_{22} - \frac{1}{R}D_{22}) - A_{22} + \frac{1}{R}B_{22} \qquad (3.6.18)$$

N_o represents a characteristic loading parameter and is defined by :

$$\frac{N_o}{I} : \frac{N_x^i}{k_x} : \frac{N_y^i}{k_y} : \frac{N_{xy}^i}{k_{xy}} \qquad (3.6.19)$$

where k_x, k_y and k_{xy} are constants

Equation (3.6.19) is written in view that only proportional combined loading is used in the experimental investigation.

The parameters a, b and c in equation (3.6.9) are :

$$a = \lambda^2 k_x + 2\lambda n k_{xy} + n^2 k_y \qquad (3.6.20)$$

$$b = 2\lambda k_{xy} + n k_y \qquad (3.6.21)$$

$$c = \lambda k_y \qquad (3.6.22)$$

Equation (3.6.9) represents a system of three linear homogeneous equations in three unknowns, hence nontrivial solutions exist if and only if :

$$\begin{vmatrix} F_{11} - a N_o & F_{12} & F_{13} + c N_o \\ F_{21} & F_{22} - a N_o & F_{23} - b N_o \\ F_{31} + c N_o & F_{32} - b N_o & F_{33} - a N_o \end{vmatrix} = 0 \qquad (3.6.23)$$

or :

$$F_1 N_o^3 + F_2 N_o^2 + F_3 N_o + F_4 = 0 \qquad (3.6.24)$$

where :

$$F_1 = - a^3 + a(b^2 + c^2) \qquad (3.6.25)$$

$$F_2 = a^2(F_{11} + F_{22} + F_{33}) - b^2 F_{11} - c^2 F_{22} - ab(F_{23} + F_{32}) - bc(F_{12} + F_{21}) + ac(F_{13} + F_{31}) \qquad (3.6.26)$$

$$F_3 = a(- F_{11}F_{22} - F_{11}F_{33} - F_{22}F_{33} + F_{23}F_{32} + F_{12}F_{21} + F_{13}F_{31}) + b(F_{11}F_{23} + F_{11}F_{32} - F_{13}F_{21} - F_{31}F_{12}) + c(F_{21}F_{32} + F_{12}F_{23} - F_{31}F_{22} - F_{13}F_{22}) \qquad (3.6.27)$$

$$F_4 = F_{11}F_{22}F_{33} + F_{12}F_{23}F_{31} + F_{21}F_{13}F_{32} - F_{11}F_{23}F_{32} - F_{21}F_{12}F_{33} - F_{13}F_{31}F_{22} \qquad (3.6.28)$$

The buckling load is then the zero of equation (3.6.23) which is the characteristic equation of the buckling of a composite cylinder.

For more accurate results the analysis continues by substituting the buckling load back in equation (3.6.9) and solving this equation for λ (which has eight roots). These roots are then substituted in the solution equations (3.6.7) and then into the boundary condition equations to obtain finally the critical length of the cylinder at which the shell buckles under the critical load of equation (3.6.24). The complete analysis is then repeated with a new initial cylinder length and a new critical length is obtained and so on till a relation between the cylinder length and the buckling load is established, (Ref. 243).

In this thesis, however, the analysis stops at equation (3.6.24) as the analysis that follows that equation is rigorous and the buckling load obtained is higher than the critical load of equation (3.6.24). Bearing in mind that the non-linear behaviour of composites is not included in the preceding analysis of buckling, which would result in lower buckling loads, the present analysis seems to be justified. Non-linear composite behaviour in buckling has been studied by Morgan and Jones on cross-ply laminated plates, (Ref. 244).

3.6.5 Application to Test Specimens

The solution of Sec. (3.6.4) is coded in a computer program described in Appendix H. The results obtained from the program are summarized in table (3.6.1). In this table the buckling load is given and compared with the failure load. It is obvious that none of the specimens has suffered a buckling failure.

TABLE (3.6.1)

BUCKLING AND FAILURE LOADS
OF THE TEST SPECIMENS
(MN/m^2)

SPECIMEN	LOADING	BUCKLING LOAD	FAILURE LOAD
9B1	Torsion	106.9	60.7
10B1	Axial Compression	134.7	99.3
3B2	Axial Compression	154.7	111.2
4B3	Axial Compression	250.8	126.6
3B4	Axial Compression	235.2	169.4
4B5	Axial Compression	323.1	190.1
4B6	Torsion	73.7	49.1
5B6	Axial Compression	127.0	87.0
3P1*	Torsion	182.0	
14P1	Axial Compression	147.8	90.1

* Specimen 3P1 was not taken to failure

CHAPTER 4

POST-FAILURE BEHAVIOUR OF LAMINATED COMPOSITE STRUCTURES

4.1 INTRODUCTION

Unlike isotropic homogeneous materials, in laminated composite structures the failure of one layer in certain direction does not necessarily imply the failure of this layer in all other directions, nor does it mean the failure of the whole laminate. Consequently, it is of interest to study the behaviour of a laminated structure after the failure of one of its ply to determine the total load carrying capacity. An analogy to this problem is the problem called "post-buckling" of plates and shells where these elements can be loaded with load higher than their buckling load but at a decreased stiffness.

4.2 EXISTING METHODS FOR POST-FAILURE ANALYSIS

4.2.1 Hahn-Tsai Method

This method, (Refs. 34, 245), considers that any failed lamina will support its load, which it was carrying when it has failed, till the total laminate failure. Fig. (4.2.1) describes this theory for the case of cross-ply laminate, i.e., $(0^{\circ}/90^{\circ})$ laminate, under uniaxial tesnion.

The laminate after the failure of 90° layer will have a modulus equal to the modulus of 0° corrected for the area reduction. This method was applied only to this type of laminate under uniaxial loading condition.

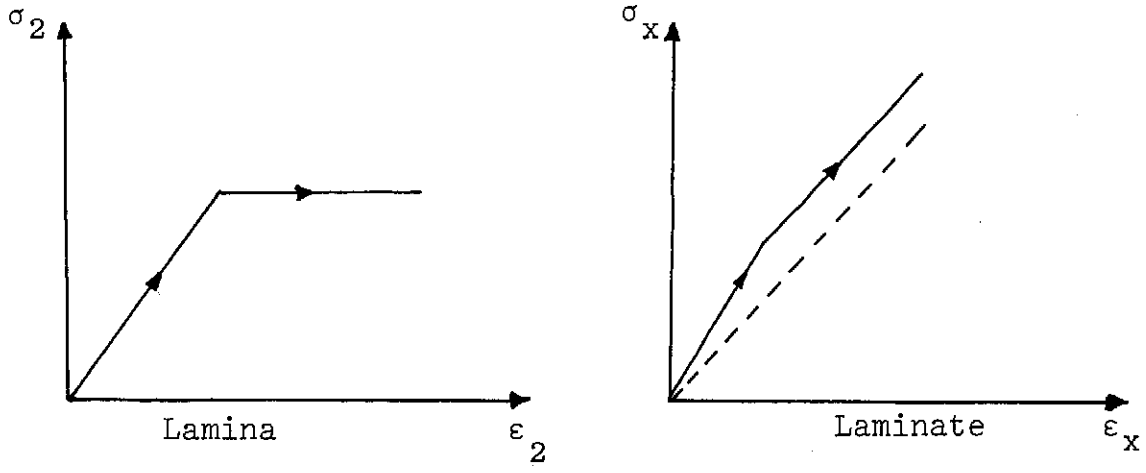

Fig. (4.2.1) Post-failure model in Hahn-Tsai method

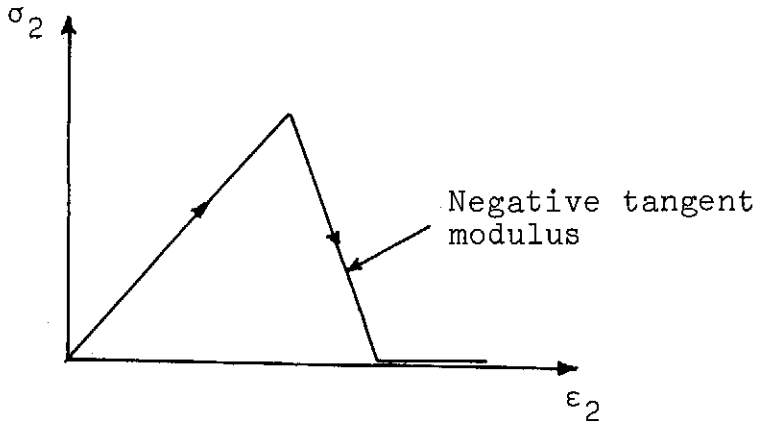

Fig. (4.2.2) Post-Failure model of Petit-Waddoups

4.2.2 Petit-Waddoups Method

In this method, (Ref. 100), the failed lamina unloads gradually. Mathematically, this is done by giving the tangent modulus a relatively high negative value as shown in Fig. (4.2.2).

4.2.3 Chiu Method

Chiu, (Ref. 246), considered the case of instantaneous unloading for the failed layers as shown in Fig. (4.2.3). He used his method for two cases only and concluded that the method's success would depend on its applicability to the general cases. The failure criterion used was Hill criterion, but Chiu determined the mode of failure by checking the strains in the individual layers. Then the failed layer unloads in the direction in which the failure has occured.

4.2.4 McLaughlin-Rosen Method

This is similar to Chiu method as it also considers instantaneous unloading for the failed plies in the direction of failure. The difference between the two is that McLaughlin and Rosen, (Ref. 247), used Hashin-Bagchi-Rosen non-linear technique (Sec. 2.3.2C) in their analysis. Unloading is performed by changing Ramberg-Osgood parameters to give essentially zero stress under large strain.

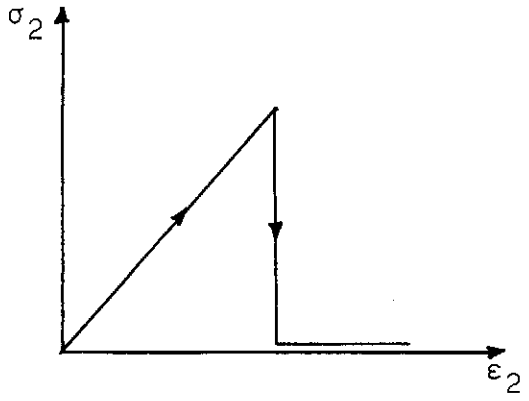

Fig. (4.2.3) Chiu model for post-failure

4.2.5 Foye Method

Foye, (Ref. 248), studied the post-yielding mechanical behaviour of symmetric laminates. He did not consider the behaviour beyond ultimate failure of a lamina. His method introduced a method to analyse the non-linear behaviour after yield has occured in any lamina of the laminate. The conclusion he derived was that more meaningful failure theory would be required for non-linear analysis.

4.2.6 Sandhu Method

Sandhu, (Refs. 103, 104), used his own failure criterion (Sec. 3.3.21) to predict the lamina failure. When the contribution to degradation is dominantly transverse or shear the lamina is assumed to be capable of sustaining longitudinal load.

4.2.7 Brown Method

This method, (Ref. 249), is similar to that of Sandhu but is more general. In addition to Sandhu's assumption Brown added another assumption which is: if the contribution to failure is dominantly longitudinal the lamina is assumed to be capable of carrying transverse load only.

4.2.8 Chou-Orringer-Rainey Method

This method, (Ref. 250), is similar to Chiu method except

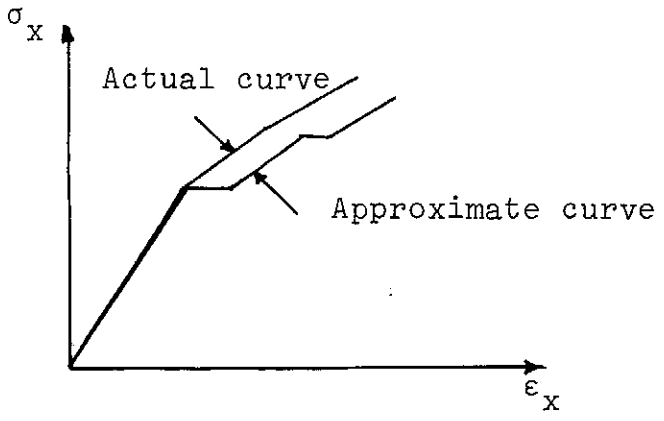

Fig. (4.2.4) Chou-Orringer-Rainey post-failure model

that it considers the non-linear behaviour, and it uses maximum stress failure criterion. It is shown schematically in Fig. (4.2.4).

This method was also used by UMIST Group, (Ref. 20).

4.2.9 Yeow-Brinson Method

Yeow and Brinson, (Ref. 251), introduced a concept different from all the aforementioned concepts and called it "the staggered-failure-surface method". The method is best explained using an example laminate. Consider a symmetric ($0^o/\pm30^o/0^o$) laminate, Fig. (4.2.5), under uniaxial tension in 0^o direction.

Failure will occur first in the $\pm30^o$ plies, but the failure planes do not coincide as failure occurs in some critical locations, i.e., the failure planes for the $+30^o$ ply will be staggered with respect to the -30^o ply failure planes. This means that the $\pm30^o$ plies can still transfer the load from ply to ply by shear stress. The method then suggests that after the failure of $\pm30^o$ plies, all stiffnesses of this failed laminae are zeroed, and only half of thickness of $\pm30^o$ is subtracted. In the example shown in Fig. (4.2.5) the thickness of the laminate before failure occurs is 8t, and becomes 6t after the failure of ±30 layers.

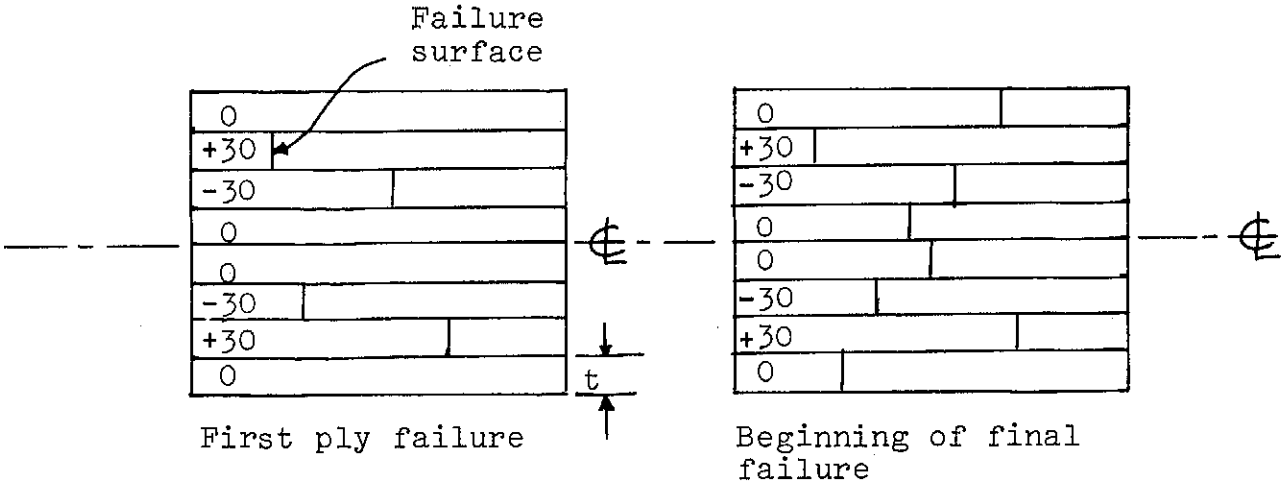

Fig. (4.2.5) Post-failure model used by Yeow and Brinson

4.2.10 Puck-Förster-Knappe Method

This method, (Refs. 179, 252), uses Puck-Schneider failure criterion. Transverse and shear failure are associated with matrix failure. At resin cracking the lamina transverse and shear elastic constants do not vanish immediately, but sink gradually towards zero with increasing strain. The overexertion factor :

$$U = \sqrt{\left(\frac{\sigma_1}{X_m}\right)^2 + \frac{\tau_{12}}{S} + \left(\frac{\sigma_2}{Y}\right)^2} - 1 \qquad (4.2.1)$$

is introduced from which the correction factor η is obtained for each step, Fig. (4.2.6). Then the reduced values ηE_2, ηG_{12} and $\eta \nu_{12}$ are used for the next step calculations.

4.2.11 Liverpool Group Method

Hull et al, (Refs. 18, 19), used Puck's failure criterion to predict the onset to non-linearity. Beyond the failure predicted by this criterion "netting" analysis is employed to predict the total failure, i.e., the resin is assumed not to transfer any load.

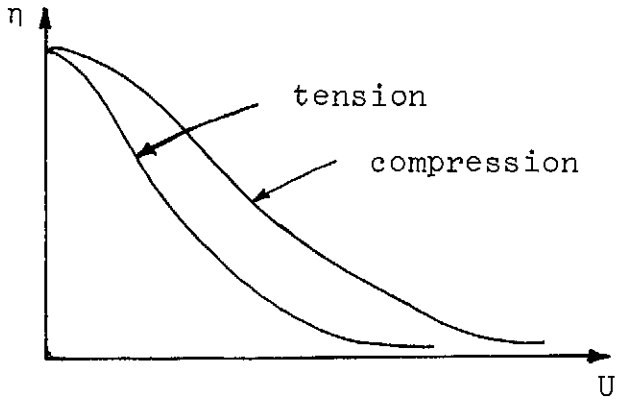

Fig. (4.2.6) Correction factor for Puck-Forster-Knappe analysis

4.2.12 Summary

There exist at least eleven different methods for the analysis of post-failure behaviour of laminated fibre reinforced composites. The difficulty in assessing these analyses comes from the obvious contradicting assumptions used by the investigators, yet they all show fair or even good agreement between their predictions and experimental results. One obvious reason for the agreement between theoretical and experimental results is that some of these techniques were compared with experimental results obtained from testing of special laminates (e.g. cross-ply laminate) under uniaxial loading. This means that some of the discussed methods lack generality.

The failure criterion chosen to predict the first ply failure, and the non-linearity considerations are important factors which affect the post-failure behaviour. Hull et al, for instance, considered the beginning of the degradation of the lamina to be the ultimate failure for the matrix material, hence they eliminated the matrix from the analysis above that level. The lamina in fact can still support load in the transverse and shear directions above that level even though degradation has initiated.

Detection of the first ply failure can be made with the use of acoustic emission technique (see Appendix F and Ref. 253), or replication technique, (Ref. 254).

4.3 A PROPOSED ANALYSIS FOR POST-FAILURE BEHAVIOUR

Before developing the present model, two of the existing post-failure methods were tested against the experimental data of Appendix B. These two methods are: Chui method and Brown method. These, in fact, represent the rest of the methods as most of the other methods are special cases of these two. In Chiu's theory, the failed lamina unloads in the direction of failure, while in Brown's theory the failed lamina unloads in two directions, one of them is the failure direction. Both of these models resulted in a step in the stress-strain curves whenever a layer failed and unloaded. But the experimental stress-strain response of the test specimens did not show any such step. Rather the response in all the specimens was smooth, though non-linear.

The present theory proposes that the failed layer does not unload instantaneously, but gradually following a decreasing exponential function as shown in Fig. (4.3.1). Furthermore, this unloading occurs only in the failure direction, and the thickness of the failed layer is not removed from the laminate because physically it is still there. In this way, when the applied load increases, and any strain in any layer reaches its maximum value, the corresponding secant modulus of this ply decreases gradually to zero when the layer strain increases to infinity.

The failure criterion, used in this analysis, is the modified maximum criterion which is also proposed in this thesis, (Sec. 3.4). The reason for choosing this criterion is very clear here, as the mode of failure and the non-linear analysis are needed for the post-failure behaviour, and this criterion provides them.

After every event of failure, as predicted when any strain reaches its maximum value, the appropriate ply in which this failure has just occured unloads as described above, then the capability of the remaining layers to carry the load is checked. If the rest part of the laminate cannot carry the load, then the laminate suffers gross failure. Mathematically, this is taken to be when the laminate stiffness matrix becomes singular, i.e., has no inverse.

4.4 APPLICATION OF THE THEORY TO THE TEST SPECIMENS

The theory proposed above was coded in the form of a computer program written in FORTRAN, (Appendix I), and was applied to the multilayered specimens of tubes B4 and B5, (Appendix A).

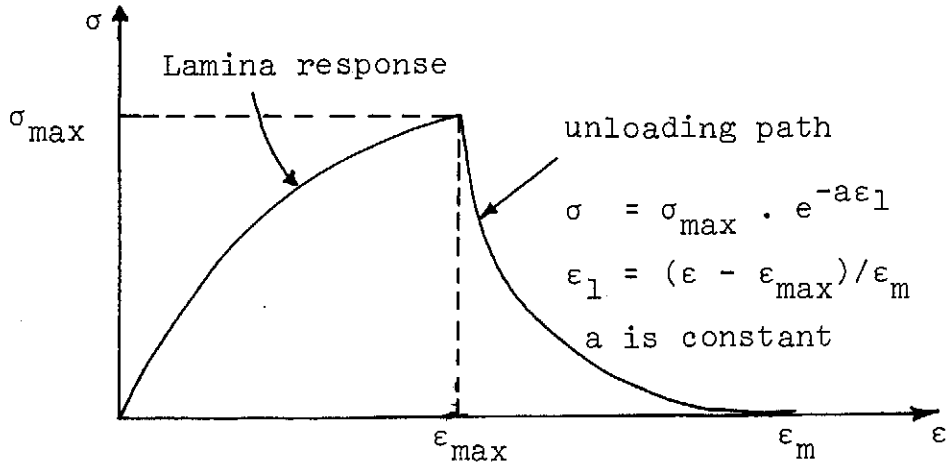

Fig. (4.3.1) Proposed post-failure model

In Fig. (4.4.1), the new method, together with Chiu's and Brown's methods, are shown applied to the test specimen 1B4 which is a laminated tube of ($\pm 85^{o}/\pm 45^{o}/\pm 85^{o}$) and was tested under internal pressure.

The three methods gave same response with the increasing load till hoop stress of 14o MN/m^2. It is to be noted here that non-linear analysis and the modified maximum strain criterion were employed with both other methods, otherwise, the use of these methods as given by their investigators would reveal different response.

At this load, the $\pm 45^{o}$ plies failed in transverse tension mode. According to Chiu's method the $\pm 45^{o}$ plies unloaded in this mode instantaneously, and this resulted in steps in the stress-strain curves. According to Brown's method, however, the $\pm 45^{o}$ layers unloaded in both transverse tension and shear loading and resulted in higher decrease in the stiffness of the laminate. With the use of gradual unloading (in transverse tension mode) of the present method the theoretical response was as smooth as the experimental curve.

According to Brown's method, at hoop stress of 183 MN/m^2, the laminate, being weaker than it actually was, suffered further failure in the $\pm 85^{o}$ plies (in transverse compression). This failure did not occur according to the other two methods until the hoop stress reached 278 MN/m^2.

Gross failure of the laminate occured according to Brown's analysis at 297 MN/m^2 hoop stress, whereas it occured at 353 MN/m^2 according to the present method and Chiu's method. The failure during the test occured at hoop stress of 340.4 MN/m^2.

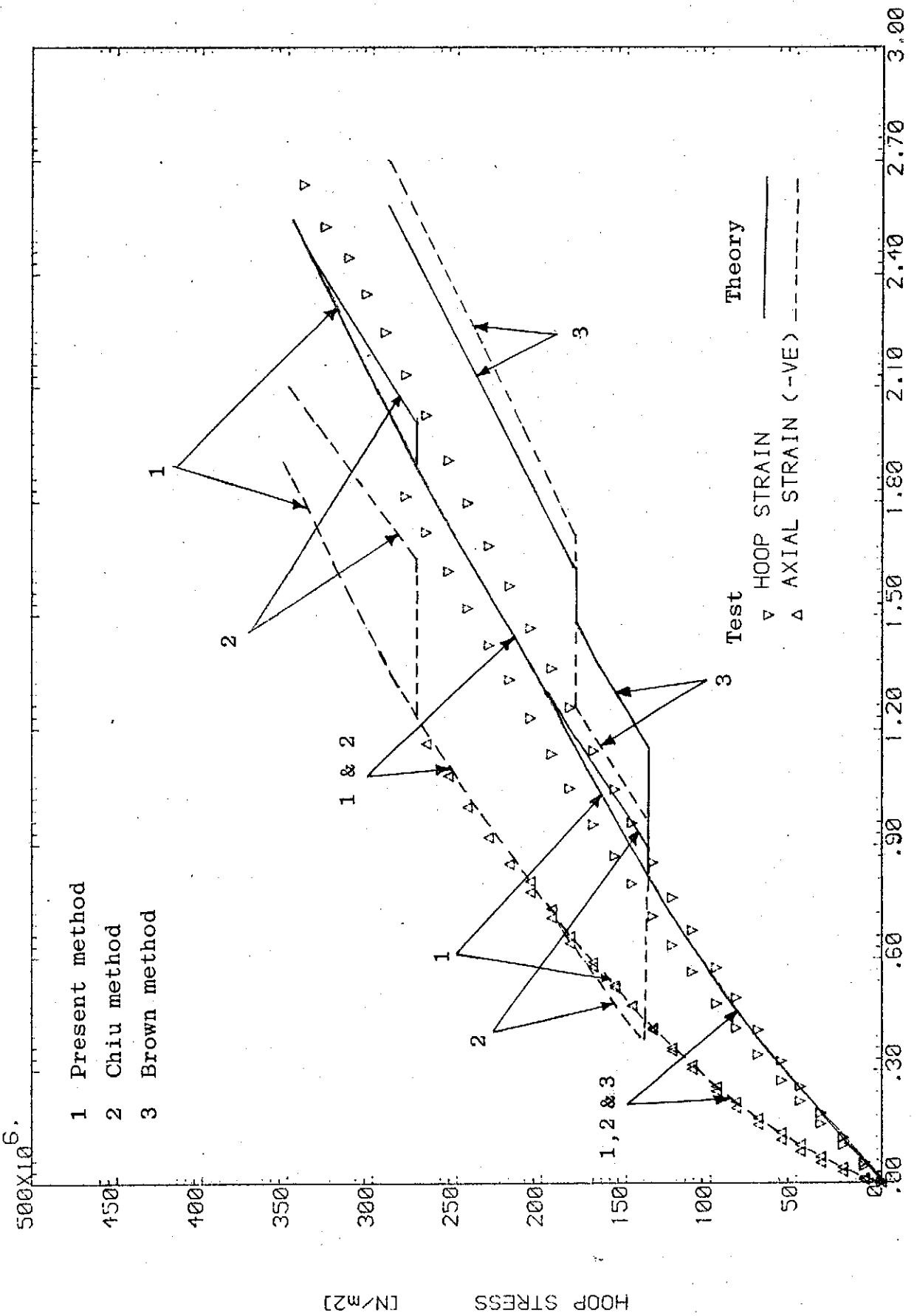

Fig. (4.4.1) Application of post-failure method to test specimen 1B4

CHAPTER 5

EXPERIMENTAL INVESTIGATION

5.1 OBJECTIVES

The main objective of the experimental investigation is to obtain experimental data for composite laminates under combined loading conditions to compare them with the different theoretical findings, hence to accept or reject the appropriate theory.

As macromechanical behaviour is adopted in this thesis, the material properties (elastic and strength properties) of a single composite layer must be determined experimentally and not from the properties of the constituents. This is another aim of the experimental research.

Sophisticated test rigs for testing composite cylinders under biaxial loadings exist at some research establishments (e.g., Refs. 40, 190, 255-257), but there is a need to develop a simple test rig, and this is the third aim of the experimental work of this thesis.

5.2 TEST EQUIPMENT

5.2.1 The Test Rig

The details of the test rig are given in Appendix J and shown in Fig. (5.2.1). Basically, the test rig consists of two end grips which are inserted inside both ends of the test tubular specimen. According to the test required, these grips are either left free so that the cylinder can slide over them (for internal pressure test), or they are connected to the cylinder to transfer the external load from the testing machine to the specimen. In this latter case, end fittings are also needed to grip the rig to the appropriate testing machine, Figs. (5.2.2) and (5.2.3). When only internal pressure loading is applied to the specimen, the end grips are stopped from moving out by two stiff parallel surfaces. The surfaces of a compression testing machine were used in this present programme, Fig. (5.2.4). The axial compression test is the easiest, as the specimen is placed without any grip on the test machine, Fig. (5.2.5). Combined loadings of internal pressure and axial load, or internal pressure and torsional load are also possible. The combination of axial and torsional loading was not possible as the existing torsional machine does not apply axial load. Only the axial load due to internal pressure

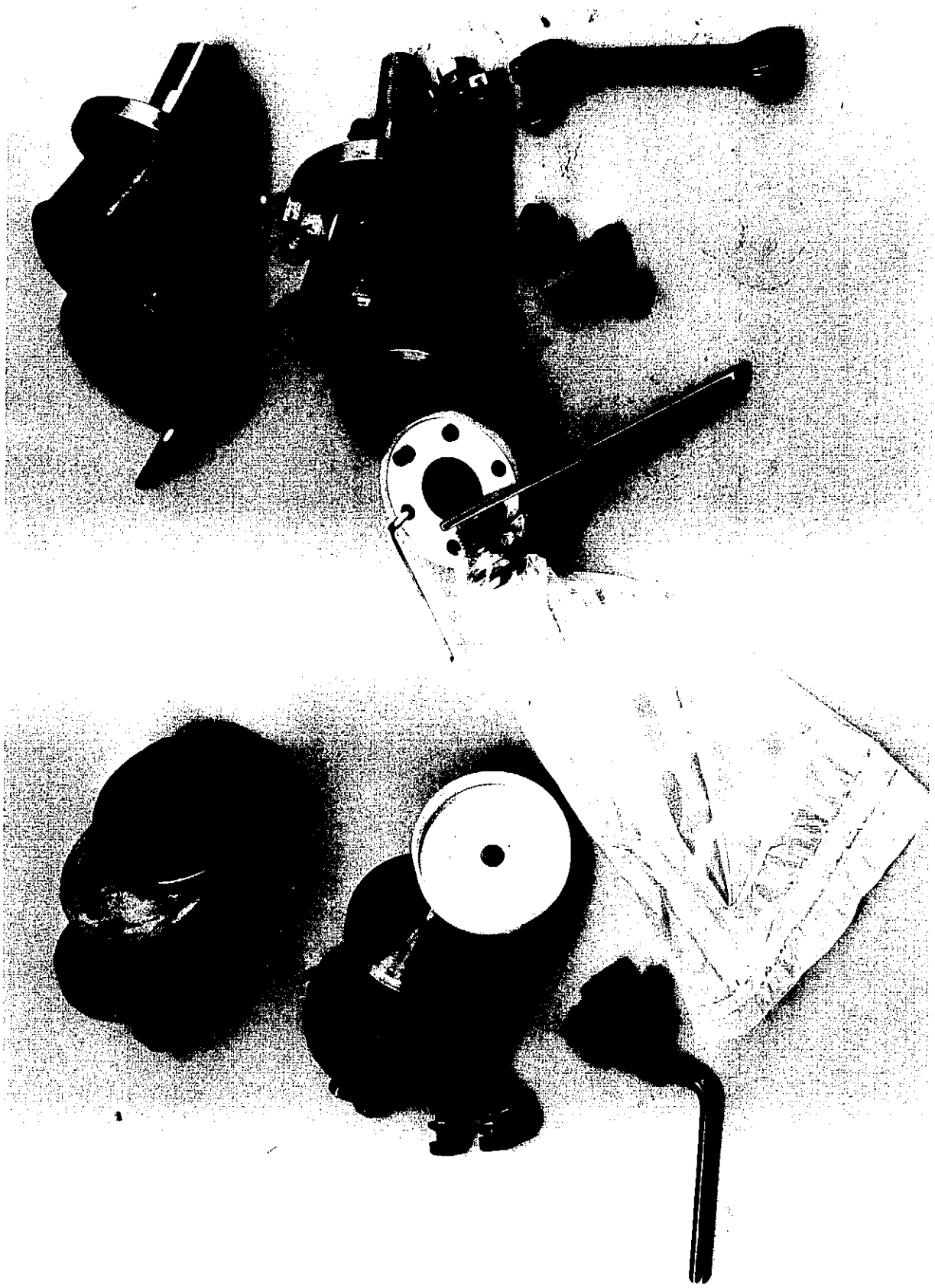

Fig.(5.2.1) Components of the test rig

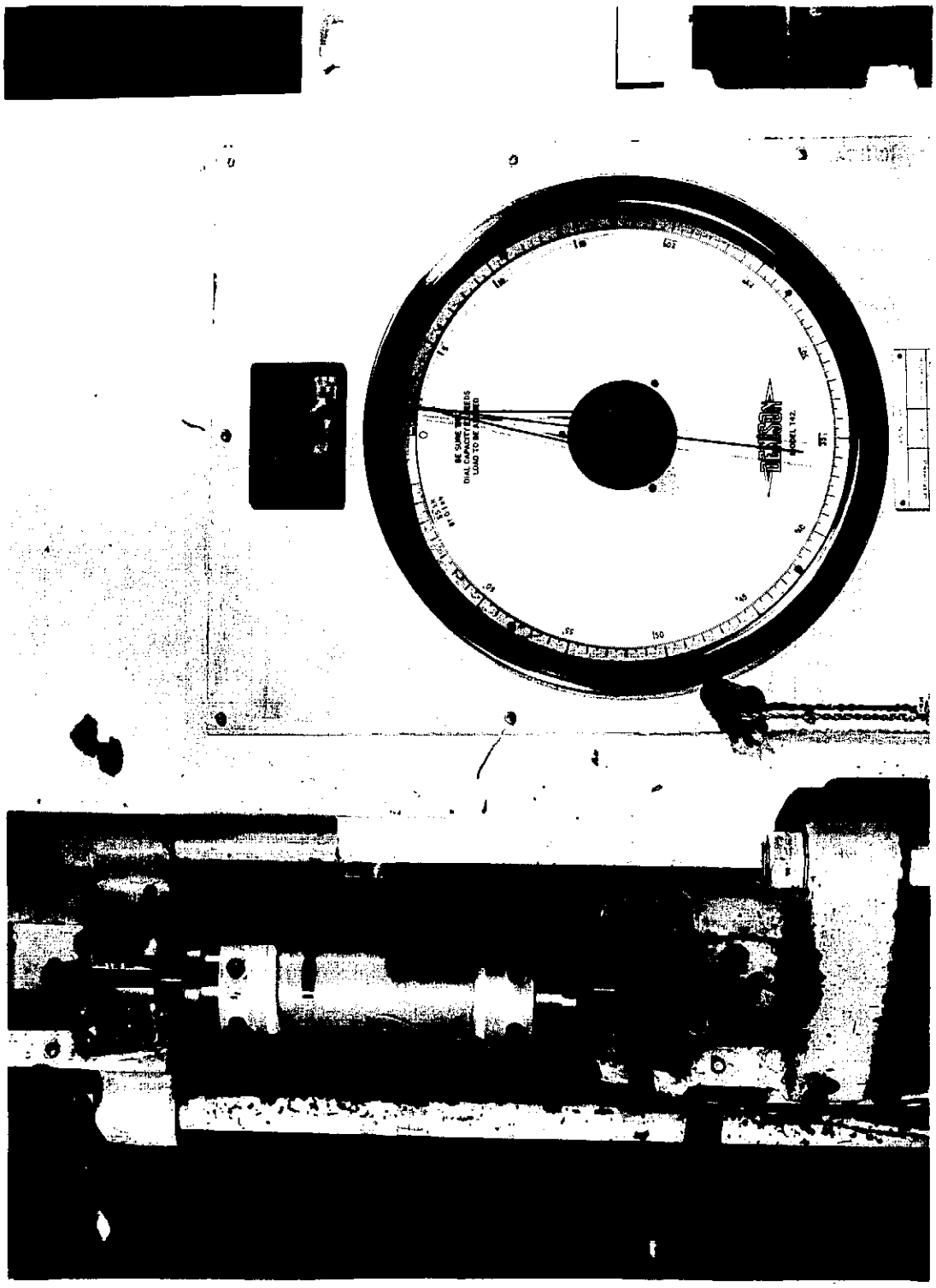

Fig.(5.2.2) Axial tension test

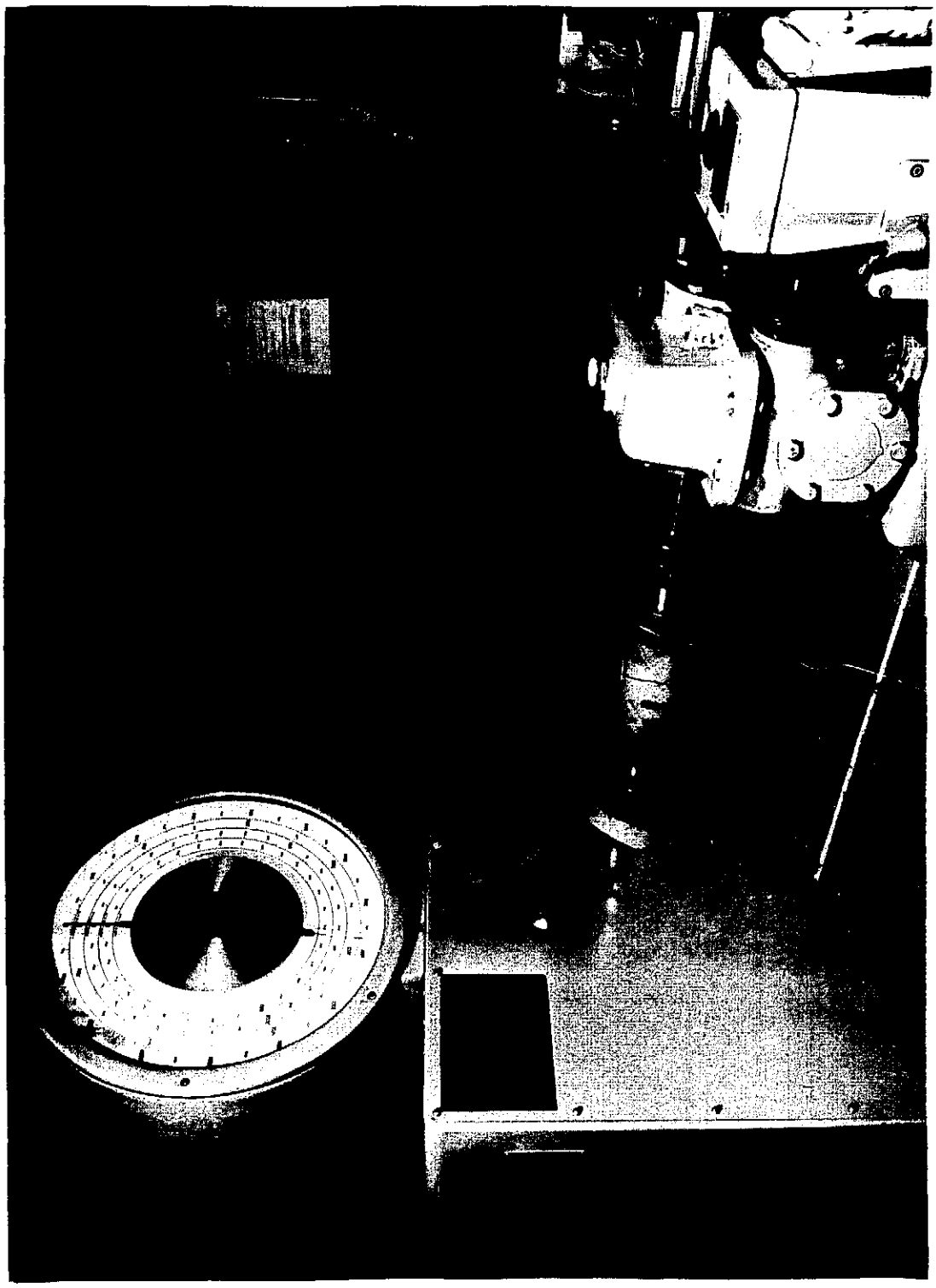

Fig.(5.2.3) Torsion test

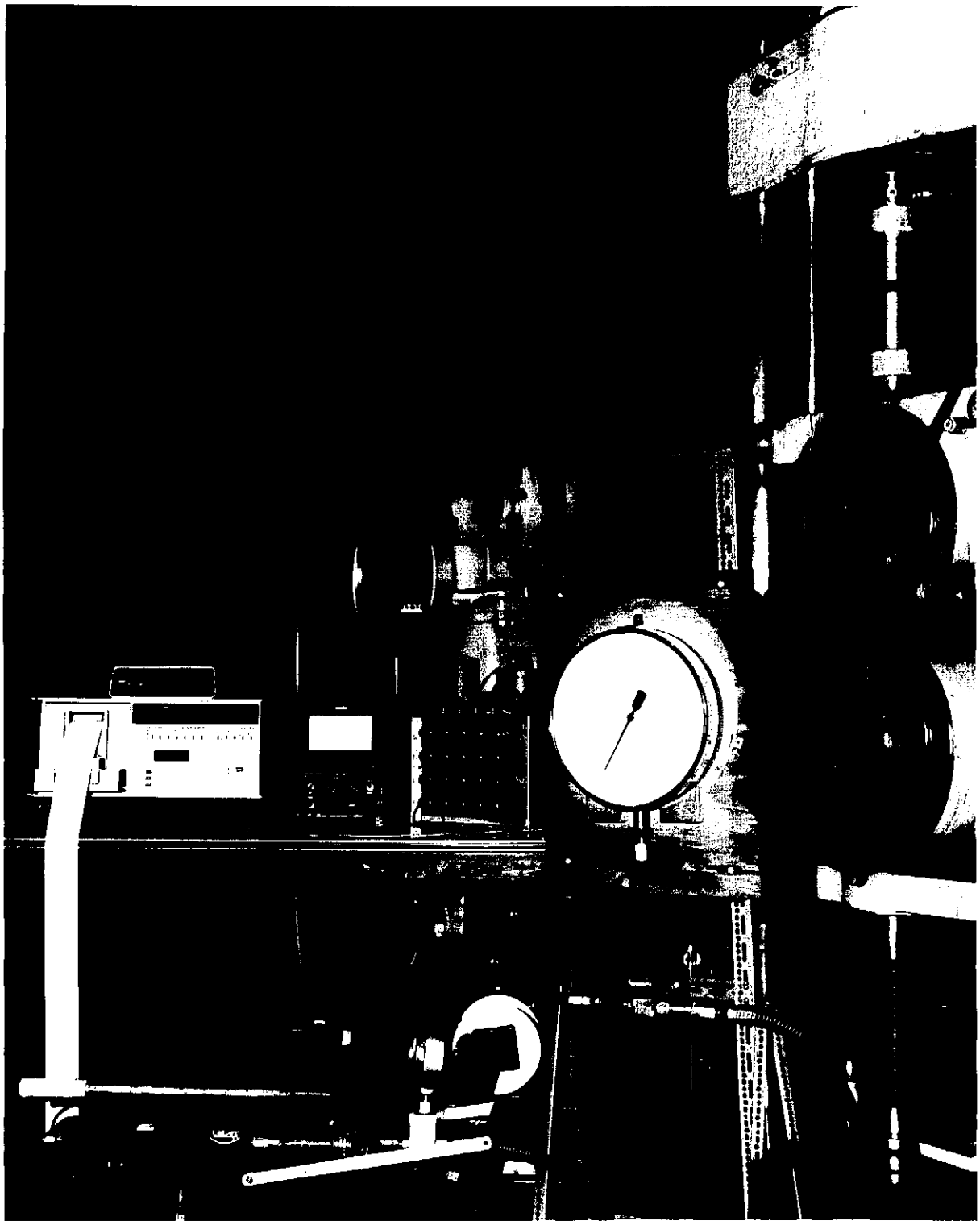

Fig.(5.2.4) Internal pressurization test

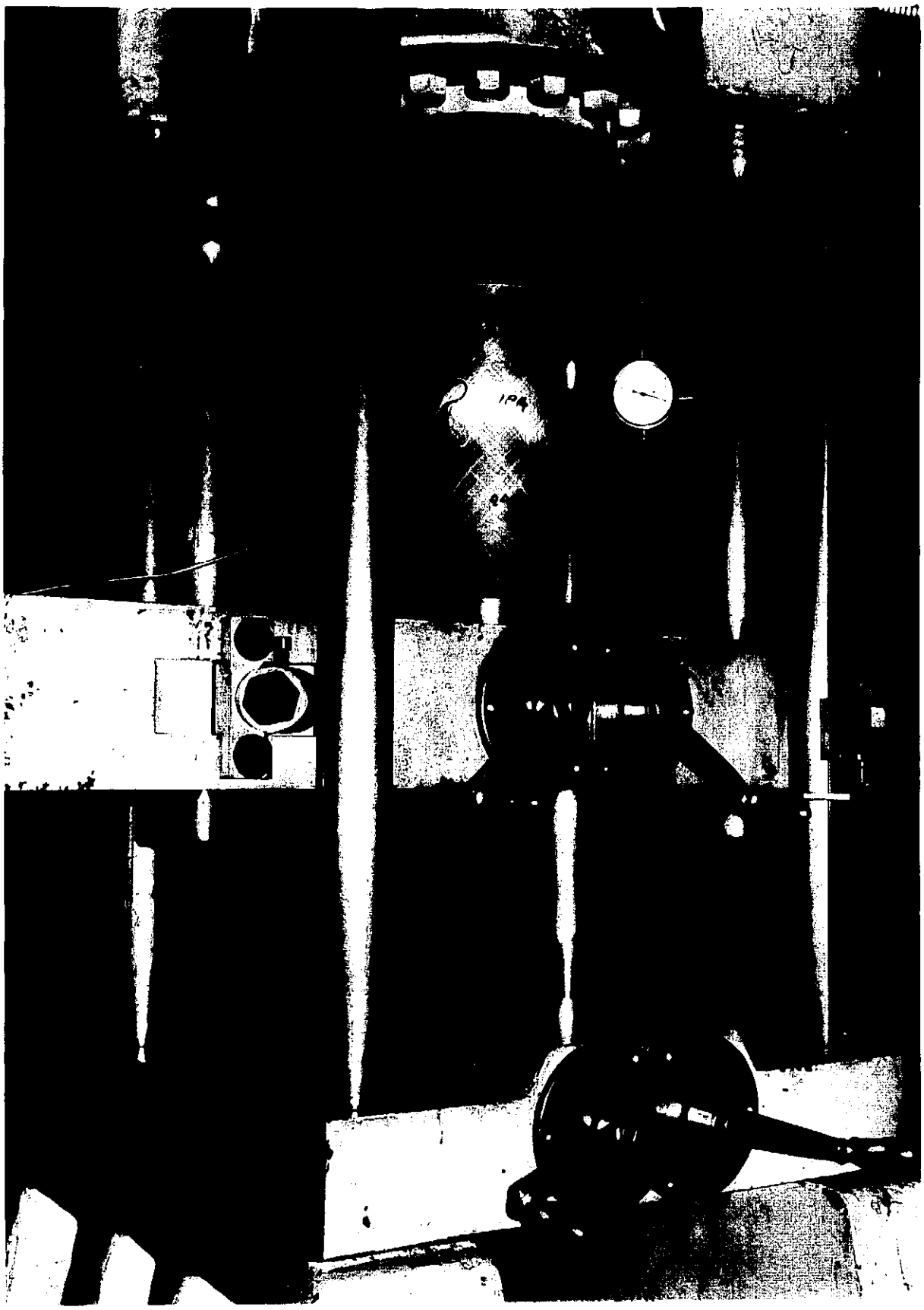

Fig.(5.2.5) Axial compression test

was possible to combine with the torsional load. Fig. (2.5.6) shows a test specimen under load ratio $\sigma_x : \sigma_y$ = 0.5 : 1.0, where the end grips are connected to the specimen, and the whole unit is free from any external load.

5.2.2 Sealing of the Test Specimen

"O" rings were used in the test rig for sealing the cylindrical specimens under internal pressure. Some specimens, however, showed large radial deflection at the "O" ring position, Fig. (2.4.4), so the "O" rings were not effective. Polythene sealing cups were cast and placed at the ends of the tube. These, due to their flexibility, opened out with the increase of pressure and prevented any oil leakage.

5.2.3 Lining of the Test Specimen

As mentioned in Sec. 3.4, the degradation in the test specimens occur well before the ultimate failure. This is due to cracks in the matrix of the specimens and at certain load, when these cracks come in one line, the specimen weeps. This weepage prevents the continuation of the test due to drop in the internal pressure. To overcome this, the tubular specimen must be lined. Different types of liners have been used. Carswell and Gemmell, (Ref. 258), for instance, used two different types, the first one was a solution of latex rubber applied to the internal surface and hardened, and the other type was a thick rubber sleeve.

In the present work, simple and cheap liners were used. The idea developed from using children's balloon, as a ready and cheap liner. Two problems were envisaged, first, the balloon did not have consistant thickness, and second, the oil of the internal pressure test affected the rubber of the balloon. Later, a stronger balloon was used. This was a Durex sheath (used usually as a contraceptive), but the oil also affected its material.

A neoprene rubber bag was later used. This was not affected by the oil, but was not flexible enough, so it was subjected to some load and failed at its neck.

Polythene bags were then used, but they were very weak at the bottom due to the seam.

The final liner which proved to be successful was a polythene sheet which was welded by an electric polythene welder. Many layers were used and many welding lines were possible as shown in Fig. (5.2.7) where all the other liners are also shown.

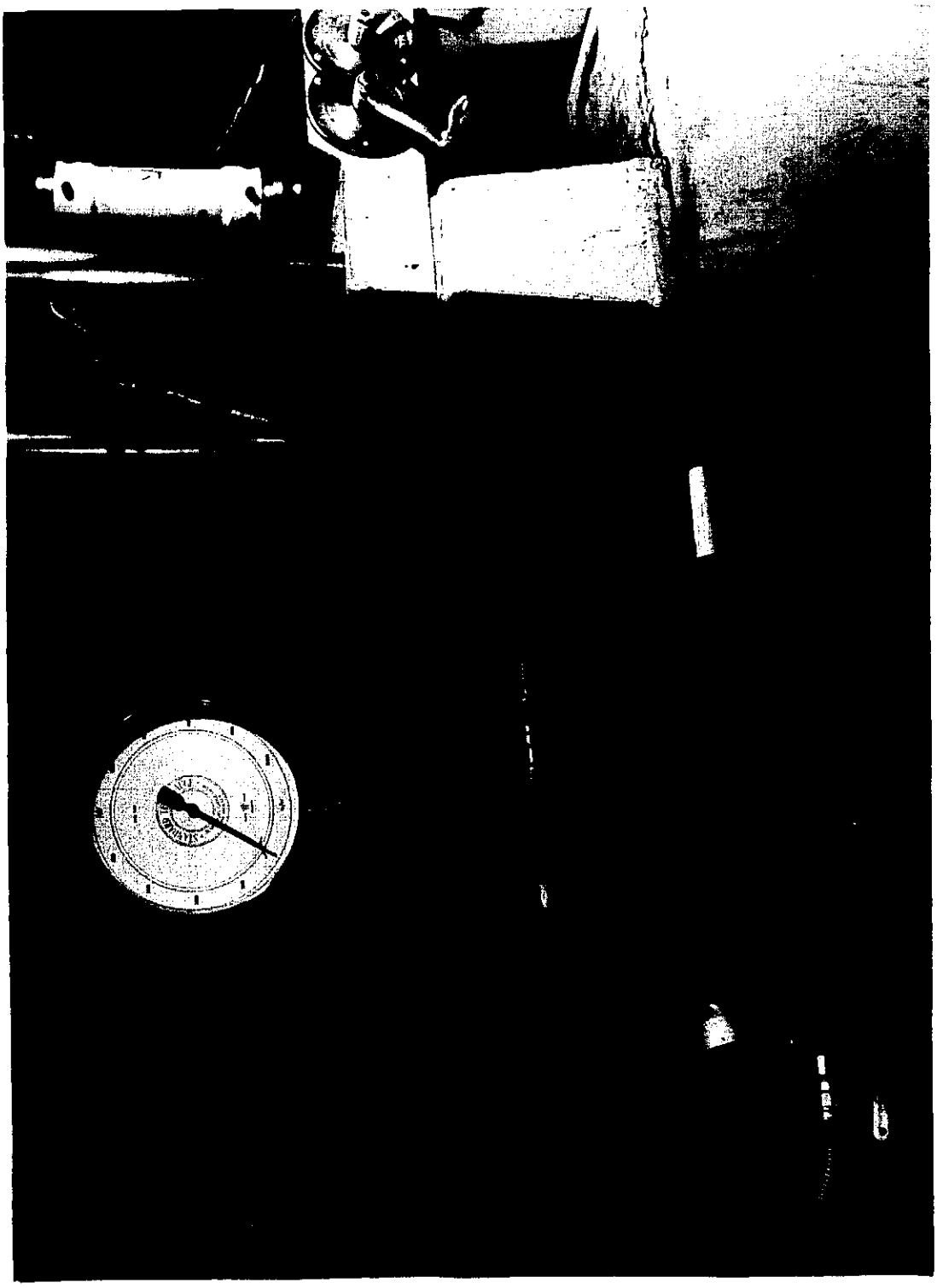

Fig.(5.2.6) Specimen under load ratio 0.5:1.0:0.0

Fig.(5.2.7) The different types of specimen liners

5.2.4 Other Equipment

In addition to the test machines and the test rig the following equipment was also used in the tests :

a) hydraulic pump for the internal pressurization tests;

b) pressure gauge (0 to 10,000 psi);

c) pressure transducer;

d) data logger;

e) digital volt meter;

f) stabilised voltage power supply;

g) strain gauge bridge zero instrument.

These are all shown in Fig. (5.2.4).

5.3 THE TEST SPECIMENS

5.3.1 Details of the Test Specimens

The dimensions, orientation and the stacking of the 50 test specimens are given in Appendix A. The specimens are all filament-wound tubes and were supplied by Bristol Aerojet Limited and Prodorite Limited in the form of long tubes.

5.3.2 Specimen Preparation

The specimens were first cut from the long tubes, then they were reinforced at their ends. These ends were then drilled (as appropraite) using a drilling jig, Fig. (5.3.1). The strain gauges were then bonded as shown in Fig. (B.1). The test rig was then assembled for every test, as described in Appendix J, and placed on the appropriate testing machine. In the case of combined loading, a loading table was arranged beforehand so that the loads can be applied simultaneously from the pump and the external load testing machine.

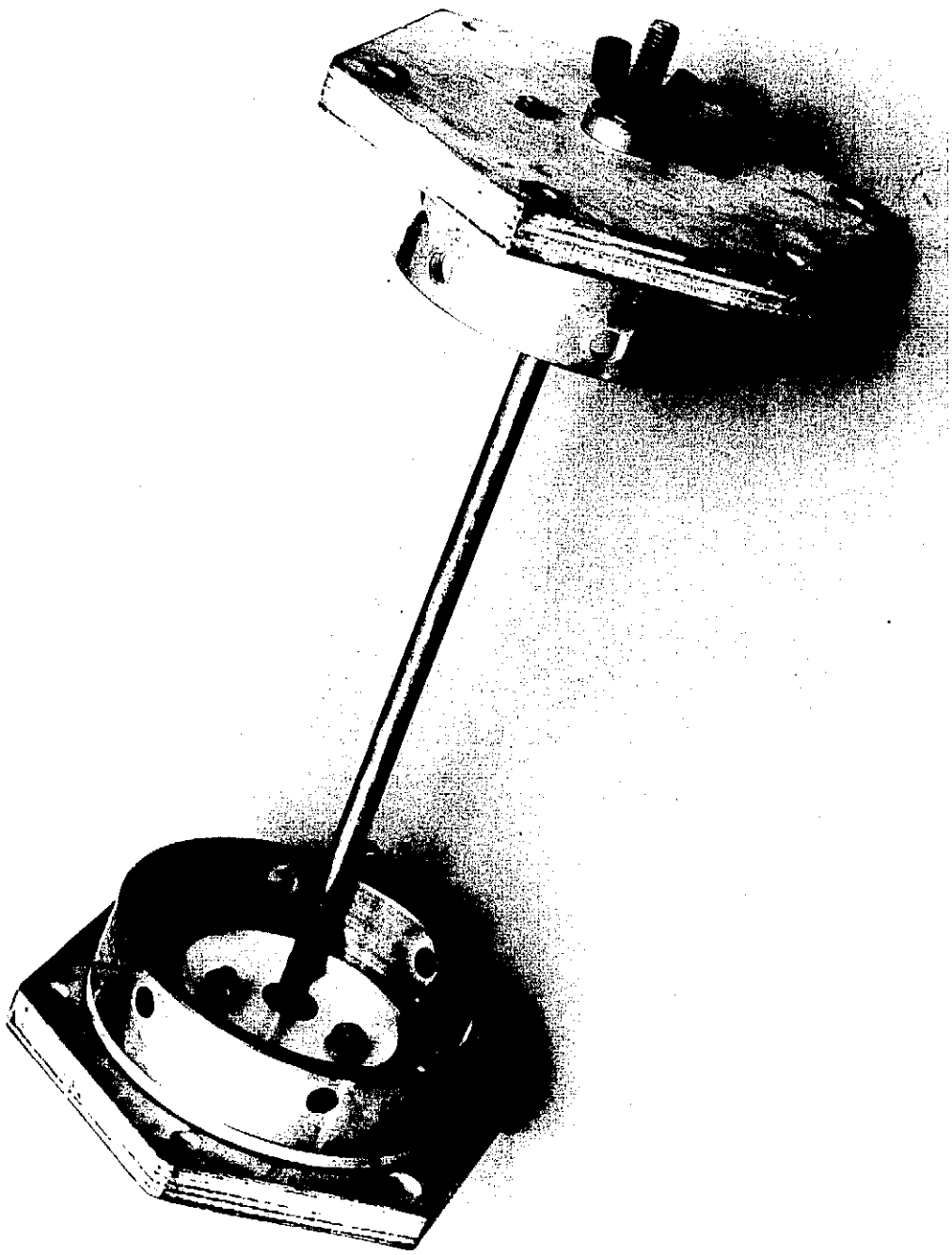

Fig.(5.3.1) The drilling jig

5.4 THE TEST RESULTS

5.4.1 The Stress-Strain Data

The stress-strain data of all the specimens are given in Appendix B. As some of these curves do not reach the ultimate failure point for some reasons given in Appendix B, the ultimate or the maximum loads are given in Table (5.4.1). Ultimate load means that failure occured at this load, whereas the maximum load is the maximum value recorded during the test before the ultimate load.

Most of the specimens failed at their test sections, Fig. (5.4.1), but some specimens failed at the end reinforcements, Table (5.4.1). In this latter case the reason for such failure was almost the same, that is the end reinforcements were not bonded properly, hence the interface between the end reinforcements and the specimen failed first, and then led to specimen failure at the holes of the bolts near the ends.

5.4.2 Single Layer Properties

The specimens of tubes B1 and B6 are $\pm 85^{\circ}$ laminates. They are as near as possible to the circumferential winding laminates. They were tested to obtain the single layer properties of Bristol Aeroject tubes. Regarding Prodorite tube, the company ceased GRP fabrication and no unidirectional tubes were supplied by them, hence the single layer properties were not obtained and the testing of Prodorite specimens did not continue.

It is to be mentioned here that the longitudinal compression properties were not obtained by test as these require either tube wound at 0°, or external pressure test for circumferentially wound tubes. Both of these were not available, and the longitudinal properties were obtained by comparison with other materials.

The longitudinal (tension and compression) properties were taken to be linear, while the transverse and the shear properties were non-linear as shown in Figs. (5.4.2) to (5.4.7). Table (5.4.2) gives the stiffnesses, the strengths and the aximum strains as obtained from specimens of tubes B1 and B6. The properties were obtained by iteration method. That is, some properties were assumed and applied to the specimens of $\pm 85^{\circ}$, when the calculated properties of $\pm 85^{\circ}$ specimens were equal to these of the tests, then the assumed properties were considered to be the single layer properties of the glass/epoxy used.

Table (5.4.1) Failure loads of the test specimens

Specimen	Loading $\sigma_x^o : \sigma_y^o : \tau_{xy}^o$	Ultimate or maximum load (MN/m^2)			Remarks on failure
1B1	0.0 : 1.0 : 0.0	max.	725.9	hoop	was not taken to failure
2B1	-1.0 : 0.0 : 0.0	max.	77.6	ax. comp.	was not taken to failure
3B1	1.0 : 0.0 : 0.0	max.	14.3	ax. tens.	was not taken to failure
4B1	0.0 : 0.0 : 1.0	max.	50.1	shear	was not taken to failure
5B1	0.0 : 1.0 : 0.0	max.	876.8	hoop	was not taken to failure
6B1	-1.0 : 0.0 : 0.0	ult.	69.0	ax. comp.	failed at the ends
7B1	0.0 : 1.0 : 0.0	max.	932.1	hoop	did not fail at this load
8B1	1.0 : 0.0 : 0.0	ult.	24.6	ax. tens.	failed at the test section
9B1	0.0 : 0.0 : 1.0	ult.	60.7	shear	failed at the test section
10B1	-1.0 : 0.0 : 0.0	ult.	99.3	ax. comp.	failed at the test section
1B2	0.0 : 1.0 : 0.0	ult.	834.9	hoop	failed at test section
2B2	0.5 : 1.0 : 0.0	ult.	80.8	hoop	failed at test section
3B2	-1.0 : 0.0 : 0.0	ult.	111.2	ax. comp.	failed at test section
4B2	1.0 : 0.0 : 0.0	ult.	33.4	ax. tens.	failed at test section
5B2	0.5 : 1.0 : 0.2	ult.	80.9	hoop	failed at test section
6B2	0.5 : 1.0 : 0.1	ult.	81.4	hoop	failed at test section
7B2	0.0 : 1.0 : 0.0	max.	371.6	hoop	was not taken to failure
8B2	0.I : 1.0 : 0.0	ult.	815.4	hoop	failed along the specimen
1B3	0.0 : 1.0 : 0.0	max.	196.0	hoop	did not fail
2B3	0.5 : 1.0 : 0.0	max.	189.1	hoop	failed at the ends
3B3	1.0 : 0.0 : 0.0	max.	79.9	ax. tens.	was not taken to failure
4B3	-1.0 : 0.0 : 0.0	ult.	126.6	ax. comp.	failed at the test section
5B3	0.5 : 1.0 : 0.1	max.	270.8	hoop	failed at the ends
6B3	-0.5 : 1.0 : 0.0	ult.	118.8	hoop	failed at test section
7B3	0.0 : 1.0 : 0.0	max.	191.6	hoop	did not fail

Table (5.4.1) Continued

Specimen	Loading $\sigma_x^o : \sigma_y^o : \sigma_{xy}^o$	Ultimate or maximum load (MN/m^2)			Remarks on failure
1B4	0.0 : 1.0 : 0.0	ult.	340.4	hoop	failed at test section
2B4	0.5 : 1.0 : 0.0	max.	248.8	hoop	failed at the ends
3B4	-1.0 : 0.0 : 0.0	max.	169.4	ax. comp.	failed at the ends
4B4	1.0 : 0.0 : 0.0	max.	120.8	ax. tens.	failed at the ends
5B4	0.5 : 1.0 : 0.1	max.	347.9	hoop	failed at the ends
6B4	0.5 : 1.0 : 0.2	max.	298.1	hoop	failed at the ends
1B5	0.0 : 1.0 : 0.0	max.	275.3	hoop	beginning of failure at test section
2B5	0.5 : 1.0 : 0.0	max.	267.1	hoop	failed at the ends
3B5	1.0 : 0.0 : 0.0	max.	71.0	ax. tens.	was not taken to failure
4B5	-1.0 : 0.0 : 0.0	ult.	190.1	ax. comp.	failed at test section
5B5	0.5 : 1.0 : 0.1	max.	277.1	hoop	failed at the ends
6B5	-0.5 : 1.0 : 0.0	ult.	158.4	hoop	failed at test section
1B6	0.0 : 0.0 : 1.0	ult.	45.6	shear	failed at test section
2B6	1.0 : 0.0 : 0.0	ult.	17.7	ax. tens.	failed at test section
3B6	1.0 : 0.0 : 0.0	ult.	22.8	ax. tens.	failed at test section
4B6	0.0 : 0.0 : 1.0	ult.	49.1	shear	failed at test section
5B6	-1.0 : 0.0 : 0.0	ult.	87.0	ax. comp.	failed at test section
6B6	0.0 : 1.0 : 0.0	max.	609.3	hoop	did not fail
7B6	0.0 : 1.0 : 0.0	max.	744.5	hoop	did not fail
3B1	0.0 : 0.0 : 1.0	max.	27.3	shear	was not taken to failure
4P1	1.0 : 0.0 : 0.0	max.	56.2	ax. tens.	was not taken to failure
13P1	0.1 : 1.0 : 0.0	max.	70.9	hoop	was not taken to failure
14P1	-1.0 : 0.0 : 0.0	ult.	90.1	ax. comp.	failed at test section

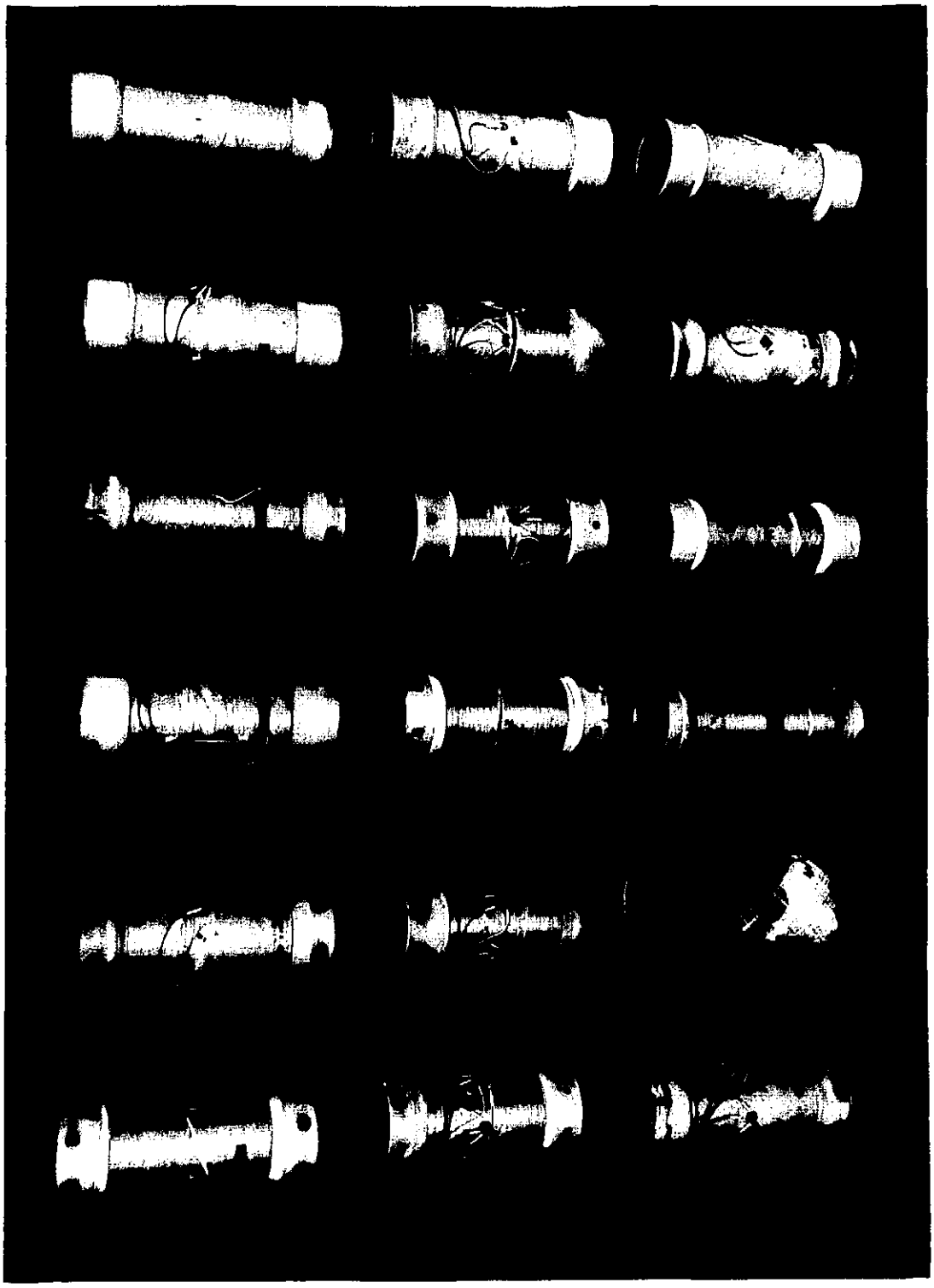

Fig.(5.4.1) Samples of the failed specimens

The longitudinal strength, X, was not obtained from the experiments as failure was not reached in this mode. Thus it was calculated from the following relation :

$$X = \sigma_f \cdot V_f + \sigma'_m \cdot (1 - V_f) \qquad (5.4.1)$$

where :

σ_f is the strength of the fibre

V_f is the volume content of the fibre

σ'_m is the stress in the matrix at the failure.

The stress σ'_m can be neglected when compared with σ_f. The fibre strength was supplied by Bristol Aerojet to be 1,992 MN/m^2 (average of five NOL ring tests).

Table (5.4.2) Single layer properties of the glass/epoxy

Property	As derived from specimens of tube B1 of V_f = 63.24%	As derived from specimens of tube B6 of V_f = 56.39%
E_1	44.50 GN/m^2	31.40 GN/m^2
E_2	13.50 GN/m^2	11.44 GN/m^2
G_{12}	5.64 GN/m^2	4.16 GN/m^2
ν_{12}	0.183	0.155
ν_{21}	0.0555	0.0565
X	1,260.0 MN/m^2	1,120.0 MN/m^2
X'	765.0 MN/m^2	680.0 MN/m^2
Y	24.1 MN/m^2	22.4 MN/m^2
Y'	98.0 MN/m^2	86.0 MN/m^2
S	48.0 MN/m^2	41.2 MN/m^2
ε_{1t}	2.83%	3.57%
ε_{1c}	1.72%	2.16%
ε_{2t}	0.198%	0.243%
ε_{2c}	1.25%	1.16%
γ_u	4.25%	3.31%

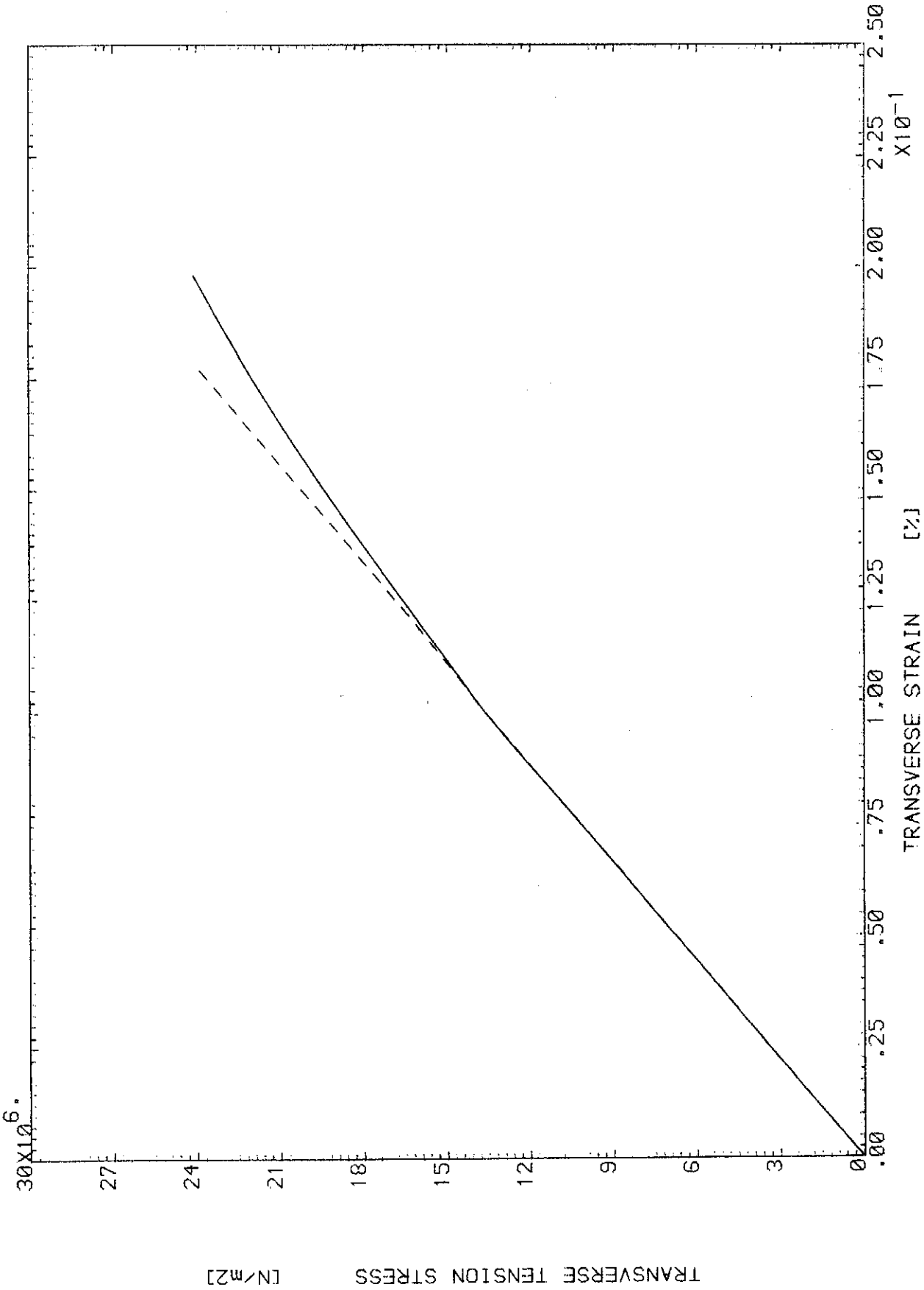

Fig.(5.4.2) LAMINA TRANSVERSE TENSION RESPONSE, V.F.= 63.24 %

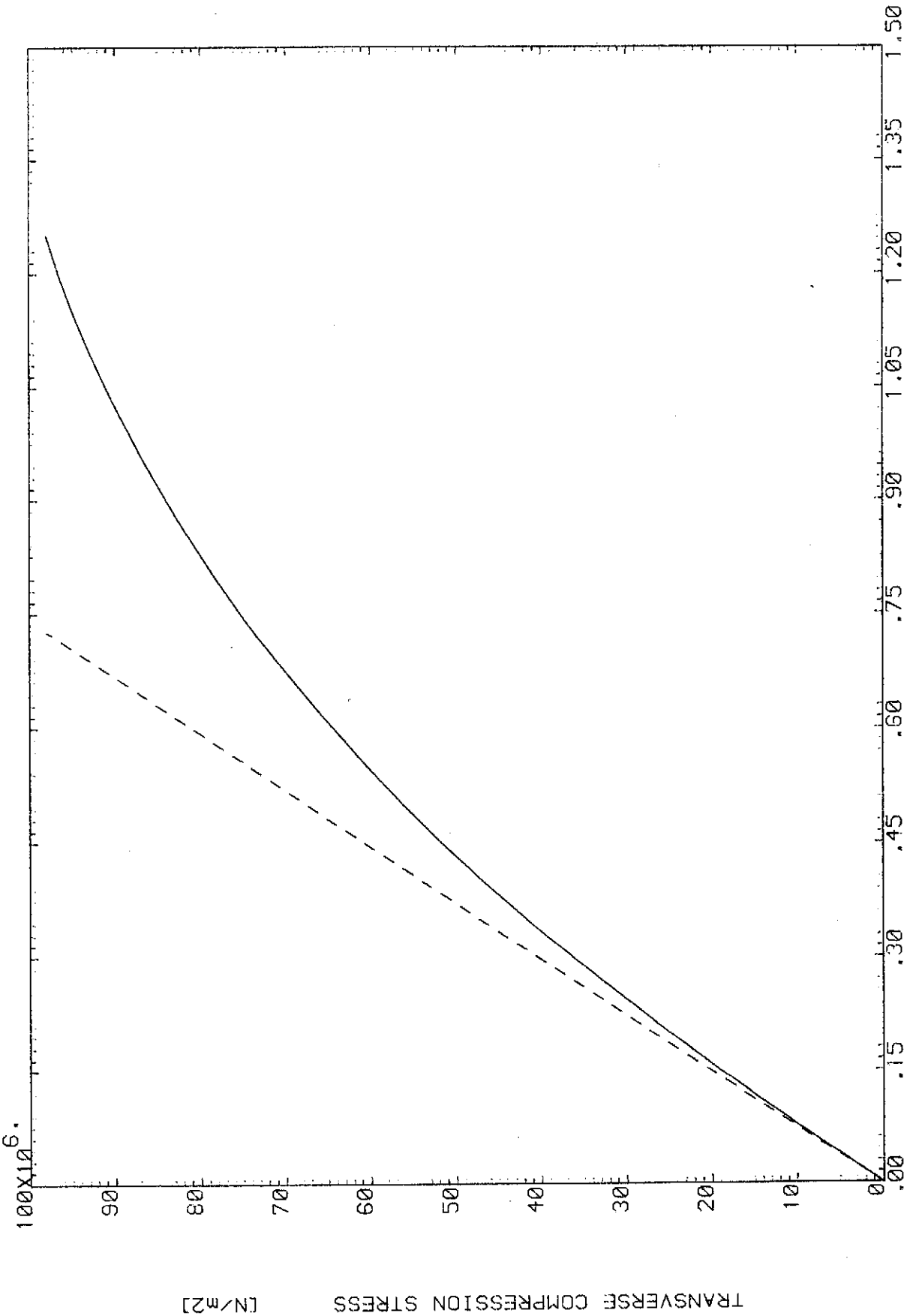

Fig.(5.4.3) LAMINA TRANSVERSE COMPRESSION RESPONSE, V.F.= 63.24 %

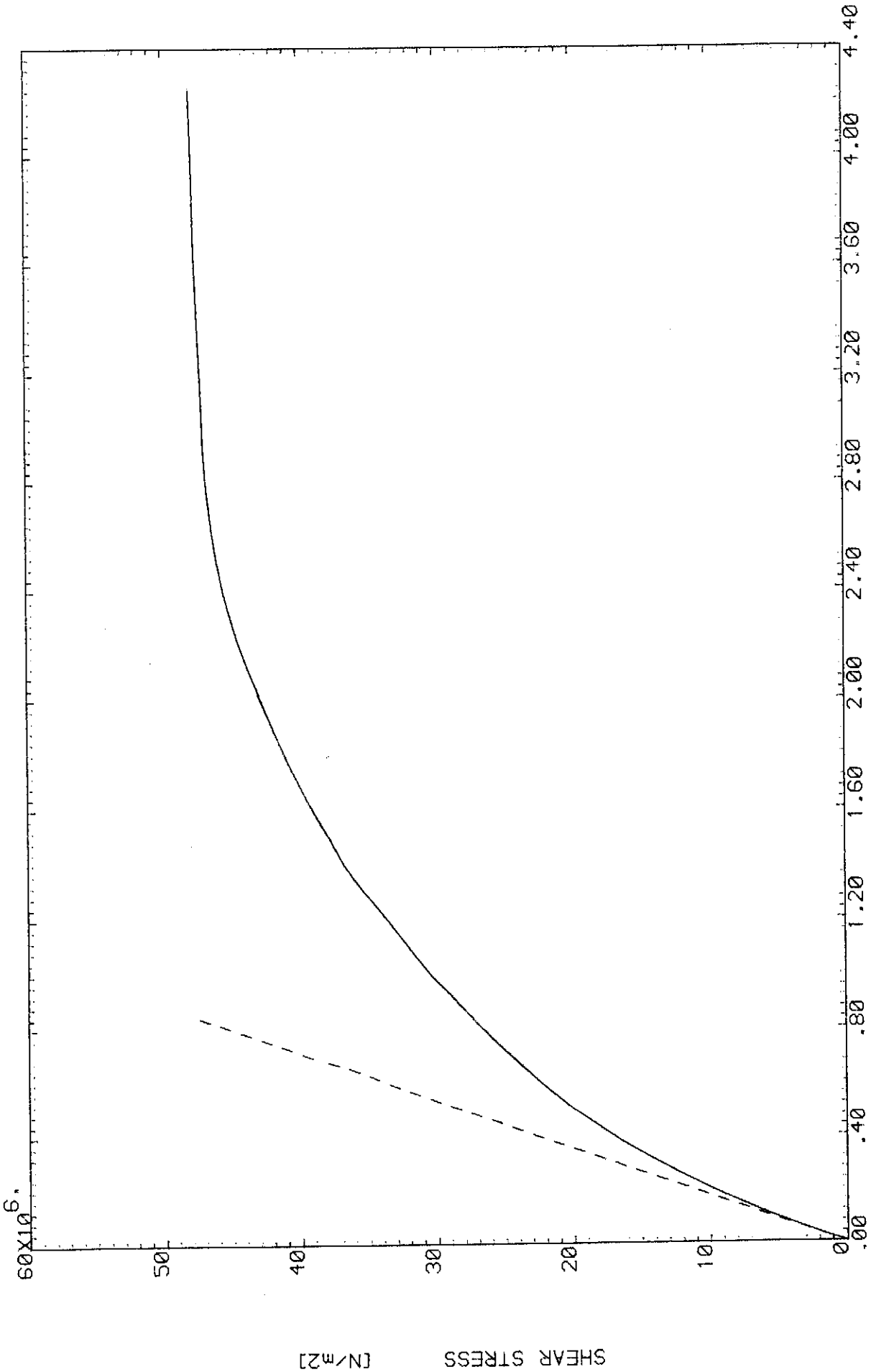

Fig.(5.4.4) LAMINA SHEAR RESPONSE, V.F.= 63.24 %

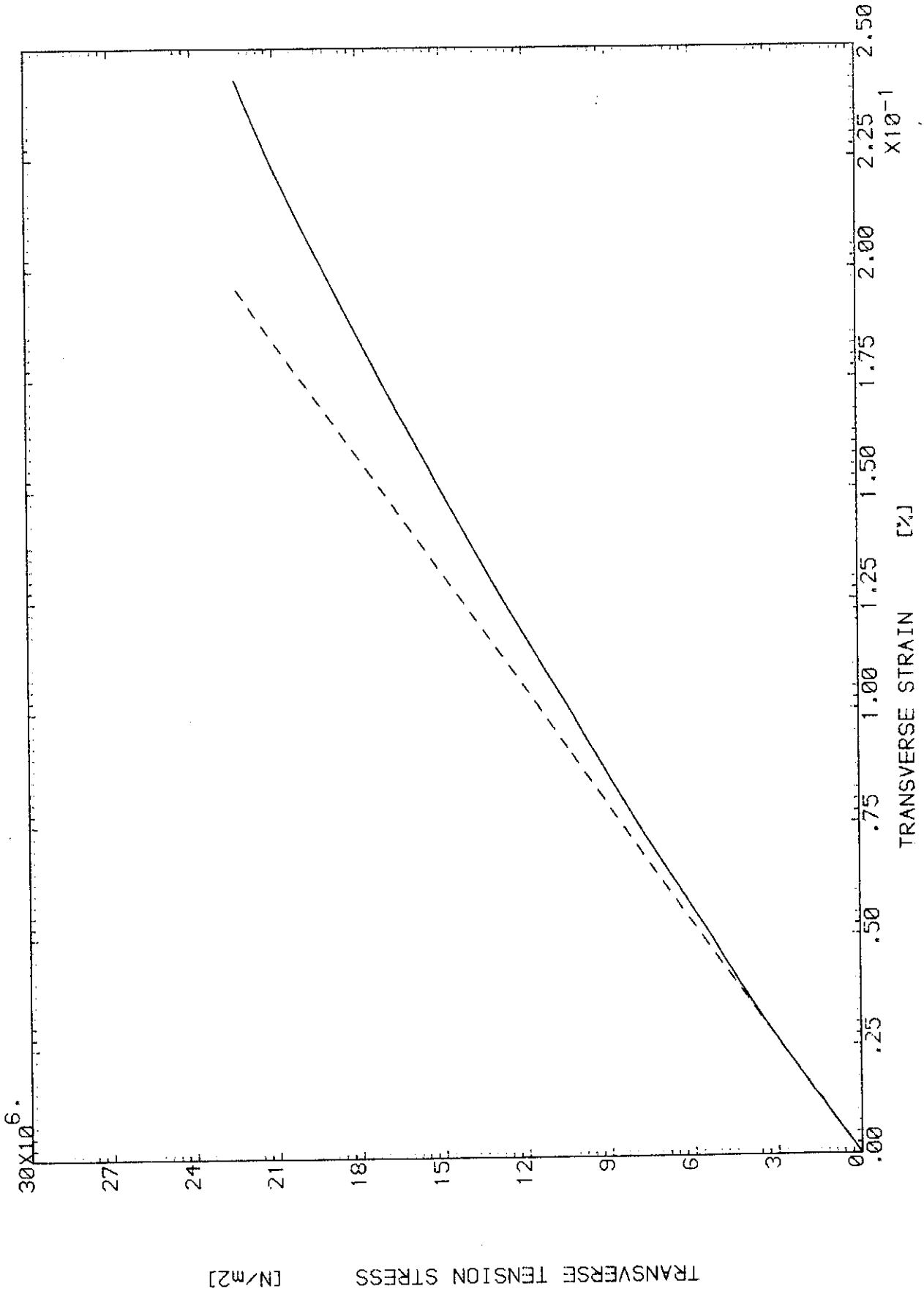

Fig.(5.4.5) LAMINA TRANSVERSE TENSION RESPONSE, V.F.= 56.39 %

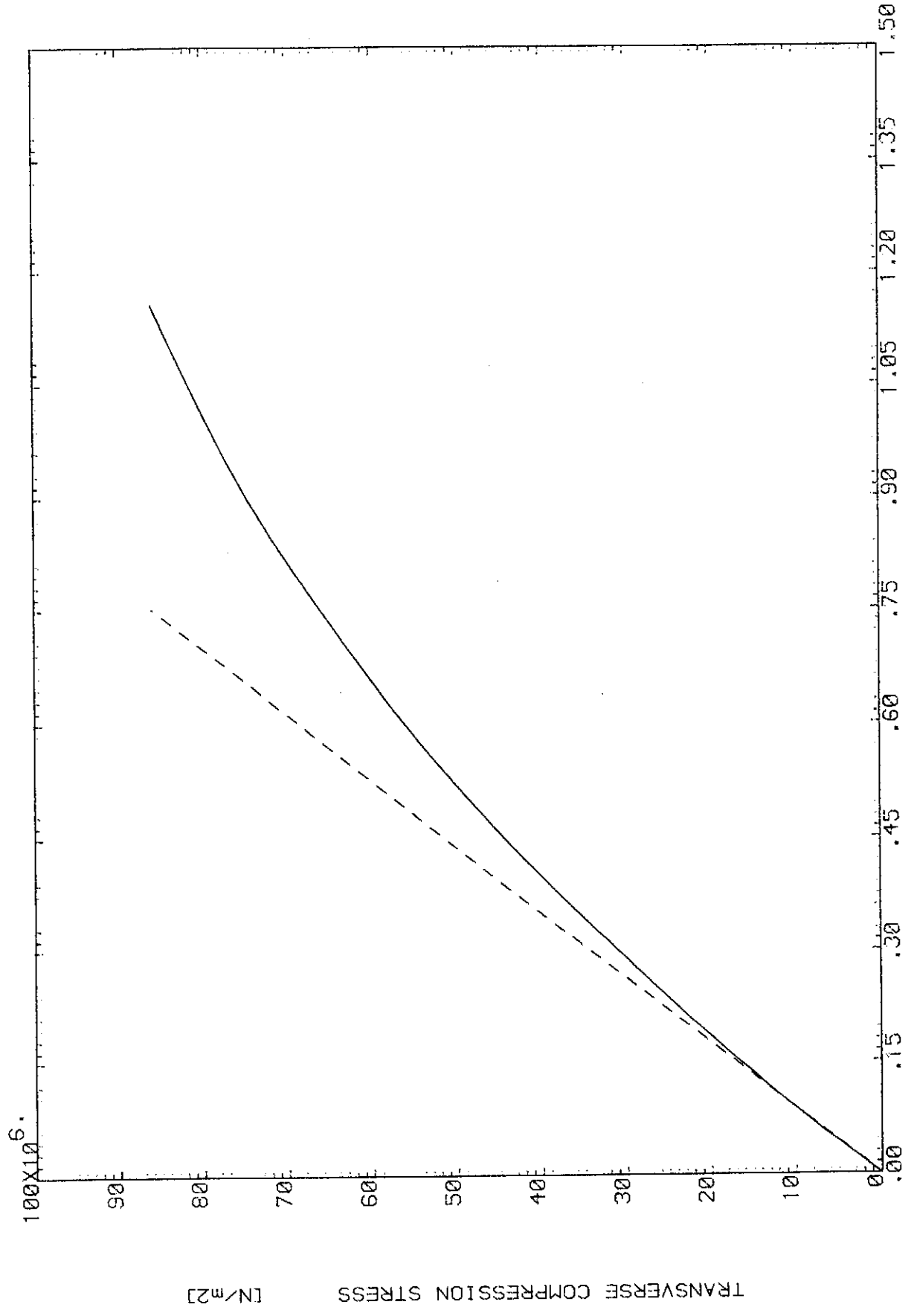

Fig.(5.4.6) LAMINA TRANSVERSE COMPRESSION RESPONSE, V.F.= 56.39 %

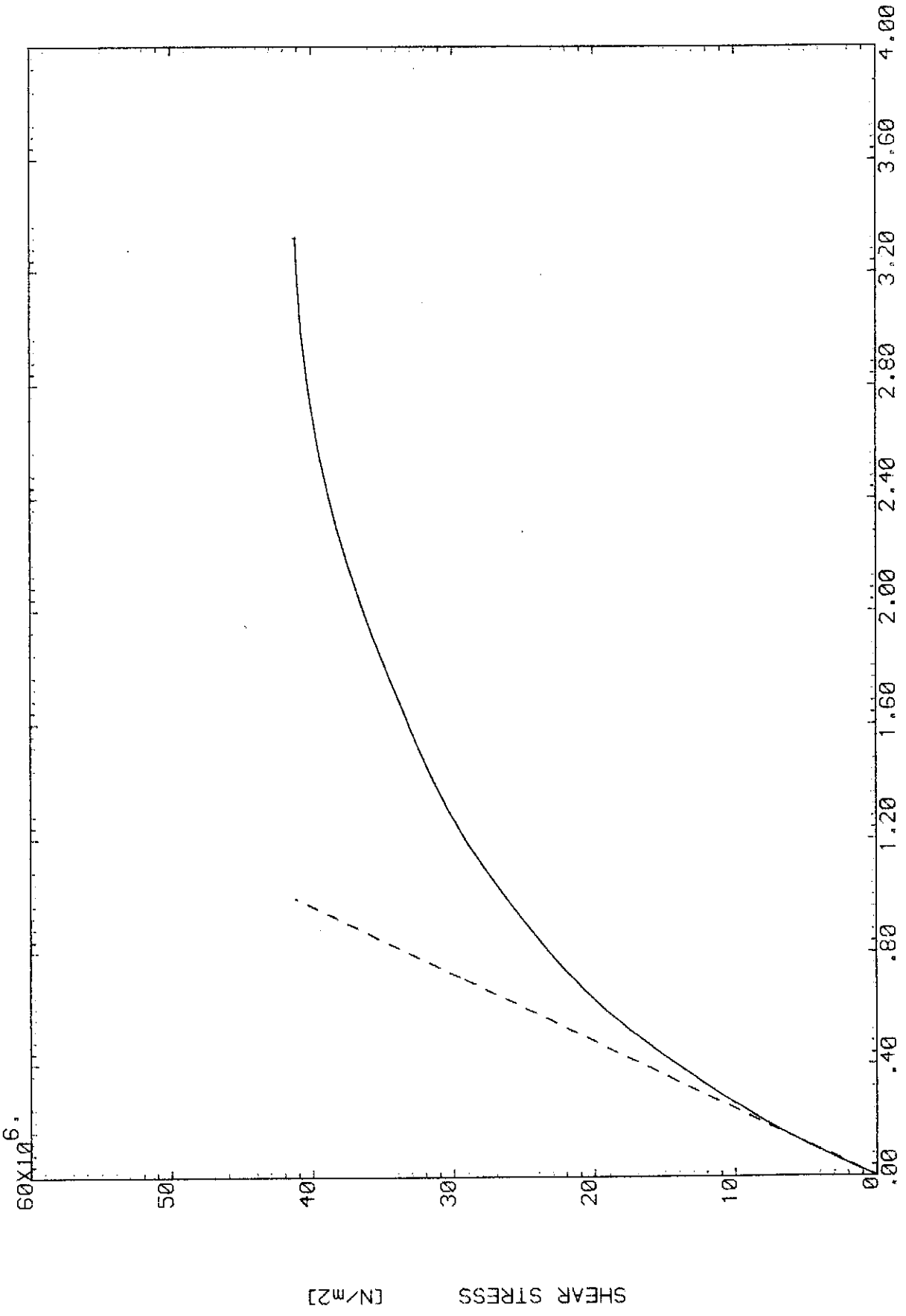

Fig.(5.4.7) LAMINA SHEAR RESPONSE, V.F.= 56.39 %

CHAPTER 6

CONCLUSIONS

Tubular specimens are the most adequate type of specimens to characterize laminated composites under combined loading conditions. With proper design of the test specimens all the difficulties can be overcome and membrane stress state can be obtained in the middle of the specimens.

The non-linear behaviour of the composite lamina is a very important phenomenon to understand both the behaviour of the laminate and the failure of laminated structures.

A modified maximum strain failure criterion is presented here for the prediction of the failure of a lamina in a laminated composite structure, and for the prediction of the behaviour of this structure after that failure. The new criterion takes into account the non-linear behaviour of the lamina and proposes a new method to analyse the laminate non-linear behaviour using secant modulus technique.

The new failure criterion also introduces two levels of failures. The first level is associated with the beginning of failure, or the yield, and the second level is associated with the ultimate failure of the lamina.

The failure criterion also proposed that after the failure of a ply in certain mode, it unloads in this mode only according to an exponential function. Total failure of the laminate occurs when the laminate, after the failure of some of its plies, cannot support the applied load.

Experimental results obtained from testing tubular composite specimens compared well with the theoretical predictions of the new failure criterion. Comparison of the new failure criterion with the previous failure criteria showed that the maximum strain theory predicts a higher failure load, while other theories are conservative.

The test rig developed in this work is simple and effective. The polythene bag used as a liner in the test specimen proved to be very effective in addition to being very cheap.

Acoustic emission, C-scanning and photomicrographic tests gave some information about the failure but they were not very useful as they are only qualitative tests.

REFERENCES

1. ASHTON, J.E. HALPIN, J.C. PETIT, P.H. — "Primer on Composite Materials: Analysis" Technomic Publishing Co., 1969.

2. JONES, R.M. — "Mechanics of Composite Materials" McGraw-Hill Book Company, 1975.

3. WINFIELD, A.G. — "Jute Reinforced Polyester Projects for UNIDO/Government of India" Plastics and Rubber International, Vol.4, No.1, Jan./Feb. 1979, pp.23-28.

4. NOTON, B.R. (Editor) — "Engineering Applications of Composites" Vol.3 of "Composite Materials", edited by L.J. Broutman and R.H. Krock, Academic Press, 1974.

5. PHILLIPS, L.N. — "Carbon-Fibre Reinforced Plastics - The First Fifteen Years" Plastics and Rubber International Vol.3, No.6, Nov./Dec. 1978, pp. 239-243.

6. SALKIND, M.J. — "Fibre Composite Structures" Proceedings of the 1975 International Conference on Composite Materials, ICCM/1, 1975, Vol.2, pp.5-30.

7. KELLY, A. — "Composites - A Decade of Progress" Composites, Vol.10, No.1, Jan. 1979, pp.2-3.

8. PHILLIPS, L.N. — "C.F.R.P. - A Decade of Progress" Composites, Vol.10, No.4, Oct. 1979, pp.195-196.

9. HOLLAWAY, L. — "Glass Reinforced Plastics in Construction" Surrey University Press, 1978.

10. "Composites News"
All issues of Composites since Vol.1, 1969.

11. THOMPSON, E.R. "Aerospace Highlights of 1978: Materials"
Astronautics and Aeronautics, Vol.16, No.12, Dec.1978, pp.66-68.

12. STRATTON, W.K. "Aerospace Highlights of 1979: Materials"
Astronautics and Aeronautics, Vol.17, No.12, Dec.1979, pp.72-73.

13. PHILLIPS, L.N. "Quiet Revolution: An Update of Carbon Fibres for Aircraft Structures"
Shell Aviation News, No.443, 1977, pp.8-13.

13. (a) BEDWELL, M. "Mechanical Engineering Applications"
Chapter 5 of "Carbon Fibres in Engineering"
edited by M. Langley, McGraw Hill, 1973.

14. GOTCH, T.M. "The Design and Manufacture of the British Rail High Speed Train Cab"
Plastics and Rubber International, Vol.4, No.3, May/June 1979, pp.119-124.

15. "GRP in the Boat Building Industry"
Proceedings of the Conference organised by the Plastics and Rubber Institute, Sept. 1978.

16. "Around Industry: Materials, Machinery and Applications"
Plastics and Rubber International, Vol.5, No.2, April 1980, pp.48-52.

17. BRODIE, I.
"The Sandwich that Flies"
Telegraph Sunday Magazine, No.188, April 27, 1980, pp.50-59.

18. HULL, D.
LEGG, M.J.
SPENCER, B.
"Failure of Glass/Polyester Filament Wound Pipe"
Composites, Vol.9, No.1, Jan.1978, pp.17-24.

19. SPENCER, B.
HULL, D.
"Effect of Winding Angle on the Failure of Filament Wound Pipes"
Composites, Vol.9, No.4, Oct.1978, pp.263-271.

20. ECKOLD, G.C.
LEADBETTER, D.
SODEN, P.D.
GRIGGS, P.R.
"Lamination Theory in the Prediction of Failure Envelopes for Filament Wound Materials Subjected to Biaxial Loading"
Composites, Vol.9, No.4, Oct.1978, pp.243-246.

21. SODEN, P.D.
LEADBETTER, D.
GRIGGS, P.R.
ECKOLD, G.C.
"The Strength of a Filament Wound Composite Under Biaxial Loading"
Composites, Vol.9, No.4, Oct.1978, pp.247-250.

22. GRESZCZUK, L.B.
"Theoretical and Experimental Studies on Properties and Behaviour of Filamentary Composites"
Proceedings of the 21st SPI Conference, Feb.1966.

23. ROSEN, B.W.
DOW, N.F.
HASHIN, Z.
"Mechanical Properties of Fibrous Composites"
NASA CR-31, April 1964.

24. TSAI, S.W.
"Structural Behaviour of Composite Materials"
NASA CR-71, July 1964.

25. TSAI, S.W.
ADAMS, D.F.
DONER, D.R.
"Analysis of Composite Structures"
NASA CR-620, Nov.1966.

26. LIN, T.H.
SALINAS, D.
ITO, Y.M.
"Elastic-Plastic Analysis of Unidirectional Composites"
J. of Composite Materials, Vol.6, 1972, pp.48, 60.

27. GRESZCZUK, L.B.
"Effect of Voids on Strength Properties of Composites"
Proceedings of the 22nd SPI Conference, Feb.1967.

28. LARDER, R.A.
BEADLE, C.W.
"The Stochastic Finite Element Simulation of Parallel Fiber Composites"
J. of Composite Materials, Vol.10, 1976, pp.21-31.

29. WHITNEY, J.M.
RILEY, M.B.
"Elastic Properties of Fiber Reinforced Composite Materials"
AIAA Journal, Vol.4, No.9, Sept.1966, pp.1537-1542.

30. TSAI, S.W.
"Formulas for the Elastic Properties of Fiber-Reinforced Composites"
Monsanto/Washington University ONR/ARPA Association, HPC 68-61, June 1968.

31. DIMMOCK, J.
ABRAHAMS, M.
"Prediction of Composite Properties from Fibre and Matrix Properties"
Composites, Vol.1, No.2, Dec.1969, pp.87-93.

32. CHAMIS, C.C.
SENDECKYJ, G.P.
"Critique on Theories Predicting Themoelastic Properties of Fibrous Composites"
J. of Composite Materials, Vol.2, No.3, July 1968, pp.332-358.

33. TETLOW, R.
"Fibre-Reinforced Plastics"
Unpublished Lecture Notes, College of Aeronautics, Cranfield Institute of Technology, 1977.

34. TSAI, S.W.
"Strength Characteristics of Composite Materials"
NASA CR-224, April 1965.

35. YURENKA, S. (Editor) "Composite Materials: Testing and Design (1st Conference)" ASTM, STP 460, 1969.

36. CORTEN, H.T. (Editor) "Composite Materials: Testing and Design (Second Conference)" ASTM, STP 497, 1972.

37. ELLIOTT, S.Y. (Editor) "Composite Materials: Testing and Design (Third Conference)" ASTM, STP 546, 1974.

38. "Composite Materials: Testing and Design (Fourth Conference)" ASTM, STP 617, 1977.

39. "Designing with Fibre Reinforced Materials" I.Mech.E. Conference, Sept. 1977.

40. COLE, B.W. PIPES, R.B. "Filamentary Composite Laminates Subjected to Biaxial Stress Fields" AFFDL-TR-73-115, June 1974.

41. WU, E.M. THOMAS, R.L. "Off-Axis Test of a Composite" J. of Composite Materials, Vol.2, 1968, pp.523-526.

42. RICHARDS, G.L. AIRHART, T.P. ASHTON, J.E. "Off-Axis Tensile Coupon Testing" J. of Composite Materials, Vol.3, 1969, pp.586-589.

43. PAGANO, N.J. HALPIN, J.C. "Influence of End Constraints in Testing of Anisotropic Bodies" J. of Composite Materials, Vol.2, 1968, pp.18-31.

44. RIZZO, R.R. "More on the Influence of End Constraints on Off-Axis Tensile Tests" J. of Composite Materials, Vol.3, 1969, pp.202-212.

45. WHITNEY, J.M.
BROWNING, C.E.
"Free Edge Delamination of Tensile Coupons"
J. of Composite Materials, Vol.6, 1972, pp.300-303.

46. GRIMES, G.C.
PAPE, B.J.
FERGUSON, J.H.
"Investigation of Structural Design Concepts for Fibrous Aircraft Structures"
AFFDL-TR-67-29, 1967.

47. BERT, C.W.
MAYBERRY, B.L.
BAY, J.D.
"Behaviour of Fiber-Reinforced Plastic Laminates under Biaxial Loading"
ASTM STP 460, 1969, pp.362-380.

48. HALPIN, J.C.
PAGANO, N.J.
WHITNEY, J.M.
WU, E.M.
"Characerization of Anisotropic Composite Materials"
ASTM STP 460, 1969, pp.37-47.

49. BERT, C.W.
"Experimental Characterization of Composites"
Chapter 9 of Vol.8 of "Composite Materials", edited by L.J. Broutman and R.H. Krock, Academic Press, 1975.

50. BERT, C.W.
"Static Testing Techniques for Filament-Wound Composite Materials"
Composites, Vol.5, No.1, Jan.1974, pp.20-26.

51. CHIAO, C.C.
MOORE, R.L.
CHIAO, T.T.
"Measurement of Shear Properties of Fibre Composites: Part 1: Evaluation of Test Methods"
Composites, Vol.8, July 1977, pp.161-169.

52. YEOW, Y.T.
BRINSON, H.F.
"A Comparison of Simple Shear Characterization Methods for Composite Materials"
Composites, Vol.9, No.1, Jan.1978, pp.49-55.

53. TERRY, G. "A Comparative Investigation of Some Methods of Unidirectional, In-Plane Shear Characterization of Composite Materials" Composites, Vol.10, No.4, Oct.1979, pp.233-237.

54. ENIE, R.B. RIZZO, R.R. "Three-Dimensional Laminate Moduli" J. of Composite Materials, Vol.4, 1970, pp.150-154.

55. ROSEN, B.W. "On Some Symmetry Conditions for Three-Dimensional Fibrous Composites" J. of Composite Materials, Vol.5, 1971, pp.279-282.

56. RYBICKI, E.F. "Approximate Three-Dimensional Solutions for Symmetric Laminates Under Inplane Loading" J. of Composite Materials, Vol.5, 1971, pp.354-360.

57. KO, H.Y. STURE, S. "Three-Dimensional Mechanical Characterization of Anisotropic Composites" J. of Composite Materials, Vol.8, 1974, pp.178-190.

58. FEWS, R.C. TETLOW, R. "The Analysis and Design of Filament Wound Pressure Vessels" Final Report, College of Aeronautics, Memo 7707, Cranfield Institute of Technology, March 1978.

59. TETLOW, R. "Structural Engineering Design and Applications" Chapter 4 of "Carbon Fibres in Engineering", edited by M. Langley, McGraw Hill, 1973.

60. TETLOW, R. "Design Charts for Composite Materials" Lecture Notes, Short Course on "Design with Fibre Reinforced Plastics", Cranfield Institute of Technology, 1978.

61. TSAI, S.W.
HALPIN, J.C.
PAGANO, N.J.
"Composite Materials Workshop"
Technomic Publishing Co., 1968.

62. CALCOTE, L.R.
"The Analysis of Laminated Composite Structures"
Van Nostrand Reinhold Co., 1969.

63. REUTER, R.C.
"Concise Property Transformation Relations for an Anisotropic Lamina"
J. of Composite Materials, Vol.5, April 1971, pp.270-272.

64. SHERRER, R.E.
"Filament-Wound Cylinders with Axial-Symmetric Loads"
J. of Composite Materials, Vol.1, 1967, pp.344-355.

65. FRANKLIN, H.G.
"Membrane Solution of Fibre-Reinforced Corrugated Shells of Revolution"
J. of Composite Materials, Vol.1, 1967, pp.382-388.

66. DONG, S.B.
PISTER, K.S.
TAYLOR, R.L.
"On the Theory of Laminated Anisotropic Shells and Plates"
J. of the Aerospace Sciences, Vol.29, 1962, pp.969-975.

67. DONG, R.G.
DONG, S.B.
"Analysis of Slightly Anisotropic Shells"
AIAA Journal, Vol.1, No.11, Nov.1963, pp.2565-2569.

68. PAGANO, N.J.
HALPIN, J.C.
WHITNEY, J.M.
"Tension Buckling of Anisotropic Cylinders"
J. of Composite Materials, Vol.2, No.2, April 1968, pp.154-167.

69. WHITNEY, J.M.
HALPIN, J.C.
"Analysis of Laminated Anisotropic Tubes Under Combined Loading"
J. of Composite Materials, Vol.2, No.3, July 1968, pp.360-367.

70. RIZZO, R.R.
VICARIO, A.A.
"A Finite Element Analysis of Laminated Anisotropic Tubes"
J. of Composite Materials, Vol.4, July 1970, pp.344-359.

71. RIZZO, R.R.
VICARIO, A.A.
"A Finite Element Analysis for Stress Distribution in Gripped Tubular Specimens"
ASTM STP 497. pp.68-88.

72. PAGANO, N.J.
WHITNEY, J.M.
"Geometric Design of Composite Cylinderical Characterization Specimens"
J. of Composite Materials, Vol.4, July 1970, pp.360-378.

73. PAGANO, N.J.
"Stress Gradients in Laminated Composite Cylinders"
J. of Composite Materials, Vol.5, April 1971, pp.260-265.

74. WHITNEY, J.M.
"On the Use of Shell Theory for Determining Stresses in Composite Cylinders"
J. of Composite Materials, Vol.5, July 1971, pp.340-353.

75. WHITNEY, J.M.
PAGANO, N.J.
PIPES, R.B.
"Design and Fabrication of Tubular Specimens for Composite Characterization"
ASTM STP 497, 1971, pp.52-67.

76. VLASOV, V.Z.
"General Theory of Shells and its Application in Engineering"
NASA TT F-99, 1964.

77. AMBARTSUMYAN, S.A.
"Theory of Anisotropic Shells"
NASA TT F-118, 1964.

78. CHENG, S.
HO, B.P.C.
"Stability of Heterogeneous Aeolotropic Cylindrical Shells Under Combined Loading"
AIAA Journal, Vol.1, No.4, April 1963, pp.892-898.

79. FLUGGE, W.
"Stresses in Shells"
Springer-Verlag, 1962.

80. CHAO, C.C.
SUN, C.T.
KOH, S.L.
"Strength Optimization for Cylindrical Shells of Laminated Composites"
J. of Composite Materials, Vol.9, 1975, pp.53-66.

81. WIDERA, O.E.
CHUNG, S.W.
"A Theory for Non-Homogeneous Anisotropic Cylindrical Shells"
J. of Composite Materials, Vol.6, Jan.1972, pp.14-30.

82. REUTER, R.C.
"Analysis of Shells Under Internal Pressure"
J. of Composite Materials, Vol.6, Jan.1972, pp.94-113.

83. ZIEN, H.M.
"Bending of Laminated Anisotropic Composite Cylinders"
J. of Composite Materials, Vol.7, 1973, pp.394-398.

84. BERT, C.W.
"Structural Theory for Laminated Anisotropic Elastic Shells"
J. of Composite Materials, Vol.1, 1967, pp.414-423.

85. WHITNEY, J.M.
SUN, C.T.
"A Refined Theory for Laminated Anisotropic Cylindrical Shells"
J. of Applied Mechanics, Vol.41, No.2, June 1974, pp.471-476.

86. WIDERA, G.E.O.
LOGAN, D.L.
"Layered Cylindrical Pressure Vessels"
J. of Pressure Vessel Technology, vol. 101, Feb. 1979, pp.80-86.

87. BERT, C.W.
GUESS, T.R.
"Mechanical Behaviour of Carbon/Carbon Filamentary Composites"
ASTM STP 497, 1972, pp.89-106.

88. BERT, C.W. "Analysis of Shells" Chapter (5) of Vol.(7) of "Composite Materials" edited by L.J. Broutman and R.H. Krock, Academic Press, 1975.

89. LOVE, A.E.H. "A Treatise on the Mathematical Theory of Elasticity" Dover Publication, 1944.

90. HAHN. H.T. PAGANO, N.J. "Curing Stresses in Composite Laminates" J. of Composite Materials, Vol.9, Jan.1975, pp.91-106.

91. PIPES, R.B. VINSON, J.R. CHOU, T.W. "On the Hygrothermal Response of Laminated Composite Systems" J. of Composite Materials, Vol.10, April, 1976, pp.129-148.

92. PAGANO, N.J. HAHN, H.T. "Evaluation of Composite Curing Stresses" ASTM STP 617, 1977, pp.317-329.

93. ISHIKAWA, T. KOYAMA, K. KOBAYASHI, S. "Thermal Expansion Coefficients of Unidirectional Composites" J. of Composite Materials, Vol.12, April 1978, pp.153-168.

94. CHAMIS, C.C. SENDECKYJ, G.P. "Critique on Theories Predicting Thermoelastic Properties of Fibrous Composites" J. of Composite Materials, Vol.2, 1968, pp.332-358.

95. QUINN, J.A. "Fibreglass Composites: Design Data" Fibreglass Limited.

96. "Crystic Monograph No.2: Polyester Handbook" Scott Bader Company Limited, 1977.

97. "Technical Bulletin: Preliminary Data Sheet T2" Honeywill-Atlas Limited.

98. HAHN, H.T.
TSAI, S.W.
"Nonlinear Elastic Behaviour of Unidirectional Composite Laminae"
J. of Composite Materials, vol.7, Jan.1973, pp.102-118.

99. HAHN, H.T.
"Nonlinear Behaviour of Laminated Composites"
J. of Composite Materials, vol.7, April 1973, pp.257-271.

100. PETIT, P.H.
WADDOUPS, M.E.
"A Method of Predicting the Nonlinear Behaviour of Laminated Composites"
J. of Composite Materials, vol.3, Jan. 1969, pp.2-19.

101. PETIT, P.H.
"Ultimate Strength of Laminated Composites".
AFML, General Dynamics, FZM-4977-Dec.1967.

102. HASHIN, Z.
BAGCHI, D.
ROSEN, B.W.
"Non-Linear Behaviour of Fiber Composite Laminates"
NASA CR-2313, April 1974.

103. SANDHU, R.S.
"Nonlinear Behaviour of Unidirectional and Angle Ply Laminates"
J. of Aircraft, vol.13, no.2, Feb.1974, pp.104-111.

104. SANDHU, R.S.
"Ultimate Strength Analysis of Symmetric Laminates"
AFFDL-TR-73-137, Feb.1974.

105. JONES, R.M.
NELSON, D.A.R.
"A New Material Model for the Nonlinear Biaxial Behaviour of ATJ-S Graphite"
J. of Composite Materials, vol.9, 1975, pp.10-27.

106. JONES, R.M.
NELSON, D.A.R.
"Further Characteristics of a Nonlinear Material Model for ATJ-S Graphite"
J. of Composite Materials, vol.9, 1975, pp.251-265.

107. JONES, R.M.
NELSON, D.A.R.
"Material Models for Nonlinear Deformation of Graphite"
AIAA Journal, vol.15, June 1976, pp.709-717.

108. JONES, R.M.
NELSON, D.A.R.
"Theoretical-Experimental Correlation of Material Models for Nonlinear Deformation of Graphite"
AIAA Journal, vol.15, Oct.1976, pp.1427-1435.

109. JONES, R.M.
MORGAN, H.S.
"Analysis of Nonlinear Stress-Strain Behaviour of Fiber-Reinforced Composite Materials"
Proceedings of AIAA/ASM/SAE 17th Structures, Structural Dynamics and Materials Conference. 1976, pp.174-183.

110. JONES, R.M.
MORGAN, H.S.
"Analysis of Nonlinear Stress-Strain Behaviour of Fiber-Reinforced Composite Materials"
AIAA Journal, vol.15, Dec.1977, pp.1669-1676.

111. MORGAN, H.S.
JONES, R.M.
"Analysis of Nonlinear Stress-Strain Behaviour of Laminated Fiber-Reinforced Composite Materials"
Proceedings of the 1978 International Conference on Composite Materials, ICCM2, April 1978, pp.337-352.

112. AMIJIMA, S.
ADACHI, T.
"Nonlinear Stress-Strain Response of Laminated Composites"
J. of Composite Materials, vol.13, July 1979, pp.206-218.

113. ADAMS, D.F.
"Inelastic Analysis of a Unidirectional Composite Subjected to Transverse Normal Loading"
J. of Composite Materials, vol.4, 1970, pp.310-328.

114. HUANG, W.C.
"Plastic Behaviour of Some Composite Materials"
J. of Composite Materials, vol.5, 1971, pp.320-328.

115. HUANG, W.C.
"Elastoplastic Transverse Properties of a Unidirectional Fibre Reinforced Composite"
J. of Composite Materials, vol.7, 1973, pp.482-498.

116. ALLRED, R.E.
HOOVER, W.R.
HORAK, J.A.
"Elastic-Plastic Poisson's Ratio of Borsic-Aluminium"
J. of Composite Materials, vol.8, 1974, pp.15-28.

117. HAHN, H.T.
"On Elastic-Plastic Poisson's Ratio"
J. of Composite Materials, vol.8, 1974, pp.313-317.

118. RAMSEY, J.E.
WASZCZAK, J.P.
KLOUMAN, F.L.
"An Investigation of the Nonlinear Response of Metal-Matrix Composite Laminates"
Paper 75-787, AIAA/ASME/SAE 16th Structures, Structural Dynamics, and Materials Conference, May 1975.

119. STANTON, E.
"A General Three-Dimensional Computational Model for Non-linear Composite Structures and Materials"
Paper 77-360, AIAA/ASME 18th Structures, Structural Dynamics, and Materials Conference, March 1977.

120. CRADDOCK, J.N.
ZAK, A.R.
"Nonlinear Response of Composite Materials Structures"
J. of Composite Materials, vol.11, 1977, pp.204-221.

121. VAN DREUMEL, W.H.M.
KAMP, J.L.M.
"Non Hookean Behaviour in the Fibre Direction of Carbon-Fibre Composites and the Influence of Fibre Waviness on the Tensile Properties"
J. of Composite Materials, vol.11, 1977, pp.461-469.

122. McKAGNE, E.L.
LEMON, G.H.
KAMINSKI, B.E.
"Development of Engineering Data for Advanced Composite Materials"
AFML-TR-70-108, vol.1, 1970.

123. DANIEL, I.M.
MULLINEAUX, J.L.
AHIMAZ, F.J.
LIBER, T.
"The Embedded Strain Gage Technique for Testing Boron/ Epoxy Composites"
ASTM STP 497, 1972, pp.257-272.

124. DONNELL, L.H.
"Stability of Thin-Walled Tubes Under Torsion"
NACA Report No. 479, 1933.

125. HERRMANN, L.R.
CHAN, S.T.K.
"Mechanical Property Tests for Cylindrical Orthotropic Materials"
J. of Composite Materials, vol.3, Jan. 1969, pp.136-147.

126. VICARIO, A.A.
RIZZO, R.R.
"Effect of Length on Laminated Thin Tubes Under Combined Loading"
J. of Composite Materials, vol.4, 1970, pp.273-277.

127. WHITNEY, J.M.
GRIMES, G.C.
FRANCIS, P.H.
"Effect of End Attachment on the Strength of Fiber-Reinforced Composite Cylinders"
Experimental Mechanics, vol.13, no.5, May 1973, pp.185-192.

128. REUTER, R.C.
GUESS, T.R.
"Analysis, Testing, and Design of Filament Wound, Carbon-Carbon Burst Tubes"
ASTM STP 546, 1974, pp.67-83.

129. WALTZ, T.L.
VINSON, J.R.
"Interlaminar Stresses in Laminated Cylindrical Shells of Composite Materials"
Paper 75/755, AIAA/ASME/SAE 16th Structures, Structural Dynamics, and Materials Conference, 1975.

130. PIPES, R.B.
WHITNEY, J.M.
"Analysis of the Anisotropic Cylinder of Finite Length"
Fibre Science and Technology, vol.12, no.5, Sept.1979, pp.327-339.

131. GUESS, T.R.
HAIZLIP, C.B.
"End-Grip Configurations for Axial Loading of Composite Tubes" Experimental Mechanics, vol.20, no.1, Jan.1980, pp.31-36.

132. LEMOINE, L.
"Effects of Geometric and Material Non-Linearities on the Deflections of Filament Wound Motor Chambers" Paper 78/1565, AIAA/SAE 14th Joint Propulsion Conference, July 1978.

133. TIMOSHENKO, S.
"Theory of Plates and Shells" McGraw-Hill Co., 1940.

134. RABENSTEIN, A.L.
"Introduction to Ordinary Differential Equations" Academic Press, 1966.

135. MILLER, R.J.
"End Plugs for External Pressure Tests of Composite Cylinders" ASTM STP 460, 1969.

136. SANDHU, R.S.
"A Survey of Failure Theories of Isotropic and Anisotropic Materials" AFFDL-TR-72-71, Jan.1972.

137. FRANKLIN, H.G.
"Classic Theories of Failure of Anisotropic Materials" Fibre Science and Technology, vol.1, 1968, pp.137-150.

138. BERT, C.W.
MAYBERRY, B.L.
RAY, J.D.
"Behaviour of Fiber-Reinforced Plastic Laminates Under Uniaxial, Biaxial, and Shear Loadings" U.S. Army Aviation Material Laboratories, TR 68-86, Jan.1969.

139. KAMINSKI, B.E.
LANTZ, R.B.
"Strength Theories of Failure for Anisotropic Materials" ASTM STP 460, 1969, pp.160-169.

140. SENDECKJI, G.P.
"A Brief Survey of Empirical Multidirectional Strength Criteria for Composites" ASTM STP 497, 1972, pp.41-51.

141. VICARIO, A.A.
TOLAND, R.H.
"Failure Criteria and Failure Analysis of Composite Structural Components"
Chapter 2 of vol.7 of "Composite Materials" edited by L.J.Broutman and R.H. Krock, Academic Press, 1975.

142. ROWLANDS, R.E.
"Flow and Failure of Biaxially Loaded Composites: Experimental-Theoretical Correlation"
In: "Inelastic Behaviour of Composite Materials" edited by C.T. Herakovich, ASME AMD vol.13,1975.

143. ROWLANDS, R.E.
"Analytical-Experimental Correlation of the Biaxial State of Stress in Composite Materials"
AFFDL-TR-75-11, April 1975.

144. HÜTTER, U.
SCHELLING, H.
KRAUSS, H.
"An Experimental Study to Determine Failure Envelope of Composite Materials with Tubular Specimens Under Combined Loads and Comparison Between Several Classical Criteria."
Paper 3, AGARD-CP-163, Oct.1964.

145. SNELL, M.B.
"Strength and Elastic Response of Symmetric Angle-Ply CFRP"
Composites, vol.9, no.3, July 1978, pp.167-176.

146. STOWELL, E.Z.
LIU, T.S.
"On the Mechanical Behaviour of Fibre-Reinforced Crystalline Materials"
J. of Mechanics and Physics of Solids, vol.9, no.4, 1961, pp.242-260.

147. KELLY, A.
DAVIES, G.J.
"The Principles of the Fibre Reinforcement of Metals"
Metallurgical Reviews, vol.10, no.37, 1965, pp.1-77.

148. EL-HOSSEINY, F.
PAGE, D.H.
"The Mechanical Properties of Single Wood Pulp Fibres: Theories of Strength"
Fibre Science and Technology, vol.8, no.1, Jan.1965, pp.21-31

149. HOLISTER, G.S.
THOMAS, C.
"Fibre Reinforced Materials"
Elsevier Publishing Co. 1966.

150. PRAGER, W.
"Plastic Failure of Fiber-Reinforced Materials"
J. of Applied Mechanics, vol.36, no.3, Sep.1969, pp.542-544.

151. HAHN, H.T.
TSAI, S.W.
"Graphical Determination of Stiffness and Strength of Composite Laminates"
J. of Composite Materials, vol.8, April 1974, pp.160-177.

152. HU, L.W.
"Modified Tresca's Yield Condition and Associated Flow Rules for Anisotropic Materials and Applications"
J. of the Franklin Institute, vol.265, 1958, pp.187-204

153. WASTI, S.T.
"The Plastic Bending of Transversely Anisotropic Circular Plates"
International J. of Mechanical Sciences, vol.12, 1970, pp.109-112.

154. LANCE, R.H.
ROBINSON, D.N.
"A Maximum Shear Stress Theory of Plastic Failure of Fiber-Reinforced Materials"
J. of Mechanics and Physics of Solids, vol.19, 1971, pp.49-60.

155. CAPURSO, M.
"Yield Conditions for Incompressible Isotropic and Orthotropic Materials with Different Yield Stress in Tension and Compression"
Meccanica, vol.2, no.2, June 1967, pp.118-125.

156. HILL, R.
"The Mathematical Theory of Plasticity"
Oxford University Press, 1950.

157. AZZI, V.D.
TSAI, S.W.
"Anisotropic Strength of Composites"
Experimental Mechanics, vol.5, 1965, pp.283-288.

158. TSAI, S.W.
AZZI, V.D.
"Strength of Laminated Composite Materials"
AIAA J., vol.4, no.2, Feb.1966, pp.296-301.

159. TSAI, S.W.
"Strength Theories of Filamentary Structures"
Chapter 1 of "Fundamental Aspects of Fibre Reinforced Plastic Composites" edited by R.T.Schwartz and H.S. Schwartz, Wiley Interscience, 1968.

160. JONES, B.H.
"Determination of Design Allowables for Composite Materials"
ASTM STP 460, 1969, pp.307-320.

161. BRANDMAIER, H.E.
"Optimum Filament Orientation Criteria"
J. of Composite Materials, vol.4, July 1970, pp.422-425.

162. HARRIS, B.
"The Strength of Fibre Composites"
Composites, vol.3, July 1972, pp.152-167.

163. AGARWAL, B.D.
NARANG, J.N.
"Strength and Failure Mechanism of Anisotropic Composites"
Fibre Science and Technology, vol.10, 1977, pp.37-52.

164. JOHNSON, A.F.
"Engineering Design Properties of GRP"
The British Plastics Federation, 1978.

165. MARIN, J.
"Theories of Strength for Combined Stresses and Nonisotropic Materials"
J. of the Aeronautical Sciences, vol.24, no.4, April 1957, pp.265-268.

166. TOPPING, A.D.
"Marin's Strength Hypothesis"
J. of the Aeronautical Sciences, vol.25, no.1, Jan.1958, pp.59-60.

167. COLEMAN, J.J.
"An Evaluation of the Criticisms by Topping of Marin's Strength Hypothesis"
J. of the Aeronautical Sciences, vol.25, no.7, June 1958, p.408.

168. STASSI-D'ALIA, F.
"Limiting Conditions of Yielding of Thick-Walled Cylinders and Spherical Shells"
University of Palermo (Italy), Final Report, 1959.

169. NORRIS, C.B.
McKINNON, P.F.
"Compression, Tension and Shear Tests on Yellow-Poplar Plywood Panels of Sizes that do not Buckle with Tests Made at Various Angles to the Face Gain".
Report No. 1328, Forest Product Laboratory, 1946.

170. NORRIS, C.B.
"Strength of Orthotropic Materials Subjected to Combined Stresses"
Report No. 1816, Forest Product Laboratory, 1962.

171. FISCHER, L.
"Optimization of Orthotropic Laminates"
J. of Engineering for Industry, vol.89, Aug.1967, pp.399-402.

172. YAMADA, S.E.
SUN, C.T.
"Analysis of Laminated Strength and Its Distribution"
J. of Composite Materials, vol.12, July 1978, pp.275-284.

173. GRIFFITH, J.E.
BALDWIN, W.M.
"Failure Theories for Generally Orthotropic Materials"
Development in Theoretical and Applied Mechanics, vol.1 (Proceedings of the 1st Southeastern Conference on Theoretical and Applied Mechanics, 1972), Plenum Press, 1963, pp.410-420.

174. CHAMIS, C.C.
"Failure Criteria for Filamentary Composites"
NASA TN-D-5367, 1969. Also
ASTM STP 460, 1969, pp.336-351.

175. CHAMIS, C.C.
"Impetus of Composite Mechanics on Test Methods for Fiber Composites"
Paper 30, US/USSR Seminar on Fracture of Composite Materials, Sept.1978, pp.329-348.

176. HOFFMAN, O.
"The Brittle Strength of Orthotropic Materials".
J. of Composite Materials, Vol.1, 1967, pp.200-206.

177. PUCK, A.
SCHNEIDER, W.
"On failure Mechanisms and Failure Criteria of Filament-Wound Glass/Resin Composites"
Plastics and Polymers, Vol.37, no.2, Feb.1969, pp.33-43.

178. McCRUM, N.G.
"A Review of the Science of Fibre Reinforced Plastics".
H.M. Stationery Office, London, 1971.

179. GREENWOOD, J.H.
"German Work on GRP Design".
Composites, Vol.8, no.3, July 1977, pp.175-184.

180. DODDS, R.
"Transverse Fibre Debonding in Reinforced Thermosets - A Review"
RAPRA Members J., Vol.4, May/June 1976, pp.49-56.

181. WU, E.M.
"Failure Criteria to Fracture Mode Analysis of Composite Laminates"
Paper 2, AGARD-CP-153, Oct.1974.

182. HAGA, O.
HAYASHI, N.
KASUYA, K.
"Failure Criterion of Glass Fibre Reinforced Plastic Laminates"
J. of Japan Society of Materials Science, Vol.25 , June 1976, pp.516-520.

183. GOL'DENBLAT, I.I.
KOPNOV, V.A.
"Strength of Glass-Reinforced Plastics in the Complex Stress State"
Polymer Mechanics (translation of Mekhanika Polimerov), vol.1, 1966, pp.54-59.

184. ASHKENAZI, E.K.
"Problems of the Anisotropic of Strength"
Polymer Mechanics, Vol.1, 1966, pp.60-70.

185. MALMEISTER, A.
"Geometry of Theories of Strength"
Polymer Mechanics, Vol.2, 1967, pp.324-331.

186. NIKOLAEV, V.P.
"Strength of Reinforced Materials in Plane Stressed State"
Strength of Materials (Translation of Problemy Prochnosti), Vol.10, no.3, 1978, pp.336-340.

187. TSAI, S.W.
WU, E.M.
"A General Theory of Strength for Anisotropic Materials"
J. of Composite Materials, Vol.5, no.1, Jan.1971, pp.58-80.

188. WU, E.M.
"Phenomenological Anisotropic Failure Criterion"
Chapter 9 of Vol.2, of "Composite Materials", edited by L.J. Broutman and R.H. Krock, Academic Press, 1974.

189. WU, E.M.
"Optimal Experimental Measurements of Anisotropic Failure Tensors"
J. of Composite Materials, Vol.6, Oct.1972, pp.472-489.

190. WU, E.M.
JERINA, K.L.
"Computer-Aided Mechanical Testing of Composites"
Materials Research and Standards, Vol.12, Feb.1972, pp.13-18.

191. JERINA, K.L.
HALPIN, J.C.
"Strength of Molded Discontinuous Fibre Composites"
AFML-TR-72-148, Oct.1972.

192. COLLINS, B.R.
CRANE, R.L.
"A Graphical Representation of the Failure Surface of a Composite"
J. of Composite Materials, Vol.5, July 1971, pp.408-413.

193. NARAYANASWAMI, R.
ADELMAN, H.M.
"Evaluation of the Tensor Polynomial and Hoffman Strength Theories for Composite Materials"
J. of Composite Materials, Vol.11, Oct. 1977, pp.366-377.

194. COLLINS, B.R.
THOMAS, R.L.
"The General Plane Stress Failure of Boron Aluminium Composites"
AFML-TR-73-137, Nov.1973.

195. THOMAS, R.L.
"Strength Characteristics of Boron Aluminium Composite Subjected to Combined Stresses"
AFML-TR-74-214, Oct.1974.

196. TENNYSON, R.C.
"Experimental Evaluation of the Tensor Polynomial Failure Criterion for Designing Composite Structures"
NASA-CR-155219, Oct.1977.

197. TENNYSON, R.C.
MacDONALD, D.
NANYARO, A.P.
"Evaluation of the Tensor Polynomial Failure Criterion for Composite Materials"
J. of Composite Materials, Vol.12, Jan.1978, pp.63-75.

198. HUANG, C.L.
KIRMSER, P.G.
"A Criterion of Strength for Orthotropic Materials"
Fibre Science and Technology, Vol.8, 1975, pp.103-112.

199. PUPPO, A.H.
EVENSEN, H.A.
"Strength of Anisotropic Materials under Combined Stresses"
AIAA J., Vol.10, no.4, April 1972, pp.468-474.

200. WU, E.M.
SCHEUBLEIN, J.K.
"Laminate Strength - A Direct Characterization Procedure"
ASTM STP 546, 1974, pp.188-206.

201. WU, E.M.
SCHEUBLEIN, J.K.
"Basic Failure of Composites"
AFML-TR-73-272, Nov.1973.

202. CHOU, P.C.
McNAMEE, B.M.
CHOU, D.K.
"The Yield Criterion of Laminated Media"
J. of Composite Materials, Vol.7, Jan.1973, pp.22-35.

203, SCHNEIDER, W.
BARDENHEIER, R.
"Versagens Kriterien für Kunststoffe"
J. of Materials Technology, Vol.6, 1975, pp.269-280 and pp.339-348.

204. SENDECKYI, G.P.
MADDUX, G.E.
TRACY, N.A.
"Comparison of Holographic, Radiographic, and Ultrasonic Techniques for Damage Detection in Composite Materials".
Proceedings of the 1978 International Conference on Composite Materials, ICCM/2, pp.1037-1056.

205. KULKAMI, S.V.
PIPES, R.B.
RAMKUMAR, R.L.
SCOTT, W.R.
"The Analytical, Experimental, and Nondestructive Evaluation of the Criticality of an Interlaminal Defect in a Composite Laminate"
ICCM/2, 1978, pp.1057-1071.

206. SCHWALBE, H.J.
"Acoustic Emission as an Aid for Inspecting GFRP Pressure Tubes"
ICCM/2, 1978, pp.1093-1104.

207. KIMPARA, I.
TAKEHANA, M.
SUZUZI, T.
"Analysis of Thickness-Direction Ultrasonic Wave Propagation of Fibreglass Reinforced Plastics Laminates"
ICCM/2, 1978, pp.1105-1122.

208. HARRIGAN, W.C.
"Ultrasonic Inspection of Graphite-Aluminium Composites"
ICCM/2, 1978, pp.1123-1140.

209. SALKIND, M.J.
"Early Detection of Fatigue Damage in Composite Materials"
Paper 75-772, AIAA/ASME/SAE 16th Structures, Structural Dynamics, and Materials Conference, 1975.

210. DEAN, D.S.
"The Non-Destructive Testing of Solid Propellant Rocket Motors"
5th AGARD Colloquium, 1962, pp.483-493. (Pergamon Press, 1963)

211. VAN DREUMEL, W.H.M.
"Ultrasonic Scanning for Quality Control of Advanced Fibre Composites"
NDT International, Vol.11, no.5, Oct.1978, pp.233-235.

212. HARTBOWER, C.E.
REUTER, W.G.
MORAIS, C.F.
CRIMMINS, P.P.
"Use of Acoustic Emission for the Detection of Weld and Stress Corrosion Cracking"
ASTM STP 505, 1972, pp.187-221.

213. BIRCHON, D.
"Structural Validation - A Positive Approach to NDT"
CME, June 1972, pp.54-60.

214. STONE, D.E.W.
CLARKE, B.
"Ultrasonic Attenuation as a Measure of Void Content in Carbon-Fibre Reinforced Plastics"
Non-Destructive Testing Vol.8, no.3, June 1975, pp.137-145.

215. PRAKASH, R.
"Non-Destructive Testing and Fatigue Behaviour of Carbon-Fibre Reinforced Polymer"
Ph.D. Thesis, Cranfield Institute of Technology, 1975.

216. LIPTAI, R.G.
HARRIS, D.O.
TATRO, C.A.
"An Introduction to Acoustic Emission"
ASTM STP 505, 1972, pp.3-10 and pp.336-337.

217. SIMS, G.D.
DEAN, G.D.
READ, B.E.
WESTERN, B.C.
"Assessment of Damage in GRP Laminates by Stress Wave Emission and Dynamic Mechanical Measurements"
J. of Materials Science, Vol.12, 1977, pp.2329-2342.

218. STONE, D.E.W.
DINGWALL, P.F.
"Acoustic Emission Parameters and their Interpretation"
RAE TR-76121, 1976.

219. MEHAN, R.L.
MULLIN, J.V.
"Analysis of Composite Failure Mechanisms Using Acoustic Emission"
J. of Composite Materials, Vol.5, July 1971, pp.266-269.

220. FITZ-RANDOLPH, J.
PHILLIPS, D.C.
BEAUMONT, P.W.R.
TETELMAN, A.S.
"Acoustic Emission Studies of a Boron-Epoxy Composite"
J. of Composite Materials, Vol.5, Oct.1971, pp.542-548.

221. HARRIS, D.O.
TETELMAN, A.S.
DARWISH, F.A.
"Detection of Fiber Cracking by Acoustic Emission"
ASTM STP 505, 1972, pp.238-249.

222. LIPTAI, R.G.
"Acoustic Emission from Composite Materials"
ASTM STP 497, 1972, pp.285-298.

223. CHIAO, T.T.
HAMSTAD, M.A.
MARCON, M.A.
HANAFEE, J.E.
"Filament-Wound Kevlar 49/Epoxy Pressure Vessels"
NASA CR-134506, Nov.1973.

224. HAMSTAD, M.A.
CHIAO, T.T.
"Acoustic Emission Produced During Burst Tests of Filament-Wound Bottles"
J. of Composite Materials, Vol.7, July 1973, pp.320-332.

225. HAMSTAD, M.A.
CHIAO, T.T.
"Acoustic Emission from Stress Rupture and Fatigue of an Organic Fiber Composite"
ASTM STP 580, 1975, pp.191-201.

226. HENNEKE, E.G.
HERRING, H.W.
"Spectrum Analysis of Acoustic Emissions from Boron-Aluminium Composites"
ASTM STP 580, 1975, pp.202-214.

227. PIPES, R.B.
BALLINTYN, N.J.
SCOTT, W.R.
CARLYLE, J.M.
"Acoustic Emission Response Characteristics of Metal Matrix Composites"
ASTM STP 617, 1977, pp.153-169.

228. BUNSELL, A.R.
"Acoustic Emission for Proof Testing of Carbon Fibre Reinforced Plastics"
NDT International, Vol.10, no.1, Feb.1977, pp.21-25.

229. MURR, L.E.
"Electron Optical Applications in Materials Science"
McGraw Hill Book Co., 1970.

230. GUESS, T.R.
GERSTLE, F.P.
"Deformation and Fracture of Resin Matrix Composites in Combined Stress States"
J. of Composite Materials, Vol.11, April 1974, pp.146-163.

231. GUESS, T.R.
"Biaxial Testing of Composite Cylinders: Experimental-Theoretical Comparison"
Composites, Vol.11, no.3, July 1980, pp.139-148.

232. TENNYSON, R.C.
"Buckling of Laminated Composite Cylinders: A Review"
Composites, Vol.6, 1975,pp.17-24.

233. CHEHILL, D.S.
CHENG, S.
"Elastic Buckling of Composite Cylindrical Shells Under Torsion"
J. of Spacecraft and Rockets, Vol.5, No.8, Aug.1968, pp.973-978

234. HO, B.P.C.
CHENG, S.
"Some Problems in Stability of Heterogeneous Aeolotropic Cylindrical Shells Under Combined Loading"
AIAA J., Vol.1, No.7, July 1963, pp.1603-1607.

235. TSAI, J.
"Effect of Heterogeneity on the Stability of Composite Cylindrical Shells Under Axial Compression"
AIAA J., Vol.4, No.6, June 1966, pp.1058-1062.

236. WHITNEY, J.M.
SUN, C.T.
"Buckling of Composite Cylindrical Characterization Specimens"
J. of Composite Materials, Vol.9, April 1975, pp.138-148.

237. HERANO, Y.
"Buckling of Angle-Ply Laminated Circular Cylindrical Shells"
J. of Applied Mechanics, Vol.46, March 1979, pp.233-234.

238. CHAO, T.L.
"Minimum Weight Design of Stiffened Fiber Composite Cylinders"
AFML-TR-69-251, Sep.1969.

239. BOOTON, M.
TENNYSON, R.C.
"Buckling of Imperfect Anisotropic Circular Cylinders under Combined Loading"
AIAA J., Vol.17, No.3, March 1979, pp.278-287. Also Paper 78-514, AIAA/ASME 19th Structures, Structural Dynamics and Materials Conference, April 1978.

240. JONES, R.M.
HENNEMANN, C.F.
"Effect of Prebuckling Deformations on Buckling of Laminated Composite Circular Cylindrical Shells"
Paper 78-516, AIAA/ASME 19th Structures, Structural Dynamics and Materials Conference, April 1978.

241. JONES, R.M.
MORGAN, H.S.
"Buckling of Laminated Circular Cylindrical Shells with Different Moduli in Tension and Compression"
ICCM/1, 1975, pp.318-343.

242. MARLOWE, D.E.
SUSHINSKY, G.F.
DEXTER, H.B.
"Elastic Torsional Buckling of Thin-Walled Composite Cylinders"
ASTM STP 546, 1974, pp.84-108.

243. LEI, M.M.
CHENG, S.
"Buckling of Composite and Homogeneous Isotropic Cylindrical Shells under Axial and Radial Loading"
J. of Applied Mechanics, Vol.36, Dec. 1969, pp.791-798.

244. MORGAN, H.S.
JONES, R.M.
"Buckling of Rectangular Cross-Ply Laminated Plates with Non-Linear Stress-Strain Behaviour."
J. of Applied Mechanics, Vol.46, Sept.1979, pp.637-643.

245. HAHN, H.T.
TSAI, S.W.
"On the Behaviour of Composite Laminates After Initial Failures"
J. of Composite Materials, Vol.8, July 1974, pp.280-305.

246. CHIU, K.D.
"Ultimate Strengths of Laminated Composites"
J. of Composite Materials, Vol.3, July 1969, pp.578-582.

247. McLAUGHLIN, P.V.
ROSEN, B.W.
"Combined Stress Effects Upon Failure of Fibre Composites"
Materials Sciences Corporation Report TFR/7404/1112, 1974.

248. FOYE, R.L.
"Theoretical Post-Yielding Behaviour of Composite Laminates"
J. of Composite Materials, Vol.7, 1973, pp.178-193 and pp.310-319.

249. BROWN, G.E.
"Progressive Failure of Advanced Composite Laminates Using the Finite Element Method."
M.Sc. Thesis, University of Utah, 1976.

250. CHOU, S.C.
ORRINGER, O.
RAINEY, J.H.
"Post-Failure Behaviour of Laminates"
J. of Composite Materials, Vol.10, Oct.1976, pp.371-381 and Vol.11, Jan.1977, pp.71-78.

251. YEOW, Y.T.
BRINSON, H.F.
"An Experimental Investigation on the Tensile Moduli and Strengths of Graphite/Epoxy Laminates"
Experimental Mechanics, Vol.17, Nov.1977, pp.401-408.

252. FÖRSTER, R.
KNAPPE, W.
"Spannungs-und Bruchanalyse an Glasfaser/Kunststoff-Wickelkorpern"
Kunststoff, Vol.60, 1970, pp.1053-1059.

253. KIM, R.Y.
HAHN, H.T.
"Effect of Curing Stresses on the First Ply Failure in Composite Laminates"
J. of Composite Materials, Vol.13, Jan. 1979, pp.2-16.

254. FRANCIS, P.H.
WALRATH, D.E.
WEED, D.N.
"First Ply Failure of G/E Laminates under Biaxial Loadings"
Fibre Science and Technology, Vol.12, 1979, pp.97-110.

255. SANDHU, R.S.
MONFORT, J.B.
HUSSONG, F.E.
ZINK, E.E.
"Laminate Tubular Specimens Subjected to Biaxial Stress States"
AFFDL-TR-73-7, 1973 and 1975.

256. NAGY, A.
LINDHOLM, U.S.
"Hydraulic Grip System for Composite Tube Specimens"
AFML-TR-73-239, 1973.

257. CHIAO, T.T.
HAMSTAD, M.A.
"Testing of Fibre Composite Materials"
ICCM-1, 1975, pp.884-915.

258. CARSWELL, W.S.
GEMMELL, R.
"Effect of Resin Flexibility on the Strength of Glass Filament-Wound Tubes"
National Engineering Laboratory Report No. 643, Aug.1977.

APPENDIX A

DATA OF THE TEST SPECIMENS

A.1 TYPES OF SPECIMENS

The specimens for the experimental investigation were supplied by two different manufacturers, Bristol Aeroject Limited and Prodorite Limited. In both cases the specimens were circular cylindrical specimens made on a mandrel by the filament winding technique, and then post-cured at high temperature.

Bristol Aeroject Limited supplied six long tubes of glass/epoxy, whereas Prodorite Limited provided one long tube of glass/polyester. Table (A.1) gives more details about the materials of the tubes.

A.2 SPECIMENS ORIENTATION AND STOCKING

Two of Bristol Aeroject tubes were used for unidirectional characterization of the composites. They were not unidirectional but as near as possible as the winding machines could not produce hoop winding. Two other tubes were angle-ply tubes, whereas the last two were multilayered tubes. The Prodorite tube was angle-ply at $\pm 45^{o}$. Table (A.2) gives more details about the orientation and the stacking sequence of the tubes, where "B" denotes Bristol Aeroject tubes and "P" denotes Prodorite tube.

The Bristol Aeroject tubes were made on mandrel of constant diameter. The Prodorite tube was made on a tapered mandrel which has difference of 1 mm between its ends over 6 m long.

A.3 SPECIMEN DIMENSIONS

The long tubes supplied by the manufacturers were cut into many specimens for different loading ratios. The thickness of the tubes was found tobe varying along the length of the tube. Thus, it was more appropriate to measure the thickness of each specimen after cutting it from the tube. The thickness of each specimen was measured at 24 positions and the average was calculated. Tables (A.3) - (A.9) give dimensions of all specimens as shown in Fig. (A.1). Each specimen has been given an identification number which indicates to the tube it was cut from, e.g., specimen 3B4 is specimen No. 3 of tube B4. Dimensions of the end reinforcements are also given

in the Tables.

A.4 SPECIMEN VOLUME FRACTIONS

During the testing of specimens cut from tube B1 and specimens cut from tube B6 the properties obtained were different although these specimens had the same orientation. The differences in properties were considered to be due to difference in the fibre contents in each composite tube. To verify this point, the volume fractions of all specimens were determined. Volume fraction is a measure of the fibre contents in a composite by volume, i.e., the volume fraction V_f is given by :

$$V_f = \frac{\text{Volume of fibres}}{\text{Total volume of composite}} \qquad (A.1)$$

or

$$V_f = \frac{\text{Volume of fibres}}{\text{Volume of fibres + Volume of matrix}} \qquad (A.2)$$

or

$$V_f = \frac{\frac{W_f}{\rho_f}}{\frac{W_f}{\rho_f} + \frac{W_m}{\rho_m}} \qquad (A.3)$$

where :

W_f is the weight of fibres;

ρ_f is the density of fibres;

W_m is the weight of matrix; and

ρ_m is the density of matrix.

Thus, to obtain V_f the weight of the fibres in a sample composite must be obtained. This is done by "burn off" test in which the sample is kept under high temperature till the matrix is burnt and the remaining fibres are weighed.

In this work a "Polymer Burn Off Furnace" was used. This was a small oven heated electrically. The sample was placed inside a little crucible which was put on a holder inside the

furnace. Two crucibles could be positioned at once inside the furnace allowing the matrix of two samples to burn off overnight at 480°C.

Since the samples used were small, the weight had to be determined using precision balance. The balance used was an Oertling balance with accuracy of within 0.1 mg.

The test procedure was to weigh the crucible first, then the crucible with the sample, from which the weight of the sample was calculated. Once the matrix burned off, the furnace was switched off and the sample was left to cool inside, otherwise, if the crucible had been removed while hot there would have been possible error in the after burn off weight due to condenced mist on the surface of the crucible. The weight of the fibres and of the matrix were calculated using the after burn off weight. Then, using equation (A.3) the volume fraction was calculated.

Three samples from each tube were cut for this burn off test and the volume fraction was taken to be the average of the three, Table (A.10). The densities of the fibres and the matrix were considered as follows, (Refs. 95-97).

$$\rho_f = 2.56 \text{ g/cm}^3$$

$$\rho_m = 1.19 \text{ g/cm}^3$$

In case of tube B4 and B5 which are multilayered specimens there was a need to know the thickness of each layer in the laminate. This was done after the burn off test by separating the unbonded fibres of each layer and then weighing the sample again. In this way it was possible to know the percentage of the $\pm 45^\circ$ layer in the laminate which helped to calculate the thickness of the different layers in these multilayered laminated tubes, Table (A.11).

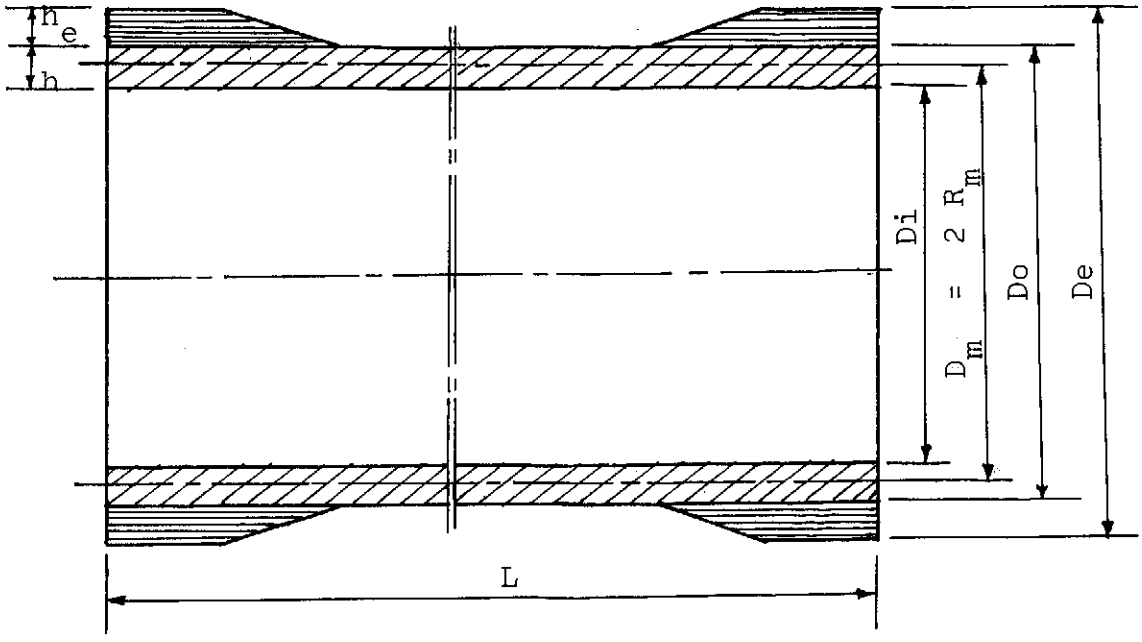

Fig. (A.1) Dimension of the test specimen

TABLE (A.1)

Details of the materials used in manufacturing of the test specimens

MANUFACTURER	No. OFF	FIBRE	RESIN	SURFACE TISSUE	CATALYST	ACCELERATOR	POST CURING
Bristol Aeroject Limited	6	Glass Fibre Silenka 051L, 600 tex	Araldite MY.750/ HT.972 (DDM)	Not Used			2 hours at 120°C
Prodorite Limited	1	"E" glass	Atlac 382-05	"C" Veil Glass	M.E.K.P.	Cobalt	3 hours at 80°C

TABLE (A.2)

Orientation and stacking sequence of the test specimens

TUBE	INSIDE DIAMETER (D_i) mm	TOTAL AVERAGE THICKNESS (h) mm	ORIENTATION AND STACKING SEQUENCE (Angles measured from axis of tube)	NUMBER OF SPECIMENS TESTED
B1	77.8	1.4638	10 layers @ $\pm 85^{\circ}$	10
B2	77.8	1.4528	4 layers @ $\pm 70^{\circ}$	8
B3	77.8	3.1783	8 layers @ $\pm 45^{\circ}$	9
B4	77.8	2.2405	2 layers @ $\pm 85^{\circ}$ 4 layers @ $\pm 45^{\circ}$ 2 layers @ $\pm 85^{\circ}$	6
B5	77.8	3.7198	2 layers @ $\pm 85^{\circ}$ 8 layers @ $\pm 45^{\circ}$ 2 layers @ $\pm 85^{\circ}$	6
B6	77.8	0.9488	10 layers @ $\pm 85^{\circ}$	7
P1	99.5 - 100.5	3.5592	4 layers @ $\pm 45^{\circ}$	4

TABLE (A.3)

Dimensions of the specimens cut from tube B1

(All dimensions in "mm")

SPECIMEN	AVERAGE THICKNESS (h)	STANDARD DEVIATION from h	MEAN DIAMETER (D_m)	MEAN RADIUS (R_m)	OUTSIDE DIAMETER (D_o)	TOTAL LENGTH (L)	ENDS OUTER DIAMETER (D_e)	THICKNESS OF END REINFORCEMENT (h_e)
1B1	1.436	0.0547	79.236	39.618	80.672	303	86.0	2.5
2B1	1.450	0.0498	79.250	39.625	80.700	295	88.0	3.5
3B1	1.463	0.0449	79.263	39.631	80.726	300	89.0	4.0
4B1	1.473	0.0532	79.273	39.636	80.746	300	90.5	4.5
5B1	1.497	0.0514	79.297	39.648	80.794	302	86.0	2.5
6B1	1.450	0.0498	79.250	39.625	80.700	258	88.0	3.5
7B1	1.436	0.0547	79.236	39.618	80.672	303	86.0	2.5
8B1	1.463	0.0449	79.263	39.631	80.726	300	89.0	4.0
9B1	1.473	0.0532	79.273	39.636	80.746	300	90.5	4.5
10B1	1.436	0.0547	79.236	39.618	80.672	303	85.0	2.0

TABLE (A.4)

Dimensions of the specimens cut from tube B2

(All dimensions in "mm")

SPECIMEN	AVERAGE THICKNESS (h)	STANDARD DEVIATION from h	MEAN DIAMETER (D_m)	MEAN RADIUS (R_m)	OUTSIDE DIAMETER (D_o)	TOTAL LENGTH (L)	ENDS OUTER DIAMETER (D_e)	THICKNESS OF END REINFORCEMENT (h_e)
1B2	1.473	0.0750	79.273	39.636	80.746	260	86.0	2.5
2B2	1.433	0.0877	79.233	39.616	80.666	258	86.0	2.5
3B2	1.458	0.0747	79.258	39.629	80.716	250	90.0	4.0
4B2	1.445	0.0843	79.245	39.622	80.690	255	90.0	4.0
5B2	1.452	0.0894	79.252	39.626	80.704	258	89.5	4.0
6B2	1.456	0.0960	79.256	39.628	80.712	258	89.5	4.0
7B2*	1.321		79.096	39.548	80.417	127		
8B2*	1.321		79.096	39.548	80.417	127		

* These specimens are from different batch and were tested on old rig.

TABLE (A.5)

Dimensions of the specimens cut from tube B3

(All dimensions in "mm")

SPECIMEN	AVERAGE THICKNESS (h)	STANDARD DEVIATION from h	MEAN DIAMETER (D_m)	MEAN RADIUS (R_m)	OUTSIDE DIAMETER (D_o)	TOTAL LENGTH (L)	ENDS OUTER DIAMETER (D_e)	THICKNESS OF END REINFORCEMENT (h_e)
1B3	3.330	0.1690	81.130	40.565	84.460	255	92.5	4.0
2B3	3.205	0.0982	81.005	40.502	84.210	255	92.5	4.0
3B3	3.102	0.1279	80.902	40.451	84.004	255	97.5	6.5
4B3	3.084	0.1208	80.884	40.442	83.968	255	97.5	6.5
5B3	3.108	0.1283	80.908	40.454	84.016	255	94.0	5.0
6B3	3.241	0.1530	81.041	40.521	84.282	255	94.0	5.0
7B3*	2.603		80.378	40.189	82.982	127		

* This specimen is from different batch and was tested on old rig.
Specimens 8B3 and 9B3 have same dimensions as specimen 7B3.

TABLE (A.6)

Dimensions of the specimens cut from tube B4
(All dimensions in "mm")

SPECIMEN	AVERAGE THICKNESS (h)	STANDARD DEVIATION from h	THICKNESS OF ±85° LAYER	THICKNESS OF ±45° LAYER	MEAN DIAMETER (D_m)	MEAN RADIUS (R_m)	OUTSIDE DIAMETER (D_o)	TOTAL LENGTH (L)	ENDS OUTER DIAMETER (D_e)	THICKNESS OF END REINFORCEMENT (h_e)
1B4	2.284	0.1488	0.330	1.625	80.084	40.042	82.368	258	88.0	2.5
2B4	2.227	0.1092	0.321	1.584	80.027	40.014	82.254	255	87.5	2.5
3B4	2.194	0.1496	0.317	1.561	79.994	39.997	82.188	255	91.5	4.5
4B4	2.175	0.1537	0.314	1.547	79.975	39.987	82.150	261	91.5	4.5
5B4	2.233	0.1745	0.322	1.589	80.033	40.016	82.266	258	91.2	4.0
6B4	2.330	0.1699	0.336	1.658	80.130	40.065	82.460	258	91.2	4.0

TABLE (A.7)

Dimensions of the specimens cut from tube B5
(All dimensions in "mm")

SPECIMEN	AVERAGE THICKNESS (h)	STANDARD DEVIATION from h	THICKNESS OF ±85° LAYER	THICKNESS OF ±45° LAYER	MEAN DIAMETER (D_m)	MEAN RADIUS (R_m)	OUTSIDE DIAMETER (D_o)	TOTAL LENGTH (L)	ENDS OUTER DIAMETER (D_e)	THICKNESS OF END REINFORCEMENT (h_e)
1B5	3.834	0.1785	0.335	3.165	81.634	40.817	85.468	258	93.0	3.5
2B5	3.681	0.1068	0.321	3.038	81.481	40.741	85.162	258	93.0	3.5
3B5	3.686	0.1173	0.322	3.042	81.486	40.743	85.172	255	95.5	5.0
4B5	3.645	0.1030	0.318	3.009	81.445	40.722	85.090	255	95.5	5.0
5B5	3.688	0.1143	0.322	3.044	81.488	40.744	85.176	258	94.0	4.5
6B5	3.785	0.1409	0.330	3.124	81.585	40.792	85.370	253	94.0	4.5

TABLE (A.8)

Dimensions of the specimens cut from tube B6
(All dimensions in "mm")

SPECIMEN	AVERAGE THICKNESS (h)	STANDARD DEVIATION from h	MEAN DIAMETER (D_m)	MEAN RADIUS (R_m)	OUTSIDE DIAMETER (D_o)	TOTAL LENGTH (L)	ENDS OUTER DIAMETER (D_e)	THICKNESS OF END REINFORCEMENT (h_e)
1B6	0.9313	0.0838	78.731	39.366	79.663	217	85.5	3.0
2B6	0.9430	0.0802	78.743	39.371	79.686	218	85.5	3.0
3B6	0.9573	0.0630	78.757	39.379	79.715	217	85.5	3.0
4B6	0.9223	0.1003	78.722	39.361	79.645	216	85.5	3.0
5B6	0.9446	0.0869	78.745	39.372	79.689	218	85.5	3.0
6B6	0.9869	0.0905	78.787	39.393	79.774	222	84.0	2.0
7B6	0.9562	0.0772	78.756	39.378	79.712	222	84.0	2.0

TABLE (A.9)

Dimensions of the specimens cut from tube P1
(All dimensions in "mm")

SPECIMEN	INSIDE DIAMETER (D_i)	AVERAGE THICKNESS (h)	STANDARD DEVIATION from h	MEAN DIAMETER (D_m)	MEAN RADIUS (R_m)	OUTSIDE DIAMETER (D_o)	TOTAL LENGTH (L)	ENDS OUTER DIAMETER (D_e)	THICKNESS OF END REINFORCEMENT (h_e)
3P1	99.60	3.468	0.227	103.068	51.534	106.536	298	116.5	4.5
4P1	99.65	3.567	0.109	103.217	51.608	106.784	300	116.5	4.4
13P1	100.20	3.575	0.212	103.775	51.887	107.350	275	114.0	3.3
14P1	100.30	3.627	0.170	103.927	51.963	107.554	296	116.5	4.4

TABLE (A.10)

Summary of "burn off" test and volume fraction calculations
(Weight is given in "g")

TUBE	SAMPLE	WEIGHT OF CRUCIBLE	WEIGHT OF (CRUCIBLE + SAMPLE)	WEIGHT OF SAMPLE	AFTER BURN OFF WEIGHT	WEIGHT OF FIBRES (W_f)	WEIGHT OF MATRIX (W_m)	VOLUME FRACTION (V_f) %
P1	A	17.6822	19.9859	2.3037	19.2929	1.6107	0.6930	51.93
	B	19.7739	22.8680	3.0941	21.9898	2.2159	0.8782	53.98
	C	19.7743	21.4709	1.6966	20.9167	1.1424	0.5542	48.93
	Average V_f = 51.61%, Standard deviation = 2.54%							
B1	A	19.7745	20.5798	0.8053	20.4114	0.6369	0.1684	63.74
	B	17.6810	18.3185	0.6375	18.1826	0.5014	0.1361	63.13
	C	17.6816	18.5566	0.8750	18.3681	0.6864	0.1886	62.85
	Average V_f = 63.24%, Standard deviation = 0.45%							
B2	A	17.6820	18.2171	0.5351	18.0747	0.3937	0.1414	56.41
	B	17.6812	18.1673	0.4861	18.0258	0.3442	0.1419	53.00
	C	17.6817	18.3412	0.6595	18.1748	0.4927	0.1668	57.86
	Average V_f = 55.76%, Standard deviation = 2.49%							

TABLE (A.10) Continued

TUBE	SAMPLE	WEIGHT OF CRUCIBLE	WEIGHT OF (CRUCIBLE + SAMPLE)	WEIGHT OF SAMPLE	AFTER BURN OFF WEIGHT	WEIGHT OF FIBRES (W_f)	WEIGHT OF MATRIX (W_m)	VOLUME FRACTION (V_f) %
B3	A	19.7748	21.2165	1.4417	20.8954	1.1215	0.3202	61.95
	B	19.7739	20.8983	1.1244	20.6402	0.8659	0.2585	60.89
	C	19.7743	20.7588	0.9845	20.5276	0.7523	0.2322	60.10
	Average V_f = 60.98%, Standard deviation = 0.93%							
B4	A	17.6821	18.5734	0.8913	18.3722	0.6913	0.2000	61.64
	B	17.6809	18.4794	0.7985	18.2961	0.6148	0.1837	60.87
	C	17.6813	18.2624	0.5811	18.1232	0.4414	0.1397	59.49
	Average V_f = 60.67%, Standard deviation = 1.09%							
B5	A	19.7753	21.2275	1.4522	20.9064	1.1323	0.3199	62.60
	B	19.7741	21.1432	1.3691	20.8449	1.0704	0.2987	62.49
	C	19.7745	21.1123	1.3378	20.8063	1.0317	0.3061	61.04
	Average V_f = 61.91%, Standard deviation = 0.77%							

TABLE (A.10) Continued

TUBE	SAMPLE	WEIGHT OF CRUCIBLE	WEIGHT OF (CRUCIBLE + SAMPLE)	WEIGHT OF SAMPLE	AFTER BURN OFF WEIGHT	WEIGHT OF FIBRES (W_f)	WEIGHT OF MATRIX (W_m)	VOLUME FRACTION (V_f) %
B6	A	19.7745	20.6491	0.8746	20.4162	0.6423	0.2323	56.24
	B	19.7739	20.4783	0.7044	20.2905	0.5173	0.1871	56.24
	C	19.7732	20.5775	0.8043	20.3672	0.5936	0.2107	56.70
	Average V_f = 56.39%, Standard deviation = 0.27%							

TABLE (A.11)

Angle-ply ratio in multilayered tubes
(weight is given in "g")

TUBE	SAMPLE	WEIGHT OF CRUCIBLE	AFTER BURN OFF WEIGHT	WEIGHT OF FIBRES	WEIGHT OF (CRUCIBLE + ANGLE-PLY FIBRES)	WEIGHT OF ANGLE-PLY FIBRES	ANGLE-PLY RATIO * %
B4	A	17.6821	18.3722	0.6913	18.1850	0.5041	72.92
	B	17.6809	18.2961	0.6148	18.1157	0.4344	70.66
	C	17.6813	18.1232	0.4414	17.9896	0.3083	69.85
	Average angle-ply ratio = 71.14%, Standard deviation = 1.59%						
B5	A	19.7753	20.9064	1.1323	20.7181	0.9440	83.37
	B	19.7741	20.8449	1.0704	20.6475	0.8730	81.56
	C	19.7745	20.8063	1.0317	20.6276	0.8530	82.68
	Average angle-ply ratio = 82.54%, Standard deviation = 0.91%						

$$* \text{ Angle-ply ratio} = \frac{\text{weight of fibres in } \pm\theta}{\text{weight of fibres in laminate}}$$

APPENDIX B

EXPERIMENTAL STRESS-STRAIN DATA FOR THE TEST SPECIMENS

B.1 THE LOAD MEASUREMENTS

The internal pressure was measured using a pressure transducer which was calibrated before the tests by means of a standard dead-weight calibrator. It behaved linearly giving output of 1 V for every 2,000 psi.

The axial load (tension or compression) and the torsional load were read directly from the indicators of the appropriate testing machines as their calibrations did not reveal linear relations between the input and the output.

The laminate stresses were then calculated from equation (2.2.38). In the cases of combined loadings of certain ratio $\sigma_x^o : \sigma_y^o : \tau_{xy}^o$ the ratio P : p : T was established from equation (2.2.38) and the specimen dimension (Appendix A) prior to the test. The specimen was then loaded with these loads simultaneously.

B.2 THE STRAIN MEASUREMENTS

The strain readings were obtained using strain gauges available in the workshop of the Aircraft Design Department. The strain gauges were bonded on the specimens as shown in Fig. (B.1), noting that not all the specimens had all these strain gauges. In fact, the majority of the specimens had strain gauges at their centres, only few specimens from tube B1 had additional strain gauges at 50 mm from the centre to ensure that the strain distribution along the test section is constant. The strain gauges used had gauge factor ranging from 2.0 to 2.145.

B.3 EXPERIMENTAL STRESS-STRAIN CURVES

The xperimental stress-strain curves for the test specimens are shown in Figs. (B.2) to (B.49). It should be noted that it was not possible to record the strains at the ultimate failure. In some cases the strain gauges debonded during the test before reaching the ultimate load. In some other cases these gauges reached their maximum allowable strains

before final failure. What can be concluded from these remarks is that the stress-strain curves presented here do not reach ultimate failure of the test specimens. The failure loads were, of course, recorded and are given in Chapter 5.

As shown in the figures, there were sometimes different readings for the strains from the two strain gauges which measured the same strain. One may suggest that the average of the two readings should be plotted, but it was preferred to plot them as they were obtained to give a true picture of the tests. There are many reasons, however, for the difference in the values of strains, some of these reasons are :

1. local miasalignment of fibres,
2. local high/low fibre content,
3. local greater/smaller wall thickness,
4. misalignment of strain gauges,
5. gauges not bonded properly.

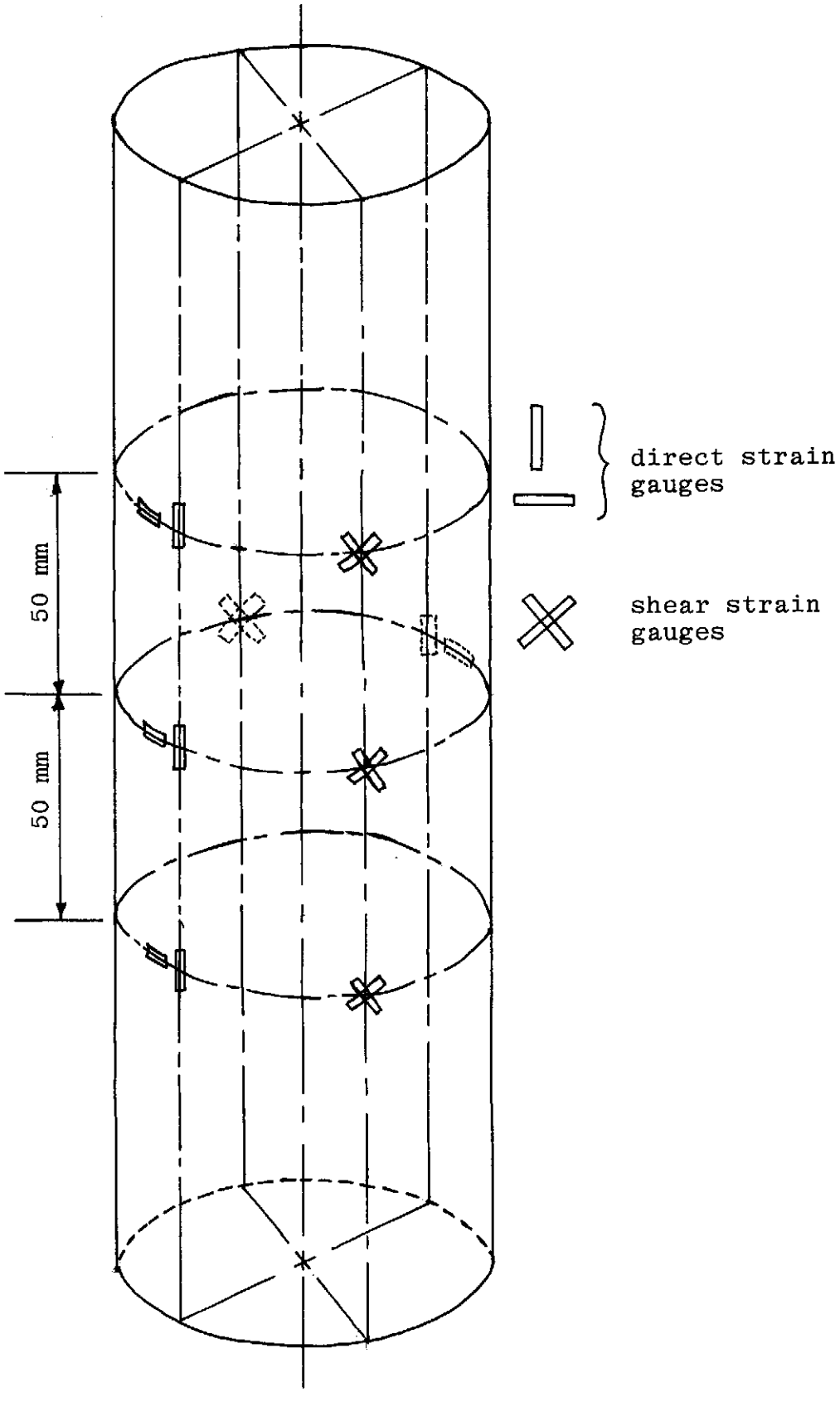

Fig.(B.1) Strain gauges arrangement

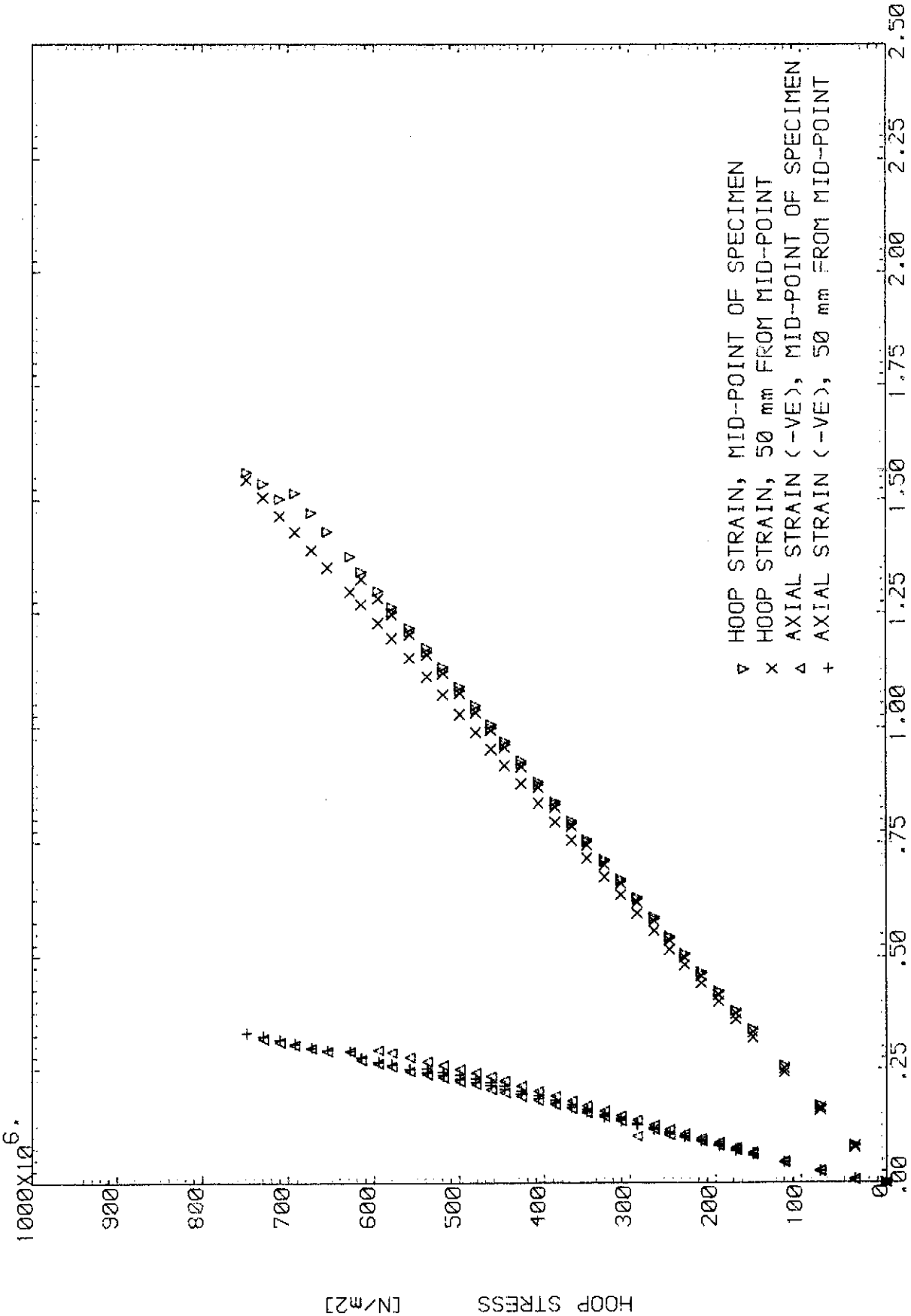

Fig.(B.2) INTERNAL PRESSURE TEST OF SPECIMEN 181 (SX:SY:SXY=0.0:1.0:0.0)

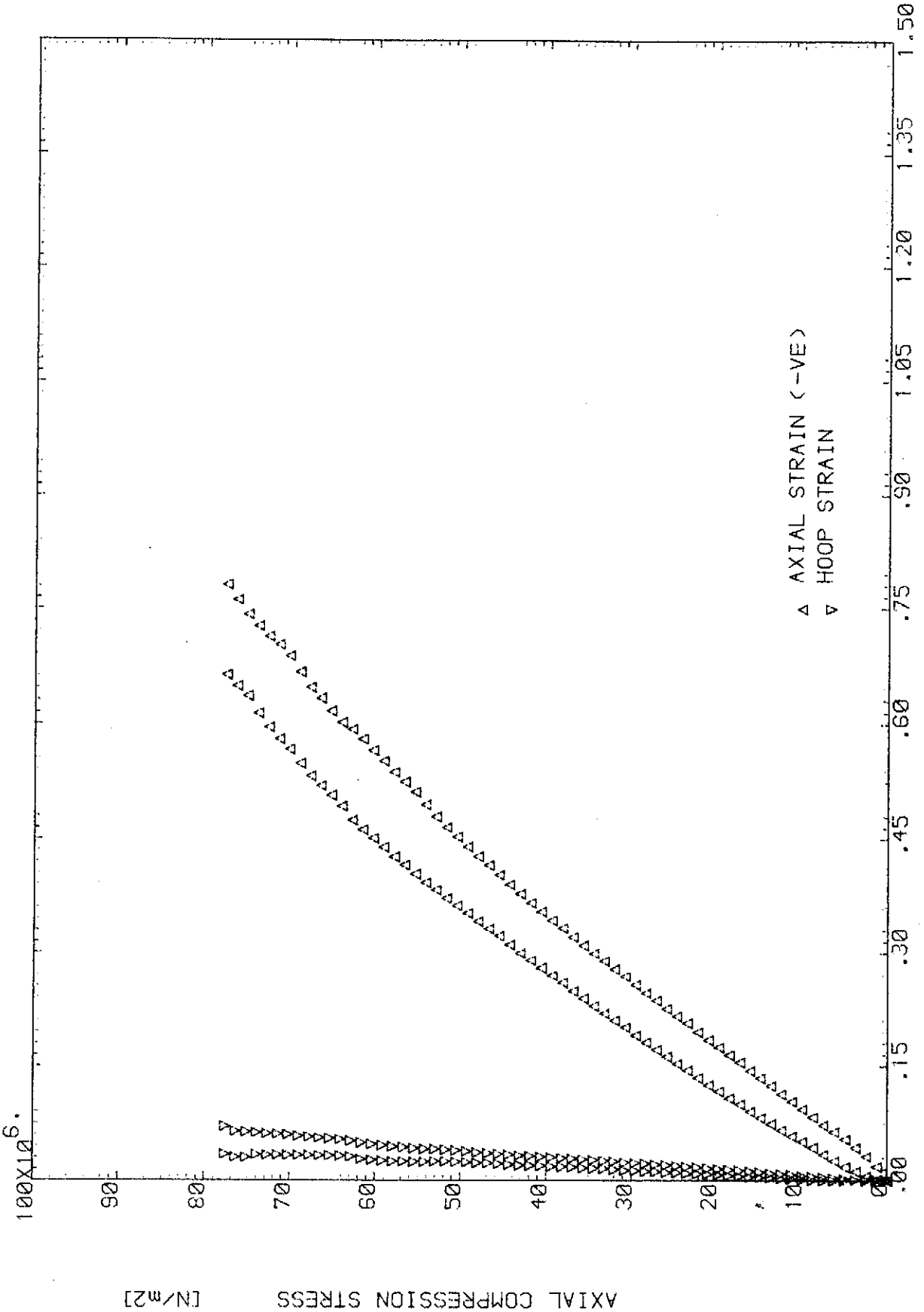

Fig.(B.3) AXIAL COMPRESSION TEST OF SPECIMEN 2B1 (SX:SY:SXY=-1.0:0.0:0.0)

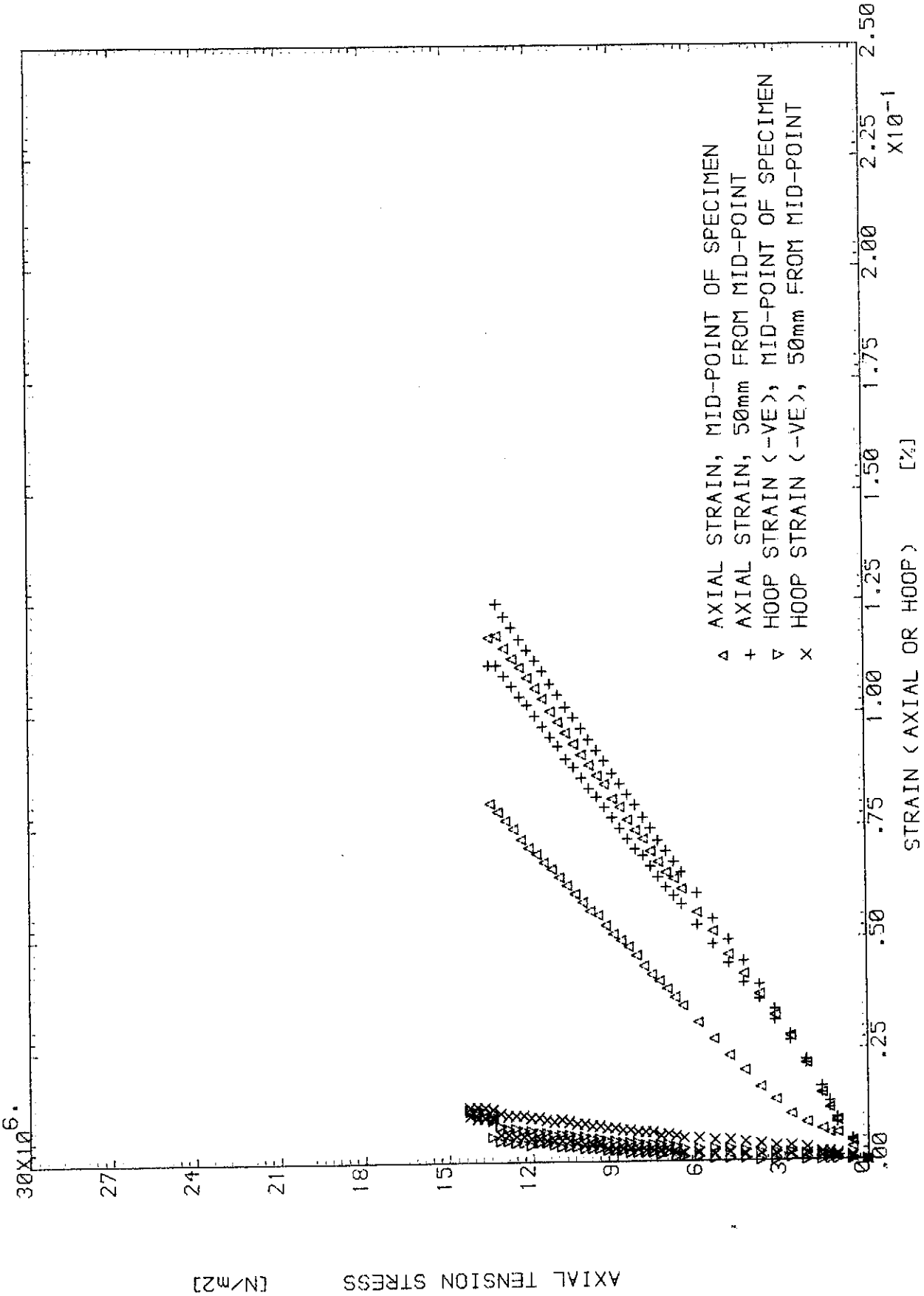

Fig.(B.4) AXIAL TENSION TEST OF SPECIMEN 3B1 (SX:SY:SXY=1.0:0.0:0.0)

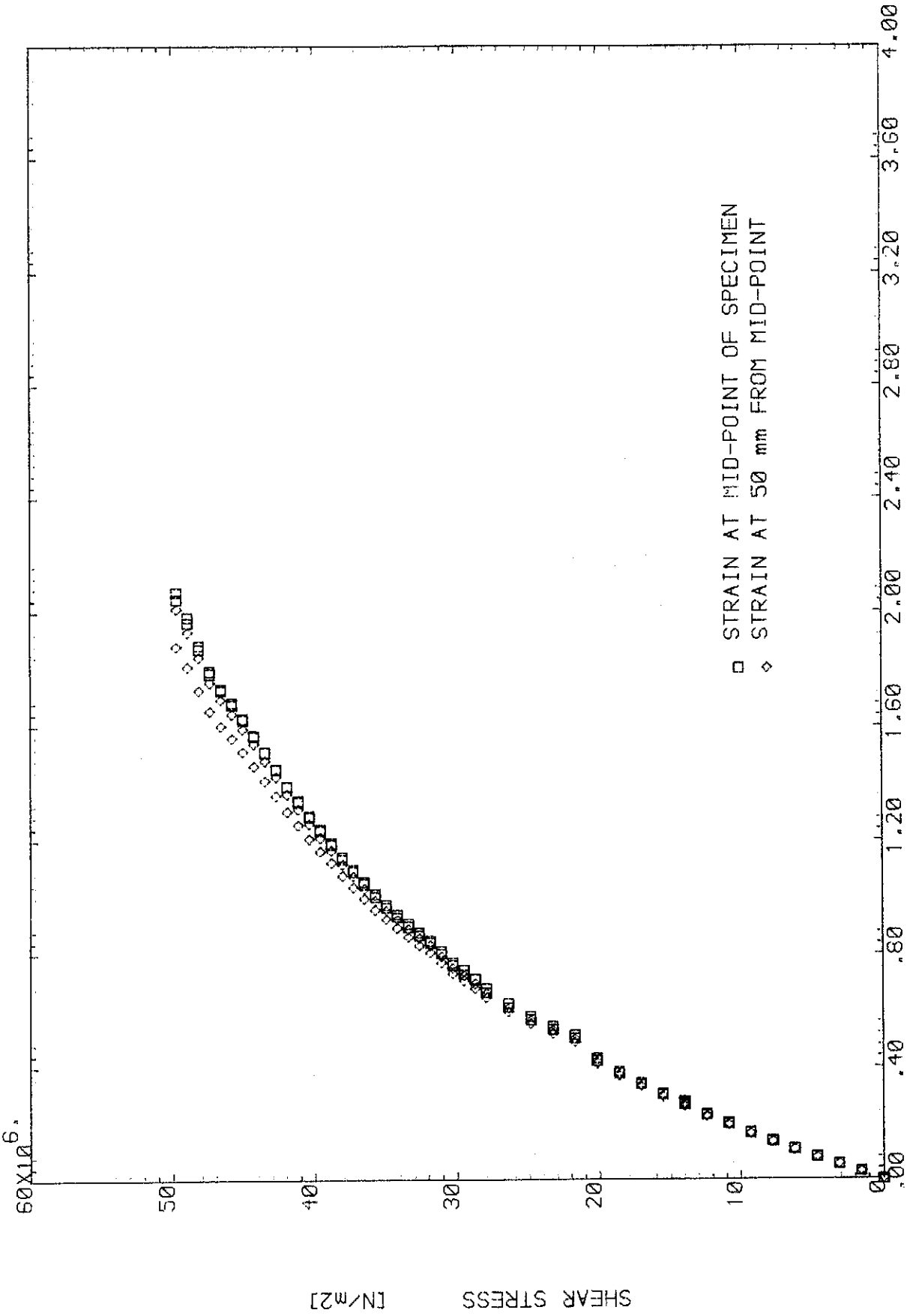

Fig.(B.5) TORSION TEST OF SPECIMEN 4B1 (SX:SY:SXY=0.0:0.0:1.0)

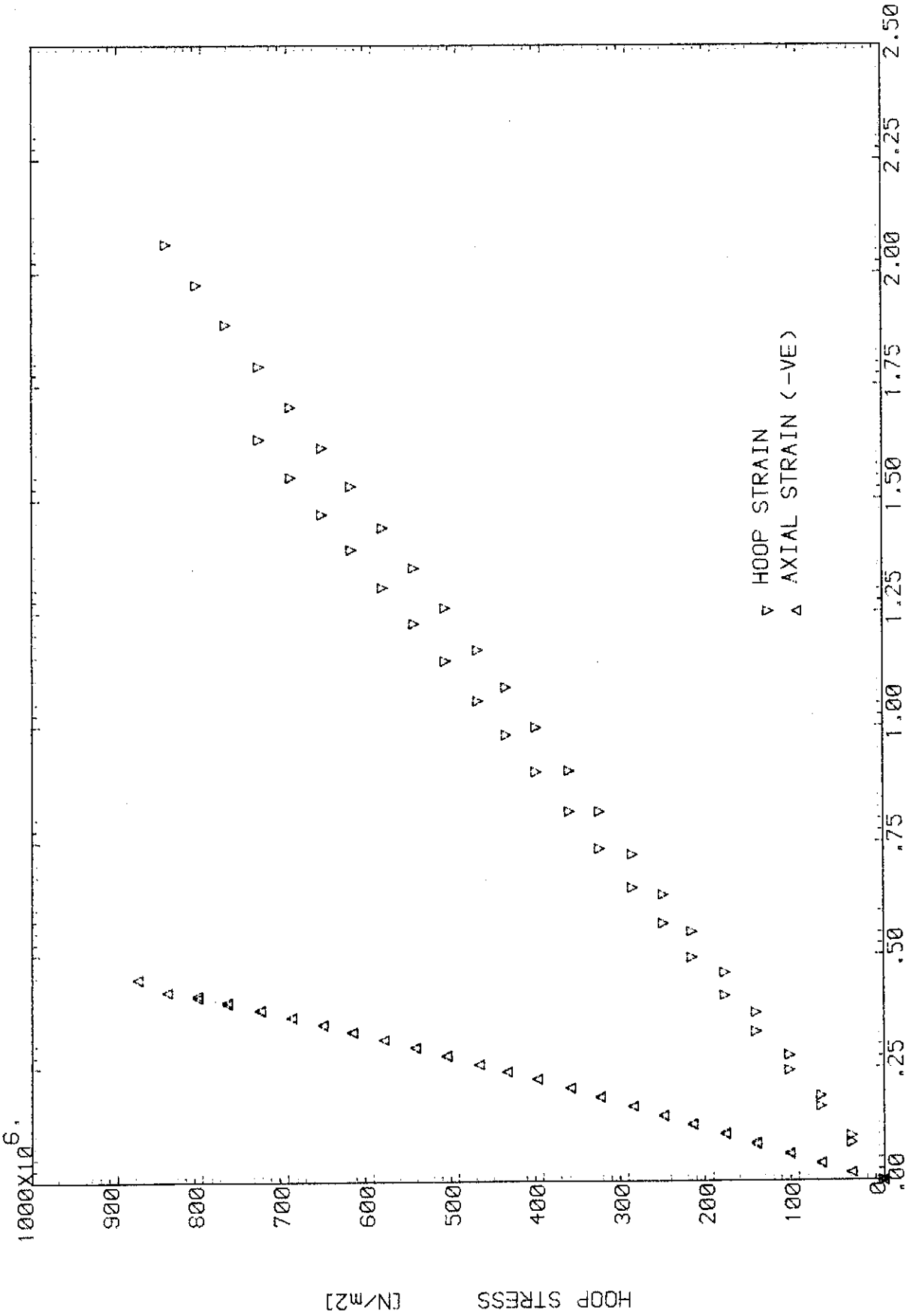

Fig.(B.6) INTERNAL PRESSURE TEST OF SPECIMEN 5B1 (SX:SY:SXY=0.0:1.0:0.0)

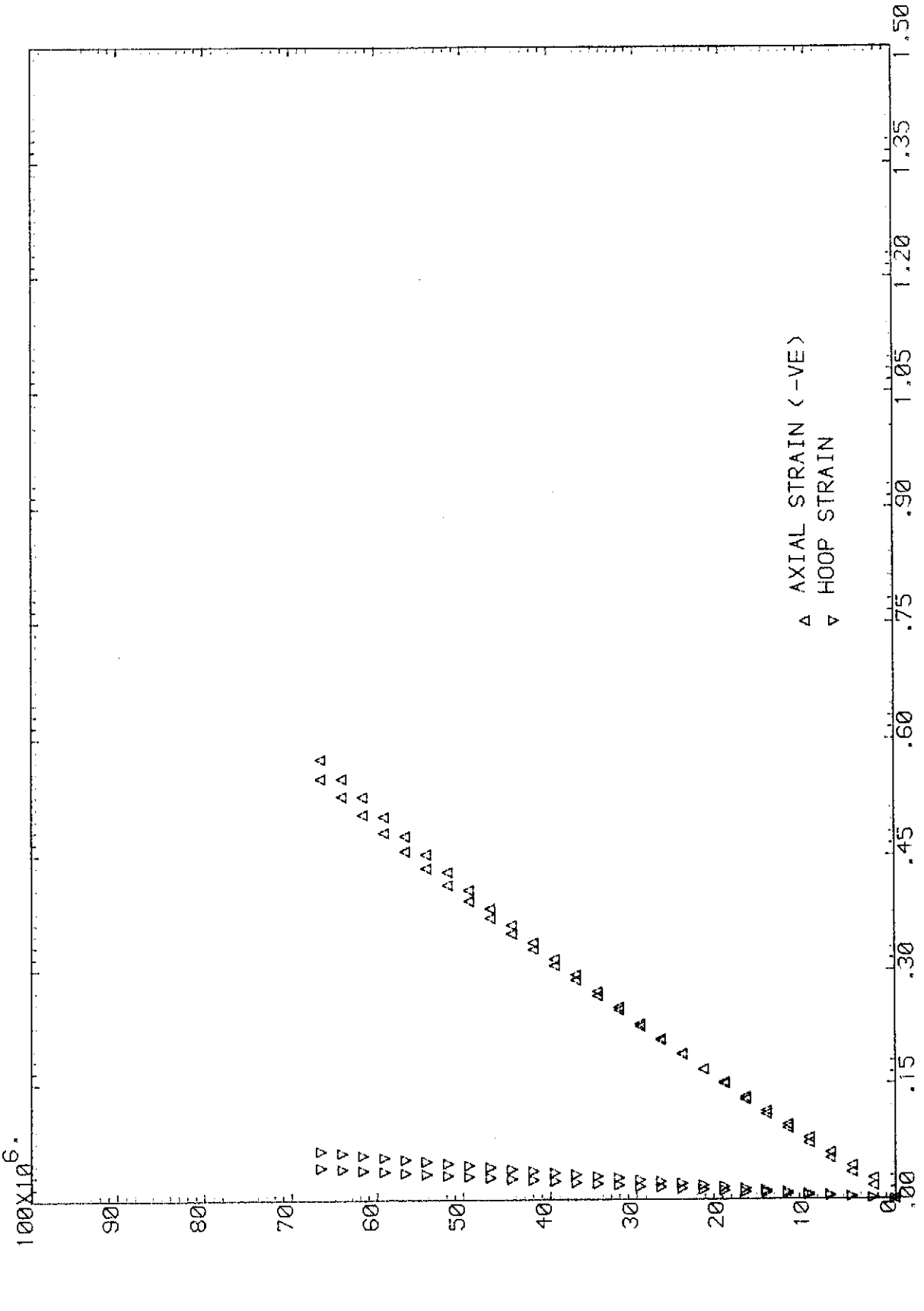

Fig.(B.7) AXIAL COMPRESSION TEST OF SPECIMEN 6B1 (SX:SY:SXY=-1.0:0.0:0.0)

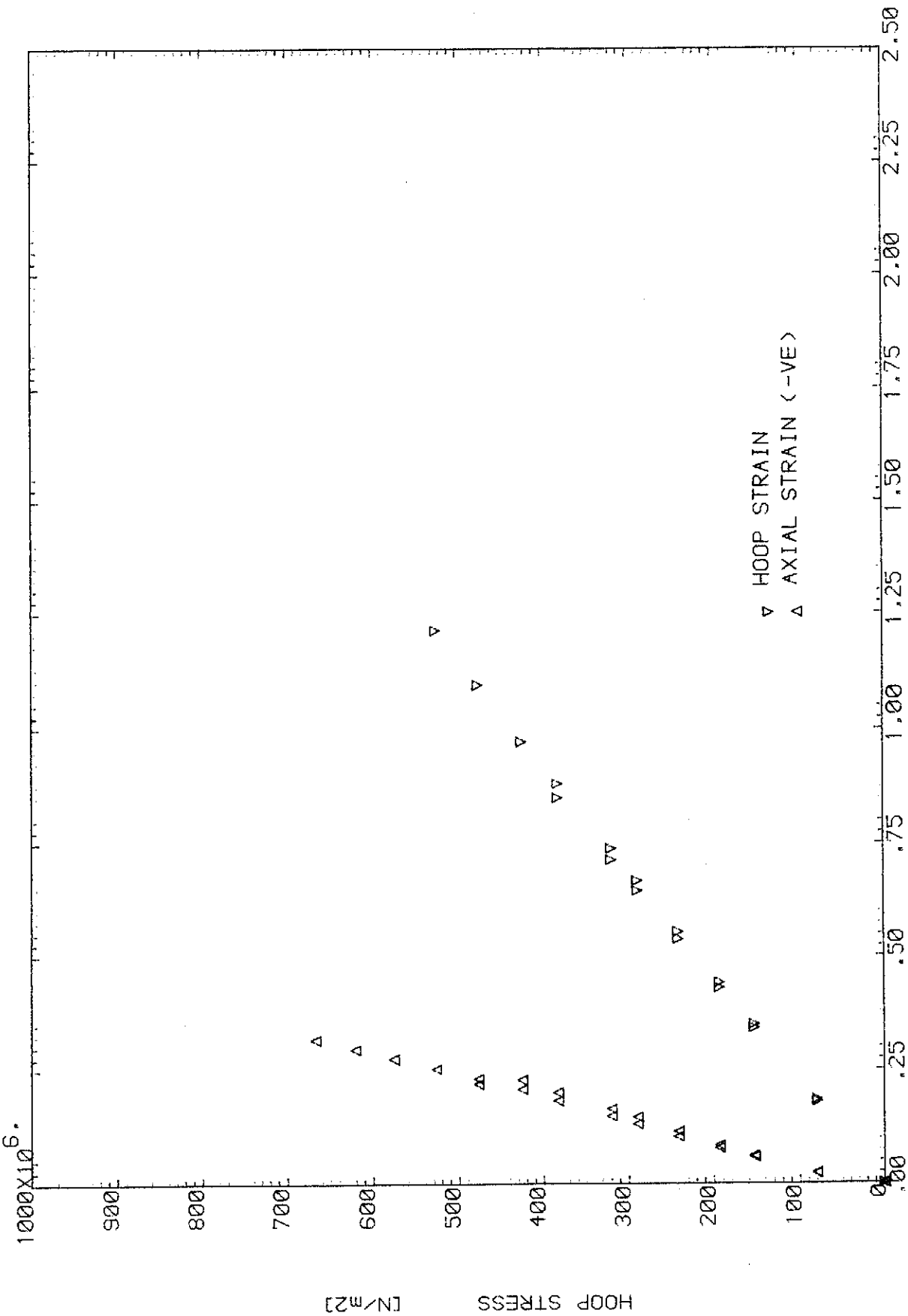

Fig.(B.8) INTERNAL PRESSURE TEST OF SPECIMEN 7B1 (SX:SY:SXY=0.0:1.0:0.0)

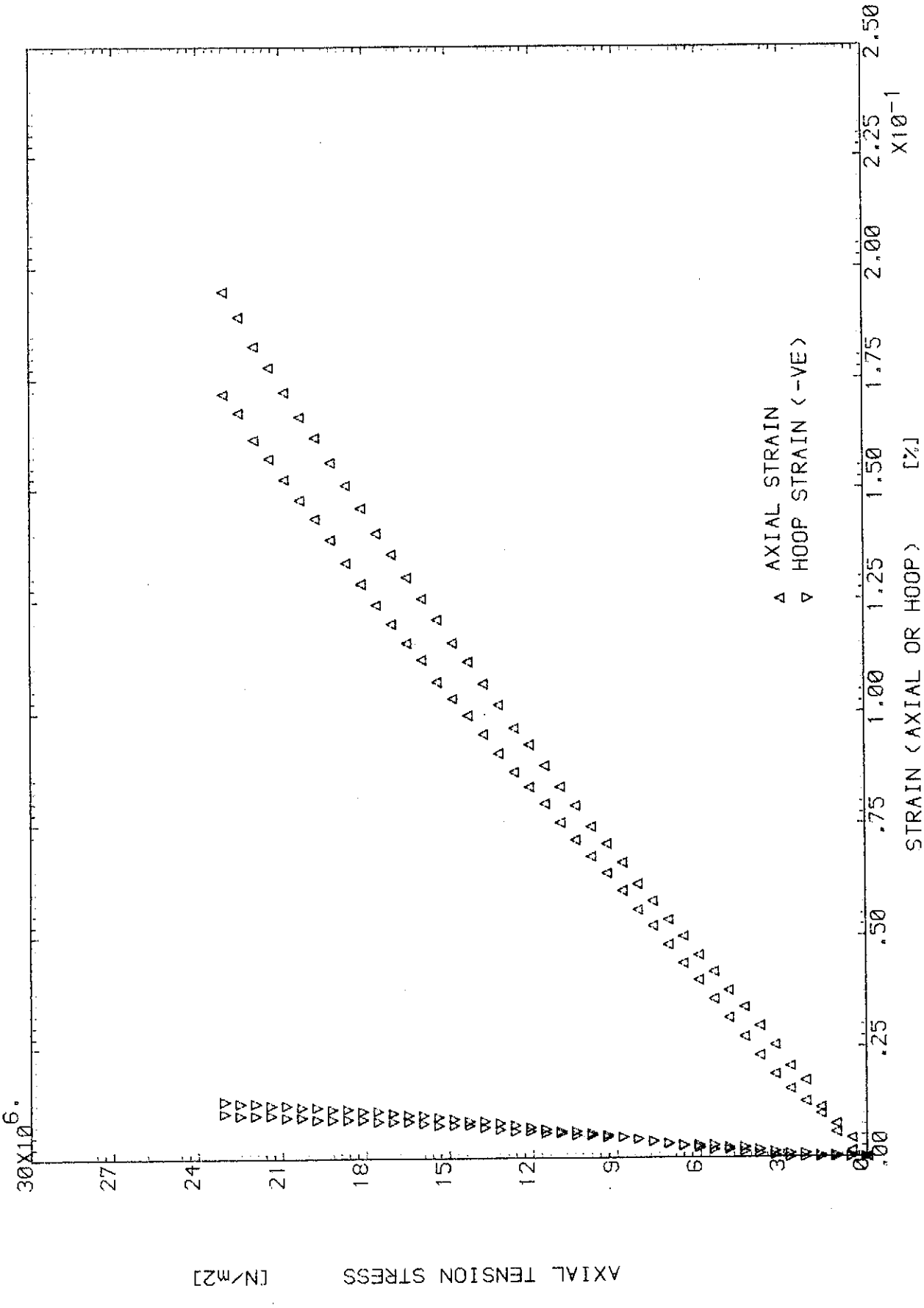

Fig.(B.9) AXIAL TENSION TEST OF SPECIMEN 8B1 (SX:SY:SXY=1.0:0.0:0.0)

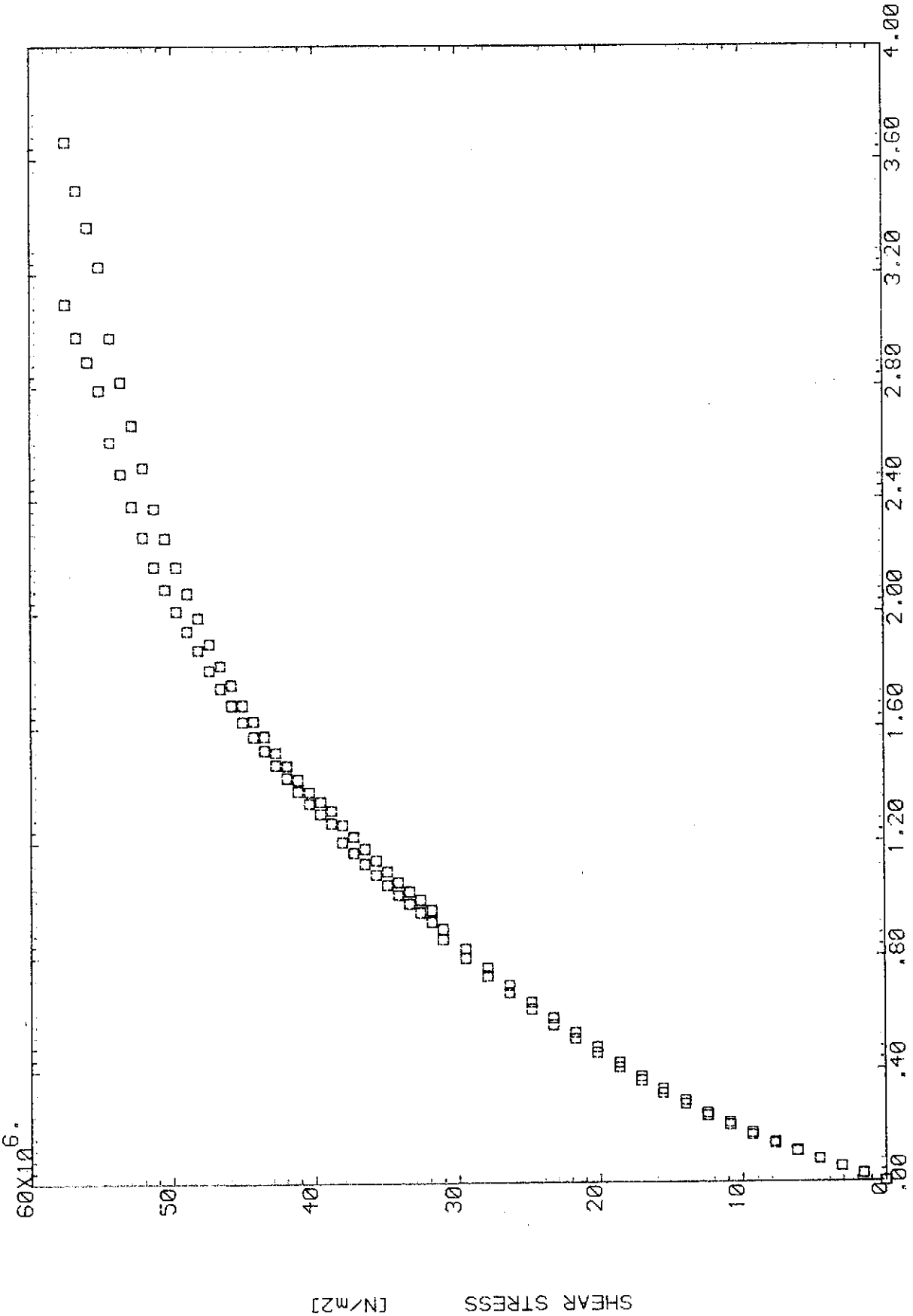

Fig.(B.10) TORSION TEST OF SPECIMEN 9B1 (SX:SY:SXY=0.0:0.0:1.0)

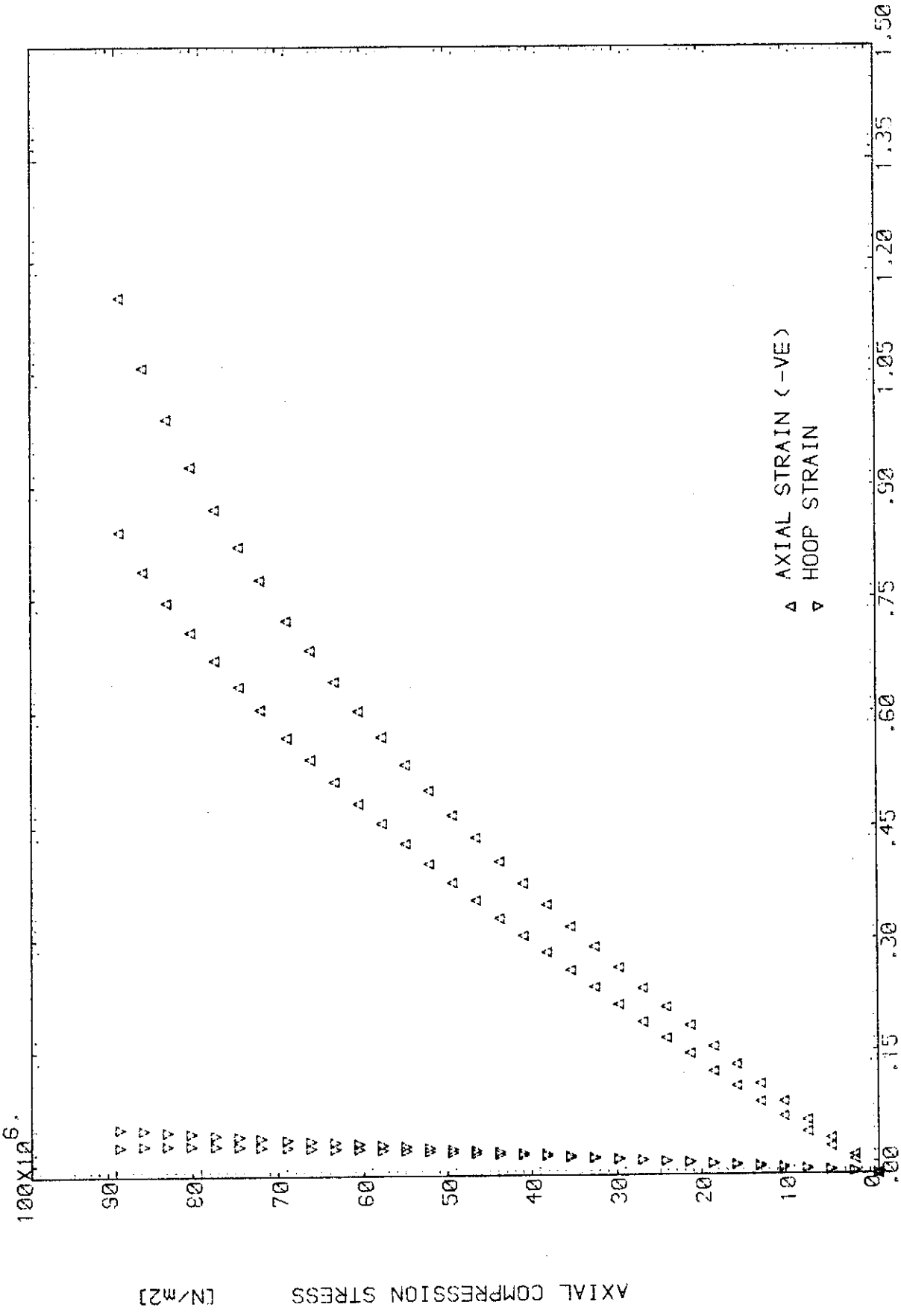

Fig.(B.11) AXIAL COMPRESSION TEST OF SPECIMEN 10B1 (SX:SY:SXY=-1.0:0.0:0.0)

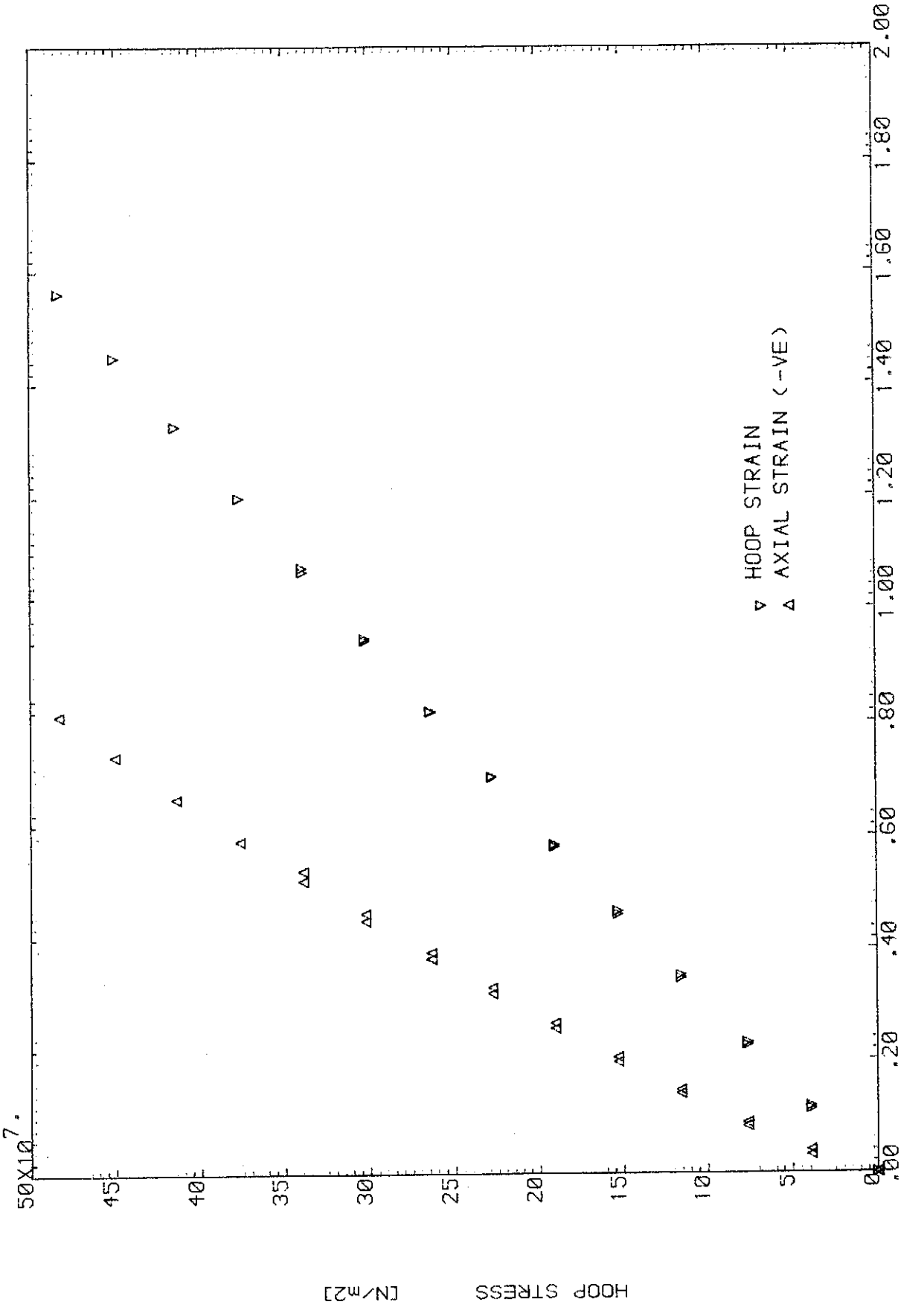

Fig.(B.12) BIAXIAL TEST OF SPECIMEN 1B2 (SX:SY:SXY=0.0:1.0:0.0)

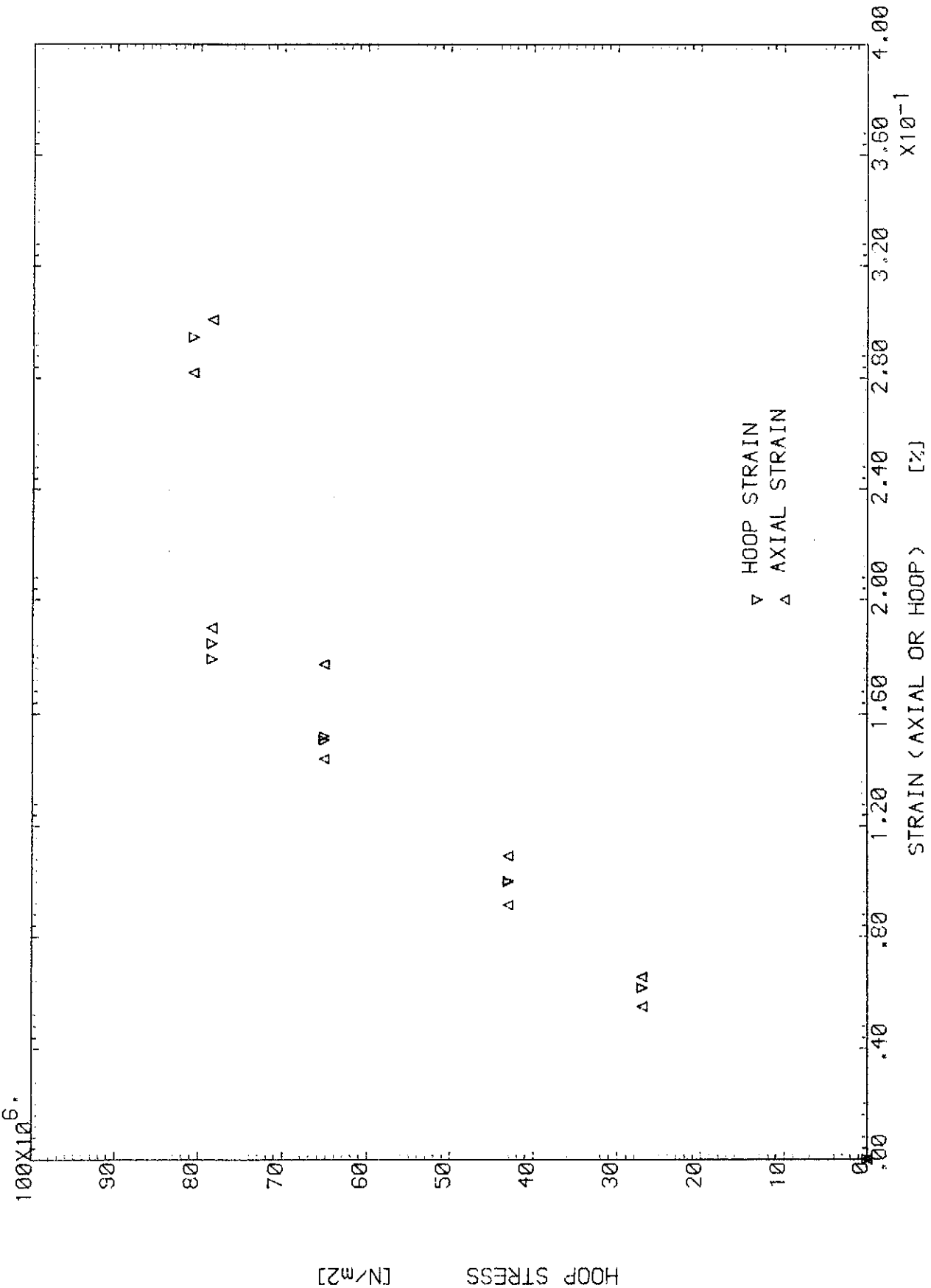

Fig.(B.13) BIAXIAL TEST OF SPECIMEN 2B2 (SX:SY:SXY=0.5:1.0:0.0)

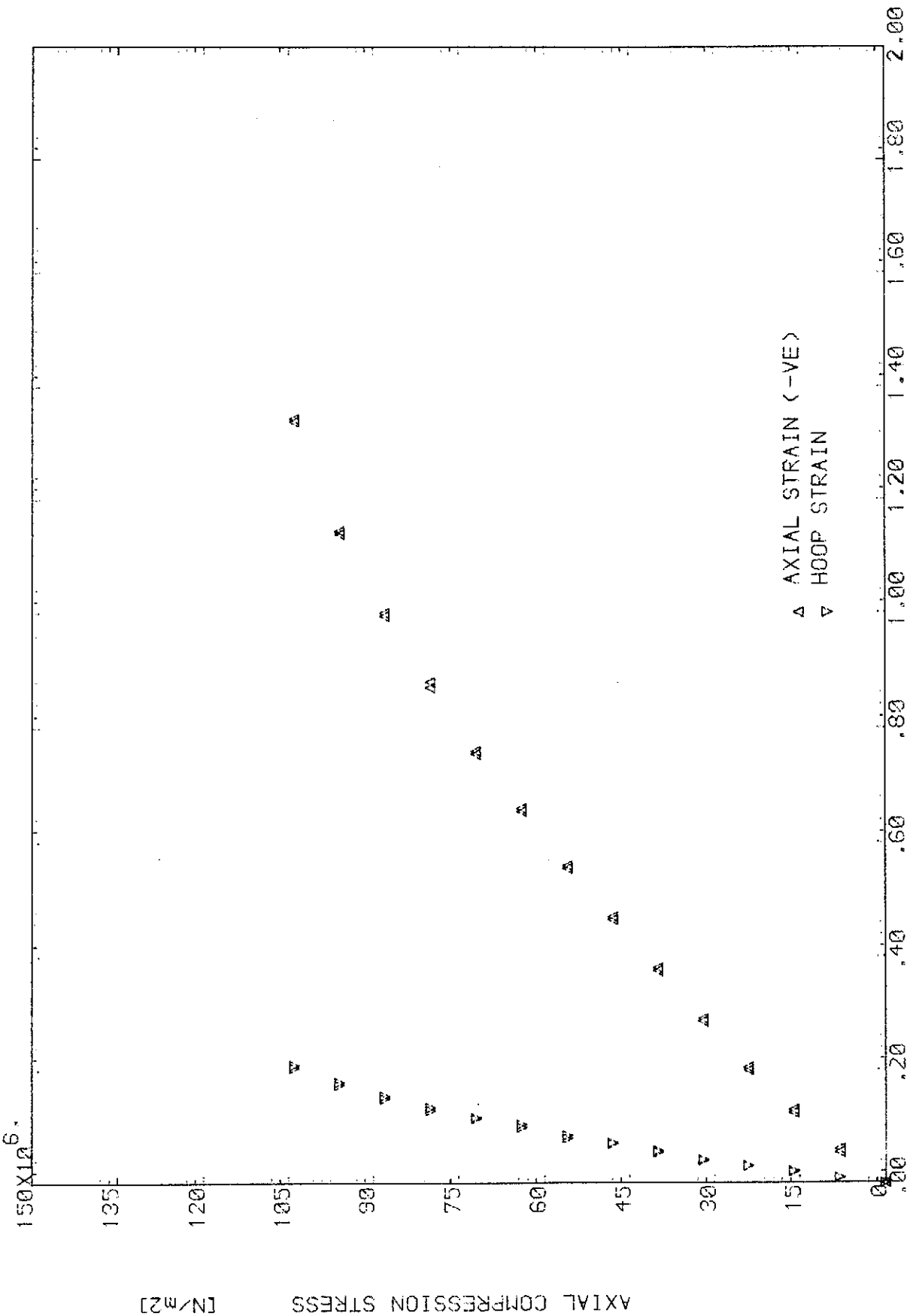

Fig.(B.14) BIAXIAL TEST OF SPECIMEN 3B2 (SX:SY:SXY=-1.0:0.0:0.0)

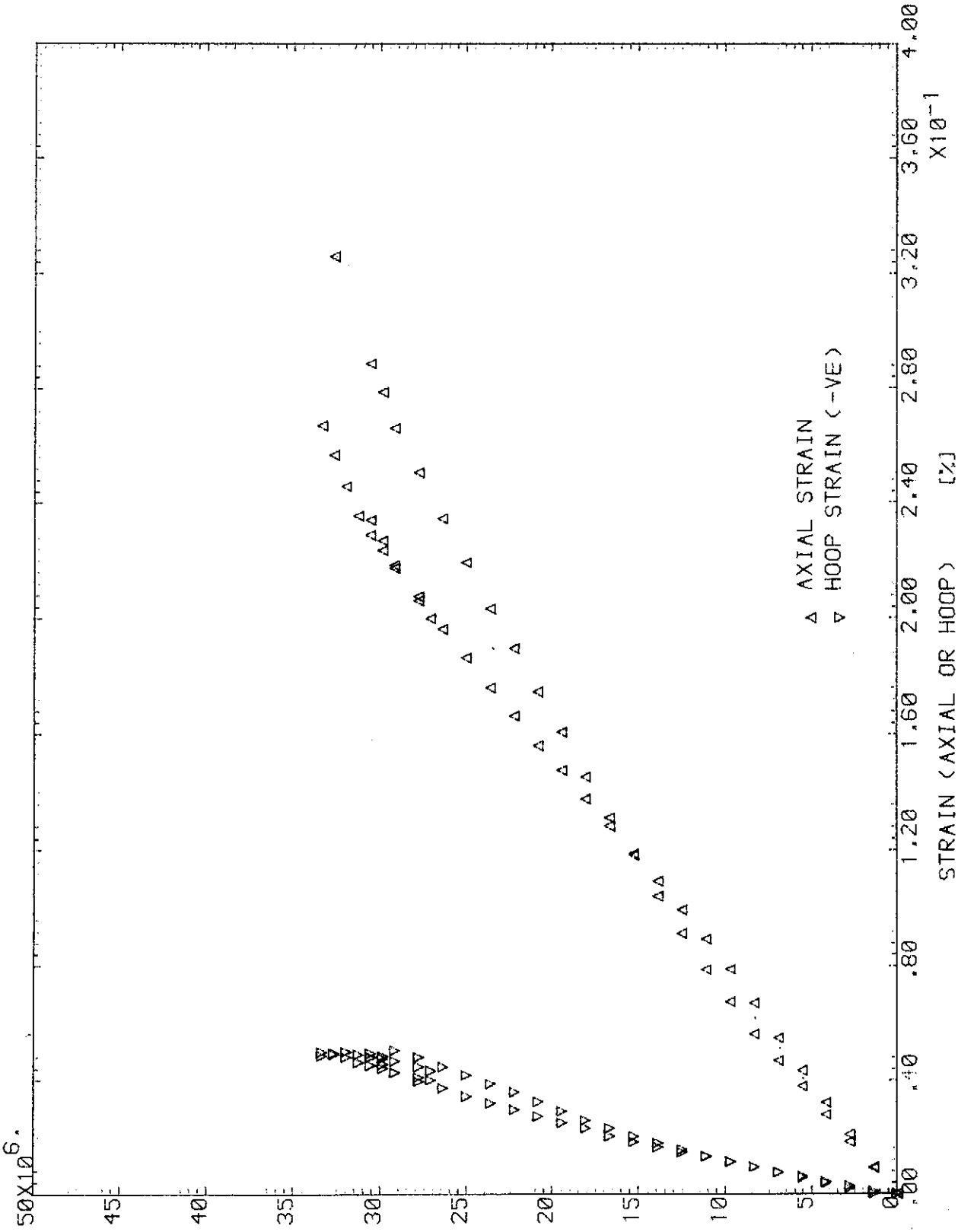

Fig.(B.15) BIAXIAL TEST OF SPECIMEN 4B2 (SX:SY:SXY=1.0:0.0:0.0)

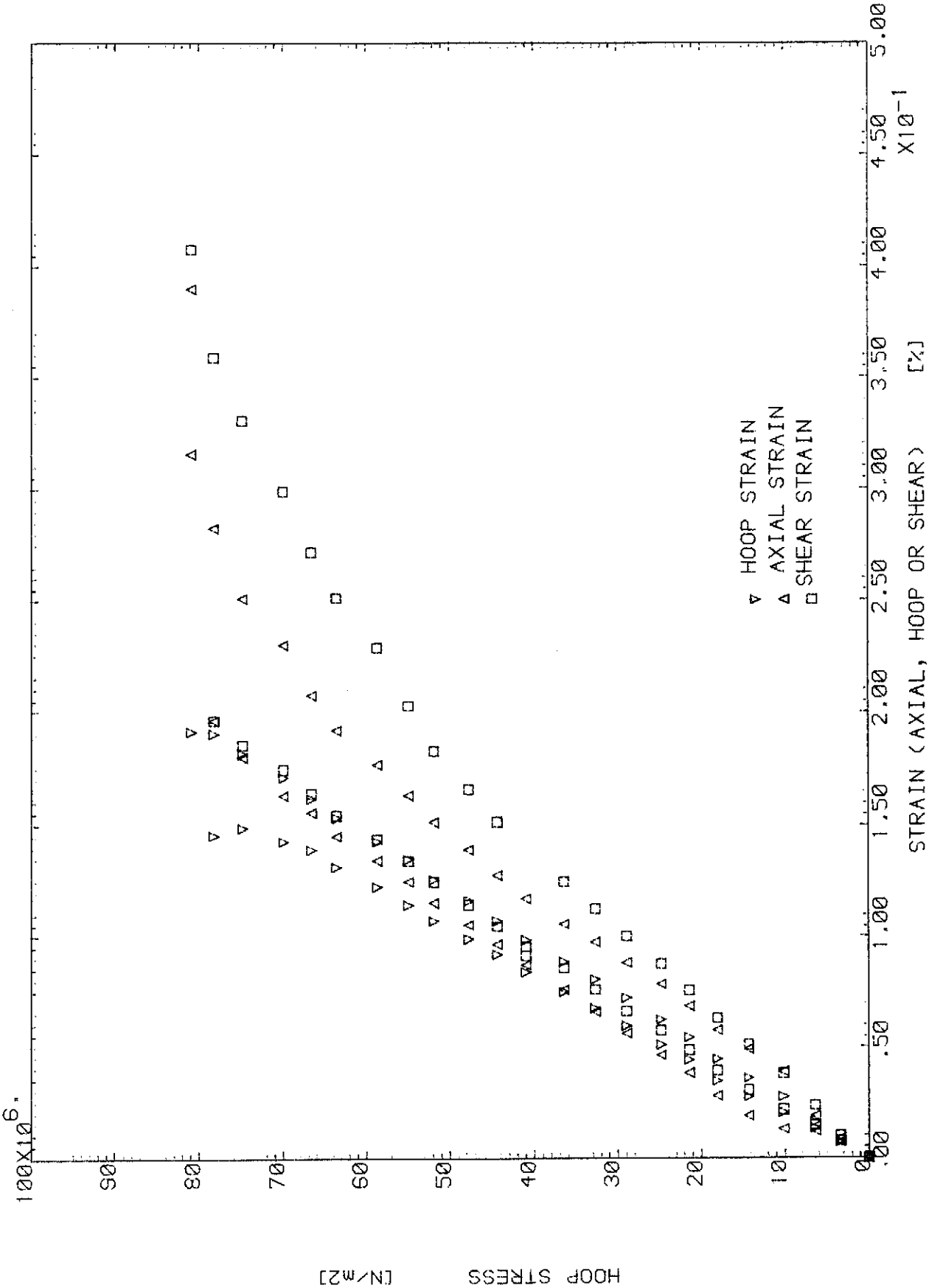

Fig.(B.16) BIAXIAL TEST OF SPECIMEN 5B2 (SX:SY:SXY=0.5:1.0:0.2)

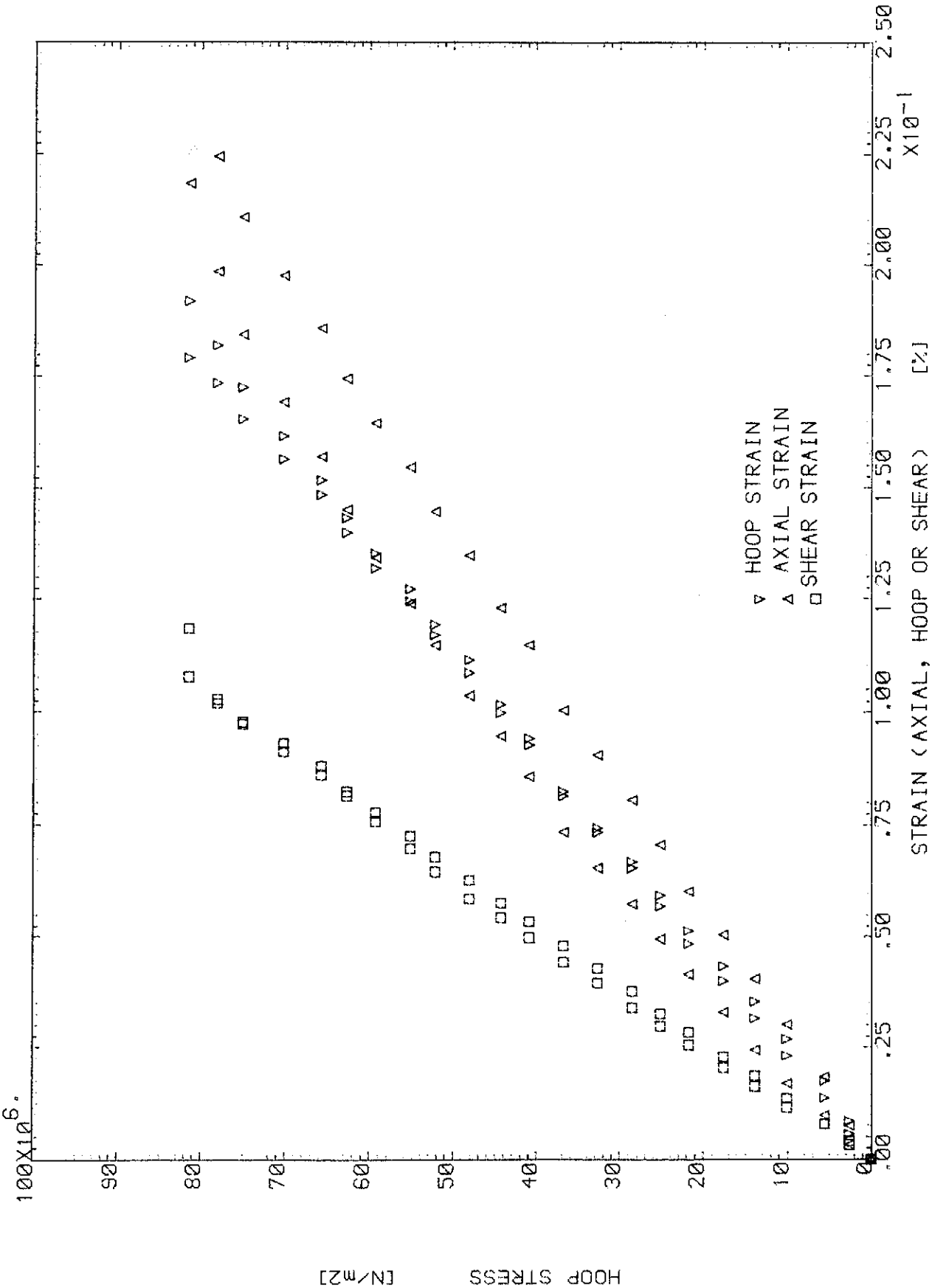

Fig.(B.17) BIAXIAL TEST OF SPECIMEN 6B2 (SX:SY:SXY=0.5:1.0:0.1)

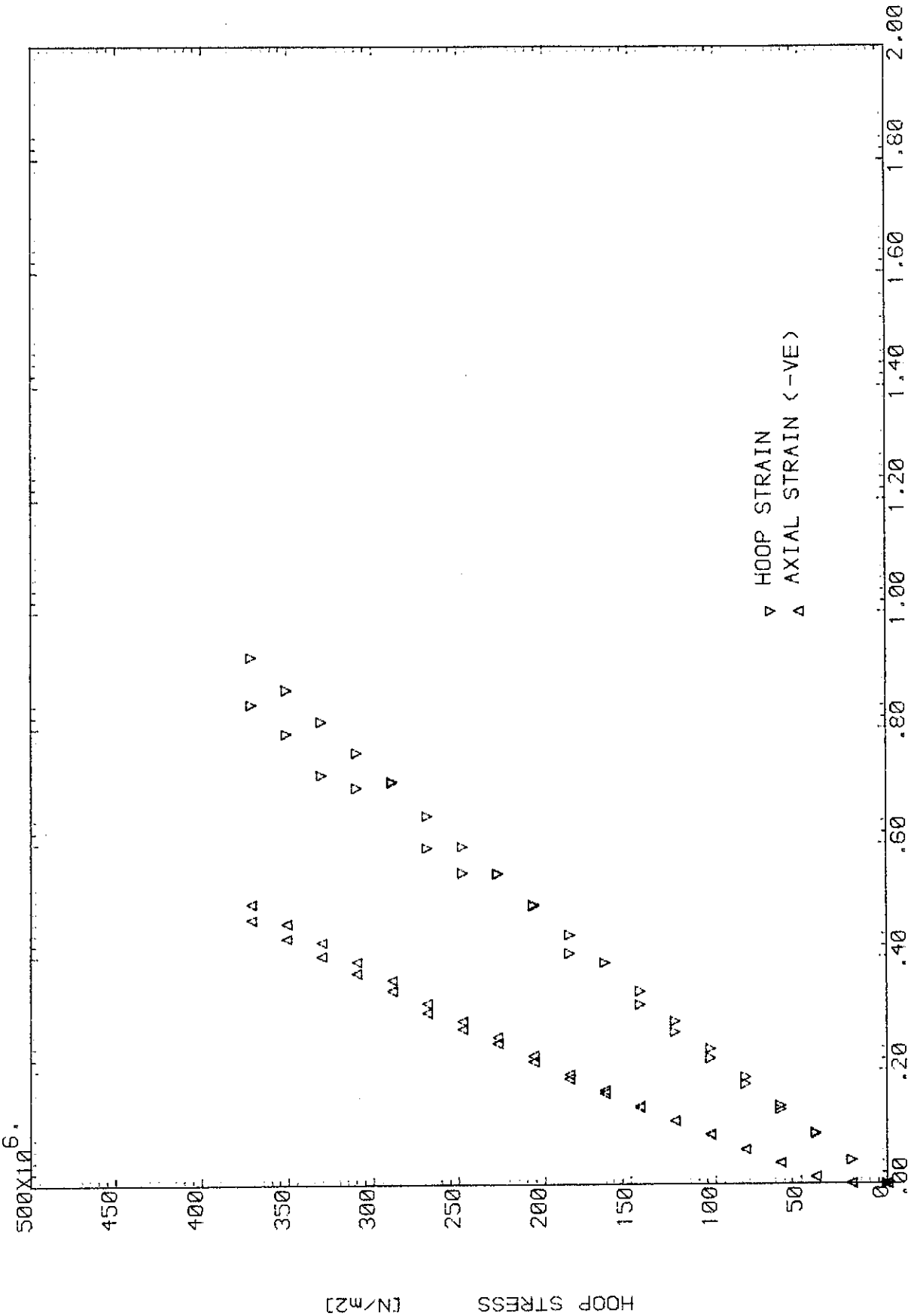

Fig.(B.18) BIAXIAL TEST OF SPECIMEN 7B2 (SX:SY:SXY=0.0:1.0:0.0)

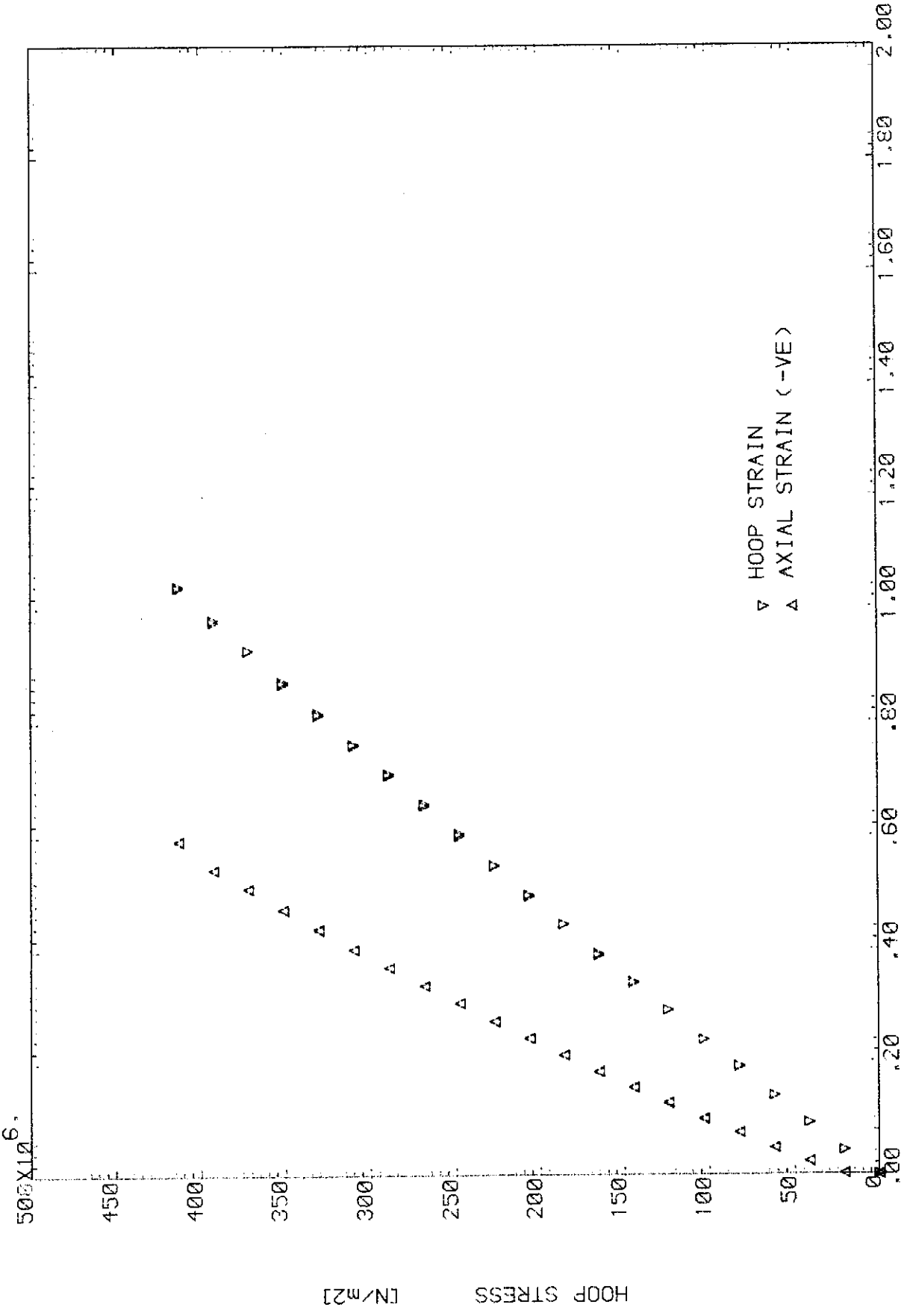

Fig.(B.19) BIAXIAL TEST OF SPECIMEN 8B2 (SX:SY:SXY=0.0:1.0:0.0)

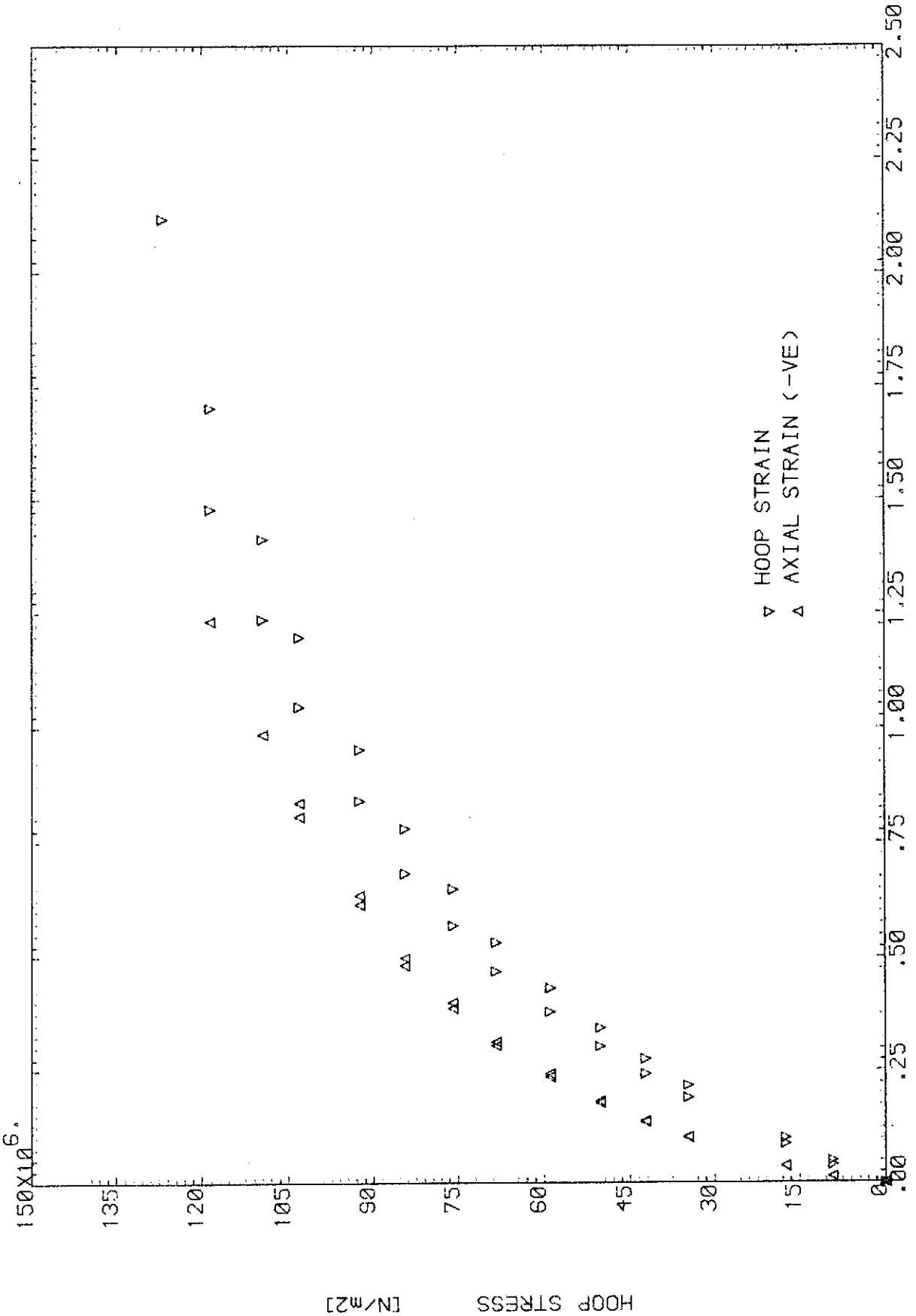

Fig.(B.20) BIAXIAL TEST OF SPECIMEN 1B3 (SX:SY:SXY=0.0:1.0:0.0)

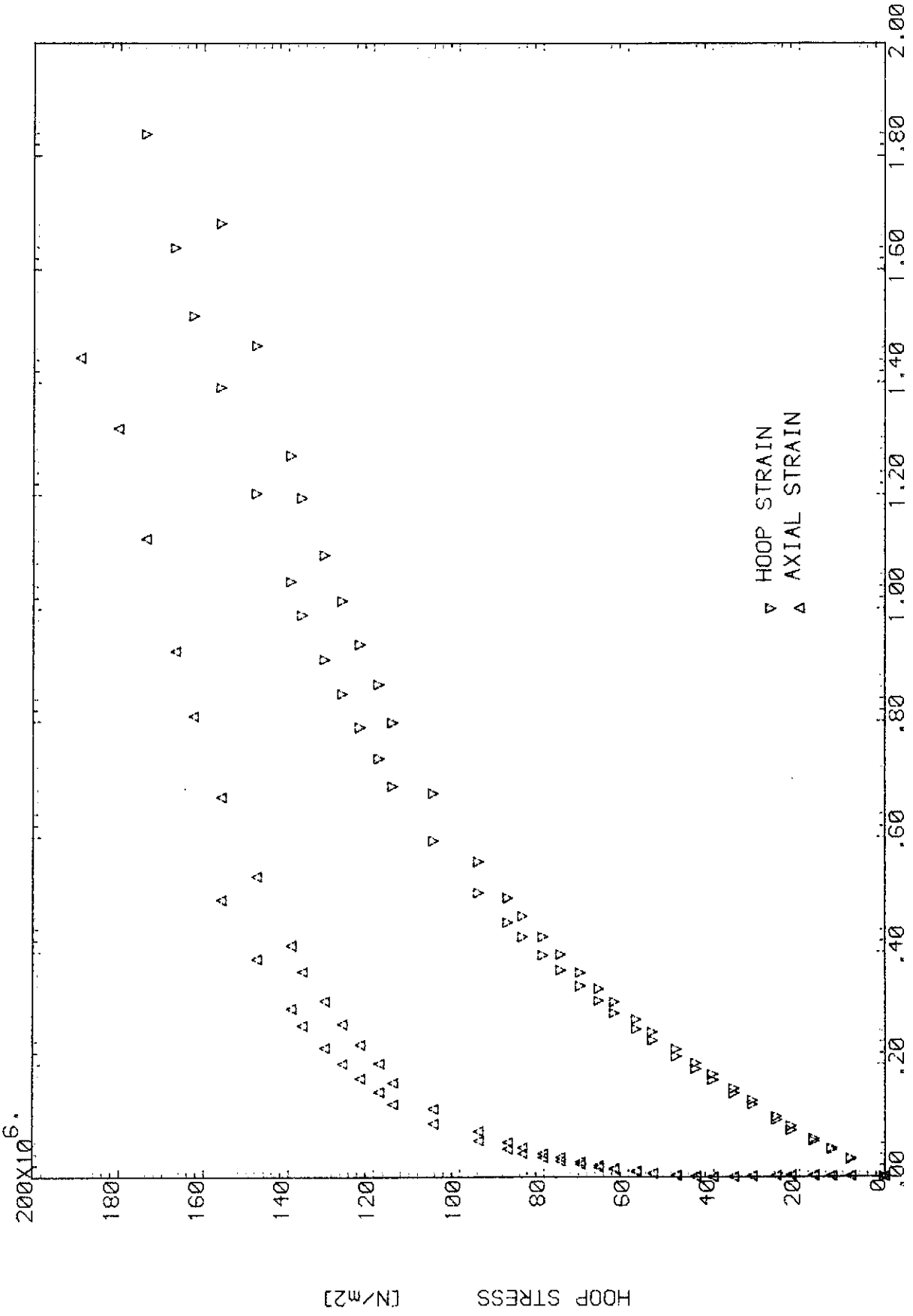

Fig.(B.21) BIAXIAL TEST OF SPECIMEN 2B3 (SX:SY:SXY=0.5:1.0:0.0)

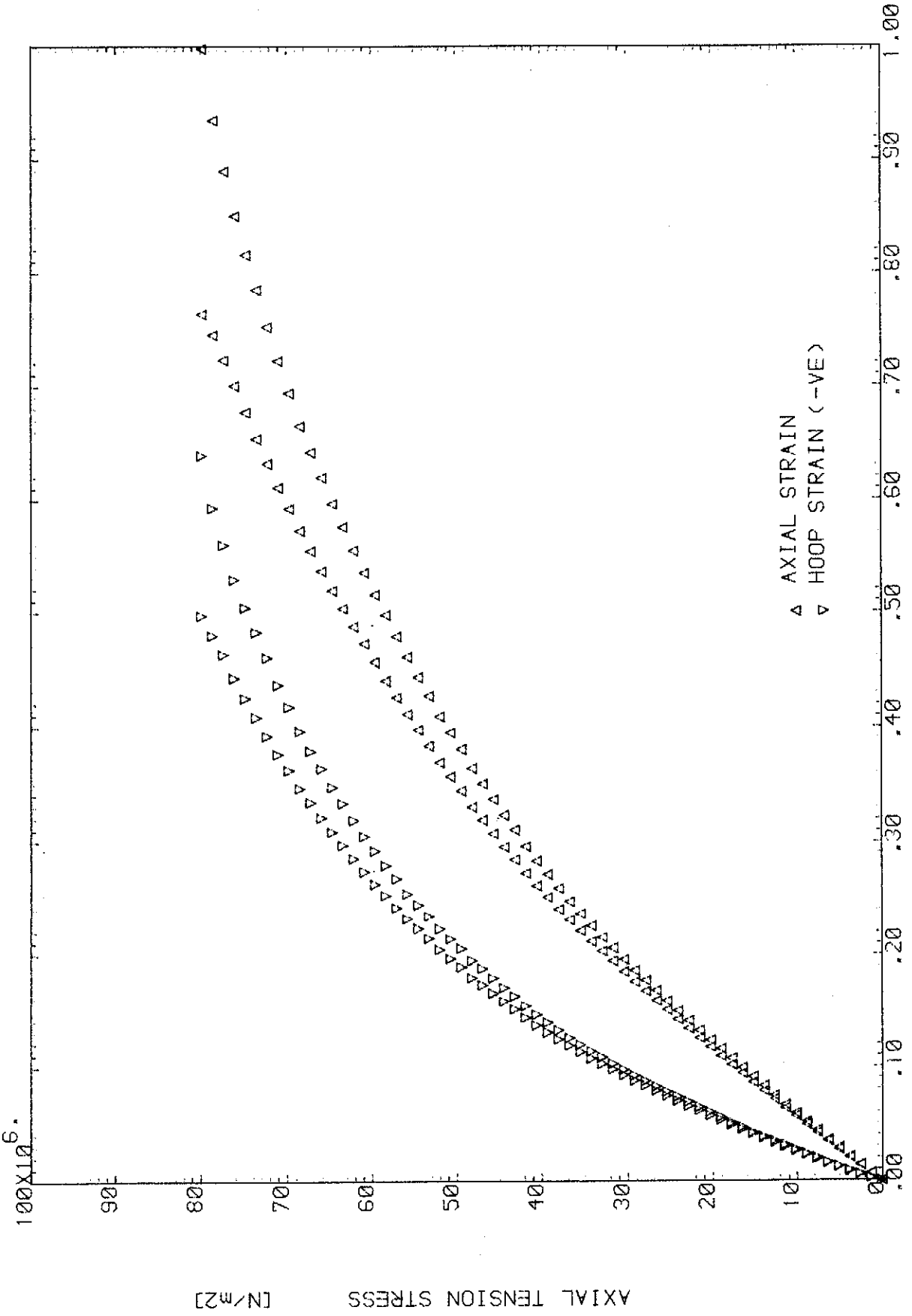

Fig.(B.22) BIAXIAL TEST OF SPECIMEN 3B3 (SX:SY:SXY=1.0:0.0:0.0)

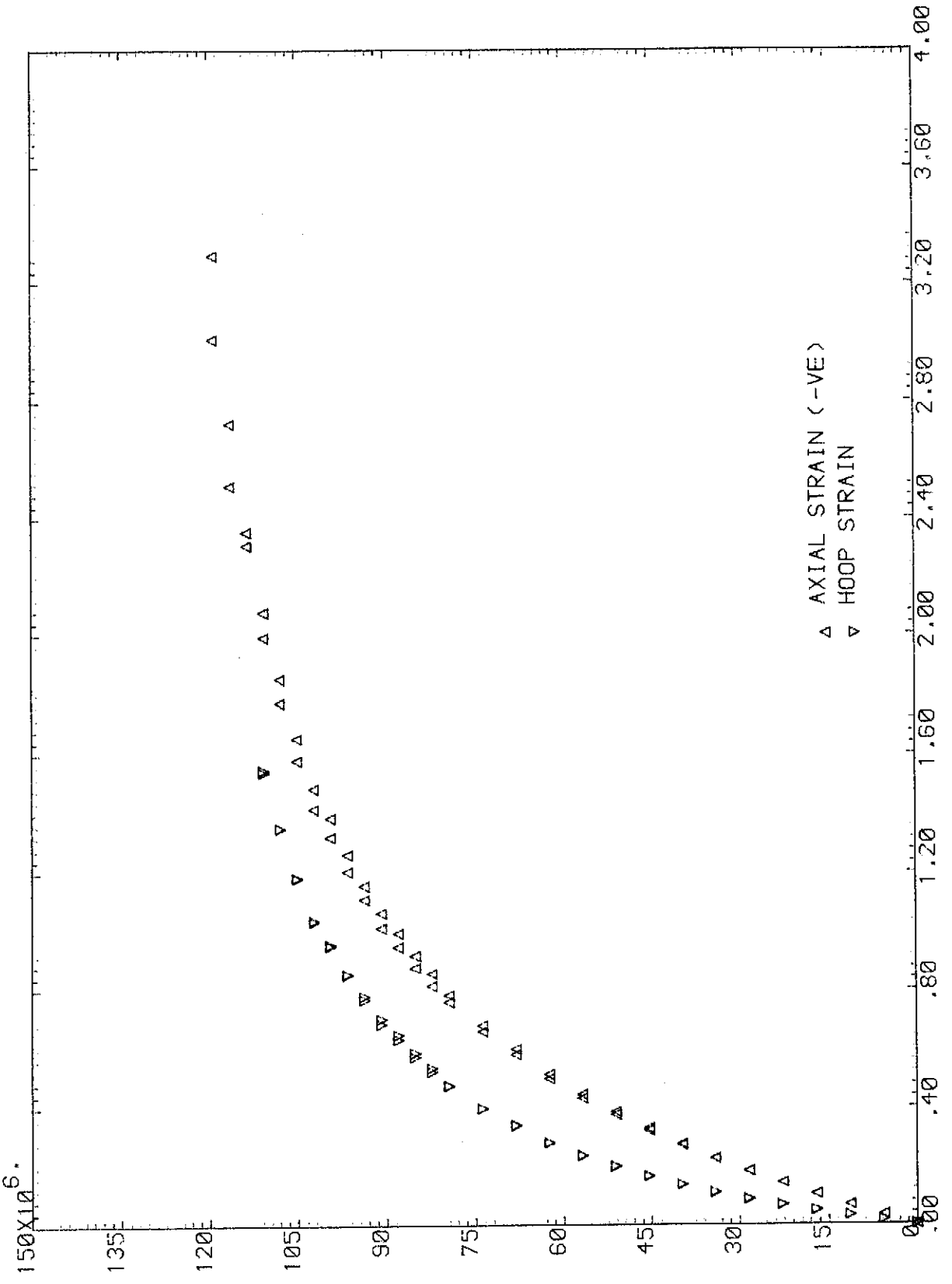

Fig.(B.23) BIAXIAL TEST OF SPECIMEN 4B3 (SX:SY:SXY=-1.0:0.0:0.0)

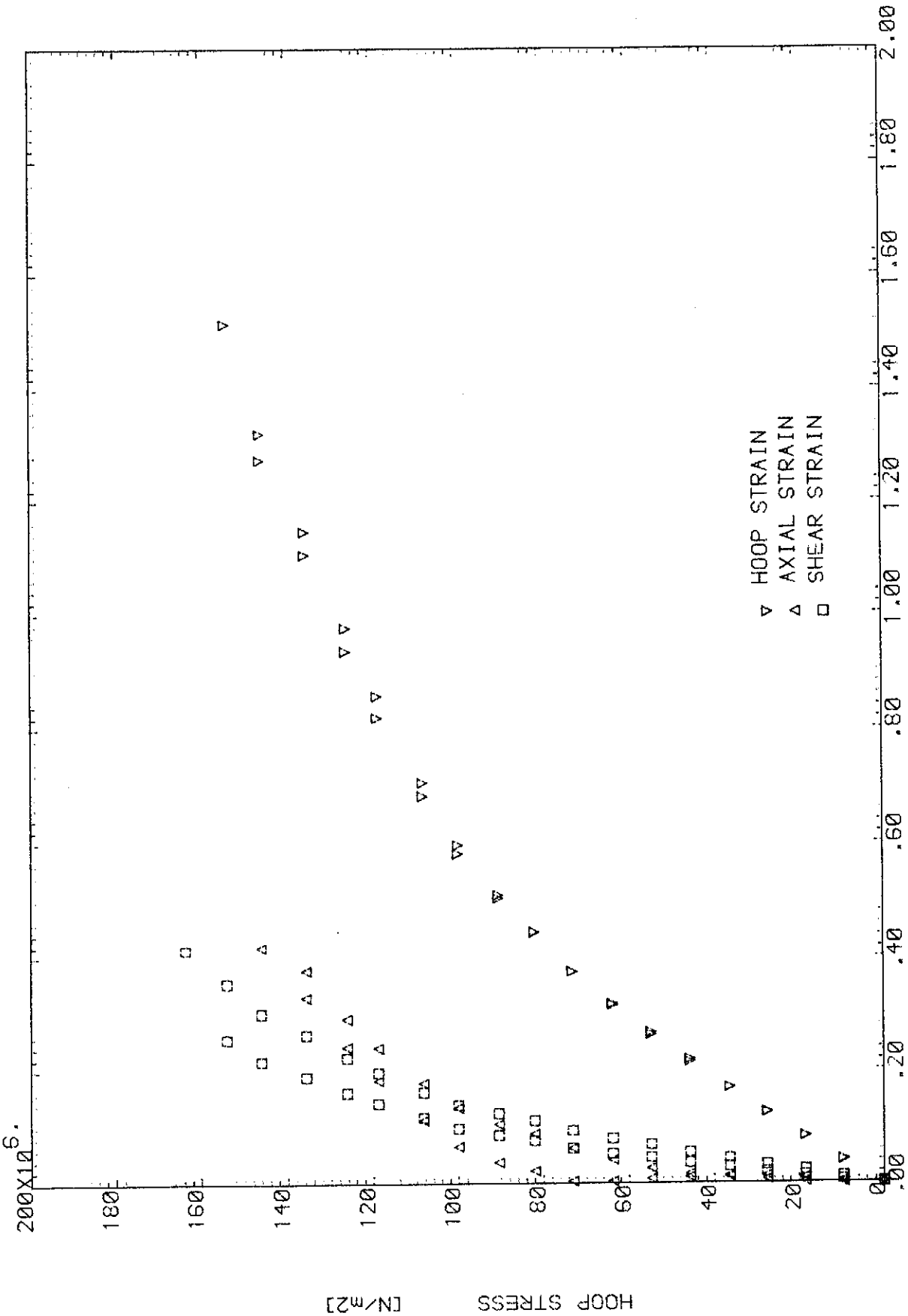

Fig.(B.24) BIAXIAL TEST OF SPECIMEN 5B3 (SX:SY:SXY=0.5:1.0:0.1)

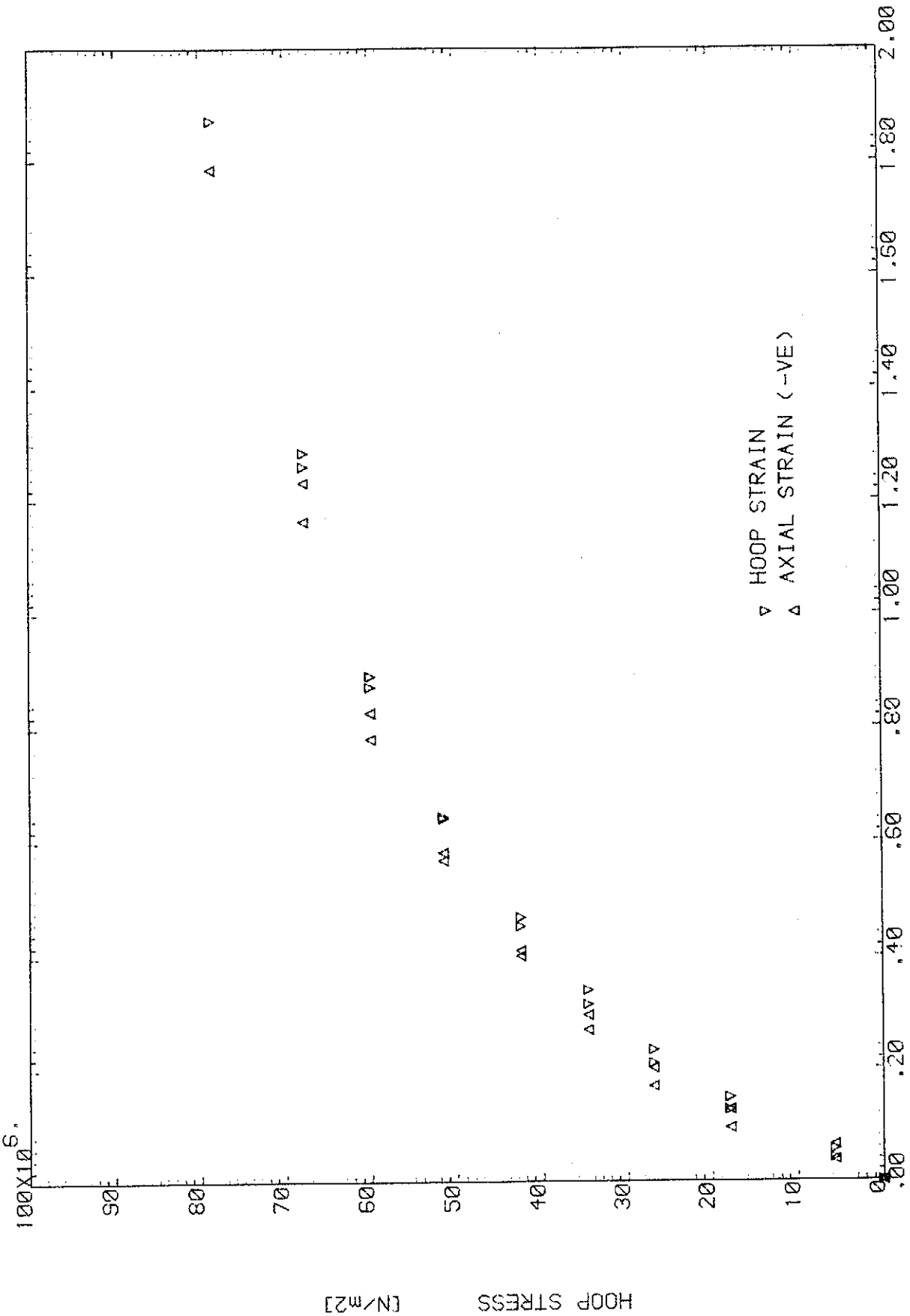

Fig.(B.25) BIAXIAL TEST OF SPECIMEN 6B3 (SX:SY:SXY=-0.5:1.0:0.0)

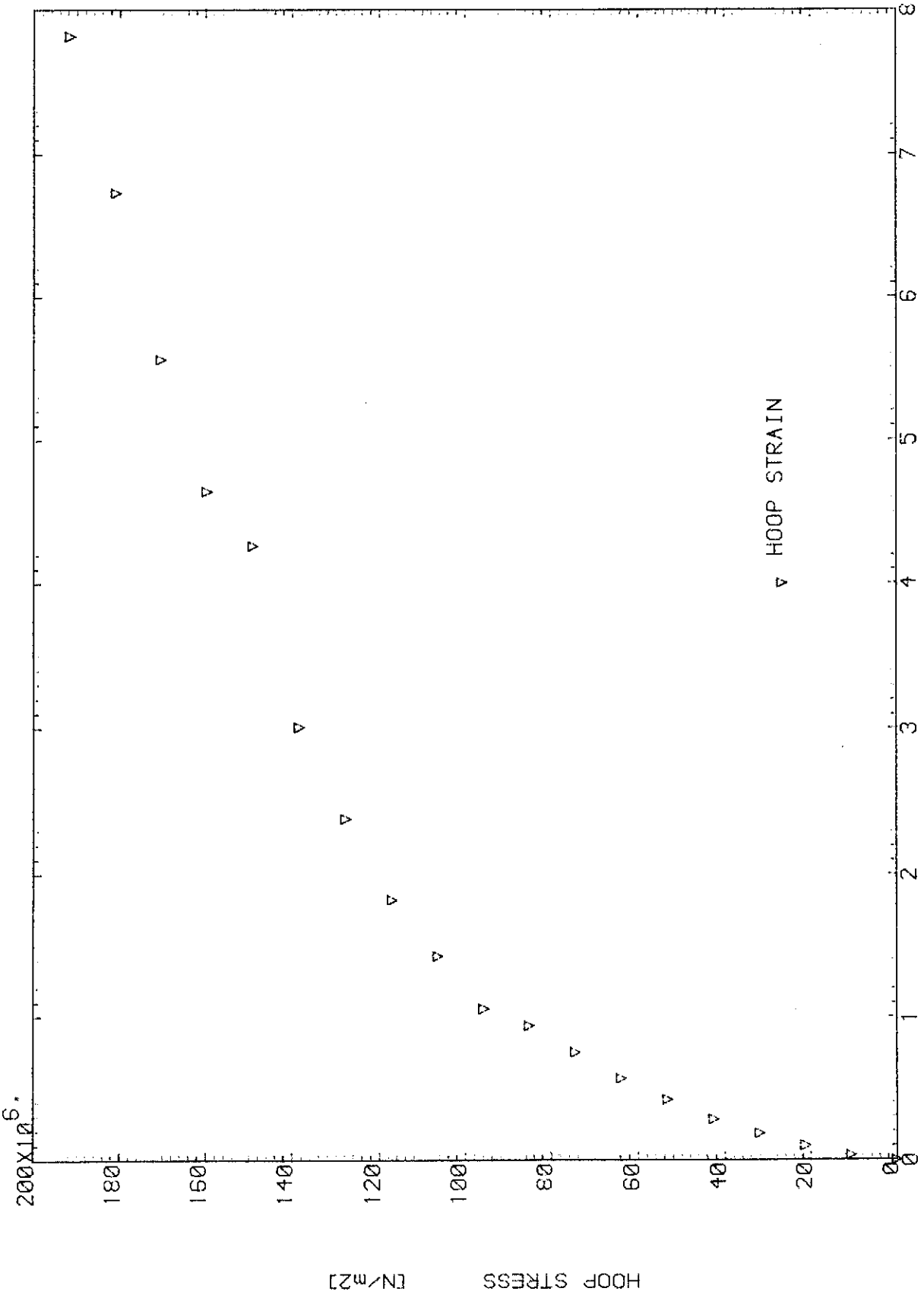

Fig.(B.26) BIAXIAL TEST OF SPECIMEN 7B3 (SX:SY:SXY=0.0:1.0:0.0)

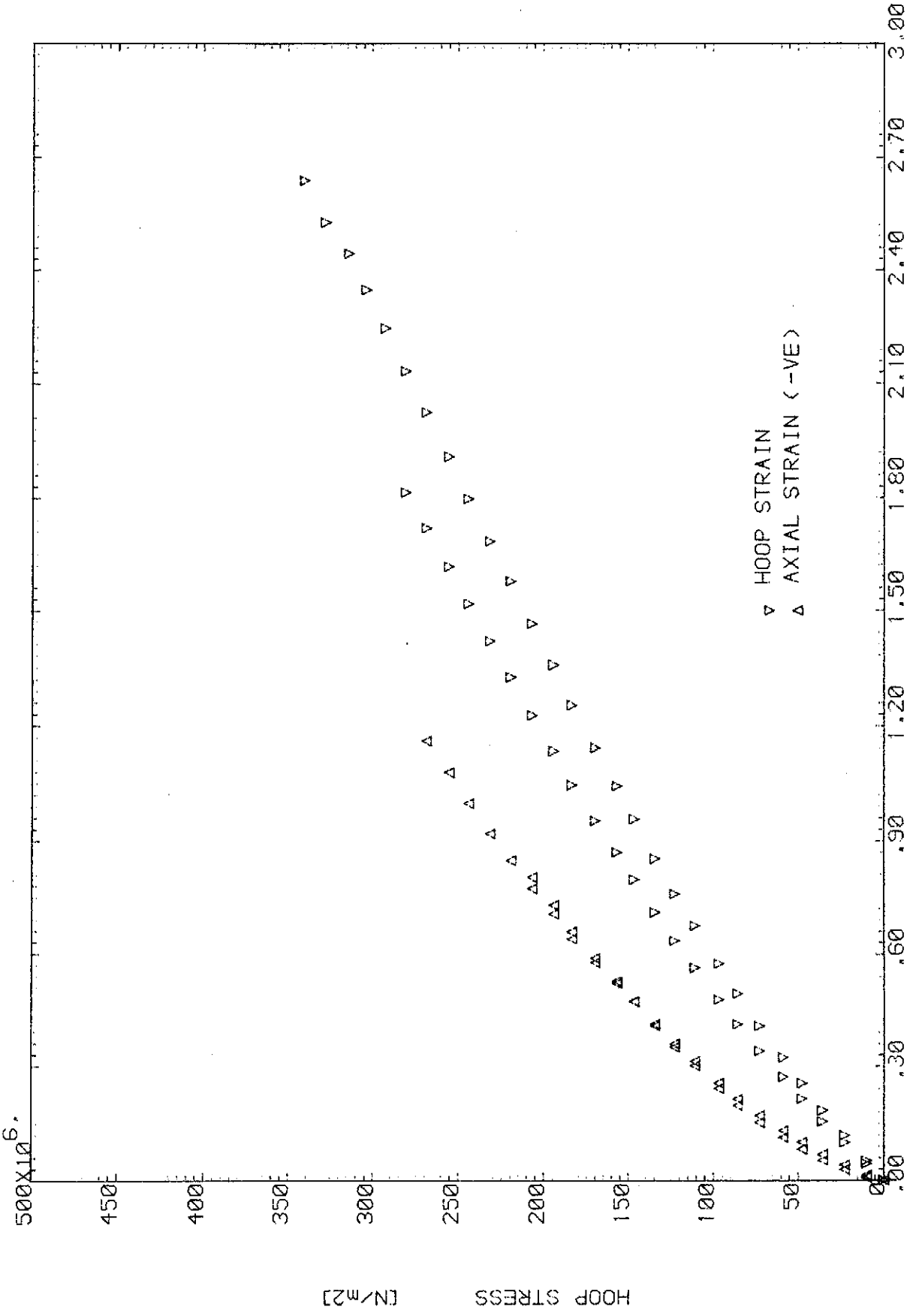

Fig.(B.27) BIAXIAL TEST OF SPECIMEN 1B4 (SX:SY:SXY=0.0:1.0:0.0)

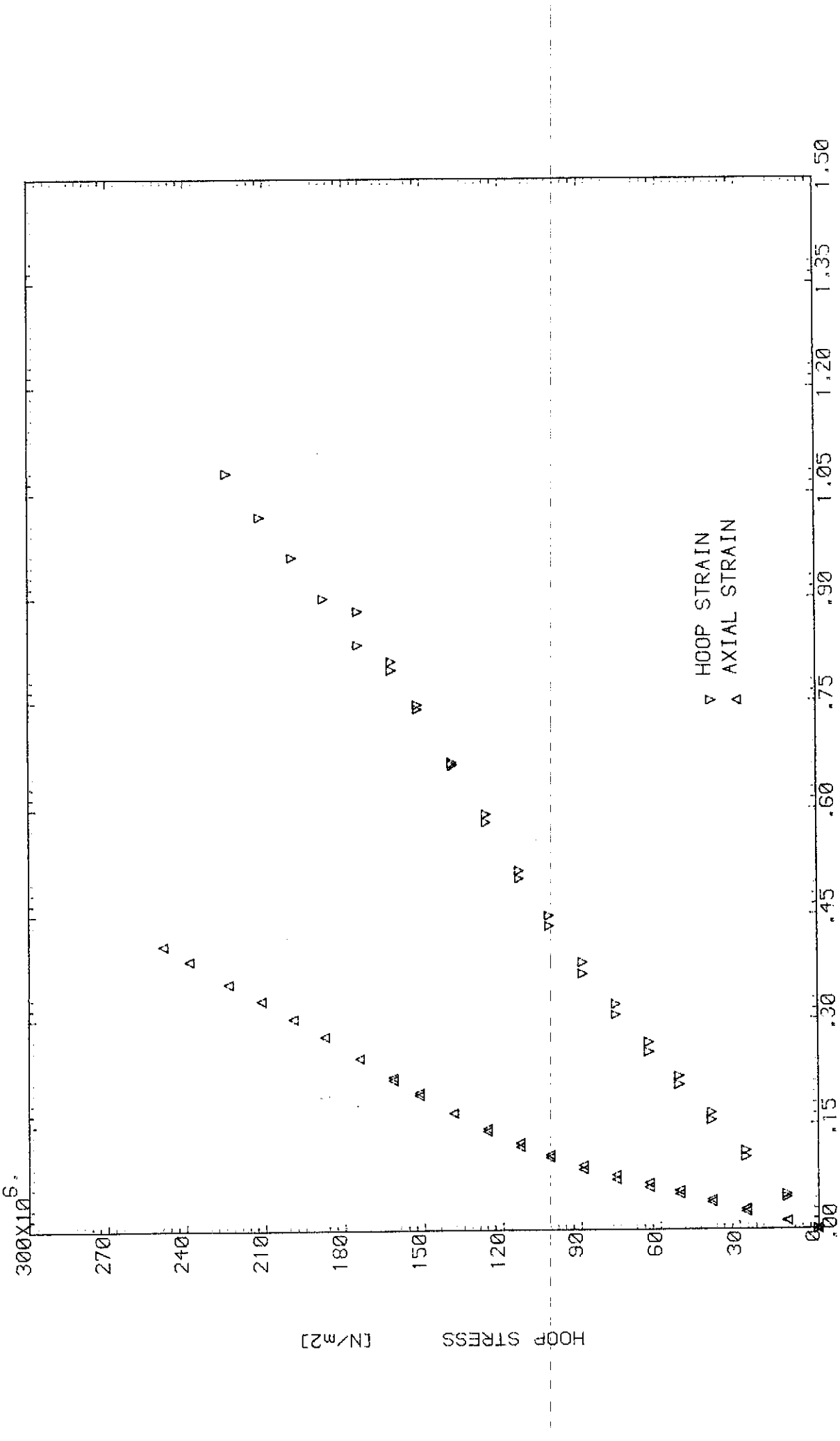

Fig.(B.28) BIAXIAL TEST OF SPECIMEN 2B4 (SX:SY:SXY=0.5:1.0:0.0)

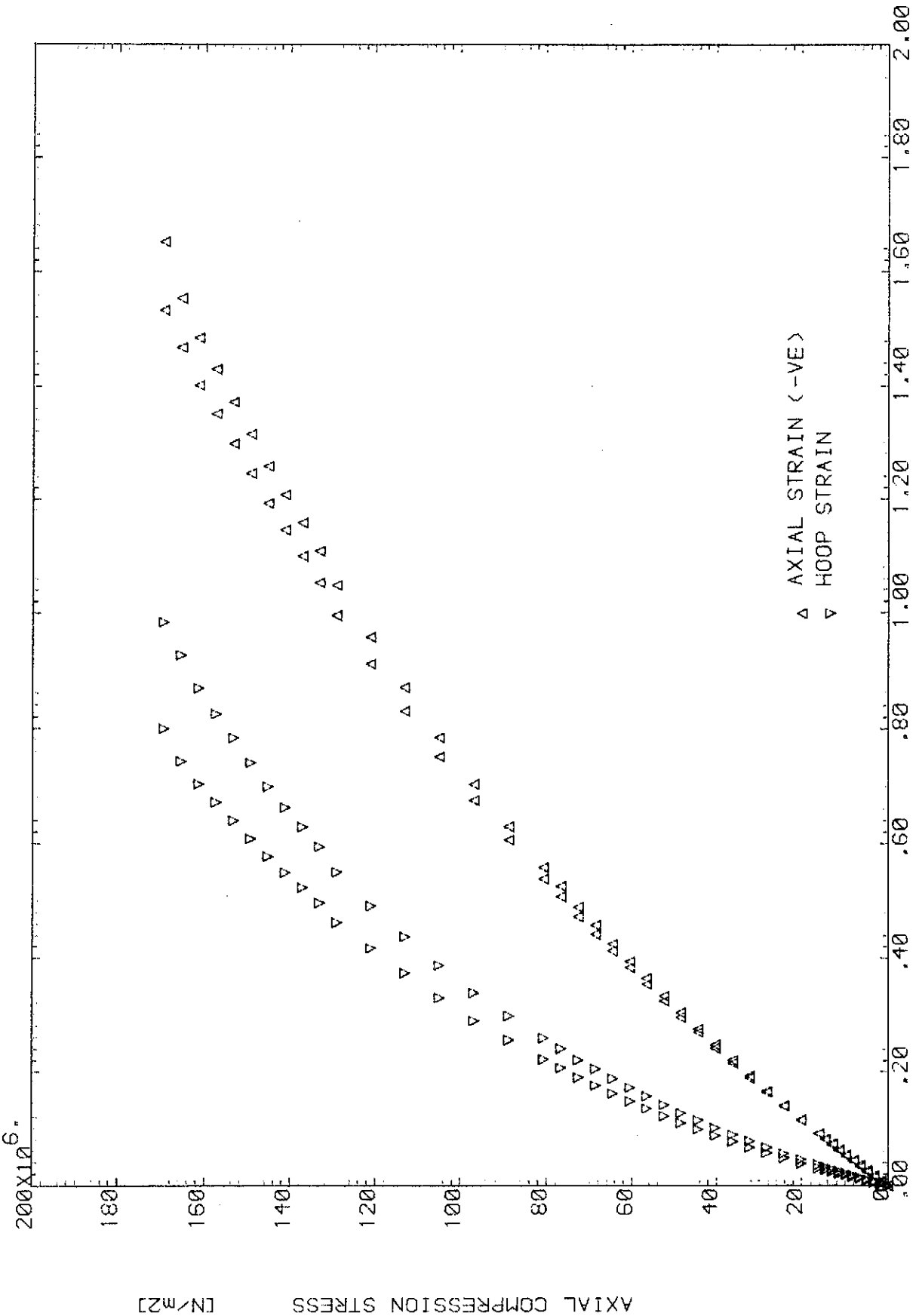

Fig.(B.29) BIAXIAL TEST OF SPECIMEN 3B4 (SX;SY;SXY=-1.0;0.0;0.0)

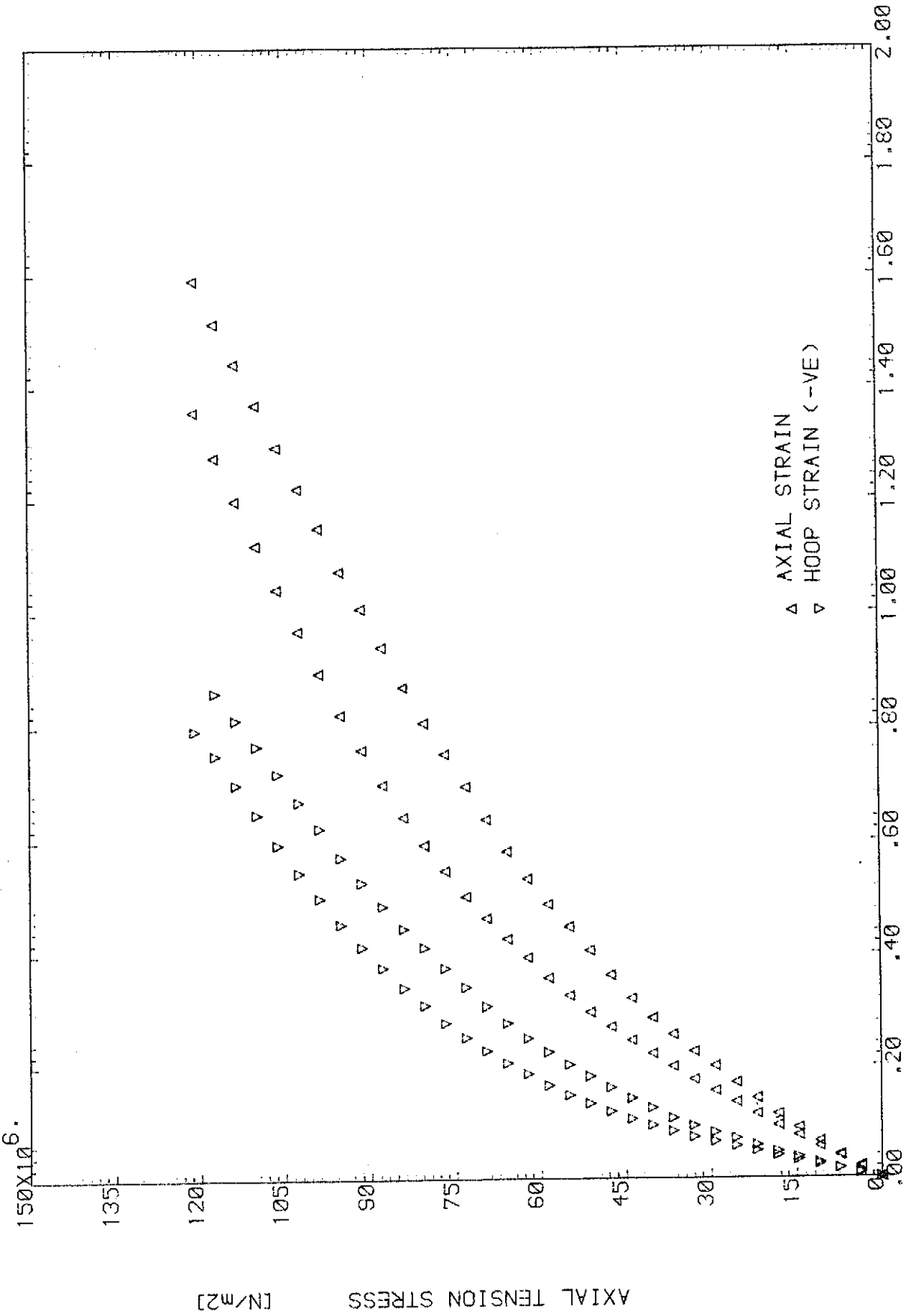

Fig.(B.30) BIAXIAL TEST OF SPECIMEN 4B4 (SX:SY:SXY=1.0:0.0:0.0)

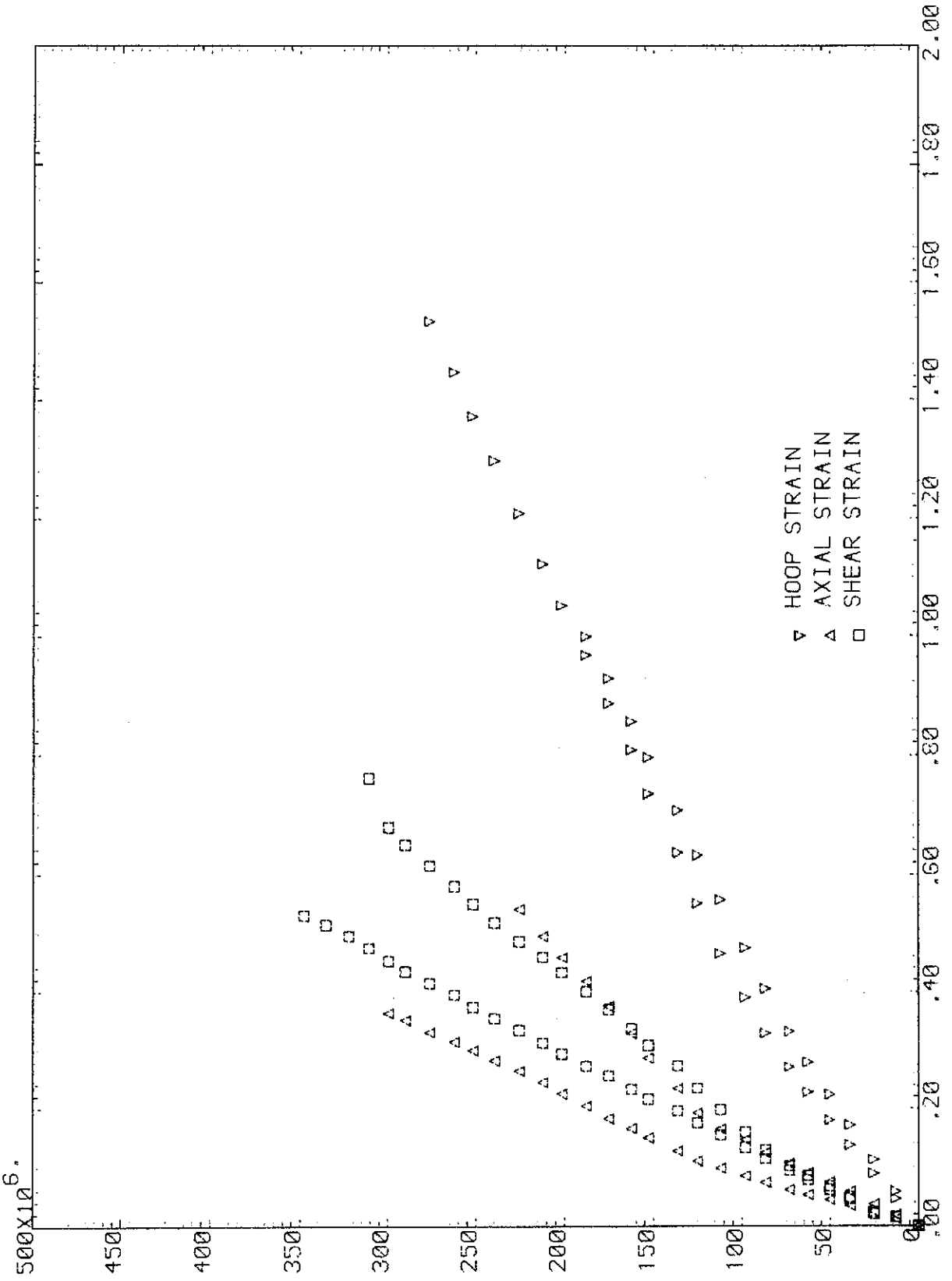

Fig.(B.31) BIAXIAL TEST OF SPECIMEN 5B4 (SX:SY:SXY=0.5:1.0:0.1)

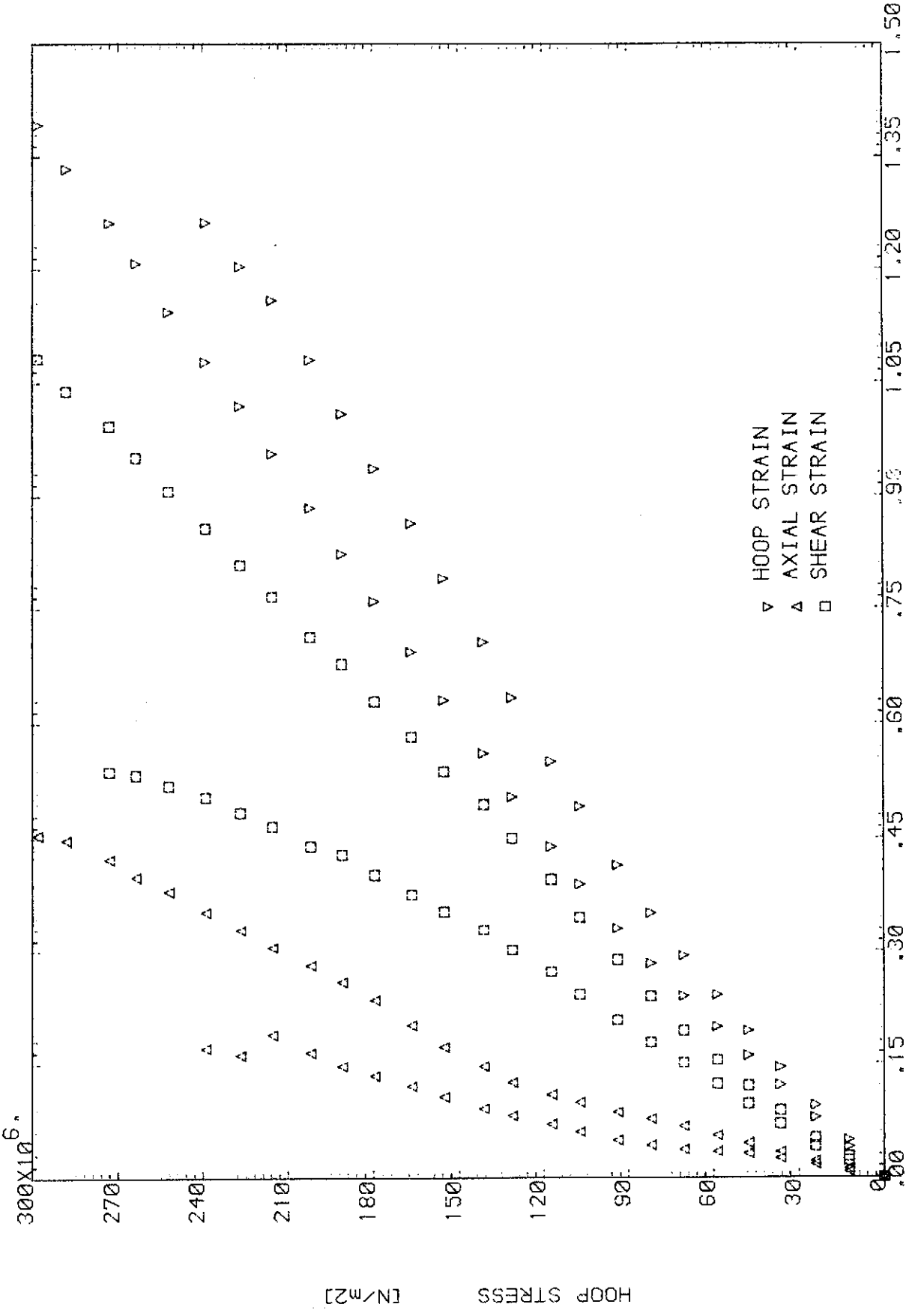

Fig.(B.32) BIAXIAL TEST OF SPECIMEN 6B4 (SX:SY:SXY=0.5:1.0:0.2)

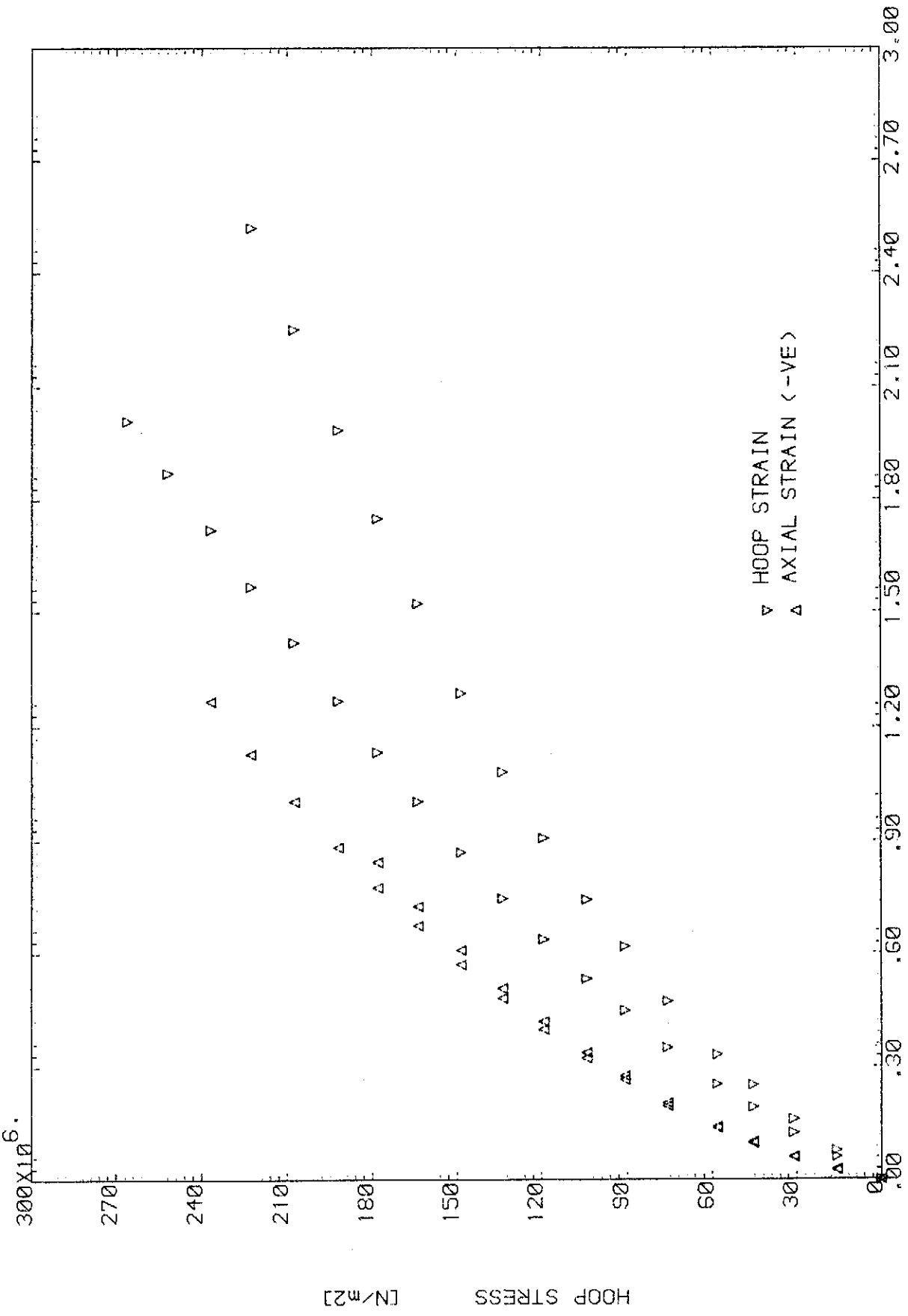

Fig.(B.33) BIAXIAL TEST OF SPECIMEN 1B5 (SX:SY:SXY=0.0:1.0:0.0)

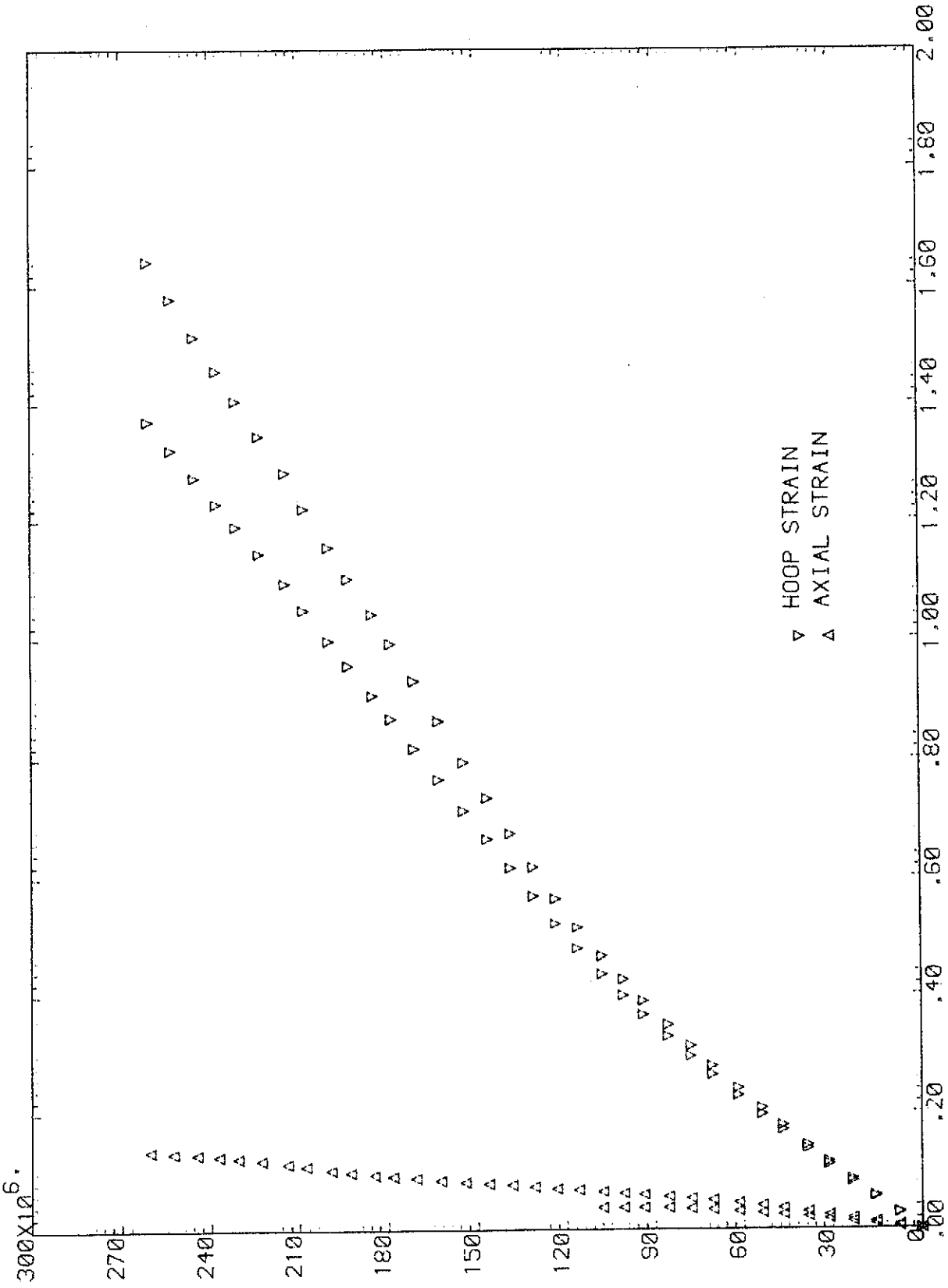

Fig.(B.34) BIAXIAL TEST OF SPECIMEN 2B5 (SX:SY:SXY=0.5:1.0:0.0)

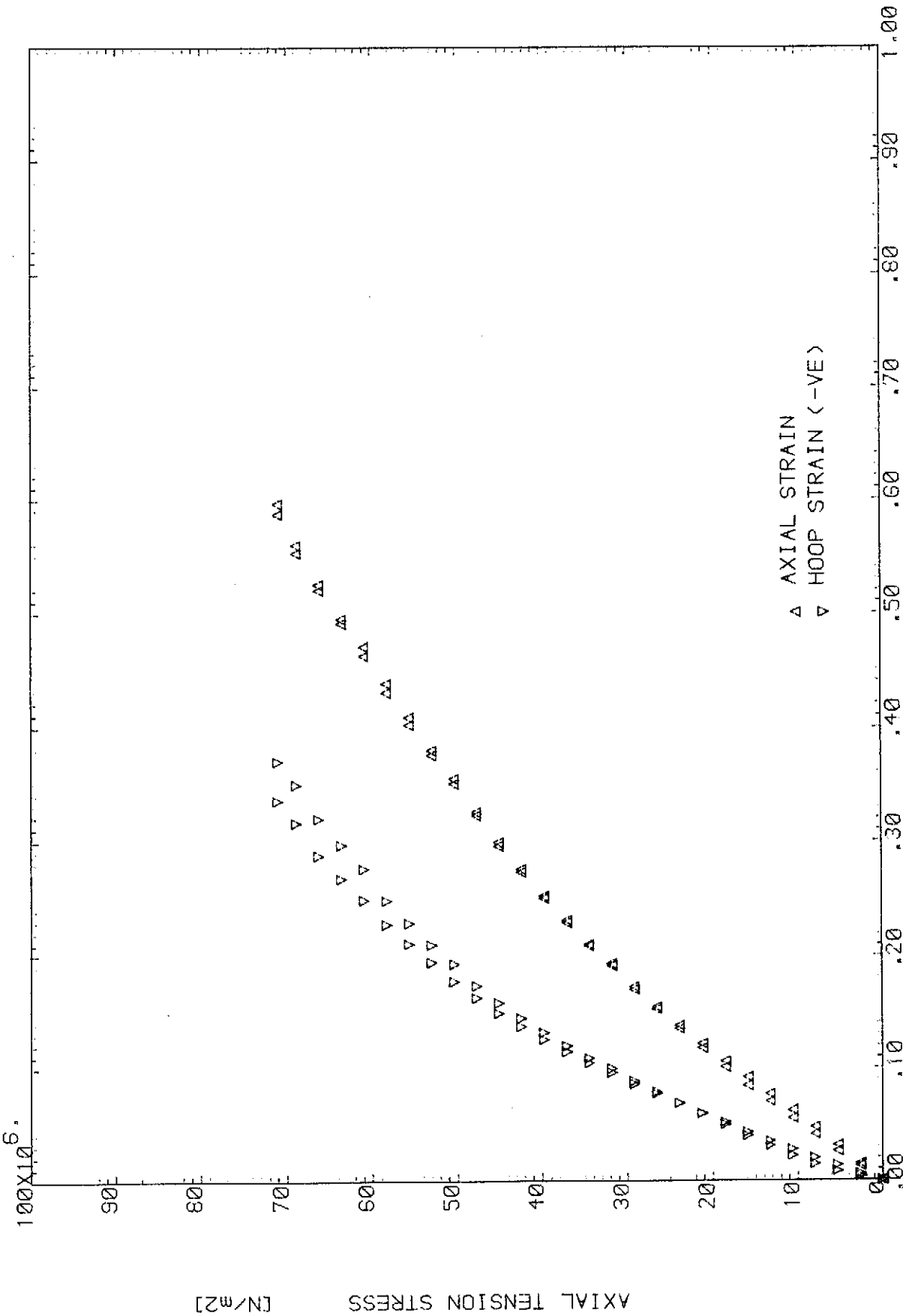

Fig.(B.35) BIAXIAL TEST OF SPECIMEN 3B5 (SX;SY;SXY=1.0;0.0;0.0)

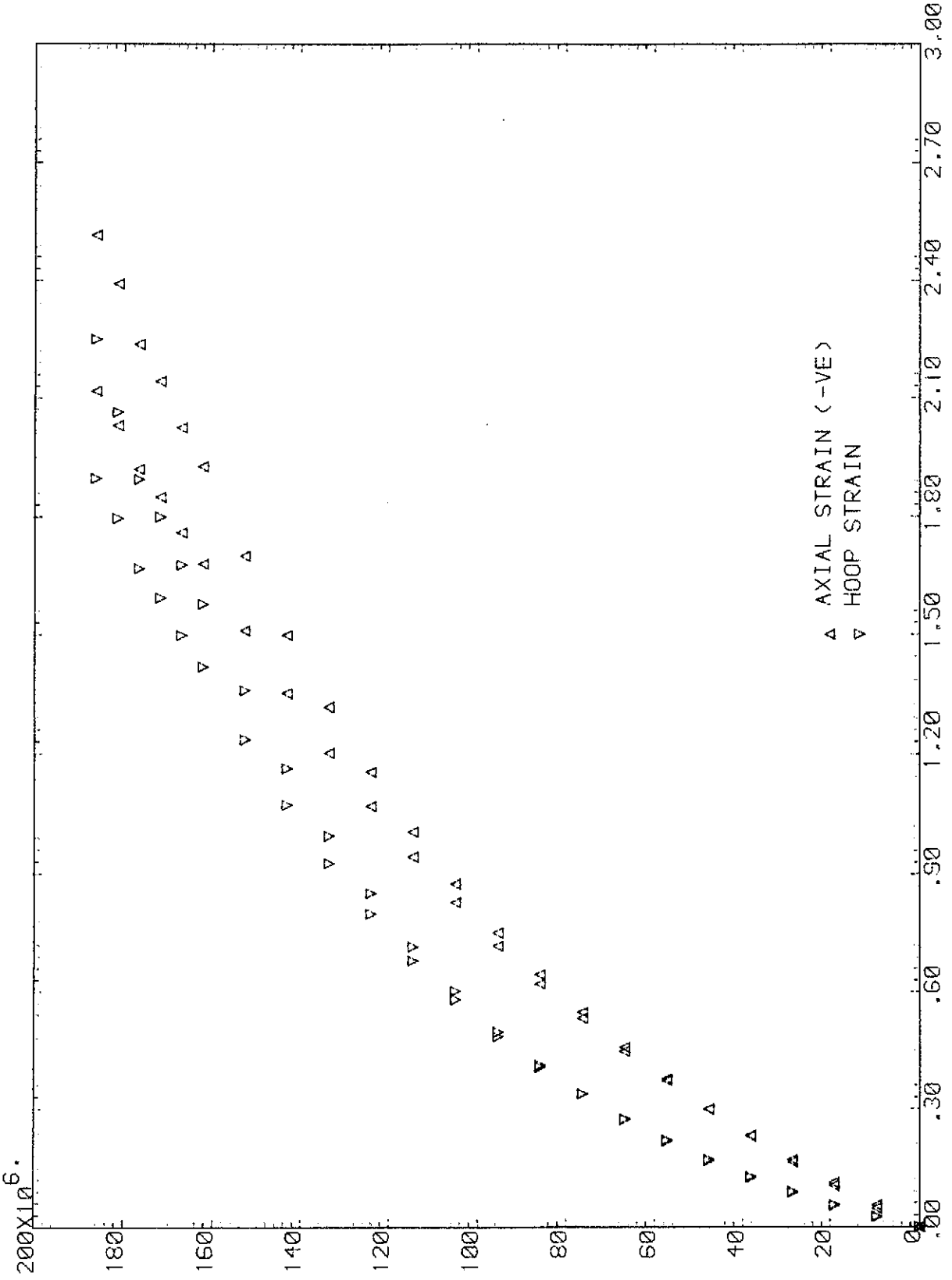

Fig.(B.36) BIAXIAL TEST OF SPECIMEN 4B5 (SX;SY;SXY=-1.0;0.0;0.0)

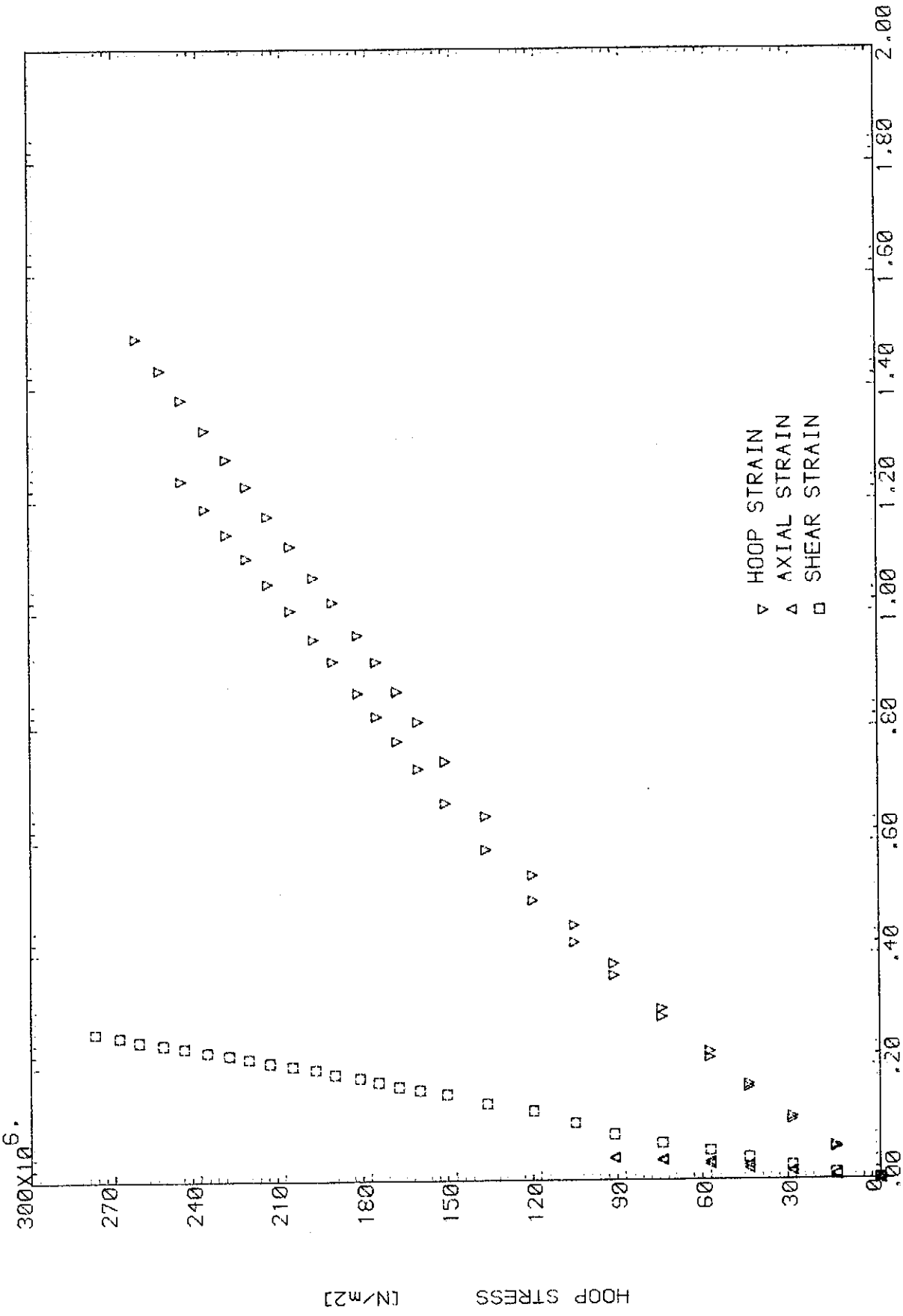

Fig.(B.37) BIAXIAL TEST OF SPECIMEN 5B5 (SX:SY:SXY=0.5:1.0:0.1)

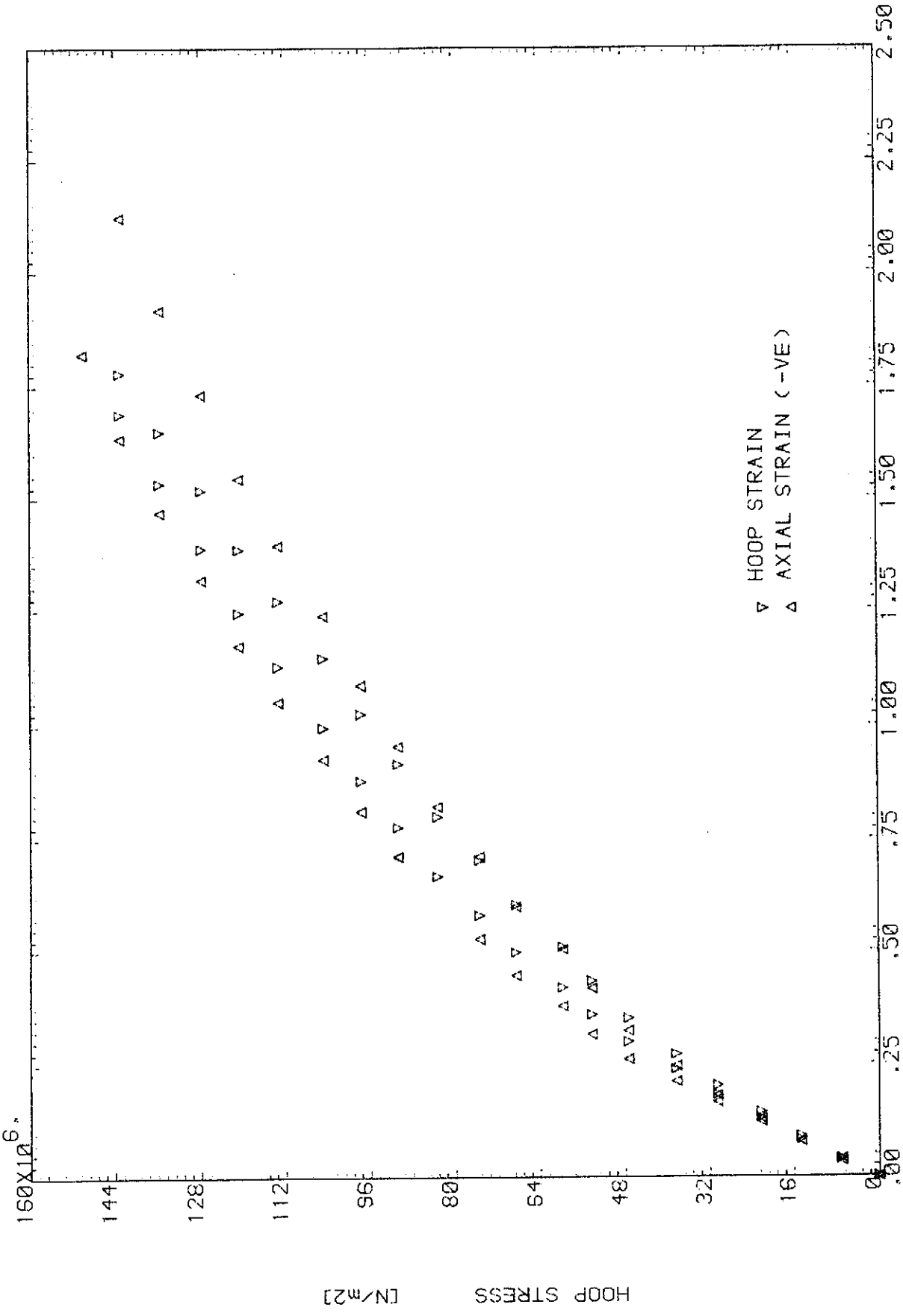

Fig.(B.38) BIAXIAL TEST OF SPECIMEN 6B5 (SX:SY:SXY=-0.5:1.0:0.0)

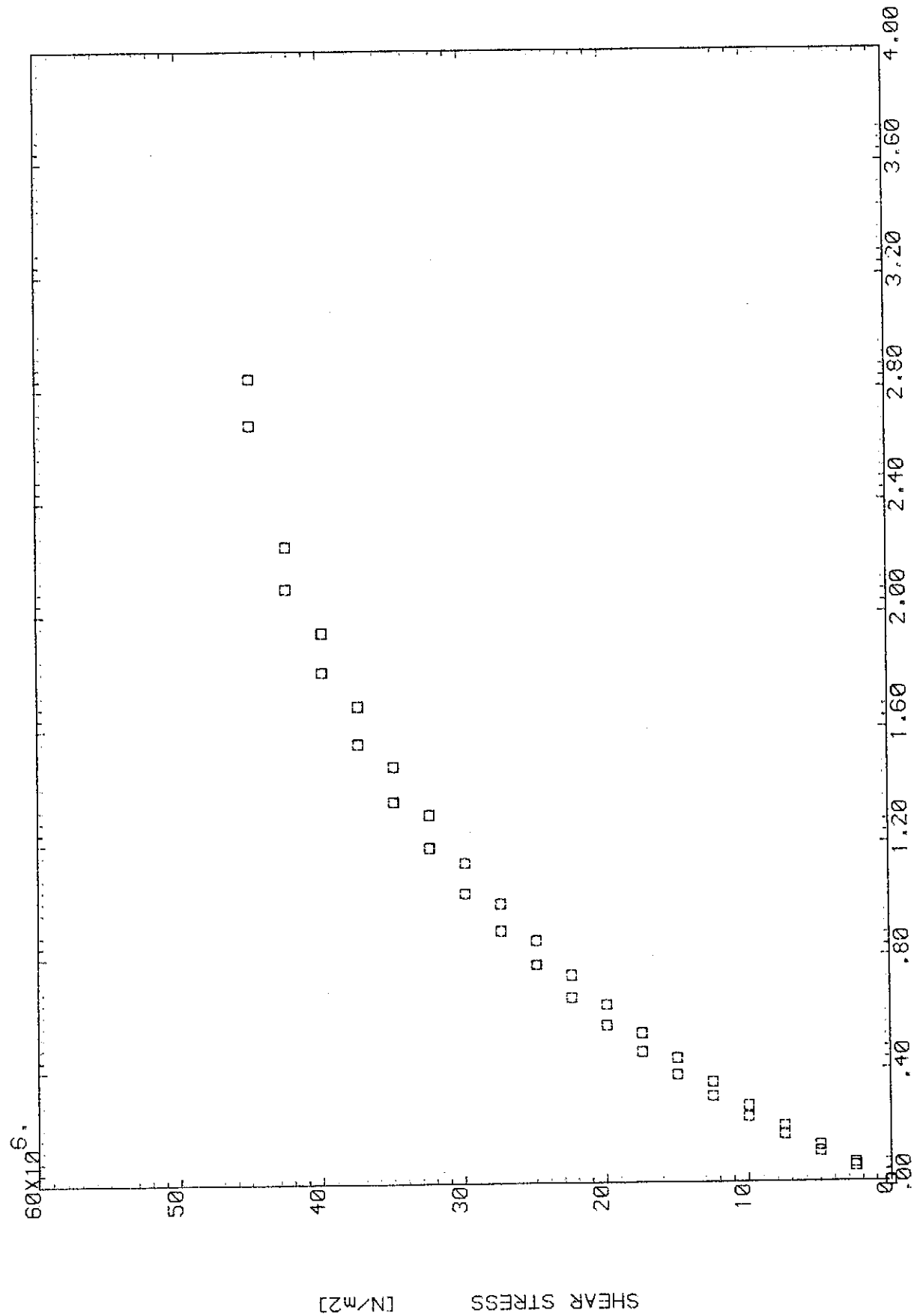

Fig.(B.39) TORSION TEST OF SPECIMEN 186 (SX:SY:SXY=0.0:0.0:1.0)

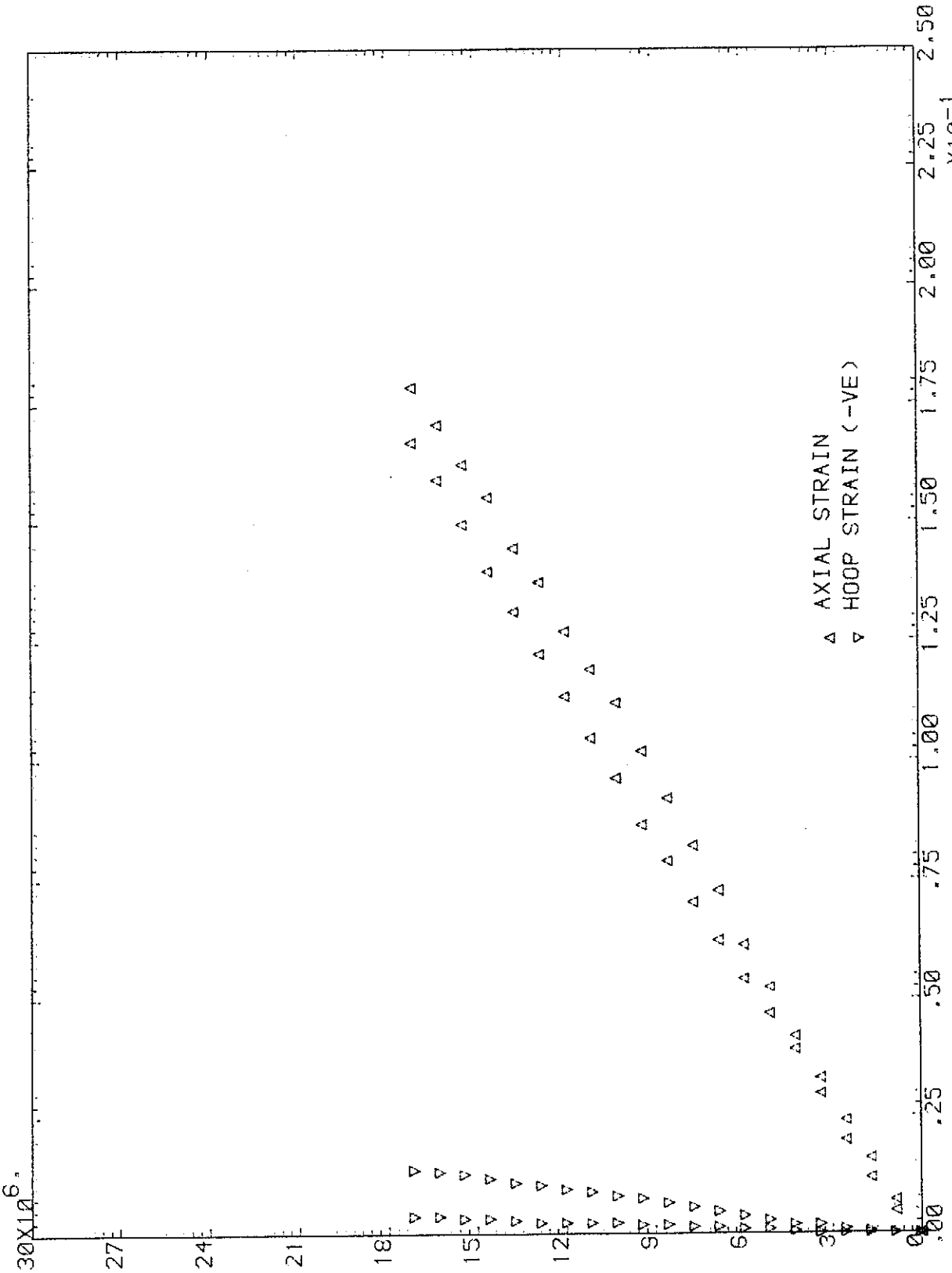

Fig.(B.40) AXIAL TENSION TEST OF SPECIMEN 2B6 (SX:SY:SXY=1.0:0.0:0.0)

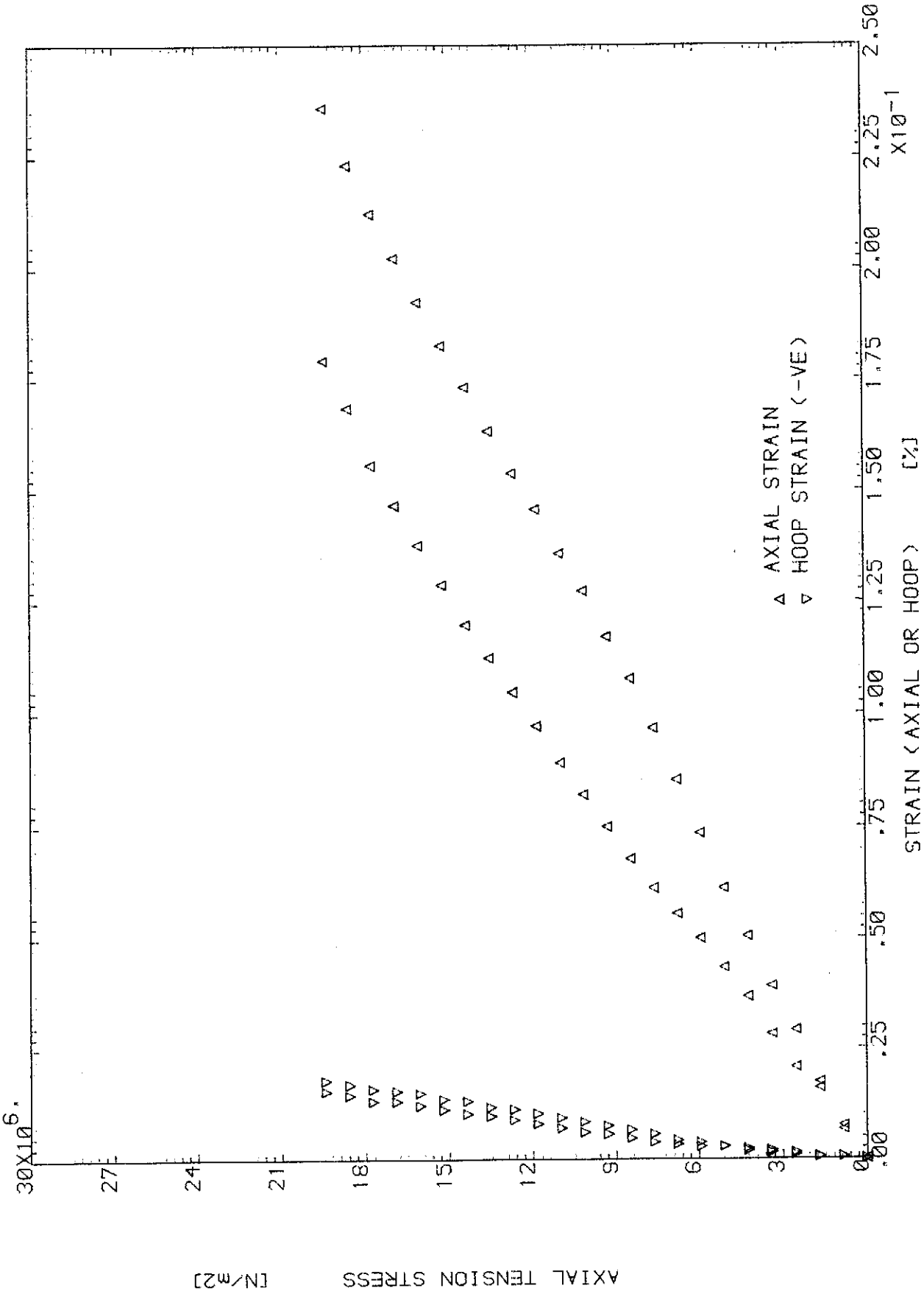

Fig.(B.41) AXIAL TENSION TEST OF SPECIMEN 3B6 (SX;SY;SXY=1.0;0.0;0.0)

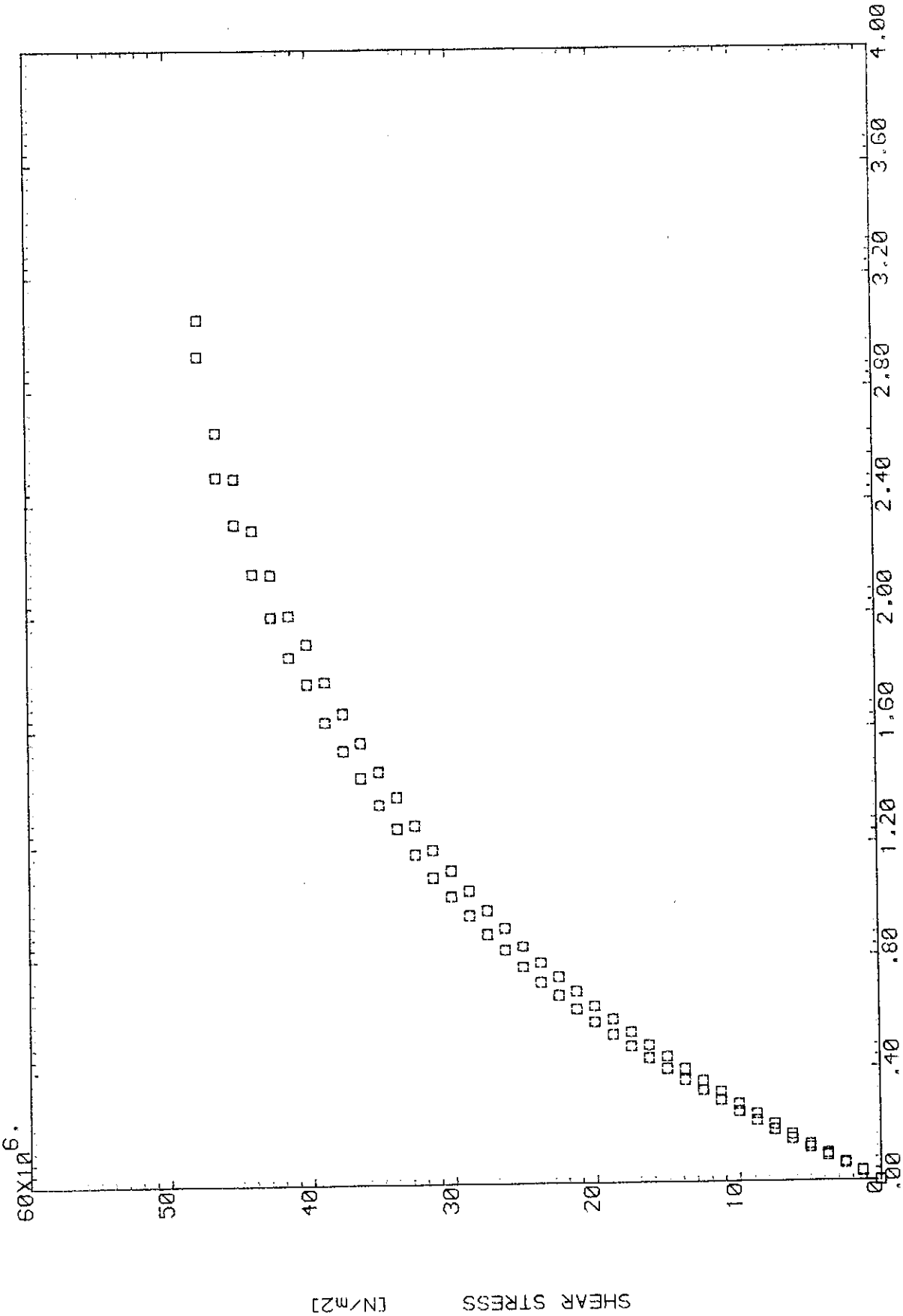

Fig.(B.42) TORSION TEST OF SPECIMEN 4B6 (SX:SY:SXY=0.0:0.0:1.0)

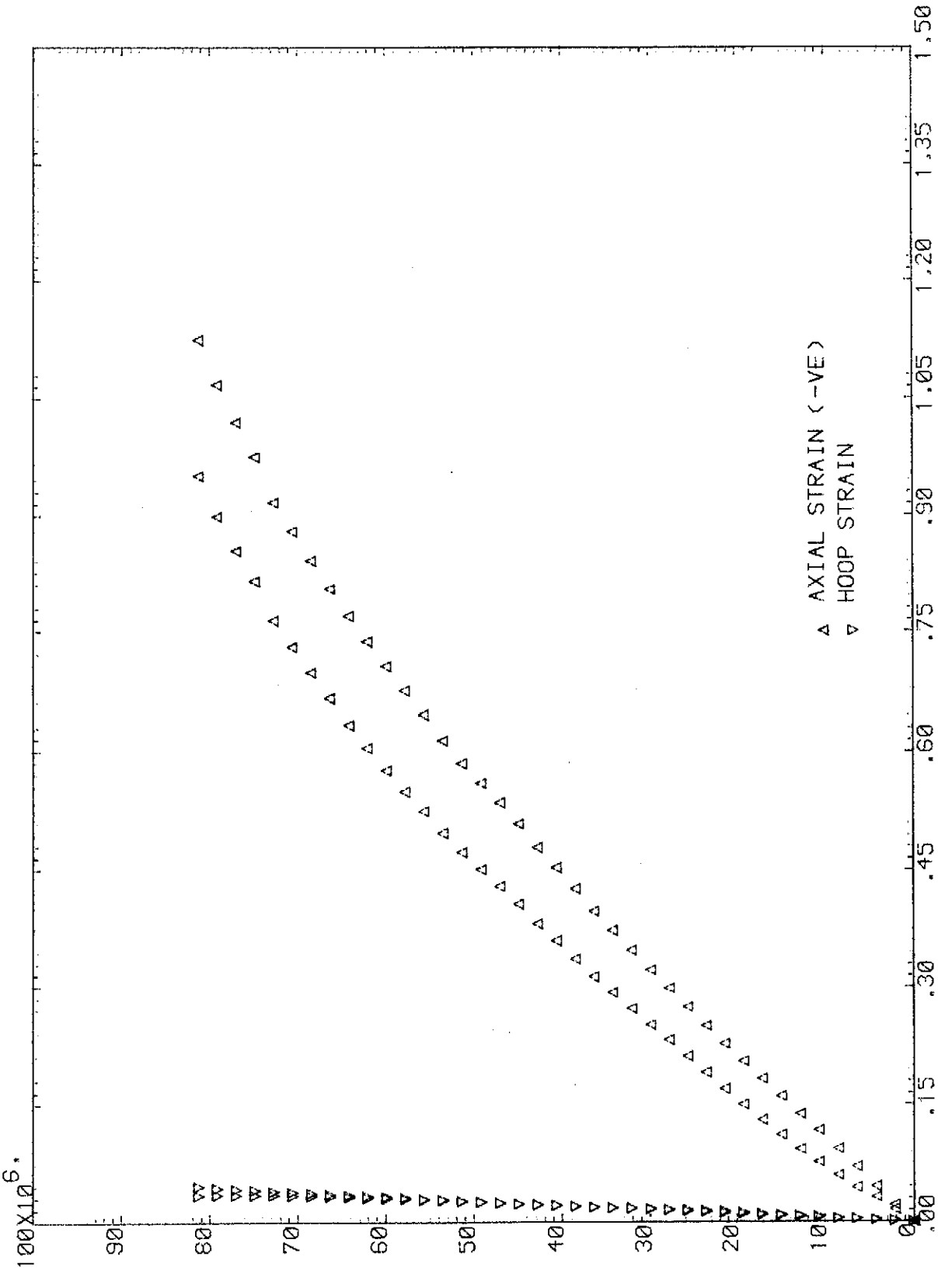

Fig.(B.43) AXIAL COMPRESSION TEST OF SPECIMEN 5B6 (SX:SY:SXY=-1.0:0.0:0.0)

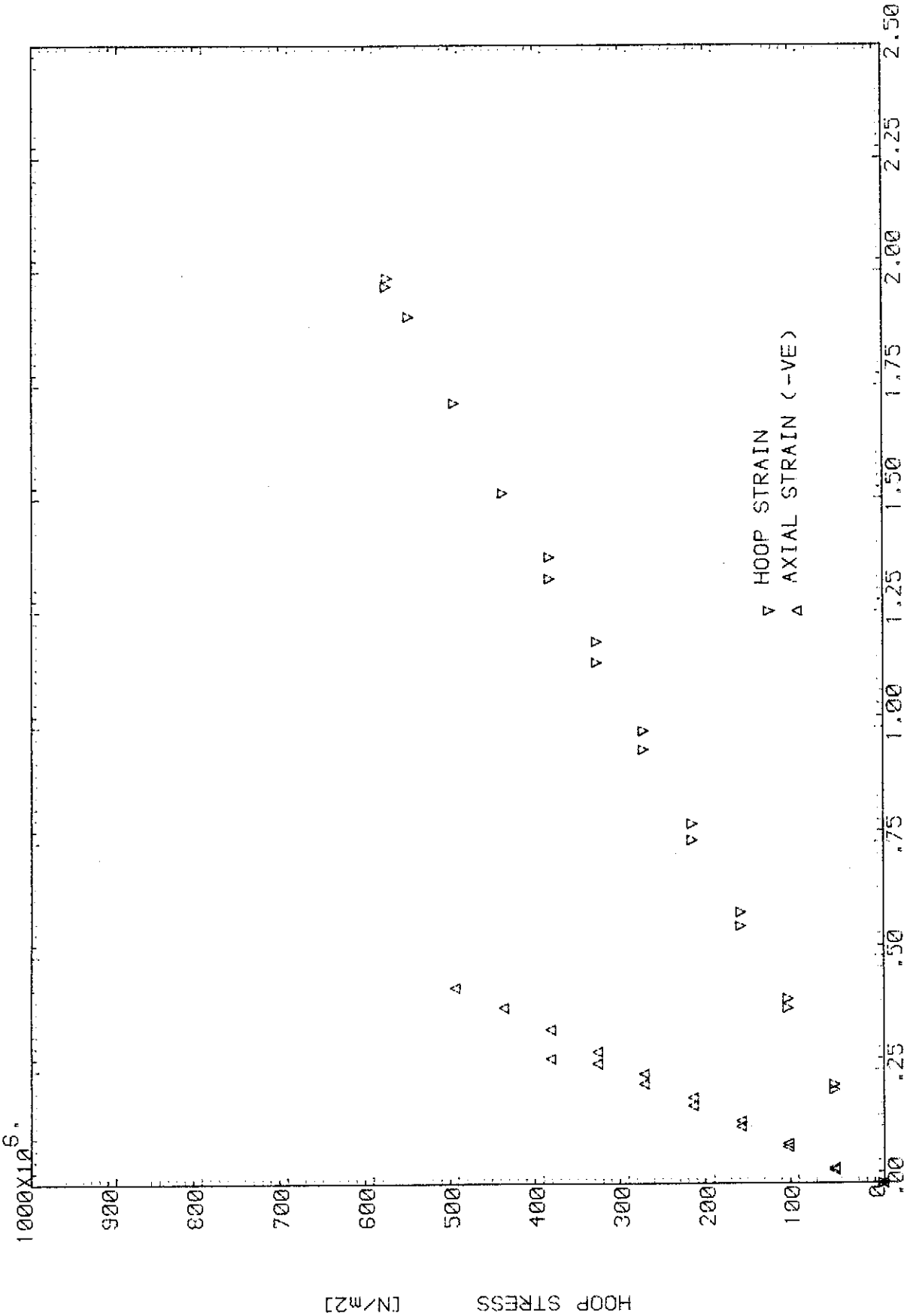

Fig.(B.44) INTERNAL PRESSURE TEST OF SPECIMEN 6B6 (SX:SY:SXY=0.0:1.0:0.0)

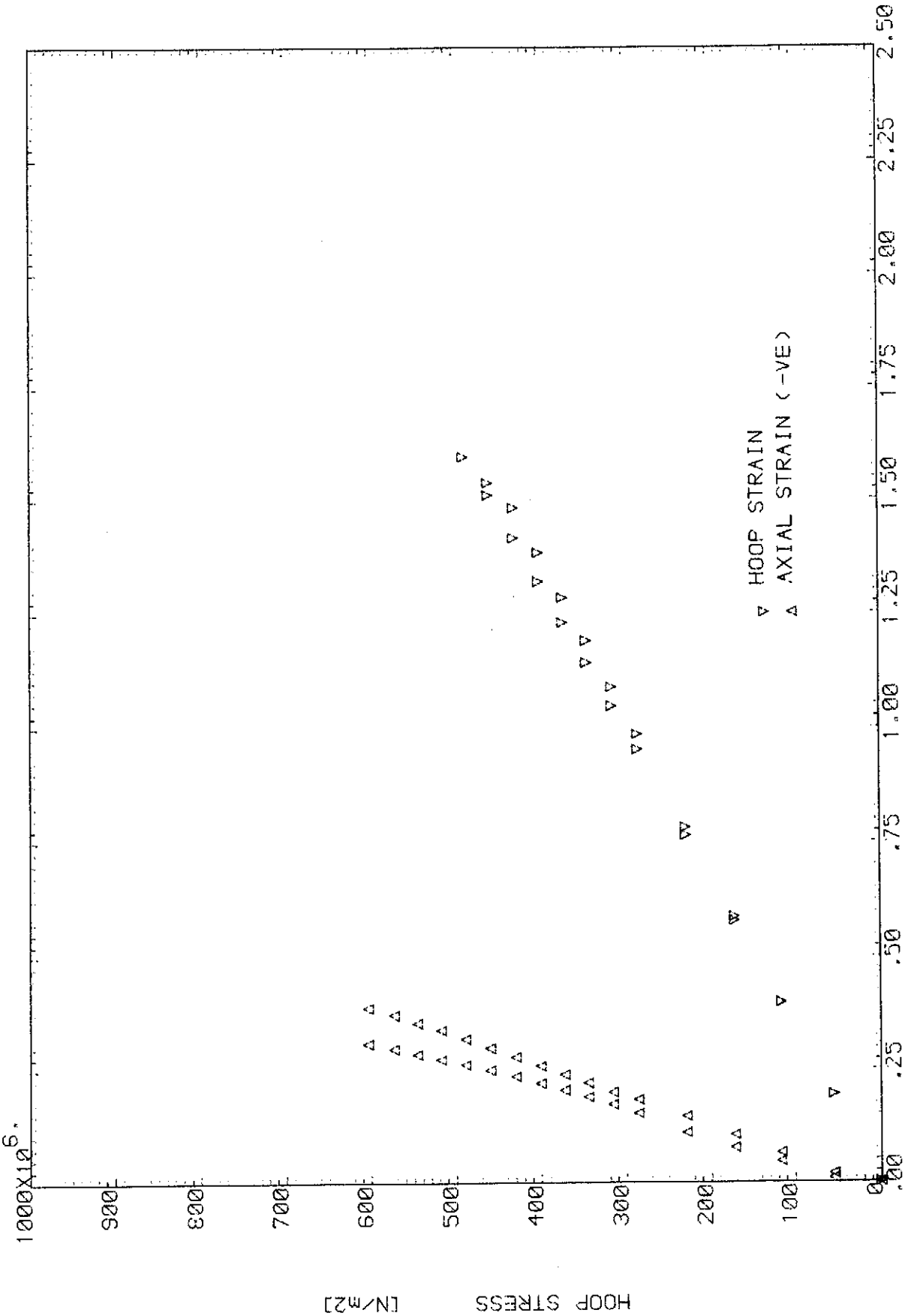

Fig.(B.45) INTERNAL PRESSURE TEST OF SPECIMEN 7B6 (SX:SY:SXY=0.0:1.0:0.0)

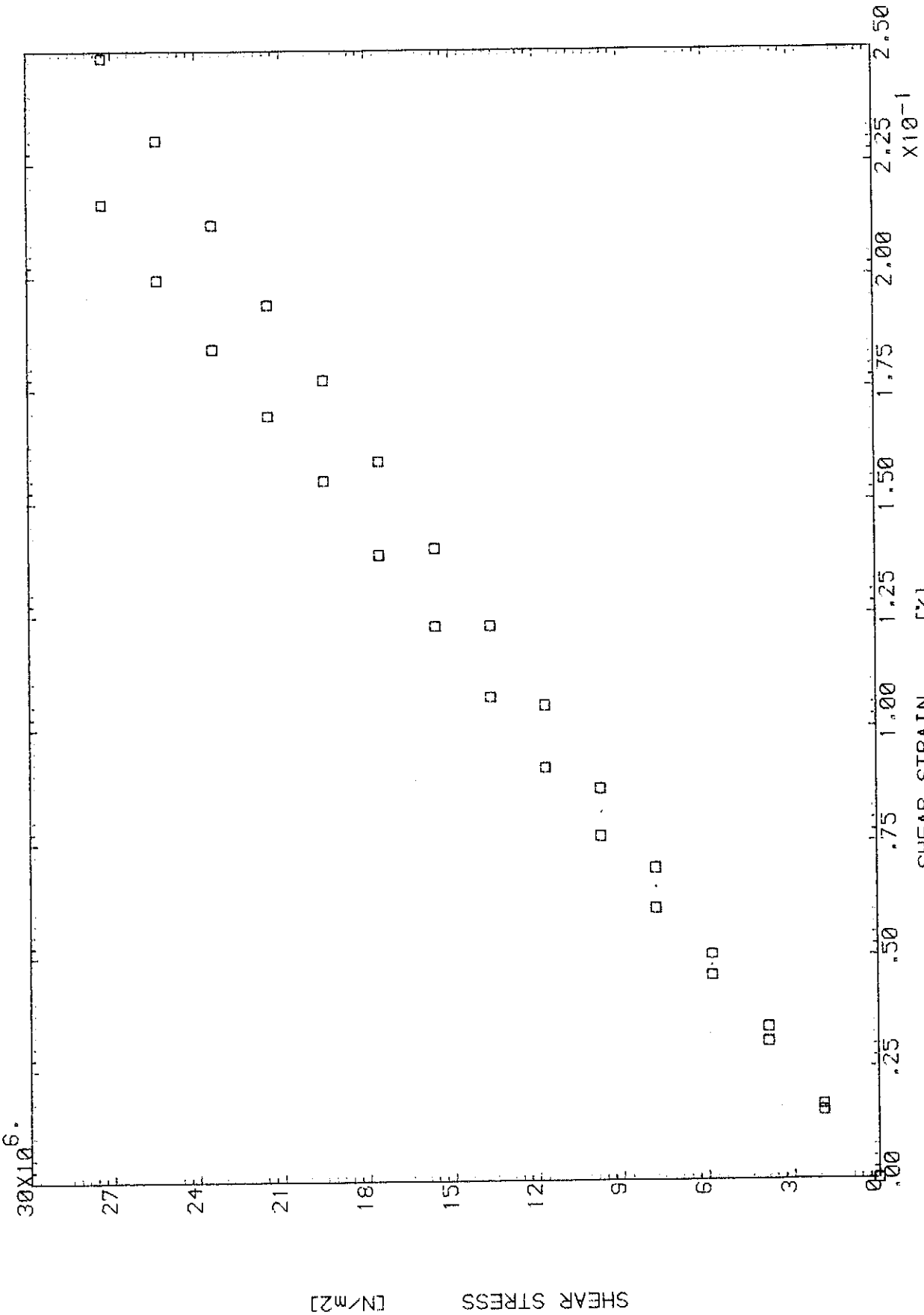

Fig.(B.46) TORSION TEST OF SPECIMEN 3P1 (SX:SY:SXY=0.0:0.0:1.0)

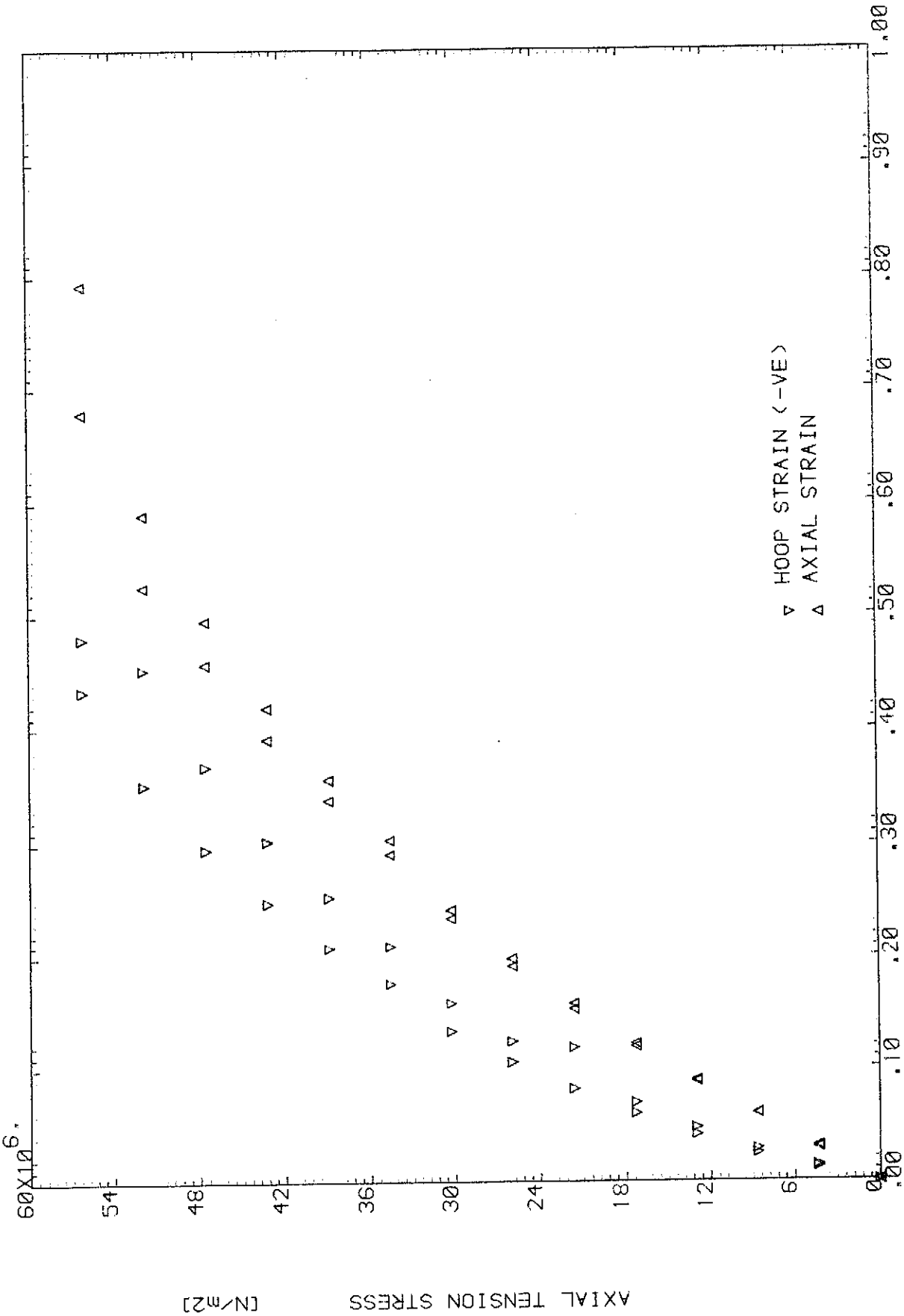

Fig.(B.47) BIAXIAL TEST OF SPECIMEN 4P1 (SX:SY:SXY=1.0:0.0:0.0)

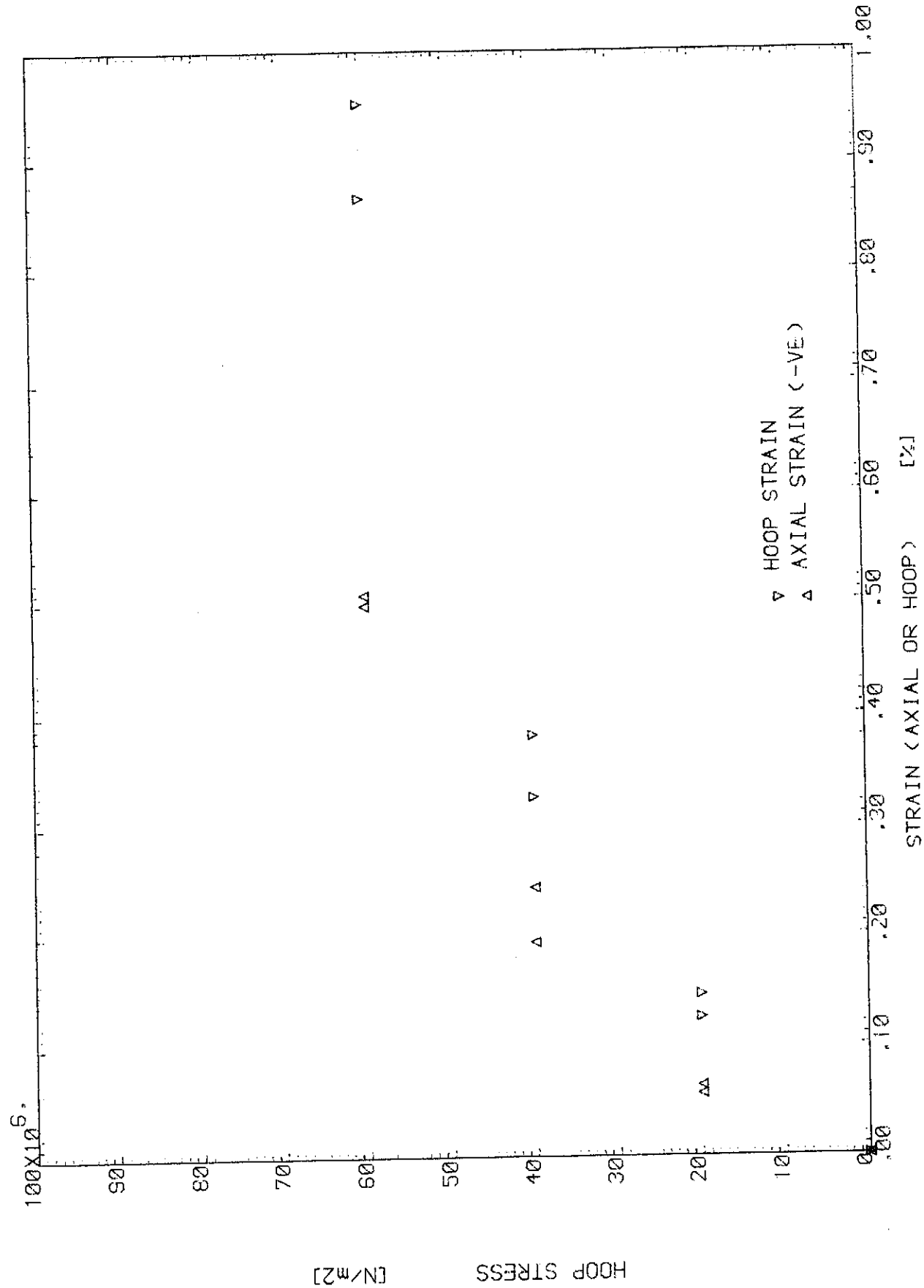

Fig.(B.48) BIAXIAL TEST OF SPECIMEN 13P1 (SX:SY:SXY=0.0:1.0:0.0)

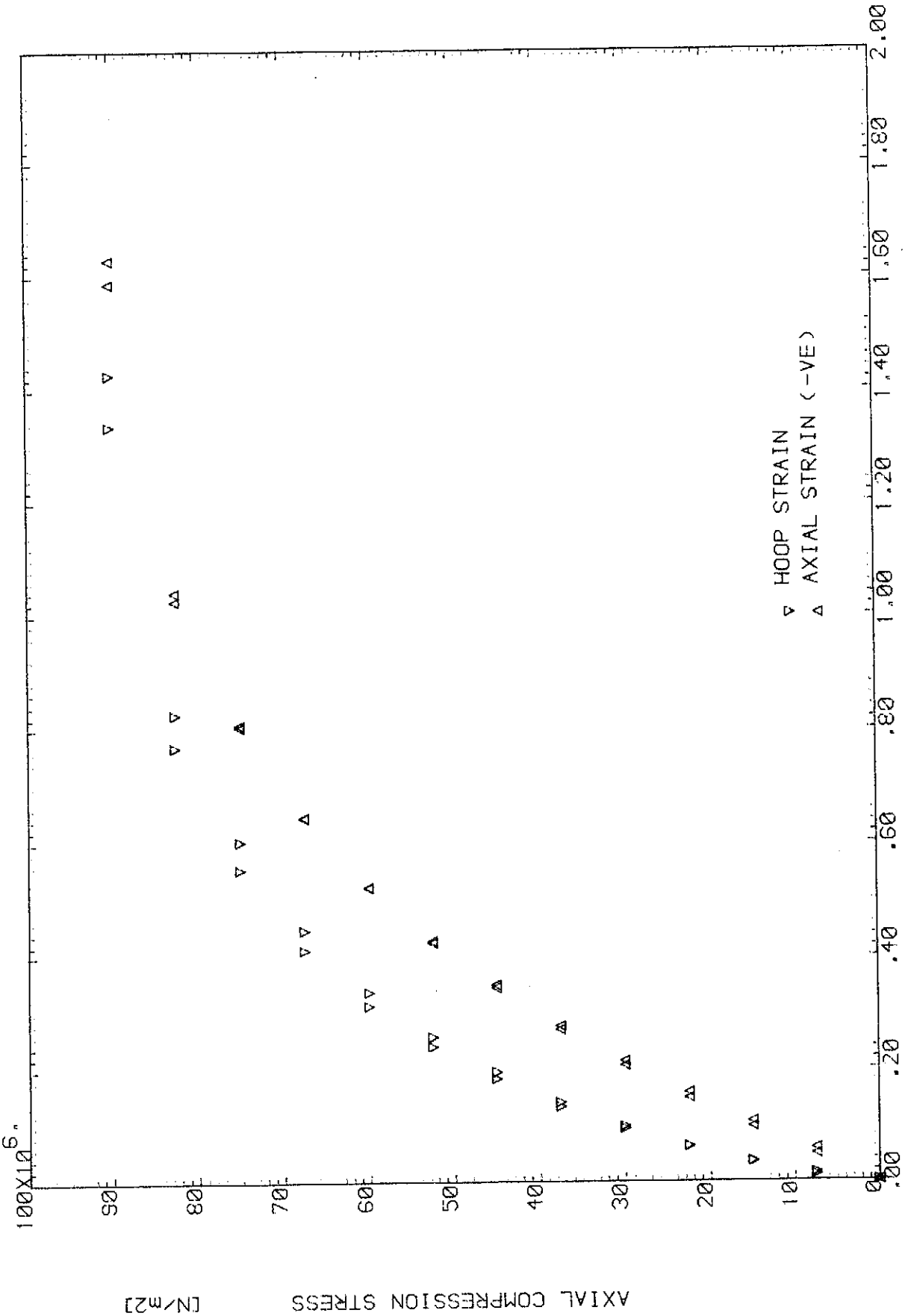

Fig.(B.49) BIAXIAL TEST OF SPECIMEN 14P1 (SX:SY:SXY=-1.0:0.0:0.0)

APPENDIX C

STRESS AND STRENGTH CALCULATIONS OF LAMINATED COMPOSITE STRUCTURES

C.1 INTRODUCTION

This Appendix describes the general computer program which was developed to calculate the stress and strength of a laminated composite structure under combined loadings. The theoretical background for the linear stress calculations is that of Sec. 2.2., while the non-linear stress calculations are based on the analysis of Sec. 2.3.3. The strength calculations are based on the proposed modified maximum strain criterion, (see Sect. 3.4). In addition to that there is an option to calculate the strength according to six other widely used failure criteria. These are the maximum stress, the maximum strain, Azzi-Tsai, Hoffman, Tsai-Wu, and Puppo-Evensen failure criteria, (see Sec. 3.3). There is also an option to calculate the strength for one loading case, or to calculate the strength for the whole loading spectrum for fixed value of the laminate shear load, and in this latter case the failure envelope is plotted.

The program can give the stress and strain distributions across the thickness of the laminate if the user wanted these distributions. Other intermediate calculations can also be printed out.

Non-linearity is allowed in all directions of the lamina with an option to have different non-linear behaviour for tension and compression. Thus, up to five non-linear stress-strain data are needed for every material used, viz., the longitudinal tensile response, the longitudinal compression response, the transverse tensile response, the transverse compression response, and the shear response.

C.2 NOTES ABOUT THE STRENGTH CALCULATIONS

C.2.1 The Limit Criteria

In the cases of maximum stress and maximum strain criteria the failure load is calculated by one of the following methods:

a) for one loading case: the ratios of the strengths to their corresponding stresses (or strains) are calculated to find the smallest of these ratios. This smallest ratio multiplied by the applied load gives the failure load, (see Subroutine FAIL).

b) for the whole loading spectrum: the equations of the six straight lines which defines the failure in the six different modes are written from equation (2.2.39) for the case of maximum stress criterion, or from equation (2.2.36) for the case of maximum strain criterion. Then these lines are drawn by giving values to σ_x^o and obtaining the corresponding values of σ_y^o, (see subroutines MAXIFAIL and MAXIMUM)

C.2.2 Other Criteria

When the stresses in lamina σ_1, σ_2 and σ_{12} are obtained under the loads σ_x^o, σ_y^o and σ_{xy}^o, the stresses σ_2 and σ_3 are replaced by $\alpha\ \sigma_1$ and $\beta\ \sigma_1$ respectively. Then, the stress at failure σ_{1f} is the stress which satisfies the appropriate failure equation. Hence, $\sigma_{2f} = \alpha \cdot \sigma_{1f}$ and $\sigma_{12f} = \beta \cdot \sigma_{1f}$. The laminate loads at failure are : $\sigma_{xf} = \gamma \cdot \sigma_x^o$, $\sigma_{yf} = \gamma \cdot \sigma_y^o$ and $\sigma_{xyf} = \gamma \cdot \sigma_{xy}^o$ where $\gamma = \sigma_{1f}/\sigma_1$, (see subroutine FAILURE)

The above method was used for both the cases of single loading and whole loading spectrum. In the latter case the laminate loads are changed at the end of every case to obtain the failure for a new load case, (see subroutine LOAD RATIO)

C.2.3 The Modified Maximum Strain Criterion

Since this criterion considers the non-linear behaviour of the composite, incremental load technique is employed. When any strain component increases its limit, failure occurs. To determine the exact loading at which failure occurs the load increment is reduced to 1/100 of its original value. But because this is an expensive operation in terms of computing time, the reduction is made step by step. First the load increment is reduced to 1/10 of its original value, then when the failure is detected it is reduced again to 1/10 of its new value.

C.3 THE COMPUTER PROGRAM

The computer program which calculates the stress and strength of laminated composites is written in FORTRAN programming language and consists of the following segments:

a) The MASTER segment form the lamination theory and calculates the stresses and strains in the individual plies. It also deals with the non-linear analysis and the modified maximum strain failure criterion.

b) Subroutine TRANSFORMATION transforms the properties of the layers from their own axes to the laminate axes.

c) Subroutine FAIL finds the failure load according to maximum stress and maximum strain criteria in the single loading case.

d) Subroutine MAXIFAIL plots the failure envelopes for the maximum stress and maximum strain criteria.

e) Subroutine MAXIMUM finds the equations of the failure in the different modes for maximum stress and maximum strain criteria.

f) Subroutine FAILURE calculates and plots the failure envelopes for Azzi-Tsai, Hoffman, Tsai-Wu and Puppo-Evensen Criteria.

g) Subroutine LOAD RATION changes the load ratio to cover the whole spectrum of loading.

h) Function HILL and function AZZI deals with Hill-Tsai-Azzi failure cirterion.

i) Subroutine HOFFMAN and function HOFF deals with Hoffman failure theory.

j) Subroutine WU and function WUTSAI deals with Tsai-Wu failure equation.

k) Subroutine PUPPO and subroutine EVENSEN deals with Puppo-Evensen failure theory.

l) Subroutine AXES draws the axes for the failure envelopes.

m) Subroutine NONLINEAR deals with the non-linear data of the plies.

n) Subroutine MAXIMUM VALUE finds the biggest number in an array.

o) Supporting subroutines: these are standard subroutines from the different libraries at Cranfield Computer Centre :

   * CC936N, WINDOW, CHASIZ, PICCLE, GRASYM, DASHED, GRAPOL, MOVTO2, LINBY2, CHAHOL, CHAINT, CHAFIX, SYMBOL, AXIPOS, AXISCA, GRID, and CHAANG are all GINO-F and GINOGRAF subroutines and are used here to plot the failure envelopes.

* FMOVE copies an array into another array.

* F01AAF calculates the inverse of a matrix.

* F01CKF calculates the multiplication of two matrices.

* AMIN1 finds the smallest number of a group of numbers.

* E02BAF computes a least-squares approximation to any arbitrary set of data points by a cubic spline.

* E02BBF computes a cubic spline from its B-spline representation.

C.4 DATA INPUT DESCRIPTION

1st data card: (FORMAT: 10I0, 2F0.0)

NM NL IP IW IZ NON1T NON1C NON2T
NON2C NON12 R DEF

where : NM = the number of different materials used, (max 2);

NL = the number of layers in the laminate, (max 10);

IP = 1 if the failure envelopes are to be plotted, otherwise IP = 0;

IW = 1 if the data is to be output, otherwise IW = 0;

IZ = 1 if the stress and strain distributions across the thickness are required, otherwise IZ = 0;

NON1T = 1 if the longitudinal tensile response is non-linear, otherwise NON1T = 0;

NON1C = 1 if the longitudinal compression response is non-linear and different from the longitudinal tensile behaviour. If it is non-linear and similar to that of the tensile response then NON1C = 2, otherwise NON1C = 0;

NON2T = 1 if the transverse tensile response is non-linear, otherwise NON2T = 0;

NON2C = 1 if the transverse compression response is non-linear and different from the transverse tensile behaviour. If it is non-linear and similar to that of the tensile response then NON2C = 2, otherwise NON2C = 0;

NON12 = 1 if the shear response is non-linear, otherwise NON12 = 0;

R = the mean radius of the cylinder; and

DEF = the difference in strain used by the iteration technique.

2nd data card: (FORMAT: 6I0)

I1 I2 I3 I4 I5 I6

These parameters determines which strength criterion is wanted to predict the failure. Every parameter takes the value 1 or 0. The value 1 means that this particular criterion is wanted to calculate the failure load, otherwise the value 0 is used. The parameters are arranged in this sequence: maximum stress, maximum strain, Azzi-Tsai-Hill, Hoffman, Tsai-Wu and Puppo-Evensen criteria.

3rd set of cards: (FORMAT: I0, 2F0.0, 2I0)

These are NL cards, a card per layer as follows :

NL cards

L	TL	THET	NS	KIND
L	TL	THET	NS	KIND
---	---	---	---	---

where:

L = layer material number;

TL = thickness of layer;

THET = angle of layer with x-axis (in degree);

NS = number of sub-layers for this layer;

KIND = 2 for angle-ply layer, otherwise KIND = 1.

N.B. The angle-ply layer is input as two layers, one is with $+\theta$ angle and the other is with $-\theta$, then the program divides each of these two layers into NS sub-layers and arranges them in the sequence : $+\theta, -\theta, +\theta, -\theta, +\theta, -\theta, \ldots$.

4th set of cards: (FORMAT: 2A8, 4F0.0)

These are NM cards, one card per material as follows :

AA ELL ETT GGLT PLT

where :

AA = the material name;

ELL = longitudinal Young's modulus;

ETT = transverse Young's modulus;

GGLT = shear modulus; and

PLT = major Poisson's ratio

5th set of cards: (FORMAT: 5F0.0)
These are also NM cards, a card per material :

XT XC YT YC ST

where :

XT = the longitudinal tensile strength;

XC = the longitudinal compression strength;

YT = the transverse tensile strength;

YC = the transverse compression strength; and

ST = the shear strength

If I1 = I3 = I4 = I5 = 0, this set of cards is omitted.

6th set of cards: (FORMAT: 5F0.0)
These are NM cards, one card per material :

EXT EXC EYT EYC EST

where :

EXT = the maximum tensile strain in the fibre direction;

EXC = the maximum compression strain in the fibre direction;

EYT = the maximum tensile strain in the transverse direction;

EYC = the maximum compression strain in the transverse direction; and

EST = the maximum shear strain

If I2 = NON1T = NON1C = NON2T = NON2C = NON12 = 0, then this set of cards is omitted.

7th_set_of_cards : (FORMAT: 6F0.0)

These are also NM cards as follows :

F12

where: F12 = the interaction strength parameter of Tsai-Wu failure theory.

If I5 = 0, this set of cards is omitted.

8th_set_of_cards : (FORMAT: 6F0.0)

This is one card for the laminate strengths of Puppo-Evensen criterion as follows :

XLT XLC YLT YLC SLT SLC

where :

XLT = the laminate tensile strength in x-direction;

XLC = the laminate compression strength in x-direction;

YLT = the laminate tensile strength in y-direction;

YLC = the laminate compression strength in y-direction;

SLT = the positive shear strength; and

SLC = the negative shear strength.

If I6 = 0, then this card is omitted.

9th_set_of_cards :

This is only one card, but the data required follows the value of IP :

If IP = 0, then the data is as follows : (FORMAT: 6F0.0)

SX SY SXY DSX DSY DSXY

where :

SX = the external laminate load in x-direction;

SY = the external laminate load in y-direction;

SXY = the external laminate shear load;

DSX = the load increment in x-direction;

DSY = the load increment in y-direction; and

DSXY = the incremental shear load.

If IP = 1, then the data is as follows : (FORMAT: 8F0.0, 2I0)

SXY SXMAX SXMIN SYMAX SYMIN FACT XL YL
NX NY

where :

SXY = the value of laminate shear load for which the failure envelope is to be plotted;

SXMAX = the maximum value of load on x-axis;

SXMIN = the minimum value of load on x-axis;

SYMAX = the maximum value of load on y-axis;

SYMIN = the minimum value of load on y-axis;

FACT = is a factor to scale the results;

XL = the length of x-axis (in mm);

YL = the length of y-axis (in mm), (max. 22o);

NX = number of interval on x-axis; and

NY = number of interval on y-axis.

10th set of cards :

For every non-linear stress-strain curve the following data are required :

NP NC		(FORMAT: 2I0)
X(I)	I = 1, NP	(FORMAT: 10F0.0)
Y(I)	I = 1, NP	(FORMAT: 10F0.0)
P(I)	I = 1, NC-1	(FORMAT: 10F0.0)

where :

NP = number of data points;

NC = number of splines for this curve;

X's = the values of the strains at the points;

Y's = the values of the stresses at the points; and

P's = the values of the strains at which the splines intersect.

C.5 THE PROGRAM LISTING

```
      LIBRARY(SUBGROUPCRAN)
      LIBRARY(SUBGROUPNAGF)
      LIBRARY(SUBGROUPGRAF)
      LIBRARY(SUBGROUPGINO)
      PROGRAM(STIF)
      COMPRESS INTEGER AND LOGICAL
      EXTENDED DATA
      INPUT 1=CR0
      OUTPUT 2=LP0
      END
C
      MASTER STRESS CALCULATIONS
C     -------------------------
      COMMON/BLOCK1/T(3,3),TT(6,4)/BLOCK2/SX,SXY,SY1,SY2,SY3/
     *BLOCK3/F(3),STR(3),WK(3),X7(50),Y7(50),F1(2),F2(2),F6(2),
     *F11(2),F22(2),F66(2),F12(2),XLT,YLT,SLT,XLC,YLC,SLC,YMAX/
     *BLOCK4/XT(2),XC(2),YT(2),YC(2),ST(2),SC(2),P(3,3)/
     *BLOCK5/EXT(2),EXC(2),EYT(2),EYC(2),EST(2),ESC(2),TI(3,3)/
     *BLOCK6/SXMAX,SXMIN,SYMAX,SYMIN,IP,XL,YL,NX,NY,NN,CC,DD,FACT
     */BLOCK7/SPC(3,10)
      DIMENSION EL(10),ET(10),PLT(2),GLT(10),C(4,1),CK(3,3,10),SK(3,3
     *,10),L(10),TL(10),THETA(10),TK(3,3,10),TTC(6,1),QK(3,3,10),Z(21),
     *Z1(20),Z2(21),HS(20),A(3,3),B(3,3),Q(3,3),S(3,3),AA(2,5),THET(10)
     *,STRN(3),KIND(10),NS(10),EP(3),STRESS(3,10),STRAIN(3,10)
     *,ELL(2),ETT(2),GGLT(2),PP(3,3,10),TTI(3,3,10)
     *,P1T(10),C1T(10),P1C(10),C1C(10),P2T(10),C2T(10),P2C(10),C2C(10),
     *P12(10),C12(10)
C
C     FORMATS:
C     --------
1     FORMAT(10I0,2F0.0)
2     FORMAT(2A8,4F0.0)
3     FORMAT(I0,2F0.0,2I0)
4     FORMAT(8F0.0,2I0)
5     FORMAT(6F0.0)
6     FORMAT(6I0)
51    FORMAT(5X,'ANALYSIS OF FILAMENT-WOUND TUBE OF R=' ,1PE9.3,'  AND',
     *I3,' LAYERS:'//5X,'LAYER',4X,'LAYER',5X,'LAYER',4X,'LAYER MATERIAL
     *'/6X,'NO.',3X,'THICKNESS',3X,'ANGLE',10X,'NO.'/)
52    FORMAT(6X,I2,4X,1PE9.3,2X,0PF6.2,10X,I2)
53    FORMAT(/26X,'MATERIAL PROPERTIES'//5X,'NO.',5X,
     *'MATERIAL',11X,'EL',8X,'ET',7X,'GLT',5X,'NULT')
54    FORMAT(5X,I2,4X,2A8,3(1PE10.2),2X,0PF5.3)
55    FORMAT(' EX=',1PE10.2,2X,'EY=',1PE10.2,2X,'NUXY=',0PF6.3,2X,
     *'NUYX=',0PF6.3,2X,'GXY=',1PE10.2)
56    FORMAT(3(1PE10.2))
57    FORMAT(/5X,3HNO.,4X,1HX,9X,2HX',8X,1HY,9X,2HY',8X,1HS)
```

```
58    FORMAT(//5X,'LAMINATE STRESSES:',3(1PE12.4)/5X,'LAMINATE STRAINS :
     *',3(1PE12.4))
59    FORMAT(5X,I2,6(1PE10.2))
60    FORMAT(/5X,3HNO.,3X,3HEU1,7X,4HEU1',6X,3HEU2,7X,4HEU2',6X,4HEU12)
63    FORMAT(/5X,'LAYER NO. ',I2/5X,'.............')
82    FORMAT(//'  FAILURE BY MAXIMUM STRESS CRITERION:'/2X,35('-'))
83    FORMAT(//'  FAILURE BY MAXIMUM STRAIN CRITERION:'/2X,35('-'))
84    FORMAT(' FACTOR',4X,'*******LAYER STRESSES*******',2X,
     *'********EXTERNAL LOAD********')
85    FORMAT(//' FAILURE BY HILL-TSAI-AZZI CRITERION:'/1X,35('-'))
86    FORMAT(//' FAILURE BY HOFFMAN CRITERION:'/1X,28('-'))
87    FORMAT(//' FAILURE BY TSAI-WU CRITERION, WITH F12=',1PE10.2,' :'/
     *1X,39('-'))
88    FORMAT(//' FAILURE BY PUPPO-EVENSEN CRITERION:'/1X,34('-')/
     *' FACTOR1 FACTOR2     GAMA     ******EXTERNAL LOADS********')
89    FORMAT(/' LAMINATE STRENGTH:'/' XLT=',1PE9.2,' XLC=',1PE9.2,
     *' YLT=',1PE9.2,' YLC=',1PE9.2,' SLT=',1PE9.2,' SLC=',1PE9.2)
90    FORMAT(2X,'S1 EXCEEDS MAX. AT MODE S2 EXCEEDS MAX. AT MODE S12 EXC
     *EEDS MAX. AT MODE')
91    FORMAT(2X,'E1 EXCEEDS MAX. AT MODE E2 EXCEEDS MAX. AT MODE E12 EXC
     *EEDS MAX. AT MODE')
92    FORMAT(' STRESS',3(1PE10.2),'STRAIN',3(1PE10.2))
93    FORMAT(/5X,'LINEAR ANALYSIS:'/5X,16('=')/5X,'LAMINATE PROPERTIES:'
     *)
94    FORMAT(/5X,'LAMINATE PROPERTIES (SECANT MODULI):')
95    FORMAT(' LAYER ',I2,' FAILED IN MODE ',I2,' AT LOAD:',3(1PE12.4))
97    FORMAT(' STRESSES AND STRAINS IN ANGLE PLY LAYER'/5X,'Z/H',11X,
     *'SX',10X,'SY',10X,'SXY',9X,'EPX',9X,'EPY',9X,'EPXY')
98    FORMAT(F12.8,6(1PE12.4))
99    FORMAT(' LAYER ',I2,' IS SIMILAR TO LAYER ',I2,' (ANGLE PLY)')
100   FORMAT(/5X,'STRENGTH CALCULATIONS:'/5X,22('='))
181   FORMAT(/5X,'NONLINEAR ANALYSIS:'/5X,19('='))
C
C     DATA INPUT:
C     -----------
      READ(1,1)NM,NL,IP,IW,IZ,NON1T,NON1C,NON2T,NON2C,NON12,R,DEF
      NON=1
      IF(NON1T.EQ.0.AND.NON1C.EQ.0.AND.NON2T.EQ.0.AND.NON2C.EQ.0.
     *AND.NON12.EQ.0)NON=0
      IF(IW.EQ.1)WRITE(2,51)R,NL
      READ(1,6)I1,I2,I3,I4,I5,I6
      READ(1,3)(L(K),TL(K),THET(K),NS(K),KIND(K),K=1,NL)
      IF(IW.EQ.1)WRITE(2,52)(K,TL(K),THET(K),L(K),K=1,NL)
      READ(1,2)(AA(1,I),AA(2,I),ELL(I),ETT(I),GGLT(I),PLT(I),I=1,NM)
      IF(IW.EQ.1)WRITE(2,53)
      IF(IW.EQ.1)WRITE(2,54)(I,AA(1,I),AA(2,I),ELL(I),ETT(I),GGLT(I),
     *PLT(I),I=1,NM)
      IF(I1.EQ.0.AND.I3.EQ.0.AND.I4.EQ.0.AND.I5.EQ.0)GO TO 30
      READ(1,5)(XT(I),XC(I),YT(I),YC(I),ST(I),I=1,NM)
      IF(IW.EQ.1)WRITE(2,57)
      IF(IW.EQ.1)WRITE(2,59)(I,XT(I),XC(I),YT(I),YC(I),ST(I),I=1,NM)
```

```
30    IF(I2.EQ.0.AND.NON.EQ.0)GO TO 31
      READ(1,5)(EXT(I),EXC(I),EYT(I),EYC(I),EST(I),I=1,NM)
      IF(IW.EQ.1)WRITE(2,60)
      IF(IW.EQ.1)WRITE(2,59)(I,EXT(I),EXC(I),EYT(I),EYC(I),EST(I)
     *,I=1,NM)
31    IF(I5.EQ.0)GO TO 48
      READ(1,5)(F12(I),I=1,NM)
48    IF(I6.EQ.0)GO TO 32
      READ(1,5)XLT,XLC,YLT,YLC,SLT,SLC
      IF(IW.EQ.1)WRITE(2,89)XLT,XLC,YLT,YLC,SLT,SLC
32    IF(IP.EQ.0)GO TO 34
      READ(1,4)SXY,SXMAX,SXMIN,SYMAX,SYMIN,FACT,XL,YL,NX,NY
C
      CALL CC936N
      CALL WINDOW(2)
      CALL CHASIZ(2.5,2.5)
      YMAX=YT(1)
      XMAX2=SXMAX/2.*FACT
      XMIN2=ABS(SXMIN)/2.*FACT
      CC=(SXMAX-SXMIN)/NX
      DD=(SYMAX-SYMIN)/NY
      IFR=0
      GO TO 33
34    READ(1,5)SX,SY,SXY,DSX,DSY,DSXY
      F(1)=SX
      F(2)=SY
      IFR=1
33    PI=4.*ATAN(1.)
      DO 390 I=1,NM
      XC(I)=-XC(I)
      YC(I)=-YC(I)
      SC(I)=-ST(I)
      EXC(I)=-EXC(I)
      EYC(I)=-EYC(I)
      ESC(I)=-EST(I)
390   CONTINUE
      WX,WY=1.
      DFF=ETT(1)*EYT(1)/3.
      PI8=PI/8.
      PI90=PI/2.
      PI270=PI90*3.
      PI360=PI*2.
      F(3)=SXY
      DO 47 K=1,NL
      THETA(K)=PI*THET(K)/180.
47    CONTINUE
      ID=0
      IDD=0
      LFF=0
      IWRT=0
C
```

```
C     CURVE FITTING FOR NONLINEAR DATA:
C     ---------------------------------
      IF(NON1T.EQ.0)GO TO 106
      CALL NONLINEAR(NC1T,XO1T,YO1T,XM1T,P1T,C1T)
      GO TO 206
106   XO1T,XM1T=EXT(1)
206   IF(NON1C.EQ.0)GO TO 107
      IF(NON1C.EQ.2)GO TO 108
      CALL NONLINEAR(NC1C,XO1C,YO1C,XM1C,P1C,C1C)
      GO TO 207
108   NC1C=NC1T
      XO1C=XO1T
      YO1C=YO1T
      XM1C=XM1T
      DO 109 I=1,10
      P1C(I)=P1T(I)
      C1C(I)=C1T(I)
109   CONTINUE
      GO TO 207
107   XO1C,XM1C=ABS(EXC(1))
207   IF(NON2T.EQ.0)GO TO 101
      CALL NONLINEAR(NC2T,XO2T,YO2T,XM2T,P2T,C2T)
      GO TO 210
101   XO2T,XM2T=EYT(1)
210   IF(NON2C.EQ.0)GO TO 102
      IF(NON2C.EQ.2)GO TO 103
      CALL NONLINEAR(NC2C,XO2C,YO2C,XM2C,P2C,C2C)
      GO TO 211
103   NC2C=NC2T
      XO2C=XO2T
      YO2C=YO2T
      XM2C=XM2T
      DO 104 I=1,10
      P2C(I)=P2T(I)
      C2C(I)=C2T(I)
104   CONTINUE
      GO TO 211
102   XO2C,XM2C=ABS(EYC(1))
211   IF(NON12.EQ.0)GO TO 105
      CALL NONLINEAR(NC12,XO12,YO12,XM12,P12,C12)
      GO TO 208
105   XO12,XM12=EST(1)
208   CONTINUE
C
      IF(I4.EQ.0.AND.I5.EQ.0)GO TO 22
      DO 13 I=1,NM
      F1(I)=1./XT(I)-1./ABS(XC(I))
      F2(I)=1./YT(I)-1./ABS(YC(I))
      F6(I)=1./ST(I)-1./ABS(SC(I))
      F11(I)=1./(XT(I)*ABS(XC(I)))
      F22(I)=1./(YT(I)*ABS(YC(I)))
      F66(I)=1./(ST(I)*ABS(SC(I)))
13    CONTINUE
```

```
C
22    DO 45 K=1,NL
      LK=L(K)
      EL(K)=ELL(LK)
      ET(K)=ETT(LK)
      GLT(K)=GGLT(LK)
45    CONTINUE
      EP1=0.
      EP2=0.
      EP12=0.
      LOOP=0
C
C     LAYER COMPLIANCE MATRIX:
C     ------------------------
20    DO 12 K=1,NL
      LK=L(K)
      SK(1,1,K)=1./EL(K)
      SK(2,2,K)=1./ET(K)
      SK(3,3,K)=1./GLT(K)
      SK(1,2,K),SK(2,1,K)=-PLT(LK)/EL(K)
      CALL FMOVE(SK(1,1,K),T,9)
C
C     LAYER STIFFNESS MATRIX:
C     -----------------------
      IFAIL=0
      CALL F01AAF(T,3,3,TI,3,WK,IFAIL)
      CALL FMOVE(TI,CK(1,1,K),9)
      C(1,1)=CK(1,1,K)
      C(2,1)=CK(1,2,K)
      C(3,1)=CK(2,2,K)
      C(4,1)=CK(3,3,K)
      AM=COS(THETA(K))
      AN=SIN(THETA(K))
      CALL TRANSFORMATION(AM,AN)
      CALL FMOVE(T,TK(1,1,K),9)
      IFAIL=0
      CALL F01CKF(TTC,TT,C,6,1,4,WK,3,1,IFAIL)
      QK(1,1,K)=TTC(1,1)
      QK(1,2,K),QK(2,1,K)=TTC(2,1)
      QK(1,3,K),QK(3,1,K)=TTC(3,1)
      QK(2,2,K)=TTC(4,1)
      QK(2,3,K),QK(3,2,K)=TTC(5,1)
      QK(3,3,K)=TTC(6,1)
12    CONTINUE
C
C     LAMINATE STIFFNESS MATRIX:
C     --------------------------
      IWR=0
      H=0.
```

```
      DO 14 K=1,NL
14    H=H+TL(K)
      Z(1)=-H/2.
      Z2(1)=Z(1)**2
      KK=2
      DO 15 K=1,NL
      MM=KK+NS(K)-1
      TLL=TL(K)/NS(K)
      DO 46 M=KK,MM
      Z(M)=Z(M-1)+TLL
      Z2(M)=Z(M)**2
46    CONTINUE
      KK=KK+NS(K)
15    CONTINUE
      DO 16 K=1,MM-1
      Z1(K)=(Z(K+1)+Z(K))/2.
      HS(K)=Z2(K+1)-Z2(K)
16    CONTINUE
      DO 18 I=1,3
      DO 18 J=1,3
      NN=0
      MM=0
      LL=0
      A(I,J)=0.
      B(I,J)=0.
      DO 19 K=1,NL
      A(I,J)=A(I,J)+QK(I,J,K)*TL(K)
      KKK=KIND(K)
      GO TO (121,122),KKK
121   NN=MM+1
      MM=NN
      GO TO 123
122   IF(LL.EQ.2)GO TO 126
      LL=LL+1
      NN=NN+1
      GO TO 127
126   LL=1
      NN=MM+1
127   MM=NN+2*NS(K)-2
123   DO 124 M=NN,MM,2
      B(I,J)=B(I,J)+QK(I,J,K)*HS(M)
124   CONTINUE
19    CONTINUE
      A(I,J)=A(I,J)/H
      B(I,J)=B(I,J)/2./R/H
18    CONTINUE
      Q(1,1)=A(1,1)
      Q(1,2)=A(1,2)-B(1,2)
      Q(1,3)=A(1,3)+B(1,3)
      Q(2,1)=A(2,1)
      Q(2,2)=A(2,2)-B(2,2)
```

```
      Q(2,3)=A(2,3)+B(2,3)
      Q(3,1)=A(3,1)
      Q(3,2)=A(3,2)-B(3,2)
      Q(3,3)=A(3,3)+B(3,3)
C
C     LAMINATE COMPLIANCE MATRIX:
C     ---------------------------
      IFAIL=0
      CALL F01AAF(Q,3,3,S,3,WK,IFAIL)
      EX=1./S(1,1)
      EY=1./S(2,2)
      PXY=-S(1,2)/S(1,1)
      PYX=-S(2,1)/S(2,2)
      GXY=1./S(3,3)
      IF(IFR.EQ.0)GO TO 155
      IFAIL=0
      CALL F01CKF(EP,S,F,3,1,3,WK,3,1,IFAIL)
      DP1=ABS(EP(1)-EP1)
      DP2=ABS(EP(2)-EP2)
      DP12=ABS(EP(3)-EP12)
      IF(DP1.LE.DEF.AND.DP2.LE.DEF.AND.DP12.LE.DEF)LOOP=1
      EP1=EP(1)
      EP2=EP(2)
      EP12=EP(3)
155   IF(IWRT.EQ.0.AND.LOOP.EQ.0)GO TO 151
      IF(IWRT.EQ.1.AND.LOOP.EQ.1)GO TO 152
      GO TO 154
151   WRITE(2,93)
      WRITE(2,55)EX,EY,PXY,PYX,GXY
      IF(IFR.EQ.1)WRITE(2,58)F,EP
      IWR=1
      GO TO 154
152   WRITE(2,58)F,EP
      WRITE(2,94)
153   WRITE(2,55)EX,EY,PXY,PYX,GXY
      IWR=1
154   CONTINUE
C
C     LAYER STRESS/STRAIN CALCULATIONS:
C     ---------------------------------
      NN=0
      MM=0
      LL=0
      DO 27 K=1,NL
      IF(IWR.EQ.1.AND.IFR.EQ.1)WRITE(2,63)K
      IC=0
      KKK=KIND(K)
      GO TO (141,142),KKK
141   NN=MM+1
      MM=NN
      GO TO 143
```

```
142   IF(LL.EQ.2)GO TO 146
      LL=LL+1
      NN=NN+1
      GO TO 147
146   LL=1
      NN=MM+1
147   MM=NN+2*NS(K)-2
      IF(IZ.EQ.1.AND.IWR.EQ.1)WRITE(2,97)
      DO 145 I=1,3
      DO 145 J=1,10
      SPC(I,J)=0.
145   CONTINUE
143   IF(IFR.EQ.0)MM=1
      DO 144 M=NN,MM,2
      ZR=Z1(M)/R
      ZH=Z1(M)/H
      IC=IC+1
      DO 21 J=1,3
      B(1,J)=S(1,J)
      B(2,J)=S(2,J)-ZR*S(2,J)
      B(3,J)=S(3,J)+ZR*S(3,J)
21    CONTINUE
      CALL FMOVE(QK(1,1,K),T,9)
      IFAIL=0
      CALL F01CKF(TI,T,B,3,3,3,WK,3,1,IFAIL)
      IF(IZ.EQ.0)GO TO 50
      IF(IWR.EQ.0)GO TO 50
      IFAIL=0
      CALL F01CKF(STR,TI,F,3,1,3,WK,3,1,IFAIL)
      IFAIL=0
      CALL F01CKF(STRN,B,F,3,1,3,WK,3,1,IFAIL)
      DO 301 I=1,3
      IF(F(I).EQ.0.)GO TO 302
      STR(I)=STR(I)/F(I)
302   IF(EP(I).EQ.0.)GO TO 301
      STRN(I)=STRN(I)/EP(I)
301   CONTINUE
      WRITE(2,98)ZH,STR,STRN
50    CONTINUE
      CALL FMOVE(TK(1,1,K),T,9)
      IFAIL=0
      CALL F01CKF(P,T,TI,3,3,3,WK,3,1,IFAIL)
      IF(IFR.EQ.0)CALL FMOVE(P,PP(1,1,K),9)
      IF(IFR.EQ.1)GO TO 132
      CALL FMOVE(SK(1,1,K),T,9)
      IFAIL=0
      CALL F01CKF(TI,T,P,3,3,3,WK,3,1,IFAIL)
      CALL FMOVE(TI,TTI(1,1,K),9)
132   CONTINUE
      IF(IFR.EQ.1)CALL F01CKF(STR,P,F,3,1,3,WK,3,1,IFAIL)
      IF(KKK.EQ.1)GO TO 144
```

```
      IF(IFR.EQ.0)GO TO 144
      CALL FMOVE(STR,SPC(1,IC),3)
144   CONTINUE
      IF(IFR.EQ.0)GO TO 27
      IF(KKK.EQ.2)CALL MAXIMUM VALUE(IC,STR)
      CALL FMOVE(STR,STRESS(1,K),3)
      CALL FMOVE(SK(1,1,K),T,9)
      IFAIL=0
      CALL F01CKF(STRN,T,STR,3,1,3,WK,3,1,IFAIL)
      IF(IWR.EQ.1)WRITE(2,92)STR,STRN
      CALL FMOVE(STRN,STRAIN(1,K),3)
27    CONTINUE
C
C     NONLINEAR ANALYSIS:
C     -------------------
      IF(IFR.EQ.0)GO TO 23
      IF(LOOP.EQ.1)GO TO 160
      GO TO 161
160   F111=F(1)
      F222=F(2)
      F333=F(3)
      GO TO 28
161   IF(NON.EQ.0)GO TO 23
      DO 112 K=1,NL
      IF(THET(K).EQ.-THET(K-1).AND.KIND(K).EQ.KIND(K-1))GO TO 112
      K1=K+1
      CALL FMOVE(STRAIN(1,K),STRN,3)
      IF(STRN(1).LT.0.0)GO TO 113
      IF(STRN(1).LE.XO1T)GO TO 114
      ND=1
      IF(STRN(1).GT.XM1T)GO TO 162
      STRN(1)=STRN(1)-XO1T
      IFAIL=0
      CALL E02BBF(NC1T,P1T,C1T,STRN(1),S1T,IFAIL)
      STRN(1)=STRN(1)+XO1T
      S1T=S1T+YO1T
      EL(K)=S1T/STRN(1)
      IF(KIND(K).EQ.2)EL(K1)=EL(K)
      GO TO 114
113   IF(ABS(STRN(1)).LE.XO1C)GO TO 114
      ND=-1
      IF(ABS(STRN(1)).GT.XM1C)GO TO 162
      STRN(1)=ABS(STRN(1))-XO1C
      IFAIL=0
      CALL E02BBF(NC1C,P1C,C1C,STRN(1),S1C,IFAIL)
      STRN(1)=STRN(1)+XO1C
      S1C=S1C+YO1C
      EL(K)=S1C/STRN(1)
      IF(KIND(K).EQ.2)EL(K1)=EL(K)
      GO TO 114
162   IF(IDD.EQ.0.OR.IDD.EQ.1)GO TO 115
```

```
      WRITE(2,95)K,ND,F111,F222,F333
      IF(KIND(K).EQ.2)WRITE(2,95)K1,ND,F111,F222,F333
      LFF=1
      GO TO 116
114   IF(STRN(2).LT.0.0)GO TO 110
      IF(STRN(2).LE.XO2T)GO TO 111
      ND=2
      IF(STRN(2).GT.XM2T)GO TO 163
      STRN(2)=STRN(2)-XO2T
      IFAIL=0
      CALL E02BBF(NC2T,P2T,C2T,STRN(2),S2T,IFAIL)
      STRN(2)=STRN(2)+XO2T
      S2T=S2T+YO2T
      ET(K)=S2T/STRN(2)
      IF(KIND(K).EQ.2)ET(K1)=ET(K)
      GO TO 111
110   IF(ABS(STRN(2)).LE.XO2C)GO TO 111
      ND=-2
      IF(ABS(STRN(2)).GT.XM2C)GO TO 163
      STRN(2)=ABS(STRN(2))-XO2C
      IFAIL=0
      CALL E02BBF(NC2C,P2C,C2C,STRN(2),S2C,IFAIL)
      STRN(2)=STRN(2)+XO2C
      S2C=S2C+YO2C
      ET(K)=S2C/STRN(2)
      IF(KIND(K).EQ.2)ET(K1)=ET(K)
      GO TO 111
163   IF(IDD.EQ.0.OR.IDD.EQ.1)GO TO 115
      WRITE(2,95)K,ND,F111,F222,F333
      IF(KIND(K).EQ.2)WRITE(2,95)K1,ND,F111,F222,F333
      LFF=1
      GO TO 116
111   IF(ABS(STRN(3)).LE.XO12)GO TO 116
      ND=12
      IF(ABS(STRN(3)).GT.XM12)GO TO 164
      STRN(3)=ABS(STRN(3))-XO12
      IFAIL=0
      CALL E02BBF(NC12,P12,C12,STRN(3),S12,IFAIL)
      STRN(3)=STRN(3)+XO12
      S12=S12+YO12
      GLT(K)=S12/STRN(3)
      IF(KIND(K).EQ.2)GLT(K1)=GLT(K)
      GO TO 116
164   IF(IDD.EQ.0.OR.IDD.EQ.1)GO TO 115
      WRITE(2,95)K,ND,F111,F222,F333
      IF(KIND(K).EQ.2)WRITE(2,95)K1,ND,F111,F222,F333
      LFF=1
116   CONTINUE
      GO TO 112
115   ID=1
112   CONTINUE
```

```
      IF(IWRT.EQ.0.AND.LOOP.EQ.0)GO TO 23
117   IWRT=1
      N7=0
      IF(LFF.EQ.0)GO TO 166
      LFF=0
      IDD,ID=0
      GO TO 119
166   IF(ID.EQ.1)GO TO 165
      IF(IFR.EQ.1)GO TO 20
      GO TO 28
165   DSX=DSX/10.
      DSY=DSY/10.
      DSXY=DSXY/10.
      IDD=IDD+1
      ID=0
28    CONTINUE
      IF(IFR.EQ.0)GO TO 118
      F(1)=F111+DSX
      F(2)=F222+DSY
      F(3)=F333+DSXY
      GO TO 22
118   IFR=1
      CALL PICCLE
      NN=7
      CALL AXES
      F(1),SX=WX
      F(2),SY=0.
      DSX=DFF
      DSY,DSXY=0.
      ANGLE=0.
      GO TO 22
119   IF(IP.EQ.0)GO TO 39
      IF(F111.GT.SXMAX.OR.F111.LT.SXMIN.OR.F222.GT.SYMAX.OR.F222.LT.
     *SYMIN)GO TO 189
      N7=N7+1
      X7(N7)=F111
      Y7(N7)=F222
189   ANGLE=ANGLE+PI8
      IF(ANGLE.GE.PI360)GO TO 188
      IF(ANGLE.EQ.PI90.OR.ANGLE.EQ.PI270)GO TO 171
      TANA=ABS(TAN(ANGLE))
      F(1)=WY/(TANA+WY/WX)
      F(2)=TANA*F(1)
      IF(ANGLE.GT.PI90.AND.ANGLE.LT.PI270)F(1)=-F(1)
      IF(ANGLE.GT.PI)F(2)=-F(2)
      DSX=DFF
      IF(ANGLE.GT.PI90.AND.ANGLE.LT.PI270)DSX=-DFF
      DSY=DSX*F(2)/F(1)
      GO TO 172
171   F(1)=0.
      DSX=0.
```

```
      F(2)=WY
      IF(ANGLE.EQ.PI270)F(2)=-WY
      DSY=DFF
      IF(ANGLE.EQ.PI270)DSY=-DFF
172   DSXY=0.
      GO TO 22
188   DO 391 I=1,N7
      X7(I)=X7(I)/FACT
      Y7(I)=Y7(I)/FACT
391   CONTINUE
      CALL GRASYM(X7,Y7,N7,4,0)
      GO TO 120
C
C     STRENGTH CALCULATIONS:
C     ----------------------
23    IF(I1.EQ.0.AND.I2.EQ.0.AND.I3.EQ.0.AND.I4.EQ.0.AND.I5.EQ.0.AND.
     *I6.EQ.0)GO TO 205
      WRITE(2,100)
      YMAX=YT(1)
      XMAX2=SXMAX/2.*FACT
      XMIN2=ABS(SXMIN)/2.*FACT
C
C     MAXIMUM STRESS THEORY:
C     ----------------------
      IF(I1.EQ.0) GO TO 200
      WRITE(2,82)
      N=1
      DO 17 K=1,NL
      LK=L(K)
      K1=K-1
      WRITE(2,63)K
      IF(THET(K).EQ.-THET(K1).AND.KIND(K).EQ.KIND(K1))GO TO 156
      GO TO 157
156   WRITE(2,99)K,K1
      GO TO 17
157   IF(IP.EQ.1)GO TO 36
      CALL FMOVE(STRESS(1,K),STR,3)
      CALL FAIL(XT(LK),YT(LK),ST(LK),XC(LK),YC(LK),SC(LK),STR,SX,SY,SXY
     *,N)
      GO TO 17
36    WRITE(2,90)
      NN=1
      CALL AXES
      CALL FMOVE(PP(1,1,K),P,9)
      CALL MAXIFAIL(K,N,LK,XMAX2,XMIN2,KIND(K),THET(K))
17    CONTINUE
200   CONTINUE
C
```

```
C     MAXIMUM STRAIN THEORY:
C     ----------------------
      IF(I2.EQ.0)GO TO 201
      WRITE(2,83)
      N=2
      DO 190 K=1,NL
      LK=L(K)
      K1=K-1
      WRITE(2,63)K
      IF(THET(K).EQ.-THET(K1).AND.KIND(K).EQ.KIND(K1))GO TO 191
      GO TO 192
191   WRITE(2,99)K,K1
      GO TO 190
192   IF(IP.EQ.1)GO TO 37
      CALL FMOVE(STRAIN(1,K),STRN,3)
      CALL FAIL(EXT(LK),EYT(LK),EST(LK),EXC(LK),EYC(LK),ESC(LK),STRN,
     *SX,SY,SXY,N)
      GO TO 190
37    WRITE(2,91)
      NN=2
      CALL PICCLE
      CALL AXES
      CALL FMOVE(TTI(1,1,K),TI,9)
      CALL MAXIFAIL(K,N,LK,XMAX2,XMIN2,KIND(K),THET(K))
190   CONTINUE
201   CONTINUE
C
C     HILL-TSAI-AZZI THEORY:
C     ----------------------
      IF(I3.EQ.0)GO TO 202
      WRITE(2,85)
      N=1
      DO 193 K=1,NL
      LK=L(K)
      K1=K-1
      WRITE(2,63)K
      IF(THET(K).EQ.-THET(K1).AND.KIND(K).EQ.KIND(K1))GO TO 194
      GO TO 195
194   WRITE(2,99)K,K1
      GO TO 193
195   WRITE(2,84)
      IF(IP.EQ.1)GO TO 196
      F(1)=SX
      F(2)=SY
      F(3)=SXY
      CALL FMOVE(STRESS(1,K),STR,3)
      GO TO 40
196   CALL FMOVE(PP(1,1,K),P,9)
      NN=3
      CALL PICCLE
      CALL AXES
40    CALL FAILURE(K,N,LK,KIND(K),THET(K))
193   CONTINUE
202   CONTINUE
```

```
C
C     HOFFMAN THEORY:
C     ---------------
      IF(I4.EQ.0)GO TO 203
      WRITE(2,86)
      N=2
      DO 183 K=1,NL
      LK=L(K)
      K1=K-1
      WRITE(2,63)K
      IF(THET(K).EQ.-THET(K1).AND.KIND(K).EQ.KIND(K1))GO TO 184
      GO TO 185
184   WRITE(2,99)K,K1
      GO TO 183
185   WRITE(2,84)
      FF1=ABS(XC(LK))-XT(LK)
      FF2=ABS(YC(LK))-YT(LK)
      IF(IP.EQ.1)GO TO 186
      F(1)=SX
      F(2)=SY
      F(3)=SXY
      CALL FMOVE(STRESS(1,K),STR,3)
      GO TO 41
186   CALL FMOVE(PP(1,1,K),P,9)
      NN=4
      CALL PICCLE
      CALL AXES
41    CALL FAILURE(K,N,LK,KIND(K),THET(K))
183   CONTINUE
203   CONTINUE
C
C     TSAI-WU THEORY:
C     ---------------
      IF(I5.EQ.0)GO TO 204
      WRITE(2,87)F12(LK)
      N=3
      DO 173 K=1,NL
      LK=L(K)
      K1=K-1
      WRITE(2,63)K
      IF(THET(K).EQ.-THET(K1).AND.KIND(K).EQ.KIND(K1))GO TO 174
      GO TO 175
174   WRITE(2,99)K,K1
      GO TO 173
175   WRITE(2,84)
      IF(IP.EQ.1)GO TO 176
      F(1)=SX
      F(2)=SY
      F(3)=SXY
      CALL FMOVE(STRESS(1,K),STR,3)
      GO TO 42
```

```
176   CALL FMOVE(PP(1,1,K),P,9)
      NN=5
      CALL PICCLE
      CALL AXES
42    CALL FAILURE(K,N,LK,KIND(K),THET(K))
173   CONTINUE
204   CONTINUE
C
C     PUPPO-EVENSEN THEORY:
C     ---------------------
      IF(I6.EQ.0)GO TO 205
      WRITE(2,88)
      N=4
      IF(IP.EQ.1)GO TO 43
      F(1)=SX
      F(2)=SY
      F(3)=SXY
      GO TO 44
43    CALL PICCLE
      NN=6
      CALL AXES
44    CALL FAILURE(1,N,1,1,1)
205   CONTINUE
      IF(NON.EQ.0)GO TO 180
      WRITE(2,181)
      GO TO 117
C
180   IF(IP.EQ.0)GO TO 39
120   CALL DEVEND
39    STOP OK
      END
C
      SUBROUTINE TRANSFORMATION(AM,AN)
C     -------------------------------
      COMMON/BLOCK1/ T(3,3),TT(6,4)
      DO 1 I=1,3
      DO 1 J=1,3
1     T(I,J)=0.
      DO 2 I=1,6
      DO 2 J=1,4
2     TT(I,J)=0.
      AM2=AM**2
      AN2=AN**2
      AM3=AM**3
      AN3=AN**3
      AM4=AM2**2
      AN4=AN2**2
      AMAN=AM*AN
      AMAN2=2.*AMAN
      AM2AN2=AM2*AN2
      AMAN22=AM2-AN2
```

```
      T(1,1),T(2,2)=AM2
      T(1,2),T(2,1)=AN2
      T(1,3)=-AMAN2
      T(2,3)=AMAN2
      T(3,1)=AMAN
      T(3,2)=-AMAN
      T(3,3)=AMAN22
      TT(1,1),TT(4,3)=AM4
      TT(1,2),TT(4,2)=2.*AM2AN2
      TT(1,3),TT(4,1)=AN4
      TT(1,4),TT(4,4)=4.*AM2AN2
      TT(2,1),TT(2,3),TT(6,1),TT(6,3)=AM2AN2
      TT(2,2)=AM4+AN4
      TT(2,4)=-TT(1,4)
      TT(3,1)=-AM3*AN
      TT(3,2)=AMAN*AMAN22
      TT(3,3)=AM*AN3
      TT(3,4)=2.*TT(3,2)
      TT(5,1)=-TT(3,3)
      TT(5,2)=-TT(3,2)
      TT(5,3)=-TT(3,1)
      TT(5,4)=-TT(3,4)
      TT(6,2)=-TT(1,2)
      TT(6,4)=AMAN22**2
      RETURN
      END
C
      SUBROUTINE FAIL(XT,YT,ST,XC,YC,SC,STR,SX,SY,SXY,N)
C     ------------------------------------------------
      DIMENSION STR(3)
      X=XT
      Y=YT
      SS=ST
      IF(STR(1).LT.0.)X=XC
      IF(STR(2).LT.0.)Y=YC
      IF(STR(3).LT.0.)SS=SC
      IF(ABS(STR(1)).LT.1.E-10)STR(1)=1.E-10
      IF(ABS(STR(2)).LT.1.E-10)STR(2)=1.E-10
      IF(ABS(STR(3)).LT.1.E-10)STR(3)=1.E-10
      R1=X/STR(1)
      R2=Y/STR(2)
      R3=SS/STR(3)
      RM=AMIN1(R1,R2,R3)
      SXF=RM*SX
      SYF=RM*SY
      SXYF=RM*SXY
      IF(RM.EQ.R1)KK=11
      IF(RM.EQ.R2)KK=22
      IF(RM.EQ.R3)KK=12
      GO TO(1,2)N
1     WRITE(2,3)SXF,SYF,SXYF,KK
```

```
      GO TO 5
2     WRITE(2,4)SXF,SYF,SXYF,KK
3     FORMAT(21H LAYER FAILS AT LOAD:,3(1PE10.2),
     *6H  AS S,I2,14H  REACHES MAX.)
4     FORMAT(21H LAYER FAILS AT LOAD:,3(1PE10.2),
     *6H  AS E,I2,14H  REACHES MAX.)
5     RETURN
      END
C
      SUBROUTINE MAXIFAIL(K,N,LK,XMAX2,XMIN2,KIND,THET)
C     ------------------------------------------------
      COMMON/BLOCK2/SX,SXY,SY1,SY2,SY3/BLOCK4/XT(2),XC(2),YT(2),YC(2),
     *ST(2),SC(2),P(3,3)/BLOCK6/SXMAX,SXMIN,SYMAX,SYMIN,IP,XL,YL,NX,NY,
     *NN,CC,DD,FACT/BLOCK5/EXT(2),EXC(2),EYT(2),EYC(2),EST(2),ESC(2),
     *TI(3,3)
      DIMENSION X1(5),X2(5),X3(5),X4(5),X5(5),X6(5),Y1(5),Y2(5),
     *Y3(5),Y4(5),Y5(5),Y6(5)
      N1,N2,N3,N4,N5,N6=0
      SX=SXMAX*FACT
100   IF(N.EQ.2)GO TO 111
      CALL MAXIMUM(P,XT(LK),YT(LK),ST(LK),1,2,3)
      GO TO 112
111   CALL MAXIMUM(TI,EXT(LK),EYT(LK),EST(LK),1,2,3)
112   SY1=SY1/FACT
      SY2=SY2/FACT
      SY3=SY3/FACT
      IF(SY1.GT.SYMAX.OR.SY1.LT.SYMIN)GO TO 101
      N1=N1+1
      X1(N1)=SX
      Y1(N1)=SY1
101   IF(SY2.GT.SYMAX.OR.SY2.LT.SYMIN)GO TO 102
      N2=N2+1
      X2(N2)=SX
      Y2(N2)=SY2
102   IF(SY3.GT.SYMAX.OR.SY3.LT.SYMIN)GO  TO 103
      N3=N3+1
      X3(N3)=SX
      Y3(N3)=SY3
103   IF(N.EQ.2)GO TO 113
      CALL MAXIMUM(P,XC(LK),YC(LK),SC(LK),-1,-2,-3)
      GO TO 114
113   CALL MAXIMUM(TI,EXC(LK),EYC(LK),ESC(LK),-1,-2,-3)
114   SY1=SY1/FACT
      SY2=SY2/FACT
      SY3=SY3/FACT
      IF(SY1.GT.SYMAX.OR.SY1.LT.SYMIN)GO TO 104
      N4=N4+1
      X4(N4)=SX
      Y4(N4)=SY1
104   IF(SY2.GT.SYMAX.OR.SY2.LT.SYMIN)GO  TO 105
      N5=N5+1
```

```
      X5(N5)=SX
      Y5(N5)=SY2
105   IF(SY3.GT.SYMAX.OR.SY3.LT.SYMIN)GO TO 106
      N6=N6+1
      X6(N6)=SX
      Y6(N6)=SY3
106   IF(SX.LT.0.0)GO TO 107
      GO TO 108
107   SX=SX-XMIN2
      GO TO 109
108   SX=SX-XMAX2
109   IF(SX.GE.SXMIN*FACT)GO TO 100
      IF(K.EQ.1)GO TO  118
      DASH=FLOAT(K)
      REP=DASH*2.
      CALL DASHED(-1,REP,DASH,0.)
      GO TO 119
118   CALL DASHED(0,10.,10.,0.)
119   IF(N1.EQ.0)GO TO 120
      DO 201 I=1,5
      X1(I)=X1(I)/FACT
      Y1(I)=Y1(I)/FACT
201   CONTINUE
      CALL GRASYM(X1,Y1,N1,1,0)
      CALL GRAPOL(X1,Y1,N1)
120   IF(N2.EQ.0)GO TO 121
      DO 202 I=1,5
      X2(I)=X2(I)/FACT
      Y2(I)=Y2(I)/FACT
202   CONTINUE
      CALL GRASYM(X2,Y2,N2,2,0)
      CALL GRAPOL(X2,Y2,N2)
121   IF(N3.EQ.0)GO TO 122
      DO 203 I=1,5
      X3(I)=X3(I)/FACT
      Y3(I)=Y3(I)/FACT
203   CONTINUE
      CALL GRASYM(X3,Y3,N3,3,0)
      CALL GRAPOL(X3,Y3,N3)
122   IF(N4.EQ.0)GO TO 123
      DO 204 I=1,5
      X4(I)=X4(I)/FACT
      Y4(I)=Y4(I)/FACT
204   CONTINUE
      CALL GRASYM(X4,Y4,N4,4,0)
      CALL GRAPOL(X4,Y4,N4)
123   IF(N5.EQ.0)GO TO 124
      DO 205 I=1,5
      X5(I)=X5(I)/FACT
      Y5(I)=Y5(I)/FACT
205   CONTINUE
```

```
      CALL GRASYM(X5,Y5,N5,5,0)
      CALL GRAPOL(X5,Y5,N5)
124   IF(N6.EQ.0)GO TO 125
      DO 206 I=1,5
      X6(I)=X6(I)/FACT
      Y6(I)=Y6(I)/FACT
206   CONTINUE
      CALL GRASYM(X6,Y6,N6,6,0)
      CALL GRAPOL(X6,Y6,N6)
125   CONTINUE
      DDD=YL+65.+5.*K
      CALL MOVTO2(55.,DDD)
      CALL LINBY2(20.,0.)
      GO TO(131,132),KIND
131   CALL CHAHOL(' LAYER *.')
      CALL CHAINT(K,2)
      CALL CHAHOL('          ANGLE=   *.')
      CALL CHAFIX(THET,6,2)
      GO TO 133
132   CALL CHAHOL(' LAYER *.')
      CALL CHAINT(K,2)
      K1=K+1
      CALL CHAHOL(' AND *.')
      CALL CHAINT(K1,2)
      CALL CHAHOL(' ANGLE=+/-*.')
      CALL CHAFIX(THET,6,2)
133   RETURN
      END
C
      SUBROUTINE MAXIMUM(P,X,Y,S,K1,K2,K3)
C     ------------------------------------
      DIMENSION P(3,3)
      COMMON/BLOCK2/SX,SXY,SY1,SY2,SY3
      SY1=(-P(1,1)*SX-P(1,3)*SXY+X)/P(1,2)
      SY2=(-P(2,1)*SX-P(2,3)*SXY+Y)/P(2,2)
      SY3=(-P(3,1)*SX-P(3,3)*SXY+S)/P(3,2)
      WRITE(2,200)SX,SY1,K1,SX,SY2,K2,SX,SY3,K3
200   FORMAT(2(1PE10.2),2X,I2,2(1PE10.2),2X,I2,2(1PE10.2),3X,I2)
      RETURN
      END
C
      SUBROUTINE FAILURE(K,N,LK,KIND,THET)
C     ------------------------------------
      COMMON/BLOCK3/F(3),STR(3),WK(3),X7(50),Y7(50),F1(2),F2(2),
     *F6(2),F11(2),F22(2),F66(2),F12(2),XLT,YLT,SLT,XLC,YLC,SLC,YMAX/
     *BLOCK4/XT(2),XC(2),YT(2),YC(2),ST(2),SC(2),P(3,3)/
     *BLOCK6/SXMAX,SXMIN,SYMAX,SYMIN,IP,XL,YL,NX,NY,NN,CC,DD,FACT
      IF(IP.EQ.0)GO TO 16
      N7=0
      DO 200 I=1,50
      X7(I)=0.
```

```
      Y7(I)=0.
200   CONTINUE
      F(1)=4.*YMAX
      IF(N.EQ.4)F(1)=YLT
      F(2)=0.
      DF=F(1)/10.
400   IFAIL=0
      IF(N.EQ.4)GO TO 16
      CALL F01CKF(STR,P,F,3,1,3,WK,3,1,IFAIL)
16    CONTINUE
      IF(N.NE.4)GO TO 18
      DO 17 I=1,3
      STR(I)=F(I)
17    CONTINUE
18    IF(ABS(STR(1)).LT.1.E-10)STR(1)=1.E-10
      ALF=STR(2)/STR(1)
      BET=STR(3)/STR(1)
      GO TO (1,2,3,4)N
1     X=XT(LK)
      Y=YT(LK)
      SS=ST(LK)
      IF(STR(1).LT.0.0)X=XC(LK)
      IF(STR(2).LT.0.0)Y=YC(LK)
      IF(STR(3).LT.0.0)SS=SC(LK)
      S1F=AZZI(ALF,BET,X,Y,SS)
      IF(STR(1).LT.0.0)S1F=-S1F
      GO TO 10
2     CALL HOFFMAN(F11(LK),F22(LK),F66(LK),FF1,FF2,ALF,BET,STR(1),S1F)
      GO TO 10
3     CALL WU(F1(LK),F2(LK),F6(LK),F11(LK),F22(LK),F66(LK),F12(LK),
     *ALF,BET,STR(1),S1F)
      GO TO 10
4     X=XLT
      Y=YLT
      SS=SLT
      IF(STR(1).LT.0.0)X=XLC
      IF(STR(2).LT.0.0)Y=YLC
      IF(STR(3).LT.0.0)SS=SLC
      GAMA=3.*SS*SS/X/Y
      CALL PUPPO(ALF,BET,GAMA,H,G,X,Y,SS,S1F)
      IF(STR(1).LT.0.0)S1F=-S1F
10    S2F=S1F*ALF
      S3F=S1F*BET
      GAM=S1F/STR(1)
      SXF=GAM*F(1)
      SYF=GAM*F(2)
      SXYF=GAM*F(3)
      SX=F(1)
      SY=F(2)
      SXY=F(3)
```

```
      SXFF=SXF/FACT
      SYFF=SYF/FACT
      SXYFF=SXYF/FACT
      IF(N.EQ.4)GO TO 9
      F(1)=SXF
      F(2)=SYF
      F(3)=SXYF
      IFAIL=0
      CALL F01CKF(STR,P,F,3,1,3,WK,3,1,IFAIL)
      GO TO(6,7,8)N
6     FACTOR=HILL(STR(1),STR(2),STR(3),X,Y,SS)
      GO TO 11
7     FACTOR=HOFF(F11(LK),F22(LK),F66(LK),FF1,FF2,STR(1),STR(2),STR(3))
      GO TO 11
8     FACTOR=WUTSAI(F1(LK),F2(LK),F6(LK),F11(LK),F22(LK),F66(LK),
     *F12(LK),STR(1),STR(2),STR(3))
11    WRITE(2,100)FACTOR,STR,SXF,SYF,SXYF
      GO TO 12
9     CALL EVENSEN(GAMA,H,G,SXF,SYF,SXYF,X,Y,SS,FACTR1,FACTR2)
      WRITE(2,101)FACTR1,FACTR2,GAMA,SXF,SYF,SXYF
12    IF(IP.EQ.0)GO TO 103
      IF(SXFF.GT.SXMAX.OR.SXFF.LT.SXMIN.OR.SYFF.GT.SYMAX.OR.SYFF.LT.SYMI
     *N)GO TO 310
      N7=N7+1
      X7(N7)=SXF
      Y7(N7)=SYF
310   N77=0
      CALL LOAD RATIO(F,SX,SY,DF,N7,N77)
      IF(N77.EQ.1)GO TO 319
      GO TO 400
319   DO 320 I=1,N7
      X7(I)=X7(I)/FACT
      Y7(I)=Y7(I)/FACT
320   CONTINUE
      CALL GRASYM(X7,Y7,N7,K,0)
      IF(N.EQ.4)GO TO 103
      DDD=YL+50.+5.*K
      CALL MOVTO2(55.,DDD)
      CALL SYMBOL(K)
      GO TO(131,132),KIND
131   CALL CHAHOL(' LAYER *.')
      CALL CHAINT(K,2)
      CALL CHAHOL('          ANGLE=   *.')
      CALL CHAFIX(THET,6,2)
      GO TO 103
132   CALL CHAHOL(' LAYER *.')
      CALL CHAINT(K,2)
      K1=K+1
      CALL CHAHOL(' AND *.')
      CALL CHAINT(K1,2)
      CALL CHAHOL(' ANGLE=+/-*.')
      CALL CHAFIX(THET,6,2)
100   FORMAT(1X,F6.4,2X,6(1PE10.2))
```

```
101   FORMAT(1X,2(F6.4,2X),4(1PE10.2))
103   RETURN
      END
C
      SUBROUTINE LOAD RATIO(F,SX,SY,DF,N7,N77)
C     ----------------------------------------
      DIMENSION F(3)
      IF(N7.EQ.40)GO TO 307
      IF(SX)311,317,312
311   IF(SY)313,313,314
313   F(1)=SX+DF
      F(2)=SY-DF
      RETURN
314   F(1)=SX-DF
      F(2)=SY-DF
      RETURN
312   IF(SY)315,318,316
315   F(1)=SX+DF
      F(2)=SY+DF
      RETURN
316   F(1)=SX-DF
      F(2)=SY+DF
      RETURN
317   IF(SY)315,315,314
318   IF(N7-1)316,316,307
307   N77=1
      RETURN
      END
C
      FUNCTION HILL(S1,S2,S12,X,Y,S)
C     ------------------------------
      HILL=S1*(S1-S2)/X**2+(S2/Y)**2+(S12/S)**2
      RETURN
      END
C
      FUNCTION AZZI(ALF,BET,X,Y,S)
C     ----------------------------
      AZZI=(1.-ALF)/X**2+(ALF/Y)**2+(BET/S)**2
      IF(AZZI.LE.0.0)GO TO 1
      AZZI=1./(SQRT(AZZI))
      GO TO 3
1     WRITE(2,2)
2     FORMAT(5X,20HNO SQRT FOR NEGATIVE)
3     RETURN
      END
C
```

```
      SUBROUTINE HOFFMAN(F11,F22,F66,FF1,FF2,ALF,BET,STR,S1F)
C     ------------------------------------------------------
      A=F11*(1.-ALF)+F22*ALF**2+F66*BET**2
      B=FF1*F11+ALF*FF2*F22
      D=B*B+4.*A
      IF(D.LT.0.0)GO TO 3
      E=-B/2./A
      F=SQRT(D)/2./A
      IF(STR.LT.0.0)GO TO 1
      GO TO 2
1     S1F=E-F
      GO TO 5
2     S1F=E+F
      GO TO 5
3     WRITE(2,4)
4     FORMAT(5X,20HNO SQRT FOR NEGATIVE)
5     RETURN
      END
C
      FUNCTION HOFF(F11,F22,F66,FF1,FF2,S1,S2,S3)
C     -------------------------------------------
      HOFF=F11*S1*(S1-S2)+F22*S2**2+F66*S3**2+FF1*F11*S1+FF2*F22*S2
      RETURN
      END
C
      SUBROUTINE WU(F1,F2,F6,F11,F22,F66,F12,ALF,BET,STR,S1F)
C     ------------------------------------------------------
      A=F11+ALF**2*F22+2.*ALF*F12+BET**2*F66
      B=F1+ALF*F2+BET*F6
      D=B*B+4.*A
      IF(D.LT.0.0)GO TO 3
      E=-B/2./A
      F=SQRT(D)/2./A
      IF(STR.LT.0.0)GO TO 1
      GO TO 2
1     S1F=E-F
      GO TO 5
2     S1F=E+F
      GO TO 5
3     WRITE(2,4)
4     FORMAT(5X,20HNO SQRT FOR NEGATIVE)
5     RETURN
      END
C
      FUNCTION WUTSAI(F1,F2,F6,F11,F22,F66,F12,S1,S2,S3)
C     --------------------------------------------------
      WUTSAI=F1*S1+F2*S2+F6*S3+F11*S1**2+F22*S2**2+2.*F12*S1*S2
     **+F66*S3**2
      RETURN
      END
C
```

```
      SUBROUTINE PUPPO(ALF,BET,GAMA,H,G,X,Y,S,S1F)
C     ---------------------------------------------
      X2=X**2
      Y2=Y**2
      S2=S**2
      BET2=BET**2
      IF(GAMA.GT.1.0)GO TO 1
      S1F1=1./X2+GAMA*ALF*(ALF-1.)/Y2+BET2/S2
      IF(S1F1.LE.0.0)GO TO 2
      S1F1=1./SQRT(S1F1)
      S1F2=GAMA*(1.-ALF)/X2+ALF**2/Y2+BET2/S2
      IF(S1F2.LE.0.0)GO TO 2
      S1F2=1./SQRT(S1F2)
      S1F=S1F1
      IF(S1F2.LT.S1F1)S1F=S1F2
      GO TO 4
1     A=3./GAMA+4.
      F=1./10.*(-A+SQRT(A*A+240./GAMA))
      H=1.-0.5*F
      G=SQRT(GAMA/12.)*(3.*F/(F-4.)+1.)*F
      B=1./X2+ALF**2/Y2+BET2/S2-2.*H*ALF/X/Y
      C=2.*G*BET/S*(1./X+ALF/Y)
      S1F1=B-C
      IF(S1F1.LE.0.0)GO TO 2
      S1F1=1./SQRT(S1F1)
      S1F2=B+C
      IF(S1F2.LE.0.0)GO TO 2
      S1F2=1./SQRT(S1F2)
      S1F=S1F1
      IF(S1F2.LT.S1F1)S1F=S1F2
      GO TO 4
2     WRITE(2,3)
3     FORMAT(5X,20HNO SQRT FOR NEGATIVE)
4     RETURN
      END
C
      SUBROUTINE EVENSEN(GAMA,H,G,SX,SY,SXY,X,Y,S,FACTR1,FACTR2)
C     ----------------------------------------------------------
      IF(GAMA.GT.1.0)GO TO 1
      FACTR1=(SX/X)**2+GAMA*(-SX*SY/Y**2+(SY/Y)**2)+(SXY/S)**2
      FACTR2=GAMA*((SX/X)**2-SX*SY/X**2)+(SY/Y)**2+(SXY/S)**2
      GO TO 2
1     A=(SX/X)**2+(SY/Y)**2+(SXY/S)**2-2.*H*SX*SY/X/Y
      B=2.*G*(SXY/S)*(SX/X+SY/Y)
      FACTR1=A-B
      FACTR2=A+B
2     RETURN
      END
C
```

```
      SUBROUTINE AXES
C     ---------------
      COMMON/BLOCK6/SXMAX,SXMIN,SYMAX,SYMIN,IP,XL,YL,NX,NY,NN,CC,DD,FACT
      CALL AXIPOS(1,50.,50.,XL,1)
      CALL AXIPOS(1,50.,50.,YL,2)
      CALL AXISCA(3,NX,SXMIN,SXMAX,1)
      CALL AXISCA(3,NY,SYMIN,SYMAX,2)
      CALL GRID(-2,1,1)
      CALL MOVTO2(70.,40.)
      CALL CHAHOL('LAMINATE LOAD PER UNIT AREA IN X-DIRECTION, SX*.')
      CALL MOVTO2(30.,70.)
      CALL CHAANG(90.)
      CALL CHAHOL('LAMINATE LOAD PER UNIT AREA IN Y-DIRECTION, SY*.')
      CALL CHAANG(0.)
      CALL MOVTO2(70.,20.)
      GO TO (1,2,3,4,5,6,7)NN
1     CALL CHAHOL('MAXIMUM STRESS FAILURE ENVELOPE FOR*.')
      GO TO 11
2     CALL CHAHOL('MAXIMUM STRAIN FAILURE ENVELOPE FOR*.')
      GO TO 11
3     CALL CHAHOL('HILL-TSAI FAILURE ENVELOPE FOR*.')
      GO TO 10
4     CALL CHAHOL('HOFFMAN FAILURE ENVELOPE FOR*.')
      GO TO 10
5     CALL CHAHOL('TSAI-WU FAILURE ENVELOPE FOR*.')
      GO TO 10
6     CALL CHAHOL('PUPPO-EVENSEN FAILURE ENVELOPE FOR*.')
      GO TO 10
7     CALL CHAHOL('MODIFIED MAXIMUM STRAIN ENVELOPE FOR*.')
      GO TO 10
11    Y4=YL+65.
      Y5=YL+60.
      Y6=YL+55.
      CALL MOVTO2(55.,Y4)
      CALL SYMBOL(1)
      CALL CHAHOL('  LONGITUDINAL TENSION      *.')
      CALL SYMBOL(4)
      CALL CHAHOL('  LONGITUDINAL COMPRESSION*.')
      CALL MOVTO2(55.,Y5)
      CALL SYMBOL(2)
      CALL CHAHOL('  TRANSVERSE TENSION        *.')
      CALL SYMBOL(5)
      CALL CHAHOL('  TRANSVERSE COMPRESSION*.')
      CALL MOVTO2(55.,Y6)
      CALL SYMBOL(3)
      CALL CHAHOL('  POSITIVE SHEAR            *.')
      CALL SYMBOL(6)
      CALL CHAHOL('  NEGATIVE SHEAR*.')
10    RETURN
      END
C
```

```
      SUBROUTINE NONLINEAR(NC7,XO,YO,XM,P,C)
C     ---------------------------------------
      DIMENSION X(30),Y(30),W(30),P(10),WK(30),WRK(4,10),C(10)
      READ(1,1)NP,NC
      READ(1,2)(X(I),I=1,NP)
      READ(1,2)(Y(I),I=1,NP)
      NC3=NC+3
      NC7=NC+7
      IF(NC.EQ.1)GO TO 10
      READ(1,2)(P(I),I=5,NC3)
10    CONTINUE
      XO=X(1)
      YO=Y(1)
      XM=X(NP)
      DO 11 I=1,NP
      X(I)=X(I)-XO
      Y(I)=Y(I)-YO
      W(I)=1.
11    CONTINUE
      IFAIL=0
      CALL E02BAF(NP,NC7,X,Y,W,P,WK,WRK,C,SS,IFAIL)
1     FORMAT(2I0)
2     FORMAT(10F0.0)
      RETURN
      END
C
      SUBROUTINE MAXIMUM VALUE(N,STR)
C     -------------------------------
      COMMON/BLOCK7/SPC(3,10)
      DIMENSION  STR(3)
      DO 1 I=1,3
      STR(I)=0.
-------------------------------------------------------------------------
1     CONTINUE
      DO 3 I=1,3
      DO 2 J=1,N
      F=ABS(SPC(I,J))-ABS(STR(I))
      IF(F)4,4,5
5     STR(I)=SPC(I,J)
4     CONTINUE
2     CONTINUE
3     CONTINUE
      RETURN
      END
C
      FINISH
```

C.6 SAMPLE INPUT

```
1  2  0  0  0  0  0  0  0  0  39.626E-3   .0001
1  1  1  1  1  1
1  .7264E-3   70.   5   2
1  .7264E-3  -70.   5   2
 GLASS/EPOXY          41.88E9  13.088E9  5.344E9  .1774
1232.E6  748.E6  28.5E6  101.E6  47.E6
2.94E-2  1.79E-2  .275E-2  1.5E-2  4.04E-2
0.
  33.36E6  111.2E6  835.E6  510.E6  135.E6  135.E6
100.E6 -50.E6 0.  20.E6  -10.E6  0.
```

C.7 SAMPLE OUTPUT

```
     LINEAR ANALYSIS:
     ================
     LAMINATE PROPERTIES:
 EX=  1.28E 10  EY=  3.37E 10  NUXY= 0.150  NUYX= 0.397  GXY=  8.39E 09


     LAMINATE STRESSES:  1.0000E 07 -5.0000E 06  0.0000E 00
     LAMINATE STRAINS :  8.4202E-04 -2.6597E-04 -4.8244E-07

     LAYER NO.  1
     ............
 STRESS -4.26E 06  9.11E 06  3.82E 06STRAIN -1.40E-04  7.14E-04  7.15E-04

     LAYER NO.  2
     ............
 STRESS -4.23E 06  9.11E 06 -3.82E 06STRAIN -1.40E-04  7.14E-04 -7.14E-04

     STRENGTH CALCULATIONS:
     ======================


  FAILURE BY MAXIMUM STRESS CRITERION:
  ------------------------------------

     LAYER NO.  1
     ............
 LAYER FAILS AT LOAD:  3.13E 07 -1.56E 07  0.00E 00  AS S22  REACHES MAX.

     LAYER NO.  2
     ............
 LAYER  2 IS SIMILAR TO LAYER  1 (ANGLE PLY)
```

```
 FAILURE BY MAXIMUM STRAIN CRITERION:
 ------------------------------------

    LAYER NO.  1
    ............
LAYER FAILS AT LOAD:  3.85E 07 -1.93E 07  0.00E 00  AS E22  REACHES MAX.

    LAYER NO.  2
    ............
LAYER  2 IS SIMILAR TO LAYER  1 (ANGLE PLY)


FAILURE BY HILL-TSAI-AZZI CRITERION:
------------------------------------

    LAYER NO.  1
    ............
FACTOR    *******LAYER STRESSES*******  ********EXTERNAL LOAD********
1.0003   -1.19E 07  2.76E 07 -1.15E 07  3.03E 07 -1.52E 07  0.00E 00

    LAYER NO.  2
    ............
LAYER  2 IS SIMILAR TO LAYER  1 (ANGLE PLY)


FAILURE BY HOFFMAN CRITERION:
-----------------------------

    LAYER NO.  1
    ............
FACTOR    *******LAYER STRESSES*******  ********EXTERNAL LOAD********
0.9978   -2.09E 07  4.84E 07 -2.01E 07  5.31E 07 -2.65E 07  0.00E 00

    LAYER NO.  2
    ............
LAYER  2 IS SIMILAR TO LAYER  1 (ANGLE PLY)


FAILURE BY TSAI-WU CRITERION, WITH F12=  0.00E 00 :
---------------------------------------

    LAYER NO.  1
    ............
FACTOR    *******LAYER STRESSES*******  ********EXTERNAL LOAD********
0.9994   -1.17E 07  2.71E 07 -1.12E 07  2.97E 07 -1.48E 07  0.00E 00

    LAYER NO.  2
    ............
LAYER  2 IS SIMILAR TO LAYER  1 (ANGLE PLY)


FAILURE BY PUPPO-EVENSEN CRITERION:
-----------------------------------
FACTOR1 FACTOR2     GAMA     ******EXTERNAL LOADS********
1.0000  0.5783    5.89E-01  1.64E 08 -8.20E 07  0.00E 00
```

APPENDIX D

DESIGN OF TEST SPECIMENS

D.1 INTRODUCTION

In this appendix the computer program which was developed to design the test specimens is described. The mathematical foundations for the program are those of Sec. 2.4 where the analysis of laminated composite cylinders of finite length is presented. Some equations in Sec. 2.4 are given there without details. Therefore, before describing the computer program, some mathematical details will be given here using same notation.

D.2 MATHEMATICAL DETAILS OF SEC. 2.4

The general solution for the displacement w^o is, from equations (2.4.25), (2.4.26) and (2.4.35) :

$$w^o = e^{\alpha x}(C_1 \cos \beta x + C_2 \sin \beta x) + e^{-\alpha x} (C_3 \cos \beta x + C_4 \sin \beta x) + P + r K_1 + s K_2 \qquad (D.2.1)$$

From this equation the derivitives $w^o_{,x}$, $w^o_{,xx}$ and $w^o_{,xxx}$ are :

$$w^o_{,x} = e^{\alpha x} \left[(\alpha C_1 + \beta C_2) \cos \beta x + (\alpha C_2 - \beta C_1) \sin \beta x \right] + e^{-\alpha x} \left[(-\alpha C_3 + \beta C_4) \cos \beta x - (\alpha C_4 + \beta C_3) \sin \beta x\right] \qquad (D.2.2)$$

$$w^{o}_{,xx} = e^{\alpha x}\left[\{\alpha(\alpha C_1 + \beta C_2) + \beta(\alpha C_2 - \beta C_1)\}\cos\beta x + \{\alpha(\alpha C_2 - \beta C_1) - \beta(\alpha C_1 + \beta C_2)\}\sin\beta x\right] + e^{-\alpha x}\left[-\{\alpha(-\alpha C_3 + \beta C_4) + \beta(\alpha C_4 + \beta C_3)\}\cos\beta x + \{\alpha(\alpha C_4 + \beta C_3) - \beta(-\alpha C_3 + \beta C_4)\sin\beta x\right] \qquad (D.2.3)$$

$$w^{o}_{,xxx} = e^{\alpha x}\left[\{\alpha^2(\alpha C_1 + \beta C_2) + 2\alpha\beta(\alpha C_2 - \beta C_1) - \beta^2(\alpha C_1 + \beta C_2)\}\cos\beta x + \{\alpha^2(\alpha C_2 - \beta C_1) - 2\alpha\beta(\alpha C_1 + \beta C_2) - \beta^2(\alpha C_2 - \beta C_1)\}\sin\beta x\right] + e^{-\alpha x}\left[\{\alpha^2(-\alpha C_3 + \beta C_4) + 2\alpha\beta(\alpha C_4 + \beta C_3) - \beta^2(-\alpha C_3 + \beta C_4)\}\cos\beta x + \{-\alpha^2(\alpha C_4 + \beta C_3) + 2\alpha\beta(-\alpha C_3 + \beta C_4) + \beta^2(\alpha C_4 + \beta C_3)\}\sin\beta x\right] \qquad (D.2.4)$$

From equation (D.2.1)

$$\int w^{o}dx = \frac{1}{\alpha^2 + \beta^2}\left[e^{\alpha x}\{(\alpha C_1 - \beta C_2)\cos\beta x + (\beta C_1 + \alpha C_2)\sin\beta x\} + e^{-\alpha x}\{-(\alpha C_3 + \beta C_4)\cos\beta x + (\beta C_3 - \alpha C_4)\sin\beta x\}\right] + P\,x + r\,K_1\,x + s\,K_2\,x \qquad (D.2.5)$$

Then, from equation (2.4.21) :

$$u^o = \frac{(ae + b)}{\alpha^2 + \beta^2}\left[e^{\alpha x}\{(\alpha C_1 - \beta C_2)\cos \beta x + (\beta C_1 + \alpha C_2)\sin \beta x\} + e^{-\alpha x}\{-(\alpha C_3 + \beta C_4)\cos \beta x + (\beta C_3 - \alpha C_4)\sin \beta x\}\right] +$$

$$(af + d)\left[e^{\alpha x}\{(\alpha C_1 + \beta C_2)\cos \beta x + (\alpha C_2 - \beta C_1)\sin \beta x\} + e^{-\alpha x}\{(-\alpha C_3 + \beta C_4)\ \text{cos}\ \beta x - (\alpha C_4 + \beta C_3)\sin \beta x\}\right] +$$

$$(ae + b)Px + (ae + b)r + 1\ K_1 x + (ae + b)s\ K_2 x + K_3$$

(D.2.6)

and from equation (2.4.22) :

$$v^o = \frac{e}{\alpha^2 + \beta^2}\left[e^{\alpha x}\{(\alpha C_1 - \beta C_2)\cos \beta x + (\beta C_1 + \alpha C_2)\sin \beta x\} + e^{-\alpha x}\{-(\alpha C_3 + \beta C_4)\cos \beta x + (\beta C_3 - \alpha C_4)\sin \beta x\}\right] +$$

$$f\left[e^{\alpha x}\{(\alpha C_1 + \beta C_2)\cos \beta x + (\alpha C_2 - \beta C_1)\sin \beta x\} + e^{-\alpha x}\{(-\alpha C_3 + \beta C_4)\cos \beta x - (\alpha C_4 + \beta C_3)\sin \beta x\}\right] +$$

$$e\ P\ x + e\ r\ K_1\ x + (e\ s + 1)\ K_2\ x + K_4$$

(D.2.7)

From equations (2.4.2), (2.4.3) and (2.4.7) :

$$M_x = B_{11}\ u^o_{,x} + (B_{13} + \frac{1}{R}\ D_{13})\ v^o_{,x} + (\frac{1}{R}\ B_{12} - \frac{1}{R^2}\ D_{12})\ w^o - D_{11}\ w^o_{,xx}$$

(D.2.8)

when $u^{o}_{,x}$ and $v^{o}_{,x}$ are substituted from equations (2.4.21) and (2.4.22) the following equation is obtained :

$$M_x = t\, w^{o} + t'\, w^{o}_{,xx} + B_{11}\, K_1 + (B_{13} + \frac{1}{R} D_{13})\, K_2 \qquad (D.2.9)$$

then from equations (D.2.1) and (D.2.3) :

$$\begin{aligned} M_x = {} & t\left[e^{\alpha x}\,(C_1 \cos \beta x + C_2 \sin \beta x) + e^{-\alpha x}(C_3 \cos \beta x + C_4 \sin \beta x)\right] + \\ & t' e^{\alpha x}\left[\{\alpha(\alpha C_1 + \beta C_2) + \beta(\alpha C_2 - \beta C_1)\} \cos \beta x + \right. \\ & \left. \{\alpha(\alpha C_2 + \beta C_1) - \beta(\alpha C_1 + \beta C_2)\ \sin \beta x\right] + \\ & t' e^{-\alpha x}\left[-\{\alpha(-\alpha C_3 + \beta C_4) + \beta(\alpha C_4 + \beta C_3)\} \cos \beta x + \right. \\ & \left. \{\alpha(\alpha C_4 + \beta C_3) - \beta(-\alpha C_3 + \beta C_4)\} \sin \beta x\right] + \\ & tP + (tr + B_{11})\, K_1 + (ts + B_{13} + \frac{1}{R} D_{13})\, K_2 \end{aligned} \qquad (D.2.10)$$

Since $Q_x = M_{x,x}$, then :

$$Q_x = t\, w^{o}_{,x} + t'\, w^{o}_{,xxx} \qquad (D.2.11)$$

or, from equations (D.2.2) and (D.2.4) :

$$Q_x = t\left[e^{\alpha x}\{(\alpha C_1 + \beta C_2)\cos\beta x + (\alpha C_2 - \beta C_1)\sin\beta x\} + e^{-\alpha x}\{(-\alpha C_3 + \beta C_4)\cos\beta x - (\alpha C_4 + \beta C_3)\sin\beta x\}\right] +$$

$$t' e^{\alpha x}\left[\{\alpha^2(\alpha C_1 + \beta C_2) + 2\alpha\beta(\alpha C_2 - \beta C_1) - \beta^2(\alpha C_1 + \beta C_2)\}\cos\beta x + \{\alpha^2(\alpha C_2 - \beta C_1) - 2\alpha\beta(\alpha C_1 + \beta C_2) - \beta^2(\alpha C_2 - \beta C_1)\}\sin\beta x\right] +$$

$$t' e^{-\alpha x}\left[\{\alpha^2(-\alpha C_3 + \beta C_4) + 2\alpha\beta(\alpha C_4 + \beta C_3) - \beta^2(-\alpha C_3 + \beta C_4)\}\cos\beta x + \{-\alpha^2(\alpha C_4 + \beta C_3) + 2\alpha\beta(-\alpha C_3 + \beta C_4) + \beta^2(\alpha C_4 + \beta C_3)\}\sin\beta x\right]$$

(D.2.12)

For N_x the following equation is obtained in a similar way equation (D.2.3) was obtained :

$$N_x = A_{11}\, u^o_{,x} + (A_{13} + \frac{1}{R} B_{13})\, v^o_{,x} + (\frac{1}{R} A_{12} - \frac{1}{R^2} B_{12})\, w^o - B_{11}\, w^o_{,xx}$$

(D.2.13)

or :

$$N_x = \left[A_{11}(ae + b) + e(A_{13} + \frac{1}{R} B_{13}) + (\frac{1}{R} A_{12} - \frac{1}{R^2} B_{12})\right] w^o + \left[A_{11}(af + d) + f(A_{13} + \frac{1}{R} B_{13}) - B_{11}\right] w^o_{,xx} + A_{11} K_1 + (A_{13} + \frac{1}{R} B_{13}) K_2 \qquad \text{(D.2.14)}$$

when a, b, e, d and f are substituted from equations (2.4.17) and (2.4.19) the following equation obtained :

$$N_x = A_{11} K_1 + (A_{13} + \frac{1}{R} B_{13}) K_2 \qquad (D.2.15)$$

Similarly :

$$N_{xy} + \frac{1}{R} M_{xy} = (A_{31} + \frac{1}{R} B_{31})K_1 + (A_{33} + \frac{2}{R} B_{33} + \frac{1}{R^2} D_{33}) \qquad (D.2.16)$$

When the above equations are rearranged equations (2.4.47) to (2.4.54) are obtained.

The matrix equation (2.4.45) takes then the shape shown in Fig. (D.2.1).

D.3 THE COMPUTER PROGRAM

The computer program has been written in FORTRAN programming language and consists of a master segmant and five subroutines. The master segmant controls the subroutines while all the calculations are done by the subroutines which are :

a) Subroutine LAMINATION: this subroutine deals with the lamination theory to obtain the matrices A, B and D, and then calculates some parameters which are derived from these matrices.

b) Subroutine TRANSFORMATION: this subroutine finds the transformation matrices which transform the properties of the composite material from the principal axes to the loading axes.

c) Subroutine COEFFICIENTS: this subroutine sets up the matrix equation (2.4.45) and then finds the solution (2.4.46).

d) Subroutine DEFLECTIONS: this finds the displacements u^o, v^o and w^o.

e) Subroutine FUNCTIONS: this calculates the distribution of bending moments, shearing forces, stresses and strains along the specimen.

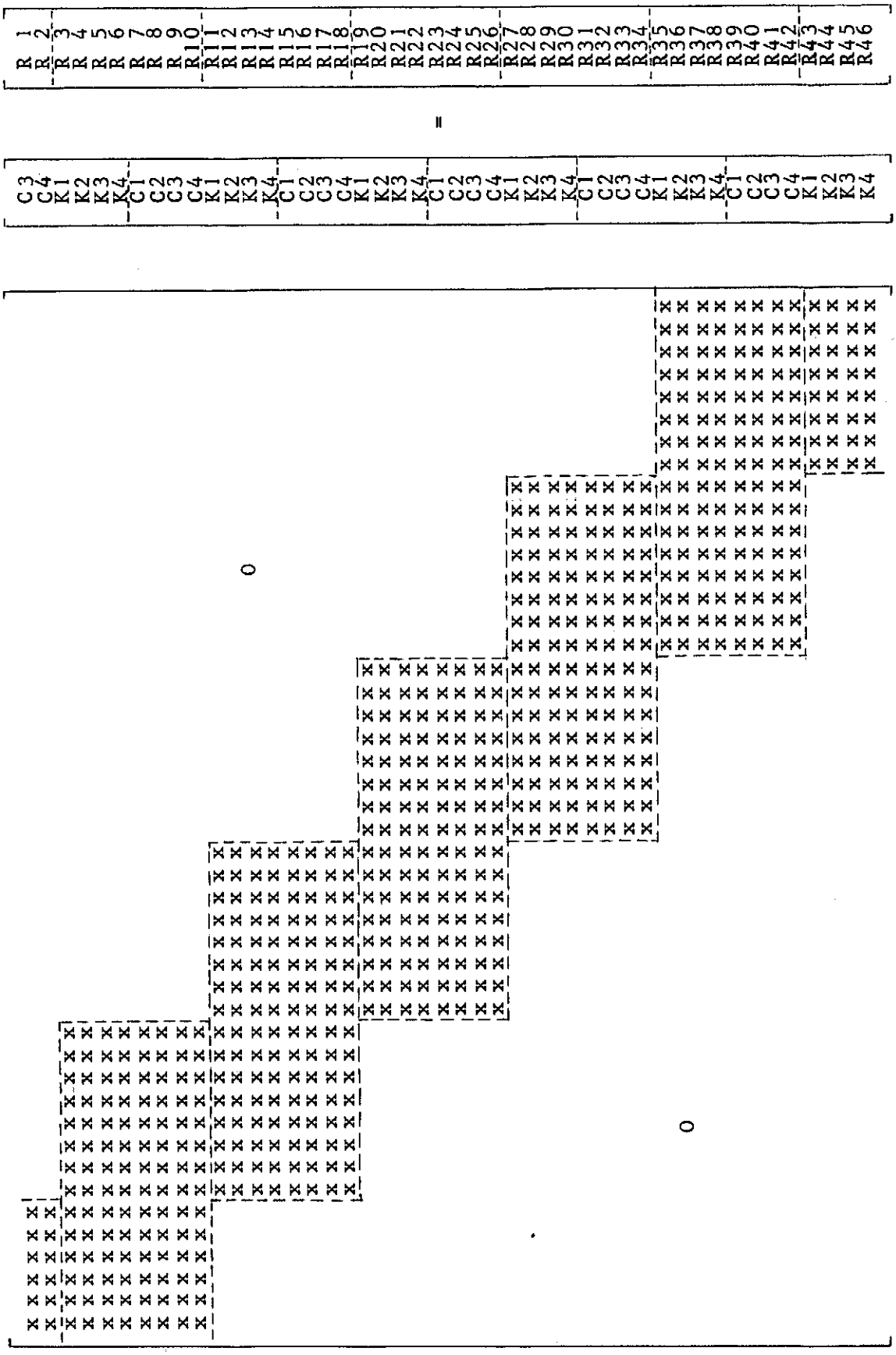

Fig.(D.2.1) The matrix equation (2.4.45) for a tube devided into six finite elements

f) Supporting subroutines: the following standard subroutines are used in the program :

FMOVE: shifts a matrix into another matrix.

F01AAF: finds the inverse of a matrix.

F01CKF: finds the multiplication of two matrices.

F04AEF: finds the solution of a matrix equation.

D.4 THE PROGRAM LISTING:

```
      LIBRARY(SUBGROUPNAGF)
      PROGRAM(STIF)
      COMPRESS INTEGER AND LOGICAL
      INPUT 1=CR0
      OUTPUT 2=LP0
      END
C
      MASTER CYLINDRICAL SHELL ANALYSIS
C     ---------------------------------
      COMMON/BLOCK3/EL(3),ET(3),PLT(3),GLT(3)
     */BLOCK2/NE,R,AL(6),NF(6),AA(3,3,6),BB(3,3,6),DD(3,3,6),F2(6),
     *F1(6),AEB(6),AFD(6),R1(6),S4(6),S3(6),T3(6),AF(6),
     *BT(6),ABM(6),ABP(6),AB(6),A3B(6),B3A(6),P(6),ANX,ANXY,ICOND
     */BLOCK4/A(3,3),B(3,3),D(3,3),WK(3)
     */BLOCK5/QKIN(3,3),QKOT(3,3),HB,IFUN,ISTRN,ISTRS,IFUN2
     *,QKR(3,3,6),ZR(6),NR(6)
      DIMENSION C(46,46),CFI(46,46),RHS(46,1),COF(46),WRK(46),CFT(46,46)
     *,ENDS(6,5)
C
C     FORMATS:
C     --------
1     FORMAT(2I0,4F0.0,6I0)
2     FORMAT(4F0.0)
9     FORMAT(1X,4(1PE12.4))
10    FORMAT(' ANALYSIS OF COMPOSITE CYLINDER WITH R= ',
     *F7.3,' DIVIDED INTO ',I2,' ELEMENTS'/' LOADED BY: P=',1PE9.2,
     *', NX=',1PE9.2,', NXY=',1PE9.2,',WITH END CONDITIONS:')
12    FORMAT(//5X,'X',9X,'W',9X,'NY',8X,'MX',8X,'MY',8X,'MXY',7X,'QX')
13    FORMAT(5X,'X',6X,'---OUTER SURFACE STRAINS----',2X,
     *'---INNER SURFACE STRAINS----')
14    FORMAT(5X,'X',6X,'---OUTER SURFACE STRESSES---',2X,
     *'---INNER SURFACE STRESSES---')
15    FORMAT(5X,'X',6X,'---MIDDLE SURFACE STRAIN---',2X,
     *'----CHANGES OF CURVATURE----')
16    FORMAT(10A8)
11    FORMAT(/' ELEMENT',I2/' ---------')
C
      READ(1,1)NM,NE,R,PR,ANX,ANXY,NP,ICOND,IFUN,ISTRN,ISTRS,IFUN2
      READ(1,2)(EL(I),ET(I),GLT(I),PLT(I),I=1,NM)
      DATA ENDS(1,1)/'  FREE ENDS                                    '/
      DATA ENDS(1,2)/'  CLAMPED ENDS-NO DISPLACEMENTS                '/
      DATA ENDS(1,3)/'  CLAMPED ENDS-AXIAL DISPLACEMENTS ONLY        '/
      DATA ENDS(1,4)/'  CLAMPED ENDS-HOOP DISPLACEMENTS ONLY         '/
      DATA ENDS(1,5)/'  CLAMPED ENDS-AXIAL AND HOOP DISPLACEMENTS    '/
      DO 5 K=1,NP
      P(K)=PR
5     CONTINUE
      CALL LAMINATION
      L=8*NE-2
```

```
      CALL COEFFICIENTS(L,C,CFI,RHS,COF,WRK,CFT)
      WRITE(2,10)R,NE,PR,ANX,ANXY
      WRITE(2,16)(ENDS(I,ICOND),I=1,6)
      IF(IFUN.EQ.1)WRITE(2,12)
      IF(IFUN2.EQ.1)WRITE(2,15)
      IF(ISTRN.EQ.1)WRITE(2,13)
      IF(ISTRS.EQ.1)WRITE(2,14)
      ALL=0.
      DO 20 N=1,NE
      M=NE+1-N
      K=L-8*(N-1)
      WRITE(2,11)M
      J=0
      X=0.
      DX=AL(N)/NF(N)
24    XO=X+ALL
      IF(N.EQ.1)GO TO 21
      GO TO 22
21    CALL DEFLECTIONS(N,0.,0.,COF(K-5),COF(K-4),COF(K-3),COF(K-2),
     *COF(K-1),COF(K),X,XO)
      GO TO 23
22    CALL DEFLECTIONS(N,COF(K-7),COF(K-6),COF(K-5),COF(K-4),COF(K-3)
     *,COF(K-2),COF(K-1),COF(K),X,XO)
23    J=J+1
      IF(J-NF(N))25,25,26
25    X=X+DX
      GO TO 24
26    CONTINUE
      ALL=ALL+AL(N)
20    CONTINUE
      STOP OK
      END
C
      SUBROUTINE LAMINATION
C     ---------------------
      COMMON/BLOCK1/T(3,3),TT(6,4)/BLOCK3/EL(3),ET(3),PLT(3),GLT(3)
     */BLOCK2/NE,R,AL(6),NF(6),AA(3,3,6),BB(3,3,6),DD(3,3,6),F2(6),
     *F1(6),AEB(6),AFD(6),R1(6),S4(6),S3(6),T3(6),AF(6),
     *BT(6),ABN(6),ABP(6),AB(6),A3B(6),B3A(6),P(6),ANX,ANXY,ICOND
     */BLOCK4/A(3,3),B(3,3),D(3,3),WK(3)
     */BLOCK5/QKIN(3,3),QKOT(3,3),HB,IFUN,ISTRN,ISTRS,IFUN2
     *,QKR(3,3,6),ZR(6),NR(6)
      DIMENSION C(4,1),CK(3,3,8),SK(3,3,8),L(8),TL(8),THETA(8),
     *THET(8),TK(3,3,8),TTC(6,1),QK(3,3,8),Z(21),Z2(21),Z1(20),
     *Z3(21),HS(20),HC(20),TI(3,3),NS(8),KIND(8)
      HB=0.
      DO 20 N=1,NE
      NR(N)=0
      READ(1,1)NL,AL(N),NF(N)
1     FORMAT(I0,F0.0,I0)
      READ(1,3)(L(K),TL(K),THET(K),NS(K),KIND(K),K=1,NL)
```

```
3     FORMAT(I0,2F0.0,2I0)
      PI=4.*ATAN(1.)
      IF(N.EQ.1)LAYER=NL
      DO 12 K=1,NL
      THETA(K)=PI*THET(K)/180.
      LK=L(K)
      SK(1,1,K)=1./EL(LK)
      SK(2,2,K)=1./ET(LK)
      SK(3,3,K)=1./GLT(LK)
      SK(1,2,K),SK(2,1,K)=-PLT(LK)/EL(LK)
      CALL FMOVE(SK(1,1,K),T,9)
      IFAIL=0
      CALL F01AAF(T,3,3,TI,3,WK,IFAIL)
      CALL FMOVE(TI,CK(1,1,K),9)
      C(1,1)=CK(1,1,K)
      C(2,1)=CK(1,2,K)
      C(3,1)=CK(2,2,K)
      C(4,1)=CK(3,3,K)
      AM=COS(THETA(K))
      AN=SIN(THETA(K))
      CALL TRANSFORMATION(AM,AN)
      CALL FMOVE(T,TK(1,1,K),9)
      IFAIL=0
      CALL F01CKF(TTC,TT,C,6,1,4,WK,3,1,IFAIL)
      QK(1,1,K)=TTC(1,1)
      QK(1,2,K),QK(2,1,K)=TTC(2,1)
      QK(1,3,K),QK(3,1,K)=TTC(3,1)
      QK(2,2,K)=TTC(4,1)
      QK(2,3,K),QK(3,2,K)=TTC(5,1)
      QK(3,3,K)=TTC(6,1)
12    CONTINUE
      IF(N.NE.1)GO TO 5
      DO 99 I=1,3
      DO 99 J=1,3
      QKIN(I,J)=QK(I,J,1)
      QKOT(I,J)=QK(I,J,NL)
99    CONTINUE
      DO 2 K=1,NL
      HB=HB+TL(K)
2     CONTINUE
      HB=HB/2.
      Z(1)=-HB
      Z2(1)=Z(1)**2
      Z3(1)=Z(1)**3
5     CONTINUE
      IF(LAYER.EQ.NL)GO TO 6
      NR(N)=1
      DO 7 I=1,3
      DO 7 J=1,3
      QKR(I,J,N)=QK(I,J,NL)
7     CONTINUE
```

```
6     CONTINUE
      KK=2
      DO 15 K=1,NL
      MM=KK+NS(K)-1
      TLL=TL(K)/NS(K)
      DO 46 M=KK,MM
      Z(M)=Z(M-1)+TLL
      Z2(M)=Z(M)**2
      Z3(M)=Z(M)**3
46    CONTINUE
      KK=KK+NS(K)
15    CONTINUE
      DO 16 K=1,MM-1
      Z1(K)=(Z(K+1)+Z(K))/2.
      HS(K)=Z2(K+1)-Z2(K)
      HC(K)=Z3(K+1)-Z3(K)
16    CONTINUE
      ZR(N)=Z1(K)
      DO 18 I=1,3
      DO 18 J=1,3
      NN=0
      MM=0
      LL=0
      A(I,J)=0.
      B(I,J)=0.
      D(I,J)=0.
      DO 19 K=1,NL
      A(I,J)=A(I,J)+QK(I,J,K)*TL(K)
      KKK=KIND(K)
      GO TO(121,122),KKK
121   NN=MM+1
      MM=NN
      GO TO 123
122   IF(LL.EQ.2)GO TO 126
      LL=LL+1
      NN=NN+1
      GO TO 127
126   LL=1
      NN=MM+1
127   MM=NN+2*NS(K)-2
123   DO 124 M=NN,MM,2
      B(I,J)=B(I,J)+QK(I,J,K)*HS(M)
      D(I,J)=B(I,J)+QK(I,J,K)*HC(M)
124   CONTINUE
19    CONTINUE
      B(I,J)=B(I,J)/2.
      D(I,J)=D(I,J)/3.
18    CONTINUE
      CALL FMOVE(A,AA(1,1,N),9)
      CALL FMOVE(B,BB(1,1,N),9)
      CALL FMOVE(D,DD(1,1,N),9)
```

```
      R2=R*R
      R3=R2*R
      A1=-(A(1,3)+B(1,3)/R)/A(1,1)
      B1=-(A(1,2)/R-B(1,2)/R2)/A(1,1)
      D1=B(1,1)/A(1,1)
      CONS=A(3,3)+2.*B(3,3)/R+B(3,3)/R2-(A(3,1)+B(3,1)/R)*
     ;       (A(1,3)+B(1,3)/R)/A(1,1)
      F2(N)=-(A(3,2)/R-B(3,2)/R3-(A(3,1)+B(3,1)/R)*(A(1,2)/R-
     ;       B(1,2)/R2)/A(1,1))/CONS
      F1(N)=-(B(1,1)*(A(3,1)+B(3,1)/R)/A(1,1)-(B(3,1)+D(3,1)/R))/CONS
      AEB(N)=A1*F2(N)+B1
      AFB(N)=A1*F1(N)+D1
      G1=D(1,1)-B(1,1)*AFB(N)-F1(N)*(B(1,3)+B(1,3)/R)
      H1=A(2,1)*AFB(N)/R+F1(N)*(A(2,3)/R+B(2,3)/R2)-F2(N)*(B(1,3)+
     ;    D(1,3)/R)-B(1,1)*AEB(N)-(B(1,2)/R+B(2,1)/R-D(1,2)/R2)
      Q1=A(2,1)*AEB(N)/R+F2(N)*(A(2,3)/R+B(2,3)/R2)+(A(2,2)/R2-B(2,2)/
     ;    R3)
      R1(N)=-A(2,1)/R/Q1
      S4(N)=(B(2,3)/R2+A(2,3)/R)/Q1
      G3(N)=B(1,1)*AEB(N)+F2(N)*(B(1,3)+D(1,3)/R)+(B(1,2)/R-D(1,2)/R2)
      T3(N)=B(1,1)*AFB(N)+F1(N)*(B(1,3)+D(1,3)/R)-D(1,1)
      GAMA=-H1/(2.*G1)
      ALAMDA=SQRT(ABS(H1**2-4.*G1*Q1))/(2.*G1)
      ZGL=SQRT(GAMA**2+ALAMDA**2)
      ZAB=SQRT(ZGL)
      TGL=ATAN2(ALAMDA,GAMA)
      TAB=TGL/2.
      AF(N)=ZAB*COS(TAB)
      BT(N)=ZAB*SIN(TAB)
      ABM(N)=AF(N)**2-BT(N)**2
      ABP(N)=AF(N)**2+BT(N)**2
      AB(N)=2.*AF(N)*BT(N)
      A3B(N)=AF(N)**3-3.*AF(N)*BT(N)**2
      B3A(N)=BT(N)**3-3.*AF(N)**2*BT(N)
      P(N)=P(N)/Q1
20    CONTINUE
      RETURN
      END
C
      SUBROUTINE TRANSFORMATION(AM,AN)
C     --------------------------------
      COMMON/BLOCK1/T(3,3),TT(6,4)
      DO 1 I=1,3
      DO 1 J=1,3
1     T(I,J)=0.
      DO 2 I=1,6
      DO 2 J=1,4
2     TT(I,J)=0.
      AM2=AM**2
      AN2=AN**2
      AM3=AM**3
```

```
      AN3=AN**3
      AN4=AN2**2
      AN4=AN2**2
      AMAN=AM*AN
      AMAN2=2.*AMAN
      AM2AN2=AM2*AN2
      AMAN22=AM2-AN2
      T(1,1),T(2,2)=AM2
      T(1,2),T(2,1)=AN2
      T(1,3)=-AMAN2
      T(2,3)=AMAN2
      T(3,1)=AMAN
      T(3,2)=-AMAN
      T(3,3)=AMAN22
      TT(1,1),TT(4,3)=AN4
      TT(1,2),TT(4,2)=2.*AM2AN2
      TT(1,3),TT(4,1)=AN4
      TT(1,4),TT(4,4)=4.*AM2AN2
      TT(2,1),TT(2,3),TT(6,1),TT(6,3)=AM2AN2
      TT(2,2)=AN4+AN4
      TT(2,4)=-TT(1,4)
      TT(3,1)=-AM3*AN
      TT(3,2)=AMAN*AMAN22
      TT(3,3)=AM*AN3
      TT(3,4)=2.*TT(3,2)
      TT(5,1)=-TT(3,3)
      TT(5,2)=-TT(3,2)
      TT(5,3)=-TT(3,1)
      TT(5,4)=-TT(3,4)
      TT(6,2)=-TT(1,2)
      TT(6,4)=AMAN22**2
      RETURN
      END
C
      SUBROUTINE COEFFICIENTS(L,C,CFI,RHS,COF,WRK,CFT)
C     ------------------------------------------------
      COMMON/BLOCK2/NE,R,AL(6),NF(6),AA(3,3,6),BB(3,3,6),DD(3,3,6),
     *F2(6),F1(6),AEB(6),AFD(6),R1(6),S4(6),S3(6),T3(6),AF(6),
     *BT(6),ABN(6),ABP(6),AB(6),A3B(6),B3A(6),P(6),ANX,ANXY,ICOND
      DIMENSION C(L,L),CFI(L,L),RHS(L,1),COF(L,1),WRK(L),CFT(L,L)
      DO 1 I=1,L
      DO 1 J=1,L
1     C(I,J)=0.
      DO 2 N=1,NE
      IF(N.EQ.NE)GO TO 5
      BL=BT(N+1)*AL(N+1)
      FL=AF(N+1)*AL(N+1)
      CS=COS(BL)
      SN=SIN(BL)
      XP=EXP(FL)
      XN=EXP(-FL)
```

```
      E1=AF(N+1)*CS-BT(N+1)*SN
      E2=BT(N+1)*CS+AF(N+1)*SN
      E3=AF(N+1)*CS+BT(N+1)*SN
      E4=BT(N+1)*CS-AF(N+1)*SN
      E5=ABN(N+1)*CS-AB(N+1)*SN
      E6=AB(N+1)*CS+ABN(N+1)*SN
      E7=ABN(N+1)*CS+AB(N+1)*SN
      E8=AB(N+1)*CS-ABN(N+1)*SN
5     IF(N.EQ.1)GO TO 3
      GO TO 4
3     COSS=COS(BT(N)*AL(N))
      SINN=SIN(BT(N)*AL(N))
      EX=EXP(-AF(N)*AL(N))
      ACOS=AF(N)*COSS
      ASIN=AF(N)*SINN
      BCOS=BT(N)*COSS
      BSIN=BT(N)*SINN
      C(1,1)=EX*(AEB(N)/ABP(N)*(-ACOS+BSIN)-AFD(N)*(ACOS+BSIN))
      C(1,2)=EX*(-AEB(N)/ABP(N)*(BCOS+ASIN)+AFD(N)*(BCOS-ASIN))
      C(1,3)=(AEB(N)*R1(N)+1.)*AL(N)
      C(1,4)=AEB(N)*S4(N)*AL(N)
      C(1,5)=1.
      C(1,6)=0.
      RHS(1,1)=-AEB(N)*AL(N)*P(N)
      C(2,1)=EX*(F2(N)/ABP(N)*(-ACOS+BSIN)-F1(N)*(ACOS+BSIN))
      C(2,2)=EX*(-F2(N)/ABP(N)*(BCOS+ASIN)+F1(N)*(BCOS-ASIN))
      C(2,3)=F2(N)*R1(N)*AL(N)
      C(2,4)=(F2(N)*S4(N)+1.)*AL(N)
      C(2,5)=0.
      C(2,6)=1.
      RHS(2,1)=-F2(N)*AL(N)*P(N)
4     M=8*N-5
      K=M-4
      IF(N.EQ.NE)GO TO 21
      IF(N.EQ.1)GO TO 31
      C(M,K)=1.
      C(M,K+1)=0.
31    C(M,K+2)=1.
      C(M,K+3)=0.
      C(M,K+4)=R1(N)
      C(M,K+5)=S4(N)
      C(M,K+6)=0.
      C(M,K+7)=0.
      C(M,K+8)=-XP*CS
      C(M,K+9)=-XP*SN
      C(M,K+10)=-XN*CS
      C(M,K+11)=-XN*SN
      C(M,K+12)=-R1(N+1)
      C(M,K+13)=-S4(N+1)
      C(M,K+14)=0.
      C(M,K+15)=0.
```

```
      RHS(M,1)=P(N+1)-P(N)
      IF(N.EQ.1)GO TO 32
      C(M+1,K)=AF(N)
      C(M+1,K+1)=BT(N)
32    C(M+1,K+2)=-AF(N)
      C(M+1,K+3)=BT(N)
      C(M+1,K+4)=0.
      C(M+1,K+5)=0.
      C(M+1,K+6)=0.
      C(M+1,K+7)=0.
      C(M+1,K+8)=-XP*E1
      C(M+1,K+9)=-XP*E2
      C(M+1,K+10)=XN*E3
      C(M+1,K+11)=-XN*E4
      C(M+1,K+12)=0.
      C(M+1,K+13)=0.
      C(M+1,K+14)=0.
      C(M+1,K+15)=0.
      RHS(M+1,1)=0.
      IF(N.EQ.1.)GO TO 33
      C(M+2,K)=(AEB(N)/ABP(N)+AFD(N))*AF(N)
      C(M+2,K+1)=(-AEB(N)/ABP(N)+AFD(N))*BT(N)
33    C(M+2,K+2)=-(AEB(N)/ABP(N)+AFD(N))*AF(N)
      C(M+2,K+3)=(-AEB(N)/ABP(N)+AFD(N))*BT(N)
      C(M+2,K+4)=0.
      C(M+2,K+5)=0.
      C(M+2,K+6)=1.
      C(M+2,K+7)=0.
      C(M+2,K+8)=-XP*(AEB(N+1)/ABP(N+1)*E3+AFD(N+1)*E1)
      C(M+2,K+9)=-XP*(-AEB(N+1)/ABP(N+1)*E4+AFD(N+1)*E2)
      C(M+2,K+10)=-XN*(-AEB(N+1)/ABP(N+1)*E1-AFD(N+1)*E3)
      C(M+2,K+11)=-XN*(-AEB(N+1)/ABP(N+1)*E2+AFD(N+1)*E4)
      C(M+2,K+12)=-(AEB(N+1)*R1(N+1)+1.)*AL(N+1)
      C(M+2,K+13)=-AEB(N+1)*S4(N+1)*AL(N+1)
      C(M+2,K+14)=-1.
      C(M+2,K+15)=0.
      RHS(M+2,1)=AEB(N+1)*AL(N+1)*P(N+1)
      IF(N.EQ.1)GO TO 34
      C(M+3,K)=(F2(N)/ABP(N)+F1(N))*AF(N)
      C(M+3,K+1)=(-F2(N)/ABP(N)+F1(N))*BT(N)
34    C(M+3,K+2)=-(F2(N)/ABP(N)+F1(N))*AF(N)
      C(M+3,K+3)=(-F2(N)/ABP(N)+F1(N))*BT(N)
      C(M+3,K+4)=0.
      C(M+3,K+5)=0.
      C(M+3,K+6)=0.
      C(M+3,K+7)=1.
      C(M+3,K+8)=-XP*(F2(N+1)/ABP(N+1)*E3+F1(N+1)*E1)
      C(M+3,K+9)=-XP*(-F2(N+1)/ABP(N+1)*E4+F1(N+1)*E2)
      C(M+3,K+10)=-XN*(-F2(N+1)/ABP(N+1)*E1-F1(N+1)*E3)
      C(M+3,K+11)=-XN*(-F2(N+1)/ABP(N+1)*E2+F1(N+1)*E4)
      C(M+3,K+12)=-F2(N+1)*R1(N+1)*AL(N+1)
```

```
      C(M+3,K+13)=-(F2(N+1)*S4(N+1)+1.)*AL(N+1)
      C(M+3,K+14)=0.
      C(M+3,K+15)=-1.
      RHS(M+3,1)=F2(N+1)*AL(N+1)*P(N+1)
      IF(N.EQ.1)GO TO 35
      C(M+4,K)=S3(N)+T3(N)*ABM(N)
      C(M+4,K+1)=T3(N)*AB(N)
35    C(M+4,K+2)=S3(N)+T3(N)*ABM(N)
      C(M+4,K+3)=-T3(N)*AB(N)
      C(M+4,K+4)=S3(N)*R1(N)+BB(1,1,N)
      C(M+4,K+5)=S3(N)*S4(N)+BB(1,3,N)+BD(1,3,N)/R
      C(M+4,K+6)=0.
      C(M+4,K+7)=0.
      C(M+4,K+8)=-XP*(S3(N+1)*CS+T3(N+1)*E5)
      C(M+4,K+9)=-XP*(S3(N+1)*SN+T3(N+1)*E6)
      C(M+4,K+10)=-XN*(S3(N+1)*CS+T3(N+1)*E7)
      C(M+4,K+11)=-XN*(S3(N+1)*SN-T3(N+1)*E8)
      C(M+4,K+12)=-(S3(N+1)*R1(N+1)+BB(1,1,N+1))
      C(M+4,K+13)=-(S3(N+1)*S4(N+1)+BB(1,3,N+1)+BD(1,3,N+1)/R)
      C(M+4,K+14)=0.
      C(M+4,K+15)=0.
      RHS(M+4,1)=S3(N+1)*P(N+1)-S3(N)*P(N)
      IF(N.EQ.1)GO TO 36
      C(M+5,K)=S3(N)*AF(N)+T3(N)*A3B(N)
      C(M+5,K+1)=S3(N)*BT(N)-T3(N)*B3A(N)
36    C(M+5,K+2)=-(S3(N)*AF(N)+T3(N)*A3B(N))
      C(M+5,K+3)=S3(N)*BT(N)-T3(N)*B3A(N)
      C(M+5,K+4)=0.
      C(M+5,K+5)=0.
      C(M+5,K+6)=0.
      C(M+5,K+7)=0.
      C(M+5,K+8)=-XP*(S3(N+1)*E1+T3(N+1)*(A3B(N+1)*CS+B3A(N+1)*SN))
      C(M+5,K+9)=-XP*(S3(N+1)*E2+T3(N+1)*(-B3A(N+1)*CS+A3B(N+1)*SN))
      C(M+5,K+10)=-XN*(-S3(N+1)*E3+T3(N+1)*(-A3B(N+1)*CS+B3A(N+1)*SN))
      C(M+5,K+11)=-XN*(S3(N+1)*E4+T3(N+1)*(-B3A(N+1)*CS-A3B(N+1)*SN))
      C(M+5,K+12)=0.
      C(M+5,K+13)=0.
      C(M+5,K+14)=0.
      C(M+5,K+15)=0.
      RHS(M+5,1)=0.
      IF(N.EQ.1)GO TO 37
      C(M+6,K)=0.
      C(M+6,K+1)=0.
37    C(M+6,K+2)=0.
      C(M+6,K+3)=0.
      C(M+6,K+4)=AA(1,1,N)
      C(M+6,K+5)=AA(1,3,N)+BB(1,3,N)/R
      C(M+6,K+6)=0.
      C(M+6,K+7)=0.
      C(M+6,K+8)=0.
      C(M+6,K+9)=0.
```

```
      C(M+6,K+10)=0.
      C(M+6,K+11)=0.
      C(M+6,K+12)=-AA(1,1,M+1)
      C(M+6,K+13)=-(AA(1,3,M+1)+BB(1,3,M+1)/R)
      C(M+6,K+14)=0.
      C(M+6,K+15)=0.
      RHS(M+6,1)=0.
      IF(N.EQ.1)GO TO 38
      C(M+7,K)=0.
      C(M+7,K+1)=0.
38    C(M+7,K+2)=0.
      C(M+7,K+3)=0.
      C(M+7,K+4)=AA(3,1,N)+BB(3,1,N)/R
      C(M+7,K+5)=AA(3,3,N)+2.*BB(3,3,N)/R+DD(3,3,N)/R/R
      C(M+7,K+6)=0.
      C(M+7,K+7)=0.
      C(M+7,K+8)=0.
      C(M+7,K+9)=0.
      C(M+7,K+10)=0.
      C(M+7,K+11)=0.
      C(M+7,K+12)=-(AA(3,1,N+1)+BB(3,1,N+1)/R)
      C(M+7,K+13)=-(AA(3,3,N+1)+2.*BB(3,3,N+1)/R+DD(3,3,N+1)/R/R)
      C(M+7,K+14)=0.
      C(M+7,K+15)=0.
      RHS(M+7,1)=0.
      GO TO 6
21    IF(ICONB.EQ.1)GO TO 10
      GO TO 11
10    IF(N.EQ.1)GO TO 51
      C(L-3,L-7)=S3(N)+T3(N)*ABM(N)
      C(L-3,L-6)=T3(N)*AB(N)
51    C(L-3,L-5)=S3(N)+T3(N)*ABM(N)
      C(L-3,L-4)=-T3(N)*AB(N)
      C(L-3,L-3)=BB(1,1,N)+S3(N)*R1(N)
      C(L-3,L-2)=S3(N)*S4(N)+BB(1,3,N)+DD(1,3,N)/R
      C(L-3,L-1)=0.
      C(L-3,L)=0.
      RHS(L-3,1)=-S3(N)*P(N)
      IF(N.EQ.1)GO TO 52
      C(L-2,L-7)=S3(N)*AF(N)+T3(N)*A3B(N)
      C(L-2,L-6)=S3(N)*BT(N)-T3(N)*B3A(N)
52    C(L-2,L-5)=-(S3(N)*AF(N)+T3(N)*A3B(N))
      C(L-2,L-4)=S3(N)*BT(N)-T3(N)*B3A(N)
      C(L-2,L-3)=0.
      C(L-2,L-2)=0.
      C(L-2,L-1)=0.
      C(L-2,L)=0.
      RHS(L-2,1)=0.
      IF(N.EQ.1)GO TO 53
      C(L-1,L-7)=0.
      C(L-1,L-6)=0.
```

```
53    C(L-1,L-5)=0.
      C(L-1,L-4)=0.
      C(L-1,L-3)=AA(1,1,N)
      C(L-1,L-2)=AA(1,3,N)+BB(1,3,N)/R
      C(L-1,L-1)=0.
      C(L-1,L)=0.
      RHS(L-1,1)=ANX
      IF(N.EQ.1)GO TO 54
      C(L,L-7)=0.
      C(L,L-6)=0.
54    C(L,L-5)=0.
      C(L,L-4)=0.
      C(L,L-3)=AA(3,1,N)+BB(3,1,N)/R
      C(L,L-2)=AA(3,3,N)+2.*BB(3,3,N)/R+BD(3,3,N)/R/R
      C(L,L-1)=0.
      C(L,L)=0.
      RHS(L,1)=0.
      GO TO 6
11    IF(N.EQ.1)GO TO 55
      C(L-3,L-7)=1.
      C(L-3,L-6)=0.
55    C(L-3,L-5)=1.
      C(L-3,L-4)=0.
      C(L-3,L-3)=R1(N)
      C(L-3,L-2)=S4(N)
      C(L-3,L-1)=0.
      C(L-3,L)=0.
      RHS(L-3,1)=-P(N)
      IF(N.EQ.1)GO TO 56
      C(L-2,L-7)=AF(N)
      C(L-2,L-6)=BT(N)
56    C(L-2,L-5)=-AF(N)
      C(L-2,L-4)=BT(N)
      C(L-2,L-3)=0.
      C(L-2,L-2)=0.
      C(L-2,L-1)=0.
      C(L-2,L)=0.
      RHS(L-2,1)=0.
      IF(ICOND.EQ.2.OR.ICOND.EQ.4)GO TO 71
      GO TO 72
71    IF(N.EQ.1)GO TO 57
      C(L-1,L-7)=(AEB(N)/ABP(N)+AFD(N))*AF(N)
      C(L-1,L-6)=(-AEB(N)/ABP(N)+AFD(N))*BT(N)
57    C(L-1,L-5)=-(AEB(N)/ABP(N)+AFD(N))*AF(N)
      C(L-1,L-4)=(-AEB(N)/ABP(N)+AFB(N))*BT(N)
      C(L-1,L-3)=0.
      C(L-1,L-2)=0.
      C(L-1,L-1)=1.
      C(L-1,L)=0.
      RHS(L-1,1)=0.
      GO TO 73
```

```
72    IF(N.EQ.1)GO TO  58
      C(L-1,L-7)=0.
      C(L-1,L-6)=0.
58    C(L-1,L-5)=0.
      C(L-1,L-4)=0.
      C(L-1,L-3)=AA(1,1,N)
      C(L-1,L-2)=AA(1,3,N)+BB(1,1,N)/R
      C(L-1,L-1)=0.
      C(L-1,L)=0.
      RHS(L-1,1)=ANX
73    IF(ICOND.EQ.2.OR.ICOND.EQ.3)GO TO 74
      GO TO 75
74    IF(N.EQ.1)GO TO 59
      C(L,L-7)=(F2(N)/ABP(N)+F1(N))*AF(N)
      C(L,L-6)=(-F2(N)/ABP(N)+F1(N))*BT(N)
59    C(L,L-5)=-(F2(N)/ABP(N)+F1(N))*AF(N)
      C(L,L-4)=(-F2(N)/ABP(N)+F1(N))*BT(N)
      C(L,L-3)=0.
      C(L,L-2)=0.
      C(L,L-1)=0.
      C(L,L)=1.
      RHS(L,1)=0.
75    IF(N.EQ.1)GO TO 60
      C(L,L-7)=0.
      C(L,L-6)=0.
60    C(L,L-5)=0.
      C(L,L-4)=0.
      C(L,L-3)=AA(3,1,N)+BB(3,1,N)/R
      C(L,L-2)=AA(3,3,N)+2.*BB(3,3,N)/R+DD(3,3,N)/R/R
      C(L,L-1)=0.
      C(L,L)=0.
      RHS(L,1)=ANXY
6     CONTINUE
2     CONTINUE
      IFAIL=0
      CALL F04AEF(C,L,RHS,L,L,1,COF,L,WRK,CFI,L,CFT,L,IFAIL)
      RETURN
      END
C
      SUBROUTINE DEFLECTIONS(N,C1,C2,C3,C4,K1,K2,K3,K4,X,X0)
C     ------------------------------------------------------
      COMMON/BLOCK2/NE,R,AL(6),NF(6),AA(3,3,6),BB(3,3,6),DD(3,3,6),
     *F2(6),F1(6),AEB(6),AFD(6),R1(6),S4(6),S3(6),T3(6),AF(6),
     *BT(6),ABM(6),ABP(6),AB(6),A3B(6),B3A(6),P(6),ANX,ANXY,ICOND
      REAL K1,K2,K3,K4
      E1=EXP(-AF(N)*X)
      E2=EXP(AF(N)*X)
      E3=COS(BT(N)*X)
      E4=SIN(BT(N)*X)
      E5=-AF(N)*C3+BT(N)*C4
      E6=AF(N)*C4+BT(N)*C3
```

```
      E7=AF(M)*C1+BT(M)*C2
      E8=AF(M)*C2-BT(M)*C1
      AF2=AF(M)**2
      BT2=BT(M)**2
      WP=P(M)+S4(M)*K2+R1(M)*K1
      W=E2*(C1*E3+C2*E4)+E1*(C3*E3+C4*E4)+WP
      W1=E2*(E7*E3+E8*E4)+E1*(E5*E3-E6*E4)
      W2=E2*((AF(M)*E7+BT(M)*E8)*E3+(AF(M)*E8-BT(M)*E7)*E4)
     ;   +E1*(-(AF(M)*E5+BT(M)*E6)*E3+(AF(M)*E6-BT(M)*E5)*E4)
      W3=E2*((AF2*E7+AB(M)*E8-BT2*E7)*E3+(AF2*E8-AB(M)*E7-BT2*E8)*E4)
     ;   +E1*((AF2*E5+AB(M)*E6-BT2*E5)*E3+(-AF2*E6+AB(M)*E5+BT2*E6)*E4)
      V=F2(M)/ABP(M)*E2*((AF(M)*C1-BT(M)*C2)*E3+(BT(M)*C1+AF(M)*C2)*E4)
     ;   +F2(M)/ABP(M)*E1*(-(AF(M)*C3+BT(M)*C4)*E3+(BT(M)*C3-AF(M)*C4)*
     ;   E4)+F1(M)*E2*(E7*E3+E8*E4)+F1(M)*E1*(E5*E3-E6*E4)+F2(M)*R1(M)*
     ;   X*K1+(F2(M)*S4(M)+1.)*X*K2+K4+F2(M)*P(M)*X
      V1=F2(M)*W+F1(M)*W2+K2
      U=AEB(M)/ABP(M)*E2*((AF(M)*C1-BT(M)*C2)*E3+(BT(M)*C1+AF(M)*C2)*E4)
     ;   +AEB(M)/ABP(M)*E1*(-(AF(M)*C3+BT(M)*C4)*E3+(BT(M)*C3-AF(M)*C4)
     ;   *E4)+AFB(M)*E2*(E7*E3+E8*E4)+AFB(M)*E1*(E5*E3-E6*E4)+(AEB(M)*
     ;   R1(M)+1.)*X*K1+AEB(M)*S4(M)*X*K2+K3+AEB(M)*P(M)*X
      U1=AEB(M)*W+AFB(M)*W2+K1
      CALL FUNCTIONS(M,WP,W,W1,W2,W3,V,V1,U,U1,X0)
      RETURN
      END
C
      SUBROUTINE FUNCTIONS(M,WP,W,W1,W2,W3,V,V1,U,U1,X0)
C     ------------------------------------------------
      COMMON/BLOCK2/NE,R,AL(6),NF(6),AA(3,3,6),BB(3,3,6),DD(3,3,6),
     *F2(6),F1(6),AEB(6),AFB(6),R1(6),S4(6),S3(6),T3(6),AF(6),
     *BT(6),ABN(6),ABP(6),AB(6),A3B(6),B3A(6),P(6),ANX,ANXY,ICOND
     */BLOCK4/A(3,3),B(3,3),D(3,3),WK(3)
     */BLOCK5/QKIN(3,3),QKOT(3,3),HB,IFUN,ISTRN,ISTRS,IFUN2
     *,QKR(3,3,6),ZR(6),NR(6)
      REAL NX,NY,NXY,MX,MY,MXY
      DIMENSION DEF(3),CUR(3),E(3),F(3)
     *,EPIN(3),EPOT(3),STIN(3),STOT(3),EPR(3),STR(3)
      CALL FMOVE(AA(1,1,M),A,9)
      CALL FMOVE(BB(1,1,M),B,9)
      CALL FMOVE(DD(1,1,M),D,9)
      DEF(1)=U1
      DEF(2)=W/R
      DEF(3)=V1
      CUR(1)=-W2
      CUR(2)=-W/R/R
      CUR(3)=V1/R
      IFAIL=0
      CALL F01CKF(E,A,DEF,3,1,3,WK,3,1,IFAIL)
      IFAIL=0
      CALL F01CKF(F,B,CUR,3,1,3,WK,3,1,IFAIL)
      NX=E(1)+F(1)
      NY=E(2)+F(2)
```

```
      MXY=E(3)+F(3)
      IFAIL=0
      CALL F01CKF(E,B,DEF,3,1,3,WK,3,1,IFAIL)
      IFAIL=0
      CALL F01CKF(F,D,CUR,3,1,3,WK,3,1,IFAIL)
      MX=E(1)+F(1)
      MY=E(2)+F(2)
      MXY=E(3)+F(3)
      QX=S3(M)*W1+T3(M)*W3
      EPOT(1)=DEF(1)+HB*CUR(1)
      EPOT(2)=DEF(2)+HB*CUR(2)
      EPOT(3)=DEF(3)+HB*CUR(3)
      EPIN(1)=DEF(1)-HB*CUR(1)
      EPIN(2)=DEF(2)-HB*CUR(2)
      EPIN(3)=DEF(3)-HB*CUR(3)
      IF(NR(M).EQ.0)GO TO 2
      EPR(1)=DEF(1)+ZR(M)*CUR(1)
      EPR(2)=DEF(2)+ZR(M)*CUR(2)
      EPR(3)=DEF(3)+ZR(M)*CUR(3)
      CALL FMOVE(QKR(1,1,M),A,9)
      IFAIL=0
      CALL F01CKF(STR,A,EPR,3,1,3,WK,3,1,IFAIL)
2     CONTINUE
      IFAIL=0
      CALL F01CKF(STOT,QKOT,EPOT,3,1,3,WK,3,1,IFAIL)
      IFAIL=0
      CALL F01CKF(STIN,QKIN,EPIN,3,1,3,WK,3,1,IFAIL)
      WRITE(2,10)
10    FORMAT(/)
      IF(IFUN.EQ.1)WRITE(2,1)XO,W,MY,MX,MY,MXY,QX
      IF(IFUN2.EQ.1)WRITE(2,1)XO,DEF,CUR
      IF(ISTRN.EQ.1)WRITE(2,1)XO,EPOT,EPIN
      IF(ISTRS.EQ.1)WRITE(2,1)XO,STOT,STIN
      IF(NR(M).EQ.1.AND.ISTRS.EQ.1)WRITE(2,1)XO,STR
1     FORMAT(7(1PE10.2))
      RETURN
      END
      FINISH
```

D.5 INPUT DATA DESCRIPTION

The data, whether real or integer, is in a free format. Any consistent unit can be used in the program. There are some restrictions on some data as described below. The parameters which start with an integer are input as integers. Other parameters are real. The data cards must be in the following order :

1st data card : the problem control card

NM NE R PR ANX ANXY NP ICOND IFUN ISTRN ISTRS IFUN2

where :

NM = the number of different materials used, (max. 3);

NE = number of finite elements in the tube, (max. 6);

R = mean radius of the cylinder;

PR = the internal pressure;

ANX = the axial load;

ANXY = the torsional load;

NP = number of elements subjected to internal pressure;

ICON = integer determines the end condition, it takes any of the following value :

1 for free ends;

2 for completely restricted ends;

3 for clamped ends with axial displacement allowed;

4 for clamped ends with hoop displacement allowed;

5 for clamped ends with axial and hoop displacements allowed.

IFUN = 1 if w^{o}, N_y, M_x, M_y, M_{xy} and Q_x are to be output, otherwise IFUN = 0;

ISTRN = 1 if the outer and inner surface strains are to be output, otherwise ISTRN = 0;

ISTRS = 1 if the outer and inner surface stresses are to be output, otherwise ISTRS = 0; and

IFUN2 = 1 if the middle surface strains and the changes of curvature are to be output, otherwise IFUN2 = 0.

2nd_set_of_cards : the materials properties cards

These are NM cards, a card per material where on each card the following properties are input :

EL ET GLT PLT

where :

EL = Young's modulus in the fibre direction;

ET = Young's modulus in the transverse direction;

GLT = shear modulus; and

PLT = Poisson's ratio

3rd_set_of_cards : the elements data cards

These are NE sets of cards, one set per element as follows :

NL AL NF

NL cards

L TL THET NS KIND

L TL THET NS KIND

. . . . . .

where :

NL = number of layers, (max. 8);

AL = length of element;

NF = number of finite element for this element;

L = layer material number;

TL = thickness of layer;

THET = angle of layer with x-axis (in degree);

NS = number of sub-layers for this layer;

KIND = 2 for angle-ply layer, otherwise KIND = 1.

N.B. The angle-ply layer is input as two layers, one is with θ angle and the other is with $-\theta$, then within the program each of these layers is divided into NS sublayers and arranged to be in the sequence $+\theta$, $-\theta$, $+\theta$, $-\theta$, $+\theta$, $-\theta$, ...

D.6 SAMPLE INPUT

```
1  2  40.565E-3  30.E6  0.  0.  1  1  1  1  1  1
44.5E9  13.5E9  5.64E9  .183
2   120.E-3  12
1  1.665E-3   45.  4  2
1  1.665E-3  -45.  4  2
2    10.E-3  10
1  1.665E-3   45.  4  2
1  1.665E-3  -45.  4  2
```

D.7 SAMPLE OUTPUT

```
ANALYSIS OF COMPOSITE CYLINDER WITH R=   0.041 DIVIDED INTO  2 ELEMENTS
LOADED BY: P= 3.00E 07, NX= 0.00E 00, NXY= 0.00E 00,WITH END CONDITIONS:
 FREE ENDS


    X         W          NY         MX         MY         MXY        QX
    X       ---MIDDLE SURFACE STRAINS---  ----CHANGES OF CURVATURE----
    X       ---OUTER SURFACE STRAINS----  ---INNER SURFACE STRAINS----
    X       ---OUTER SURFACE STRESSES---  ---INNER SURFACE STRESSES---

ELEMENT 2
---------


 0.00E 00 -1.25E-04 -1.71E 05 -7.34E-10  3.89E 00 -8.76E 00  3.28E-07
 0.00E 00  1.47E-03 -3.08E-03  1.22E-15 -3.62E-02  7.60E-02  3.01E-14
 0.00E 00  1.41E-03 -2.96E-03  1.27E-15  1.53E-03 -3.21E-03  1.17E-15
 0.00E 00 -1.23E-03 -4.92E 07 -1.21E 07  3.99E-04 -5.34E 07  1.32E 07


 1.00E-03 -6.74E-05 -9.21E 04 -1.78E 00  1.26E 00 -4.72E 00 -3.24E 03
 1.00E-03  7.91E-04 -1.66E-03  3.30E-06 -4.67E-02  4.09E-02  8.14E-05
 1.00E-03  7.13E-04 -1.59E-03  3.44E-06  8.68E-04 -1.73E-03  3.17E-06
 1.00E-03 -9.48E 05 -2.70E 07 -6.84E 06  9.50E 05 -2.83E 07  6.78E 06


 2.00E-03 -9.60E-06 -1.31E 04 -5.84E 00 -2.45E 00 -6.61E-01 -4.54E 03
 2.00E-03  1.13E-04 -2.37E-04  1.08E-05 -9.17E-02  5.83E-03  2.66E-04
 2.00E-03 -4.01E-05 -2.27E-04  1.13E-05  2.65E-04 -2.46E-04  1.04E-05
 2.00E-03 -3.10E 06 -5.21E 06 -1.94E 06  3.11E 06 -2.66E 06 -1.05E 04


 3.00E-03  4.83E-05  6.60E 04 -1.02E 01 -6.31E 00  3.40E 00 -3.89E 03
 3.00E-03 -5.67E-04  1.19E-03  1.89E-05 -1.42E-01 -2.93E-02  4.66E-04
 3.00E-03 -8.02E-04  1.14E-03  1.97E-05 -3.31E-04  1.24E-03  1.81E-05
 3.00E-03 -5.43E 06  1.65E 07  2.91E 06  5.44E 06  2.31E 07 -6.86E 06


 4.00E-03  1.06E-04  1.45E 05 -1.30E 01 -9.41E 00  7.47E 00 -1.28E 03
 4.00E-03 -1.25E-03  2.62E-03  2.40E-05 -1.67E-01 -6.46E-02  5.92E-04
 4.00E-03 -1.53E-03  2.51E-03  2.50E-05 -9.70E-04  2.73E-03  2.30E-05
 4.00E-03 -6.89E 06  3.86E 07  8.06E 06  6.90E 06  4.86E 07 -1.34E 07


 5.00E-03  1.64E-04  2.25E 05 -1.21E 01 -1.08E 01  1.15E 01  3.27E 03
 5.00E-03 -1.93E-03  4.05E-03  2.25E-05 -1.37E-01 -9.99E-02  5.54E-04
 5.00E-03 -2.16E-03  3.89E-03  2.34E-05 -1.70E-03  4.22E-03  2.15E-05
 5.00E-03 -6.45E 06  6.17E 07  1.38E 07  6.46E 06  7.32E 07 -1.94E 07
```

APPENDIX E

ULTRASONIC C-SCAN TEST

E.1 WHAT IS IT?

When transmitting an ultrasonic beam through a material there will be energy loss by absorption and dispersion through the thickness, (Ref. 211). In fibre-reinforced composites, the presence of voids, cracks and delaminations will cause extra energy losses which result in a decreasing amplitude of the received signal. By sacnning the material with an ultrasonic beam and simultaneously recording the value of the signal amplitude an absorption pattern is obtained. This process is usually called ultrasonic C-scan. The technique should not be considered as a quantitative analysis. It is only a useful qualitative test, (Ref. 214). Prakash, (Ref. 215), has reviewed the different techniques used in the ultrasonic testing of materials.

E.2 THE TEST EQUIPMENT

The test set-up is shown schematically in Fig. (E.1). The actual test rig was not photographed for security reason at the M.O.D. Rocket Propulsion Establishment (Westcott) where the test was conducted.

Basically, the apparatus consists of the following instruments :

1) an ultrasonic pulse generator,
2) two ultrasonic transducers, one acts as transmitter probe and the other as receiver probe,
3) an amplifier which amplifies the transducer response signal,
4) an oscilloscope to display the detected waves,
5) a signal processing unit to process the received waves,
6) a scanning unit to rotate the cylindrical specimen and to move the transmitter-receiver system along the specimen. In this way the two probes scan the whole surface of the tubular specimen,
7) an X-Y plotter to record the scanning result on a hard copy,
8) a tank of water, where the water acts as a coupling medium. The energy losses in the water are constant, then any variation in the received pulses is due to losses in the specimen.

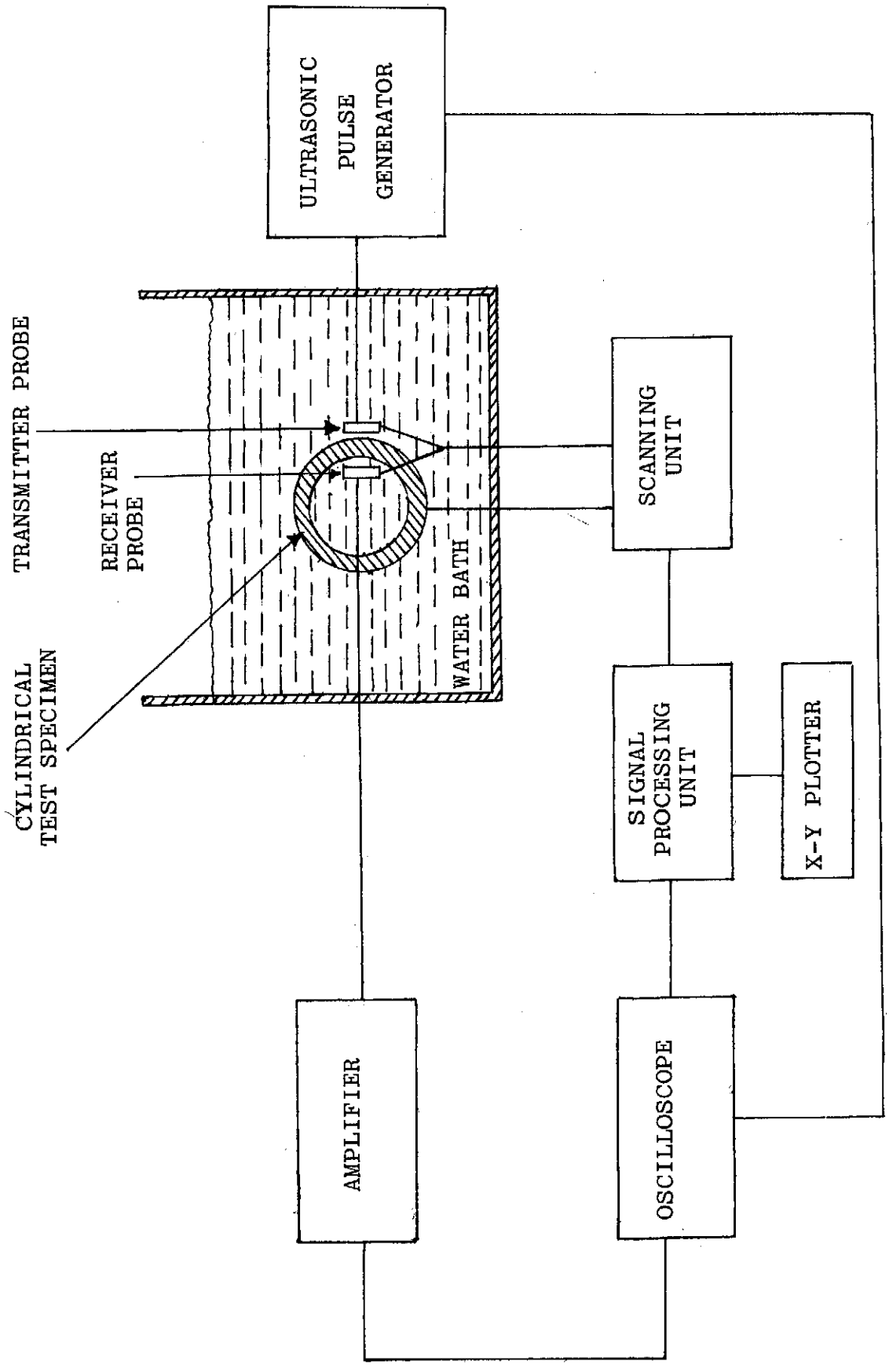

Fig.(E.1) Ultrasonic C-scan test arrangement

E.3 TESTS AND RESULTS

Three test specimens, namely 7B3, 8B3 and 9B3 (see Appendix A), were scanned ultrasonically at the M.O.D. Rocket Propulsion Establishment (Westcott). They were all scanned twice. The first ultrasonic C-scan test was conducted on the three specimens in their virgin state, whereas the second scanning was conducted on the three specimens after they were tested under internal pressure. The internal pressure test on specimen 7B3 was carried out at Cranfield, while on the specimens 8B3 and 9B3 it was conducted at Westcott where it was possible to use the acoustic emission equipment (see Appendix F). Both of 7B3 and 8B3 specimens were tested under internal pressure level which was above the linear limit and caused permanent deflections as well as cracks in the specimens, but it did not cause total failure. The cracks were detected by the acoustic emission probes as will be described in Appendix F. The 9B3 specimen, however, was taken to total failure level under internal pressure.

The charts obtained from scanning the specimens before the internal pressure tests are shown in Figs. (E.2) to (E.4). From these figures the specimens were judged to have internal defects caused during the winding of the filaments. This was expected as the tubes were of commercial quality. These defects, however, did not affect the stiffness and strength properties of the specimens as these properties were obtained experimentally and not from the properties of the constituents. The void patterns seem to run parallel to the fibres which indicate that the voids exist near the fibre cross-over areas.

The ultrasonic C-scan traces obtained from scanning the specimens after the internal pressure tests are shown in Figs. (E.5) to (E.7), from which the cracks were judged to have propagated from the voids causing internal damage in the composites even before the total failure has occurred. This was substantiated by photomicrographs made of samples taken from both virgin and tested specimens (see Appendix G). Both the ultrasonic tests and the photomicrographic evaluations indicated that damage were evident in the test specimens which had been tested under a level of internal pressure higher than the level of the limit of the linear response.

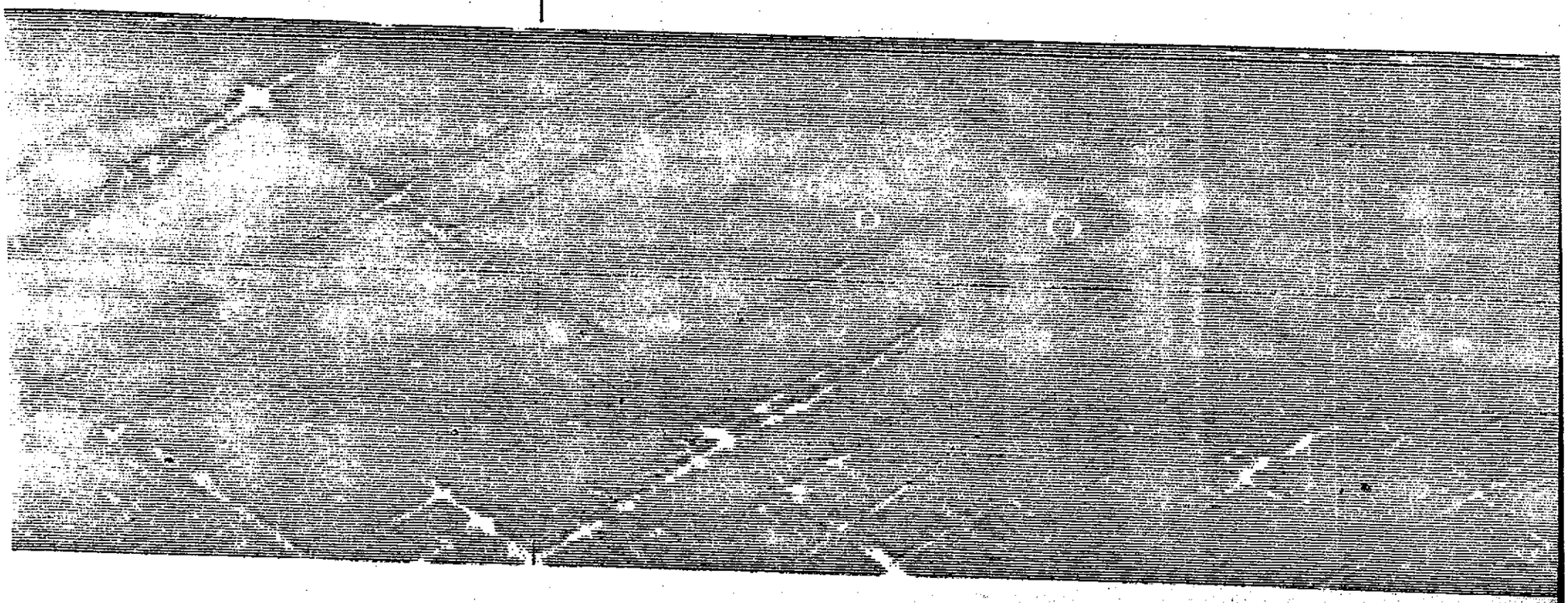

Fig.(E .2) Ultrasonic C-scan trace of specimen 7B3 before internal pressurization test

Fig.(E.3) Ultrasonic C-scan trace of specimen 8B3 before internal pressurization test

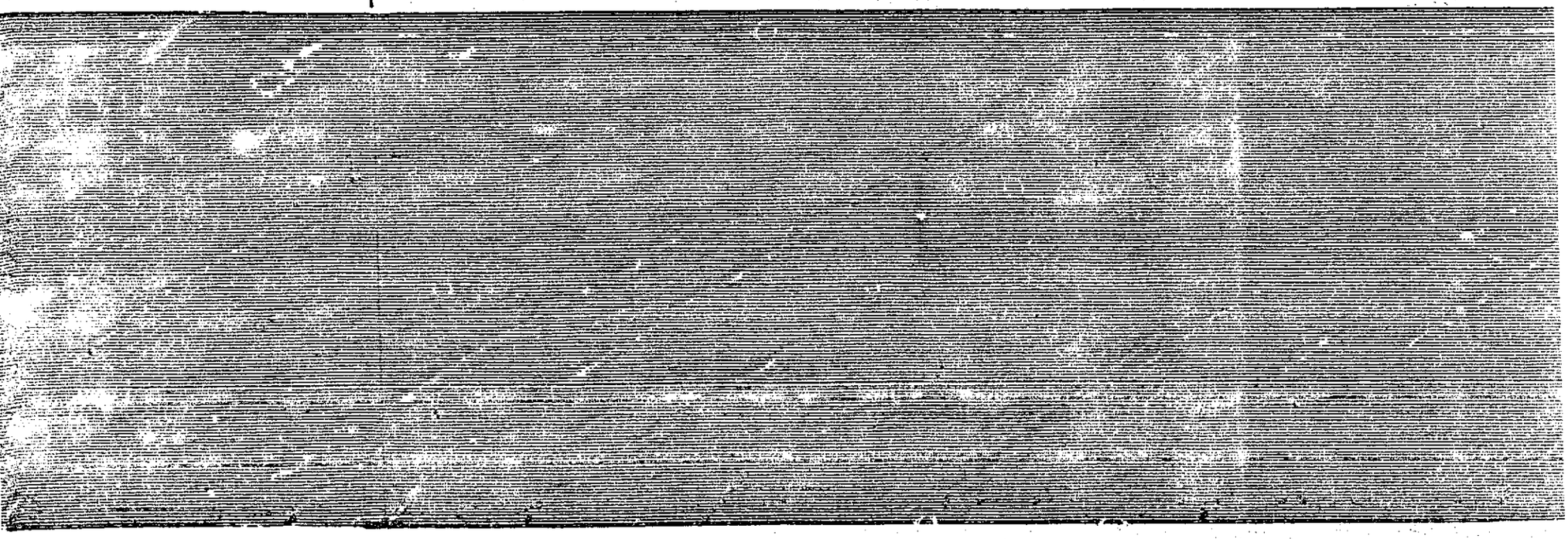

Fig.(E .4) Ultrasonic C-scan trace of specimen 9B3 before internal pressurization test

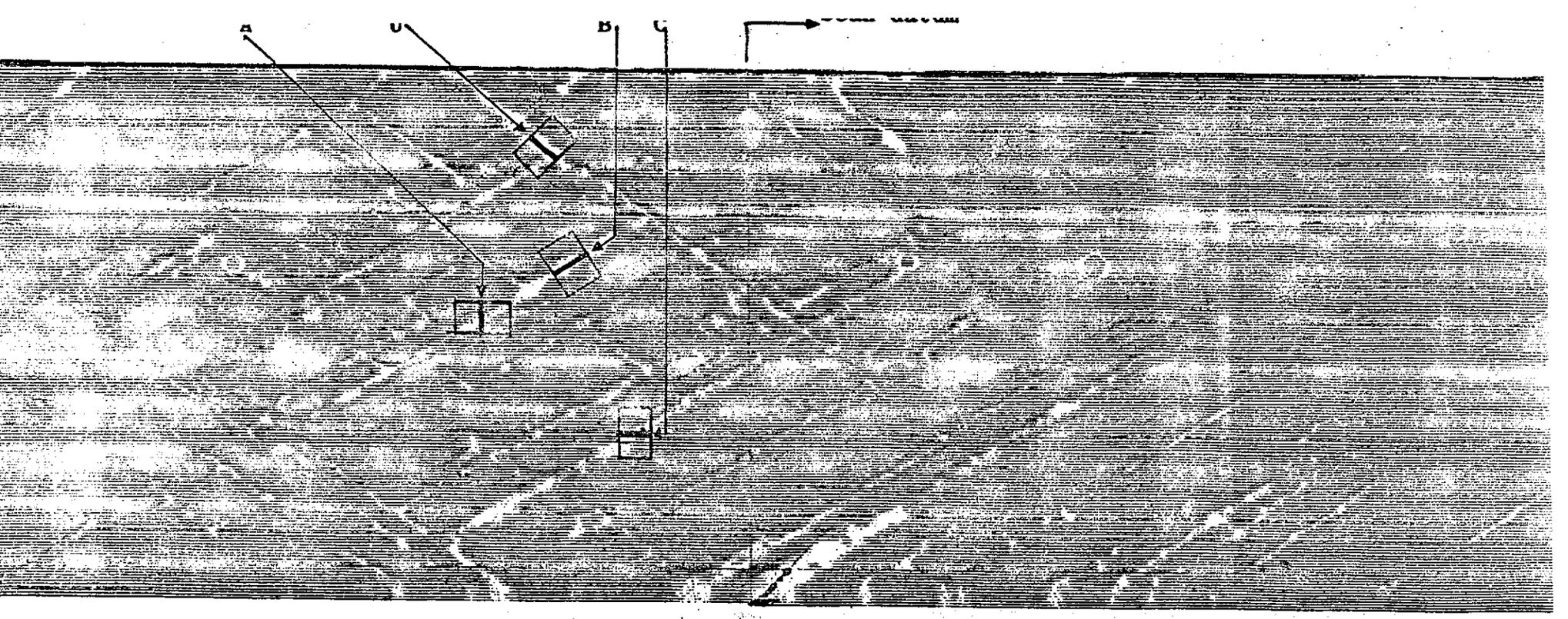

Fig.(E .5) Ultrasonic C-scan trace of specimen 7B3 after internal pressurization test

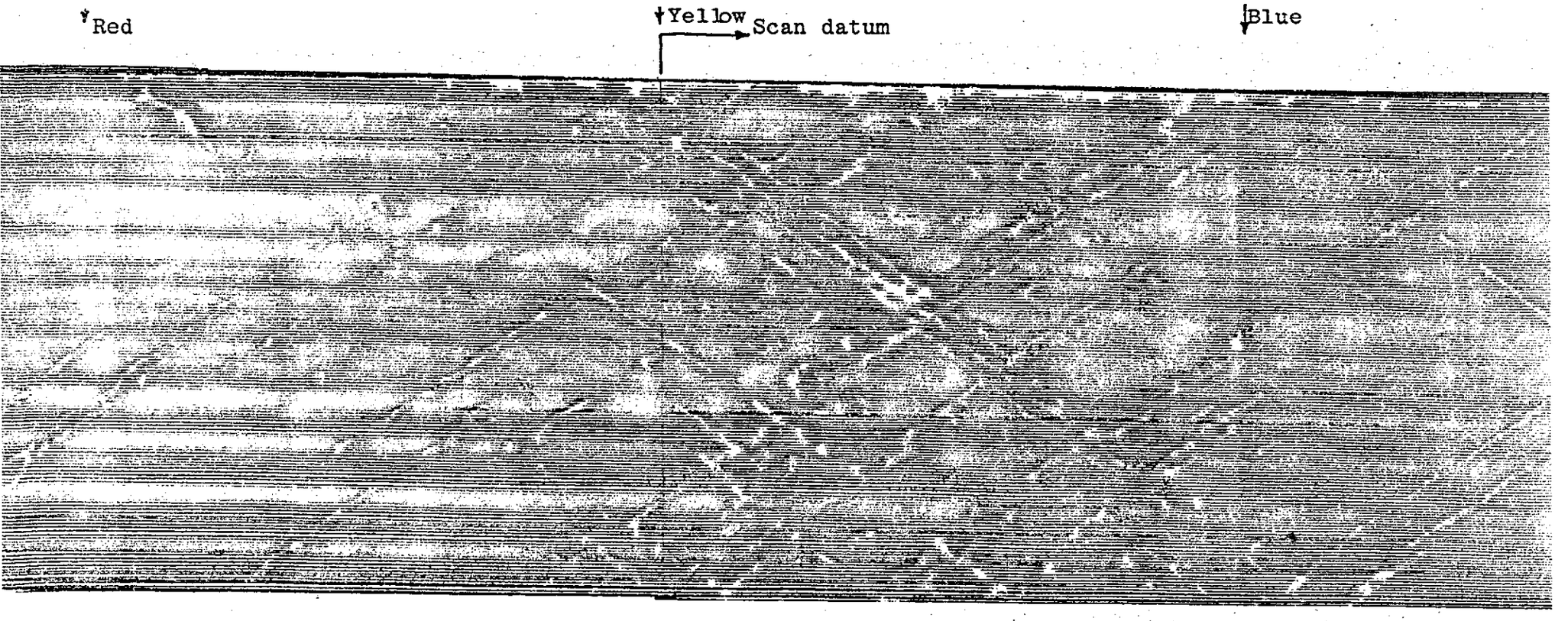

Fig.(E .6) Ultrasonic C-scan trace of specimen 8B3 after internal pressurization test

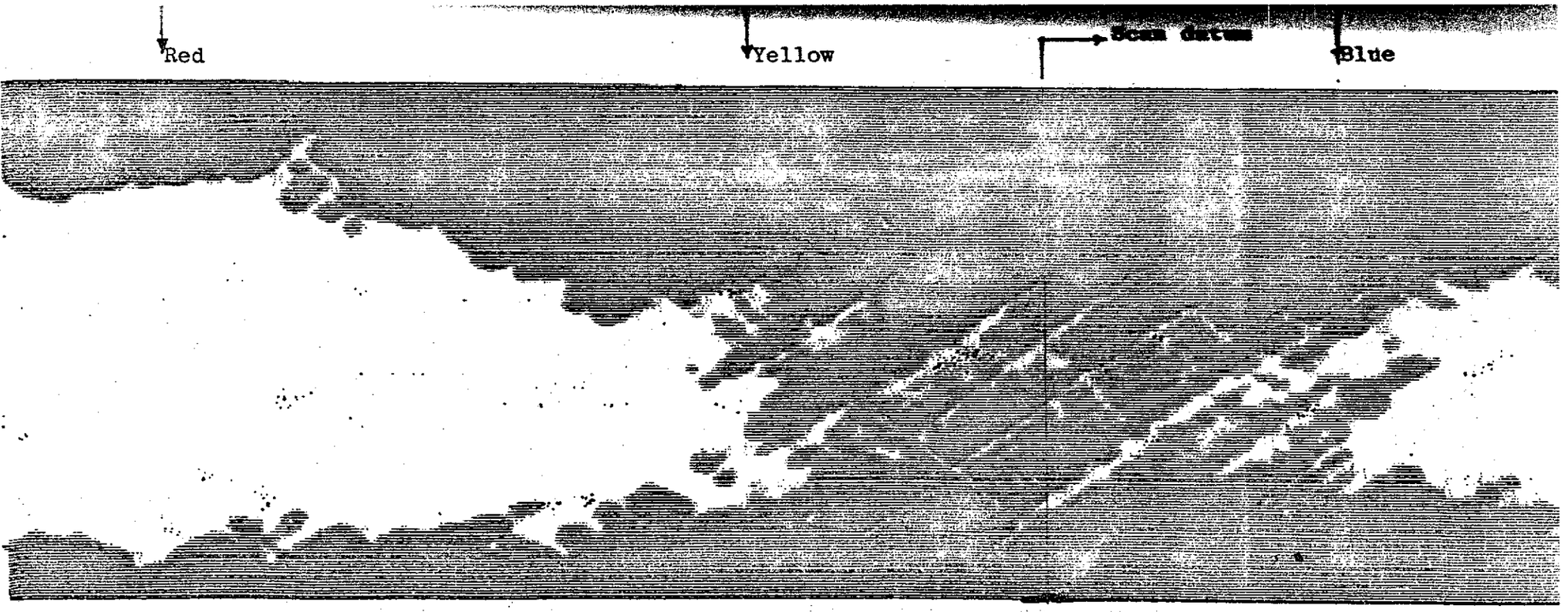

Fig.(E .7) Ultrasonic C-scan trace of specimen 9B3 after internal pressurization test

APPENDIX F

ACOUSTIC EMISSION TEST

F.1 WHAT IS IT?

Acoustic emission is a transient elastic wave generated by the rapid release of energy within a material, (Ref. 216). An alternative term is "stress wave emission", (Ref. 217). In its less conventional forms, acoustic emission can be so loud that it is audible to the unaided ear, e.g., the creaking of timber subjected to loads near failure; the sound produced by the failure of rock, (Ref. 216). Most emission, however, are either too low in amplitude or too high in frequency to be detected by the unaided ear, and therefore require the use of proper detecting equipment, (Ref. 215).

The applications of acoustic emission technique appear unlimited, (Ref. 216), but there are some limitations associated with the technique, mainly the problems created by the interpretation of the recorded emissions, (Ref. 218).

In the composite materials field, for both failure study and non-destructive evaluation of the integrity of composites, there have been considerable amount of work reproted, (Refs. 219-228). The conclusions of these reports vary. The applicability of acoustic emission to detect failure is not disputed, but there is an argument about the validity of the technique as a quantitative analysis.

F.2 THE TEST APPARATUS

A schematic diagram of the test equipment is shown in Fig. (F.1). Here again no photograph for the test rig was taken for security reason at Westcott where the test was carried out.

Essentially, the following units are needed :

1) one or more acoustic emission transducers. These are mounted on the specimen which must be stressed. To eliminate the effect of any unwanted external noise, the specimen is tested in a special, insulated test room. Tests carried out in the laboratory with too many other equipment surrounding the probes are reported to include signals other than those wanted ones, (Ref. 215),

2) a series of amplifiers and filters to amplify the signal received from the probes,

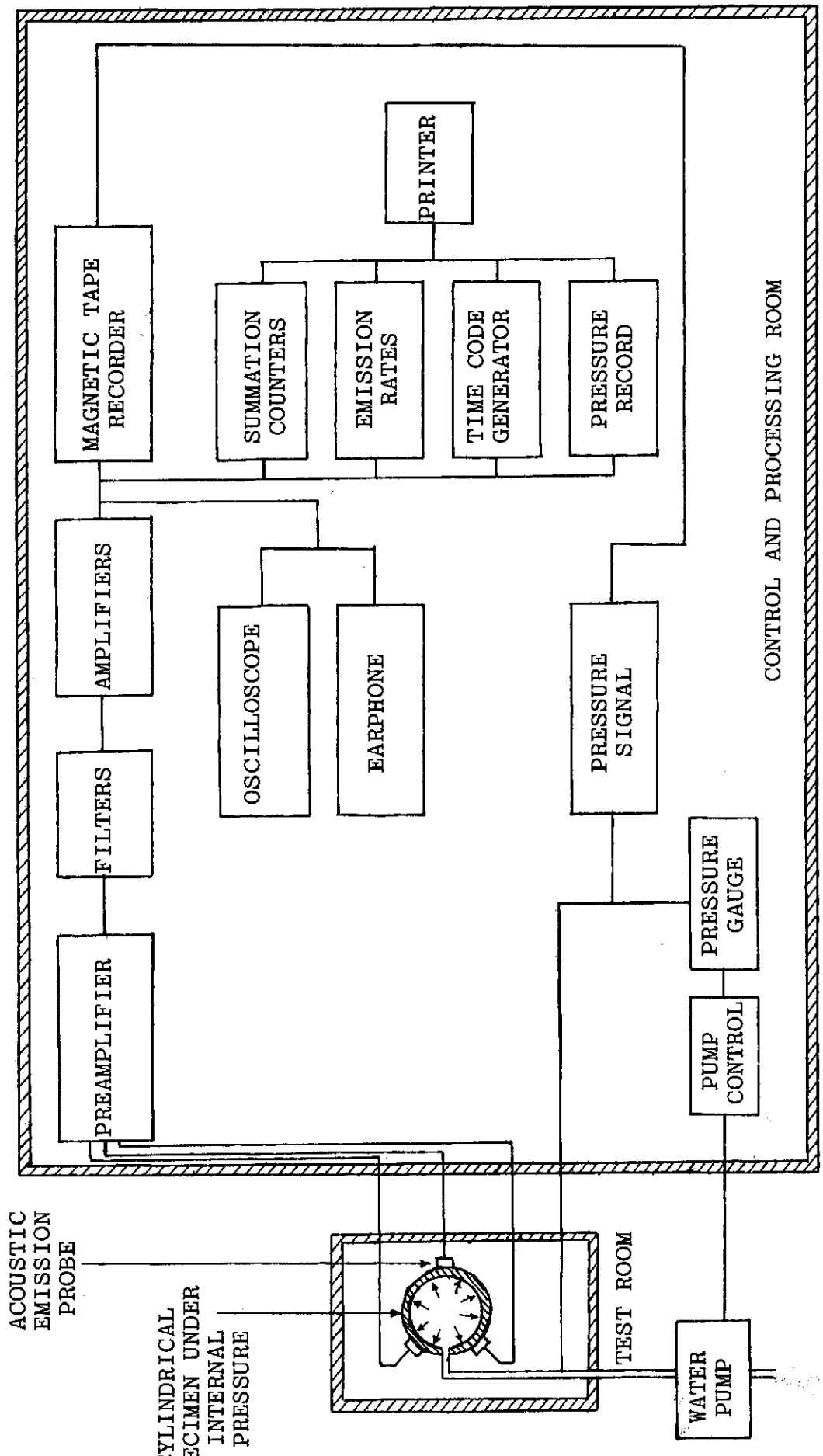

Fig.(F.1) Schematic diagram of the acoustic emission test system

3) an oscilloscope to disply the detected signals,

4) an earphone to hear the events,

5) a magnetic tape recorder to record the acoustic emission events,

6) an electronic counter to give the emission rate and the total emission count,

7) an oscillator to give the time,

8) a printer to give hard copy of the record,

9) any other equipment related to the specimen under test, e.g., a pressure gauge, etc.

F.3 TESTS AND RESULTS

Two of the test specimens, 8B3 and 9B3 (Appendix A), were tested under internal pressure loading and acoustic emission data were obtained during these tests to help understand the damage that occurs in composite materials when subjected to incremental load until final failure.

Four transducers were mounted on each specimen, three round the circumference at the gauge section of the tube, and the fourth was mounted on the top of the specimen. The probes were distinguished from the colours of their wires, namely : blue, yellow, red and green, the green probe being on the top.

The strains induced by the internal pressurization were not recorded in these tests as that would complicate the tests. The behaviour of the specimens 8B3 and 9B3 were considered to be like the behaviour of the specimen 7B3 which is given in Appendix B. This is not far from the reality as all these specimens were cut originally from same tube and were tested under similar testing conditions.

The total counts of acoustic emission emanating from the internal pressurization test of specimen 8B3 are shown in Figs. (F.2) and (F.3) for the blue and yellow probes respectively. The red and green probes, however, did not record high counts. This was because of their mounting positions on the specimen where they were away from the damaged area as can be seen in the ultrasonic C-scan traces of Fig. (E.6). The green probe, however, picked the hydraulic noise of the water. It is to be mentioned here that specimen 8B3 was not tested to total failure. It was pressurized only to a level above the linear limit.

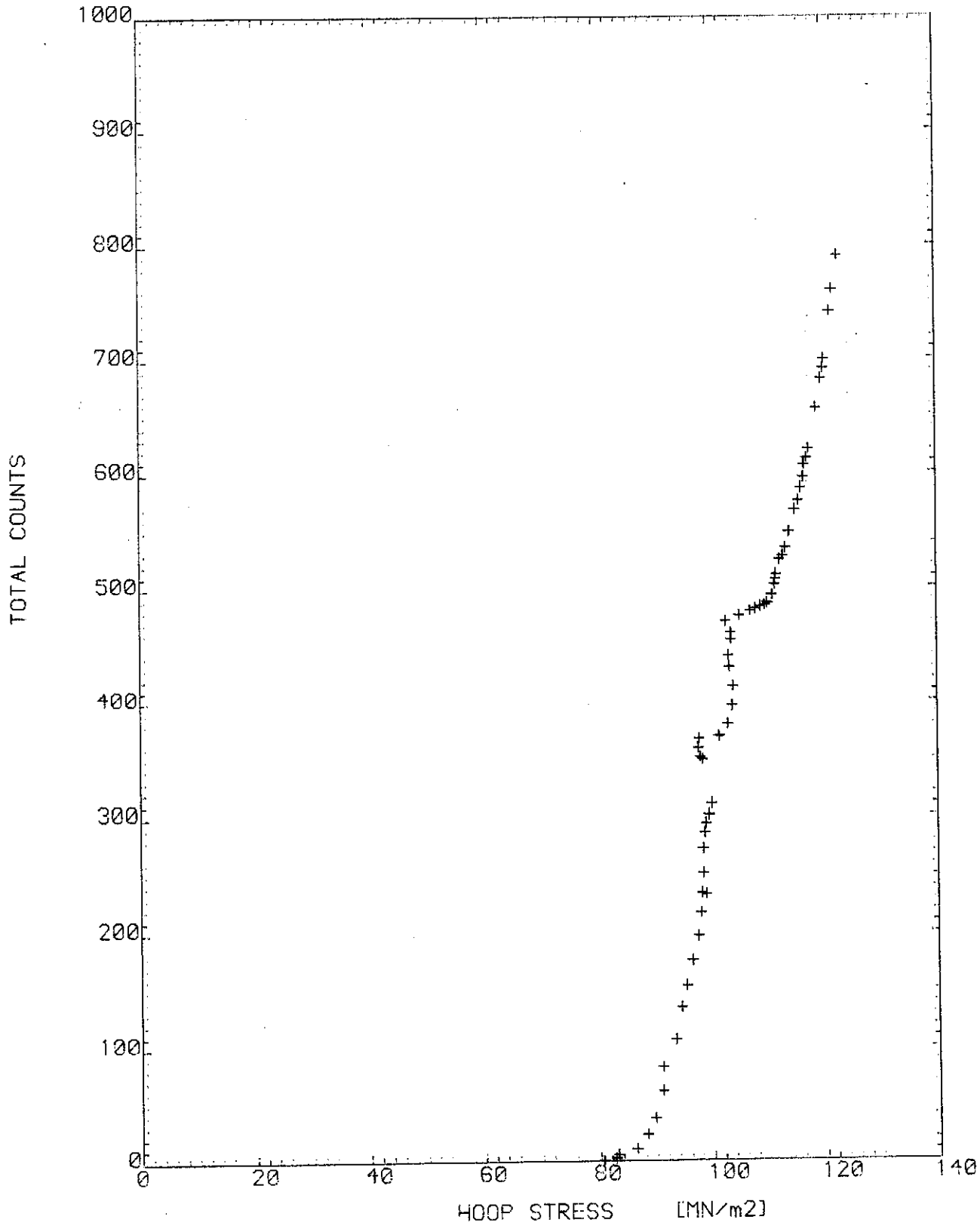

Fig.(F.2)

TOTAL COUNTS OF ACOUSTIC EMISSION, BLUE PROBE
of specimen 8B3

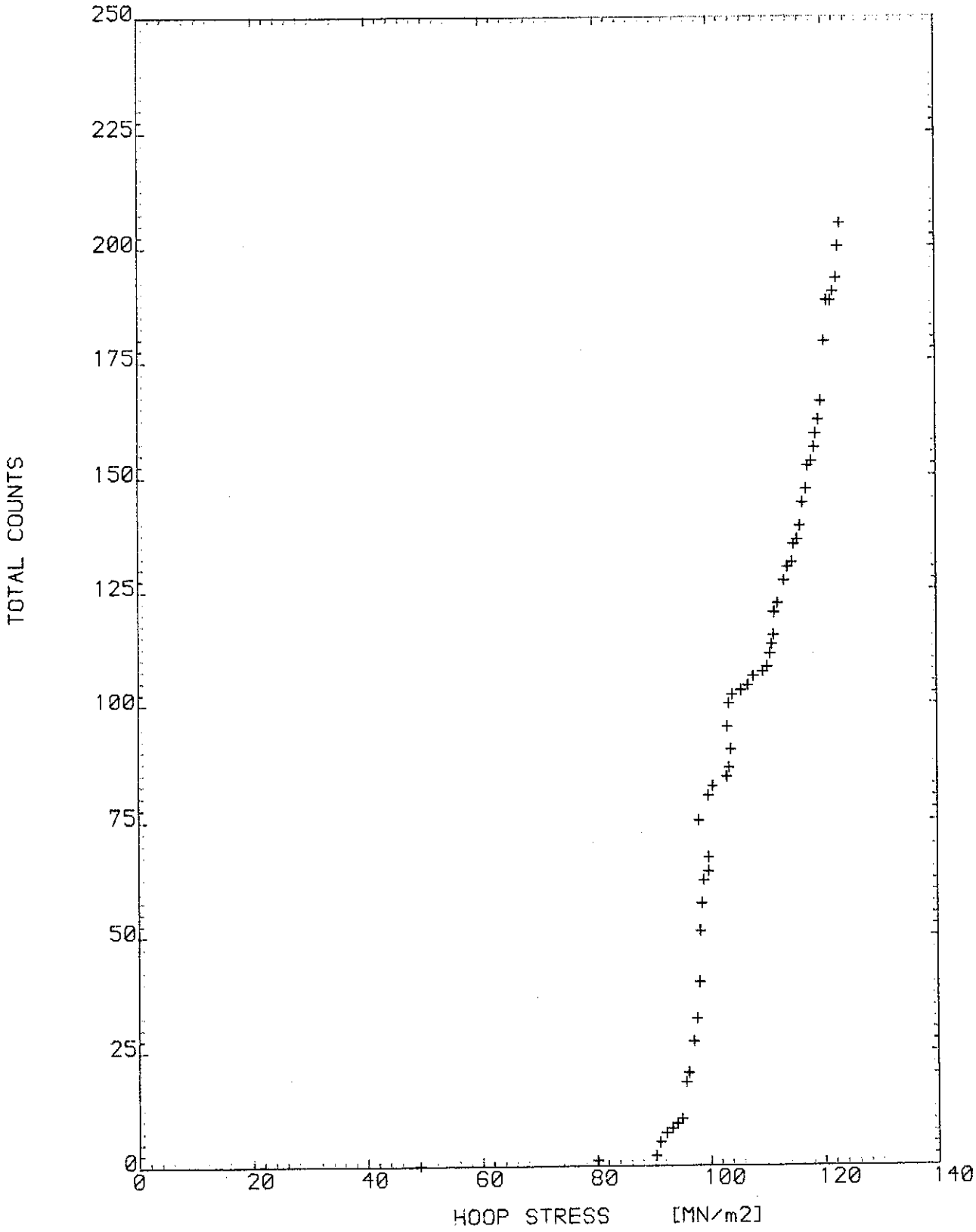

Fig.(F.3)

TOTAL COUNTS OF ACOUSTIC EMISSION, YELLOW PROBE
of specimen 8B3

The 9B3 specimen, however, was pressurized until final failure. Unfortunately, the pressure unit failed to record the pressure for this test, so the acoustic emission counts are shown versus the time in Figs. (F.4) to (F.6). As expected, the energy released in the form of stress waves in this test is much higher than that released by the previous specimen which was not taken to total failure. It is also noticed that the red probe, which was located in the failure area, gave higher response than the blue and the yellow probes which were relatively away from the damaged place, Fig. (E.7). The acoustic emission events generally accumulated a relatively steady rate with increasing load up to the ultimate load, where the fibre fractures were clearly audible.

The acoustic emission technique and the results obtained from the tests are still open for discussion, but for the purpose of this thesis it is enough to say that the degradation started in the tested specimens when the non-linear response started. This was clear from the acoustic emission charts of Figs. (F.2) to (F.6) where early acoustic emissions indicate the beginning of failure or irreversible damage. No emission, however, means that damage is not occuring and the structure is safe under the applied loading.

To conclude, it is enough to say that acoustic emission technique may offer a means to assess the degradation and the failure of composite materials, but the results obtained from the technique need interpretation. In addition, although the test equipment are not complicated, the test itself is troublesome as a quiet testing room is required to eliminate the effects of other noise sources.

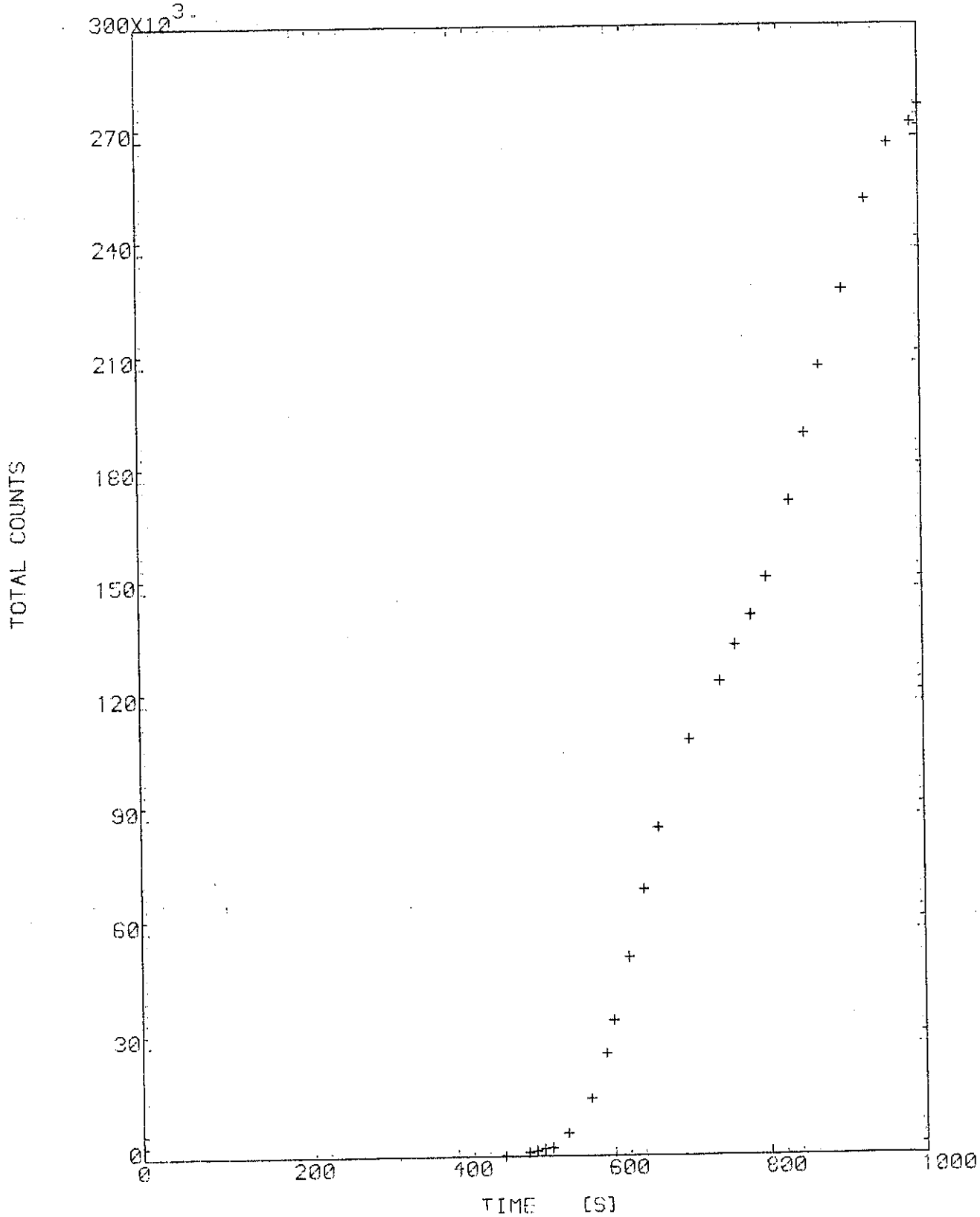

Fig.(F.4)

TOTAL COUNTS OF ACOUSTIC EMISSION, RED PROBE
of specimen 9B3

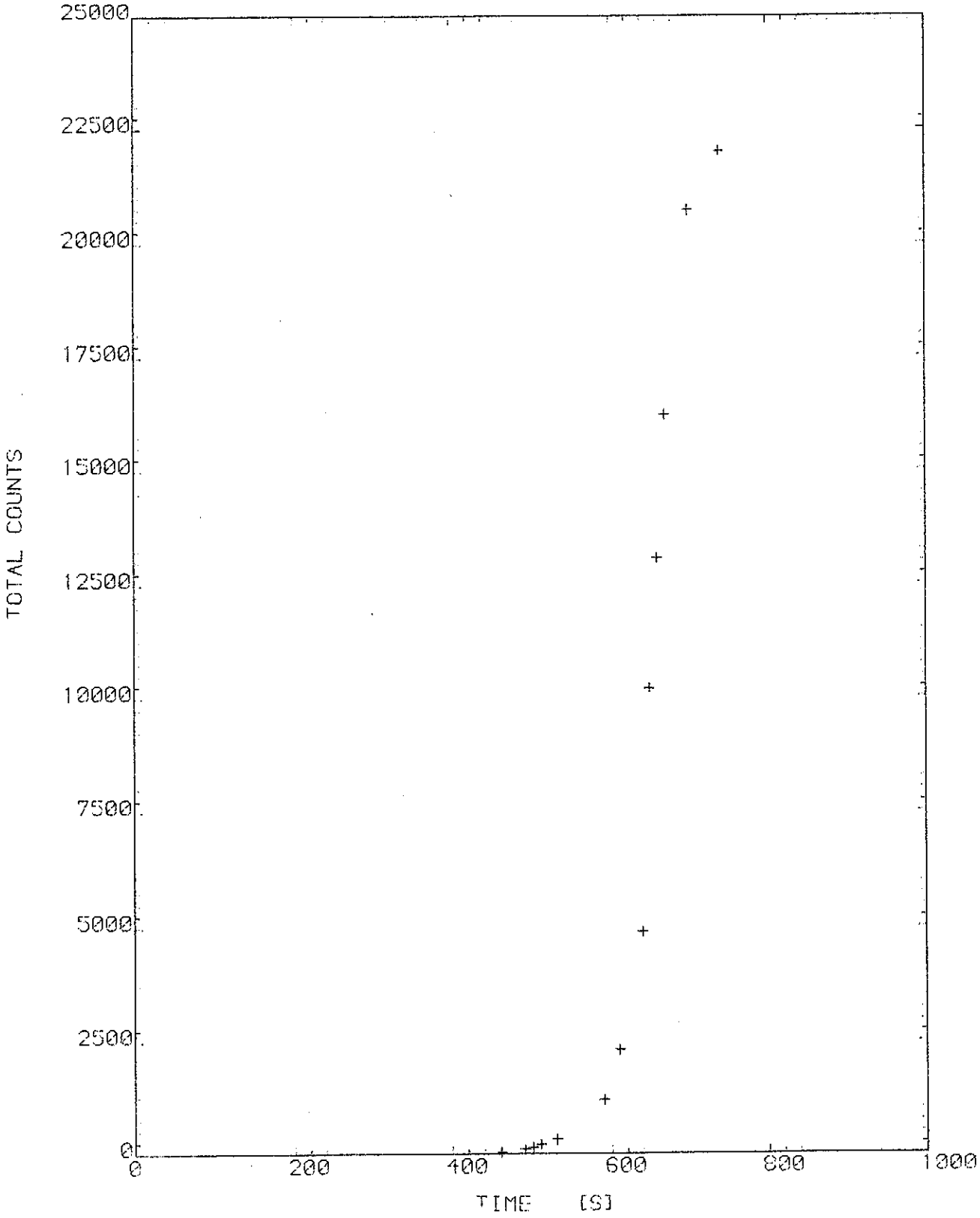

Fig.(F.5)
TOTAL COUNTS OF ACOUSTIC EMISSION, BLUE PROBE
of specimen 9B3

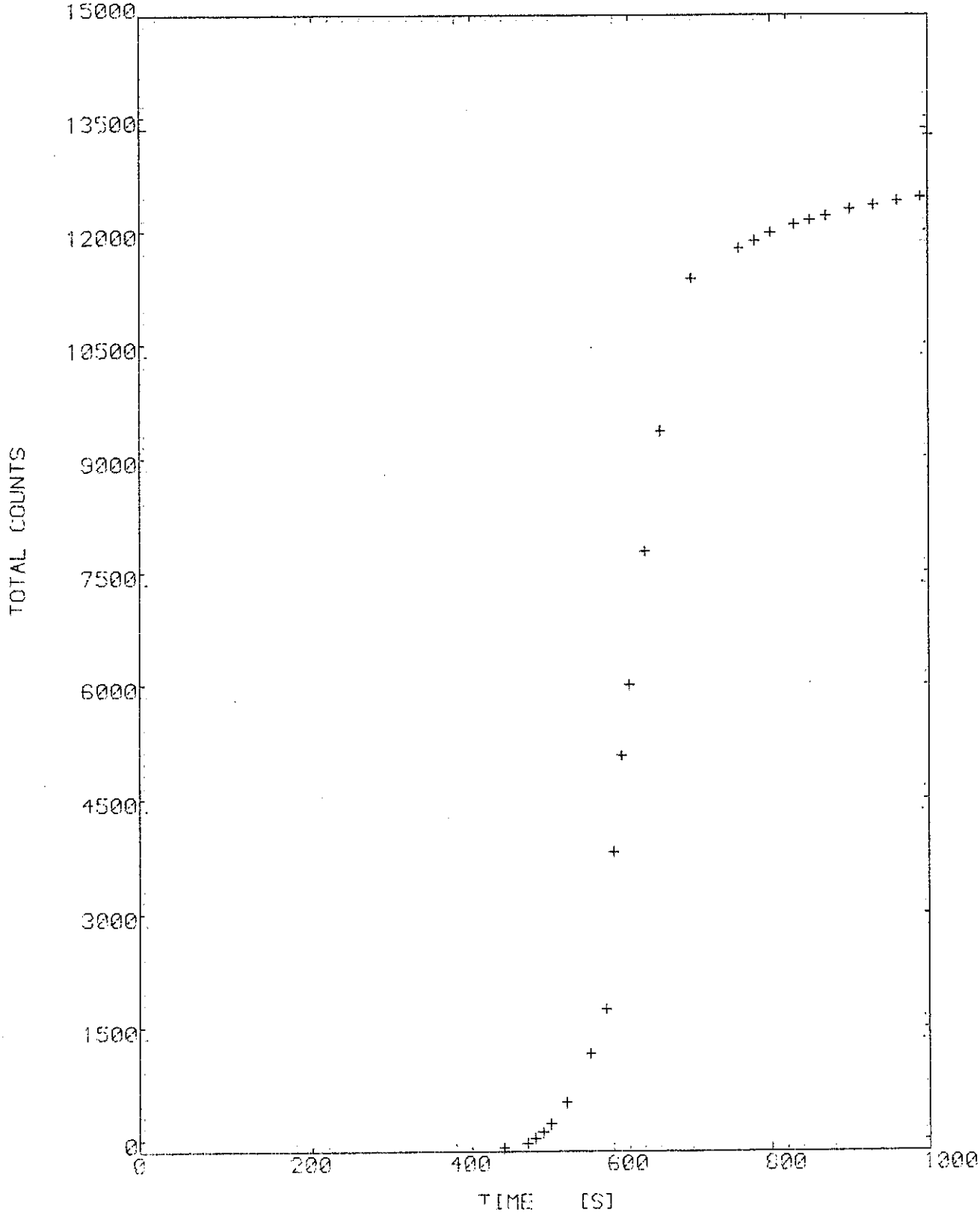

Fig.(F.6)

TOTAL COUNTS OF ACOUSTIC EMISSION, YELLOW PROBE
of specimen 9B3

APPENDIX G

PHOTOMICROGRAPHIC STUDY OF FAILURE

G.1 SCANNING ELECTRON MICROSCOPY

The scanning electron microscope (SME) images topographical details with maximum contrast and depth of field by the detection, amplification, and display of secondary electrons, (Ref. 229). The specimen under examination is scanned by a small-diameter electron probe which gives rise to secondary-emission from the specimen. This secondary-emission current is detected and causes a picture to be projected on a cathode-ray screen. The instrument has very high resolving power compared with the optical microscope due to the shorter wave-length associated with electron waves.

Because of its great depth of focus, the SEM has proved particularly useful in the examination of failure of fibre-reinforced plastics, (Ref. 215).

G.2 SAMPLE PREPARATION

While the surface of the sample is viewed directly in the SEM, the specimen size is limited by the specimen chamber. This means that large specimens must be cut into small pieces. Whether this is the case or not, all the samples examined in this study were sections of tubular specimens taken perpen-dicular to the surface of the tube in different directions (axial, hoop and winding directions). This implied that the SEM samples must be cut from the original test specimens to examine a representative damage. Cutting the microscope samples from the test specimens produces further damage which confuse the examination of the original damage. When this problem was discussed with the Materials Department it was suggested that a special technique needed to be developed to overcome this difficulty. This suggestion was not appealing as it would change the direction of the original study and the concentration would be on a supernumerary matter.

To know the level of damage produced by cutting it was decided to examine samples cut from both damaged and without damage specimens. On the other hand, two different cutting instruments were employed. These were namely: the low speed saw and the ultrasonic cutter. The low speed saw used was ISOMET 11-1180 type, Fig. (G.1), whose cutting tool is a diamond wafering circular blade which is immersed in mineral spirits to a level approximately 6 mm, and its speed ranges from 25-315 r.p.m. The sample is cut when it touches the blade near the top, so a weight is needed to press the sample down to contact the blade.

The damaged caused by cutting can be controlled in two ways: by controlling the cutting weight and/or the rotating speed. In general, the heavier the weight the greater the surface damage. Also, faster speeds tend to damage the specimen surface. The cutting of the samples was conducted at low speed using light weight.

The ultrasonic drill is designed to effectively machine hard and brittle materials. The machine uses very fine abrasive grains suspended in a liquid, such as water, between the tool and the workpiece. The tool, which is usually made of brass or mild steel, oscillates at ultrasonic frequency. The tool motion is produced by being part of a sound wave energy transmission line that causes the tool material to change its normal length by contraction and expansion. This drives the grit particles into the workpiece to remove the material according to the pattern which is controlled by the tool shape and counter. It is the abrasive which does the cutting, so it should have hardness greater than that of the workpiece material. Silicon carbide, boron carbide, and diamond are suitable for this purpose. The soft material of the tool wears very rapidly, but yields good results. The advantages of ultrasonic machining include the absence of thermal stresses, low tooling costs, and high precision work.

When the ultrasonic cutter was used to cut the GRP samples it was good for the glass but not good for the resin as its hardness (Rockwell) is only about 80, (Ref. 95). This resulted in damage in the matrix as will be shown later in the photomicrograph. Thus, only one sample, sample (U), was cut using this instrument, whereas the rest of the samples were cut with the low speed saw which gave better surfaces.

G.3 PHOTOMICROGRAPHS OF THE SAMPLES

Since there was some uncertainity about the damage caused by cutting, it was decided to cut a smple from a virgin specimen and another one from a tested specimen to compare the photomicrographs of the cross sections of these two samples to see whether they differ or not. Sample (D) was cut from tube B2 (Appendix A) perpendicular to the surface of the tube in the axial direction. Sample (E) was cut from a specimen of tube B3 which was tested under internal pressure. Sample (E) was also an axial cross section. The photomicrographs of these two samples are shown in Figs. (G.2) and (G.3) respectively.

The SEM micrograph of the untested sample (D), Fig. (G.2), showed that voids existed in the virgin tubes. These voids were the centres for cracks propagation as shown in Fig. (G.3).

Later, sample (F) was cut from untested portion of tube B3 but the section examined was taken parallel to the winding direction.

Since tube B3 is an angle ply tube of $\pm 45^{\circ}$ winding angle, the cross section showed fibres perpendicular and parallel to its plane, Fig. (G.4). This figure and Fig. (G.5), which is for the same sample but with greater magnification, show that voids appear in the matrix and between the fibres.

After these examinations, samples from specimen 7B3 were cut from areas damaged by internal pressurization test. These areas were determined from the ultrasonic C-scan trace of the specimen, Fig. (E.5). Four samples of this specimen were cut: sample (A), in the axial direction; sample (c), in the circumferential direction; sample (B), in the winding direction and sample (U), also in the winding direction but was cut by the ultrasonic cutter. The photomicrographs of these cross sections are shown in Figs. (G.6) - (G.11). From these figures the cracks in the matrix can be seen in the damaged areas. Also debonding and delamination exist in some areas. Figs. (G.10) and (G.11) show the damage caused by the ultrasonic cutter which indicate that it is not suitable for cutting GRP samples.

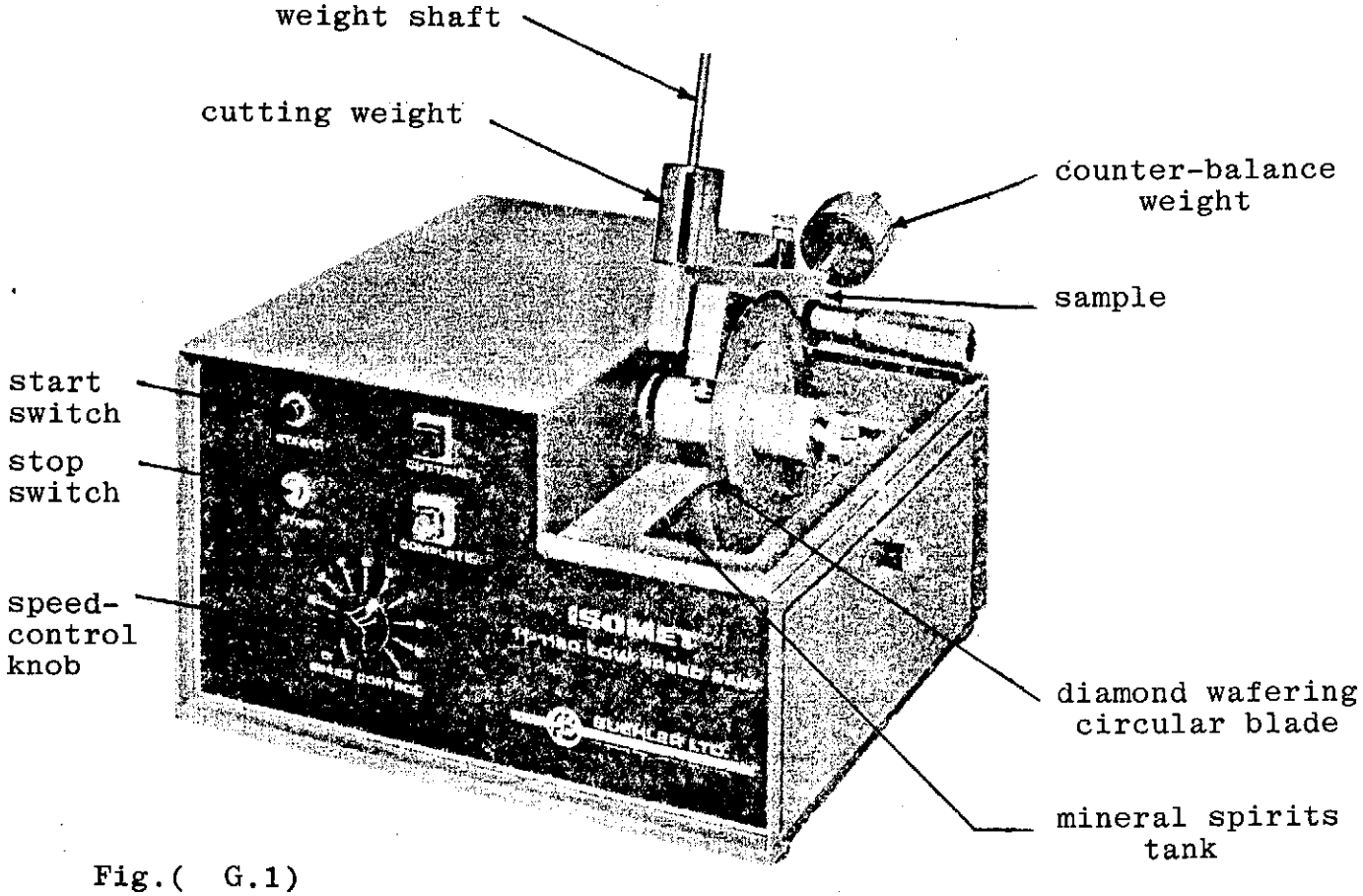

Fig.(G.1)

11-1180

ISOMET LOW SPEED SAW

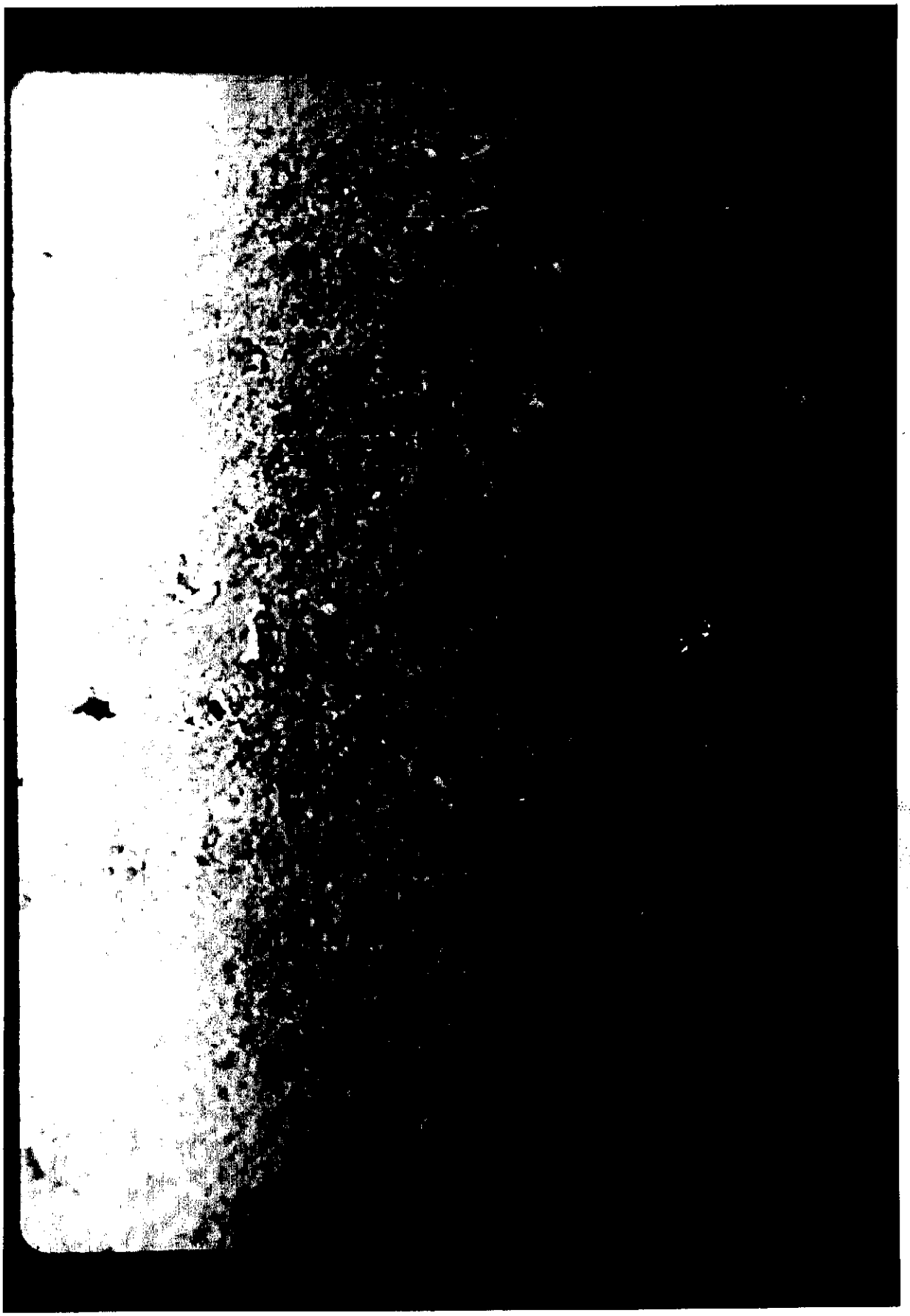

(X200)

Fig.(G.2) SEM micrograph of untested cross section (D), (cut from tube B2)

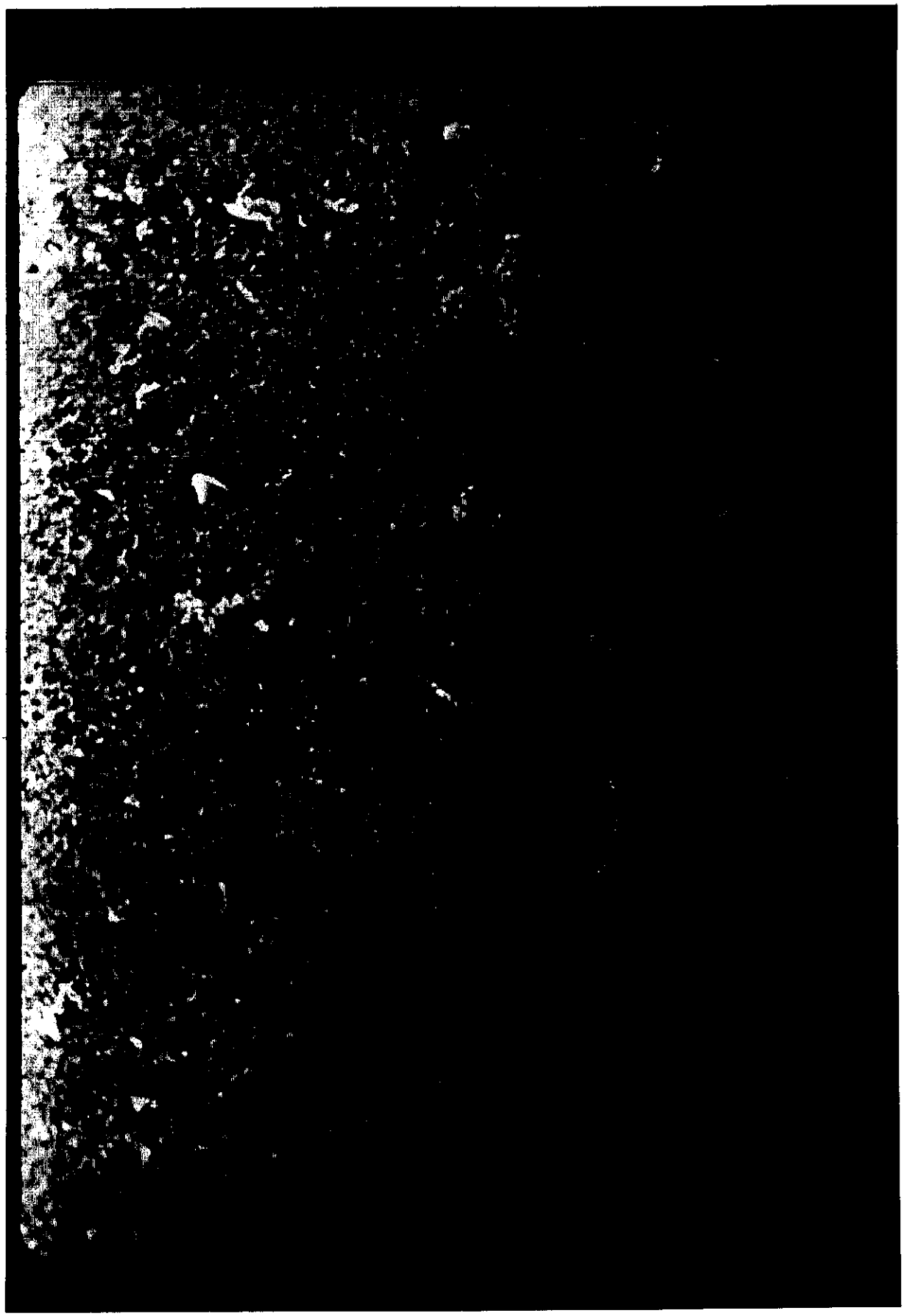

(X200)

Fig.(G.3) SEM micrograph of sample (E), (cut from a specimen of tube B3 after internal pressurization test)

(X200)

Fig.(G.4) SEM micrograph of sample (F), (cut from untested portion of tube B3)

(X500)

Fig.(G.5) SEM micrograph of sample (F) with greater magnification

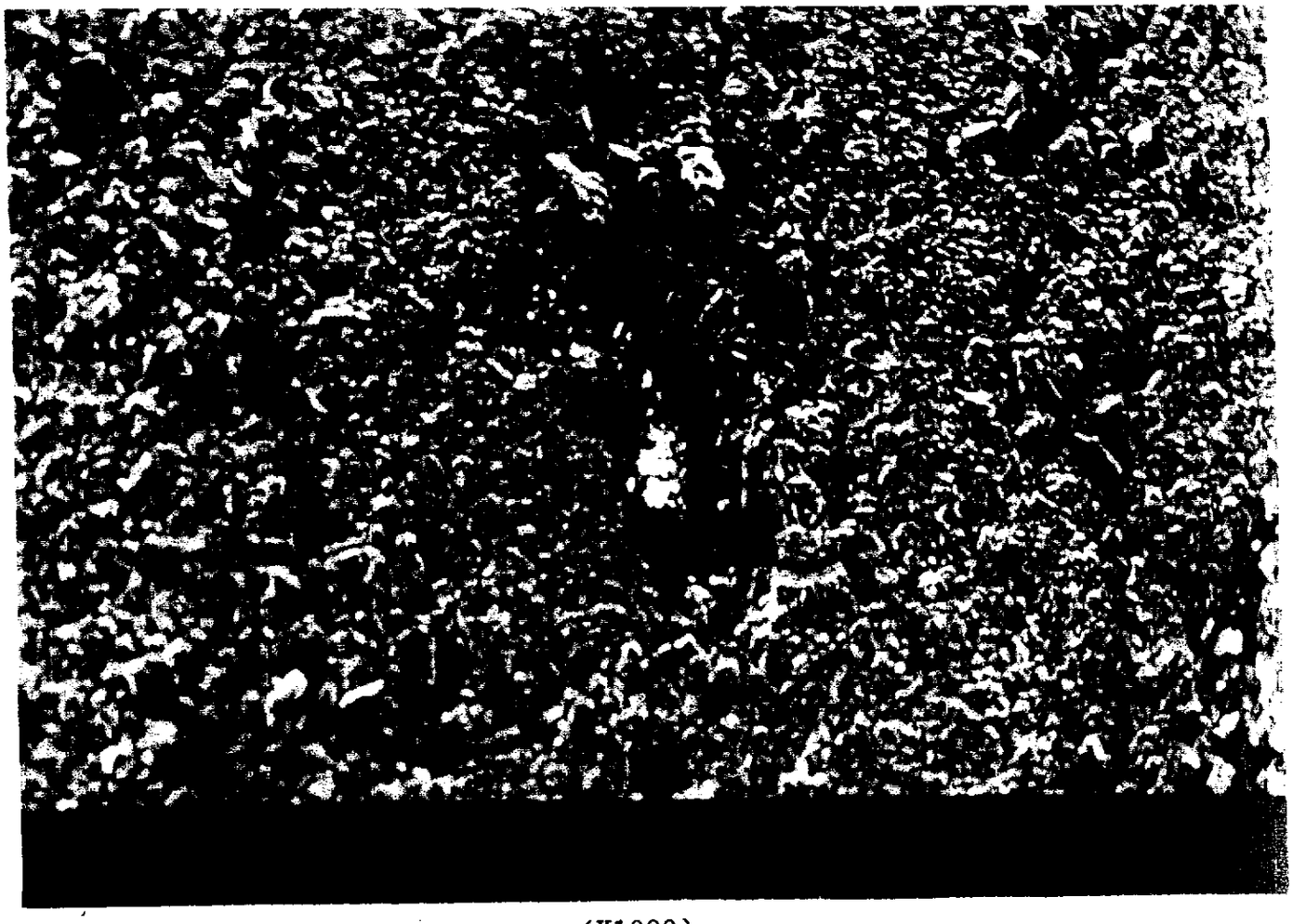

(X1000)

Fig.(G.6) SEM micrograph of sample (A)

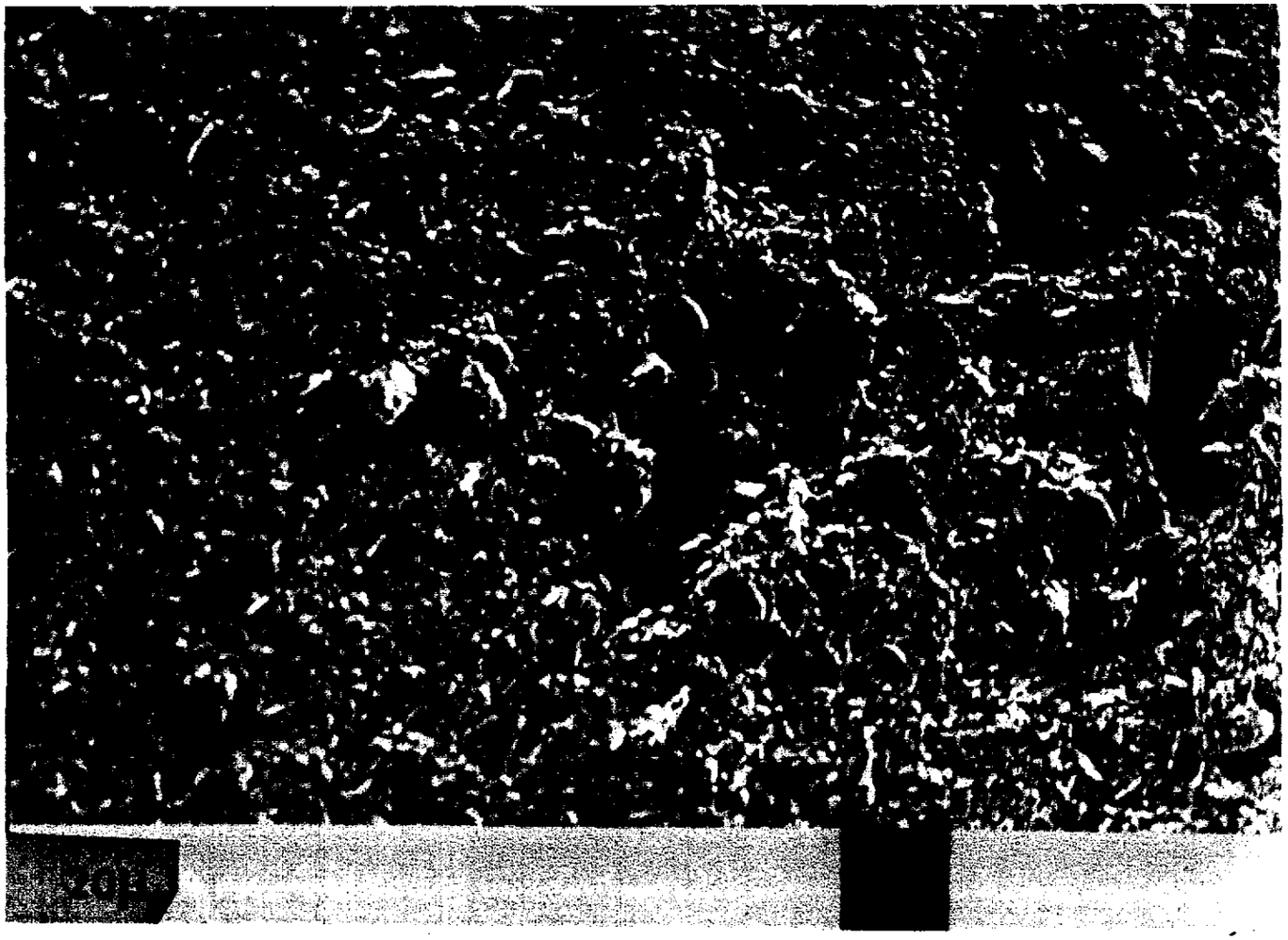

(X1000)

Fig.(G.7) SEM micrograph of sample (C)

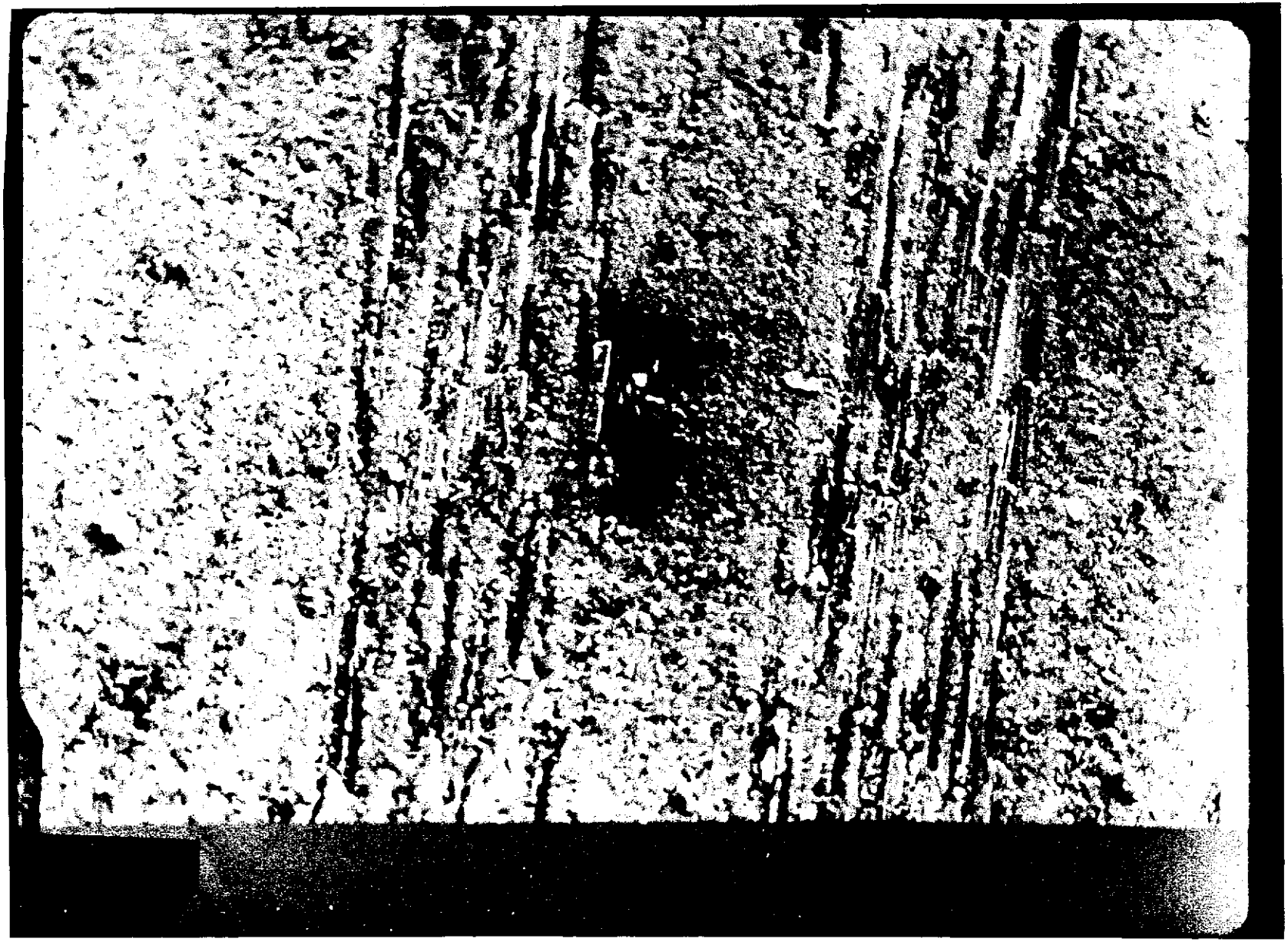

(X200)

Fig.(G.8) SEM micrograph of sample (B), (a cross section cut from specimen 7B3 in the winding direction)

(X500)

Fig.(G.9) SEM micrograph of sample (B) with greater magnification

(X200)

Fig.(G .10) SEM micrograph of sample (U), (a cross section of specimen 7B3 cut by the ultrasonic cutter in the winding direction)

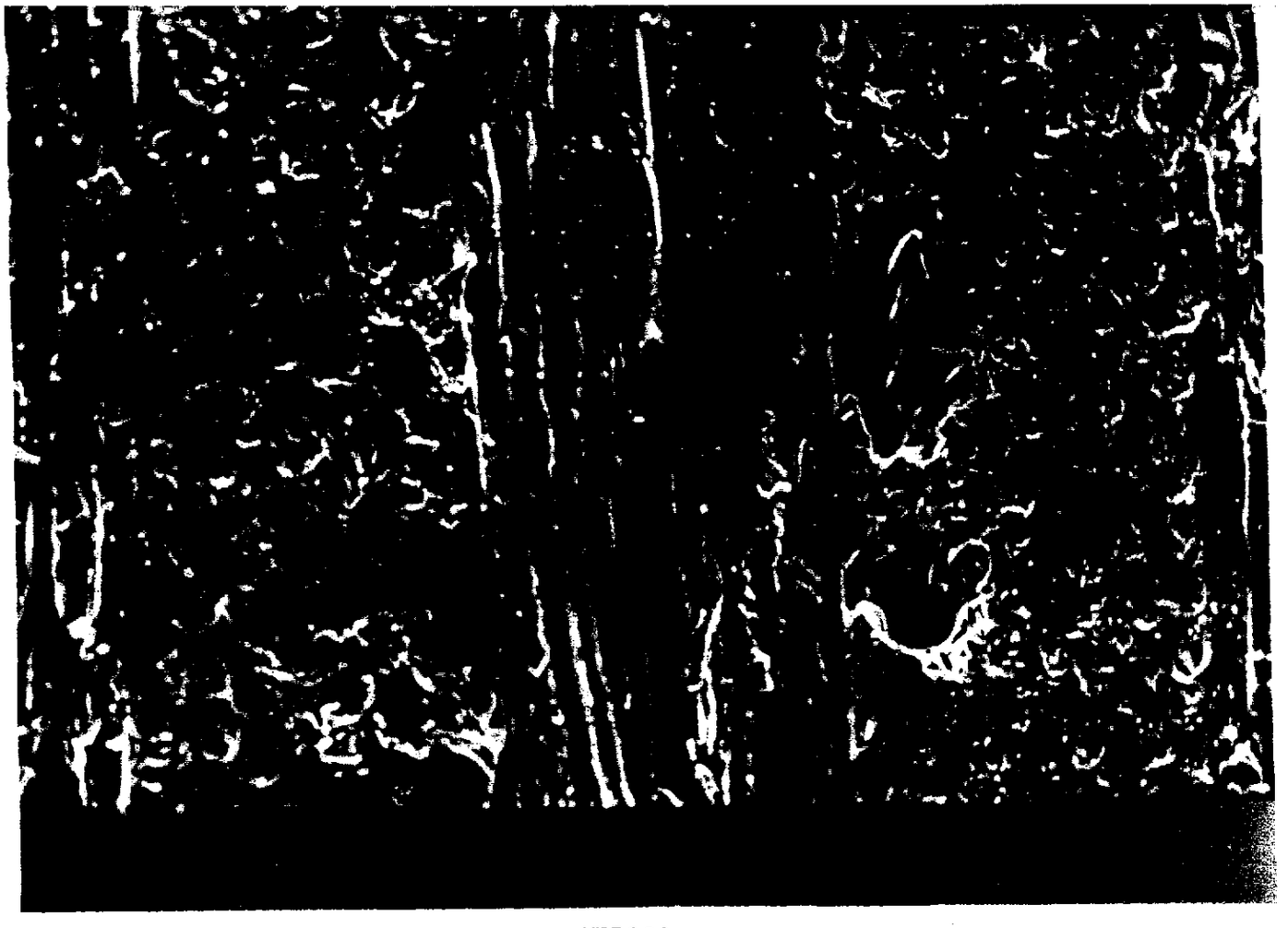

(X500)

Fig.(G.11) SEM micrograph of sample (U) with greater magnification

APPENDIX H

CALCULATION OF BUCKLING LOAD OF COMPOSITE CYLINDERS

H.1 THE COMPUTER PROGRAM

This computer program was developed in accordance with the analysis of Sec. 3.6. It is written in FORTRAN programming language and consists of a master segment and the following subroutines :

a) Subroutine LAMINATION: which uses the lamination theory to calculate the matrices A, B and D.

b) Subroutine TRANSFORMATION: which deals with the transformation of the properties of a layer to the laminate axes.

c) Subroutine MINI: this subroutine finds the smallest of the roots of equation (3.6.24).

d) Subroutine MINIMUM: this subroutine finds the buckling load which is the lowest value of N_o taken from the set of (n x m) values, where n is the number of waves in the circumferential direction and m is the number of half-waves along the length of the cylinder.

e) Standard subroutines :

FMOVE: shift an array in another array

F01AAF: calculates the inverse of a matrix

F01CKF: calculates the multiplication of two matrices

C02AEF: finds the roots of a real polynomial

X02AAF: calculates the tolerance required for C02AEF.

H.2 DATA REQUIRED BY THE PROGRAM

The data cards must be in the following order where all numbers are in a free format mode :

1st data card :

NL R AL AKX AKY AKXY MM NN

where :

NL = number of layers, (max. 8)

R = mean radius of the cylinder

AL = length of the cylinder

AKX, AKY and AKXY are the ratio of loads

MN and NN are the maximum values for m and n.

2nd data card

EL ET GLT PLT

where :

EL = Young's modulus in the fibre direction

ET = Young's modulus in the transverse direction

GLT = Shear modulus

PLT = Poisson's ratio

3rd set of cards

These are NL cards, one card for each layer :

NL Cards

T_L	THET	NS	KIND
T_L	THET	NS	KIND
--------			

where :

TL = thickness of layer

THET = angle of layer with x-axis (in degree)

NS = number of sub-layer for this layer

KIND = 2 for angle-ply layer, othewise KIND = 1

N.B. See previous Programs for NS and KIND

H.3 THE PROGRAM LISTING

```
      LIBRARY(SUBGROUPNAGF)
      PROGRAM(STIF)
      COMPRESS INTEGER AND LOGICAL
      INPUT 1=CR0
      OUTPUT 2=LP0
      END
C
      MASTER BUCKLING OF CYLINDERS
C     ----------------------------
      COMMON/BLOCK2/PI,NL,EL,ET,GLT,PLT,HB,TL(8),THET(8),
     *THETA(8),NS(8),KIND(8)/BLOCK3/A(3,3),B(3,3),D(3,3),WK(3)
     */BLOCK4/REM(21,20)
      DIMENSION F(4),RE(4),T(4)

1     FORMAT(I0,5F0.0,2I0)
2     FORMAT(4F0.0)
3     FORMAT(2F0.0,2I0)
11    FORMAT(' BUCKLING OF CYLINDER OF R= ',1PE12.4,'   H= ',1PE12.4/
     *' AND ',I2,' LAYERS OF ',4(0PF5.0,'/'),' DEG.')
15    FORMAT(' WITH LOAD RATIO: NX : NY : NXY = ',0PF4.1,' : ',0PF4.1,
     *' : ',0PF4.1/)
12    FORMAT(/)
17    FORMAT(/' SPECIMEN WILL BUCKLE AT LOAD  NO=',1PE12.4,
     *' (N= ',I2,' ,M= ',I2,' )')
18    FORMAT(/' BUCKLING LOADS:   NX=',1PE12.4,' NY=',1PE12.4,' NXY=',
     *1PE12.4)
19    FORMAT(/' BUKLING STRESSES: SX=',1PE12.4,' SY=',1PE12.4,
     *' SXY=',1PE12.4)

      READ(1,1)NL,R,AL,AKX,AKY,AKXY,MM,NN
      READ(1,2)EL,ET,GLT,PLT
      READ(1,3)(TL(K),THET(K),NS(K),KIND(K),K=1,NL)
      PI=4.*ATAN(1.)
      CALL LAMINATION
      WRITE(2,11)R,HB,NL,(THET(K),K=1,NL)
      WRITE(2,15)AKX,AKY,AKXY
      P1=.1E0
      TOL=X02AAF(P1)
      M=1
      N=0
      NNN=N+1
21    CONTINUE
      G=M*PI*R/AL
      G2=G*G
      G3=G2*G
      G4=G3*G
      GN=G*N
      G2N=G2*N
```

```
      G3N=G3*N
      N2=N*N
      N3=N2*N
      GN2=G*N2
      GN3=G*N3
      G2N2=G2*N2
      R2=R*R
      F11=-G2*A(1,1)-GN*(A(1,3)+A(3,1)-B(1,3)/R)-N2*(A(3,3)-B(3,3)/R)
      F12=-G2*(A(1,3)+B(1,3)/R)-GN*(A(1,2)+A(3,3)+B(3,3)/R)-N2*A(3,2)
      F13=-G3*B(1,1)/R-G2N/R*(2.*B(1,3)+B(3,1))-GN2/R*(B(1,2)+2.*B(3,3))
     ;     -N3/R*B(3,2)-G*(A(1,2)-B(1,2)/R)-N*(A(3,2)-B(3,2)/R)
      F21=-G2*(A(3,1)+B(3,1)/R)-GN*(A(2,1)+A(3,3)+B(2,1)/R-D(3,3)/R2)
     ;      -N2*(A(2,3)-D(2,3)/R2)
      F22=-G2*(A(3,3)+2./R*B(3,3)+D(3,3)/R2)
     ;     -GN*(A(2,3)+2./R*B(2,3)+D(2,3)/R2+A(3,2)+B(3,2)/R)
     ;     -N2*(A(2,2)+B(2,2)/R)
      F23=-G3/R*(B(3,1)+D(3,1)/R)-G2N/R*(B(2,1)+D(2,1)/R+2.*B(3,3)
     ;     +2./R*D(3,3))-GN2/R*(2.*B(2,3)+2./R*D(2,3)+B(3,2)+D(3,2)/R)
     ;     -N3/R*(B(2,2)+D(2,2)/R)-G*(A(3,2)-D(3,2)/R2)
     ;     -N*(A(2,2)-D(2,2)/R2)
      F31=-G3/R*B(1,1)-G2N/R*(B(1,3)-D(1,3)/R+2.*B(3,1))
     ;     -GN2/R*(2.*B(3,3)-2./R*D(3,3)+B(2,1))
     ;     -N3/R*(B(2,3)-D(3,3)/R)-G*A(2,1)-N*A(2,3)
      F32=-G3/R*(B(1,3)+D(1,3)/R)-G2N/R*(B(1,2)+2.*B(3,3)+2./R*D(3,3))
     ;     -GN2/R*(2.*B(3,2)+B(2,3)+D(2,3)/R)
     ;     -N3/R*B(2,2)-G*(A(2,3)+B(2,3)/R)-N*A(2,2)
      F33=-G4/R2*D(1,1)-2.*G3N/R2*(D(1,3)+D(3,1))
     ;     -G2N2/R2*(D(1,2)+D(2,1)+4.*D(3,3))
     ;     -2.*GN3/R2*(D(3,2)+D(2,3))-N4/R2*D(2,2)-G2/R*(B(1,2)+B(2,1)-
     ;     D(1,2)/R)-2.*GN/R*(B(3,2)+B(2,3)-D(3,2)/R)-N2/R*(2.*B(2,2)
     ;     -D(2,2)/R)-A(2,2)+B(2,2)/R
      AA=G2*AKX+2.*GN*AKXY+N2*AKY
      BB=2.*G*AKXY+N*AKY
      CC=G*AKY
      A2=AA*AA
      A3=A2*AA
      B2=BB*BB
      C2=CC*CC
      AB=AA*BB
      AC=AA*CC
      BC=BB*CC
      AB2=AA*B2
      AC2=AA*C2
      F1=-A3+AB2+AC2
      F2=A2*(F11+F22+F33)-BC*(F12+F21)+AC*(F13+F31)-C2*F22
     ;     -F11*B2-AB*(F23+F32)
      F3=-AA*(F11*F22+F11*F33+F22*F33-F23*F32-F13*F31-F12*F21)
     ;     +CC*(F12*F23+F21*F32-F13*F22-F22*F31)
     ;     +BB*(-F12*F31-F21*F13+F11*F23+F11*F32)
      F4=F11*F22*F33+F12*F23*F31+F21*F13*F32
     ;     -F13*F22*F31-F11*F23*F32-F12*F21*F33
```

```
      IF(F1.EQ.0.0)GO TO 27
      L,LL=4
      F(1)=F1
      F(2)=F2
      F(3)=F3
      F(4)=F4
      GO TO 28
27    IF(F2.EQ.0.0)GO TO 29
      L,LL=3
      F(1)=F2
      F(2)=F3
      F(3)=F4
      F(4)=0.
      GO TO 28
29    L,LL=2
      F(1)=F3
      F(2)=F4
      F(3)=0.
      F(4)=0.
28    CONTINUE
      IFAIL=0
      CALL C02AEF(F,LL,RE,T,TOL,IFAIL)
      CALL MINI(RE,3,REM(NNN,M))
      IF(M.EQ.MM)GO TO 22
      M=M+1
      GO TO 21
22    IF(N.EQ.NN)GO TO 23
      M=1
      N=N+1
      NNN=N+1
      GO TO 21
23    CONTINUE
      CALL MINIMUM(REM,BUKL,II,JJ)
      ANX=BUKL*AKX
      ANY=BUKL*AKY
      ANXY=BUKL*AKXY
      II=II-1
      WRITE(2,17)BUKL,II,JJ
      WRITE(2,18)ANX,ANY,ANXY
      SX=ANX/HB
      SY=ANY/HB
      SXY=ANXY/HB
      WRITE(2,19)SX,SY,SXY
      STOP OK
      END
C
      SUBROUTINE LAMINATION
C     ---------------------
      COMMON/BLOCK1/T(3,3),TT(6,4)/BLOCK2/PI,NL,EL,ET,GLT,PLT,HB,
     *TL(8),THET(8),THETA(8),NS(8),KIND(8)
     */BLOCK3/A(3,3),B(3,3),D(3,3),WK(3)
```

```
      DIMENSION C(4,1),CK(3,3,8),SK(3,3,8),Z3(21),HS(20),HC(20),TI(3,3),
     *TK(3,3,8),TTC(6,1),QK(3,3,8),Z(21),Z2(21),Z1(20)
      HB=0.
      DO 12 K=1,NL
      THETA(K)=PI*THET(K)/180.
      SK(1,1,K)=1./EL
      SK(2,2,K)=1./ET
      SK(3,3,K)=1./GLT
      SK(1,2,K),SK(2,1,K)=-PLT/EL
      CALL FMOVE(SK(1,1,K),T,9)
      IFAIL=0
      CALL F01AAF(T,3,3,TI,3,WK,IFAIL)
      CALL FMOVE(TI,CK(1,1,K),9)
      C(1,1)=CK(1,1,K)
      C(2,1)=CK(1,2,K)
      C(3,1)=CK(2,2,K)
      C(4,1)=CK(3,3,K)
      AM=COS(THETA(K))
      AN=SIN(THETA(K))
      CALL TRANSFORMATION(AM,AN)
      CALL FMOVE(T,TK(1,1,K),9)
      IFAIL=0
      CALL F01CKF(TTC,TT,C,6,1,4,WK,3,1,IFAIL)
      QK(1,1,K)=TTC(1,1)
      QK(1,2,K),QK(2,1,K)=TTC(2,1)
      QK(1,3,K),QK(3,1,K)=TTC(3,1)
      QK(2,2,K)=TTC(4,1)
      QK(2,3,K),QK(3,2,K)=TTC(5,1)
      QK(3,3,K)=TTC(6,1)
12    CONTINUE
      DO 2 K=1,NL
      HB=HB+TL(K)
2     CONTINUE
      Z(1)=-HB/2.
      Z2(1)=Z(1)**2
      Z3(1)=Z(1)**3
      KK=2
      DO 15 K=1,NL
      MM=KK+NS(K)-1
      TLL=TL(K)/NS(K)
      DO 46 M=KK,MM
      Z(M)=Z(M-1)+TLL
      Z2(M)=Z(M)**2
      Z3(M)=Z(M)**3
46    CONTINUE
      KK=KK+NS(K)
15    CONTINUE
      DO 16 K=1,MM-1
      Z1(K)=(Z(K+1)+Z(K))/2.
      HS(K)=Z2(K+1)-Z2(K)
      HC(K)=Z3(K+1)-Z3(K)
```

```
16    CONTINUE
      DO 18 I=1,3
      DO 18 J=1,3
      NN=0
      MM=0
      LL=0
      A(I,J)=0.
      B(I,J)=0.
      D(I,J)=0.
      DO 19 K=1,NL
      A(I,J)=A(I,J)+QK(I,J,K)*TL(K)
      KKK=KIND(K)
      GO TO(121,122),KKK
121   NN=MM+1
      MM=NN
      GO TO 123
122   IF(LL.EQ.2)GO TO 126
      LL=LL+1
      NN=NN+1
      GO TO 127
126   LL=1
      NN=MM+1
127   MM=NN+2*NS(K)-2
123   DO 124 M=NN,MM,2
      B(I,J)=B(I,J)+QK(I,J,K)*HS(M)
      D(I,J)=D(I,J)+QK(I,J,K)*HC(M)
124   CONTINUE
19    CONTINUE
      B(I,J)=B(I,J)/2.
      D(I,J)=D(I,J)/3.
18    CONTINUE
      RETURN
      END
C
      SUBROUTINE TRANSFORMATION(AM,AN)
C     --------------------------------
      COMMON/BLOCK1/T(3,3),TT(6,4)
      DO 1 I=1,3
      DO 1 J=1,3
1     T(I,J)=0.
      DO 2 I=1,6
      DO 2 J=1,4
2     TT(I,J)=0.
      AM2=AM**2
      AN2=AN**2
      AM3=AM**3
      AN3=AN**3
      AM4=AM2**2
      AN4=AN2**2
      AMAN=AM*AN
      AMAN2=2.*AMAN
```

```
      AM2AN2=AM2*AN2
      AMAN22=AM2-AN2
      T(1,1),T(2,2)=AM2
      T(1,2),T(2,1)=AN2
      T(1,3)=-AMAN2
      T(2,3)=AMAN2
      T(3,1)=AMAN
      T(3,2)=-ANAN
      T(3,3)=AMAN22
      TT(1,1),TT(4,3)=AM4
      TT(1,2),TT(4,2)=2.*AM2AN2
      TT(1,3),TT(4,1)=AN4
      TT(1,4),TT(4,4)=4.*AM2AN2
      TT(2,1),TT(2,3),TT(6,1),TT(6,3)=AM2AN2
      TT(2,2)=AM4+AN4
      TT(2,4)=-TT(1,4)
      TT(3,1)=-AM3*AN
      TT(3,2)=AMAN*AMAN22
      TT(3,3)=AM*AN3
      TT(3,4)=2.*TT(3,2)
      TT(5,1)=-TT(3,3)
      TT(5,2)=-TT(3,2)
      TT(5,3)=-TT(3,1)
      TT(5,4)=-TT(3,4)
      TT(6,2)=-TT(1,2)
      TT(6,4)=AMAN22**2
      RETURN
      END
C
      SUBROUTINE MINI(A,N,X)
C     ----------------------
      DIMENSION A(N)
      X=1.E50
      DO 4 I=1,N
      IF(A(I).LE.0.0)GO TO 3
      Y=A(I)-X
      IF(Y)1,1,3
1     X=A(I)
3     CONTINUE
4     CONTINUE
      RETURN
      END
C
      SUBROUTINE MINIMUN(A,X,II,JJ)
C     ---------------------------------
      COMMON/BLOCK4/REM(21,20)
      X=1.E50
      DO 4 I=1,21
      DO 4 J=1,20
      IF(REM(I,J).LE.0.0)GO TO 3
      Y=REM(I,J)-X
```

```
      IF(Y)1,1,3
1     X=REM(I,J)
      II=I
      JJ=J
3     CONTINUE
4     CONTINUE
      RETURN
      END
C
      FINISH
```

H.4 SAMPLE INPUT

```
2  39.372E-3  218.E-3   -1.  0.  0.  3  3
44.5E9  13.5E9  5.64E9  .183
.4723E-3  85.  5   2
.4723E-3 -85.  5   2
```

H.5 SAMPLE OUTPUT

```
BUCKLING OF CYLINDER OF R=   3.9372E-02   H=   9.4460E-04
AND  2 LAYERS OF   85./ -85./
WITH LOAD RATIO: NX : NY : NXY = -1.0 :  0.0 :  0.0


SPECIMEN WILL BUCKLE AT LOAD  NO=  1.1998E 05 (N=  3 ,M=  2 )

BUCKLING LOADS:   NX= -1.1998E 05 NY=  0.0000E 00 NXY=  0.0000E 00

BUKLING STRESSES: SX= -1.2701E 08 SY=  0.0000E 00 SXY=  0.0000E 00
```

APPENDIX I

ULTIMATE STRENGTH CALCULATIONS OF LAMINATED COMPOSITE STRUCTURES

I.1 INTRODUCTION

This Appendix describes the computer program which was developed to predict the progressive failure of laminated structures to arrive at the ultimate failure of such structures. The theory used in the program is given in Sec. 3.4 where a modified maximum strain failure criterion is proposed for the failure of a lamina in a laminated structure, and in Sec. 4.3 where a method for the post-failure behaviour is also proposed.

The linear and non-linear analyses of the program are those of the computer program of Appendix C. The reason for not including this program in that of Appendix C is the size of that program where its core reached about 36K.

I.2 THE COMPUTER PROGRAM

This program is also written in FORTRAN and consists of the following segments :

a) The MASTER segment forms the lamination theory and calculates the stress-strain relations in the layers of the laminate. The non-linear analysis is also dealt with in this segment.

b) Subroutine TRANSFORMATION transforms the layer properties to the laminate axes.

c) Subroutine AXES draws the axes for the laminate stress-strain curve.

d) Subroutine NONLINEAR calculates the cubic splines for the non-linear data.

e) Subroutine MAXIMUM VALUE finds the biggest number in an array.

f) Supporting subroutines: the standard subroutines used are those listed in Appendix C.

I.3 DATA INPUT DESCRIPTION

1st_data_card : (FORMAT: 8I0, 2F0.0)

NM NL IP NON1T NON1C NON2T NON2C NON12
R DEF

these are as defined in Appendix C, Sec. C.4, 1st data card except that IP = 1 if the laminate stress-strain curve is to be plotted, otherwise IP = 0.

2nd_set_of_cards : (FORMAT: I0, 2F0.0, 2I0)

This set is similar to the 3rd set of cards in the program of Appendix C, i.e.,

NL cards

L	TL	THET	NS	KIND
L	TL	THET	NS	KIND

3rd_set_of_cards: (FORMAT: 2A8, 4F0.0)

This set is similar to the 4th set of cards in the program of Appendix C, i.e.,

NM cards

AA	ELL	ETT	GGLT	PLT

4th_set_of_cards : (FORMAT: 5F0.0)

This set is similar to the 6th set of cards of Appendix C program, i.e.,

NM cards

EXT	EXC	EYT	EYC	EST

5th_set_of_cards : (FORMAT: 6F0.0)

This is one card describing the external load and the load increment, (see 9th card in Appendix C program) :

SX SY SXY DSX DSY DSXY

6th set of cards :

This is two cards describing the information needed for the stress-strain plot, if IP = 0, this set is omitted.

The first card : (FORMAT: 7F0.0, 6I0)

SXMIN SXMAX SYMIN SYMAX XL YL FACTOR
NX NY NNN I1 I2 I3

The second card : (FORMAT: 20A4)

IT

where :

SXMIN, SXMAX, SYMIN, SYMAX, XL, YL, NX, NY are as defined in Appendix C ;

FACTOR is a factor to scale the stress values;

NNN = 1 if the load in x-direction is to be plotted;

= 2 if the load in y-direction is to be plotted;

= 3 if the shear load is to be plotted;

I1 = 1 if the strain in x-direction is to be plotted, otherwise I1 = 0;

I2 = 1 if the strain in y-direction is to be plotted, otherwise I2 = 0;

I3 = 1 if the shear strain is to be plotted, otherwise I3 = 0; and

IT is the title for the stress-strain curve.

7th set of cards :

This is similar to the 10th set of cards of the program of Appendix C, i.e.,

for every non-linear curve

NP NC		(FORMAT: 2I0)
X(I)	I = 1, NP	(FORMAT: 10F0.0)
Y(I)	I = 1, NP	(FORMAT: 10F0.0)
P(I)	I = 1, NC-1	(FORMAT: 10F0.0)

I.4 THE PROGRAM LISTING

```
      LIBRARY(SUBGROUPCRAN)
      LIBRARY(SUBGROUPNAGF)
      LIBRARY(SUBGROUPGRAF)
      LIBRARY(SUBGROUPGINO)
      PROGRAM(STIF)
      COMPRESS INTEGER AND LOGICAL
      INPUT 1=CRO
      OUTPUT 2=LPO
      END
C
      MASTER STRESS CALCULATIONS
C     -------------------------
      COMMON/BLOCK1/T(3,3),TT(6,4)/BLOCK7/SPC(3,10)/
     *BLOCK6/SXMAX,SXMIN,SYMAX,SYMIN,IP,XL,YL,NX,NY,NNN,IT(20)
      DIMENSION EL(10),ET(10),PLT(10),GLT(10),C(4,1),CK(3,3,10),SK(3,3
     *,10),L(10),TL(10),THETA(10),TK(3,3,10),TTC(6,1),QK(3,3,10),Z(21),
     *Z1(20),Z2(21),HS(20),A(3,3),B(3,3),Q(3,3),S(3,3),AA(2,5),THET(10)
     *,STRN(3),KIND(10),NS(10),EP(3),STRESS(3,10),STRAIN(3,10)
     *,ELL(2),ETT(2),LF(10,3),PPLT(2),P(3,3),TI(3,3),GGLT(2),
     *P1T(10),C1T(10),P1C(10),C1C(10),P2T(10),C2T(10),P2C(10),C2C(10),
     *P12(10),C12(10),F(3),STR(3),WK(3),YP(100),X1(100),X2(100),X3(100)
     *,EXT(2),EXC(2),EYT(2),EYC(2),EST(2)
     *,PTL(10),ANDA(10),JJJ(10)
C
C     FORMATS:
C     --------
1     FORMAT(8I0,2F0.0)
2     FORMAT(2A8,4F0.0)
3     FORMAT(I0,2F0.0,2I0)
4     FORMAT(7F0.0,6I0)
5     FORMAT(6F0.0)
6     FORMAT(6I0)
7     FORMAT(20A4)
51    FORMAT(5X,'ANALYSIS OF FILAMENT-WOUND TUBE OF R= ',1PE9.3,'  AND',
     *I3,' LAYERS:'//5X,'LAYER',4X,'LAYER',7X,'LAYER',4X,'LAYER MATERIAL
     *'/6X,'NO.',3X,'THICKNESS',5X,'ANGLE',10X,'NO.'/)
52    FORMAT(6X,I2,4X,1PE9.3,4X,0PF6.2,10X,I2)
53    FORMAT(/26X,'MATERIAL PROPERTIES'//5X,'NO.',5X,
     *'MATERIAL',11X,'EL',8X,'ET',7X,'GLT',5X,'NULT')
54    FORMAT(5X,I2,4X,2A8,3(1PE10.2),2X,0PF5.3)
55    FORMAT(' EX=',1PE10.2,2X,'EY=',1PE10.2,2X,'NUXY=',0PF6.3,2X,
     *'NUYX=',0PF6.3,2X,'GXY=',1PE10.2)
56    FORMAT(3(1PE10.2))
57    FORMAT(72('-'))
58    FORMAT(/5X,'LAMINATE STRESSES:',3(1PE12.4)/5X,'LAMINATE STRAINS :'
     *,3(1PE12.4))
59    FORMAT(5X,I2,5(1PE10.2))
60    FORMAT(/5X,'NO.',3X,'EU1',7X,4HEU1',6X,'EU2',7X,4HEU2',6X,'EU12')
63    FORMAT(/5X,'LAYER NO. ',I2/5X,12('.'))
92    FORMAT(' STRESS',3(1PE10.2),'STRAIN',3(1PE10.2))
```

```
93    FORMAT(/5X,'LINEAR ANALYSIS:'/5X,16('=')/5X,'LAMINATE PROPERTIES:'
     *)
94    FORMAT(/5X,'LAMINATE PROPERTIES (SECANT MODULI):')
95    FORMAT(/' LAYER',I2,' FAILED IN MODE ',I2,' AT LOAD:',3(1PE12.4)/
     *35('*'))
97    FORMAT(//' TOTAL LAMINATE FAILURE AT LOAD:',3(1PE12.4)/31('*'))
99    FORMAT(' LAYER ',I2,' IS SIMILAR TO LAYER ',I2,' (ANGLE PLY)')
98    FORMAT(/5X,'NONLINEAR ANALYSIS:'/5X,19('='))
C
C     DATA INPUT:



C     -----------
      READ(1,1)NM,NL,IP,NON1T,NON1C,NON2T,NON2C,NON12,R,DEF
      NON=1
      IF(NON1T.EQ.0.AND.NON1C.EQ.0.AND.NON2T.EQ.0.AND.NON2C.EQ.0.
     *AND.NON12.EQ.0)NON=0
      WRITE(2,51)R,NL
      READ(1,3)(L(K),TL(K),THET(K),NS(K),KIND(K),K=1,NL)
      WRITE(2,52)(K,TL(K),THET(K),L(K),K=1,NL)
      READ(1,2)(AA(1,I),AA(2,I),ELL(I),ETT(I),GGLT(I),PPLT(I),I=1,NM)
      WRITE(2,53)
      WRITE(2,54)(I,AA(1,I),AA(2,I),ELL(I),ETT(I),GGLT(I),
     *PPLT(I),I=1,NM)
      READ(1,5)(EXT(I),EXC(I),EYT(I),EYC(I),EST(I),I=1,NM)
      WRITE(2,60)
      WRITE(2,59)(I,EXT(I),EXC(I),EYT(I),EYC(I),EST(I),I=1,NM)
      READ(1,5)SX,SY,SXY,DSX,DSY,DSXY
      IF(IP.EQ.0)GO TO  33
      READ(1,4)SXMIN,SXMAX,SYMIN,SYMAX,XL,YL,FACTOR,NX,NY,NNN,I1,I2,I3
      READ(1,7)IT
      EXPN=EXP10(FACTOR)
      SYMAX=SYMAX/EXPN
      CALL CC936N
      CALL CHASIZ(2.5,2.5)
      CALL WINDOW(2)
      CALL AXES
      YY=YL+50.
      YYY=YY+2.5
      CALL MOVTO2(50.,YY)
      CALL CHAHOL('X10*.')
      CALL MOVTO2(55.,YYY)
      CALL CHAFIX(FACTOR,3,0)
33    PI=4.*ATAN(1.)
      F111,F(1)=SX
      F222,F(2)=SY
      F333,F(3)=SXY
      DO 47 K=1,NL
      THETA(K)=PI*THET(K)/180.
      JJJ(K)=0
```

```
47    CONTINUE
      DDSX=DSX
      DDSY=DSY
      DDSXY=DSXY
      ID=0
      IDD=0
      LFF=0
      IWRT=0
      MP=0
      YP(1)=0.
      X1(1)=0.
      X2(1)=0.
      X3(1)=0.
C
C     CURVE FITTING FOR NONLINEAR DATA:
C     ---------------------------------
      IF(NON1T.EQ.0)GO TO 106
      CALL NONLINEAR(NC1T,XO1T,YO1T,XM1T,P1T,C1T)
      GO TO 206
106   XO1T,XM1T=EXT(1)
206   IF(NON1C.EQ.0)GO TO 107
      IF(NON1C.EQ.2)GO TO 108
      CALL NONLINEAR(NC1C,XO1C,YO1C,XM1C,P1C,C1C)
      GO TO 207
108   NC1C=NC1T
      XO1C=XO1T
      YO1C=YO1T
      XM1C=XM1T
      DO 109 I=1,10
      P1C(I)=P1T(I)
      C1C(I)=C1T(I)
109   CONTINUE
      GO TO 207
107   XO1C,XM1C=ABS(EXC(1))
207   IF(NON2T.EQ.0)GO TO 101
      CALL NONLINEAR(NC2T,XO2T,YO2T,XM2T,P2T,C2T)
      GO TO 210
101   XO2T,XM2T=EYT(1)
210   IF(NON2C.EQ.0)GO TO 102
      IF(NON2C.EQ.2)GO TO 103
      CALL NONLINEAR(NC2C,XO2C,YO2C,XM2C,P2C,C2C)
      GO TO 211
103   NC2C=NC2T
      XO2C=XO2T
      YO2C=YO2T
      XM2C=XM2T
      DO 104 I=1,10
      P2C(I)=P2T(I)
      C2C(I)=C2T(I)
104   CONTINUE
      GO TO 211
```

```
102   XO2C,XM2C=ABS(EYC(1))
211   IF(NON12.EQ.0)GO TO 105
      CALL NONLINEAR(NC12,XO12,YO12,XM12,P12,C12)
      GO TO 208
105   XO12,XM12=EST(1)
208   CONTINUE
C
      H=0.
      DO 14 K=1,NL
14    H=H+TL(K)
      ZKR=H/2./R
      Z(1)=-H/2.
      Z2(1)=Z(1)**2
      KK=2
      DO 15 K=1,NL
      MM=KK+NS(K)-1
      TLL=TL(K)/NS(K)
      DO 46 M=KK,MM
      Z(M)=Z(M-1)+TLL
      Z2(M)=Z(M)**2
46    CONTINUE
      KK=KK+NS(K)
15    CONTINUE
      DO 16 K=1,MM-1
      Z1(K)=(Z(K+1)+Z(K))/2.
      HS(K)=Z2(K+1)-Z2(K)
16    CONTINUE
C
      DO 13 I=1,NL
      DO 13 J=1,3
      LF(I,J)=0
13    CONTINUE
22    DO 45 K=1,NL
      LK=L(K)
      EL(K)=ELL(LK)
      ET(K)=ETT(LK)
      GLT(K)=GGLT(LK)
      PLT(K)=PPLT(LK)
      PTL(K)=ET(K)/EL(K)*PLT(K)
      IF(LF(K,1).EQ.0)GO TO  30
      EL(K)=0.
      PLT(K),PTL(K)=0.
      JJJ(K)=1
30    IF(LF(K,2).EQ.0)GO TO 31
      ET(K)=0.
      PLT(K),PTL(K)=0.
      JJJ(K)=1
31    IF(LF(K,3).EQ.0)GO TO 32
      GLT(K)=0.
      JJJ(K)=1
32    AMDA(K)=1.-PLT(K)*PTL(K)
```

```
45    CONTINUE
      EP1=0.
      EP2=0.
      EP12=0.
      LOOP=0
C
C     LAYER COMPLIANCE MATRIX:
C     ------------------------
20    DO 12 K=1,NL
      IF(JJJ(K).EQ.1)GO TO 34
      SK(1,1,K)=1./EL(K)
      SK(2,2,K)=1./ET(K)
      SK(3,3,K)=1./GLT(K)
      SK(1,2,K),SK(2,1,K)=-PLT(LK)/EL(K)
      CALL FMOVE(SK(1,1,K),T,9)
C
C     LAYER STIFFNESS MATRIX:
C     -----------------------
      IFAIL=0
      CALL F01AAF(T,3,3,TI,3,WK,IFAIL)
      GO TO 35
34    TI(1,1)=EL(K)/AMDA(K)
      TI(1,2),TI(2,1)=ET(K)*PLT(K)
      TI(2,2)=ET(K)/AMDA(K)
      TI(3,3)=GLT(K)
35    CALL FMOVE(TI,CK(1,1,K),9)
      C(1,1)=CK(1,1,K)
      C(2,1)=CK(1,2,K)
      C(3,1)=CK(2,2,K)
      C(4,1)=CK(3,3,K)
      AM=COS(THETA(K))
      AN=SIN(THETA(K))
      CALL TRANSFORMATION(AM,AN)
      CALL FMOVE(T,TK(1,1,K),9)
      IFAIL=0
      CALL F01CKF(TTC,TT,C,6,1,4,WK,3,1,IFAIL)
      QK(1,1,K)=TTC(1,1)
      QK(1,2,K),QK(2,1,K)=TTC(2,1)
      QK(1,3,K),QK(3,1,K)=TTC(3,1)
      QK(2,2,K)=TTC(4,1)
      QK(2,3,K),QK(3,2,K)=TTC(5,1)
      QK(3,3,K)=TTC(6,1)
12    CONTINUE
C
C     LAMINATE STIFFNESS MATRIX:
C     --------------------------
      IWR=0
      DO 18 I=1,3
      DO 18 J=1,3
      NN=0
      MM=0
```

```
      LL=0
      A(I,J)=0.
      B(I,J)=0.
      DO 19 K=1,NL
      A(I,J)=A(I,J)+QK(I,J,K)*TL(K)
      KKK=KIND(K)
      GO TO (121,122),KKK
121   NN=MM+1
      MM=NN
      GO TO 123
122   IF(LL.EQ.2)GO TO 126
      LL=LL+1
      NN=NN+1
      GO TO 127
126   LL=1
      NN=MM+1
127   MM=NN+2*NS(K)-2
123   DO 124 M=NN,MM,2
      B(I,J)=B(I,J)+QK(I,J,K)*HS(M)
124   CONTINUE
19    CONTINUE
      A(I,J)=A(I,J)/H
      B(I,J)=B(I,J)/2./R/H
18    CONTINUE
      Q(1,1)=A(1,1)
      Q(1,2)=A(1,2)-B(1,2)
      Q(1,3)=A(1,3)+B(1,3)
      Q(2,1)=A(2,1)
      Q(2,2)=A(2,2)-B(2,2)
      Q(2,3)=A(2,3)+B(2,3)
      Q(3,1)=A(3,1)
      Q(3,2)=A(3,2)-B(3,2)
      Q(3,3)=A(3,3)+B(3,3)
C
C     LAMINATE COMPLIANCE MATRIX:
C     ---------------------------
      IFAIL=1
      CALL F01AAF(Q,3,3,S,3,WK,IFAIL)
      IF(IFAIL.EQ.0)GO TO 132
      WRITE(2,97)F111,F222,F333
      GO TO 120
132   EX=1./S(1,1)
      EY=1./S(2,2)
      PXY=-S(1,2)/S(1,1)
      PYX=-S(2,1)/S(2,2)
      GXY=1./S(3,3)
      IFAIL=0
      CALL F01CKF(EP,S,F,3,1,3,WK,3,1,IFAIL)
      EP(2)=EP(2)*(1.-ZKR)
      EP(3)=EP(3)*(1.+ZKR)
      DP1=ABS(EP(1)-EP1)
```

```
      DP2=ABS(EP(2)-EP2)
      DP12=ABS(EP(3)-EP12)
      IF(DP1.LE.DEF.AND.DP2.LE.DEF.AND.DP12.LE.DEF)LOOP=1
      EP1=EP(1)
      EP2=EP(2)
      EP12=EP(3)
155   IF(IWRT.EQ.0.AND.LOOP.EQ.0)GO TO 151
      IF(IWRT.EQ.1.AND.LOOP.EQ.1)GO TO 152
      GO TO 154
151   WRITE(2,93)
      WRITE(2,55)EX,EY,PXY,PYX,GXY
      WRITE(2,58)F,EP
      IWR=1
      GO TO 154
152   WRITE(2,58)F,EP
      WRITE(2,94)
153   WRITE(2,55)EX,EY,PXY,PYX,GXY
      IWR=1
      IF(IP.EQ.0)GO TO 154
      MP=MP+1
      GO TO(181,182,183),NNN
181   YP(MP)=ABS(F(1))/EXPN
      GO TO 184
182   YP(MP)=ABS(F(2))/EXPN
      GO TO 184
183   YP(MP)=ABS(F(3))/EXPN
184   IF(I1.EQ.1)X1(MP)=ABS(EP(1))*100.
      IF(I2.EQ.2)X2(MP)=ABS(EP(2))*100.
      IF(I3.EQ.3)X3(MP)=ABS(EP(3))*100.
154   CONTINUE
C
C     LAYER STRESS/STRAIN CALCULATIONS:
C     ---------------------------------
      NN=0
      MM=0
      LL=0
      DO 27 K=1,NL
      IF(IWR.EQ.1)WRITE(2,63)K
      IC=0
      KKK=KIND(K)
      GO TO (141,142),KKK
141   NN=MM+1
      MM=NN
      GO TO 143
142   IF(LL.EQ.2)GOTO 146
      LL=LL+1
      NN=NN+1
      GO TO 147
146   LL=1
      NN=MM+1
147   MM=NN+2*NS(K)-2
```

```
      DO 145 I=1,3
      DO 145 J=1,10
      SPC(I,J)=0.
145   CONTINUE
143   DO 144 M=NN,MM,2
      ZR=Z1(M)/R
      IC=IC+1
      DO 21 J=1,3
      B(1,J)=S(1,J)
      B(2,J)=S(2,J)-ZR*S(2,J)
      B(3,J)=S(3,J)+ZR*S(3,J)
21    CONTINUE
      CALL FMOVE(QK(1,1,K),T,9)
      IFAIL=0
      CALL F01CKF(TI,T,B,3,3,3,WK,3,1,IFAIL)
      CALL FMOVE(TK(1,1,K),T,9)
      IFAIL=0
      CALL F01CKF(P,T,TI,3,3,3,WK,3,1,IFAIL)
      CALL F01CKF(STR,P,F,3,1,3,WK,3,1,IFAIL)
      IF(KKK.EQ.1)GO TO 144
      CALL FMOVE(STR,SPC(1,IC),3)
144   CONTINUE
      IF(KKK.EQ.2)CALL MAXIMUM VALUE(IC,STR)
      CALL FMOVE(STR,STRESS(1,K),3)
      IF(JJJ(K).EQ.1)GO TO 37
      CALL FMOVE(SK(1,1,K),T,9)
      IFAIL=0
      CALL F01CKF(STRN,T,STR,3,1,3,WK,3,1,IFAIL)
      GO TO 36
37    IF(LF(K,1).EQ.1)GO TO 38
      STRN(1)=(STR(1)-PLT(K)*STR(2))/EL(K)
      GO TO 40
38    STRN(1)=1.E10
40    IF(LF(K,2).EQ.1)GO TO 41
      STRN(2)=(STR(2)-PTL(K)*STR(1))/ET(K)
      GO TO 42
41    STRN(2)=1.E10
42    IF(LF(K,3).EQ.1)GO TO 43
      STRN(3)=STR(3)/GLT(K)
      GO TO 36
43    STRN(3)=1.E10
36    IF(IWR.EQ.1)WRITE(2,92)STR,STRN
      CALL FMOVE(STRN,STRAIN(1,K),3)
27    CONTINUE
      IF(IWR.EQ.1)WRITE(2,57)
C
C     NONLINEAR ANALYSIS:
C     -------------------
      IF(IWRT.EQ.0)WRITE(2,98)
      IF(LOOP.EQ.1)GO TO 160
      GO TO 161
```

```
160   F111=F(1)
      F222=F(2)
      F333=F(3)
      GO TO 28
C
161   DO 112 K=1,NL
      IF(THET(K).EQ.-THET(K-1).AND.KIND(K).EQ.KIND(K-1))GO TO 112
      K1=K+1
      CALL FMOVE(STRAIN(1,K),STRN,3)
      IF(LF(K,1).EQ.1)GO TO  114
      IF(STRN(1).LT.0.0)GO TO 113
      IF(STRN(1).LE.XO1T)GO TO 114
      ND=1
      IF(STRN(1).GT.XM1T)GO TO 164
      STRN(1)=STRN(1)-XO1T
      IFAIL=0
      CALL E02BBF(NC1T,P1T,C1T,STRN(1),S1T,IFAIL)
      STRN(1)=STRN(1)+XO1T
      S1T=S1T+YO1T
      EL(K)=S1T/STRN(1)
      IF(KIND(K).EQ.2)EL(K1)=EL(K)
      GO TO 114
113   IF(ABS(STRN(1)).LE.XO1C)GO TO 114
      ND=-1
      IF(ABS(STRN(1)).GT.XM1C)GO TO 164
      STRN(1)=ABS(STRN(1))-XO1C
      IFAIL=0
      CALL E02BBF(NC1C,P1C,C1C,STRN(1),S1C,IFAIL)
      STRN(1)=STRN(1)+XO1C
      S1C=S1C+YO1C
      EL(K)=S1C/STRN(1)
      IF(KIND(K).EQ.2)EL(K1)=EL(K)
114   IF(LF(K,2).EQ.1)GO TO 111
      IF(STRN(2).LT.0.0)GO TO 110
      IF(STRN(2).LE.XO2T)GO TO 111
      ND=2
      IF(STRN(2).GT.XM2T)GO TO 164
      STRN(2)=STRN(2)-XO2T
      IFAIL=0
      CALL E02BBF(NC2T,P2T,C2T,STRN(2),S2T,IFAIL)
      STRN(2)=STRN(2)+XO2T
      S2T=S2T+YO2T
      ET(K)=S2T/STRN(2)
      IF(KIND(K).EQ.2)ET(K1)=ET(K)
      GO TO 111
110   IF(ABS(STRN(2)).LE.XO2C)GO TO 111
      ND=-2
      IF(ABS(STRN(2)).GT.XM2C)GO TO 164
      STRN(2)=ABS(STRN(2))-XO2C
      IFAIL=0
      CALL E02BBF(NC2C,P2C,C2C,STRN(2),S2C,IFAIL)
```

```
      STRN(2)=STRN(2)+XO2C
      S2C=S2C+YO2C
      ET(K)=S2C/STRN(2)
      IF(KIND(K).EQ.2)ET(K1)=ET(K)
111   IF(LF(K,3).EQ.1)GO TO 116
      IF(ABS(STRN(3)).LE.XO12)GO TO 116
      ND=12
      IF(ABS(STRN(3)).GT.XM12)GO TO 164
      STRN(3)=ABS(STRN(3))-XO12
      IFAIL=0
      CALL E02BBF(NC12,P12,C12,STRN(3),S12,IFAIL)
      STRN(3)=STRN(3)+XO12
      S12=S12+YO12
      GLT(K)=S12/STRN(3)
      IF(KIND(K).EQ.2)GLT(K1)=GLT(K)
      GO TO 116
164   IF(IDD.EQ.0.OR.IDD.EQ.1)GO TO 115
      WRITE(2,95)K,ND,F111,F222,F333
      IF(KIND(K).EQ.2)WRITE(2,95)K1,ND,F111,F222,F333
      LFF=1
      IF(ND.EQ.1.OR.ND.EQ.-1)LF(K,1)=1
      IF(ND.EQ.2.OR.ND.EQ.-2)LF(K,2)=1
      IF(ND.EQ.12)LF(K,3)=1
      IF(KIND(K).EQ.1)GO TO 116
      IF(LF(K,1).EQ.1)LF(K1,1)=1
      IF(LF(K,2).EQ.1)LF(K1,2)=1
      IF(LF(K,3).EQ.1)LF(K1,3)=1
116   CONTINUE
      ND=0
      GO TO 112
115   ID=1
112   CONTINUE
C
      IWRT=1
      IF(LFF.EQ.0)GO TO 166
      LFF=0
      IDD,ID=0
      DSX=DDSX
      DSY=DDSY
      DSXY=DDSXY
      F(1)=F111
      F(2)=F222
      F(3)=F333
      GO TO 22
166   IF(ID.EQ.1)GO TO 165
      GO TO 20
165   DSX=DSX/10.
      DSY=DSY/10.
      DSXY=DSXY/10.
      IDD=IDD+1
      ID=0
```

```
28    CONTINUE
      F(1)=F111+DSX
      F(2)=F222+DSY
      F(3)=F333+DSXY
      GO TO 22
120   IF(IP.EQ.0)GO TO 39
      IF(I1.EQ.0)GO TO 118
      CALL DASHED(-1,2.,1.,0.)
      CALL GRACUR(X1,YP,MP)
118   IF(I2.EQ.0)GO TO 119
      CALL DASHED(-1,4.,2.,0.)
      CALL GRACUR(X2,YP,MP)
119   IF(I3.EQ.0)GO TO 120
      CALL DASHED(-1,6.,3.,0.)
      CALL GRACUR(X3,YP,MP)
      CALL DEVEND
39    STOP OK
      END
C
      SUBROUTINE TRANSFORMATION(AM,AN)
C     -------------------------------
      COMMON/BLOCK1/ T(3,3),TT(6,4)
      DO 1 I=1,3
      DO 1 J=1,3
1     T(I,J)=0.
      DO 2 I=1,6
      DO 2 J=1,4
2     TT(I,J)=0.
      AM2=AM**2
      AN2=AN**2
      AM3=AM**3
      AN3=AN**3
      AM4=AM2**2
      AN4=AN2**2
      AMAN=AM*AN
      AMAN2=2.*AMAN
      AM2AN2=AM2*AN2
      AMAN22=AM2-AN2
      T(1,1),T(2,2)=AM2
      T(1,2),T(2,1)=AN2
      T(1,3)=-AMAN2
      T(2,3)=AMAN2
      T(3,1)=AMAN
      T(3,2)=-AMAN
      T(3,3)=AMAN22
      TT(1,1),TT(4,3)=AM4
      TT(1,2),TT(4,2)=2.*AM2AN2
      TT(1,3),TT(4,1)=AN4
      TT(1,4),TT(4,4)=4.*AM2AN2
      TT(2,1),TT(2,3),TT(6,1),TT(6,3)=AM2AN2
      TT(2,2)=AM4+AN4
```

```
      TT(2,4)=-TT(1,4)
      TT(3,1)=-AM3*AN
      TT(3,2)=AMAN*AMAN22
      TT(3,3)=AN*AN3
      TT(3,4)=2.*TT(3,2)
      TT(5,1)=-TT(3,3)
      TT(5,2)=-TT(3,2)
      TT(5,3)=-TT(3,1)
      TT(5,4)=-TT(3,4)
      TT(6,2)=-TT(1,2)
      TT(6,4)=AMAN22**2
      RETURN
      END
C
      SUBROUTINE AXES
C     ---------------
      COMMON/BLOCK6/SXMAX,SXMIN,SYMAX,SYMIN,IP,XL,YL,NX,NY,NNN,IT(20)
      CALL AXIPOS(1,50.,50.,XL,1)
      CALL AXIPOS(1,50.,50.,YL,2)
      CALL AXISCA(3,NX,SXMIN,SXMAX,1)
      CALL AXISCA(3,NY,SYMIN,SYMAX,2)
      CALL GRID(-2,1,1)
      CALL MOVTO2(70.,40.)
      CALL CHAHOL('LAMINATE STRAIN (AXIAL, HOOP OR SHEAR)   [%]*.')
      CALL MOVTO2(30.,70.)
      CALL CHAANG(90.)
      GO TO(1,2,3),NNN
1     CALL CHAHOL('LAMINATE STRESS (AXIAL), SX*.')
      GO TO 4
2     CALL CHAHOL('LAMINATE STRESS (HOOP), SY*.')
      GO TO 4
3     CALL CHAHOL('LAMINATE STRESS (SHEAR), SXY*.')
4     CALL CHAANG(0.)
      CALL MOVTO2(70.,20.)
      CALL CHAARR(IT,20,4)
      RETURN
      END
C
      SUBROUTINE NONLINEAR(NC7,XO,YO,XM,P,C)
C     --------------------------------------
      DIMENSION X(30),Y(30),W(30),P(10),WK(30),WRK(4,10),C(10)
      READ(1,1)NP,NC
      READ(1,2)(X(I),I=1,NP)
      READ(1,2)(Y(I),I=1,NP)
      NC3=NC+3
      NC7=NC+7
      IF(NC.EQ.1)GO TO 10
      READ(1,2)(P(I),I=5,NC3)
10    CONTINUE
      XO=X(1)
      YO=Y(1)
```

```
      XM=X(NP)
      DO 11 I=1,NP
      X(I)=X(I)-XO
      Y(I)=Y(I)-YO
      W(I)=1.
11    CONTINUE
      IFAIL=0
      CALL E02BAF(NP,NC7,X,Y,W,P,WK,WRK,C,SS,IFAIL)
1     FORMAT(2I0)
2     FORMAT(10F0.0)
      RETURN
      END
C
      SUBROUTINE MAXIMUM VALUE(N,STR)
C     -------------------------------
      COMMON/BLOCK7/SPC(3,10)
      DIMENSION  STR(3)
      DO 1 I=1,3
      STR(I)=0.
1     CONTINUE
      DO 3 I=1,3
      DO 2 J=1,N
      F=ABS(SPC(I,J))-ABS(STR(I))
      IF(F)4,4,5
5     STR(I)=SPC(I,J)
4     CONTINUE
2     CONTINUE
3     CONTINUE
      RETURN
      END
C
      FINISH
```

I.5 SAMPLE INPUT

```
1  6  0  0  0  1  1  1  40.042E-3  .0001
1   .165E-3  85.  2  2
1   .165E-3 -85.  2  2
1  .8125E-3   45.   5   2
1  .8125E-3  -45.   5  2
1  .165E-3   85.   2   2
1  .165E-3  -85.   2   2
 GLASS/EPOXY         44.5E9  13.522E9  5.64E9  .183
2.83E-2  1.72E-2  .198E-2  1.25E-2  4.33E-2
  0.  50.E6  0.  0.  50.E6  0.
9  1
0. .00025 .0005 .00075 .001 .00125 .0015 .00175  .00198
0. 3.8E6  7.E6  10.4E6 13.6E6 16.6E6 19.4E6 22.E6 24.1E6
10   2
0. .0015  .003  .0045  .006  .0075  .009  .0105  .012  .0125
0. 19.E6 36.3E6 51.67E6 64.3E6 75.3E6 84.E6 91.E6 96.67E6 98.E6
.0045
17  3
0. .002  .004 .006  .008 .01 .012 .014 .016 .018
.02  .024  .028  .032  .036  .04  .0425
0. 9.8E6 17.E6 22.4E6 26.6E6 30.4E6 33.6E6 36.8E6 39.2E6 41.2E6
42.8E6 45.6E6 46.8E6 47.2E6  47.6E6  47.8E6  48.E6
.004  .028
```

I.6 SAMPLE OUTPUT

```
    ANALYSIS OF FILAMENT-WOUND TUBE OF R= 4.004E-02  AND  6 LAYERS:

    LAYER     LAYER        LAYER     LAYER MATERIAL
     NO.    THICKNESS      ANGLE          NO.

       1    1.650E-04      85.00           1
       2    1.650E-04     -85.00           1
       3    8.125E-04      45.00           1
       4    8.125E-04     -45.00           1
       5    1.650E-04      85.00           1
       6    1.650E-04     -85.00           1

                          MATERIAL PROPERTIES

    NO.      MATERIAL            EL          ET          GLT       NULT
     1      GLASS/EPOXY       4.45E 10    1.35E 10    5.64E 09    0.183

    NO.   EU1         EU1'        EU2         EU2'        EU12
     1  2.83E-02    1.72E-02    1.98E-03    1.25E-02    4.33E-02

    LINEAR ANALYSIS:
    ================
    LAMINATE PROPERTIES:
EX=  1.69E 10  EY=  2.48E 10  NUXY= 0.287  NUYX= 0.420  GXY=  1.12E 10

    LAMINATE STRESSES:  0.0000E 00  5.0000E 07  0.0000E 00
    LAMINATE STRAINS : -8.4729E-04  1.9606E-03  2.2348E-06

    LAYER NO.  1
    ------------
STRESS  9.02E 07 -6.16E 06 -2.87E 06STRAIN  2.05E-03 -8.27E-04 -5.09E-04

    LAYER NO.  2
    ------------
STRESS  9.00E 07 -6.18E 06  2.84E 06STRAIN  2.05E-03 -8.27E-04  5.04E-04

    LAYER NO.  3
    ------------
STRESS  2.86E 07  9.77E 06 -1.64E 07STRAIN  6.03E-04  6.05E-04 -2.90E-03

    LAYER NO.  4
    ------------
STRESS  2.85E 07  9.68E 06  1.63E 07STRAIN  6.01E-04  5.99E-04  2.89E-03

    LAYER NO.  5
    ------------
STRESS  8.58E 07 -6.42E 06 -2.78E 06STRAIN  1.95E-03 -8.27E-04 -4.92E-04

    LAYER NO.  6
    ------------
STRESS  8.56E 07 -6.43E 06  2.75E 06STRAIN  1.95E-03 -8.28E-04  4.87E-04
```

```
    NONLINEAR ANALYSIS:
    ===================

    LAMINATE STRESSES:  0.0000E 00  5.0000E 07  0.0000E 00
    LAMINATE STRAINS : -1.0574E-03  2.1020E-03  2.3082E-06

    LAMINATE PROPERTIES (SECANT MODULI):
EX=  1.55E 10  EY=  2.31E 10  NUXY= 0.327  NUYX= 0.489  GXY=  1.14E 10

    LAYER NO.  1
    ............
STRESS  9.63E 07 -8.20E 06 -3.50E 06STRAIN  2.20E-03 -1.03E-03 -5.72E-04

    LAYER NO.  2
    ............
STRESS  9.61E 07 -8.22E 06  3.47E 06STRAIN  2.19E-03 -1.03E-03  5.67E-04

    LAYER NO.  3
    ............
STRESS  2.72E 07  9.67E 06 -1.47E 07STRAIN  5.72E-04  5.74E-04 -3.26E-03

    LAYER NO.  4
    ............
STRESS  2.71E 07  9.57E 06  1.47E 07STRAIN  5.70E-04  5.67E-04  3.25E-03

    LAYER NO.  5
    ............
STRESS  9.16E 07 -8.46E 06 -3.40E 06STRAIN  2.09E-03 -1.03E-03 -5.54E-04

    LAYER NO.  6
    ............
STRESS  9.14E 07 -8.48E 06  3.37E 06STRAIN  2.09E-03 -1.04E-03  5.48E-04
```

```
    LAMINATE STRESSES:  0.0000E 00  1.6350E 08  0.0000E 00
    LAMINATE STRAINS : -4.9514E-03  7.9820E-03  9.6352E-06

    LAMINATE PROPERTIES (SECANT MODULI):
EX=  1.26E 10  EY=  1.99E 10  NUXY= 0.380  NUYX= 0.603  GXY=  1.09E 10

    LAYER NO.  1
    ............
STRESS  3.64E 08 -3.80E 07 -1.16E 07STRAIN  8.34E-03 -4.86E-03 -2.33E-03

    LAYER NO.  2
    ............
STRESS  3.63E 08 -3.81E 07  1.15E 07STRAIN  8.33E-03 -4.86E-03  2.31E-03

    LAYER NO.  3
    ............
STRESS  8.05E 07  2.57E 07 -3.60E 07STRAIN  1.70E-03  1.71E-03 -1.33E-02

    LAYER NO.  4
    ............
STRESS  8.01E 07  2.54E 07  3.59E 07STRAIN  1.70E-03  1.69E-03  1.33E-02
```

```
    LAYER NO.  5
    ------------
STRESS  3.46E 08 -3.89E 07 -1.14E 07STRAIN  7.94E-03 -4.86E-03 -2.27E-03

    LAYER NO.  6
    ------------
STRESS  3.46E 08 -3.89E 07  1.12E 07STRAIN  7.93E-03 -4.86E-03  2.24E-03
-------------------------------------------------------------------------

LAYER 3 FAILED IN MODE  2 AT LOAD:  0.0000E 00  1.6350E 08  0.0000E 00
**********************************

LAYER 4 FAILED IN MODE  2 AT LOAD:  0.0000E 00  1.6350E 08  0.0000E 00
**********************************

    LAMINATE STRESSES:  0.0000E 00  3.2950E 08  0.0000E 00
    LAMINATE STRAINS : -1.2801E-02  1.8957E-02  3.7576E-05

    LAMINATE PROPERTIES (SECANT MODULI):
EX=  8.73E 09  EY=  1.69E 10  NUXY= 0.339  NUYX= 0.656  GXY=  9.07E 09

    LAYER NO.  1
    ------------
STRESS  8.68E 08 -7.06E 07 -2.13E 07STRAIN  1.98E-02 -1.26E-02 -5.74E-03

    LAYER NO.  2
    ------------
STRESS  8.67E 08 -7.07E 07  2.10E 07STRAIN  1.98E-02 -1.26E-02  5.66E-03

    LAYER NO.  3
    ------------
STRESS  1.56E 08 -3.16E-03 -4.76E 07STRAIN  3.52E-03  1.00E 10 -3.27E-02

    LAYER NO.  4
    ------------
STRESS  1.56E 08 -8.99E-04  4.75E 07STRAIN  3.51E-03  1.00E 10  3.26E-02

    LAYER NO.  5
    ------------
STRESS  8.26E 08 -7.20E 07 -2.09E 07STRAIN  1.89E-02 -1.26E-02 -5.58E-03

    LAYER NO.  6
    ------------
STRESS  8.24E 08 -7.21E 07  2.06E 07STRAIN  1.88E-02 -1.26E-02  5.50E-03
-------------------------------------------------------------------------

LAYER 1 FAILED IN MODE -2 AT LOAD:  0.0000E 00  3.2950E 08  0.0000E 00
**********************************

LAYER 2 FAILED IN MODE -2 AT LOAD:  0.0000E 00  3.2950E 08  0.0000E 00
**********************************

LAYER 5 FAILED IN MODE -2 AT LOAD:  0.0000E 00  3.2950E 08  0.0000E 00
**********************************

LAYER 6 FAILED IN MODE -2 AT LOAD:  0.0000E 00  3.2950E 08  0.0000E 00
**********************************
```

APPENDIX J

DETAILS OF THE TEST RIG

J.1 THE TEST RIG

The test rig was designed to test the two types of tubes which have different diameter. The components of the rig, therefore, were designed to serve as much as possible both types of tubes. Only the components which relateto the diameter were different, Figs. (J.1) to (J.15). The end fittings for the tension testing machine are also different from those of the torsion testing machine, Figs. (J.6) and (J.7).

J.2 TEST RIG ASSEMBLY PROCEDURE

The procedure to assemble the test rig is as follows, the component numbers are those of Fig. (J.1) :

1. Put the liner holder (11) in the mouth of the polythene bag (18), then twist the mouth of the bag round the holder and place the "O" ring (23) over the bag.

2. Place the sealing cup (12) and its cover (14).

3. Place the "O" rings (26) and (27) (or 25 as appropriate) in their holders and insert the bag holder (11) in the "O" ring holder (9) (or 8 as appropriate).

4. Tighten the nut (19).

5. Insert the "O" ring (28) (or 24) and place the end grip (3) (or 2) and tighten Allen screws (21) (or 22).

6. Place the sealing cup (13) and its cover (15) over the end grip (5) (or 4 + 10) and tighten the Allen screw (29) (or screws 22).

7. Place the appropriate end fitting (6) (or 7) and tighten the bolts (20).

8. Blow the bag with air and close the oil inlet.

9. Insert both ends in the specimen (1) and tighten Allen screws (16), and the specimen is ready for biaxial test.

The above procedure can be simplified when the specimen is to be tested in uniaxial loading. In internal pressure test, for instance, the end fittings are removed and the specimen is left free to slide on the ends by removing Allen screws (16).

To insert the ends easily in the specimen the inside edges of the specimen are tapered with a file, and then greased with some oil.

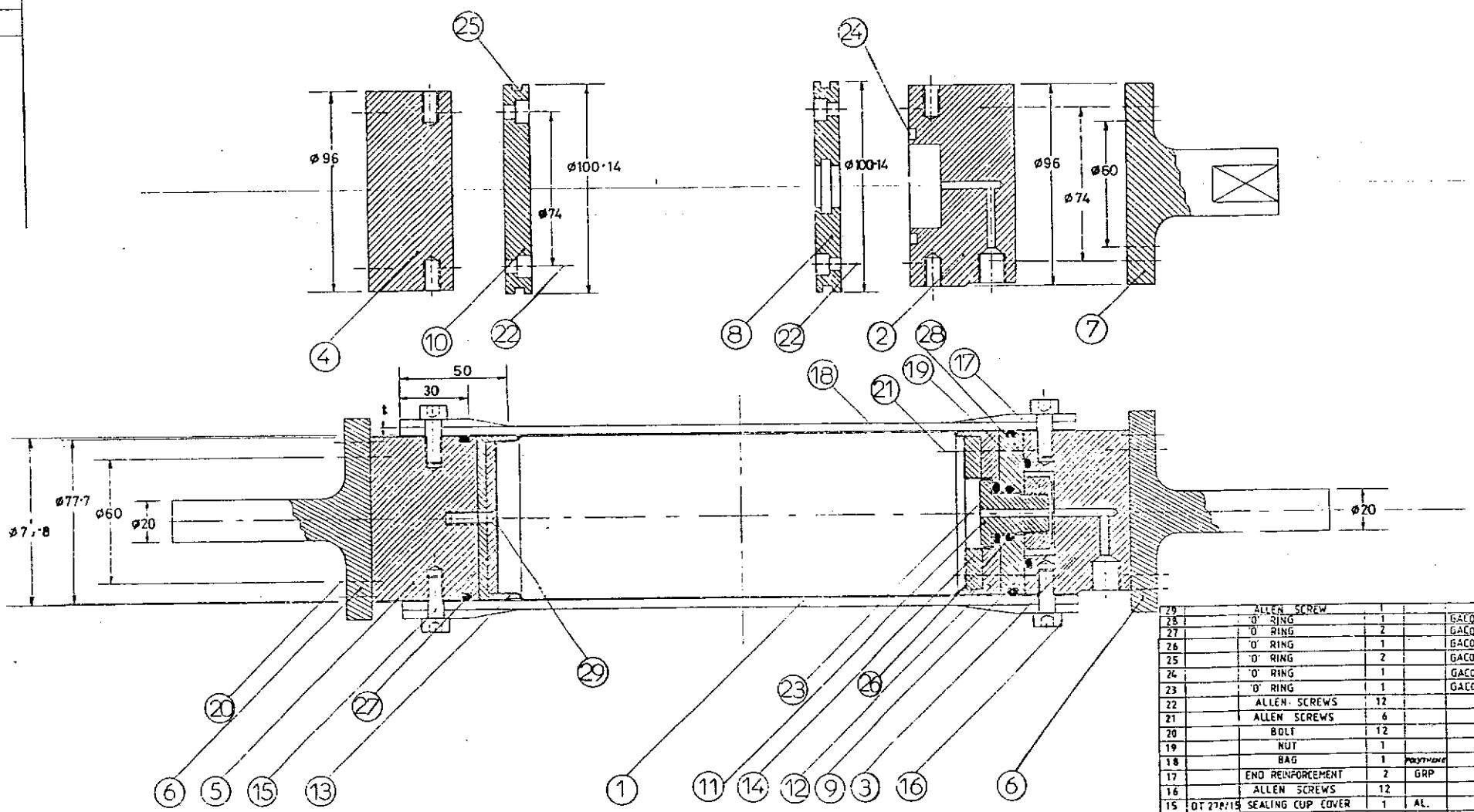

Fig.(J.1)

29		ALLEN SCREW	1			2BA
28		'O' RING	1		GACO	R 175
27		'O' RING	2		GACO	R 174
26		'O' RING	1		GACO	R 4081
25		'O' RING	2		GACO	R 4362
24		'O' RING	1		GACO	R 4175
23		'O' RING	1		GACO	R 4075
22		ALLEN SCREWS	12			1/4" B.S.F.
21		ALLEN SCREWS	6			2BA
20		BOLT	12			3/8" B.S.F.
19		NUT	1			3/4" B.S.F. 10mm THICK
18		BAG	1	POLYTHENE		
17		END REINFORCEMENT	2	GRP		
16		ALLEN SCREWS	12			3/8" B.S.F.
15	DT 278/15	SEALING CUP COVER	1	AL.		
14	DT 278/14	SEALING CUP COVER	1	M.S.		
13	DT 278/13	SEALING CUP	1	CAST POLYTHENE		
12	DT 278/12	SEALING CUP	1	CAST POLYTHENE		
11	DT 278/11	LINER HOLDER	1	M.S.		
10	DT 278/10	'O' RING HOLDER	1	M.S.		
9	DT 278/9	'O' RING HOLDER (B-TUBES)	1	M.S.		
8	DT 278/8	'O' RING HOLDER (P-TUBES)	1	M.S.		
7	DT 278/7	END FITTING (TORSION)	2	M.S.		
6	DT 278/6	END FITTING (TENSION)	2	M.S.		
5	DT 278/5	END GRIP (B-TUBES)	1	M.S.		
4	DT 278/4	END GRIP (P-TUBES)	1	M.S.		
3	DT 278/3	END GRIP (B-TUBES)	1	M.S.		
2	DT 278/2	END GRIP (P-TUBES)	1	M.S.		
1		GRP TUBE	1	GRP		FILAMENT-WOUND
ITEM	PART NO.	DESCRIPTION	NO. OFF	MATL	SPEC.	REMARKS

THIRD ANGLE PROJECTION

SHEET SIZE A1

SCALE 1:1

DRAWN M.N.NAHAS 2.3.1979

TITLE:- GRP TUBE TEST RIG (BIAXIAL LOADING)

ISSUED BY AIRCRAFT DESIGN DIVISION

CRANFIELD INSTITUTE OF TECHNOLOGY CRANFIELD.

DRAWING NO. DT 278/1

SHT 1 OF 15

DRAWING No.

ISSUE	MODIFICATION

ALL DIMENSIONS IN MILLIMETRES UNLESS OTHERWISE STATED.

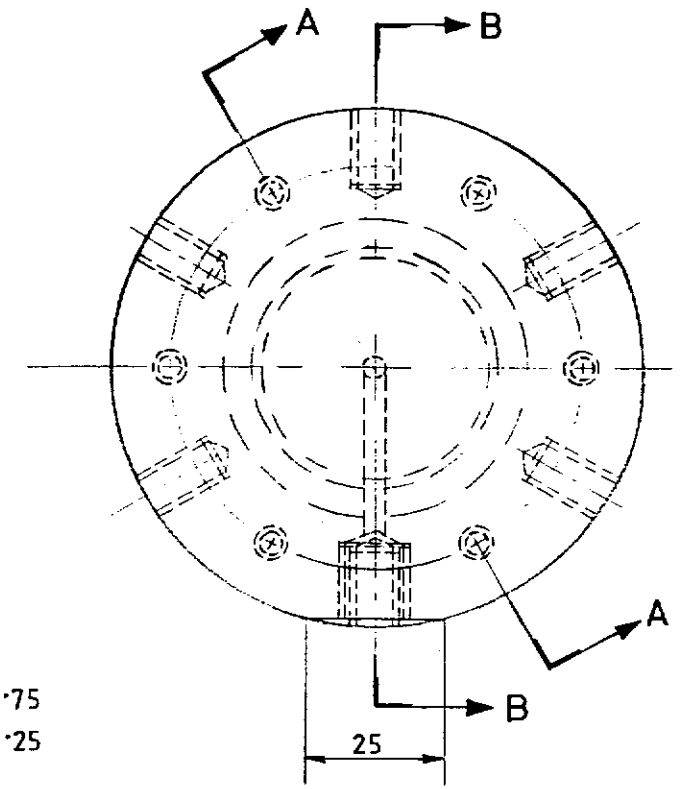

NOTE

R_1 = ·5 → ·75

R_2 = ·12 → ·25

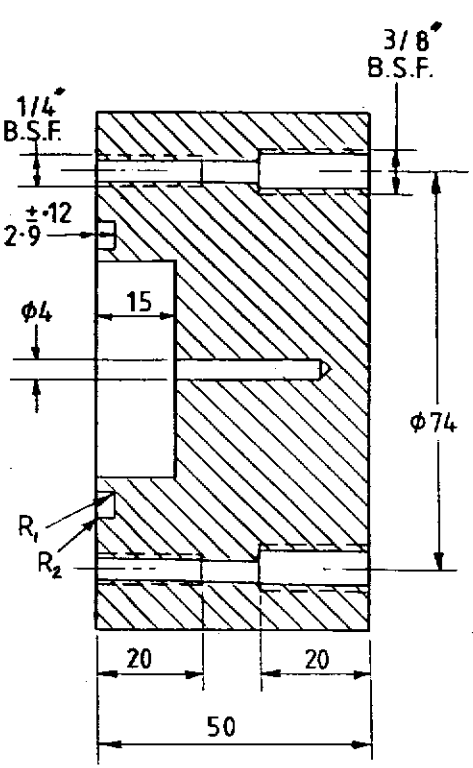

SECTION A-A

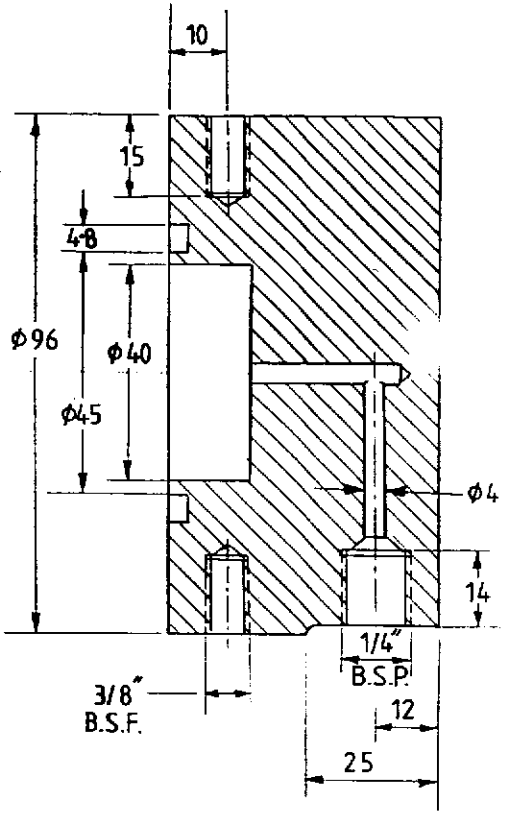

SECTION B-B

Fig.(J.2)

THIRD ANGLE PROJECTION			SHEET SIZE A 3	2		END GRIP (P-TUBES)	1	M.S.		
				ITEM	PART No.	DESCRIPTION	No. OFF	MATL	SPEC.	REMARKS
GENERAL TOLERANCE ON DIMENSIONS	JOB No.	No. OF SETS REQD	SCALE 1 : 1	DRAWN	CHKD	APPVD	STRESS APPVD	TITLE:- GRP TUBE TEST RIG (BIAXIAL LOADING)		
MACHINED				M.N. NAHAS	R.TETLOW	C.K.TROTMAN	R.TETLOW			
UNMACHINED				2.3.1979	13.3.79	13.3.79	13.3.79			
OTHER DIMENSIONS AS STATED			FINISH	ISSUED BY AIRCRAFT DESIGN DIVISION				DRAWING No. DT 278/2		
WELD WHERE SHOWN THUS				CRANFIELD INSTITUTE OF TECHNOLOGY CRANFIELD.				SHT. 2 OF 15 SHTS		
MACHINE WHERE SHOWN THUS	USED ON DRG.									

DRAWING No.	
ISSUE	MODIFICATION

ALL DIMENSIONS IN MILLIMETRES UNLESS OTHERWISE STATED.

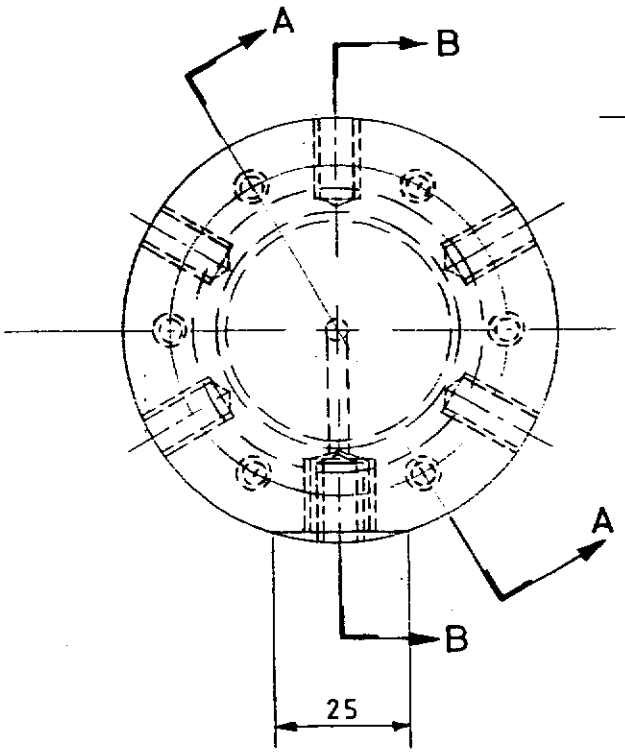

NOTE

R_1 = ·5 → ·75

R_2 = ·12 → ·25

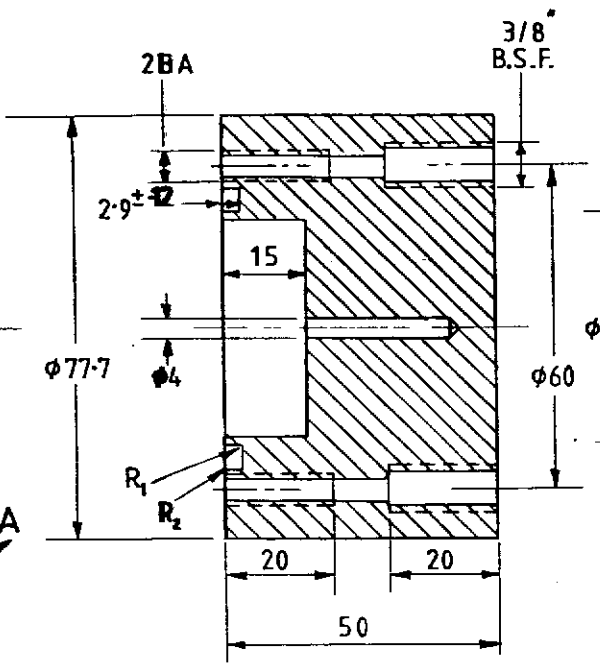

SECTION A-A

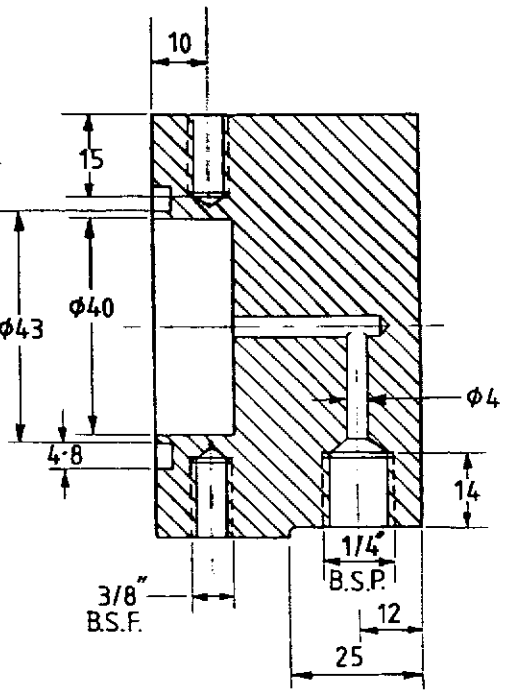

SECTION B-B

Fig.(J.3)

THIRD ANGLE PROJECTION	SHEET SIZE A 3	3		END GRIP (B-TUBES)	1	M.S.		
		ITEM	PART No.	DESCRIPTION	No. OFF	MAT'L	SPEC.	REMARKS

GENERAL TOLERANCE ON DIMENSIONS	JOB No.	No. OF SETS REQ'D	SCALE 1 : 1	DRAWN	CHK'D	APPV'D	STRESS APPVD.	TITLE:- GRP TUBE TEST RIG (BIAXIAL LOADING)
MACHINED				M. N. NAHAS	R.TETLOW	C.K.TROTMAN	R.TETLOW	
UNMACHINED				2 . 3 . 1979	13.3.79	13.3.79	13.3.79	
OTHER DIMENSIONS AS STATED			FINISH	ISSUED BY AIRCRAFT DESIGN DIVISION				DRAWING No. DT 278 / 3
WELD WHERE SHOWN THUS				CRANFIELD INSTITUTE OF TECHNOLOGY CRANFIELD.				SHT. 3 OF 15 SHEETS
MACHINE WHERE SHOWN THUS	USED ON DRG.							

DRAWING No.	
ISSUE	MODIFICATION

ALL DIMENSIONS IN MILLIMETRES UNLESS OTHERWISE STATED.

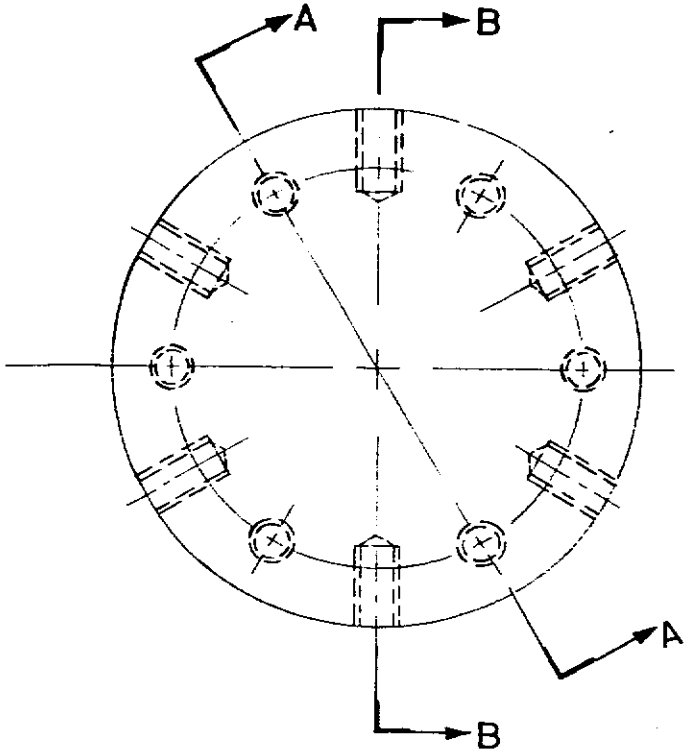

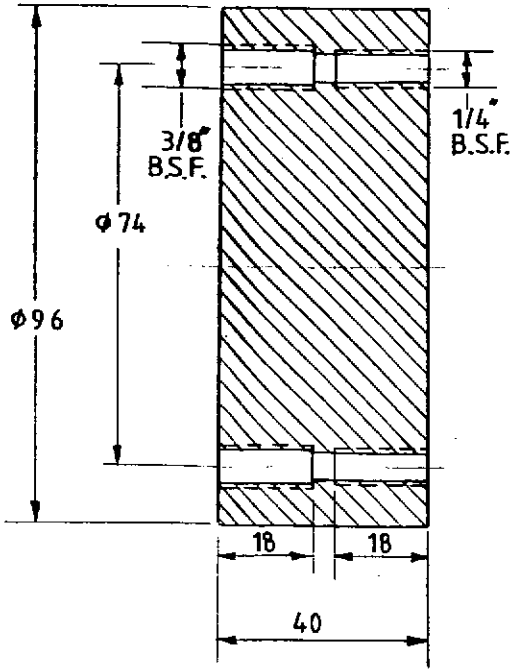

SECTION A-A

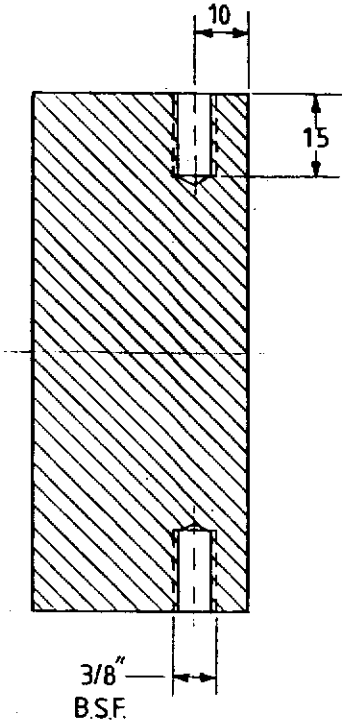

SECTION B - B

Fig.(J.4)

THIRD ANGLE PROJECTION	SHEET SIZE A 3	4		END GRIP (P-TUBES)	1	M.S.		
		ITEM	PART No.	DESCRIPTION	No. OFF	MATL	SPEC.	REMARKS

GENERAL TOLERANCE ON DIMENSIONS MACHINED UNMACHINED OTHER DIMENSIONS AS STATED	JOB No.	No. OF SETS REQD	SCALE 1 : 1	DRAWN	CHKD	APPVD	STRESS APPVD
				M. N. NAHAS	R.TETLOW	C.K.TROTMAN	R.TETLOW
				2.3.1979	13.3.79	13.3.79	13.3.79
WELD WHERE SHOWN THUS ⌒			FINISH				
MACHINE WHERE SHOWN THUS ✓	USED ON DRG.						

TITLE:- GRP TUBE TEST RIG (BIAXIAL LOADING)

ISSUED BY AIRCRAFT DESIGN DIVISION

CRANFIELD INSTITUTE OF TECHNOLOGY
CRANFIELD.

DRAWING No. DT 278 / 4

SHT. 4 OF 15 SHEETS

6480

DRAWING No.	
ISSUE	MODIFICATION

ALL DIMENSIONS IN MILLIMETRES UNLESS OTHERWISE STATED.

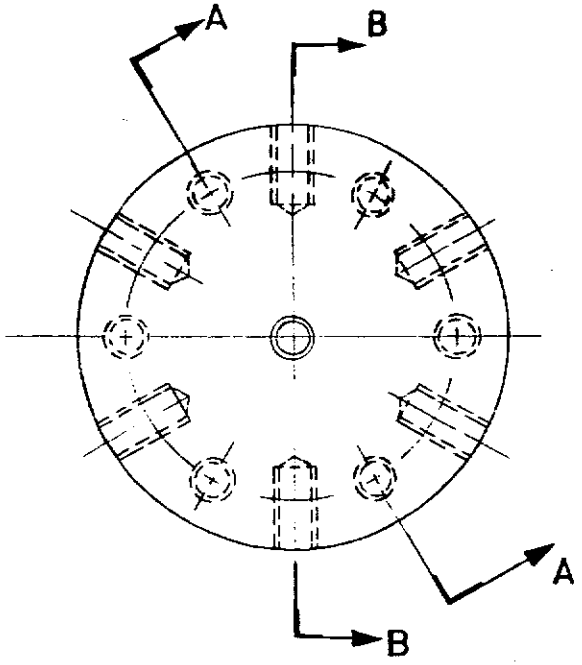

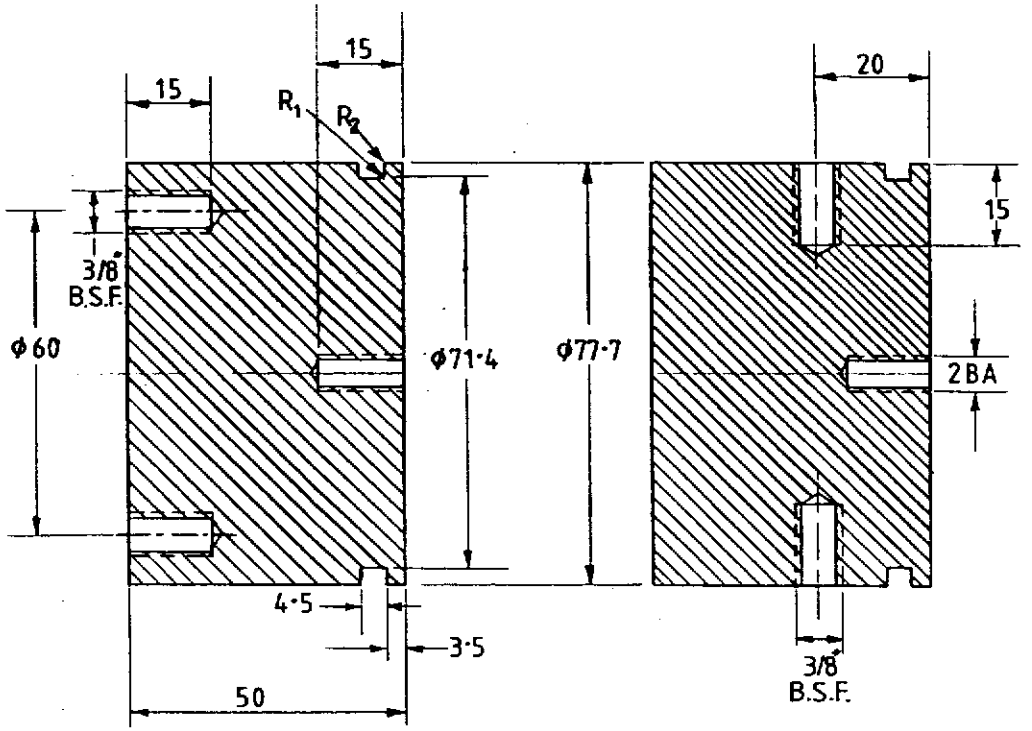

SECTION A-A

SECTION B-B

NOTE

R_1 = ·5 — ·75

R_2 = ·12 — ·25

Fig.(J.5)

- 396 -

THIRD ANGLE PROJECTION	SHEET SIZE A 3	5		END GRIP (B-TUBES)	1	M.S.		
		ITEM	PART No.	DESCRIPTION	No. OFF	MAT'L	SPEC.	REMARKS

GENERAL TOLERANCE ON DIMENSIONS MACHINED UNMACHINED OTHER DIMENSIONS AS STATED	JOB No.	No. OF SETS REQ'D	SCALE 1:1	DRAWN	CHK'D	APPV'D	STRESS APPVD.	TITLE:- GRP TUBE TEST RIG (BIAXIAL LOADING)
				M.N. NAHAS	R.TETLOW	C.K.TROMAN	R.TETLOW	
				2.3.1979	13.3.79	13.3.79	13.3.79	
WELD WHERE SHOWN THUS			FINISH	ISSUED BY AIRCRAFT DESIGN DIVISION				DRAWING No. DT 278 / 5
MACHINE WHERE SHOWN THUS	USED ON DRG.			CRANFIELD INSTITUTE OF TECHNOLOGY CRANFIELD.				SHT. 5 OF 15 SHEETS

1 2 3 4 5 6 7 8

DRAWING No.

ISSUE	MODIFICATION

ALL DIMENSIONS IN MILLIMETRES UNLESS OTHERWISE STATED.

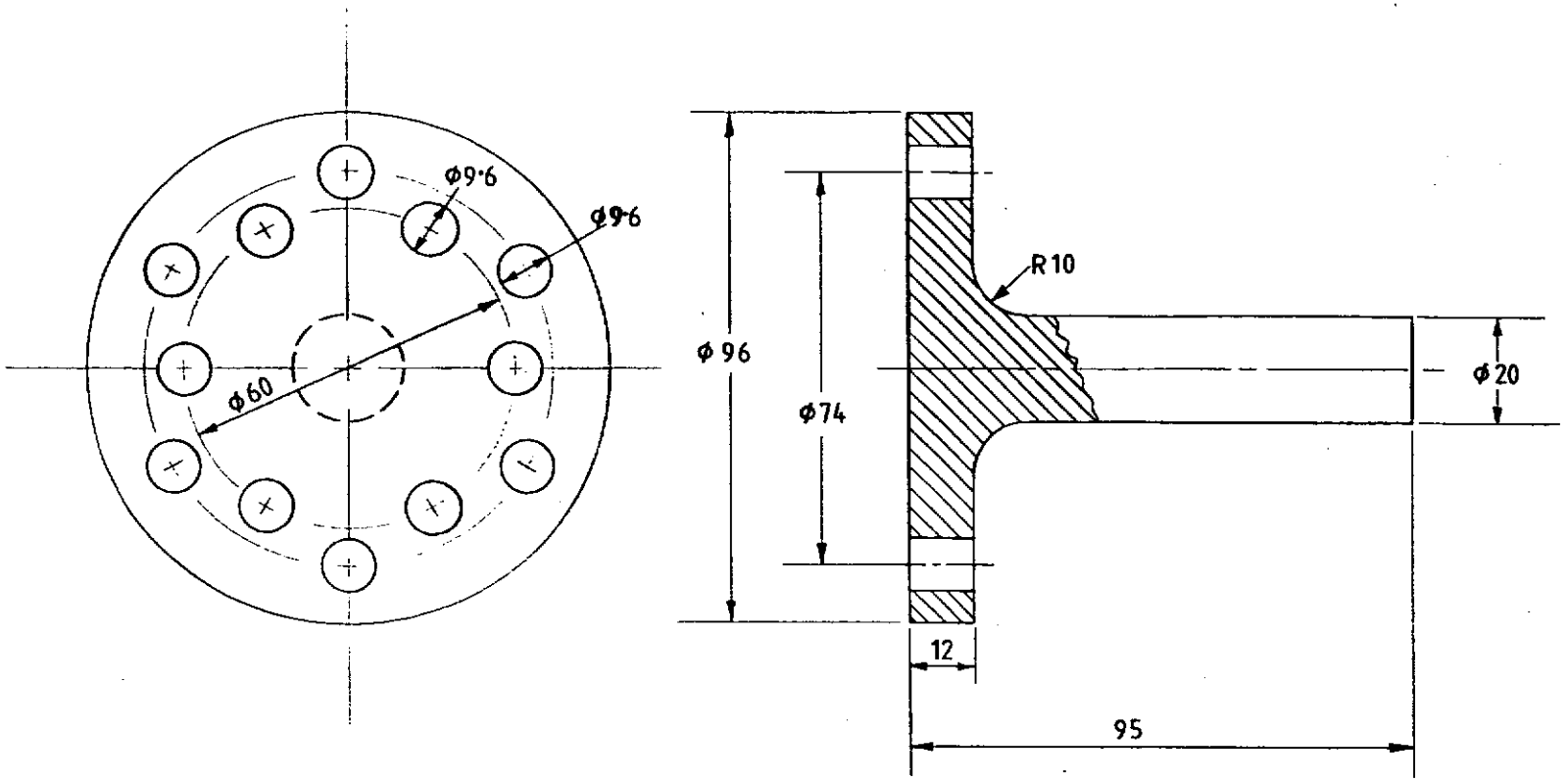

Fig.(J.6)

THIRD ANGLE PROJECTION	SHEET SIZE A 3	6		END FITTING (TENSION)	2	M.S.		
		ITEM	PART No.	DESCRIPTION	No. OFF	MAT!	SPEC.	REMARKS

GENERAL TOLERANCE ON DIMENSIONS	JOB No.	No. OF SETS REQ?	SCALE 1 : 1	DRAWN	CHK?	APPV?	STRESS APPVD.	TITLE:- GRP TUBE TEST RIG (BIAXIAL LOADING)
MACHINED				M.N. NAHAS	R.TETLOW	C.K.TROTMAN	R.TETLOW	
UNMACHINED				2.3.1979	13.3.79	13.3.79	13.3.79	
OTHER DIMENSIONS AS STATED			FINISH	ISSUED BY AIRCRAFT DESIGN DIVISION				DRAWING No. DT 278 / 6
WELD WHERE SHOWN THUS				CRANFIELD INSTITUTE OF TECHNOLOGY CRANFIELD.				SHT. 6 OF 15 SHEETS
MACHINE WHERE SHOWN THUS ✓	USED ON DRG.							

6880

1 2 3 4 5 6 7 8

DRAWING No.	
ISSUE	MODIFICATION

ALL DIMENSIONS IN MILLIMETRES UNLESS OTHERWISE STATED.

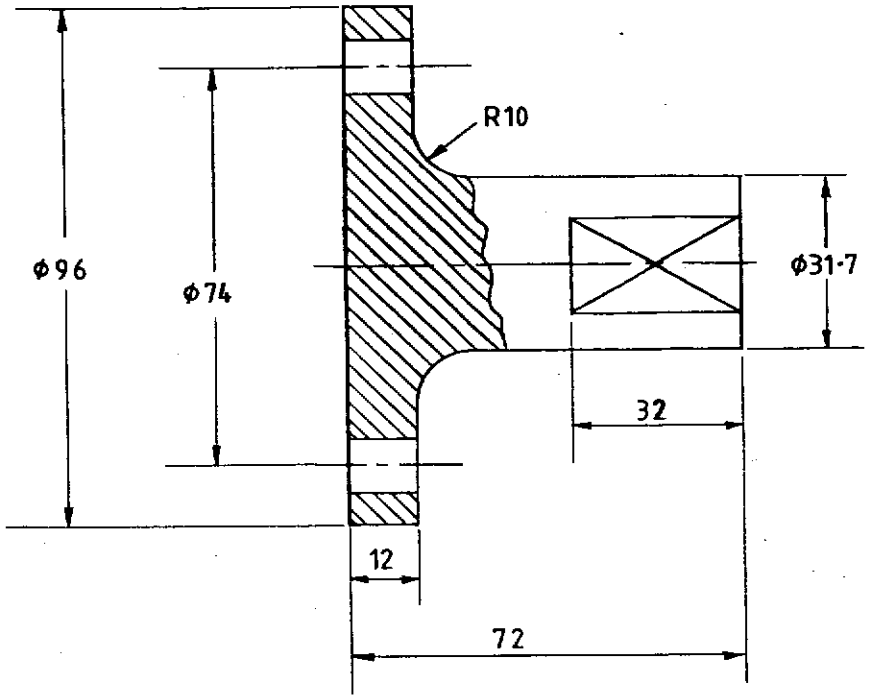

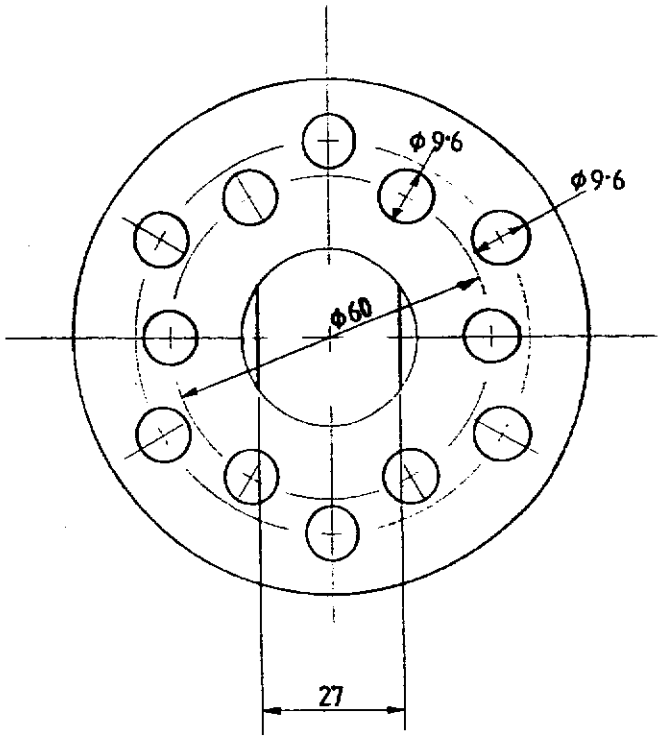

Fig.(J.7)

THIRD ANGLE PROJECTION	SHEET SIZE	ITEM	PART No.	DESCRIPTION	No. OFF	MAT'L	SPEC.	REMARKS
	A 3	7		END FITTING (TORSION)	2	M. S.		

GENERAL TOLERANCE ON DIMENSIONS	JOB No.	No. OF SETS REQ'D
MACHINED		
UNMACHINED		
OTHER DIMENSIONS AS STATED		
WELD WHERE SHOWN THUS		
MACHINE WHERE SHOWN THUS	USED ON DRG.	

SCALE	DRAWN	CHK'D	APPV'D	STRESS APPVD.
1 : 1	M.N. NAHAS	R.TETLOW	C.K.TROTMAN	R.TETLOW
	2.3.1979	13.3.79	13.3.79	13.3.79

TITLE:- GRP TUBE TEST RIG (BIAXIAL LOADING)

FINISH

ISSUED BY AIRCRAFT DESIGN DIVISION

CRANFIELD INSTITUTE OF TECHNOLOGY
CRANFIELD.

DRAWING No. DT 278 / 7

SHT. 7 OF 15 SHEETS

DRAWING No.	
ISSUE	MODIFICATION

ALL DIMENSIONS IN MILLIMETRES UNLESS OTHERWISE STATED.

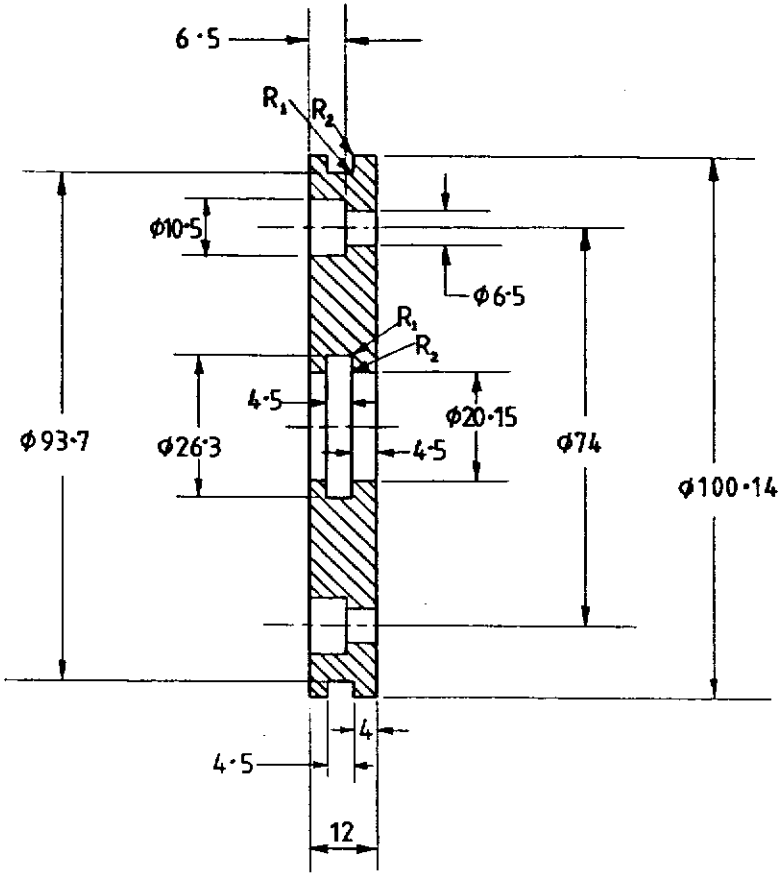

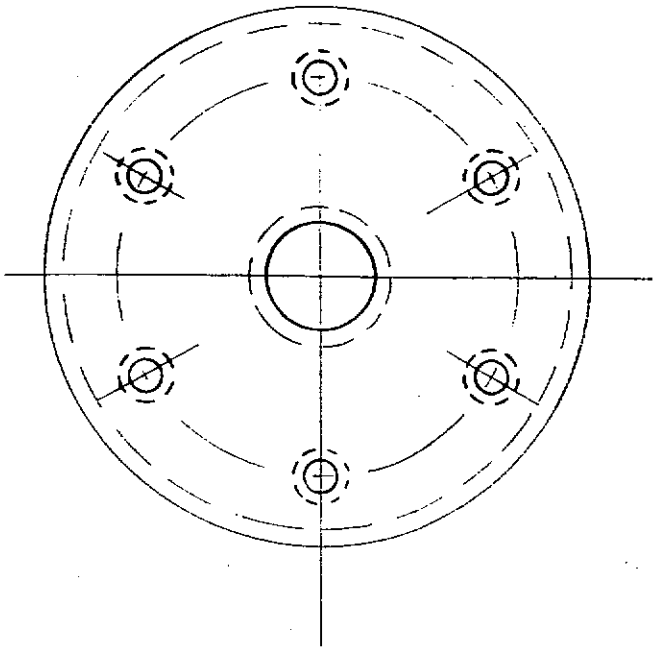

NOTE

R_1 = ·5 — ·75
R_2 = ·12 — ·25

Fig.(J.8)

THIRD ANGLE PROJECTION	SHEET SIZE A 3	8		'O' RING HOLDER (P-TUBES)	1	M.S.		
		ITEM	PART No.	DESCRIPTION	No. OFF	MAT'L	SPEC.	REMARKS

GENERAL TOLERANCE ON DIMENSIONS	JOB No.	No. OF SETS REQ'D	SCALE 1 : 1	DRAWN	CHK'D	APPV'D	STRESS APPV'D.	TITLE:- GRP TUBE TEST RIG (BIAXIAL LOADING)
MACHINED				M.N.NAHAS	R.TETLOW	C.K.TROTMAN	R.TETLOW	
UNMACHINED				2.3.1979	13.3.79	13.3.79	13.3.79	
OTHER DIMENSIONS AS STATED			FINISH	ISSUED BY AIRCRAFT DESIGN DIVISION				DRAWING No. DT 278 / 8
WELD WHERE SHOWN THUS				CRANFIELD INSTITUTE OF TECHNOLOGY CRANFIELD.				SHT. 8 OF 15 SHEETS
MACHINE WHERE SHOWN THUS	USED ON DRG.							

DRAWING No.	
ISSUE	MODIFICATION

ALL DIMENSIONS IN MILLIMETRES UNLESS OTHERWISE STATED.

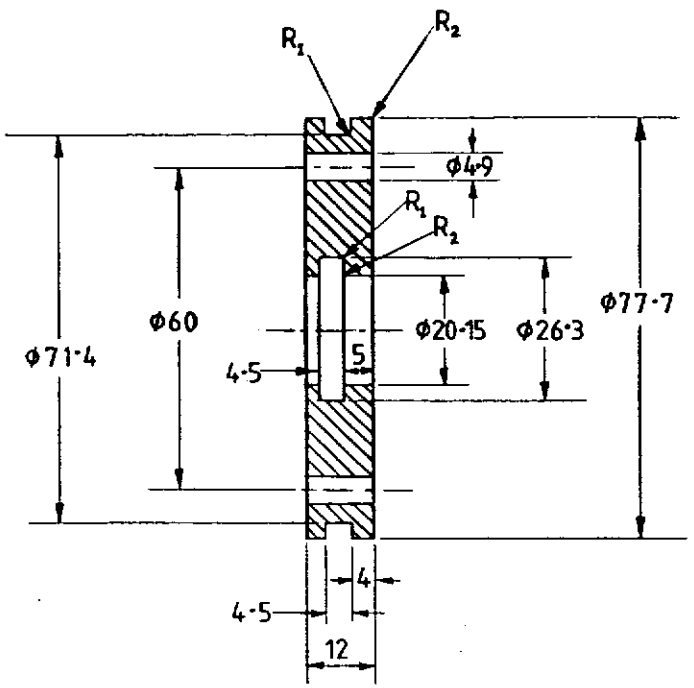

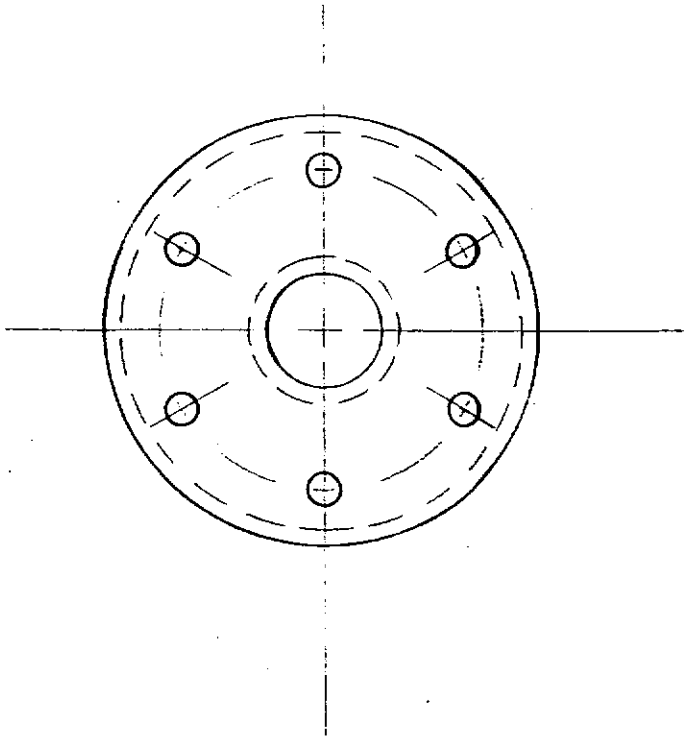

NOTE

R_1 = ·5 ⟷ ·75

R_2 = ·12 ⟷ ·25

- 400 -

Fig.(J.9)

	9		O' RING HOLDER (B-TUBES)	1	M.S.		
	ITEM	PART No.	DESCRIPTION	No. OFF	MAT'L	SPEC.	REMARKS

THIRD ANGLE PROJECTION

SHEET SIZE A 3

SCALE 1 : 1

FINISH

DRAWN	CHK'D	APPV'D	STRESS APPVD.
M.N. NAHAS	R.TETLOW	C.K.TROTMAN	R.TETLOW
2.3.1979	13.3.79	13.3.79	13.3.79

TITLE:- GRP TUBE TEST RIG (BIAXIAL LOADING)

ISSUED BY AIRCRAFT DESIGN DIVISION

CRANFIELD INSTITUTE OF TECHNOLOGY CRANFIELD.

DRAWING No. DT 278 / 9

SHT. 9 OF 15 SHEETS

GENERAL TOLERANCE ON DIMENSIONS	JOB No.	No. OF SETS REQ'D
MACHINED		
UNMACHINED		
OTHER DIMENSIONS AS STATED		
WELD WHERE SHOWN THUS		
MACHINE WHERE SHOWN THUS ✓	USED ON DRG.	

6280

ALL DIMENSIONS IN MILLIMETRES UNLESS OTHERWISE STATED.

DRAWING No.	
ISSUE	MODIFICATION

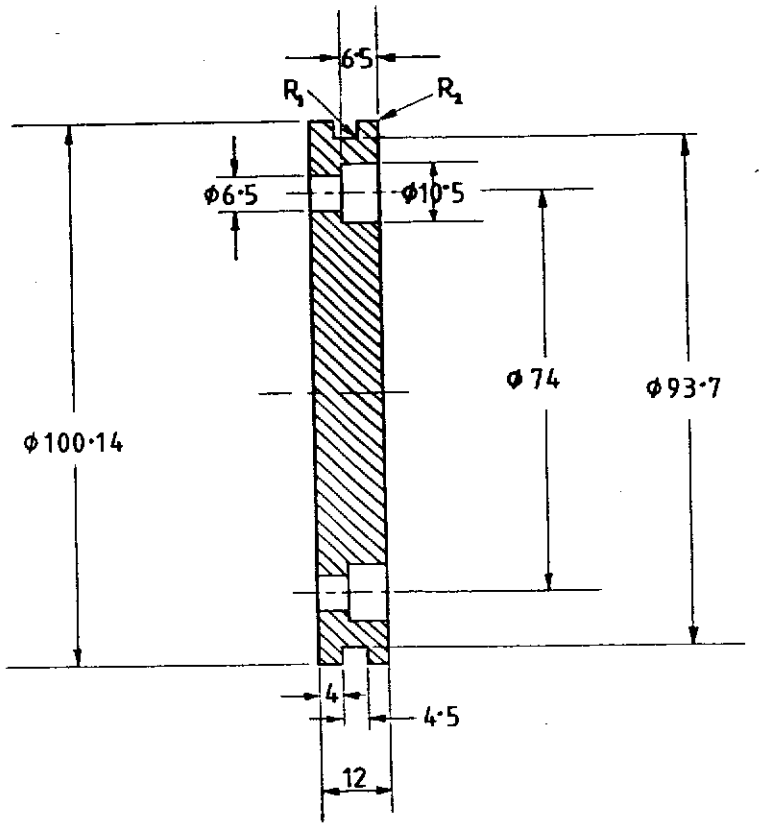

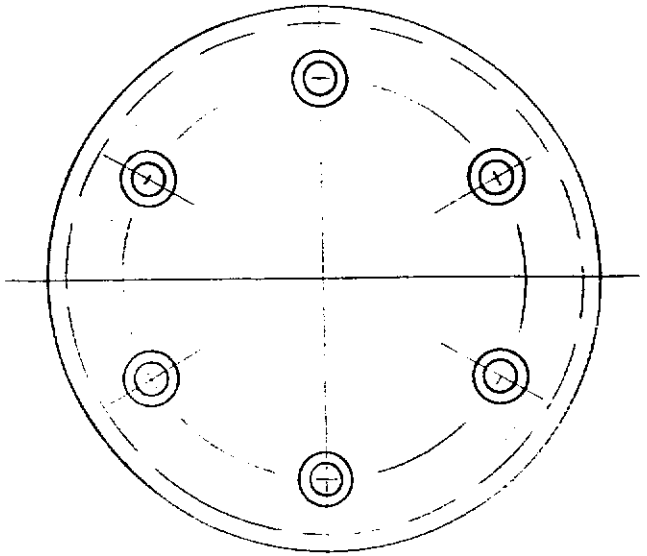

NOTE

R_1 = ·5 → ·75
R_2 = ·12 → ·25

Fig.(J.10)

ITEM	PART No.	DESCRIPTION	No. OFF	MAT'L	SPEC.	REMARKS
10		"O" RING HOLDER	1	M.S.		

THIRD ANGLE PROJECTION

SHEET SIZE A 3

SCALE 1 : 1

FINISH

	DRAWN	CHK'D	APPV'D	STRESS APPVD.
	M.N. NAHAS	R.TETLOW	C.K.TROTMAN	R.TETLOW
	2.3.1979	13.3.79	13.3.79	13.3.79

TITLE:- GRP TUBE TEST RIG (BIAXIAL LOADING)

ISSUED BY AIRCRAFT DESIGN DIVISION

CRANFIELD INSTITUTE OF TECHNOLOGY
CRANFIELD.

DRAWING No. DT 278 / 10

SHT. 10 OF 15 SHEETS

GENERAL TOLERANCE ON DIMENSIONS	JOB No.	No. OF SETS REQ'D
MACHINED		
UNMACHINED		
OTHER DIMENSIONS AS STATED		
WELD WHERE SHOWN THUS ⌐		
MACHINE WHERE SHOWN THUS ✓	USED ON DRG.	

DRAWING No.	
ISSUE	MODIFICATION

ALL DIMENSIONS IN MILLIMETRES UNLESS OTHERWISE STATED.

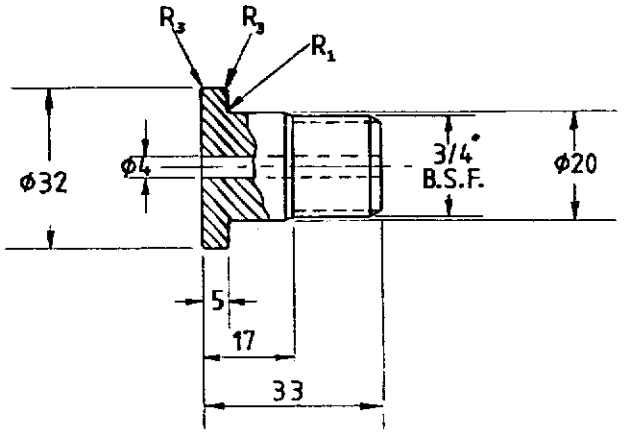

NOTE

R_1 = ·5 — ·75

R_3 = 1

Fig.(J.11)

THIRD ANGLE PROJECTION	SHEET SIZE A 3	11		LINER HOLDER	1	M.S.		
		ITEM	PART No.	DESCRIPTION	No. OFF	MAT'L	SPEC.	REMARKS

GENERAL TOLERANCE ON DIMENSIONS	JOB No.	No. OF SETS REQD
MACHINED		
UNMACHINED		
OTHER DIMENSIONS AS STATED		
WELD WHERE SHOWN THUS		
MACHINE WHERE SHOWN THUS	USED ON DRG.	

SCALE 1 : 1

FINISH

	DRAWN	CHK'D	APPV'D	STRESS APPVD.
	M. N. NAHAS	R.TETLOW	C.K.TROTMAN	R.TETLOW
	2.3.1979	13.3.79	13.3.79	13.3.79

TITLE:- GRP TUBE TEST RIG (BIAXIAL LOADING)

ISSUED BY AIRCRAFT DESIGN . DIVISION

CRANFIELD INSTITUTE OF TECHNOLOGY
CRANFIELD.

DRAWING No. DT 278 / 11

SHT. 11 OF 15 SHEETS

ALL DIMENSIONS IN MILLIMETRES UNLESS OTHERWISE STATED.

DRAWING No.	
ISSUE	MODIFICATION

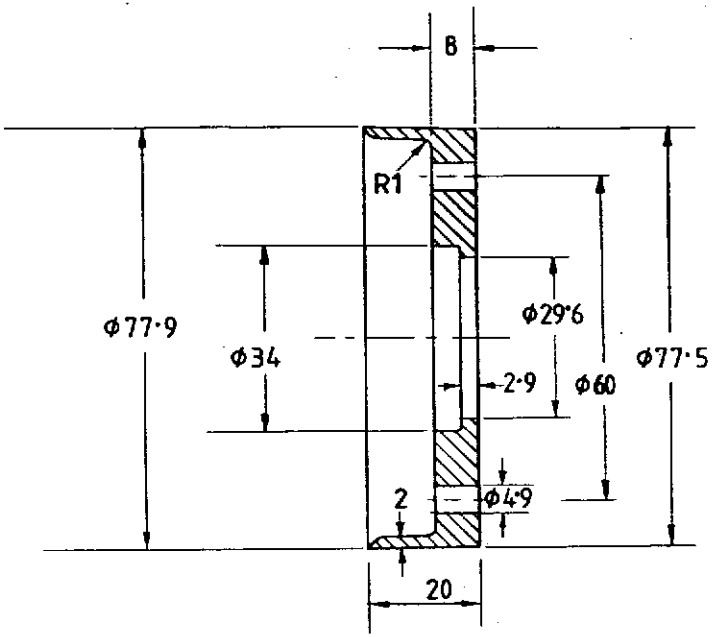

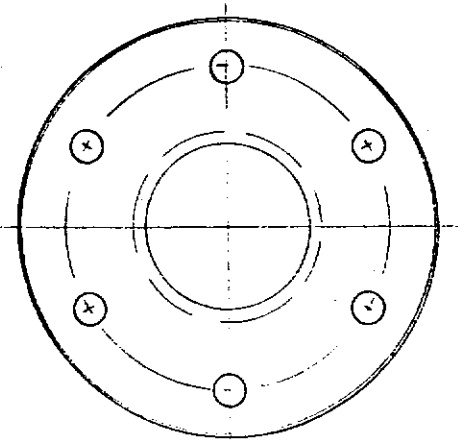

Fig.(J.12)

THIRD ANGLE PROJECTION	SHEET SIZE	ITEM	PART No.	DESCRIPTION	No. OFF	MAT'L	SPEC.	REMARKS
	A 3	12		SEALING CUP	1	CAST POLYTHENE		

GENERAL TOLERANCE ON DIMENSIONS MACHINED UNMACHINED OTHER DIMENSIONS AS STATED	JOB No.	No. OF SETS REQ'D
WELD WHERE SHOWN THUS		
MACHINE WHERE SHOWN THUS ✓	USED ON DRG.	

SCALE	DRAWN	CHK'D	APPV'D	STRESS APPVD.
1 : 1	M. N. NAHAS	R.TETLOW	C.K.TROTMAN	R.TETLOW
FINISH	2.3.1979	13.3.79	13.3.79	13.3.79

TITLE:- GRP TUBE TEST RIG (BIAXIAL LOADING)

ISSUED BY AIRCRAFT DESIGN DIVISION

CRANFIELD INSTITUTE OF TECHNOLOGY
CRANFIELD.

DRAWING No. DT 278 / 12

SHT. 12 OF 15 SHEETS

DRAWING No.

ISSUE	MODIFICATION

ALL DIMENSIONS IN MILLIMETRES UNLESS OTHERWISE STATED.

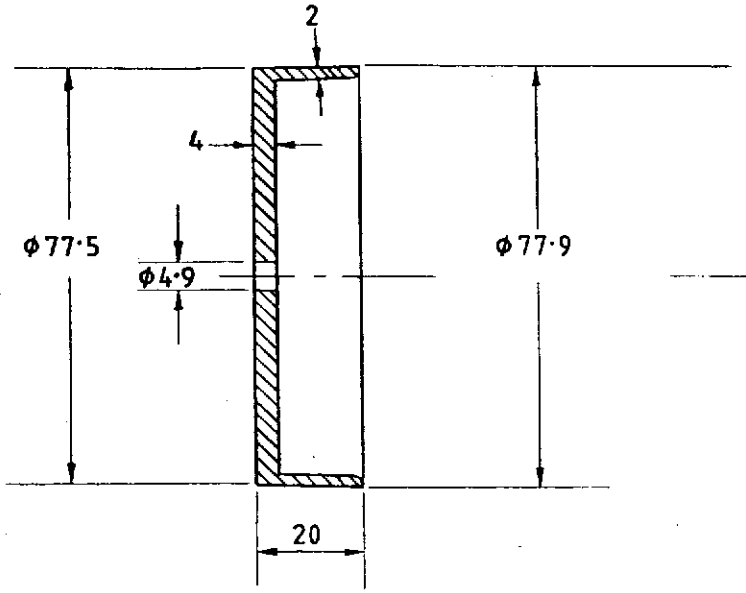

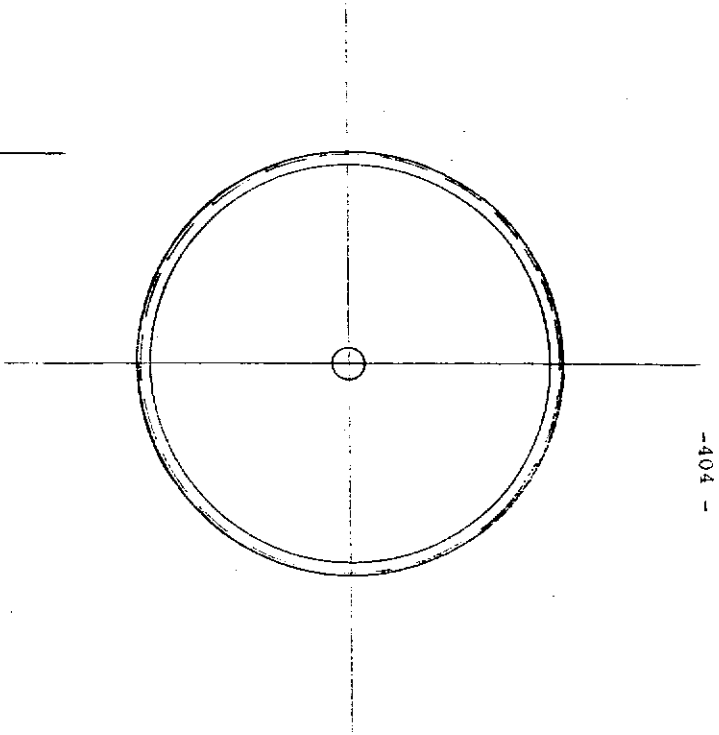

Fig.(J.13)

THIRD ANGLE PROJECTION	SHEET SIZE A 3	13		SEALING CUP	1	CAST POLYTHENE		
		ITEM	PART No.	DESCRIPTION	No. OFF	MAT'L	SPEC.	REMARKS

GENERAL TOLERANCE ON DIMENSIONS MACHINED UNMACHINED OTHER DIMENSIONS AS STATED	JOB No.	No. OF SETS REQ'D	SCALE 1 : 1	DRAWN	CHK'D	APPV'D	STRESS APPVD.	TITLE:- GRP TUBE TEST RIG (BIAXIAL LOADING)
				M.N.NAHAS	R.TETLOW	C.K.TROTMAN	R.TETLOW	
				2.3.1979	13.3.79	13.3.79	13.3.79	
WELD WHERE SHOWN THUS			FINISH	ISSUED BY AIRCRAFT DESIGN DIVISION				DRAWING No. DT 278 / 13
MACHINE WHERE SHOWN THUS ✓	USED ON DRG.			CRANFIELD INSTITUTE OF TECHNOLOGY CRANFIELD.				SHT. 13 OF 15 SHEETS

6880

DRAWING No.	
ISSUE	MODIFICATION

ALL DIMENSIONS IN MILLIMETRES UNLESS OTHERWISE STATED.

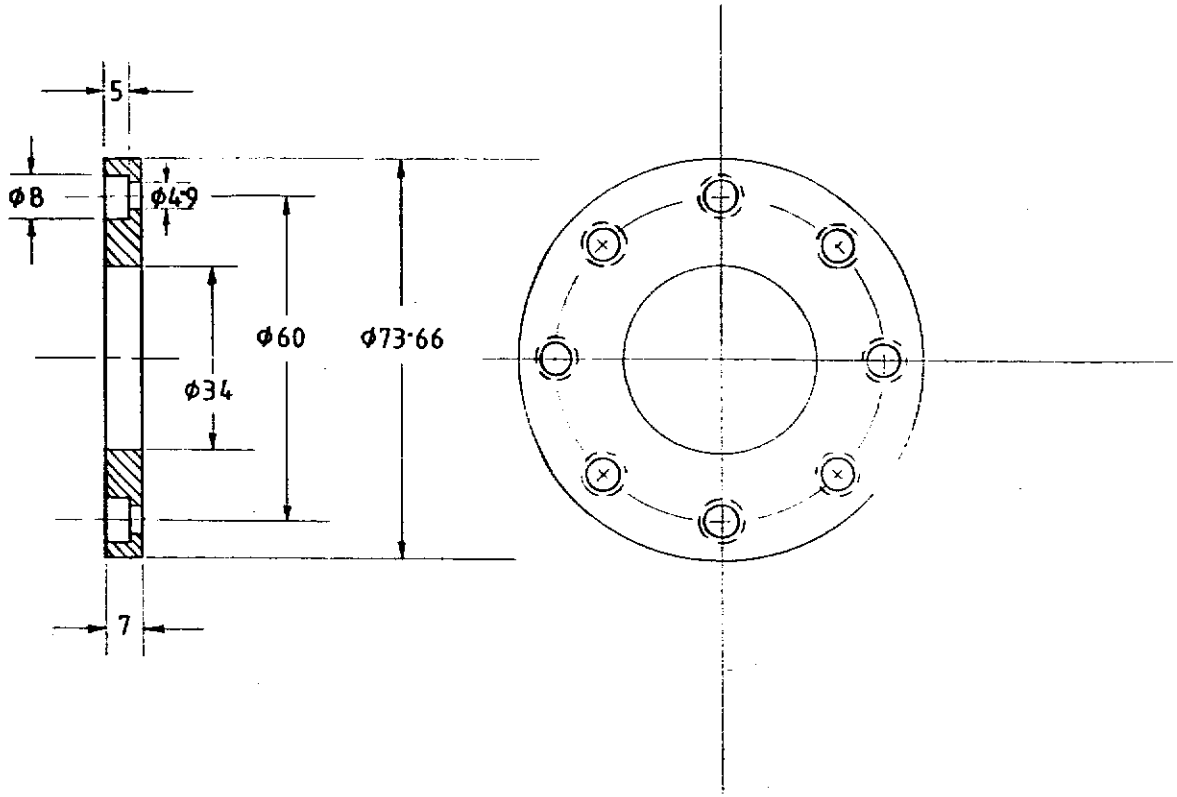

Fig.(J.14)

THIRD ANGLE PROJECTION			SHEET SIZE A 3	14		SEALING CUP COVER	1	M. S.		
				ITEM	PART No.	DESCRIPTION	No. OFF	MAT'L	SPEC.	REMARKS
GENERAL TOLERANCE ON DIMENSIONS MACHINED UNMACHINED OTHER DIMENSIONS AS STATED	JOB No.	No. OF SETS REQ'D	SCALE 1 : 1	DRAWN	CHK'D	APPV'D	STRESS APPVD.	TITLE:- GRP TUBE TEST RIG (BIAXIAL LOADING)		
				M.N. NAHAS	R.TETLOW	C.K.TRITMAN	R.TETLOW			
				2.3.1979	13.3.79	13.3.79	13.3.79			
WELD WHERE SHOWN THUS			FINISH	ISSUED BY AIRCRAFT DESIGN DIVISION				DRAWING No. DT 278 / 14		
MACHINE WHERE SHOWN THUS ✓	USED ON DRG.			CRANFIELD INSTITUTE OF TECHNOLOGY CRANFIELD.				SHT. 14 OF 15 SHEETS		

DRAWING No.	
ISSUE	MODIFICATION

ALL DIMENSIONS IN MILLIMETRES UNLESS OTHERWISE STATED.

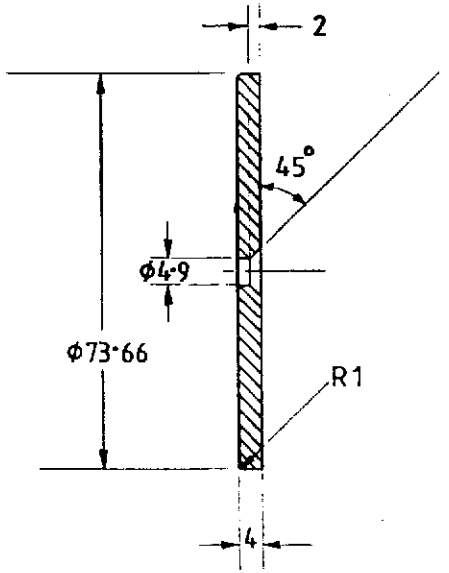

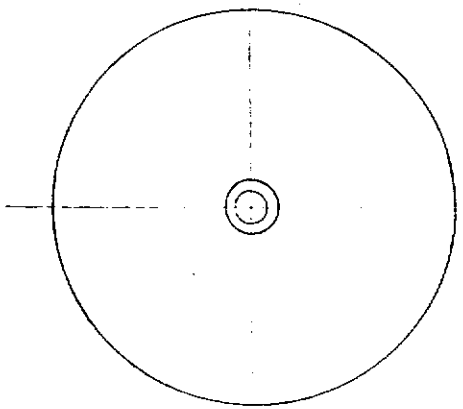

Fig.(J.15)

THIRD ANGLE PROJECTION	SHEET SIZE A 3	15		SEALING CUP COVER	1	AL.		
		ITEM	PART No.	DESCRIPTION	No. OFF	MAT'L	SPEC.	REMARKS

GENERAL TOLERANCE ON DIMENSIONS MACHINED UNMACHINED OTHER DIMENSIONS AS STATED	JOB No.	No. OF SETS REQ'D	SCALE 1 : 1	DRAWN	CHK'D	APPV'D	STRESS APPVD.	TITLE:- GRP TUBE TEST RIG (BIAXIAL LOADING)
				M.N. NAHAS	R.TETLOW	K.K.TROTMAN	R.TETLOW	
				2.3.1979	13.3.79	13.3.79	13.3.79	
WELD WHERE SHOWN THUS			FINISH	ISSUED BY AIRCRAFT DESIGN DIVISION				DRAWING No. DT 278 / 15
MACHINE WHERE SHOWN THUS	USED ON DRG.			CRANFIELD INSTITUTE OF TECHNOLOGY CRANFIELD.				SHT. 15 OF 15 SHEETS